Synthesis of main group, rare-earth, and d^0 metal complexes containing beta-hydrogen

by

KaKing Yan

A dissertation submitted to the graduate faculty

in partial fulfillment of the requirements for the degree of

DOCTOR OF PHILOSOPHY

Major: Inorganic Chemistry

Program of Study Committee:
Aaron D. Sadow, Major Professor
Andreja Bakac
William S. Jenks
Gordon J. Miller
L. Keith Woo

Iowa State University

Ames, Iowa

2013

To my dad, my mom, my sister Jen, and my grandfather

TABLE OF CONTENTS

Acknowledgements

My Ph.D journey was a long but rewarding life experience. Within these long six and a half year and over 4000 real experiments (distillation, purification etc. excluded), I could not have gone through this time without the help and assistance from a lot of people. Here, I would like to sincerely express my deepest appreciation to these fellows.

First of the pack, I would like to thank my boss, Prof. Aaron Sadow, to take a chance on me to work in his lab. I still remember there were four people interested in his group and he picked three people, Isaac, Steven and me. Thanks for being so supportive the entire time. I learned a lot from you on how to be a real scientist: never take shortcut, hard-working, and fully committed to your work.

Next, I would like to thank my committee members, Prof. Andreja Bakac, Prof. Gordie Miller, Prof. William Jenks and Prof. Keith Woo. In addition, I want to thank Prof. Victor Lin, my previous committee member. All of your valuable suggestions and helpful critiques lead me to the right direction. Moreover, I have to thank the CIF staff, the BB&B scientist and the glassblower, Steve Veysey, Dr. Dave Scott, Dr. Kamel Harrata, Dr. Shu Xu, Dr. Sarah Cady, Dr. Bruce Fulton and Trond Forre because I could not have excelled my work without running these instruments (GC, LC, X-ray and NMR) or having my glassware fixed. A special thank goes to Dr. Arkady Ellern for his time to collect and solve all my structure in an amazingly fast speed. Your help makes my work go forward. Thank you.

Also, I would like to thank all the past and present Sadow group members for your help over the years – past members included Dr. James Dunne, Ben Baird, Jiachun Su, Dr. Hung-An Ho, Dr. Steven Neal, Ryang Kim, Dr. Andrew Pawlikowski, Stephanie Smith, Dr.

Barun Jana and present members included Dr. Kuntal Manna, soon to be Dr. Debabrata Mukherjee, Sonchen Xu, Amy (B zi) Jing Zhu, Aradhanna Pinwal, Naresh Eedugurala, Nicole Lampland, Jacob Fleckenstein, Regina Reinig, Zak Weinstein, Megan Hovey, and Brad. Please forgive me if I ever gave you a bad tamper, as happiness is dropping exponentially after fifth year in grad school, you will all soon find out. Special thanks go to Andy, James, Isaac, and Steven for being there for me – still enjoy all the productive scientific discussion with you over the years. Also, if not because of the passion and enthusiasm shown by Crystal Su, I would not have joined the Sadow group. Too much to be thankful for. Forgive me if I didn't give enough credit.

To the many undergraduates who have worked in our lab over the years – Dan, David, Marlie, Tristan, Jared, Kate, Jooyoung, Brianna, Rick, Josh, Marissa, and Yitzhak, Yixin, and Jacob. Thank you all. Brianna, you have been my undergrad for ~ 2yrs, without you, work would get done so fast. Thanks for taking my bad advices and still bearing with me.

My life in Ames would not be so colorful without help and care from people outside my research group. I want to thank you my friends, Ben Tang, Isaac Ho, Yuesi Fung, Lin Liu, and Steven Tsai, my previous roommate, to get me through the tough time and all the fun weekend nights. I also want to thank you James Dunne, Ben Baird, Aaron Kemperman, Bernie Anding, Issac, and Andy Pawlikawski for good time in watching football, playing fantasy football, and bar time. Without all of you, my life here in Ames would be all about work. Also, I would like to thank you a lot of Taiwanese here in Ames, including Cedric, Mike, Dr. Song, Steven etc. to introduce me to the game of Softball. I want to thank you my family for all the support, patience, and tolerance about my lack of care to all the family

members, I deeply indebted to you all. Love you dad, mom, Jen, Grandpa, and all my family members, I wish I could have called you more and come home more often.

Finally, thank you all!

Abstract

A series of organometallic compounds containing the tris(dimethylsilyl)methyl ligand are described. The potassium carbanions $KC(SiHMe_2)_3$ and $KC(SiHMe_2)_3TMEDA$ are synthesized by deprotonation of the hydrocarbon $HC(SiHMe_2)_3$ with potassium benzyl. $KC(SiHMe_2)_3TMEDA$ crystallizes as a dimer with two types of three-center-two-electron K-H-Si interactions. Homoleptic Ln(III) tris(silylalkyl) complexes containing β-SiH groups $M\{C(SiHMe_2)_3\}_3$ (Ln = Y, Lu, La) are synthesized from salt elimination of the corresponding lanthanide halide and 3 equiv. of $KC(SiHMe_2)_3$. The related reactions with Sc yield bis(silylalkyl) ate-complexes containing either LiCl or KCl. The divalent calcium and ytterbium compounds $M\{C(SiHMe_2)_3\}_2L$ (M = Ca, Yb; L = THF_2 or TMEDA) are prepared from MI_2 and 2 equiv of $KC(SiHMe_2)_3$. The compounds $M\{C(SiHMe_2)_3\}_2L$ (M = Ca, Yb; L = THF_2 or TMEDA) and $La\{C(SiHMe_2)_3\}_3$ react with 1 equiv of $B(C_6F_5)_3$ to give 1,3-disilacyclobutane $\{Me_2Si\text{-}C(SiHMe_2)_2\}_2$ and $MC(SiHMe_2)_3HB(C_6F_5)_3L$, and $La\{C(SiHMe_2)_3\}_2HB(C_6F_5)_3$, respectively. The corresponding reactions of $Ln\{C(SiHMe_2)_3\}_3$ (Ln = Y, Lu) give the β-SiH abstraction product $[\{(Me_2HSi)_3C\}_2LnC(SiHMe_2)_2SiMe_2][HB(C_6F_5)_3]$ (Ln = Y, Lu), but the silene remains associated with the Y or Lu center. The abstraction reactions of $M\{C(SiHMe_2)_3\}_2L$ (M = Ca, Yb; L = THF_2 or TMEDA) and $Ln\{C(SiHMe_2)_3\}_3$ (Ln = Y, Lu, La) and 2 equiv of $B(C_6F_5)_3$ give the expected dicationic $M\{HB(C_6F_5)_3\}_2L$ (M = Ca, Yb; L = THF_2 or TMEDA) and dicationic mono(silylalkyl) $LnC(SiHMe_2)_3\{HB(C_6F_5)_3\}_2$ (Ln = Y, Lu, La), respectively.

Salt metathesis reactions of $Cp_2(NR_2)ZrX$ (X = Cl, I, OTf; R = *t*-Bu, $SiHMe_2$) and lithium hydrosilazide ultimately afford hydride products $Cp_2(NR_2)ZrH$ that suggest unusual

β-hydrogen elimination processes. A likely intermediate in one of these reactions, $Cp_2Zr[N(SiHMe_2)t\text{-}Bu][N(SiHMe_2)_2]$, is isolated under controlled synthetic conditions. Addition of alkali metal salts to this zirconium hydrosilazide compound produces the corresponding zirconium hydride. However as conditions are varied, a number of other pathways are also accessible, including C-H/Si-H dehydrocoupling, γ-abstraction of a CH, and β-abstraction of a SiH. Our observations suggest that the conversion of (hydrosilazido)zirconocene to zirconium hydride does not follow the classical four-center β-elimination mechanism.

Elimination and abstraction reactions dominate the chemistry of ligands containing β-hydrogen. In contrast, $Cp_2Zr\{N(SiHMe_2)_2\}H$ and $Cp_2Zr\{N(SiHMe_2)_2\}Me$ undergo selective γ-CH bond activation to yield the azasilazirconacycle $Cp_2Zr\{\kappa^2\text{-}N(SiHMe_2)SiHMeCH_2\}$, even though there are reactive β-hydrogen available for abstraction. The β-SiH groups in metallacycle provide access to new pathways for sixteen-electron zirconium alkyl compounds, in which $Cp_2Zr\{\kappa^2\text{-}N(SiHMe_2)SiHMeCH_2\}$ undergoes a rare σ-bond metathesis reaction with ethylene. The resulting vinyl intermediate undergoes β-hydrogen abstraction to reform ethylene and a silanimine zirconium species that reacts with ethylene to give a metallacyclopentane as the isolated product. The pendent β-SiH in metallocycle also reacts with paraformaldehyde through an uncatalyzed hydrosilylation to form an exocyclic methoxysilyl moiety, while the zirconium-carbon bond in metallocycle is surprisingly inert toward formaldehyde. Still, the Zr-C moiety in metallocycle is available for chemistry, and it interacts with the carbon monoxide and strong electrophile $B(C_6F_5)_3$ to provide $Cp_2Zr[\kappa^2\text{-}OC(=CH_2)SiMeHN(SiHMe_2)]$ and $Cp_2Zr[N(SiHMe_2)SiHMeCH_2B(C_6F_5)_3]$. Finally, the

frustrated Lewis-pair 2,6-lutidine-$B(C_6F_5)_3$ adduct reacts with the intra-cyclic SiH to give a transient 2,6-lutidine-stabilized silicon cation $[Cp_2ZrCH_2SiMe(2,6\text{-}Me_2\text{-}NC_6H_3)N(SiMe_2H)][HB(C_6F_5)_3]$ that slowly rearranges to give $Cp_2Zr[N(SiHMe_2)SiHMeCH_2B(C_6F_5)_3]$ and free 2,6-lutidine.

Finally, we also demonstrated a β-elimination of a cationic zirconocene disilazide compound $[Cp_2ZrN(SiHMe_2)_2]^+$ that is facilitated by DMAP (4-N,N-dimethylaminopyridine) to give $[Cp_2ZrH\{N(SiHMe_2)(SiMe_2DMAP)\}]^+$. A formal insertion reaction of a Zr-R group of $Cp_2ZrN(SiHMe_2)_2R$ (R = H, alkyl, halide, alkoxide) into a silaimine, formed by reaction of the zirconocene silazide and $B(C_6F_5)_3$, to give $[Cp_2Zr\{N(SiHMe_2)(SiRMe_2)\}]^+$. Thus, we also show the application of the β-elimination reaction in hydrosilylation of ketones and aldehydes.

Chapter 1. General introduction

Homoleptic rare-earth hydrocarbyl complexes[1]

Since the historic discovery and isolation of extremely reactive and highly pyrophoric diethyl zinc in 1849,[2] it took another decade for the isolation of another homoleptic hydrocarbyl main group complexes. However, ever since then, the traditional point of view that metal carbon is too weak and reactive to isolate slowly changed. The next decade represented a major breakthrough in metal hydrocarbyl chemistry as more and more organometallic alkyl complexes were synthesized and isolated. Although Wilkinson and Birmingham synthesized $Ln(C_5H_5)_3$ (Ln = Sc, Y, La, Ce, Pr, Nd, Sm, Gd, Dy, Er, Yb)[3] in 1954, a genuine rare-earth homoleptic hydrocarbyl with a σ-bond was synthesized in $Sc(C_6H_5)_3$ in 1968 by Hart and Saran[4] and a first structural proof of a s-bonded rare-earth alkyl was provided by Hart in $[Li(thf)_4][Lu(C_6H_3Me_2\text{-}2,6)_4]$[5].

Another major breakthrough in rare-earth σ-bonded alkyl chemistry came since the pioneer of "neopentyl"-type ligands $[CH_2CMe_3]$,[1,6] and more specifically, $[CH_2SiMe_3]$,[1,6] $[CH(SiMe_3)_2]$,[1,7] and $[C(SiMe_3)_3]$,[1,8] by Lappert[9] and Eaborn[8] that opened up organolanthanide chemistry. Shortly after, the structural characterization of the first neutral homoleptic rare-earth metal σ-bonded alkyl complexes $Ln(CH(SiMe_3)_2)_3$ (Ln = La, Sm) were reported by Hitchcock.[10] Until today, the (trimethylsilyl)methane ligand and its derivatives become the most widely used alkyl ligands in rare-earth metal chemistry. More recently, homoleptic organolanthanide alkyl chemistry is extended to t-Bu,[1,11] alkynyl,[1,12] and benzyl derivative[1,13].

"Truly" monomeric homoletpic alkyl family

$Ln(C(SiMe_3)_3)_2$

$Ln(CH(SiMe_3)_2)_3$

"Truly" polymeric homoletpic alkyl family

$(LnMe_3)_n$

$[LnC_6H_5)_3]_n$

$[Ln(C\equiv C\text{-}R)_3]_n$

Monomeric homoletpic alkyl family complexed with alkali metal or solvent moledules

$Ln(C_6H_5)_3(Do)_n$ $Ln(CH_2SiMe_3)_3(Do)$ $[Li(Do)_n][Ln(CH_2CMe_3)_4]$

$Ln(CH_2C_6H_4R)_3(Do)_n$ $[Li(Do)_n][Ln(CMe_3)_4]$

Scheme 1.1. Homoleptic organolanthanide hydrocarbyl complexes known in literature

Notably, if the term "homoletpic" is defined as purely M-C bonded components, in exclusion of alkaline-metal salt, donor solvent molecules (external and internal), and bimetallic ligand, then the only truly homoleptic organolanthanide alkyl complexes known in literature would be $LnMe_3$[1,14] $Ln(C_6H_5)_3$,[1,4] $Ln(CH(SiMe_3)_2)_3$,[1,7] $Ln(C(SiMe_3)_3)_2$[1,8] and derivatives. Due to the large ionic radii and electropositive nature of rare-earth metals, they tend to coordinate to donor molecules and form complexation with alkali-metal salt and even aggregate.[1] Therefore, it is utterly important for the availability of truly homoleptic alkyl starting materials to avoid contamination by salt or solvent molecules later in the synthetic steps. As you also note, the homoletpic rare-earth alkyls all lack β-hydrogens to avoid the facile β-H elimination known in transition metal alkyl chemistry. However, important aspects of rare earth metal-ligand bonding and reactivity may be overlooked in the absence of studies of β-hydrogen-containing complexes.

β-Agostic interaction and β-H elimination

Agostic interaction was first coined by Green to "discuss the various manifestations of covalent interactions between carbon-hydrogen groups and transition metal centers in organometallic compounds. The word agostic will be used to refer specifically to situations in which a hydrogen atom is covalently bonded simultaneously to both a carbon atom and a transition metal atom."[15] Ever since the discovery, this bonding phenomenon has been found more usual than expected. Although agostic interaction refers to M---H---C interaction, not all 3-center-2-electron bonds are agostic. For example, some of these interactions are better described as hydrogen-bonding.[16]

Experimental studies have shown that agostic complex is the ground state structure. For example, the variable temperature NMR experiments done by Brookhart demonstrated that the agostic alkyl species is at equilibrium with olefin-hydride species and olefin-ethyl species at room temperature, while the agostic alkyl complex is observed predominately at low temperature (Scheme 1.2). Thus, it suggests the 18 e^- agostic complex is the ground state structure.[17]

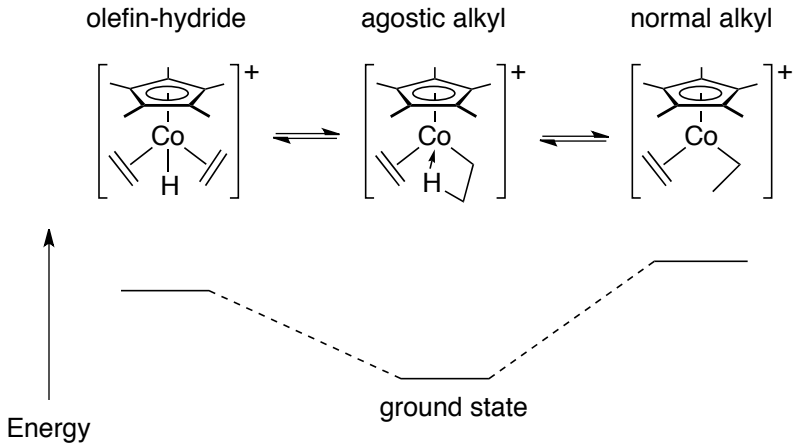

Scheme 1.2. The dynamic equilibria of $[Cp^*Co(\eta^2\text{-}C_2H_2)(\beta\text{-agostic-}C_2H_5)]^+$ [17]

Another system $(Me_2PCH_2CH_2PMe_2)TiEtCl_3$, studied by Green, showed evidence of agostic interaction by crystallography.[18] The crystal structure of $(Me_2PCH_2CH_2PMe_2)TiEtCl_3$ exhibits remarkably small angle of 85.9(6)° at the C_β while an angle close to 109° would be expected without any unusual interaction. This result provided the first clear evidence that a short Ti-H_β distance and acute angle must come from an attractive force between the titanium center and C–H bond. These two benchmark examples lay the ground for agostic development for the next 30 years.

Theoretical and experimental works done by Eisenstein,[19] McGrady,[20] and Scherer[21] have shown that there are distinct differences in term of the origin of agostic interactions in d^0 early metal, main group and late metal systems. The aogstic interaction in d^0 metal system mainly arises from hyperconjugative delocalization of electrons from M-C bond to over to the alkyl backbone and establishment of a secondary M---H_b interaction, while the agostic interaction in main group alkyl originates from electrostatic M---H---C interaction. The theory behind late metal system is more complicated since the metal center is not as Lewis acidic as d^0 metal, therefore, C_β-H_β to M π-donation, M to C_β-H_β π-back-donation, and some of C_β-H_β to M s-donation contribute to the agostic interaction. As a result, the M---H_β distance is shorter in the late metal system than the early metal system. Due to this difference, late metal alkyl systems are more prone to β-H elimination. In the benchmark study by Bercaw on a (cgc)Sc system, based on kinetic study, he proposed that early metal alkyl complexes containing β-agostic interaction are less likely to eliminate olefin and form metal hydride.[22] As a result, the agostic interaction stabilizes the catalysts resting state against β-H elimination during olefin polymerization.

On the other hand, aogstic early metal amide systems are less likely to undergo β-H elimination because they share different structural and electronic features with agostic metal alkyl.[23] For example, β-agostic amides generally contain long N-C bonds, large (~120 °) ∠M-N-C angles, and short β-C-H distances, while β-agostic alkyls contain short C-C bonds, small ∠M-C-C angles, and long β-CH bonds. Theoretic study suggested that agostic amide systems contain activated N-C_{β} bond and short M-N bond, in contrast to β-agostic alkyls, which disfavor β-elimination.

Thesis Organization

The thesis contains twelve chapters. Chapter 1 give a brief introduction of the topic discussed later. Part of chapter 2, chapter 3 and chapter 6 have already been published, and other chapters are modified from manuscripts in preparation. The thesis ends with a general conclusion in Chapter 11. All the published journal articles are modified to some degree to have a coherent description.

Chapter 2 to 4 describe preparation of organometallic chemistry of main group and lanthanide complexes with β-SiH containing $–C(SiHMe_2)_3$ ligand, and their reactions with Lewis acids to initiate β-SiH abstraction to give zwitterionic products. Chapter 5 describes our investigation of mixed alkyl silyl organomagnesium chemistry, and our effort led to the preparation of first examples of cationic magnesium silyl complexes.

The ultimate goal of this project is to eventually study reactivity of β-SiH containing d^0 silyl with Lewis acids.

Chapter 6 to 10 describes our contribution in β-SiH containing zirconocene amide chemistry. Chapter 6 illustrates a first example of β-H elimination of a d^0 amide system. This unprecedented transformation was observed in salt metathesis reactions of a hydrosilazido zirconium halide compound and lithium hydrosilazides ultimately afford hydride products that suggest unusual β-hydrogen elimination processes. Chapter 7 demonstrates a rare C-H activation of ethylene by a β-H containing azasilazirconacyle to give a zirconacyclopentane, in which all the proposed intermediates were isolated. Chapter 8 highlights the reactivity of various Lewis acids with a β-H containing azasilazirconacyle, which leads to a series of Lewis acids dependent abstraction reactions. Chapter 9 and 10 demonstrate another example of β-H elimination in a d^0 amide system that contains strong SiH bisagostic interactions. All the work described in this thesis was performed by KaKing Yan. In all chapters, X-ray crystal structures were solved by Dr. Arkady Ellern.

Reference

1 Zimmermann, M.; Anwander, R. *Chem. Rev.* **2010**, *110*, 6194-6259.

2 Frankland, P. F. *J. Chem. Soc.* **1848-1849**, *2*, 263.

3 Wilkinson, G.; Birmingham, J. M. *J. Am. Chem. Soc.* **1954**, *76*, 6210.

4 Hart, F. A.; Saran, M. S. *J. Chem. Soc., Chem. Commun.* **1968**, 1614.

5 Cotton, S. A.; Welch, A. J.; Hursthouse, M. B.; Hart, F. A. *J. Chem. Soc., Chem. Commun.* **1972**, 1225.

6 Lappert, M. F.; Pearce, R. *J. Chem. Soc., Chem. Commun.* **1973**, 126.

7 Hitchcock, P. B.; Holmes, S. A.; Lappert, M. F.; Tian, S. *J. Chem. Soc., Chem. Commun.* **1994**, 2691.

8 Eaborn, C.; Hitchcock, P. B.; Izod, K.; Smith, J. D. *J. Am. Chem. Soc.* **1994**, *116*, 12071.

9 (a) Lappert, M. F.; Pearce, R. *J. Chem. Soc., Chem. Commun.* **1973**, 126. (b) Barker, G. K.; Lappert, M. F. *J. Organomet. Chem.* **1974**, *76*, C45.

10 Hitchcock, P. B.; Lappert, M. F.; Smith, R. G.; Bartlett, R. A.; Power, P. P. *J. Chem. Soc., Chem. Commun.* **1988**, 1007.

11 Wayda, A. L.; Evans, W. J. *J. Am. Chem. Soc.* **1978**, *100*, 7119.

12 (a) Deacon, G. B.; Koplick, A. J. *J. Organomet. Chem.* **1978**, *146*, C43. (b) Deacon, G. B.; Koplick, A. J.; Raverty, W. D.; Vince, D. G. *J. Organomet. Chem.* **1979**, *182*, 121.

13 (a) Chigir, N. N.; Guzman, I. S.; Sharaev, O. K.; Tinyakova, E. I.; Dolgoplosk, B. A. *Dokl. Akad. Nauk SSSR* **1982**, *263*, 375. (b) Guzman, I. S.; Chigir, N. N.; Sharaev, O. K.; Bondarenko, G. N.; Tinyakova, E. I.; Dolgoplosk, B. A. *Dokl. Akad. Nauk SSSR* **1979**, *249*, 860. (c) Thiele, K. H.; Unverhau, K.; Geitner, M.; Jacob, K. *Z. Anorg. Allg. Chem.* **1987**, *548*, 175. (d) Manzer, L. E. *J. Organomet. Chem.* **1977**, *135*, C6. (e) Manzer, L. E. *J. Am. Chem. Soc.* **1978**, *100*, 8068.

14 Gerber, L. C. H.; Le Roux, E.; To¨rnroos, K. W.; Anwander, R. *Chem. Eur. J.* **2008**, *14*, 9555.

15 Brookhart, M.; Green, M. L. H. *J. Organomet. Chem*. **1983**, *250*, 395-408.

16 (a) Brammer, L.; Charnock, J. M.; Goggin, P. L.; Goodfellow, R. J.; Koetzle, T. F.; Orpen, A. G. *J. Chem. Soc., Chem. Commun.* **1987**, 443-445. (b) Brammer, L.; McCann, M. C.; Bullock, R. M.; McMullan, R. K.; Sherwood, P. *Organometallics* **1992**, *11*, 2339-2341.

17 Brookhart, M.; Green, M. L. H.; Pardy, R. B. A. *J. Chem. Soc., Chem. Commun.* **1983**, 691-693.

18 Dawoodi, Z.; Green, M. L. H.; Mtetwa, V. S. B.; Prout, K. *J. Chem. Soc., Chem. Commun.* **1982**, 802-803.

19 Eisenstein, O.; Jean, Y. *J. Am. Chem. Soc.* **1985**, *107*, 1177-1186.

20 McGrady, G. S.; Scherer, W. *Angew. Chem., Int. Ed.* **2004**, *43*, 1782-1806.

21 Scherer, W.; Herz, V.; Brück, A.; Hauf, C.; Reiner, F.; Altmannshofer, S.; Leusser, D.; Stalke, D. *Angew. Chem. Int. Ed.* **2011**, *50*, 2845-2849. 22 Burger, B. J.; Thompson, M. E.; Cotter, W. D.; Bercaw, J. E. *J. Am. Chem. Soc.* **1990**, *112*, 1566-1577.

22 Scherer, W.; Wolstenholme, D. J.; Herz, V.; Eickerling, G.; Brück, A.; Benndorf, P.; Roesky, P. W. *Angew. Chem. Int. Ed.* **2010**, *49*, 2242-2246.

Chapter 2: Lewis acid mediated β-hydrogen elimination on homoleptic trisalkyl lanthanide complexes containing β-hydrogen.

Modified from a paper published in *Chem. Commun.*[1] and a paper to be submitted to *J. Am. Chem. Soc.*

KaKing Yan, Jing Zhu, Andrew V. Pawlikowski, Chris Ebert, Arkady Ellern, Aaron D. Sadow

Department of Chemistry and US Department of Energy Ames Laboratory, Iowa State University, Ames IA, 50011, USA

Abstract. Homoleptic Ln(III) tris(silylalkyl) complexes containing β-SiH group $M[C(SiHMe_2)_3]_3$ {Ln = Y (**2.1a**), Lu (**2.1b**), La (**2.1c**)} were synthesized from salt elimination of the corresponding lanthanide halide and 3 equiv. of $KC(SiHMe_2)_3$. The related reaction with Sc yield bis(silylalkyl) ate-complexes containing either LiCl or KCl. The reaction of **1c** with one equiv. of $B(C_6F_5)_3$ yield $La[C(SiHMe_2)_3]_2HB(C_6F_5)_3$ (**2.3**), while the corresponding reactions of $Ln[C(SiHMe_2)_3]_3$ (Ln = Y, Lu) give partial β-SiH abstraction product $[((Me_2HSi)_3C)_2LnC(SiHMe_2)_2SiMe_2][HB(C_6F_5)_3]$ {Ln = Y (**2.4a**), Lu (**2.4b**)}. The abstraction reactions of $Ln[C(SiHMe_2)_3]_3$ **2.1** and two equiv. of $B(C_6F_5)_3$ give the expected dicationic mono(silylalkyl) $Ln[C(SiHMe_2)_3][HB(C_6F_5)_3]_2$ {Ln = Y (**2.5a**), Lu (**2.5b**), La (**2.5c**)}.

[1] *Chem. Commun.* **2009**, 656-658.

Introduction

Transition metal alkyl compounds containing β-hydrogen and at least one empty orbital in an open *cis* coordination site are susceptible to elimination. These general rules also apply to elimination reactions in main group and rare earth organometallics. While β-eliminations of alkyllithiums tend to require forcing conditions (130-150 °C in hydrocarbon solvent), the heavier congeners react more rapidly.[1] Dialkylmagnesium compounds containing β-hydrogen eliminate olefin upon thermolysis, but very little is known about eliminations of the heavier analogs.[2] Likewise, coordinatively unsaturated organolanthanides will react via β-elimination.[3] For example, isobutylene extrusion from $Cp_2ErCMe_3(THF)$ is faciliated by the addition of LiCl, presumably to open a coordination site,[3e] whereas the lutetium analog decomposes at 70-80 °C.[3c] The bridging dimers $[Cp^*OArLu]_2(m\text{-}H)(m\text{-}CH_2CH_2R)$ are coordinatively saturated and robust to elimination.[3g] Importantly, unsaturated organolanthanides are highly reactive even mediating C-C bond cleavage through β-Me eliminations.[3d,f] Although β-H elimination reactions in rare-earth alykls is less common and requires harsch condition, these reactions are typically studied to avoid β-H containing ligands. For that matter, β-hydrogen-absent alkyl ligands, such as $-CH_2SiMe_3$, $-CH(SiMe_3)_2$, and $–CH_2Ph$, have been used extensively in Group 3 and rare-earth organometallic synthesis.[4] However, valuable aspects of metal-ligand bonding and unexpected reactivity would be ignored in the absence of studies of β-hydrogen-containing complexes.

Meanwhile, β-agostic alkyl structures are considered as an "arrested" structure for β-H elimination reactions.[5] Spectroscopic data and structural features of organometallic alkyl ligands containing agostic interactions provide metrics for probing electron delocalization in

metal-ligand bonds.[6,7] Characteristic infrared (ν_{CH} ~ 2250-2800 cm^{-1}) and NMR ($^1J_{CH}$ ~ 50-100 Hz) spectroscopy of β-agostic alkyl moieties support a description of these structures as intermediate between metal hydrido(olefin) and alkyl species.[6] In d^0 and agostic compounds, the bonding is better described by delocalization of the M–C bonding electrons to involve the β-carbon.[8] Several features are commonly observed in the structures and bonding of β-agostic alkyl groups. These interactions are typically weak (< 10 kcal/mol)[2] and easily disrupted by the coordination of stronger donor ligands such as tetrahydrofuran.[9] Usually only one metal-carbon(β) interaction occurs per alkyl ligand,[10] and only one alkyl ligand is agostic per metal center, although large organo-*f*-element compounds and bimetallic species may have more.[11] Lappert's [Ln(CH(SiMe$_3$)$_2$)$_3$] [Ln = Sc, Y, Lu, La, Ce] contains one β-agostic C–Si per bis(trimethylsilyl)methyl ligand giving three total.[12] Multiple agostic interactions per metal center are more common with amido (particularly silylamido) versus alkyl ligands. Early examples of bis-β-agostic disilylamide ligands were observed in X-ray structures of Na[Ln[N(SiMe$_3$)$_2$)$_3$] (Ln = Eu, Yb) in which four methyl carbons have close contacts with the lanthanide center and three carbons have close contacts with sodium cations.[13] Recently, the β-hydrogen-containing tetramethyldisilazide ligand –N(SiHMe$_2$)$_2$ has been widely studied in d^0 metal and f-elements chemistry. Compounds ligated with –N(SiHMe$_2$)$_2$ often show multiple agostic interactions to a single metal center; for example, [Eu(N(SiHMe$_2$)^{t}Bu)$_3$] contains three mono-β-agostic ligands.[14] Rare earth *ansa*-metallocenes such as Me$_2$Si(C$_5$Me$_4$)$_2$YN(SiHMe$_2$)$_2$ ligand exhibit a rare bis-β-SiH agostic structure,[15] but interestingly the bulkier Cp*$_2$YN(SiHMe$_2$)$_2$ is only mono-β-agostic.[15c] More importantly, although early metal and rare earth silazides containing β-SiH often form agostic-type

structures, β-H elimination reactions have not been observed. For example, the β-SiH containing $Cp_2Zr[N(SiHMe_2)^tBu][CH_2SiMe_3]$ reacts at the β-SiH position by β-abstraction to give a zirconocene silanimine complex.[16] Despite the rich chemistry of tetramethyldisilazido rare earth complexes, the chemistry of the earth metals with β-SiH containing alkyl remains unexplored.

Intrigued by on the lack of study on β-SiH containing alkyl chemistry in rare-earth and main group metal, here we report the syntheses and spectroscopic characterization of homoleptic group 3 and lanthanide compounds $[Ln(C(SiHMe_2)_3)_3]$ (Ln = Y (**2.1a**), Lu (**2.1b**), La (**2.1c**)) that contain β-agostic SiH structures. These complexes are the first examples of a transition metal compound containing the bulky $C(SiHMe_2)_3$ ligand,[17] which is a smaller derivative of trisyl $C(SiMe_3)_3$ that has been used to isolate low coordinate metal alkyl compounds.[10,18] Unlike most β-agostic alkyl compounds, monomeric tris(alkyl) **2.1** contain two agostic SiH interactions in each -$C(SiHMe_2)_3$ alkyl ligand for a total of six interactions per lanthanide(III) center. Although alkali metal cations do not participate in **2.1**, but incorporation of alkali metal halides in to Sc coordination sphere was observed. Additionally, the NMR chemical shift and coupling constant data for **2.1** suggest substantial electron delocalization in each tris(dimethylsilyl)methyl ligand. Reaction of **2.1c** and $B(C_6F_5)_3$ trigger β-SiH group abstraction to provide zwitterionic lanthanide bis(alkyl) $[La\{C(SiHMe_2)_3\}][HB(C_6F_5)_3]$

Results and discussion.

2.1. Synthesis and characterization of tris(dimethylsilyl)methyl yttrium compound.

In contrast to the low yielding reaction of YCl_3 and $[LiC(SiHMe_2)_3(THF)_2]$, a suspension of YCl_3 and 3 equiv. of $[KC(SiHMe_2)_3]$ in benzene affords the homoleptic solvent-free trialkyl yttrium (**2.1a)** in excellent yield (eq 2.1).

$$YCl_3 + 3\,KC(SiHMe_2)_3 \xrightarrow[\text{r.t., 12 h}\\ \text{- 3 KCl}]{\text{benzene}} [Y\{C(SiHMe_2)_3\}_3] \quad (2.1)$$

2.1a, 82%

The room temperature ^{1}H NMR spectrum (benzene-d_6) of **2.1a** contained a multiplet at 3.85 ppm (Si-*H*, $^1J_{SiH}$ = 134 Hz) and a doublet at 3.96 ppm (Si-CH_3, $^3J_{HH}$ = 3.2 Hz). Two absorptions at 2106 and 1845 cm^{-1} (KBr) attributed to SiH vibrations were observed in the infrared spectrum (2102 and 1844 cm^{-1}, THF). The IR and low $^1J_{SiH}$ coupling constants in **2.1a** suggest agostic bonding involving the SiH moieties.[19]

Given the possibility that these interactions involve K^+ ions in 'ate'-type complexes,[20] additional investigations were required. The identity of **2.1a** as a homoleptic, salt-free tris(alkyl) compound is confirmed by elemental analysis and mass spectrometry (the parent ion was observed at m/z = 656). ICP-MS indicated that these ions are present as only trace elements.

Low temperature NMR spectroscopy indicates that each $C(SiHMe_2)_3$ alkyl interacts with the yttrium center through *two* β-agostic interactions. ^{1}H NMR spectra of **2.1a** in toluene-d_8, recorded from 320 to 190 K, are shown in Figure 2.1. As the temperature was lowered, the SiH and SiMe resonances were broadened to the coalescence point at 240 K. At 190 K, the ^{1}H NMR spectrum was sufficiently resolved for interpretation, and two $SiMe_2$ and two SiH resonances were detected. The downfield-shifted SiH at 4.71 ppm ($^1J_{SiH}$ = 190 Hz, 3

H) corresponds to one type of terminal SiH group, while the upfield chemical shift (3.40 ppm, 6 H) and low $^{1}J_{SiH}$ ($^{1}J_{SiH}$ = 108 Hz) for the other SiH resonance corresponds to the β-agostic Y···(H–Si) in **2.1a**. The 2:1 ratio corresponds to six non-classical SiH groups and three terminal SiH moieties. At 190 K in the ^{1}H NMR spectrum, the two methyl resonances at 0.47 (36 H, apparently coincident diastereotopic agostic $SiMe_2$, assigned by a ^{1}H COSY experiment) and 0.34 ppm (18 H) were too broad for additional structural assignment ($\omega_{1/2}$ = 14.9 Hz). Therefore, variable temperature $^{13}C\{^{1}H\}$ NMR was needed to characterize **2.1a**. Only one type of yttrium-bonded carbon is detected as a doublet from ambient conditions to low temperature (298 K: δ 17.3, $^{1}J_{YC}$ = 9.8 Hz; 190 K: δ 15.9,

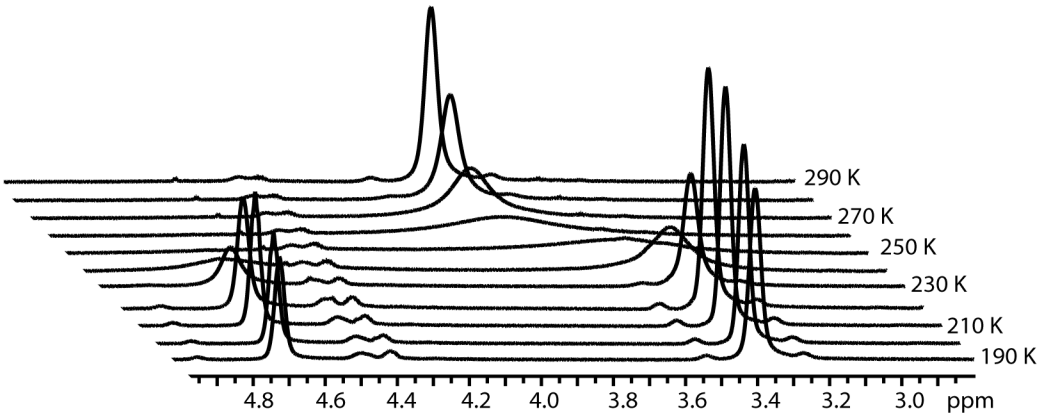

Figure 2.1. ^{1}H NMR spectra of 2.**1a** showing the splitting of Si-*H* resonances into a 2:1 ratio as temperature is lowered.

$^{1}J_{YC}$ = 9.9 Hz) in the $^{13}C\{^{1}H\}$ NMR spectra (toluene-d_8). A comparison with β-SiC agostic [$Y(CH(SiMe_3)_2)_3$] (δ 50.0, $^{1}J_{YC}$ = 30.2 Hz)[12c] highlights the unusually high field chemical shift and low $^{1}J_{YC}$ for the yttrium-bound carbon in **2.1a**. The low $^{1}J_{YC}$ of **2.1a** results from a combination of electron delocalization in the β-agostic alkyl[21] and the electropositive Si

subsituents on carbon (Bent's Rule).[22]

The $SiMe_2$ region of the VT $^{13}C\{^1H\}$ NMR spectra is also informative: as the temperature is cooled, the sharp single (δ 3.96) broadens into a resonance that begins to decoalesce at 240 K into three SiMe resonances. The expected three $^{13}C\{^1H\}$ NMR SiMe resonances were assigned using a ^1H-^{13}C HMQC experiment: resonances at 4.39 and 2.91 correspond to the two diastereotopic methyl groups in two agostic $SiHMe_2$ moieties, and the third signal at 4.60 corresponds to the two methyl carbons in the non-agostic $SiHMe_2$. At all temperatures, all three -$C(SiHMe_2)_3$ ligands are equivalent; a mirror plane bisecting each ligand relates the two agostic $SiHMe_2$ groups by symmetry and the methyl moities in the nonagostic $SiHMe_2$ group are also equivalent. These data are consistent with either pyramidal C_{3v} (**A**) or planer C_{3h}-symmetric (**B**) structures (Chart 1); **A** is favored because compounds containing agostic interactions typically exhibit distortions from VSEPR geometries and yttrium is pyramidal in $[Y(CH(SiMe_3)_2)_3]$.[6,7,12]

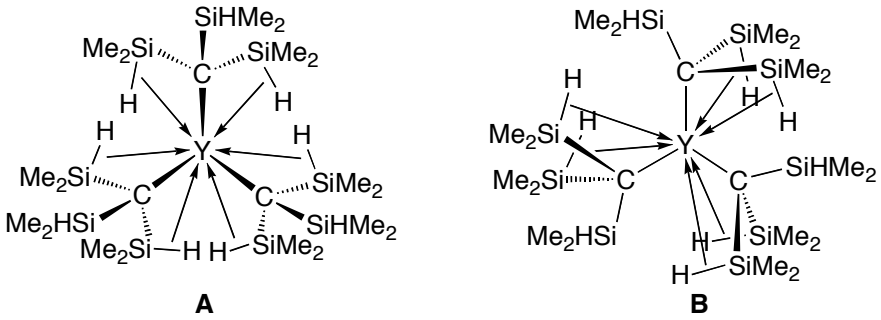

Chart 2.1. Possible structures of **2.1a**.

The methyl resonances in the $^{13}C\{^1H\}$ NMR spectra were used to model the exchange of agostic and non-agostic SiH groups from 190 to 260 K because $^3J_{HH}$ complicated simulation of the ^1H NMR spectra. The peak-widths at half-height ($\omega_{1/2}$; e.g., 3.6 Hz at 190

K) for all three SiMe resonances are identical within error, and the signals sharpen to the same extent as the low temperature limit is approached. gNMR was used to simulate the dynamic exchange of the three methyl sites; in our model, all three sites were allowed to exchange.[23] Good correlation between simulated and experimental spectra allowed the determination of rate constants for exchange. An Eyring plot provided activation parameters ($\Delta H^{\ddagger}$ = 13.4 ± 0.1 kcal/mol; $\Delta S^{\ddagger}$ of 10.9 ± 0.1 cal/mol K; $\Delta G^{\ddagger}$ = 11.3 kcal/mol at 190 K). The small positive value for $\Delta S^{\ddagger}$ is consistent with a dissociative mechanism in which one or both β-agostic interactions are disrupted, followed by -$C(SiHMe_2)_3$ rotation and re-formation of the bis-β-agostic structure (Scheme 2.1).

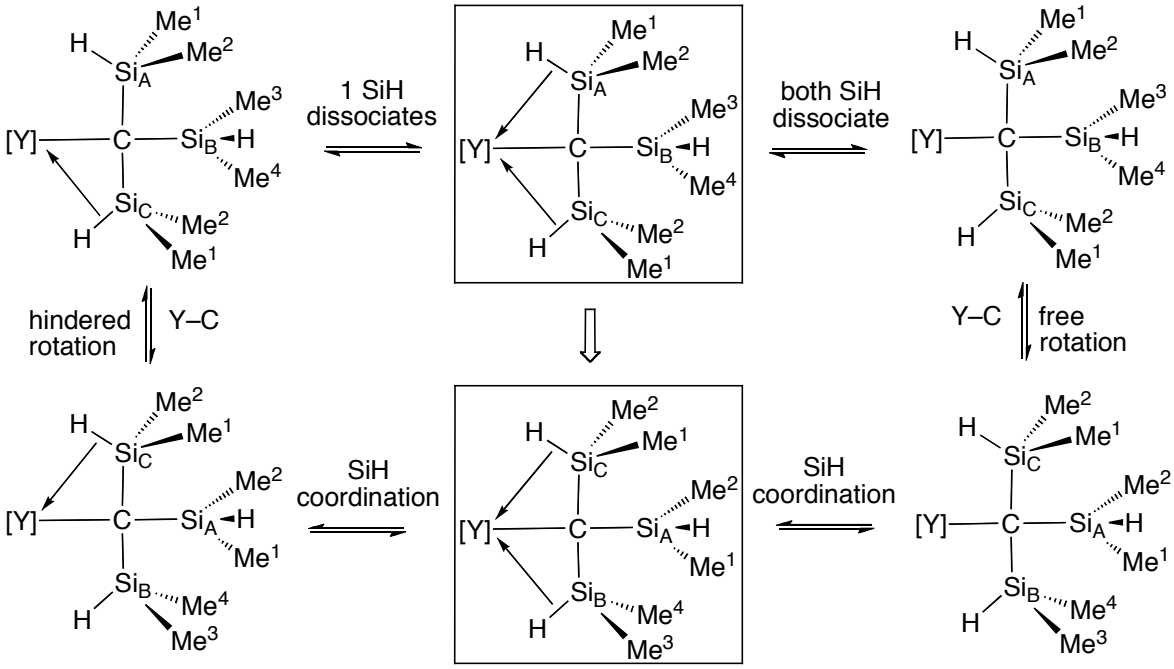

Scheme 2.1. Fischer projections illustrating two possible mechanisms for exchange of agostic and non-agostic SiH groups

The small values for the activation parameters suggest that exchange with one -$C(SiHMe_2)_3$

group is not affected by the other two ligands (i.e., the exchange processes in each ligand are not related). The strengths of β-agostic interactions have been estimated by calculations as <10 kcal/mol for non-d^0 complexes,[8] and the interactions in d^0 compounds are typically smaller (the β-agostic ethyl in Me_2YEt was calculated to be 2.4 kcal/mol).[24] Thus, the exchange process in **2.1a** proceeds with a small activation barrier. For comparison, the d^2 compounds $Cp_2M(Me_2HSiC{\equiv}CSiHMe_2)$ (M = Ti, Zr) contain one β-agostic and one non-agostic SiH that undergo exchange; for this process, $\Delta G^{\ddagger}$ values of 8.8 kcal/mol (Ti) and 14 kcal/mol (Zr) at 190 K were measured.[25] The small positive $\Delta S^{\ddagger}$ measured for **2.1a** is more consistent with exchange via dissociation of one agostic interaction rather than both. The large $\Delta H^{\ddagger}$ (relative to calculated for Me_2YEt) likely results from a combination of increased donor ability of the more polarizable Si–H[19] bond in **2.1a** compared to the β-C–H in Me_2YEt and the barrier to rotation of a bulky ligand containing an agostic SiH group.

In fact, relatively strong bis-β-agostic interactions are not disrupted by THF, which apparently does not coordinate to **2.1a**. The IR spectrum of **2.1a** in a KBr pellet and as a THF solution are very similar (vide supra), and the room temperature $^1J_{SiH}$ in benzene-d_6 and THF-d_8 are identical. The steric bulk **2.1a** also prevents coordination of THF. However, addition of LiCl to a THF-d_8 solution of **2.1a** results in a 0.7 ppm downfield change in the SiH chemical shift to 4.40 ppm and the value of $^1J_{SiH}$ increases from 130 to 162 Hz. Surprisingly, the SiMe resonances are also greatly affected by the presence of LiCl, shifting 0.32 ppm upfield to -0.07 in comparison to **2.1a**. The IR spectrum in THF only contains one ν_{SiH} at 2106 cm^{-1}, indicating that the agostic interactions are broken by LiCl coordination. ^1H NMR spectrum of $LiC(SiHMe_2)_3$ recorded in THF-d_8 matched up with the product observed

above, thus, it suggested a "reverse salt metathesis" reaction. Interestingly, no change in IR or NMR spectra of **2.1a** are observed in the presence KCl as apparently the adduct **2.1a**·KCl does not form. Salt adducts of organo-rare earth compounds can complicates their chemistry. For example, the ^{1}H NMR spectra of [Lu(CH(SiMe$_3$)$_2$)$_3$] and [Lu(CH(SiMe$_3$)$_2$)$_3$(μ-Cl)K] are identical, so the presence and quantity of the KCl-adduct is not easily determined.[12b] The diagnostic ν_{SiH} and $^{1}J_{SiH}$ in **2.1a** are clearly useful here for detecting the presence of 'ate' salts of yttrium. Additionally, compound **2.1a** is robust and does not undergo β-hydride elimination. When a solution of **2.1a** is heated at 60 °C in benzene-d_6, no change is observed after 1 day. After two days at 100 °C, HC(SiHMe$_2$)$_3$ has formed as the only product with 58% of **2.1a** remaining (as determined by ^{1}H NMR spectroscopy).

2.2. Synthesis and characterization of tris(dimethylsilyl)methyl lanthanum and lutetium compounds.

Similarly, the solvent-free homoleptic tris(alkyl) lutetium and lanthanum analogs M[C(SiHMe$_2$)$_3$]$_3$ (**1**; M = Lu (**2.1b**), La (**2.1c**)) are synthesized with the same salt elimination approach of **2.1a** using the corresponding lanthanide halides (eq 2.2). Notably, the reaction time for **2.1c** (1.5 h) is much shorter than both **2.1a** and **2.1b**.

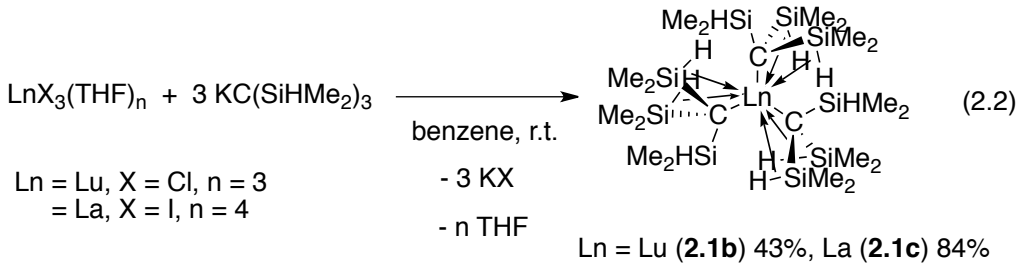

(2.2)

The compounds are isolated by extraction with pentane and crystallization as colorless to pale yellow block crystals in good yield. In the ^{1}H NMR spectra, the complexes show one set of doublet for $SiMe_2$ group (**2.1b**: δ 0.41, $^{3}J_{HH}$ = 3.3 Hz; **2.1c**: δ 0.37, $^{3}J_{HH}$ = 3.2 Hz) and one multiplet resonance of SiH (**2.1b**: δ 4.04, $^{1}J_{SiH}$ = 134 Hz; **2.1c**: δ 4.15, $^{1}J_{SiH}$ = 137 Hz) at room temperature. The similarity of the ^{1}H NMR spectra of **2.1b** and **2.1c** compared to **2.1a** suggested that both **2.1b** and **2.1c** could be fluxional at ambient temperature; thus, they were subject to variable-temperature NMR experiment. Low temperature NMR spectroscopy indicates that each -$C(SiHMe_2)_3$ alkyl ligand interacts with Ln center through two β-agostic interactions. ^{1}H NMR spectra of **2.1b** and **2.1c** in toluene-d_8 were recorded from 298 to 190 K. As the temperature was lowered, the SiH resonance broadened to the coalescence point at 233 K, while the $SiMe_2$ resonance remained relatively sharp. At 203 K, the resonances were sufficiently resolved and two SiH resonances and three $SiMe_2$ resonances were observed. The downfield SiH resonance (**2.1b**: δ 4.77, $^{1}J_{SiH}$ = 183 Hz; **2.1c**: δ 4.78, $^{1}J_{SiH}$ = 186 Hz) is assigned to the terminal SiH, while the other upfield SiH resonance (**2.1a**: δ 3.40, $^{1}J_{SiH}$ = 109 Hz; **2.1b**: δ 3.61, $^{1}J_{SiH}$ = 105 Hz; **2.1c**: δ 4.04, $^{1}J_{SiH}$ = 114 Hz) corresponds to the β-agostic Ln---H—Si. The 2:1 ratio in ^{1}H NMR integration of the SiH resonances reveals six non-classical (3-center-2-electron) SiH groups and three terminal (2-center-2-electron) SiH moieties. Both ^{1}H and $^{13}C\{^{1}H\}$ NMR spectra at 190 K contain three SiMe resonances. The COSY experiments suggested two of the SiMe resonances are the diastereotopic β-agosic SiMe groups. In $^{13}C\{^{1}H\}$ NMR spectra at 190 K, three SiMe resonances were observed at 4.14, 3.76 and 2.36 ppm for **2.1b** and 4.42, 3.40, and 2.25 ppm for **2.lc**. Also, only one type of Ln-bounded C resonances by $^{13}C\{^{1}H\}$ NMR spectroscopy were detected for **2.1b** (δ_{LuC} at

25°C: 16.8) and **2.1c** (δ_{LaC} at 25 °C: 31.8). In comparison, The Ln-bounded C resonances were observed at 57.4 ppm for $Lu[CH(SiMe_3)_2]_3$[4d] and 75.2 ppm for $La[CH(SiMe_3)_2]_3$,[4c] which are significantly downfield compared to those of $Ln[C(SiHMe_2)_3]_3$. We reason such upfield chemical shift on Ln-C due to the electron delocalization throughout the entire agostic $C(SiHMe_3)_3$ ligand framework (negative hyperconjugative delocalization).[8] Furthermore, while the $^1J_{SiH}$ vary significantly between agostic and nonagostic SiHs, the ^{29}Si NMR chemical shifts do not differ much. For example, the ^{29}Si NMR resonances of the agostic SiH are -14.6 and -9.3 ppm and those of nonagostic SiH are -13.3 and -18.5 ppm for **2.1b** and **2.1c** at 190 K, respectively.

Two absorption bands are observed in IR (**2.1b**: 2107 and 1859 cm^{-1}; **2.1c**: 2108 and 1826 cm^{-1}). The integration of the two bands is roughly 1:2 ratio that suggests the series of complexes contain one nonagostic SiH and two agostic SiHs for each $–C(SiHMe_2)_3$ ligand. The spectroscopic assignment is further supported by the crystal structures of **2.1b** and **2.1c**. Multiple samples of crystals of **2.1a** were studied by X-ray diffraction. Although high-resolution data was obtained, a suitable solution could not be found. Furthermore, while the general molecular features of compounds **2.1b** and **2.1c** are similar (from spectroscopy above and X-ray diffraction studies), the crystallographic motifs are not equivalent. Compound **2.1c** crystallizes in a triclinic P-1 space group with a single molecule in the asymmetric unit and two molecules in the unit cell, whereas compound **2.1b** crystallizes in $P2_1/n$ space group with 4 independent molecules in the asymmetric unit and 16 molecules per unit cell.

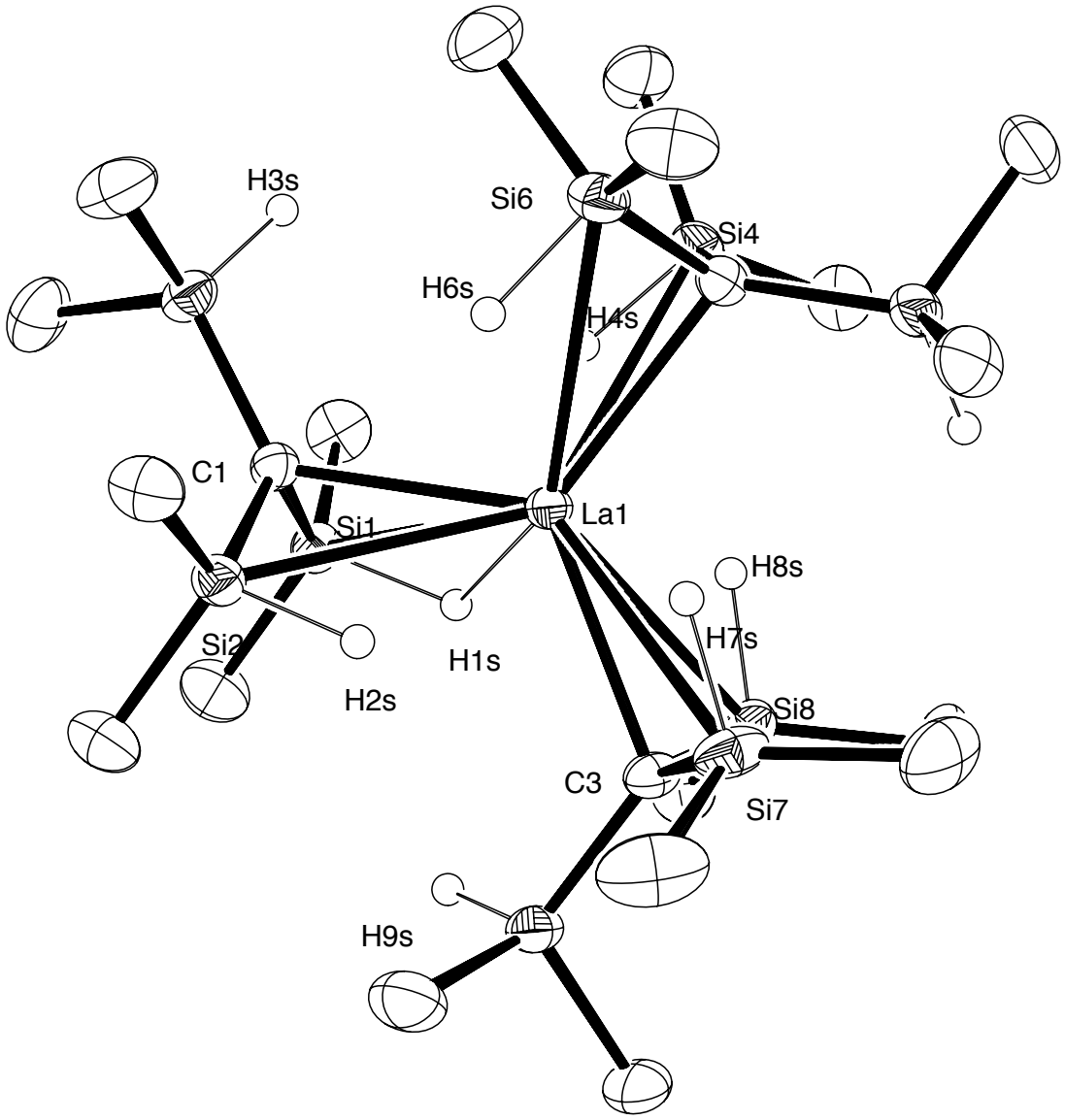

Figure 2.2. ORTEP diagram of $La[C(SiHMe_2)_3]_3$ (**2.1c**). Ellipsoids are plotted at 50% probability. Hydrogen atoms bonded to carbon are not illustrated. Hydrogen atoms bonded to silicon were located objectively in the Fourier difference map. Significant interatomic distances (Å): La1-C1, 2.6953(17); La1-C2, 2.6791(16); La1-C3, 2.6850(16); C1-Si1, 1.8389(17); C1-Si2, 1.8275(17). Significant interatomic angles (°): La1-C1-Si1, 88.30(6);

La1-C1-Si2, 88.54(6); La1-C1-Si3, 126.16(8); C1-La1-C2, 119.70(5); C1-La1-C3, 119.23(5); C2-La1-C3, 120.99(5).

The X-ray structure of **2.1b** is illustrated in figure **2.2**, and the lutetium tris(alkyl) **2.1b** is isostructural. The structural feature is consistent with two β-agostic SiH interaction on each $C(SiHMe_2)_3$ ligand, evident by the short La-$Si_{\beta\text{-agostic}}$ distance (avg. 3.229 A) and small La-C-$Si_{\beta\text{-agostic}}$ angle (avg. 89.34 °). The La-C distances of **2.1c** are 2.6953(17), 2.6791(16), 2.6850(16) Å. The other homoleptic La trisalkyls resolved by X-ray include $La[CH(SiHMe_2)_2]_3$, $La(CH_2Ph)_3(THF)_3$ and $La(CH_2C_6H_4\text{-}4\text{-}Me)_3(THF)_3$. The La-C distances of **2.1c** are not significantly different than those of $La(CH_2Ph)_3(THF)_3$[4e] (2.645(2) Å) and $La(CH_2C_6H_4\text{-}4\text{-}Me)_3(THF)_3$ (avg. 2.626(2) Å).[4g] However, the La-C bond lengths are longer than those of $La[CH(SiMe_3)_2]_3$ (2.515(9) A) by ~0.16 Å.[4c] The average torsion angle $\angle_{\text{La-C-Si-H}}$ ranges of the agostic $SiHMe_2$ is 7.10 °, which is significantly distorted from the nonagostic $SiHMe_2$ group (avg. ∠La-C-Si-H = 42.05 °). Another important feature of $La[C(SiHMe_2)_3]_3$ is its planarity on the metal center ($\Sigma\angle_{\text{C-La-C}}$: 359.92(15)°), deviated from the pyramidal geometry common to Ln trisalkyl or trisamido complexes, ex. $La[CH(SiMe_3)_2]_3$, which was suggested to minimize the ligand-ligand repulsions. However, in case of $Ln[C(SiHMe_2)_3]_3$, the adoption of planarity helps maximize the metal-ligand interaction by β-SiH agostic interactions. Meanwhile, the sum of the angles of Si-C-Si angles for each -$C(SiHMe_2)_3$ are 351.0 °, 349.2 °, and 352.0 °. This implies the C center of each -$C(SiHMe_2)_3$ is rather planar than tetrahedral (would be ~328 °), thus, this also suggests the strong La—H—Si diagostic interactions greatly distort the hybridization of the orbital on the C center. Such planarity with two $SiHMe_2$ gorups of each $C(SiHMe_2)_3$ ligand pointing to La center and one $SiHMe_2$

pointing away La center also minimizes the inter-ligand repulsion. The average La-H distance on the agostic La—H—Si interaction is 2.47(2) Å, but the Si-H distances of the agostic SiH (avg. 1.49(2) Å) is in average slightly elongated compared to nonagostic SiH (1.36(2), 1.40(2), 1.45(2) Å).

Similar structural features are also observed in the crystal structure of **2.1b**. It also features short Lu-$Si_{b\text{-agostic}}$ distance (avg. 3.020 Å) and small Lu-C-$Si_{b\text{-agostic}}$ angle (avg. 87.20 °) that are consistent of two β-agostic SiH interaction on each $C(SiHMe_2)_3$ ligand on Lu. The average Lu-Si distance and Lu-C-Si angle for the nonagostic Lu-C-Si group are 3.924 Å and 129.29 °. Furthermore, The average Lu-H distance on the agostic Lu—H—Si interaction is 2.317 Å, but the Si-H distances do not vary much between the agostic SiH and nonagostic SiH. The average Lu-C distance of **2.1b** is 2.502(2). There are only ample examples of homoletptic trisalkyl Lu complexes in literature resolved by X-ray crystallography. Within those, Lu-C bonds in **2.1b** are about ~0.15 Å longer than those in $Lu(CH_2SiMe_3)_3(THF)_2$ (2.364-2.380(18) Å)[4h] and ~0.1 Å longer than those in $Lu(CH_2Ph)_3(THF)_3$ (2.404(7)-2.413(5) Å). [4i] Notably, THF molecules were not obtained in the coordination sphere in the complexes from smaller (Y, Lu) to biggest lanthanides (La), which suggests the sterically hindered $C(SiHMe_2)_3$ group effectively protect the metal ions.

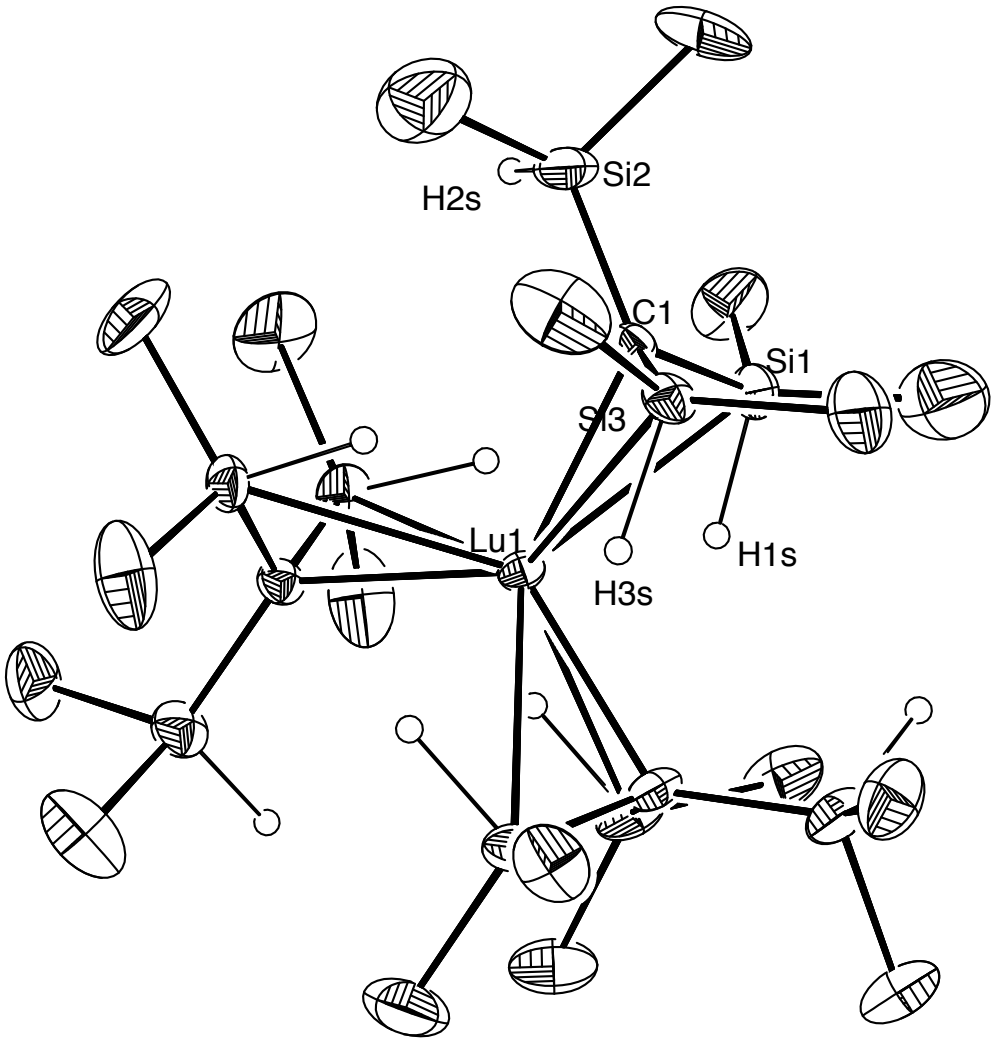

Figure 2.3. ORTEP diagram of $Lu[C(SiHMe_2)_3]_3$ (**2.1b**). Ellipsoids are plotted at 35% probability. Hydrogen atoms bonded to carbon are not illustrated. Hydrogen atoms bonded to silicon were located objectively in the Fourier difference map. Significant interatomic distances (Å): La1-C1, 2.6953(17); La1-C2, 2.6791(16); La1-C3, 2.6850(16); C1-Si1, 1.8389(17); C1-Si2, 1.8275(17). Significant interatomic angles (°): La1-C1-Si1, 88.30(6);

La1-C1-Si2, 88.54(6); La1-C1-Si3, 126.16(8); C1-La1-C2, 119.70(5); C1-La1-C3, 119.23(5); C2-La1-C3, 120.99(5).

2.3. Synthesis and characterization of bis(dimethylsilyl)methyl scandium ate compounds.

Furthermore, we attempted to synthesize the related homoleptic scandium trisalkyl, but the desired compound was not obtained. The reaction of $ScCl_3(THF)_3$ with either two or three equiv. of $KC(SiHMe_2)_3$ in benzene yields bisalkyl ate-Sc-LiCl adduct, $Sc[C(SiHMe_2)_3]_2(\mu\text{-}Cl)_2Li(THF)_2$ with LiCl bridged between Sc-Cl (confirmed by X-ray structure, see supplementary information). The origin of the lithium is believed to come from contamination in the synthesis of benzyl potassium (*n*-BuLi + KOtBu + toluene) used to deprotonate $HC(SiHMe_2)_3$ in that particular experiment. Similar LiCl coordination to lanthanide metal alkyl was previously observed.[4j]

Another attempt to synthesize homoletpic tris(alkyl) $ScC[C(SiHMe_2)_3]_3$ employed lithium-free $KC(SiHMe_2)_3$(tmeda) to avoid lithium contaimation. Instead, the KCl-ate dimer adduct $[Sc[C(SiHMe_2)_3]_2(\mu\text{-}Cl)_2K(tmeda)_2]_2$ (**2.2-KCl-tmeda**) formed as pale yellow crystals, but its good solubility in pentane contributed the low isolation yield in 20.5% (eq 2.3).

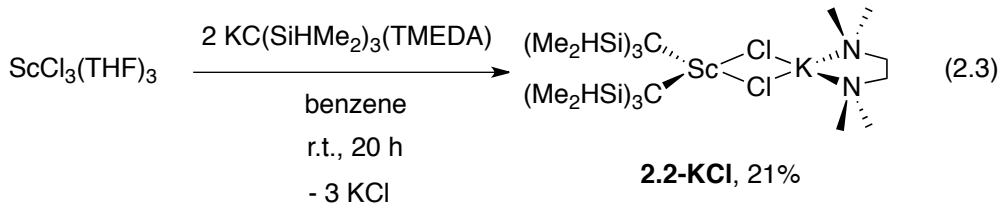

(2.3)

The ^1H NMR spectrum in benzene-d_6 contained a multiplet at 4.86 ppm (Si–H, $^1J_{SiH}$ = 156 Hz) and a doublet at 0.61 ppm (Si–CH_3, $^3J_{HH}$ = 3.1 Hz). The $^{13}C\{^1H\}$ NMR also contains one

SiMe resonance at 2.85 ppm, while the other $Ln[C(SiHMe_2)_3]_3$ exhibits more upfield $^{13}C\{^1H\}$ NMR chemical shift on LnC resonance than other homoleptic Ln trisalkyls, ScC resonance of **2.2-KCl-tmeda** was detected at 34.0 ppm. In comparison, the ScC resonance of $Sc[CH_2SiMe_2Ph]_3THF_2$[26] is quite comparable at 37.0 ppm, but that of $[Li_3ScMe_6(THF)_{1.2}]$[27] is significantly more upfield at 14.2 ppm. That suggests the incorporation of an alkali metal salt and being dimeric greatly affect the electronic property in the alkyl ligand.

Two absorptions at 2090 and 1844 cm^{-1} (KBr) observed in the infrared spectrum were attributed to SiH vibrations. The IR data and low $^1J_{SiH}$ coupling constant suggest agostic interaction involving the SiH moieties and Sc center. X-ray quality crystals were obtained from a concentrated pentane solution of **2.2-KCl-tmeda** cooled to -30 °C. Although there is disorder on the crystal structure, the dimeric **2.2-KCl-tmeda** (SAD238) containing bridging motif between Sc-Cl and two KCl molecules are unambiguously established. **2.2-KCl-tmeda** forms an ate complex with a alkali metal halide capped with one TMEDA in a bidentate coordination mode (see supplementary information).

2.4. Reactions of 1 with one equiv. of $B(C_6F_5)_3$.

Alkyl group abstraction by organometallic Lewis acids represents the most general methodology to generate cationic complexes that are important catalysts in polymerization. However, β-H abstraction by Lewis acid is represents a rare event compared to the alkyl group abstraction.[28] We have found previously that $M[C(SiHMe_2)_3]_2THF_2$ (M: Ca, Yb) react with $B(C_6F_5)_3$ via a β-H abstraction pathway to give zwitterionic hydroborate species. Similar to Ca and Yb, the reaction of **2.1c** with 1 equiv. of $B(C_6F_5)_3$ in benzene cleanly rapidly yields $La[C(SiHMe_2)_3]_2[HB(C_6F_5)_3]$ (**2.3**) and 0.5 equiv. of cyclosilabutane

$[(Me_2HSi)_2C{=}SiMe_2]_2$,[17b] a head-to-tail dimer of silene $(Me_2HSi)_2C{=}SiMe_2$ (eq 2.4). Although the conversion is quantitative by NMR spectroscopy, the isolation yield is low as **2.3** is sparingly soluble in pentane that hammers its isolation from the disilacyclobutane by-product.

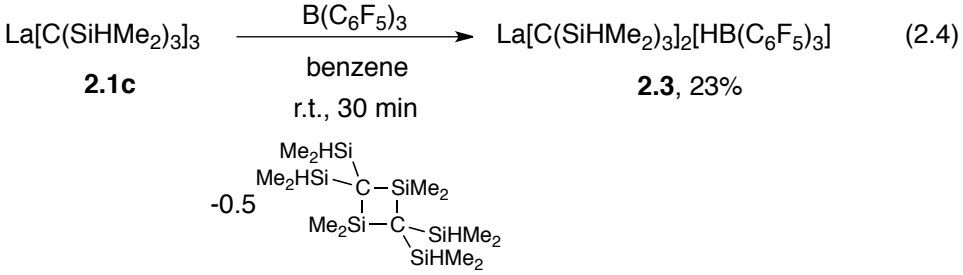

The ^{1}H NMR spectrum contained a slightly upfield-shifted $SiMe_2$ group at 0.21 ppm and a downfield-shifted SiH resonance at 4.45 ppm ($^1J_{SiH}$ = 135.2 Hz). The $^1J_{SiH}$ constant of $[La(C(SiHMe_2)_3)_2][HB(C_6F_5)_3]$ is smaller than the isoelectronic $Yb[C(SiHMe_2)_3]_2(THF)_2$ (133.5 Hz vs. 150.4 Hz), reflecting a more electron and coordinatively unsaturated metal center in the absence of the coordination of Lewis bases (ie. THF). Two ν_{SiH} bands were detected in IR at 2109 and 1787 cm^{-1} in an approximately 1:2 ratio that suggests the β-SiH diagostic structure in **2.1c** maintains in **2.3**. The β-H abstraction was also evident by the observation of a doublet resonance in ^{11}B NMR spectrum (δ -18.0, $^1J_{BH}$ = 62.0 Hz). Interestingly, the ^{11}B NMR resonance is more downfield and the $^1J_{BH}$ coupling constant is smaller in comparison to other organometallic compounds containing non-coordinated $HB(C_6F_5)_3$. Also, one low energy ν_{BH} band was observed at 2261 cm^{-1} that supports a B---H---La bridging motif in **2.3**.

Although **2.1c** is structurally similar to **2.1a** (at least spectroscopically) and **2.1b,** reactions of $B(C_6F_5)_3$ and **2.1a** and **2.1b** result in dissimilar organometallic products. By

monitoring a micromolecular scale reaction in benzene-d_6 at room temperature, very small amount of the disilacyclobutane was detected, while both **2.1a** and **2.1b** were fully consumed (eq 2.5).

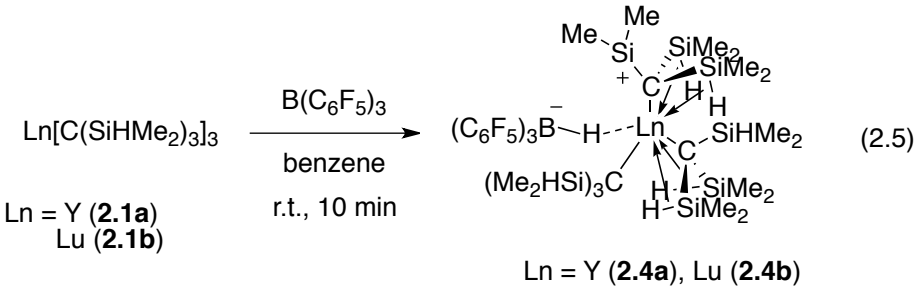

(2.5)

In the ^{1}H NMR spectra, two doublets (**2.4a**, 0.28 ppm ($^3J_{HH}$ = 3.5 Hz), 0.16 ppm ($^3J_{HH}$ = 3.0 Hz); **2.4b**, 0.26 ppm ($^3J_{HH}$ = 3.6 Hz), 0.19 ppm ($^3J_{HH}$ = 3.1 Hz)), one singlet (**2.4a**, 0.43 ppm; **2.4b**, 0.41 ppm), and two broad singlets (**2.4a**, 0.70 and 0.52 ppm; **2.4b**, 0.69 and 0.52 ppm) integrated as 18:18:6:6:6 were observed. Also, three sets of SiH resonances were also detected (**2.4a**, 4.33 ppm ($^1J_{SiH}$ = 188.1 Hz), 4.18 ppm ($^1J_{SiH}$ = 131.9 Hz), 4.12 ppm, ($^1J_{SiH}$ = 91.4 Hz); **2.4b**, 4.92 ppm ($^1J_{SiH}$ = 84.8 Hz), 4.55 ppm ($^1J_{SiH}$ = 131.0 Hz), 4.32 ppm ($^1J_{SiH}$ = 187.6 Hz)). The COSY experiments show cross peaks between the two upfield $SiMe_2$ doublets (18 H each) and two of the SiH resonances ($^1J_{SiH}$ 131-188 Hz), and another cross peak between the two broad singlets (6 H each) and the SiH resonance with low $^1J_{SiH}$ (~90 Hz). Also, a resonance at ~3 ppm in ^{1}H NMR spectrum was observed that shows correlation to a broad ^{11}B NMR resonance at -16.4 ppm in ^{1}H-^{11}B HMQC experiment, which indicates the products contain $HB(C_6F_5)_3$. These results support that one SiH group in **2.1a** and **2.1b** is abstracted by $B(C_6F_5)_3$ to generate two diastereotopic $SiHMe_2$ groups and $SiMe_2$ group. Without detection of significant amount of the disilacyclobutane, the β-H abstraction product

of $-C(SiHMe_2)_3$ ligand, we propose the products as $[Y\{C(SiHMe_2)_3\}_2C(SiHMe_2)SiMe_2][HB(C_6F_5)_3]$ (**2.4a**) and $[Lu\{C(SiHMe_2)_3\}_2C(SiHMe_2)SiMe_2][HB(C_6F_5)_3]$ (**2.4b**). ^1H-^{29}Si HMBC experiments suggest the Ln-C-Si moiety unlikely carries silene-type character. For example, the ^{29}Si NMR chemical shifts of the $SiMe_2$ group are 0.2 ppm for **2.4a** and 0.7 ppm for **2.4b**, and the ^{13}C NMR shifts of *C*($SiMe_2$) carbon are 28.9 and 28.3 ppm for **2.4a** and **2.4b**, respectively. Therefore, we cannot rule out possible F---Si^+Me_2 interaction. Attempts to grow X-ray quality crystals only resulted in amorphous solid precipitation. The proposed β-H abstraction pathway without silene elimination in **2.4a** and **2.4b** was further confirmed by addition of 1 equiv. of DMAP (N,N-dimethylaminopyridine) to a benzene-d_6 solution of **2.4a** that gives **2.1a** quantitatively and presumably DMAP-$B(C_6F_5)_3$ Lewis adduct (eq 2.6).[29]

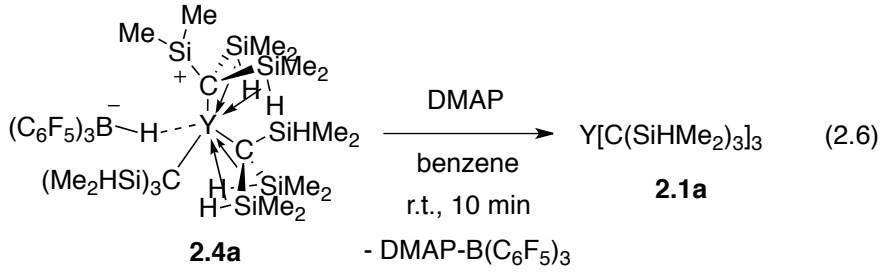

A control reaction between $Y[C(SiHMe_2)_3]_3$ and DMAP-$B(C_6F_5)_3$ does not lead to any β-abstraction. And it suggests the reversible β-H shuttling process between Si and B.

2.5. Reactions of 1 with two equiv. of $B(C_6F_5)_3$.

Reactions of **2.1** and 2 equiv. of $B(C_6F_5)_3$] are less trivial. In all cases, the reactions afford dicationic $[Ln\{C(SiHMe_2)_3\}][\{HB(C_6F_5)_3\}_2]$ (Ln = Y (**2.6a**), Lu (**2.6b**), La (**6c**); eq 2.7).

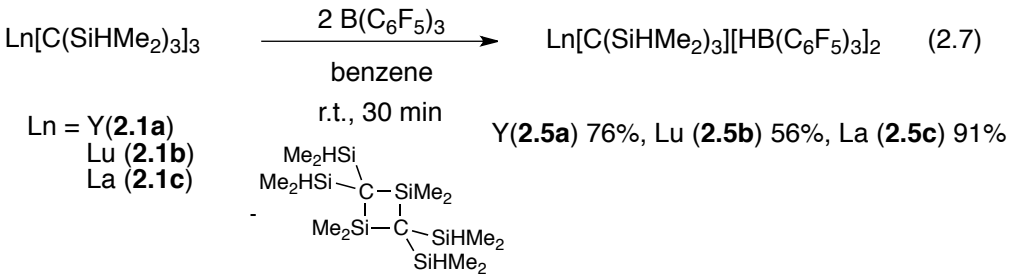

The room temperature ^{1}H NMR spectra contain only resonances for the SiMe (**2.6a**, 0.13 ppm; **2.6b**, 0.13 ppm; **2.6c**, 0.00 ppm) and SiH (**2.6a**, 4.62 ppm, $^{1}J_{SiH}$ = 120 Hz; **2.6b**, 5.12 ppm, $^{1}J_{SiH}$ = 136 Hz; **2.6c**, 4.38 ppm, $^{1}J_{SiH}$ = 135 Hz). Notably, the $^{1}J_{SiH}$ coupling constant of **2.6c** is only slightly lower than mono-zwitterionic **2.4**, although metal center in **2.6c** is expected to be more electrophilic (formally a dicationic species). Similar to **2.4** and **2.5**, the ^{11}B NMR resonances for **2.6** are more downfield than literature reported noncontacted ion-pair, therefore, **2.6** may better be categorized as dizwitterionic compounds. The unusually upfield ^{13}C resonances of *C*(SiHMe$_2$)$_3$ in **1** were not observed here for **2.6** (**2.6a**, 55.3 ppm; **2.6b**, 50.0 ppm; **2.6c**, 56.9 ppm), although the $^{1}J_{YC}$ coupling constant remains low (15.7 Hz). Furthermore, reactions of 3 equiv. of B(C$_6$F$_5$)$_3$ with **2.1** *only* yielded **2.6**. In comparison, reaction of 2 equiv. of B(C$_6$F$_5$)$_3$ with Yb[C(SiHMe$_2$)$_3$]$_2$(THF)$_2$ leads to alkyl group-free dizwitterionic Yb product.[30]

Conclusion

New solvent-free homoleptic trisalkyl lanthanide compounds containing C(SiHMe$_2$)$_3$ ligand were synthesized, which contained nine β-hydrogens. However, these compounds are resistant towards β-H elimination even in elevated temperatures. Two features in these complexes inhibit β-hydride elimination: first, three 'ancillary' bulky C(SiHMe$_2$)$_3$ ligands

create a crowded lanthanide center. Second, the product of elimination would give a silene $(Me_2HSi)_2C{=}SiMe_2$ that is not stabilized by π-donation from a metal center. Six SiH β-agostic interactions were detected and characterized by spectroscopy and crystallography that inhibit β-H elimination. However, addition of Lewis acid $B(C_6F_5)_3$ facilitates β-hydrogen abstraction to give "olefinic" organic product $(Me_2HSi)_2C{=}SiMe_2$ and hydridoborate organometallic counterparts. More importantly, reaction of $B(C_6F_5)_3$ with free ligand $HC(SiHMe_2)_3$ did not lead to any observable reaction. This suggests β-SiH hydrogens are activated by lanthanide centers and exhibit hydridic character on the basis of their reactions with Lewis acids. Compounds **2.1** contain open coordination sites on Lewis acidic metal centers and accessible β-hydrogens that form agostic interactions. However, these alkyls are clearly deactivated against β-elimination. Most likely, the M···Si interactions and delocalization of charge on the $C(SiHMe_2)_3$ ligand, as evidenced by X-ray structures and IR spectroscopy, increase the barrier to β-hydride elimination. Our observations also confirmed with Bercaw's postulation that β-agostic interaction provides ground state stabilization against β-H elimination.[31]

Experimental

General. All manipulations were performed under a dry argon atmosphere using standard Schlenk techniques or under a nitrogen atmosphere in a glovebox unless otherwise indicated. Water and oxygen were removed from benzene, toluene, pentane, diethyl ether, and tetrahydrofuran solvents using an IT PureSolv system. Benzene-d_6 and tetrahydrofuran-d_8 were heated to reflux over Na/K alloy and vacuum-transferred. The compounds

$ScCl_3(THF)_3$,[32] $LaI_3(THF)_4$,[33] $LuCl_3(THF)_3$, $KC(SiHMe_2)_3$,[30] $KC(SiHMe_2)_3(TMEDA)$,[30] $B(C_6F_5)_3$[34] were prepared following literature procedures.

^1H, $^{13}C\{^1H\}$, ^{11}B and $^{29}Si\{^1H\}$ NMR spectra were collected on an Agilent MR400 spectrometer. ^{11}B NMR spectra were referenced to an external sample of $BF_3{\cdot}Et_2O$. ^{15}N chemical shifts were determined either by ^1H-^{15}N HMBC experiments on a Bruker Avance II 700 spectrometer with a Bruker Z-gradient inverse TXI $^1H/^{13}C/^{15}N$ 5mm cryoprobe or by ^1H-^{15}N CIGARAD experiments on an Agilent MR400 spectrometer; ^{15}N chemical shifts were originally referenced to liquid NH_3 and recalculated to the CH_3NO_2 chemical shift scale by adding -381.9 ppm. Assignments of resonances are supported by ^1H-^1H and heteronuclear correlation NMR experiments. Infrared spectra were measured on a Bruker IFS66v FTIR. Elemental analyses were performed using a Perkin-Elmer 2400 Series II CHN/S. X-ray diffraction data was collected on a Bruker APEX II diffractometer.

$Y[C(SiHMe_2)_3]_3$ (2.1a). Anhydrous YCl_3 (0.046 g, 0.24 mmol) and $KC(SiHMe_2)_3$ (0.163 g, 0.71 mmol) were stirred in 10 ml of benzene at 25 °C for 12 h. The benzene was removed under vacuum, and the resulting brown residue was extracted with pentane (3 × 10 ml). The pentane was allowed to evaporation, affording a sticky yellow solid. This solid was re-recystallized at -30 °C from a minimal amount of pentane to obtain 0.13 g of **2.1a** (0.20 mmol, 82%) as colorless microcrystals. ^1H NMR (benzene-d_6, 400 MHz, 25 °C): δ 3.85 (m, 3 H, $^1J_{SiH}$ = 134 Hz, Si*H*Me_2), 0.394 (d, 18 H, $^3J_{HH}$ = 3.2 Hz, SiC*H*$_3$). ^1H NMR (THF-d_8, 400 MHz, 25 °C): δ 3.70 (m, 3 H, $^1J_{SiH}$ = 137.4 Hz, Si*H*Me_2), 0.315 (d, 18 H, $^3J_{HH}$ = 3.2 Hz, SiC*H*$_3$). ^1H NMR (toluene-d_8, 400 MHz, -83 °C): δ 4.70 (3 H, $^1J_{SiH}$ = 190 Hz, Si*H*Me_2), 3.40 (6 H, $^1J_{SiH}$ = 109 Hz, Si*H*Me_2), 0.472 (36 H, SiC*H*$_3$), 0.344 (18 H, SiC*H*$_3$). $^{13}C\{^1H\}$ NMR

(benzene-d_6, 100 MHz, 25 °C): δ 3.96 (Si*C*H$_3$), 17.3 (d, $^1J_{YC}$ = 9.8 Hz, Y*C*). ^{13}C{^{1}H} NMR (THF-d_8, 100 MHz, 25 °C): δ 3.67 (Si*C*H$_3$), 17.5 (d, $^1J_{YC}$ = 9.8 Hz, Y*C*). ^{13}C{^{1}H} NMR (toluene-d_8, 100 MHz, -83 °C): δ 16.07 (d, $^1J_{YC}$ = 9.9 Hz, Y*C*), 4.60 (Si*C*H$_3$), 4.39 (Si*C*H$_3$), 2.92 (Si*C*H$_3$). ^{29}Si{^{1}H} NMR (benzene-d_6, 79.5 MHz, 25 °C): δ -13.3 (*Si*HMe$_2$). ^{29}Si{^{1}H} NMR (THF-d_8, 79.5 MHz, 25 °C): δ -15.3 (*Si*HMe$_2$).^{29}Si{^{1}H} NMR (toluene-d_8, 79.5 MHz, -83 °C): δ -12.3 (*Si*HMe$_2$), -15.2 (*Si*HMe$_2$). IR (KBr): 2954 s, 2899 s, 2105 s (SiH), 1846 s (SiH), 1599 w, 1493 w, 1416 m, 1253 s, 1203 m, 1069 s, 957 s, 887 s, 883 s, 779 s, 690 s cm^{-1}. IR (THF, cm^{-1}): 2980 s, 2682 w, 2102 w (SiH), 1967 w (THF), 1844 w (SiH), 1460 s, 1365 m, 1289 m, 1252 s, 1181 s, 1069 s, 957 s, 837 s, 690 m. Calcd for $C_7H_{21}Si_3Y$: C, 38.37; H, 9.66. Found: C, 38.80; H, 9.21. EI-MS (*m*/*z*, assignment, %): 467 ([M – (C(SiHMe$_2$)$_3$)]$^+$, 8), 276 ([M – (C(SiHMe$_2$)$_3$)$_2$]$^+$, 10), 188 ([C(SiHMe$_2$)$_2$(SiMe$_2$)]$^+$, 100), 129 ([C(SiHMe$_2$)(SiMe$_2$)]$^+$, 18), 174 (68), 72 ([CH(SiHMe$_2$)]$^+$, 16), 59 ([SiHMe$_2$]$^+$, 11). CI-MS (*m*/*z*, %, assignment): 656 ([M]$^+$, 2), 467 ([M – H - (C(SiHMe$_2$)$_3$)]$^+$, 14), 189 ([C(SiHMe$_2$)$_3$ – H]$^+$, 100), 176 (100).

[Lu(C(SiHMe$_2$)$_3$)$_3$] (2.1b). LuCl$_3$(THF)$_3$ (0.486 g, 0.977 mmol) and KC(SiHMe$_2$)$_3$ (0.687 g, 3.005 mmol) were stirred in 10 ml of benzene at 25 °C for 12 h. The benzene was removed under vacuum, and the resulting brown residue was extracted with pentane (3 × 5 ml). The pentane was allowed to evaporation, affording a sticky yellow solid. This solid was re-recystallized at -30 °C from a minimal amount of pentane to obtain g of **2.1b** as colorless microcrystals. (0.315 g, 0.424 mmol, 43.4%). ^{1}H NMR (benzene-d_6, 600 MHz, 25 °C): δ 4.04 (m, $^1J_{SiH}$ = 134.1 Hz, 9 H, SiH), 0.41 (d, $^3J_{HH}$ = 3.3 Hz, 54 H, SiMe). ^{1}H NMR (toluene-d_8, 600 MHz, -80 °C): δ 4.77 (m, $^1J_{SiH}$ = 182.5 Hz, 3 H, SiH), 3.61 (6 H, $^1J_{SiH}$ = 104.6 Hz,

SiH), 0.52 (s br, 18 H, $SiCH_3$), 0.49 (s br, 18 H, $SiCH_3$), 0.37 (18 H, $SiCH_3$). $^{13}C\{^1H\}$ NMR (benzene-d_6, 150 MHz, 25 °C): δ 16.8 (LuC), 3.9 (SiMe). $^{13}C\{^1H\}$ NMR (toluene-d_8, 150 MHz, -80 °C): δ 13.99 (LuC), 4.14 (anagostic SiMe), 3.76 (agostic SiMe), 2.36 (agostic SiMe). $^{29}Si\{^1H\}$ NMR (benzene-d_6, 119.3 MHz, 25 °C): δ -13.8. $^{29}Si\{^1H\}$ NMR (toluene-d_8, 119.3 MHz, -80 °C): δ -13.3 (anagostic SiH), -14.6 (agostic SiH). IR (KBr, cm^{-1}): 2953 m, 2899 m, 2107 s br (ν_{SiH}), 1859 s br (ν_{SiH}), 1417 w, 1253 s, 1073 s br, 957 s, 885 s br, 833 s, 779 s, 690 s. Anal. Calcd for $C_{21}H_{63}Si_9Lu$: C, 33.93; H, 8.54. Found: C, 34.15; H, 8.20.

[La(C(SiHMe$_2$)$_3$)$_3$] (2.1c). $LaI_3(THF)_4$ (0.365g, 0.452 mmol) and $KC(SiHMe_2)_3$ (0.310 g, 1.356 mmol) were stirred in 10 ml of benzene at 25 °C for 1.5 h. The benzene was removed under vacuum, and the resulting brown residue was extracted with pentane (3 × 5 ml). The pentane was allowed to evaporation, affording a sticky yellow solid of spectroscopically pure **2.1c** (0.269 g, 0.380 mmol, 84.0 %). This solid was re-recystallized at -30 °C from a minimal amount of pentane to obtain **2.1c** as colorless crystals. ^1H NMR (benzene-d_6, 600 MHz, 25 °C): δ 4.15 (m, $^1J_{SiH}$ = 136.5 Hz, 9 H, SiH), 0.37 (d, $^3J_{HH}$ = 3.2 Hz, 54 H, $SiMe_2$). ^1H NMR (toluene-d_8, 600 MHz, -80 °C): δ 4.78 (m, $^1J_{SiH}$ = 185.7 Hz, 3 H, SiH), 4.04 (6 H, $^1J_{SiH}$ = 113.8 Hz, SiH), 0.55 (s br, 18 H, $SiCH_3$), 0.49 (s br, 18 H, $SiCH_3$), 0.42 (18 H, $SiCH_3$). $^{13}C\{^1H\}$ NMR (benzene-d_6, 150 MHz, 25 °C): δ 31.8 (LaC), 3.6 (SiMe). $^{13}C\{^1H\}$ NMR (toluene-d_8, 150 MHz, -80 °C): δ 30.15 (LaC), 4.42 (anagostic SiMe), 3.40 (agostic SiMe), 2.25 (agostic SiMe). $^{29}Si\{^1H\}$ NMR (benzene-d_6, 119.3 MHz, 25 °C): δ -13.1. $^{29}Si\{^1H\}$ NMR (toluene-d_8, 119.3 MHz, -80 °C): δ -9.3 (agostic SiH), -18.5 (anagostic SiH). IR (KBr, cm^{-1}): 2953 s, 2900 m, 2108 s (ν_{SiH}), 1826 s br (ν_{SiH}), 1590 w, 1415 w, 1254 s, 1025 s br, 889

s br, 835 s, 777 s, 689 s. Anal. Calcd for $C_{21}H_{63}Si_9La$: C, 35.66; H, 8.98. Found: C, 36.56; H, 9.24.

[Sc(C(SiHMe$_2$)$_3$)$_2$Cl$_2$K(tmeda)] (2.2-KCl). $ScCl_3(THF)_3$ (0.205 g, 2.194 mmol) and $KC(SiHMe_2)_3(TMEDA)$ (0.109 g, 4.388 mmol) were stirred in 40 ml of benzene at 25 °C for 20 h. The benzene was removed under vacuum, and the light yellow residue was extracted with pentane (2 × 20 ml). The pentane was concentrated to 10 ml and cooled to -30 °C to yield **2.2-KCl** as pale yellow crystals (0.108 g, 0.166 mmol, 20.5%). ^{1}H NMR (benzene-d_6, 600 MHz, 25 °C): δ 4.86 (m, $^1J_{SiH}$ = 155.7 Hz, 6 H, SiH), 1.95 (s, 4 H, NCH_2), 1.94 (s, 12 H, NMe), 0.61 (d, $^3J_{HH}$ = 3.1 Hz, 36 H, SiMe). $^{13}C\{^1H\}$ NMR (benzene-d_6, 150 MHz, 25 °C): δ 57.77 (NCH_2), 46.01 (NMe), 33.97 (ScC), 2.85 (SiMe). $^{29}Si\{^1H\}$ NMR (benzene-d_6, 119.3 MHz, 25 °C): δ -16.8. $^{15}N\{^1H\}$ NMR (C_6D_6, 61 MHz): δ -360.9. IR (KBr, cm^{-1}): 2952 s, 2899 m, 2830 m, 2780 m, 2090 s br (ν_{SiH}), 1844 m br (ν_{SiH}), 1462 m, 1295 m, 1251 s, 1024 s br, 879 s br, 840 s, 781 s, 673 s. Anal. Calcd for $C_{22}H_{62}KSi_6N_2Cl_2Sc$: C, 38.96; H, 9.21; N, 4.13. Found: C, 39.55; H, 8.96; N, 4.42.

[La{C(SiHMe$_2$)$_3$}$_2$][HB(C$_6$F$_5$)$_3$] (2.3). $B(C_6F_5)_3$ (0.090 g, 0.127 mmol) was added to a benzene (4 ml) solution of **1c** (0.068 g, 0.134 mmol) in small portions. The resulting yellow mixture was stirred at room temperature for 30 min. The solvent was evaporated under reduced pressure to give a yellow paste. The residue was washed with pentane (2 x 5ml) and the volatiles were evaporated to dryness in vacuo to give **2.3** as an off-white solid (0.031 g, 0.030 mmol, 23.3%). ^{1}H NMR (benzene-d_6, 600 MHz, 25 °C): δ 4.45 (m, $^1J_{SiH}$ = 135.2 Hz, 6 H, SiH), 0.21 (d, $^3J_{HH}$ = 3.4 Hz, 36 H, SiMe). $^{13}C\{^1H\}$ NMR (benzene-d_6, 150 MHz, 25 °C): δ 150.2 (br, C_6F_5), 148.7 (br, C_6F_5), 141.0 (br, C_6F_5), 139.0 (br, C_6F_5), 137.3 (br, C_6F_5), 48.1

(LaC), 2.2 (SiMe). ^{11}B NMR (benzene-d_6, 119.3 MHz, 25 °C): δ -18.0 (d, $^1J_{BH}$ = 62.0 Hz). ^{19}F NMR (benzene-d_8, 564 MHz, 25 °C): δ -137.0 (s br, 6 F, *ortho*-F), -158.7 (s br, 3 F, *para*-F), -163.3 (s br, 6 F, *meta*-F). ^{29}Si{^{1}H} NMR (benzene-d_6, 119.3 MHz, 25 °C): δ -11.1 (*Si*HMe$_2$). IR (KBr, cm^{-1}): 2958 m, 2904 w, 2261 m br (ν_{BH}), 2109 m br (ν_{SiH}), 1787 m br (ν_{SiH}), 1646 m, 1603 w, 1516 s, 1467 s br, 1372 m, 1283 s, 1258 s, 1110 s br, 1079 s br, 959 s br, 896 s br, 837 s br, 786 s, 673 m. Anal. Calcd for $BC_{32}F_{15}H_{43}Si_6La$: C, 37.28; H, 4.20. Found: C, 37.81; H, 4.00.

[Y(C(SiHMe$_2$)$_3$)$_2$C(SiHMe$_2$)SiMe$_2$][HB(C$_6$F$_5$)$_3$] (2.4a). ^{1}H NMR (benzene-d_6, 600 MHz, 25 °C): δ 4.33 (m, 3 H, $^1J_{SiH}$ = 188.1 Hz, Si*H*Me$_2$), 4.18 (m, 3 H, $^1J_{SiH}$ = 131.9 Hz, Si*H*Me$_2$), 4.12 (m br, 2 H, $^1J_{SiH}$ = 91.4 Hz, Si*H*Me$_2$), 3.40-2.79 (m br, 1 H, *H*B), 0.70 (s br, 6 H, C(SiH*Me*$_2$)$_2$), 0.52 (s br, 6 H, C(SiH*Me*$_2$)$_2$), 0.43 (s, 6 H, Si*Me*$_2$), 0.28 (d, 18 H, $^3J_{HH}$ = 3.5 Hz, YC(SiH*Me*$_2$)$_3$), 0.16 (d, 18 H, $^3J_{HH}$ = 3.0 Hz, YC(SiH*Me*$_2$)$_3$). ^{13}C{^{1}H} NMR (benzene-d_6, 100 MHz, 25 °C): δ 150.3 (br, C_6F_5), 148.8 (br, C_6F_5), 141.1 (br, C_6F_5), 139.4 (br, C_6F_5), 139.0 (br, C_6F_5), 137.3 (br, C_6F_5), 31.9 (Y*C*(SiHMe$_2$)$_3$), 28.9 (Y*C*(SiHMe$_2$)$_2$SiMe$_2$), 4.4 (C(SiH*Me*$_2$)$_2$) 3.9 (C(SiH*Me*$_2$)$_2$), 8.9 (Si*Me*$_2$), 1.7 (YC(SiH*Me*$_2$)$_3$), 2.5 (YC(SiH*Me*$_2$)$_3$). ^{11}B NMR (benzene-d_6, 119.3 MHz, 25 °C): δ -16.8 (s br). ^{19}F NMR (benzene-d_8, 564 MHz, 25 °C): δ -135.5 (s br, 6 F, *ortho*-F), -157.7 (s br, 3 F, *para*-F), -161.3 (s br, 6 F, *meta*-F). ^{29}Si{^{1}H} NMR (benzene-d_6, 119.3 MHz, 25 °C): δ 0.2 (*Si*Me$_2$), -4.1 (C(*Si*HMe$_2$)$_2$), -10.0 (YC(*Si*HMe$_2$)$_3$), -16.4 (YC(*Si*HMe$_2$)$_3$). IR (KBr, cm^{-1}): 2958 s, 2907 m, 2252 s br (ν_{BH}), 2160 s (ν_{SiH}), 2139 s (ν_{SiH}), 1790 s br (ν_{SiH}), 1648 s, 1607 m, 1517 s, 1467 s br, 1375 s, 1282 s, 1258 s, 1192 m, 1115 s br, 1085 s br, 995 s br, 898 s br, 833 s br, 787 s, 683 s. Anal. Calcd for $BC_{39}F_{15}H_{63}Si_9Y$: C, 40.06; H, 5.43. Found: C, 40.68; H, 4.72.

[Lu(C(SiHMe$_2$)$_3$)$_2$C(SiHMe$_2$)SiMe$_2$][HB(C$_6$F$_5$)$_3$] (2.4b). ^{1}H NMR (benzene-d_6, 600 MHz, 25 °C): δ 4.92 (m, 2 H, $^1J_{SiH}$ = 84.8 Hz, C(Si*H*Me$_2$)$_2$SiMe$_2$), 4.55 (m, 3 H, $^1J_{SiH}$ = 131.0 Hz, Si*H*Me$_2$), 4.32 (m br, 3 H, $^1J_{SiH}$ = 187.6 Hz, Si*H*Me$_2$), 3.90-3.20 (m br, 1 H, HB), 0.69 (s br, 6 H, C(SiH*Me*$_2$)$_2$), 0.52 (s br, 6 H, C(SiH*Me*$_2$)$_2$), 0.41 (s, 6 H, Si*Me*$_2$), 0.26 (d, 18 H, $^3J_{HH}$ = 3.6 Hz, C(SiH*Me*$_2$)$_3$), 0.19 (d, 18 H, $^3J_{HH}$ = 3.1 Hz, C(SiH*Me*$_2$)$_3$). ^{13}C{^{1}H} NMR (benzene-d_6, 100 MHz, 25 °C): δ 150.34 (br, C$_6$F$_5$), 148.80 (br, C$_6$F$_5$), 141.14 (br, C$_6$F$_5$), 139.00 (br, C$_6$F$_5$), 139.0 (br, C$_6$F$_5$), 137.38 (br, C$_6$F$_5$), 33.16 (Lu*C*(SiHMe$_2$)$_3$), 28.32 (Lu*C*(SiHMe$_2$)$_2$SiMe$_2$), 4.97 (C(SiH*Me*$_2$)$_2$) 4.52 (C(SiH*Me*$_2$)$_2$), 8.80 (Si*Me*$_2$), 2.55 (C(SiH*Me*$_2$)$_3$), 1.71 (C(SiH*Me*$_2$)$_3$), -1.16 (*C*(SiHMe$_2$)$_3$). ^{11}B NMR (benzene-d_6, 119.3 MHz, 25 °C): δ -15.8 (d, $^1J_{BH}$ = 66.5 Hz). ^{19}F NMR (benzene-d_8, 564 MHz, 25 °C): δ -135.5 (s br, 6 F, *ortho*-F), -157.7 (s br, 3 F, *para*-F), -161.3 (s br, 6 F, *meta*-F). ^{29}Si{^{1}H} NMR (benzene-d_6, 119.3 MHz, 25 °C): δ 0.7 (SiMe$_2$), -1.7 (C(*Si*HMe$_2$)$_2$), -9.2 (C(SiHMe$_2$)$_3$), -17.8 (C(SiHMe$_2$)$_3$).

[LaC(SiHMe$_2$)$_3$][HB(C$_6$F$_5$)$_3$]$_2$ (2.5c). B(C$_6$F$_5$)$_3$ (0.130 g, 0.184 mmol) was added to a benzene (4 ml) solution of **2.1c** (0.193 g, 0.377 mmol) in small portions. The resulting yellow mixture was stirred at room temperature for 30 min. The solvent was evaporated under reduced pressure to give a yellow paste. The residue was washed with pentane (3 x 5 ml) and the volatiles were evaporated to dryness in vacuo to give **2.5c** as an off-white solid (0.226 g, 0.167 mmol, 90.6%). ^{1}H NMR (benzene-d_6, 600 MHz, 25 °C): δ 4.38 (m, $^1J_{SiH}$ = 134.7 Hz, 3 H, SiH), 2.27-2.96 (br q, 1 H, HB), 0.00 (d, $^3J_{HH}$ = 3.6 Hz, 18 H, SiMe). ^{13}C{^{1}H} NMR (benzene-d_6, 150 MHz, 25 °C): δ 149.9 (br, C$_6$F$_5$), 148.4 (br, C$_6$F$_5$), 141.2 (br, C$_6$F$_5$), 139.5 (br, C$_6$F$_5$), 138.9 (br, C$_6$F$_5$), 137.2 (br, C$_6$F$_5$), 56.9 (LaC), 1.4 (SiMe). ^{11}B NMR

(benzene-d_6, 119.3 MHz, 25 °C): δ -17.7 (d, $^1J_{BH}$ = 58.4 Hz). ^{19}F NMR (benzene-d_8, 564 MHz, 25 °C): δ -137.0 (br, 6 F, *ortho*-F), -158.7 (br, 3 F, *para*-F), -163.3 (6 F, *meta*-F). ^{29}Si{^{1}H} NMR (benzene-d_6, 119.3 MHz, 25 °C): δ -10.3. IR (KBr, cm^{-1}): 2961 m, 2249 vbr (ν_{BH}), 2116 m br (ν_{SiH}), 1647 m, 1605 w, 1517 s, 1467 s br, 1376 m, 1269 m, 1115 s br, 957 s br, 900 s br, 841 s, 790 s, 673 m. Anal. Calcd for $B_2C_{48}F_{30}H_{35}Si_3La$: C, 40.41; H, 2.47. Found: C, 40.84; H, 2.59.

[YC(SiHMe$_2$)$_3$][HB(C$_6$F$_5$)$_3$]$_2$ (2.5a). $B(C_6F_5)_3$ (0.107 g, 0.209 mmol) was added to a benzene (2 ml) solution of **2.1a** (0.064 g, 0.097 mmol) in small portions. The resulting yellow mixture was stirred at room temperature for 30 min. The solvent was evaporated under reduced pressure to give a yellow paste. The residue was washed with pentane (3 x 5 ml) and the volatiles were evaporated to dryness in vacuo to give **2.5a** as a white solid (0.097 g, 0.074 mmol, 76.2%). ^{1}H NMR (benzene-d_6, 600 MHz, 25 °C): δ 4.62 (m, $^1J_{SiH}$ = 120.0 Hz, 3 H, SiH), 2.94-2.33 (br q, 1 H, HB), 0.13 (s br, 18 H, SiMe). ^{1}H{^{11}B} NMR (benzene-d_6, 125 MHz, 25 °C): δ 2.65 (s, br, HB). ^{13}C{^{1}H} NMR (benzene-d_6, 150 MHz, 25 °C): δ 150.38 (br, C_6F_5), 148.83 (br, C_6F_5), 139.89 (br, C_6F_5), 138.90 (br, C_6F_5), 137.28 (br, C_6F_5), 55.32 (d, $^1J_{YC}$ = 15.7 Hz, YC), 1.24 (SiMe). ^{11}B NMR (benzene-d_6, 119.3 MHz, 25 °C): δ -16.1 (br). ^{19}F NMR (benzene-d_8, 564 MHz, 25 °C): δ -135.8 (s vbr, 6 F, *ortho*-F), -155.2 (s br, 3 F, *para*-F), -161.4 (s br, 6 F, *meta*-F). ^{29}Si{^{1}H} NMR (benzene-d_6, 119.3 MHz, 25 °C): δ -7.3. IR (KBr, cm^{-1}): 2963 w, 2341 w br (ν_{BH}), 2120 w br (ν_{SiH}), 1647 m, 1609 w, 1520 s, 1466 s br, 1370 m, 1288 m, 1270 m, 1196 w, 1096 s br, 972 s br, 895 s, 838 s br, 806 s, 773 m, 738 m, 687 m.

[LuC(SiHMe$_2$)$_3$][HB(C$_6$F$_5$)$_3$]$_2$ (2.5b). B(C$_6$F$_5$)$_3$ (0.206 g, 0.403 mmol) was added to a benzene (4 ml) solution of **2.1b** (0.139 g, 0.187 mmol) in small portions. The resulting yellow mixture was stirred at room temperature for 30 min. The solvent was evaporated under reduced pressure to give a yellow paste. The residue was washed with pentane (3 x 5 ml) and the volatiles were evaporated to dryness in vacuo to give **2.5b** as a white solid (0.145 g, 0.104 mmol, 55.8%). ^{1}H NMR (benzene-d_6, 600 MHz, 25 °C): δ 5.12 (m, $^1J_{SiH}$ = 136.3 Hz, 3 H, SiH), 3.86-3.03 (br q, 1 H, HB), 0.13 (s br, 18 H, SiMe). ^{1}H{^{11}B} NMR (benzene-d_6, 125 MHz, 25 °C): δ 3.57 (s, br, HB). ^{13}C{^{1}H} NMR (benzene-d_6, 150 MHz, 25 °C): δ 150.43 (br, C$_6$F$_5$), 149.78 (br, C$_6$F$_5$), 148.91 (br, C$_6$F$_5$), 147.95 (br, C$_6$F$_5$), 138.88 (br, C$_6$F$_5$), 137.31 (br, C$_6$F$_5$), 50.02 (br, LuC), 1.50 (SiMe). ^{11}B NMR (benzene-d_6, 119.3 MHz, 25 °C): δ -15.5 (br). ^{19}F NMR (benzene-d_8, 564 MHz, 25 °C): δ -136.1 (s vbr, 6 F, *ortho*-F), -154.9 (s br, 3 F, *para*-F), -161.3 (s br, 6 F, *meta*-F). ^{29}Si{^{1}H} NMR (benzene-d_6, 119.3 MHz, 25 °C): δ -6.1. IR (KBr, cm^{-1}): 2962 w, 2287 w vbr (ν_{BH}), 2117 w br (ν_{SiH}), 1647 m, 1607 w, 1519 s, 1467 s br, 1375 m, 1288 m, 1269 m, 1097 s br, 972 s br, 838 s br, 774 m, 687 m.

Reference

1 Finnegan, R. A.; Kutta, H. W. *J. Org. Chem.* **1965**, *30*, 4138-4144. b) Glaze, W. H.; Lin, J.; Felton, E. G. *J. Org. Chem.* **1965**, *30*, 1258-1259. c) Glaze, W. H.; Adams, G. M. *J. Am. Chem. Soc.* **1966**, *88*, 4653-4656. d) Glaze, W. H.; Lin, J.; Felton, E. G. *J. Org. Chem.* **1966**, *31*, 2643-2645.

2 Lindsell, W. E. Magnesium, calcium, strontium, and barium. In *Comprehensive organometallic chemistry: the synthesis, reactions, and structures of organometallic*

compounds, Wilkinson, G.; Stone, F. G. A.; Abel, E. W. 1st ed.; Pergamon Press: Oxford, 1982; Vol. 1, 155-252.

3 a) Wayda, A. L.; Evans, W. J. *J. Am. Chem. Soc.* **1978**, *100*, 7119-7121. b) Evans, W. J.; Wayda, A. L.; Hunter, W. E.; Atwood, J. L. *J. Chem. Soc., Chem. Commun.* **1981**, 292-293. c) Herbert, S.; Wolfgang, G.; Norbert, B. *Angew. Chem. Int. Eng. Ed.* **1981**, *20*, 119-120. d) Watson, P. L.; Roe, D. C. *J. Am. Chem. Soc.* **1982**, *104*, 6471-6473. e) Evans, W. J.; Meadows, J. H.; Wayda, A. L.; Hunter, W. E.; Atwood, J. L. *J. Am. Chem. Soc.* **1982**, *104*, 2015-2017. f) Watson, P. L.; Parshall, G. W. *Acc. Chem. Res.* **1985**, *18*, 51-56. g) Schaverien, C. J. *Organometallics* **1994**, *13*, 69-82. h) Burger, B. J.; Thompson, M. E.; Cotter, W. D.; Bercaw, J. E. *J. Am. Chem. Soc.* **1990**, *112*, 1566-1577.

4 a) Jeske, G.; Lauke, H.; Mauermann, H.; Swepston, P. N.; Schumann, H.; Marks, T. J. *J. Am. Chem. Soc.* **1985**, *107*, 8091-8103. b) den Haan, K. H.; de Boer, J. L.; Teuben, J. H.; Spek, A. L.; Kojic-Prodic, B.; Hays, G. R.; Huis, R. *Organometallics* **1986**, *5*, 1726-1733. c) Hitchcock, P. B.; Lappert, M. F.; Smith, R. G.; Barlett, R. A.; Power, P. P. *J. Chem. Soc., Chem. Commun.* **1988**, 1007-1009. d) Schaverien, C. J.; Nesbitt, G. J. *J. Chem. Soc. Dalton Trans.* **1992**, 157-167. e) Meyer, N.; Roesky, P. W.; Bambirra, S.; Meetsma, A.; Hessen, B.; Saliu, K.; Takats, J. *Organometallics* **2008**, *27*, 1501-1505. f) Carver, C. T.; Monreal, M. J.; Diaconescu, P. L. *Organometallics* **2008**, *27*, 363-370. g) Bambirra, S.; Meetsma, A.; Hessen, B. *Organometallic* **2006**, *25*, 3454-3462. h) Schumann, H., Freckmann, D. M. M.; Dechert, S. *Z. Anorg. Allg. Chem.* **2002**, *628*, 2422-2426. i) Meyer, N.; Roesky, P.; Bambirra, S.; Meetsma, A.; Hessen, B.; Saliu, K.; Takats, J. *Organometallic* **2008**,

27, 1501-1505. j) Atwood, J. A.; Lappert, M. F.; Smith, R. G.; Zhang, H. *J. Chem. Soc., Chem. Commun.* **1988**, 1308-1309.

5 Dawoodi, Z.; Green, M. L. H.; Mtetwa, V. S. B.; Prout, K. *J. Chem.* Soc., *Chem. Commun.***1982**, 802-803.

6 a) Brookhart, M.; Green, M. L. H.; Wong, L. L. *Prog. Inorg. Chem.* **1988**, *36*, 1-124. b) Brookhart, M.; Green, M. L. H.; Parkin, G. *Proc. Natl. Acad. Sci.* **2007**, *104*, 6908-6914.

7 a) Clot, E.; Eisenstein, O. *Structure and Bonding* **2004**, *113*, 1-36. b) Demolliens, A.; Jean, Y.; Eisenstein, O. *Organometallics* **1986**, *5*, 1457-1464.

8 McGrady, G. S.; Scherer, W. *Angew. Chem., Int. Ed.* **2004**, *43*, 1782-1806.

9 Jordan, R. F.; Bradley, P. K.; Baenziger, N. C.; LaPointe, R. E. *J. Am. Chem. Soc.* **1990**, *112*, 1289-1291.

10 Eaborn, C.; Hitchcock, P. B.; Izod, K.; Smith, J. D. *J. Am. Chem. Soc.* **1994**, *116*, 12071-12072.

11 Klooster, W. T.; Lu, R. S.; Anwander, R.; Evans, W. J.; Koetzle, T. F.; Bau, R. *Angew. Chem. Int. Ed.* **1998**, *37*, 1268-1270.

12 (a) Barker, G. K.; Lappert, M. F. *J. Organomet. Chem*. **1974**, *76*, C45-C46. (b) Schaverien, C. J.; Orpen, A. G. *Inorg. Chem*. **1991**, *30*, 4968-4978. (c) Avent, A. G.; Caro, C. F.; Hitchcock, P. B.; Lappert, M. F.; Li, Z. N.; Wei, X. H. *J. Chem. Soc., Dalton Trans*. **2004**, 1567-1577.

13 Tilley, T. D.; Andersen, R. A.; Zalkin, A. *Inorg. Chem*. **1984**, *23*, 2271-2276.

14 Rees, W. S.; Just, O.; Schumann, H.; Weimann, R. *Angew. Chem. Int. Ed. Engl*. **1996**, *35*, 419-422.

15 a) Herrmann, W. A.; Eppinger, J.; Runte, O.; Spiegler, M.; Anwander, R. *Organometallics* **1997**, *16*, 1813-1815. b) Eppinger, J.; Spiegler, M.; Hieringer, W.; Herrmann, W. A.; Anwander, R. *J. Am. Chem. Soc.* **2000**, *122*, 3080-3096. c) Klimpel, M. G.; Gorlitzer, H. W.; Tafipolsky, M.; Spiegler, M.; Scherer, W.; Anwander, R. *J. Organomet. Chem*. **2002**, *647*, 236-244.

16 Procopio, L. J., Carroll, P. J., Berry, D. H. *J. Am. Chem. Soc.* **1991**, *113*, 1870-1872.

17 a) Eaborn, C.; Hitchcock, P.; Lickiss, P. *J. Organomet. Chem*. **1983**, *252*, 281-288. b) Hawrelak, E. J.; Ladipo, F. T.; Sata, D.; Braddock-Wilking, J. *Organometallics* **1999**, *18*, 1804-1807.

18 (a) Eaborn, C.; Retta, N.; Smith, J. D. *J. Organomet. Chem*. **1980**, *190*, 101-106. b) Buttrus, N. H.; Eaborn, C.; Hitchcock, P. B.; Smith, J. D.; Sullivan, A. C. *J. Chem. Soc., Chem. Commun*. **1985**, 1380-1381. c) Eaborn, C.; Hitchcock, P. B.; Izod, K.; Lu, Z. R.; Smith, J. D. *Organometallics* **1996**, *15*, 4783-4790. (e) LaPointe, . *Inorg. Chim. Acta*. **2003**, *345*, 359-362.

19 Corey, J. Y.; Braddock-Wilking, J. *Chem. Rev*. **1999**, *99* 175-292.

20 Anwander, R. *in Lanthanides: Chemistry and Use in Organic Synthesis,* ed. S. Kobayashi, Springer, Berlin, **1999**.

21 Casey, C. P.; Tunge, J. A.; Lee, T.-Y.; Fagan, M. A. *J. Am. Chem. Soc*. **2003**, *125*, 2641-2651.

22 Bent, H. A. *Chem. Rev*. **1961**, *61*, 275-311.

23 Budzelaar, P.H.M. gNMR v. 5.0, IvorySoft.

24 Margl, P.; Deng, L.; Ziegler, T. *Organometallics* **1998**, *17*, 933-946.

25 Peulecke, N.; Ohff, A.; Kosse, P.; Tillack, A.; Spannenberg, A.; Kempe, R.; Baumann, W.; Burlakov, V. V.; Rosenthal, U. *Chemistry - A European Journal* **1998**, *4*, 1852-1861.

26 26 Emslie, D. J. H.; Piers, W. E.; Parvez, M.; MacDonald, R. *Organometallics* **2002**, *21*, 4226-4240.

27 27 Kramer, M. U.; Robert, D.; Arndt, S.; Zeimentz, P. M.; Spaniol, T. P.; Yahia, A.; Maron, L.; Eisenstein, O.; Okuda, J. *Inorg. Chem.* **2008**, 47, 9265-9278.

28 Walker, D. A.; Woodman, T. J.; Hughes, D. L.; Bochmann, M. *Organometallics* **2001**, *20*, 3772–3776. (b) Milione, S.; Grisi, F.; Centore, R.; Tuzi, A. Organometallics **2006**, *25*, 266-274. (c) Dagorne, S.; Bellemin-Laponnaz, S.; Welter, R. *Organometallics* **2004**, *23*, 3053-5061. (d) Zhu, J.; Mukherjee, D.; Sadow, A. D. *Chem. Commun.* 2012, 48, 464-466.

29 Geier, S. J.; Gille, A. L.; Gilbert, T. M.; Stephan, D. W. *Inorg. Chem.* **2009**, *48*, 10466-10474.

30 See Ch 3 and Yan, K.; Upton, B. M.; Ellern, A.; Sadow, A. D. *J. Am. Chem. Soc.* **2009**, *131*, 15110-15111.

31 Burger, B. J.; Thompson, M. E.; Cotter, W. D.; Bercaw, J. E. *J. Am. Chem. Soc.* **1990**, *112*, 1566-1577.

32 Manxzer, L. E.; Deaton, J.; Sharp, P.; Schrock, R. R. *Inorg. Syn.* **1982**, *21*, 135-140.

33 Izod, K.; Liddle, S. T.; Clegg, W. *Inorg. Chem.* **2004**, *43*, 214-218.

34 Massey, A. G.; Park, A. J., *J. Organomet. Chem.* **1964**, *2*, 245-250.

Supplementary material

Table 1. Rate constants for agostic and nonagostic SiH exchange obtained from simulation of $^{13}C\{^{1}H\}$ NMR spectra over the temperature range 190 – 260 K. [3]

T (K)	k (s^{-1})
190	0
200	1.47
210	12.1
220	59.9
230	231
240	785
250	2350
260	7710

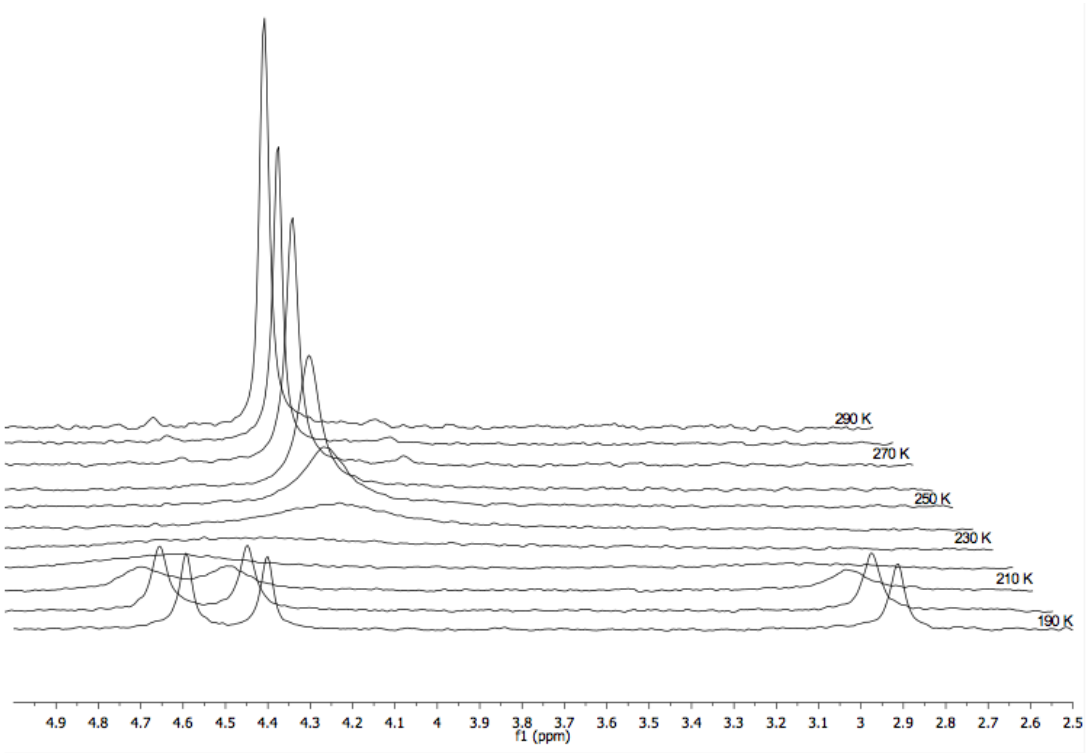

Figure 1. Stack plot of methyl region of $^{13}C\{^{1}H\}$ NMR spectra, acquired from 290 – 190 K.

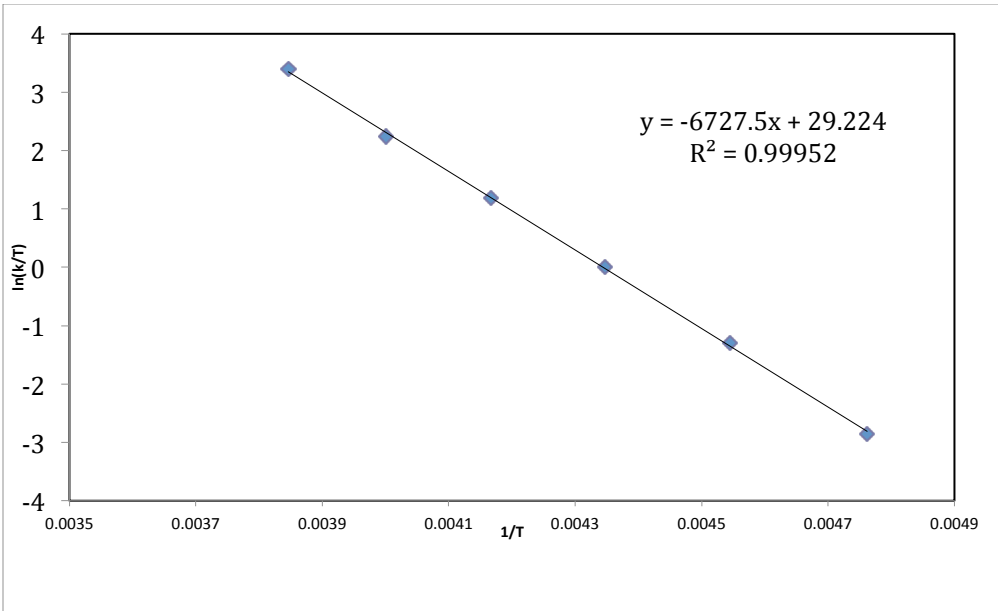

Figure 2. Eyring plot of the VT ^{13}C NMR data from gNMR program.[3]

Determination of Potassium and Chlorine by LA-ICP-MS

ICP-MS was employed to qualitatively determine whether chlorine and potassium were present as part of a stoichiometric compound. Measurements are taken using a Finnigan Element 1 ICP-MS (Table 1). Due to the air sensitivity of **2**, solution phase ICP-MS is not a feasible method, and instead laser ablation (LA-ICP-MS) methods were investigated. A pressed pellet of the sample was ablated with a LSX-500 (CETAC Technologies, Omaha NE) laser ablation system under an argon atmosphere.

Ablation was achieved by rastering the sample at 10 Hz with a 100 μm spot size. The material was ablated for 150 seconds at 9 mJ per pulse. Pure argon carrier gas was used at 1.03 L/minute, adjusted for maximum sensitivity. Five separate measurements were taken, each was background corrected and the data was averaged for reporting.

To determine whether chlorine and potassium were present at a high enough content to be part of the molecular structure of the sample, yttrium and silicon were also measured as internal standards. However, since no appropriate matrix-matched external standard exists, a different method of approximating an external standard is necessary. Therefore, an aqueous standard was prepared from stock solutions (Plasmachem Associates Inc, Bradley Beach NJ). The external standard contained 20.0 ppb Y and Si, and 22.8 ppb K and Cl in 1% (v/v) nitric acid. An Apex desolvation system (Elemental Scientific Inc, Omaha NE) was then used to remove solvent and approximate a dry load before entering the plasma. Sample gas rate was 0.80 L/minute during sample uptake with an additional 0.175 L/min added after desolvation, adjusted for maximum sensitivity and elimination of polyatomics.

The atomic ratios in the sample of Y/K, Si/K, Y/Cl and Si/Cl are all sufficiently high to lead to the conclusion that potassium and chlorine are not present in the material in a

stoichiometric amount (Table 2). The raw data show that silicon and yttrium were far more abundant in the sample than in the external standard. Likewise the ratio data show chlorine and potassium were far less present in the sample than the primary elements. Five separate trials of each measurement are averaged in the data. The most uncertain ratio found is Y/Cl, which shows chlorine still to be present at 1.1% the abundance of yttrium. Measurements by LA-ICP-MS confirm that potassium and chlorine are only contained in the substance at trace amounts.

Table 1 ICP-MS operating conditions

ICP-MS device	**Finnigan Element 1**
Forward Power	**1200 W**
Reflected Power	**8-9 W**
Cooling Gas	**16.00 L min^{-1}**
Auxiliary Gas	**0.80-0.85 L min^{-1}**
Sample Gas	**0.95 L min^{-1} aqueous, 1.03 L min^{-1} LA**
Resolution	**4000 (medium resolution)**
Isotopes Measured	**^{28}Si, ^{35}Cl, $^{39}K^{*}$, ^{89}Y**

Table 1: $^{*39}K^{+}$ was integrated only over half the peak to avoid a common interference ion, $^{1}H^{38}Ar^{+}$. The integrated signal was then doubled to readjust the data.

Table 2 Atomic ratios of present and trace elements

2a. Raw Data	Sample (cps)	Ext. Std. (cps)	Sample/Std.	2b. Ratios	Average	St. Dev.	RSD
Si	**2.47e6**	**1.14e4**	**2.17e2**	**Y/K**	**104000**	**9000**	**8.71**
Cl	**2.60e5**	**1.90e5**	**1.37e0**	**Si/K**	**217000**	**34000**	**15.9**
K	**1.24e6**	**1.07e9**	**1.16e-3**	**Y/Cl**	**88.1**	**9.0**	**10.2**
Y	**4.74e8**	**4.52e6**	**1.05e2**	**Si/Cl**	**182**	**18**	**9.61**

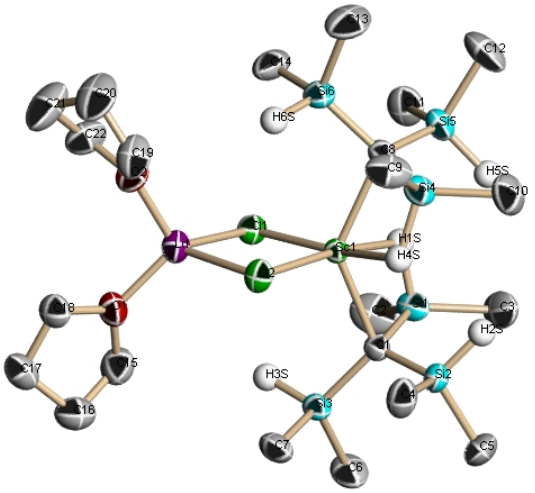

Ortep diagram for **2-LiCl-THF$_2$**.

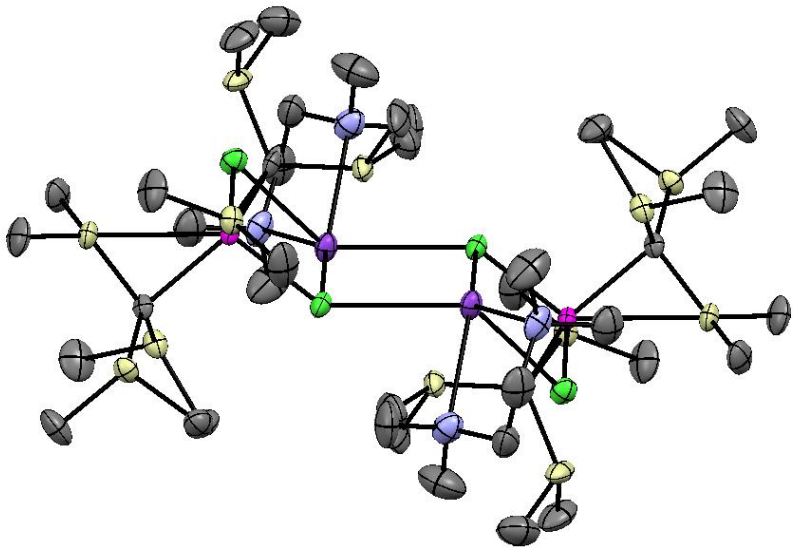

Ortep diagram for **2-KCl-tmeda**.

Chapter 3: Intermolecular β-hydrogen abstraction in ytterbium, calcium and potassium tris(dimethylsilyl)methyl compounds.

KaKing Yan, George Schoendorff, Brianna M. Upton, Arkady Ellern, Theresa L. Windus, and Aaron D. Sadow

Modified from a paper published in *J. Am. Chem. Soc.*[2] and a paper published in *Organometallics*[3]

Department of Chemistry and US Department of Energy Ames Laboratory, Iowa State University, Ames IA, 50011, USA

Abstract. A series of organometallic compounds containing the tris(dimethylsilyl)methyl ligand are described. The potassium carbanions $KC(SiHMe_2)_3$ and $\{KC(SiHMe_2)_3TMEDA\}_2$ are synthesized by deprotonation of the hydrocarbon $HC(SiHMe_2)_3$ with potassium benzyl. $\{KC(SiHMe_2)_3TMEDA\}_2$ crystallizes as a dimer with two types of 3-center-2-electron K-H-Si interactions: side-on coordination of SiH (∠K-H-Si = 102(2)°) and more obtuse K-H-Si structures (∠K-H-Si ~ 150°). The divalent calcium and ytterbium compounds $M\{C(SiHMe_2)_3\}_2L$ (M = Ca, Yb; L = THF_2 or TMEDA) are prepared from MI_2 and 2 equiv of $KC(SiHMe_2)_3$. Low $^1J_{SiH}$ coupling constants in the NMR spectra, low energy ν_{SiH} bands in the IR spectra, and short M-Si distances and small M-C-Si angles in the crystal structures suggest β-agostic interactions on each $C(SiHMe_2)_3$ ligand. The IR assignments of $M\{C(SiHMe_2)_3\}_2L$ (L = THF_2 or TMEDA) are supported by DFT calculations. The compounds $M\{C(SiHMe_2)_3\}_2L$ react with 1 or 2 equiv of $B(C_6F_5)_3$ to give 1,3-

[2] *J. Am. Chem. Soc.* **2009**, *131*, 15110-15111.

[3] *Organometallics* **2013**, *32*, 1300-1316.

disilacyclobutane $\{Me_2Si\text{-}C(SiHMe_2)_2\}_2$ and $MC(SiHMe_2)_3HB(C_6F_5)_3L$ or $M\{HB(C_6F_5)_3\}_2L$, respectively. In addition, $M\{C(SiHMe_2)_3\}_2L$ compounds react with BPh_3 to give β-H abstracted products. The compounds $M\{C(SiHMe_2)_3\}_2THF_2$ react with $SiMe_3I$ to yield Me_3SiH and disilacyclobutane as the products of β-H abstraction, while $M\{C(SiHMe_2)_3\}_2TMEDA$ and Me_3SiI form a mixture of Me_3SiH and the alkylation product $Me_3SiC(SiHMe_2)_3$ in a 1:3 ratio.

Introduction

Isolable and thermally robust organotransition-metal compounds tend not to contain β-hydrogen-containing alkyl ligands, as these groups are susceptible to intramolecular reaction pathways including β-hydrogen elimination and β-hydrogen abstraction.[1] However, this easily-identified structural feature is not the only requirement for classical intramolecular β-H elimination; at least one vacant orbital or coordination site must be located *cis* to the alkyl ligand, the accepting orbital must have the appropriate energy, the symmetry of the orbitals involved should be matched throughout the reaction, and the overall thermodynamics must favor elimination and/or subsequent products. The pathway for β-hydrogen elimination of an alkyl ligand is the microscopic reverse of olefin insertion, and thus both the forward and reverse directions of these reactions are chemically important.[2]

Likewise, there are specific requirements for β-hydrogen abstraction. Intramolecular β-hydrogen abstraction requires a sufficiently basic X^- ligand, also located *cis* to the alkyl ligand, to allow the conjugate acid HX to be a leaving group. Note that β-elimination and intramolecular β-abstraction are electronically dissimilar in terms of the formal polarization

of the β-hydrogen: a hydride is transferred to the metal center in the former reaction, whereas a proton is transferred in the latter transformation. In an interesting contrast to transition metal chemistry, many main group and rare earth alkyls are reticent to undergo β-hydrogen eliminations and abstractions despite highly polarized M-C bonds that give strongly basic ligands, potentially open coordination sites resulting from flexible coordination geometries and labile metal-ligand interactions, and often highly Lewis acidic metal centers.

For example, β-hydrogen elimination of alkyllithiums takes place at 130-150 °C in refluxing hydrocarbons;[3] the sodium congeners react more rapidly, requiring less forcing conditions,[4] while compounds such as *tert*-buyl potassium readily eliminate isobutylene as one of a number of reaction pathways.[5] Likewise, β-H-containing dialkylmagnesium compounds form olefins upon thermolysis, however *n*-butylcalcium chloride persists in refluxing tetrahydrofuran.[6] Coordinatively unsaturated organolanthanides also undergo β-elimination less readily than organotransition-metal analogs.[7] In a representative example, isobutylene elimination from isolable $Cp_2ErCMe_3(THF)$ is facilitated by LiCl at elevated temperatures.[8] Despite the hints that group 1, group 2 and rare earth alkyls containing β-hydrogen are metastable, most main group and rare earth organometallic compounds still avoid gratuitous β-hydrogen in their ligands.[9] Thus, β-hydrogen-free benzyl,[10] allyl,[11] CH_2SiMe_3,[12] $CH(SiMe_3)_2$,[13] and the ultra-bulky trisyl $C(SiMe_3)_3$ ligands[14] and their derivatives are commonly employed in starting material syntheses and in the preparation of homoleptic alkyl compounds. Such ligands have allowed the preparation of dialkyl calcium and ytterbium compounds, such as $Ca\{C(SiMe_3)_3\}_2$,[15] $Yb\{C(SiMe_3)_3\}_2$,[16]

$Ca\{C(SiMe_3)_2Ph\}_2$,[10] $Ca\{CH(SiMe_3)_2\}_2(C_4H_2O_2)_2$,[17] and $Yb\{C(SiMe_3)_2SiMe_2X\}_2$ (X = OMe, CH_2CH_2OEt, $CH{=}CH_2$, hexahydro-2H-pyrimido[1,2-a]pyrimidine).[18]

However, β-hydrogens are important in chemical transformations, particularly catalytic reactions involving β-hydrogen abstraction such as Meerwein-Ponndorf-Verley carbonyl reductions/Oppenauer alcohol oxidations and Tishchenko ester syntheses (Scheme 3.1).[19]

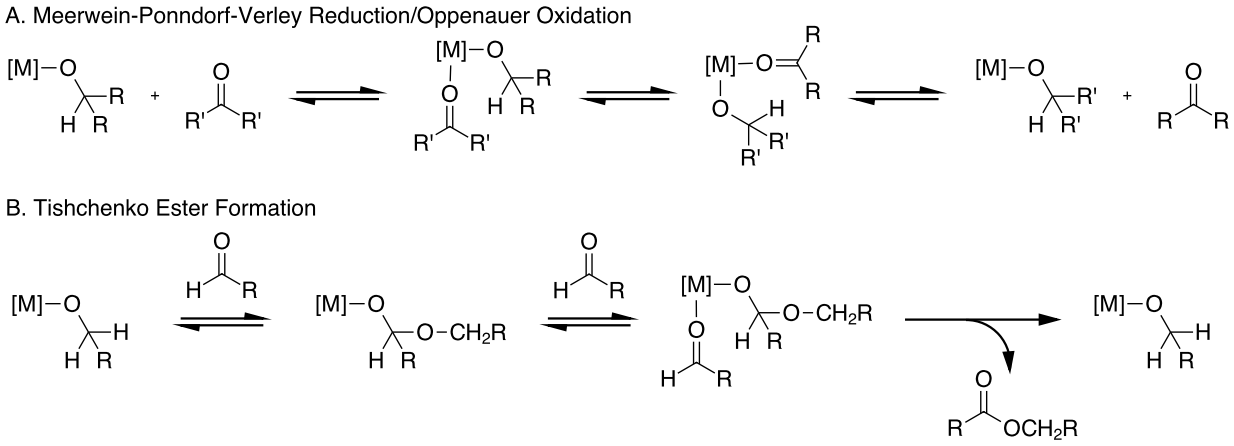

Scheme 3.1. Main group and rare earth-catalyzed (A) Meerwein-Ponndorf-Verley reduction/Oppenauer oxidation and (B) Tishchenko ester formation that are proposed to involve β-hydrogen abstractions.

These reactions involve β-hydrogen on main group and rare earth alkoxides rather than alkyls. The important point here is that β-hydrogens are particularly reactive, even though the elimination pathway is not facile in such main group and rare earth metal alkoxides. Secondly, β-agostic alkyl compounds provide key information as models for intermediates in olefin insertion reactions.[20] β-hydrogen-containing silazides, such as $N(SiHMe_2)t$-Bu and $N(SiHMe_2)_2$, have rich rare earth and early transition-metal chemistry that centers on the spectroscopic and structural features and reactivity of the SiH

moiety.[21,22,23] Thus, a significant amount of chemistry comes from β-SiH containing amido, β-CH containing alkoxide, and β-CH containing alkyl compounds.

Fewer alkyl groups contain β-SiH moieties, and therefore we targeted ligands for rare earth and main group compounds that contain M-C bonds and β-SiH groups. Lappert described the preparation and the reaction of Me_2HSiCH_2MgBr and $RhCl(PPh_3)_3$ that gives $RhH(PPh_3)_4$.[24] Eaborn has prepared analogs of trisyl $HC(SiMe_3)_3$ containing dimethylsilyl groups $HC(SiHMe_2)_3$ and $HC(SiHMe_2)(SiMe_3)_2$.[25] Ladipo demonstrated that the central CH is acidic and readily deprotonated by lithium diisopropylamide.[26]

Recently, we reported homoleptic tris(alkyl)yttrium complex $Y\{C(SiHMe_2)_3\}_3$ and bis(alkyl) calcium(II) and ytterbium(II) compounds $M\{C(SiHMe_2)_3\}_2THF_2$ (M = Ca, Yb) containing the $C(SiHMe_2)_3$ ligand.[27] These molecules contain spectroscopic and structural signatures associated with β-agostic Si-H-M interactions, but do not undergo β-H elimination even though they are (at least formally) coordinatively unsaturated. Upon thermolysis to 100 °C, only $HC(SiHMe_2)_3$ is observed. Although the classical intramolecular β-hydrogen elimination is inhibited in the sterically hindered -$C(SiHMe_2)_3$, addition of external Lewis acids results in abstraction of the β-hydrogen rather than the $C(SiHMe_2)_3$ group. This abstraction is distinguished from the intramolecular β-hydrogen abstraction described above, in that the hydrogen is formally removed as a hydride rather than as a proton.

A few examples of intermolecular β-hydrogen abstractions from alkyl ligands have been reported, particularly for aluminum and zinc alkyls.[28] Recently, β-hydrogen abstractions from zinc alkyls were shown to be favored by pre-coordination of the organometallic compound and the Lewis acid.[29] Therefore, we wanted to explore the structures of starting

materials and β-abstraction products and the effects of the Lewis acid and ancillary ligands in our calcium and ytterbium system. We have observed interesting structural and spectroscopic effects in these organometallic compounds containing the $C(SiHMe_2)_3$ ligands, and we have discovered that the M-C bond (rather than the β-SiH) reactivity is enhanced by TMEDA as an ancillary ligand.

Results and discussion

3.1. Synthesis of $KC(SiHMe_2)_3$ and $\{KC(SiHMe_2)_3TMEDA\}_2$.

The reaction of $HC(SiHMe_2)_3$ and potassium benzyl in THF for 18 h provides $KC(SiHMe_2)_3$ (**3.1**) as a red solid (eq 3.1). The red material is insoluble in pentane, and the compound solidifies upon washing with that solvent.

$$HC(SiHMe_2)_3 + KCH_2C_6H_5 \xrightarrow[\text{THF, 18 h}]{} \underset{\textbf{3.1}}{KC(SiHMe_2)_3} + C_6H_5CH_3 \quad (3.1)$$

The ^{1}H NMR spectrum of $KC(SiHMe_2)_3$ contained resonances at 4.59 ppm ($^1J_{SiH}$ = 154 Hz) and 0.46 ppm ($^3J_{HH}$ = 3.2 Hz) assigned to SiH and SiMe groups, respectively; the $^{13}C\{^1H\}$ NMR spectrum contained signals at 2.61 and 5.19 ppm; and the $^{29}Si\{^1H\}$ NMR spectrum contained one signal at -23.3 ppm. Signals for residual or coordinated THF are not detected, and combustion analysis is consistent with the formulation $KC(SiHMe_2)_3$. Thus, NMR spectroscopy is consistent with the presence of a C_3 axis that relates the three $SiHMe_2$ groups in **3.1**. The unexpected red color, the slightly low $^1J_{SiH}$ coupling constant, and the IR spectrum with ν_{SiH} bands at 2108 and 1973 cm^{-1} hint at an interesting structure. A UV-vis spectrum of **3.1** dissolved in benzene contained a stronger band (λ_{max}: 352 nm, ε = 450

$L \cdot mol^{-1} \cdot cm^{-1}$) and a broad and weaker band better described as a shoulder that tails from 450 to 550 nm (ε = 32.1 $L \cdot mol^{-1} \cdot cm^{-1}$ at 480 nm).

$\{KC(SiHMe_2)_3TMEDA\}_2$ ($\{$**3.1**$\cdot$TMEDA$\}_2$) is prepared by addition of TMEDA to $KC(SiHMe_2)_3$ in benzene, and this compound is a red solid that is soluble in pentane and benzene. The solution-phase NMR spectra are incommensurate with the results of an X-ray structure determination (the solid-phase structure is shown in equation 3.2), and this discrepancy suggests a fluxional solution-phase structure.

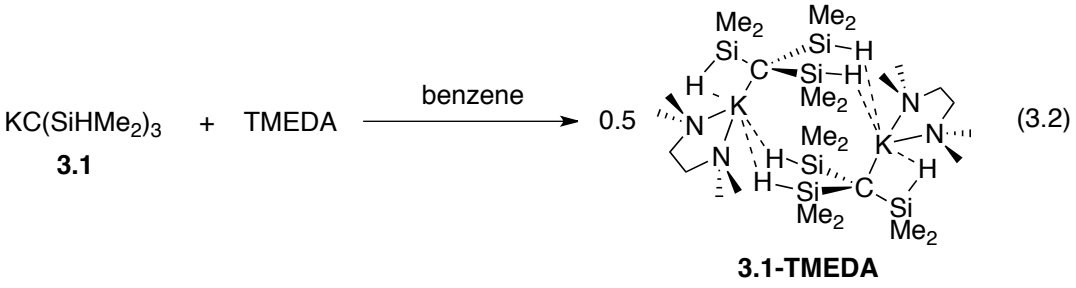

(3.2)

As in **3.1**, the ^1H, $^{13}C\{^1H\}$, and ^{29}Si NMR spectra of (**1**$\cdot$TMEDA)$_2$ suggest a three-fold rotation axis that relates the $SiHMe_2$ groups in the alkyl ligand. Thus, the ^1H NMR spectrum of (**3.1**$\cdot$TMEDA)$_2$ contained resonances at 4.80 ppm ($^1J_{SiH}$ = 154 Hz) and 0.52 ppm ($^3J_{SiH}$ = 3.5 Hz); the $^{13}C\{^1H\}$ NMR spectrum contained signals at 5.32 and 5.19 ppm, assigned to SiMe and KC groups, respectively; and the $^{29}Si\{^1H\}$ NMR spectrum contained one signal at -23.7 ppm. As in the TMEDA-free potassium alkyl, the ^1H NMR data ($^1J_{SiH}$ = 154 Hz) and FTIR ν_{SiH} bands (2105, 2035, 1962 cm^{-1} in KBr) suggest potassium-silylhydride interactions. Assignment of the ν_{SiH} signals was facilitated by the corresponding spectrum of (**3.1-*d*$_2$**$\cdot$TMEDA)$_2$, in which new peaks at 1533, 1462, and 1414 cm^{-1} were observed and the bands assigned to ν_{SiH} were absent. However, ^1H NMR spectra acquired even at 185 K were broad, and a spectrum consistent with a static structure was not observed.

X-ray quality crystals are grown from concentrated pentane solution, and a solution from the diffraction study reveals that (**3.1**·TMEDA)$_2$ is dimeric in the solid state (Figure 3.1). The two KC(SiHMe$_2$)$_3$ units of the dimer are related by a crystallographically imposed inversion center. Each potassium center is coordinated by a bidentate TMEDA ligand, the central carbon and one 'side-on' Si-H moiety from the C(SiHMe$_2$)$_3$ ligand, and two hydrogens from two H-Si groups in the second C(SiHMe$_2$)$_3$ group of the dimer.

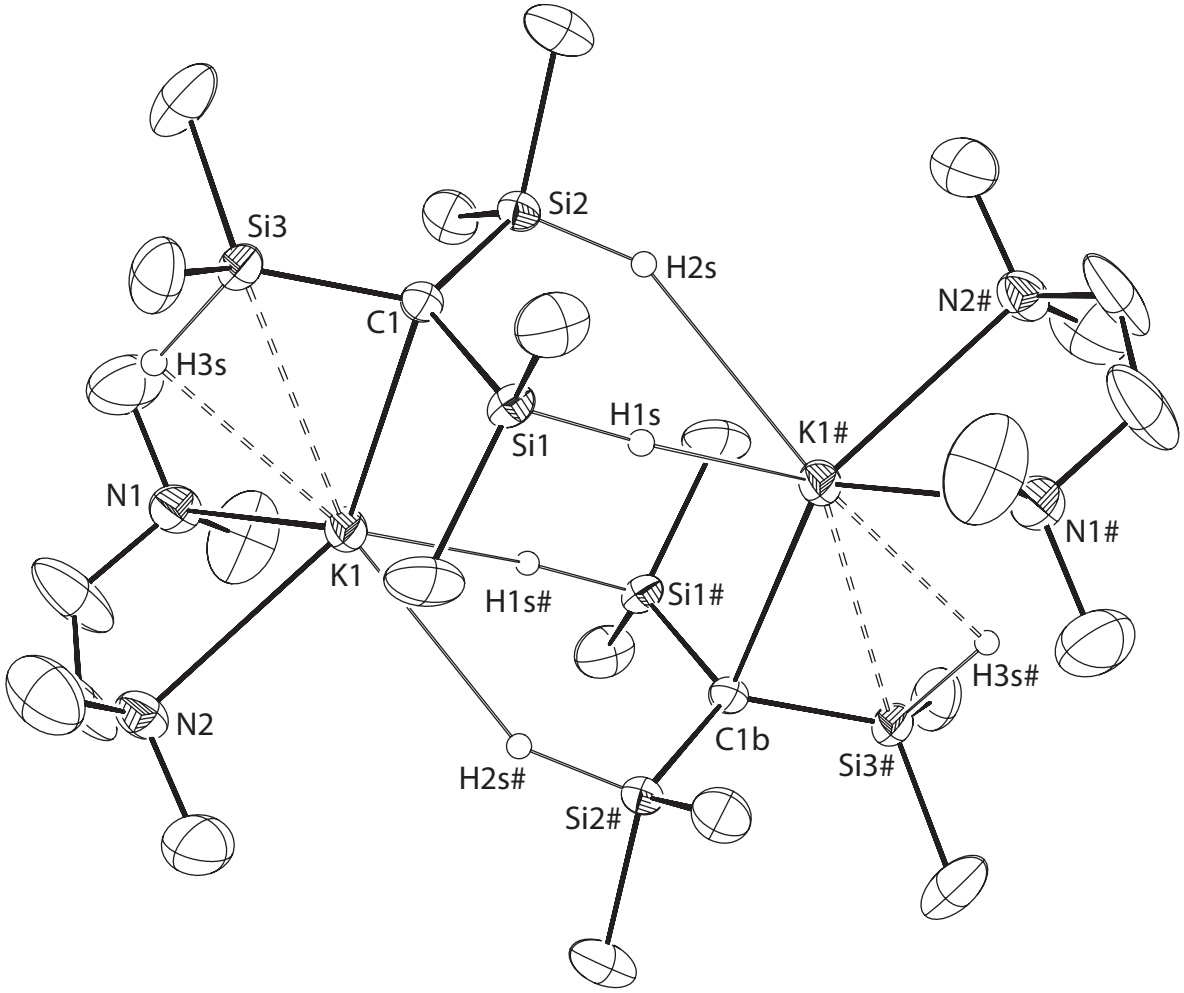

Figure 3.1. ORTEP diagram of {KC(SiHMe$_2$)$_3$TMEDA}$_2$ ({**3.1**·TMEDA}$_2$). Ellipsoids are plotted at 35% probability. Hydrogen atoms bonded to carbon are not illustrated. Hydrogen

atoms bonded to silicon were located objectively in the Fourier difference map. Significant interatomic distances (Å): K1-C1, 3.030(5); K1-H3s, 2.80(5); K1-Si3, 3.450(2); K1-Si1#, 3.983(2); K1-H1s#, 2.68(5); K1-Si2#, 4.096(2); K1-H2s#, 2.85(4). Significant interatomic angles (°): K1-C1-Si1, 95.8(2); K1-C1-Si2, 98.1(2); K1-C1-Si3, 87.2(2); K1-H1s#-Si1#, 156(3); K1-H2s#-Si2# 149(3); K1-H3s-Si3, 102(2).

The potassium-carbon distance of 3.030(5) Å is shorter than the related distance in potassium trisyl $KC(SiMe_3)_3$ of 3.10(1) Å; the structure of $KC(SiMe_3)_3$ consists of linear chains of alternating $C(SiMe_3)_3$ groups and K atoms.[14c] The K-C distance in chains of $KC(SiHMe_2)(SiPhMe_2)_2$ of 3.167(8) Å is also longer;[25b] in that compound, there are close potassium contacts to the silicon (K···Si, 3.457 Å) and hydrogen (K···H, 2.57(9) Å). The potassium in the literature compound is also coordinated by two phenyl groups of the next alkyl potassium repeat unit. The K-C interatomic distances in these compounds are within the sum of van der Waals radii of C and K (4.45 Å).[30] The central carbon are typically planar in tris(silyl) carbanions as well as phenylsubstituted carbanions;[31] thus, the carbon and three subsitutents are nearly planar in (**1**·TMEDA)$_2$, and the sum of the Si-C-Si angles is 358.8°.

There are three non-equivalent close contacts between potassium and hydrogen (bonded to silicon) in (**3.1**·TMEDA)$_2$. The side-on interaction involves short K···H and short K···Si interatomic distances of 2.80(5) and 3.450(2) Å. For comparison, the sum of H and K van der Waals radii are 3.84 Å, and the sum of H and K covalent radii are 2.34 Å.[32] Likewise, the sum of Si and K van der Waals radii are 4.85 Å, and the sum of Si and K covalent radii is 3.23 Å. The side-on interaction is further identified by an acute K1-C1-Si3 angle of 87.2(2)°, while the other K1-C1-Si1 and K1-C1-Si2 angles are greater than 90° at

95.8(2) and 98.1(2)°. As a result, the plane of the CSi_3 moiety is tilted toward the agostic SiH with respect to the potassium-carbon vector.

Four K···H–Si end-on interactions connect the two $KC(SiHMe_2)_3$ units to form the dimeric structure of (**3.1**·TMEDA)$_2$, and two of these interactions are equivalent to the two other interactions by crystallographically imposed symmetry. Thus, the K1-Si1# distance is 3.983(2) Å, and the K1-Si2# distance is 4.096(2). The bridging hydrogen atoms were located in the electron-density map, and the related K1-H1s# and K1-H2s# distances are 2.68(5) and 2.85(5) Å. The K1-H1s#-Si1# angle of 156(3)° is greater than the K1-H2s#-Si2# angle of 149(3). Thus, the potassium compound (**3.1**·TMEDA)$_2$ contains two types of three-center-two-electron potassium-hydrosilyl interactions that are best described as agostic and anagostic.[33] The two potassium atoms of the dimer are separated by a distance of 4.890(2) Å, which is within the sum of van der Waals radii (5.50 Å) but longer than the sum of covalent radii (4.06 Å); a K–K bond is not chemically reasonable in (**3.1**·TMEDA)$_2$.

The connectivity of this structure contrasts with that of $LiC(SiHMe_2)_3THF_2$ and $LiC(SiMe_3)_3$TMEDA that are disproportionated Li dimers $[Li(L)_4][Li(C(SiHMe_2)_3)_2]$.[14,26] The potassium alkyl $KC(SiHMe_2)(SiMe_2Ph)_2$ contains a similar K(η^2-SiH) interaction with a K···H distance of 2.57(9) A.[25b]

3.2. Synthesis of M{C(SiHMe$_2$)$_3$}$_2$THF$_2$ and M{C(SiHMe$_2$)$_3$}$_2$TMEDA (M = Ca, Yb).

Bis(tris(dimethylsilyl)methyl)calcium and ytterbium compounds are synthesized by salt metathesis reactions of MI_2 and $KC(SiHMe_2)_3$. Reactions in tetrahydrofuran provide the THF adducts $Ca\{C(SiHMe_2)_3\}_2THF_2$ (**3.2·THF$_2$**, 58.7%) and $Yb\{C(SiHMe_2)_3\}_2THF_2$ (**3.3·THF$_2$**, 49.6%).[Error! Bookmark not defined.b] The diamine adducts $Ca\{C(SiHMe_2)_3\}_2$TMEDA

(**3.2·TMEDA**, 23.7%) and Yb{C(SiHMe$_2$)$_3$}$_2$TMEDA (**3.3·TMEDA**, 29.8%) are prepared from MI$_2$, 2 equiv of KC(SiHMe$_2$)$_3$, and excess TMEDA in benzene (eq 3.3).

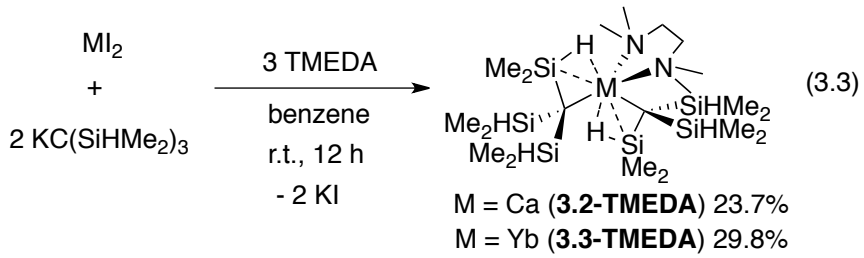

(3.3)

In general, the spectroscopic properties of M{C(SiHMe$_2$)$_3$}$_2$TMEDA and M{C(SiHMe$_2$)$_3$}$_2$THF$_2$ are similar, but a few features associated with the Si-H groups appear to be influenced by the donor ligand and metal center. The ^{1}H NMR spectra for M{C(SiHMe$_2$)$_3$}$_2$TMEDA (M = Ca, Yb) each contained one SiH resonance (Ca: δ 4.81, $^1J_{SiH}$ = 154 Hz; Yb: δ 4.76 $^1J_{SiH}$ = 148 Hz), and these spectral features are similar to those of the THF analogues M{C(SiHMe$_2$)$_3$}$_2$THF$_2$ (Ca: δ 4.78, $^1J_{SiH}$ = 152 Hz; Yb: δ 4.78 $^1J_{SiH}$ = 150 Hz). The lowest $^1J_{SiH}$ coupling constant was detected for the ytterbium compound **3.3·TMEDA**, while the largest $^1J_{SiH}$ was observed for calcium **3.2·TMEDA**. Although these values are likely affected by several time-averaged factors resulting from fluxional exchange, **3.3·TMEDA** consistently exhibits the extreme of spectroscopic values (see below). The ^{29}Si NMR spectra of TMEDA and bis(tetrahydrofuran) compounds **3.3** and **3.4** each contained a single resonance at ~ –20 ppm. Additionally, singlet resonances in both ^{1}H and ^{13}C{^{1}H} NMR spectra of **3.2·TMEDA** and **3.3·TMEDA**, assigned to the *N*-methyl and methylene groups of the TMEDA ligand, suggested bidentate coordination of TMEDA to ytterbium and calcium metal centers, respectively.

Three slightly broad bands were observed in the IR spectra of **3.2·TMEDA** and **3.3·TMEDA** in the region associated with SiH stretching modes (Table 3.1). Three bands contrast the two ν_{SiH} bands for $KC(SiHMe_2)_3$. The IR spectra of **3.2-*d*$_6$·TMEDA** and **3.3-*d*$_6$·TMEDA** provide further support for the ν_{SiH} assignments (see Table 3.1). Additionally, the NMR spectra suggest equivalent $SiHMe_2$ groups; the comparison of IR and NMR spectra indicates fluxionality on the NMR timescale. We assigned the two higher energy bands to terminal and weakly activated Si-H, whereas the lowest energy bands are associated with the Si-H bonds of silicon and hydrogen atoms that most closely approach the metal centers. These assignments are supported by DFT calculations (see below). The frequencies of the terminal SiH (high ν_{SiH}) are approximately constant for all compounds, but the low energy ν_{SiH} bands vary significantly. The signals are similar for THF-coordinated Ca and Yb compounds (~1900 cm^{-1}), lower energy in $Ca\{C(SiHMe_2)_3\}_2TMEDA$ (1861 cm^{-1}), and lowest in $Yb\{C(SiHMe_2)_3\}_2TMEDA$ (1846 cm^{-1}). Based on the inequivalent SiH bands in the IR spectra, we attempted to resolve the ^1H NMR spectra of **3.2-3.3·THF$_2$** and **3.2-3.3·TMEDA** with variable-temperature measurements from 185-298 K in toluene-d_8. However, spectra acquired even at 195 K contained equivalent and broad resonances associated with the $SiHMe_2$ groups.

Table 3.1. Infrared spectroscopic data for tris(dimethylsilyl)methyl potassium, calcium, and ytterbium with THF and TMEDA ligands (KBr, cm^{-1}).

Compound	high ν_{SiH}	intermediate ν_{SiH}	low ν_{SiH}
$HC(SiHMe_2)_3$:[25a]	2090	n.a.	n.a.

$HC(SiDMe_2)_3$	1534	n.a.	n.a.
$KC(SiHMe_2)_3$ (**3.1**)	2108	n.a.	1973
$KC(SiDMe_2)_3$ (**3.1-d_3**)	1532	n.a.	1417
$\{KC(SiHMe_2)_3TMEDA\}_2$ ($\{$**3.1·TMEDA**$\}_2$)	2105	2035	1962
$\{KC(SiDMe_2)_3TMEDA\}_2$ ($\{$**3.1-d_3·TMEDA$\}_2$**)	1533	1462	1414
$Ca\{C(SiHMe_2)_3\}_2THF_2$ (**3.2·THF$_2$**)	2107	2066	1905
$Ca\{C(SiDMe_2)_3\}_2THF_2$ (**3.2-d_6·THF$_2$**)	1530	1493	1409
$Ca\{C(SiHMe_2)_3\}_2THF_2$ asym:	2087	2050	1887
(**3.2$_{CALC}$·THF$_2$**) sym:	2090	2050	1881
$Yb\{C(SiHMe_2)_3\}_2THF_2$ (**3.3·THF$_2$**)	2101	2065	1890
$Yb\{C(SiDMe_2)_3\}_2THF_2$ (**3.3-d_6·THF$_2$**)	1506 sh	1492	1410
$Yb\{C(SiHMe_2)_3\}_2THF_2$	2074	2047	1893
(**3.3$_{CALC}$·THF$_2$**) C_1-symmetric	2090	2051	1878
3.2·TMEDA	2105	2038	1861
3.2-d_6·TMEDA	1510 sh	1493	1411
3.3·TMEDA	2080	2038	1846
3.3-d_6·TMEDA	1505 sh	1494	1380
$CaC(SiHMe_2)_3HB(C_6F_5)_3THF_2$ (**3.4·THF$_2$**)	2077	2042	1957
$YbC(SiHMe_2)_3HB(C_6F_5)_3THF_2$ (**3.5·THF$_2$**)	2074	n.a.	1921
(**3.4·TMEDA**)	2094	2026	1918
(**3.5·TMEDA**)	2094	2027	1899

Recrystallization of $Yb\{C(SiHMe_2)_3\}_2TMEDA$ from a concentrated pentane solution at -30 °C provides X-ray quality crystals, and an ORTEP diagram is shown in Figure 2.

Although previously reported THF-adducts **3.2·THF$_2$** and **3.3·THF$_2$** have similar structures to the ytterbium diamine adduct described here, the features of the M–C(SiHMe$_2$)$_3$ interactions (Tables 3.2 and 3.3) interestingly correlate with spectroscopic trends (Table 3.1) for the THF and TMEDA adducts.

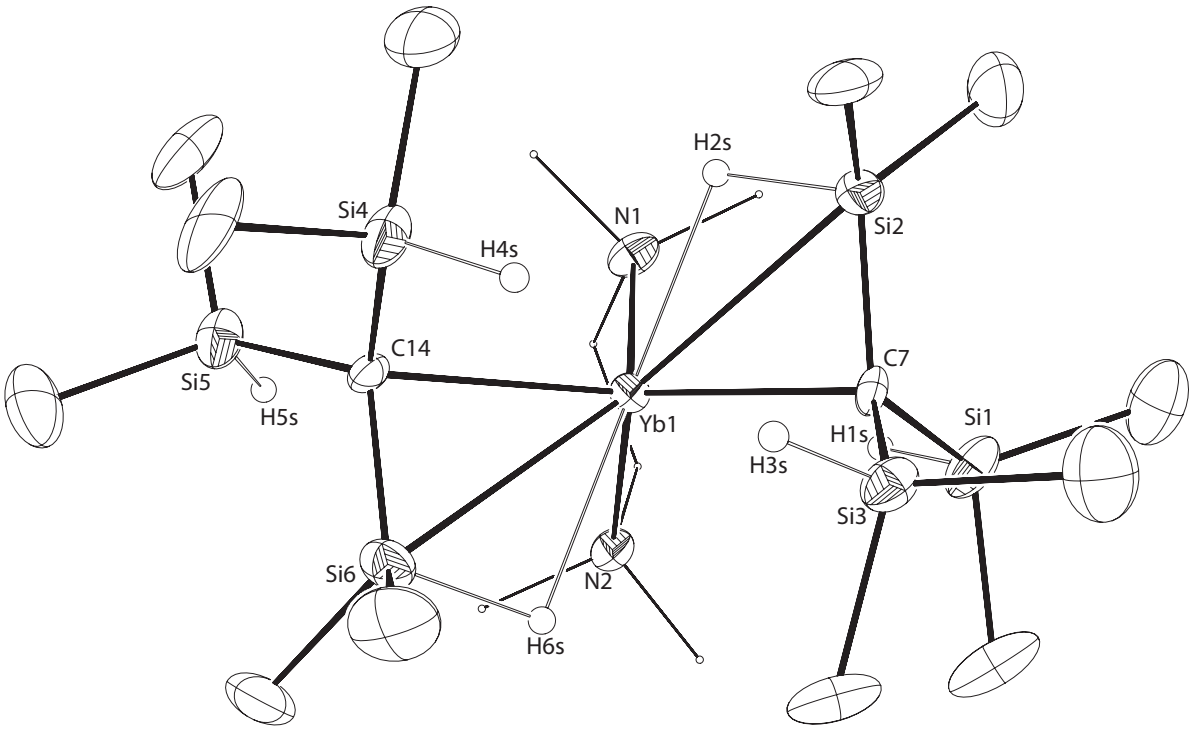

Figure 3.2. ORTEP diagram of Yb{C(SiHMe$_2$)$_3$}$_2$TMEDA (**3.3·TMEDA**). Carbon atoms on the TMEDA are plotted as points and hydrogen atoms on TMEDA and silyl methyl groups are not illustrated. Interatomic distances (Å): Yb1-C7, 2.68(1); Yb1-C14, 2.67(1); Yb1-Si1, 3.374(4); Yb1-Si2, 3.191(4); Yb1-Si3, 3.977(4); Yb1-Si4, 3.559(4); Yb1-Si5, 4.002(4); Yb1-Si6, 3.142(4); Yb1-H2s, 2.4(1); Yb1-H6s, 2.5(1). Interatomic angles (°): N1-Yb1-N2, 71.5(3); C7-Yb1-C14, 121.8(3); Si1-C7-Si2, 116.7(6); Si1-C7-Si3, 117.2(6); Si2-C7-Si3,

114.4(6); Si4-C14-Si5, 114.0(6); Si4-C14-Si6, 113.2(2); Si5-C15-Si6, 114.8(6); Yb1-H2s-Si2, 44(4); Yb1-H6s-Si6, 52(4).

The formally four-coordinate ytterbium center adopts a distorted tetrahedral geometry containing an acute ∠N-Yb-N angle of 71.5(3)° and an obtuse ∠C-Yb-C angle of 121.8(3)°. All of the $SiHMe_2$ groups in the $C(SiHMe_2)_3$ ligands are oriented with hydrogen directed toward the interior of the molecule and the methyl groups pointing outward. The hydrogen atoms bonded to silicon were located objectively in the difference Fourier map; the positions of the $SiMe_2$ atoms and the electron density map provide a reasonable estimate of the hydrogen position, subject to the normal limitations associated with X-ray diffraction. Still, the angles and distances of the $C(SiHMe_3)_3$ ligands show distortions associated with β-agostic structures. In particular, three categories of Yb-Si distances are easily identified as long (~4 Å), intermediate (3.4-3.5 Å), and short (3.14-3.19 Å). For comparison, the Yb-Si distance in $Cp^*YbSi(SiMe_3)_3$ is 3.032(2) Å.[34] The Yb-C-Si angles in **3.3·TMEDA** may also be categorized as obtuse (~120°), intermediate (95-102), and acute (86-88°), and these angles correlate with the Yb-Si distances. However, the C-Si distances in the CSi_3 moieties (C7-Si1, C7-Si2, C7-Si3 and C14-Si4, C14-Si5, C14-Si6) are identical within 3σ error.

Table 3.2. Significant interatomic distances from the single crystal diffraction studies of $Ca\{C(SiHMe_2)_3\}_2THF_2$ (**3.2·THF$_2$**), $Yb\{C(SiHMe_2)_3\}_2THF_2$ (**3.3·THF$_2$**), $Yb\{C(SiHMe_2)_3\}_2TMEDA$ (**3.3·TMEDA**), $CaC(SiHMe_2)_3HB(C_6F_5)_3)THF_2$ (**3.4·THF$_2$**), and $YbC(SiHMe_2)_3HB(C_6F_5)_3THF_2$ (**3.5·THF$_2$**), as well as from density function theory modeling of $Ca\{C(SiHMe_2)_3\}_2THF_2$ (**3.2$_{calc}$·THF$_2$**) and $Yb\{C(SiHMe_2)_3\}_2THF_2$ (**3.3$_{calc}$·THF$_2$**).

Compound	agostic M-Si	intermediate M-Si	long M-Si	M-C bond
$Ca\{C(SiHMe_2)_3\}_2THF_2$ (**3.2·THF$_2$**)	Ca1-Si2 3.216(2)	Ca1-Si3 3.571(2)	Ca1-Si1 3.642(3)	Ca1-C7 2.616(7)
(**3.2$_{calc}$·THF$_2$**)	3.209	3.660	3.721	2.579
$Yb\{C(SiHMe_2)_3\}_2THF_2$ (**3.3·THF$_2$**)	Yb1-Si1 3.180(1)	Yb1-Si3 3.515(2)	Yb1-Si2 3.617(2)	Yb1-C1 2.596(4)
(**3.3$_{calc}$·THF$_2$**) C_1	3.272 3.286	3.624 3.654	3.785 3.699	2.602 2.598
$Yb\{C(SiHMe_2)_3\}_2TMEDA$ (**3.3·TMEDA**)	Yb1-Si6 3.142(4)	Yb1-Si1 3.374(4)	Yb1-Si3 3.977(4)	Yb1-C7 2.68(1)
	Yb1-Si2 3.191(4)	Yb1-Si4 3.559(4)	Yb1-Si5 4.002(4)	Yb1-C14 2.67(1)
$CaC(SiHMe_2)_3HB(C_6F_5)_3)THF_2$ (**3.4·THF$_2$**)	Ca1-Si3 3.097(1)	Ca1-Si2 3.097(1)	Ca1-Si1 3.912(1)	Ca1-C1 2.566(3)
$YbC(SiHMe_2)_3HB(C_6F_5)_3THF_2$ (**3.5·THF$_2$**)	Yb1-Si1 3.1016(7)	Yb1-Si2 3.0925(7)	Yb1-Si3 3.937(1)	Yb1-C27 2.593(2)

Table 3.3. Significant interatomic angles from the single crystal diffraction studies of $Ca\{C(SiHMe_2)_3\}_2THF_2$ (**3.2·THF$_2$**), $Yb\{C(SiHMe_2)_3\}_2THF_2$ (**3.3·THF$_2$**), $Yb\{C(SiHMe_2)_3\}_2TMEDA$ (**3.3·TMEDA**), $CaC(SiHMe_2)_3HB(C_6F_5)_3THF_2$ (**3.4·THF$_2$**) and $YbC(SiHMe_2)_3HB(C_6F_5)_3THF_2$ (**3.5·THF$_2$**), as well as from density function theory modeling of $Ca\{C(SiHMe_2)_3\}_2THF_2$ (**3.2$_{calc}$·THF$_2$**) and $Yb\{C(SiHMe_2)_3\}_2THF_2$ (**3.3$_{calc}$·THF$_2$**).

Compound	agostic M-C-Si	intermediate M-C-Si	obtuse M-C-Si
$Ca\{C(SiHMe_2)_3\}_2THF_2$ (**3.2·THF$_2$**)	Ca1-C7-Si2 90.7(3)	Ca1-C7-Si3 105.1(3)	Ca1-C7-Si1 108.4(3)
$Ca\{C(SiHMe_2)_3\}_2THF_2$ (**3.2$_{calc}$·THF$_2$**)	90.730	109.358	111.747
$Yb\{C(SiHMe_2)_3\}_2THF_2$ (**3.3·THF$_2$**)	Yb1-C1-Si1 90.6(1)	Yb1-C1-Si3 103.9(2)	Yb1-C1-Si2 108.7(2)
$Yb\{C(SiHMe_2)_3\}_2THF_2$ (**3.3$_{calc}$·THF$_2$**) C_1	92.407 93.037	106.949 108.099	113.896 110.556
$Yb\{C(SiHMe_2)_3\}_2TMEDA$ (**3.3·TMEDA**)	Yb1-C14-Si6 86.2(4)	Yb1-C7-Si1 95.1(5)	Yb1-C7-Si3 120.7(5)
	Yb1-C7-Si2 88.1(4)	Yb1-C14-Si4 102.0(5)	Yb1-C14-Si5 123.3(5)
$CaC(SiHMe_2)_3HB(C_6F_5)_3THF_2$ (**3.4·THF$_2$**)	Ca1-C1-Si3 88.2(1)	Ca1-C1-Si2 88.1(1)	Ca1-C1-Si1 125.2(1)
$YbC(SiHMe_2)_3HB(C_6F_5)_3THF_2$ (**3.5·THF$_2$**)	Yb1-C27-Si1 87.43(9)	Yb1-C27-Si2 87.22(9)	Yb1-C27-Si3 125.3(1)

In **3.3·TMEDA**, the $SiHMe_2$ groups associated with the most acute M-C-Si angles, Yb-C7-Si2 and Yb-C14-Si6, also have small Yb-C-Si-H torsion angles showing that the Yb-C and Si-H bonds are co-planar. In particular, the Yb1-C14-Si6-H6s torsion angle is 3.75°,

and the Yb1-C7-Si2-H2s is 3.31°. The torsion angles for the other Yb-C-Si-H are greater than 20°. Together, short Yb-Si distances and acute Yb-C-Si angles, along with small Yb-C-Si-H torsion angles and short Yb-H distances, provide structural support for two mono-agostic $C(SiHMe_2)_3$ ligands bonded to ytterbium center in **3.3·TMEDA**. Similar features are observed in **3.2·THF$_2$** and **3.3·THF$_2$**.

In fact, comparisons with THF adducts of Ca and Yb reveal that the ytterbium TMEDA adduct contains shorter M-Si distances, even though the ionic radius of six-coordinate Ca(II) (1.00 Å) is 0.02 Å shorter than that of Yb(II) (1.02 Å).[35] For example, the shortest Yb-Si distance in **3.3·TMEDA** is 3.142(4) Å, whereas the shortest M-Si distances in THF adducts are 3.216(2) Å (Ca) and 3.180(1) Å (Yb). Likewise, the most acute M-C-Si angle is found in the ytterbium TMEDA adduct of 86.2(4)° in comparison to the Ca value of 90.7(3)° and Yb angle of 90.6(1)° in the THF adducts. These structural features nicely parallel the trends observed in the IR, where **3.3·TMEDA** contains the lowest energy ν_{SiH}. The M-C distances, however, are long in the TMEDA adduct (Yb-C7, 2.68(1); Yb-C14, 2.67(1) Å). These interatomic distance are longer by ~0.2 Å than those found in the corresponding $C(SiMe_3)_3$ compound $Yb\{C(SiMe_3)_3\}_2$ (2.490(8) and 2.501(9) Å)[16] and even ~0.1 Å longer than in $Yb\{C(SiHMe_2)_3\}_2THF_2$ (2.596(4) Å).

Clearly, the donor ligands THF and TMEDA influence the spectroscopic and structural properties of compounds **3.2** and **3.3**, particularly the characteristics associated with the tris(dimethylsilyl)methyl-metal interaction. We were therefore curious which donor would bind preferentially. Reaction of 1 equiv of TMEDA and **3.2·THF$_2$** in benzene-d_6 quantitatively provides **3.2·TMEDA** and 2 equiv of THF (eq 3.4).

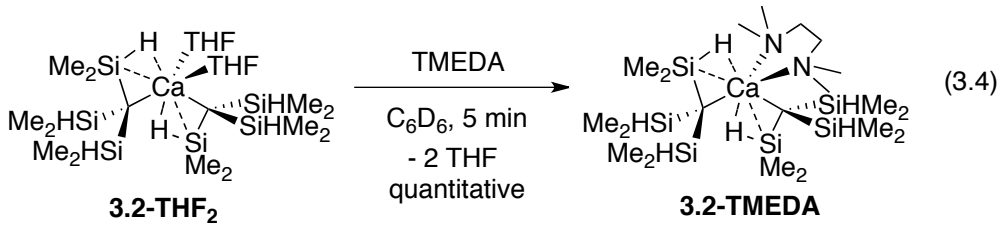

3.2-THF$_2$ **3.2-TMEDA**

In contrast, addition of excess THF (>5 equiv) to **3.3·TMEDA** provides the mixed donor compound {Yb[C(SiHMe$_2$)$_3$]$_2$THF}$_2$TMEDA ({**3.3·THF}$_2$TMEDA**), which is also isolated in quantitative yield (eq 3.5).

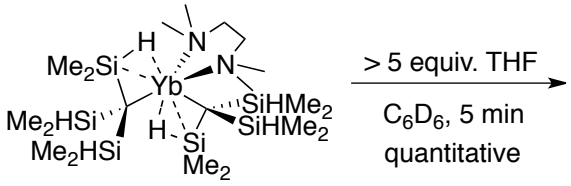

0.5 (Yb(C(SiHMe$_2$)$_3$)$_2$THF)$_2$TMEDA (3.5)

3.3-TMEDA **(3.3-THF)$_2$TMEDA**

The thermal stabilities of **3.3·TMEDA** and **3.3·THF$_2$** were examined to further compare the effects of THF and TMEDA as ligands in these bis(alkyl) divalent metal compounds. Thermolysis of both compounds at 120 °C in benzene-d_6 yields the hydrocarbon HC(SiHMe$_2$)$_3$ as the only ^{1}H NMR spectroscopically active material; however **3.3·TMEDA** is consumed in 6 h, whereas the THF adduct requires 96 h to form HC(SiHMe$_2$)$_3$. The source of the hydrogen *H*C(SiHMe$_2$)$_3$ is unknown. The deuterated solvent is dried and distilled from NaK alloy prior to thermolysis, and the interior surface of a Teflon-sealed J. Young style NMR tube is silylated with CHCl$_3$/Me$_3$SiCl. These compounds are highly air- and moisture sensitive, and benzene-d_6 solutions are 90% decomposed to HC(SiHMe$_2$)$_3$ upon 30 s of air exposure. Their persistence in sealed NMR tubes at room and moderate temperatures (60 °C) argues against adventitious hydrolysis in the high temperature reactions. Thermolysis of **3.3·(THF-*d*$_8$)$_2$** provides HC(SiHMe$_2$)$_3$, ruling out THF as the source of hydrogen. Thermolysis of Yb{C(SiDMe$_2$)$_3$}$_2$THF$_2$ affords HC(SiDMe$_2$)$_3$; this experiment rules out the

silicon-hydride as the source of hydrogen by intramolecular or intermolecular β-hydrogen abstraction. A related decomposition of Cp*La(CH(SiMe$_3$)$_2$)$_2$THF produces H$_2$C(SiMe$_3$)$_2$, in which the proton source is proposed to be the C$_5$Me$_5$ ligand; that is not a possibility in this case.[36]

3.3. Density Functional Theory Calculations of Ca{C(SiHMe$_2$)$_3$}$_2$THF$_2$ and Yb{C(SiHMe$_2$)$_3$}$_2$THF$_2$.

Both Ca{C(SiHMe$_2$)$_3$}$_2$THF$_2$ (**3.2·THF$_2$**) and Yb{C(SiHMe$_2$)$_3$}$_2$THF$_2$ (**3.3·THF$_2$**) were modeled using Density Functional Theory (DFT) employing the B3LYP functional. DFT optimizations were performed for gas-phase species and compared with solid state results to help elucidate the locations of the hydrogens. The calculations also facilitate assignments of infrared bands to particular structural motifs; indeed, the calculations show that the SiH groups with short M-SiH distances also have low energy ν_{SiH} bands. The large size of the compounds limits the methods available for the calculations; X-ray coordinates were used as the starting geometries for optimizations. Our first calculations employed the constraint of C_2 symmetry. C_2-optimized structures contain very small imaginary frequencies in the Hessian calculations (**3.2$_{calc}$·THF$_2$**: –19, –28 cm^{-1}; **3.3$_{calc}$·THF$_2$**: –20, –24, –38 cm^{-1}). These imaginary frequencies correspond to a rotational motion of the SiH(CH$_3$)$_2$ groups around the C-Si bonds that results in breaking of the C_2 symmetry. The Yb complex **3.3$_{calc}$·THF$_2$**, re-optimized without symmetry constraints (C_1 symmetry) to examine the effect of this rotation, retains the imaginary frequencies (–35, –23, and –18 cm^{-1}). Further geometry optimizations were not performed because the magnitudes of the imaginary frequencies are small and the computational cost for these calculations are large. Furthermore, the small magnitude of the imaginary frequencies indicates that this region of the potential energy

surface is relatively flat, thus a structure with a positive definite Hessian is difficult to locate. Also, because the potential energy surface (PES) is relatively flat, the imaginary modes introduce only a small error in the calculated energy. Finally, the C_1-optimized Yb complex and C_2-optimized **3.3$_{calc}$·THF$_2$** have similar ν_{SiH} values, similar Si-H distances, and similar Si-C distances.

Despite these minor difficulties, the optimized gas-phase structures reproduce the general features of the structures obtained from crystallography (see Tables 3.2 and 3.3 for crystallographic and DFT-calculated distances and angles). Each $C(SiHMe_2)_3$ ligand contains one $SiHMe_2$ group with short M-H and M-Si distances and acute M-C-Si angles consistent with a β-agostic SiH. The optimized Ca-C distance of 2.58 Å is shorter than the experimental distance in **3.2·THF$_2$** of 2.616(7) Å (see Table 3.2), whereas the calculated Yb-C distance (2.60 Å) is similar to the experimental distance 2.596(4) Å. The shortest optimized M-Si distances in each molecule are reproduced well for Ca and slightly longer than experiment for Yb (Ca-Si: calc. 3.21, expt. 3.216(2) Å; Yb-Si: calc. 3.27, expt. 3.180(1) Å).

The DFT calculations support a relationship between Si-H and Yb-H distances. The calculation of **3.2$_{calc}$·THF$_2$** clearly shows a long Si-H distance is associated with a short Ca-H distance; likewise **3.3$_{calc}$·THF$_2$** contains long Si-H distances for the hydrogen atoms that have close contacts to the ytterbium center. Furthermore, the calculated vibrational frequencies (see Table 3.1) show that the longest Si-H distances are the moieties with the lowest energy ν_{SiH}. However, the Si-H distances in the X-ray structures are identical within 3σ error. Although **3.3·THF$_2$** contains a seemingly long Si-H distance for the hydrogen that has a short Yb-H distance, that observation may be fortuitous.

Table 3.4. M-H and Si-H distances in **3.2·THF$_2$**, **3.2$_{calc}$·THF$_2$**, **3.3$_{calc}$·THF$_2$** and **3.3$_{calc}$·THF$_2$**.

Compound	Si-H	M-H
3.2·THF$_2$	Si1-H1s: 1.42(6)	Ca1-H1s: 3.37(2)
	Si2-H2s: 1.39(6)	Ca1-H2s: 2.53(7)
	Si3-H3s: 1.46(6)	Ca1-H3s: 3.86(6)
3.2$_{calc}$·THF$_2$ (C_2 symmetry)	1.541	2.562
	1.507	3.936
	1.500	3.744
3.3·THF$_2$	Si1-H1s: 1.48(3)	Yb1-H1s: 2.50(3)
	Si2-H2s: 1.36(4)	Yb2-H2s: 3.56(4)
	Si3-H3s: 1.42(4)	Yb3-H3s: 3.59(4)
3.3$_{calc}$·THF$_2$ (C_1 symmetry)	1.541 and 1.538	2.651 and 2.679
	1.500 and 1.502	3.881 and 3.665
	1.506 and 1.507	3.916 and 3.991
3.3·TMEDA	Si1-H1s: 1.6(1) Si4-H4s: 1.4(1)	Yb1-H1s: 2.9(1) Yb1-H4s: 3.4(1)
	Si2-H2s: 1.5(1) Si6-H6s: 1.6(1)	Yb1-H2s: 2.4(1) Yb1-H6s: 2.5(1)
	Si3-H3s: 1.4(1) Si5-H5s: 1.6(1)	Yb1-H3s: 4.2(1) Yb1-H5s: 4.0(1)

For comparison, in-depth studies of monoagostic and diagostic tetramethyldisilazide compounds of lanthanum, lutetium, yttrium, and scandium reveal ~0.05 Å lengthened Si-H distances.[23d] In computationally-modeled compounds such as $\{H_2Si(C_5H_4)_2\}LaN(SiHMe_2)_2$, the β-diagostic interaction is described as a donor-acceptor pair, with both the Si and H contributing to the donor orbitals and the lanthanum *s* and *d* orbitals as the acceptor.

In the present system, the Kohn-Sham orbitals show that the HOMO and HOMO-1 (-0.1828 and -0.1919 Hartree) are largely centered on the carbon bonded to the calcium center. An Edminston-Ruedenberg energy localization of the orbitals provides a localized orbital picture (the HOMO is shown in Figure 3.3a).[37] The next lower set of orbitals involves bonding from the central carbon to the silicon centers, followed by Si-C bonding to the methyl groups. The Si-H bonding orbitals are still lower in energy. The Kohn-Sham

canonical orbitals corresponding to terminal silicon-hydrogen bonding are grouped by energy in two sets (-0.4790 and -0.4779 Hartree; -0.3147 and -0.3136 Hartree); the Si-H bonds associated with the β-agostic structures are barely stabilized versus the latter set (-0.3231 and -0.3175 Hartree) and significantly higher energy than the former.

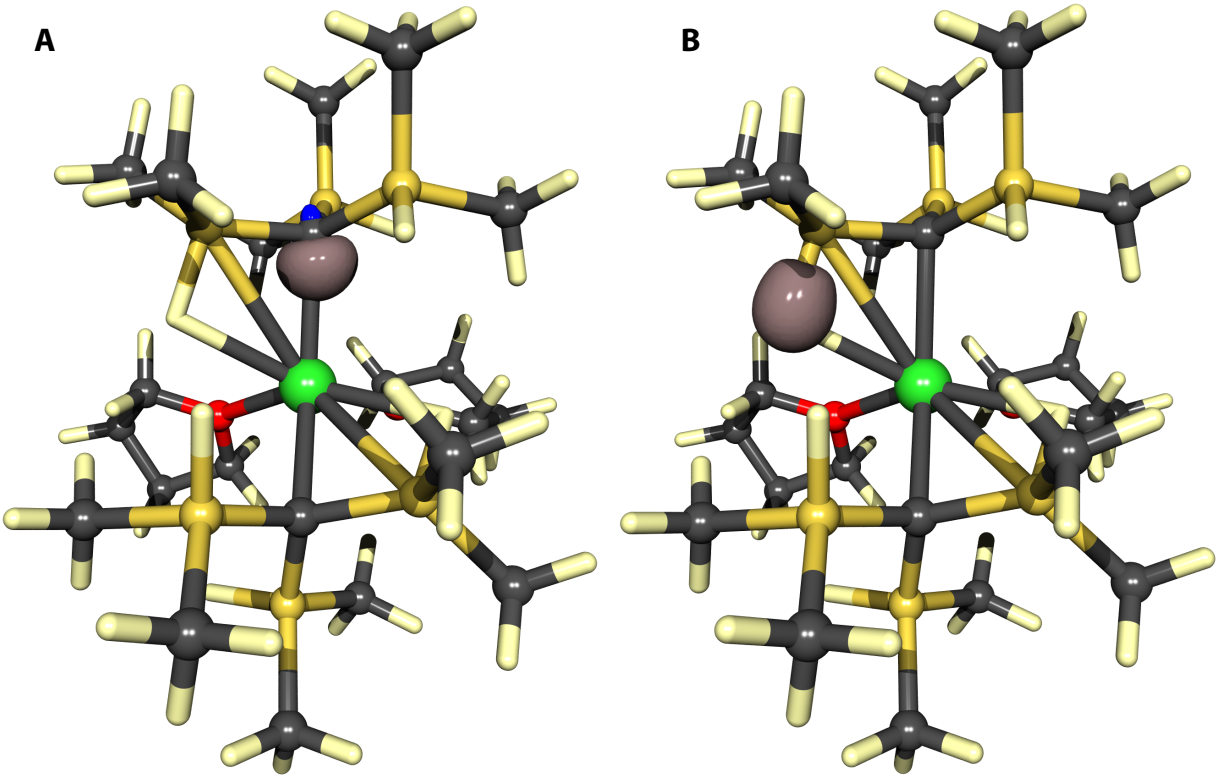

Figure 3.3. Rendered image of localized orbitals of the HOMO (**A**) and occupied Si-H bonding orbital associated with the β-agostic SiH (**B**) are illustrated. Ca, Si, C, O and H are shown as light green, teal, grey, red and white, respectively. The localized orbital is shown in green.

3.4. β-Hydrogen Abstraction Reactions.

Reactions of $M\{C(SiHMe_2)_3\}_2L_2$ and $B(C_6F_5)_3$.

The identity of the organic thermolysis product as $HC(SiHMe_2)_3$ argues against β-hydrogen elimination as the kinetically favored reaction pathway. While β-hydrogen eliminations are notoriously slow for rare earth and main group metal compounds as noted in the introduction, **3.2-3.3·THF$_2$** and **3.2-3.3·TMEDA** contain (presumably) hydridic β-hydrogen bonded to silicon and Lewis acid sites on the metal that might act as intramolecular hydride acceptors via β-elimination or through intermolecular reactions involving β-hydride abstraction. Therefore, reactions of **3.2-3.3·THF$_2$** and **3.2-3.3·TMEDA** with the Lewis acids $B(C_6F_5)_3$, BPh_3, and Me_3SiI were explored to test nucleophilicity of the central carbanion versus the peripheral β-hydrogen.

Reactions of **3.2-3.3·THF$_2$** and $B(C_6F_5)_3$ occur through β-hydrogen abstraction to form $MC(SiHMe_2)_3\{HB(C_6F_5)_3\}THF_2$ (M = Ca (**3.4·THF$_2$**); Yb (**3.5·THF$_2$**)), as previously communicated.[27d] Similarly, the TMEDA adducts and $B(C_6F_5)_3$ react to give $MC(SiHMe_2)_3\{HB(C_6F_5)_3\}$TMEDA (M = Ca (**3.4·TMEDA**); Yb (**3.5·TMEDA**)) and 0.5 equiv of 1,3-disilacyclobutane $\{Me_2Si\text{-}C(SiHMe_2)_2\}_2$, which is the head-to-tail dimer of the silene $Me_2Si{=}C(SiHMe_2)_2$ (eq 3.6).

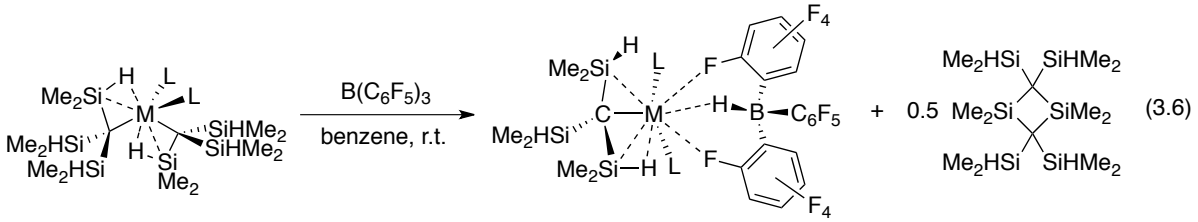

M = Ca, L = THF (**3.2-THF$_2$**)
M = Ca, L$_2$ = TMEDA (**3.2-TMEDA**)
M = Yb, L = THF (**3.3-THF$_2$**)
M = Yb, L$_2$ = TMEDA (**3.3-TMEDA**)

M = Ca, L = THF (**3.4-THF$_2$**)
M = Ca, L$_2$ = TMEDA (**3.4-TMEDA**)
M = Yb, L = THF (**3.5-THF$_2$**)
M = Yb, L$_2$ = TMEDA (**3.5-TMEDA**)

These reactions are best monitored initially by ^{11}B NMR spectroscopy, in which sharp upfield doublet resonances (**3.4·THF$_2$**: –21.3 ppm, $^1J_{BH}$ = 76.2 Hz; **3.4·TMEDA**: –21.8 ppm, $^1J_{BH}$ = 75.0 Hz; **3.5·THF$_2$**: –20.8 ppm, $^1J_{BH}$ = 72.8 Hz; **3.5·TMEDA**: –21.4 ppm, $^1J_{BH}$ = 71.6

Hz) are consistent with formation of an anionic, four-coordinate boron center that is bonded to hydrogen. In the $^{1}H\{^{11}B\}$ NMR spectra, singlets were assigned to the boron hydride (**3.4·THF$_2$**: 2.63 ppm; **3.4·TMEDA**: 2.64 ppm; **3.5·TMEDA**: 3.22 ppm), and cross-peaks in ^{1}H-^{11}B HMQC experiments supported these assignments. The general NMR features of the $C(SiHMe_2)_3$ ligand were similar in **3.4-3.5·THF$_2$** and **3.4-3.5·TMEDA**. In the ^{1}H NMR spectra, upfield doublets (~0.3 ppm, $^{3}J_{SiH}$ ~ 3 Hz) were assigned to methyl groups of the $SiHMe_2$, whereas the SiH multiplets were characterized by signals from 4.4 – 4.6 ($^{1}J_{SiH}$ 145-149 Hz). Table 3.5 lists the SiH resonances and $^{1}J_{SiH}$ coupling constants for the dialkyl compounds and the (alkyl)hydridoborate complexes for comparison. The signals in the zwitterionic compounds are ca. 0.2 ppm upfield in comparison to the dialkyl, and the coupling constants are reduced by ~5 Hz.

Table 3.5. Spectroscopic features of dialkyl and monoalkyl ytterbium and calcium compounds.

Compound	δ SiH	$^{1}J_{SiH}$	Compound	δ SiH	$^{1}J_{SiH}$
3.2·THF$_2$	4.78	152.1	**3.4·THF$_2$**	4.55	148.9
3.3·THF$_2$	4.78	150.4	**3.5·THF$_2$**	4.61	146.4
3.2·TMEDA	4.81	154	**3.4·TMEDA**	4.44	144.9
3.3·TMEDA	4.76	148	**3.5·TMEDA**	4.51	147.0

Interestingly, the trend in the IR spectra is somewhat opposite to that of the NMR, in that the ν_{SiH} bands in the zwitterionic compounds appeared at higher energy relative to their dialkyl precursors (see Table 3.1). Three ν_{SiH} signals were observed in **3.4·THF$_2$** and **3.4-**

3.5·TMEDA, but only two bands were observed for **3.5·THF$_2$**. As in the dialkyl compounds, the lowest energy bands were assigned to the β-agostic SiH. The spectrum for the ytterbium compound **3.5·TMEDA** contained the lowest energy band, and the trend of stretching frequency for the zwitterionic compounds **3.5·TMEDA** < **3.4·TMEDA** ~ **3.5·THF$_2$** < **3.4·THF$_2$** is similar to the dialkyl compounds **3.3·TMEDA** < **3.2·TMEDA** < **3.3·THF$_2$** < **3.2·THF$_2$**.

X-ray quality crystals were obtained for **3.4·THF$_2$** and **3.5·THF$_2$**, and the general structural features and connectivity of these zwitterionic compounds are similar (see Figure 3.4 for the ORTEP diagram of **3.4·THF$_2$**)[27b] Based on the similar structural features of these two crystallographically characterized compounds and the similar overall spectroscopic features for **3.4-3.5·THF$_2$** and **3.4-3.5·TMEDA**, the connectivity of these compounds is assigned as shown in equation 3.6.

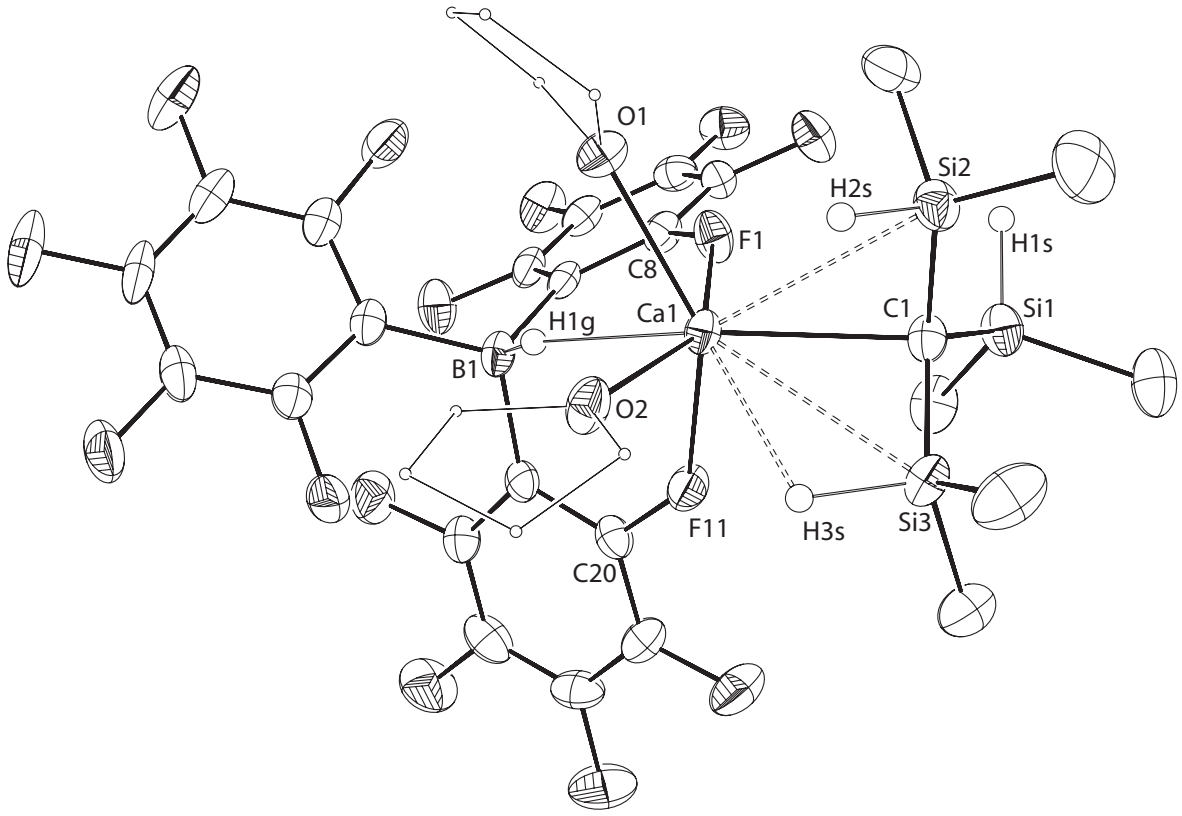

Figure 3.4. ORTEP diagram of $CaC(SiHMe_2)_3\{\kappa^3\text{-H},o\text{-F},o\text{-F-}HB(C_6F_5)_3\}THF_2$ **(3.4·THF$_2$)**. See Tables 3.2, 3.3, and 3.4 for significant interatomic distances and angles.

The solid-state structure of **3.4·THF$_2$** confirms that calcium interacts with one $HB(C_6F_5)_3$ group and one tris(dimethylsilyl)methyl ligand, as well as two THF ligands. The Ca-C distance for **3.4·THF$_2$** (2.566(3) Å) is 0.05 Å shorter than the neutral compound **3.2·THF$_2$** (2.616(7) Å). This contrasts to the pair of Yb analogs, in which the Yb-C distances are identical in the neutral and zwitterionic compounds. Additionally, the zwitterionic nature of **3.4·THF$_2$** affects Ca-Si and Ca-O distances. For example, the Ca1-Si3 distance of 3.097(1) Å (associated with the proposed β-agostic structure) is ~0.1 Å shorter than that of the agostic Ca1-Si2 distance in **3.2·THF$_2$** (3.216(2) Å). The hydrogen bonded to silicon (H3s) was located in the Fourier difference map at the position expected for a roughly tetrahedral silicon

center. That SiH is directed toward the Ca center such that the Ca1-C1-Si3-H3s torsion angle is -3(1)°. Furthermore, a second short calcium-silicon distance (Ca1-Si2 = 3.097(1) Å) is also observed; however in this case, the torsion angle is 37(1)°.

The Ca center is further coordinated by two *ortho*-F atoms from two C_6F_5 groups in a bidentate $HB(C_6F_5)_3$ ligand, with Ca-F distances of 2.412(2) and 2.437(2) Å. The hydrogen bonded to boron was located objectively in the difference Fourier map, and its position is consistent with one expected for a tetrahedral boron center. From this, the H1g-Ca1 distance of 2.45(3) Å is significantly (0.45 Å) longer than the sum of covalent radii of Ca and H (1.99 Å), suggesting that the Ca-H interaction is likely weak. The ν_{BH} in this series of compounds (Table 3.6) also suggested weak M···H···B interaction (see below). A similar structural motif was reported for the coordination of $HB(C_6F_5)_3$ to a samarium(III) center in $Cp^*_2Sm\{\kappa^3$-H,F,F-$HB(C_6F_5)_3\}$.[38] In that compound, the Sm-H distance is 2.45(5) Å, the B-H distance is 1.18(5) Å and the infrared spectrum contains a ν_{BH} band at 2290 cm^{-1}.

Reactions of **3.2-3.3·THF$_2$** and 2 equiv of $B(C_6F_5)_3$ in benzene provide $M\{HB(C_6F_5)_3\}_2THF_2$ (M = Ca (**3.6·THF$_2$**); Yb (**3.7·THF$_2$**)) along with 1 equiv of 1,3-disilacyclobutane $\{Me_2Si\text{-}C(SiHMe_2)_2\}_2$ (eq 3.7). The "dizwitterionic" TMEDA adducts (**3.6·TMEDA**) and (**3.7·TMEDA**) are prepared analogously from **3.2-3.3·TMEDA**. These products are consistent with β-abstraction of one hydrogen from each $C(SiHMe_2)_3$ ligand. Expectedly, the monoalkyl compounds **3.4** and **3.5** react with one equiv of $B(C_6F_5)_3$ to provide **3.6** and **3.7**.

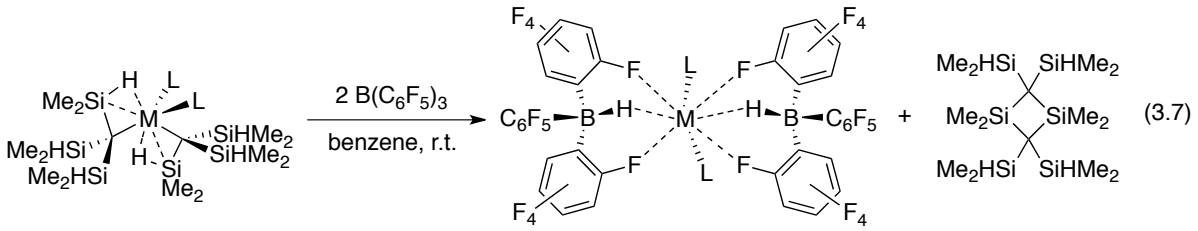

M = Ca, L = THF (**3.2-THF$_2$**)
M = Ca, L_2 = TMEDA (**3.2-TMEDA**)
M = Yb, L = THF (**3.3-THF$_2$**)
M = Yb, L_2 = TMEDA (**3.3-TMEDA**)

M = Ca, L = THF (**3.6-THF$_2$**)
M = Ca, L_2 = TMEDA (**3.6-TMEDA**)
M = Yb, L = THF (**3.7-THF$_2$**)
M = Yb, L_2 = TMEDA (**3.7-TMEDA**)

The TMEDA adducts of **3.6** and **3.7** precipitate from benzene whereas $\{Me_2Si\text{-}C(SiHMe_2)_2\}_2$ is soluble, thus allowing facile separation of products. However, the poor solubility of **3.6-3.7·TMEDA** in aromatic and aliphatic solvents limits solution-phase characterization.

The ν_{BH} stretching frequencies in monoalkyl hydridoborate compounds **3.4-3.5** and bis(hydridoborates) **3.6-3.7** vary from 2293 to 2383 cm^{-1} (Table 3.6). For comparison, the ν_{BH} in $Cp^*_2Sc(\kappa_2\text{-}C_6F_5)BH(C_6F_5)_2$ is 2410 cm^{-1},[39] and in that compound an X-ray structural analysis indicates that the boron-hydride distance is to long to allow a scandium-hydrogen bonding interaction. The ν_{BH} values are generally blue-shifted in the bis(hydridoborate) compounds versus the mono(hydridoborate) compounds. The exception is **3.6·THF$_2$**, in which the ν_{BH} is 21 cm^{-1} lower energy. The variation in the ν_{BH} values suggests that there is some M···H···B interaction in these compounds (which is also suggested by X-ray crystallography). However, the fluxionality of these compounds limits further conclusions on the strength of the interaction.

Table 3.6. Comparison of B-H stretching bands (KBr, cm^{-1}) from IR spectra of mono and bis(hydridoborate) compounds.

$MC(SiHMe_2)_3\{HB(C_6F_5)_3\}L_2$	ν_{BH}	$M\{HB(C_6F_5)_3\}_2L_2$	ν_{BH}
3.4·THF$_2$	2329	**3.6·THF$_2$**	2308
3.5·THF$_2$	2310	**3.7·THF$_2$**	2377
3.4·TMEDA	2302	**3.6·TMEDA**	2383
3.5·TMEDA	2293	**3.7·TMEDA**	2305

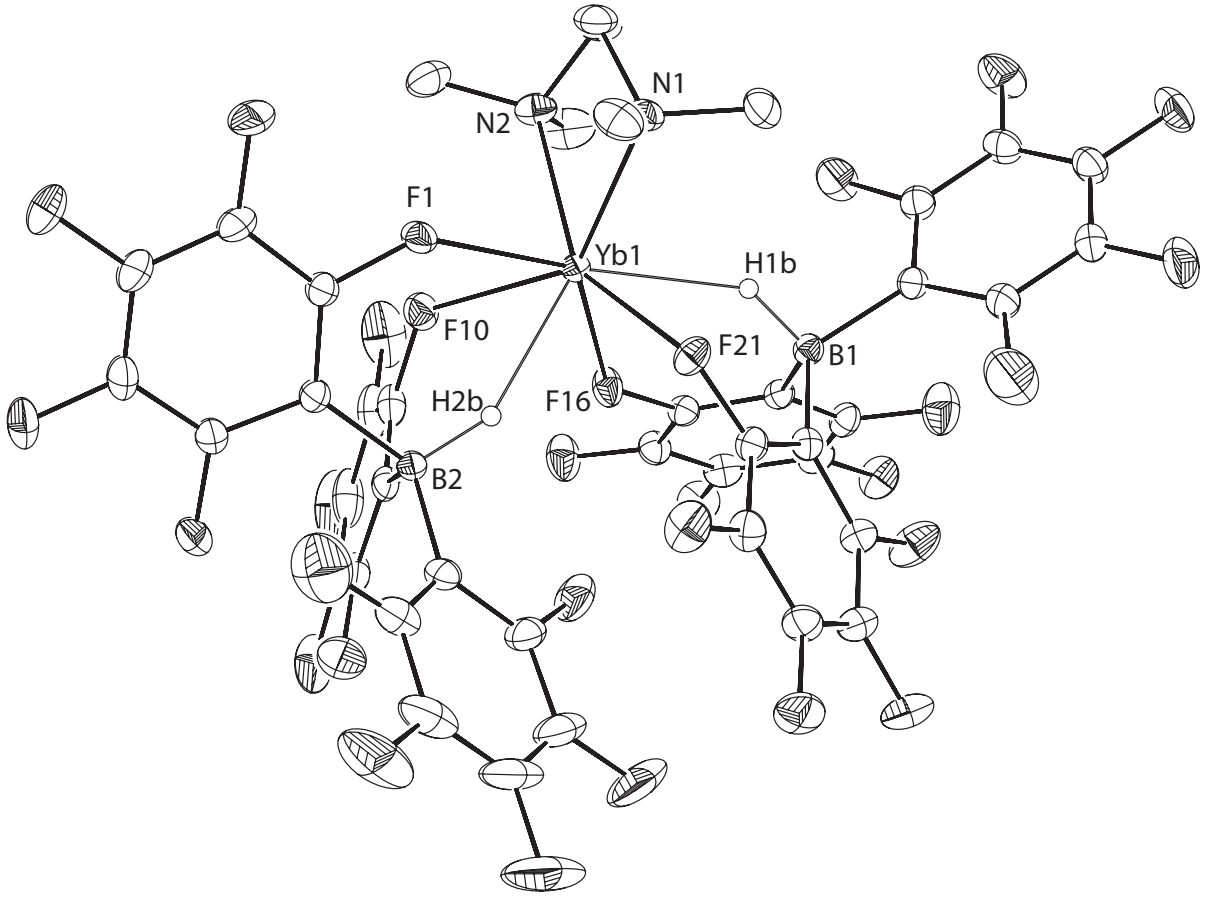

Figure 3.5. ORTEP diagram of Yb{κ^3-HB(C_6F_5)$_3$}$_2$TMEDA (**3.7·TMEDA**). Ellipsoids are plotted at 35% probability, and hydrogen atoms on the TMEDA ligand are not illustrated for clarity.

Both bis(hydridoborate) Yb complexes **3.7·THF$_2$** and **3.7·TMEDA** crystallize from benzene solution. X-ray crystallography reveals that the Yb center is coordinated to four *ortho*-F atoms from four C_6F_5 rings (two from each HB(C_6F_5)$_3$ ligand) as well as a bidentante TMEDA ligand or two THF ligands in the two compounds (Figure 3.5). As in the mono(hydridoborate) structures discussed above, the boron-hydrogen point toward the ytterbium centers. The crystallographically-characterized calcium analog **3.6·THF$_2$** is isostructural with **3.7·THF$_2$**.

The SiH groups in **3.2-3.3·THF$_2$** and **3.2-3.3·TMEDA** have sufficient nucleophilic character to react with the strong Lewis acid B(C_6F_5)$_3$, but the SiH moieties do not react with calcium(II) or ytterbium(II) centers in any of the neutral, cationic, or dicationic compounds **3.2-3.7·THF$_2$** or **3.3-3.7·TMEDA** even though the THF and TMEDA ligands are sufficiently labile to undergo substitution. The only hint of possible β-elimination comes from the thermolysis of **3.4·THF$_2$**, which gives HC($SiHMe_2$)$_3$ and the disilacyclobutane species in a 4:3 ratio after 5 d at 80 °C. Disilacyclobutane could form through a β-elimination process, although dissociation of B(C_6F_5)$_3$ from (Me_2HSi)$_3$CCaHB(C_6F_5)$_3$ followed by β-abstraction is more likely.

Reactions of M{C($SiHMe_2$)$_3$}$_2$L$_2$ and 1 equiv BPh$_3$.

The compounds **3.2-3.3·THF$_2$** and **3.2-3.3·TMEDA** also react with the much weaker Lewis acid BPh_3. This observation is unexpected because, as noted above, the calcium(II) and ytterbium(II) centers in **3.2-3.7** are not sufficient Lewis acids to mediate β-hydrogen elimination or abstraction. The $M(HBPh_3)$ and $MHB(C_6F_5)_3$ products from the abstractions have dissimilar connectivity in the solid state (see below). In addition, BPh_3 abstractions afford a mixture of species whereas $B(C_6F_5)_3$ provides a single product. In addition, the product distributions from reactions of BPh_3 and **3.2-3.3·TMEDA** in comparison to **3.2-3.3·THF$_2$** and BPh_3 are different. For example, **3.3·TMEDA** and BPh_3 react in benzene to give 0.5 equiv of $Yb(HBPh_3)_2TMEDA$ (**3.9·TMEDA**), leaving 0.5 equiv of **3.3·TMEDA** unreacted (eq 3.8). In contrast, **3.2-3.3·THF$_2$** and 1 equiv of BPh_3 react to give a mixture of dialkyl starting material, $MC(SiHMe_2)_3(HBPh_3)(THF)_n$ (**3.10-3.11·THF$_n$**) and $M(HBPh_3)_2THF$ (**3.8-3.9·THF**) in a 1:2:1 ratio, along with disilacyclobutane (eq 3.9).

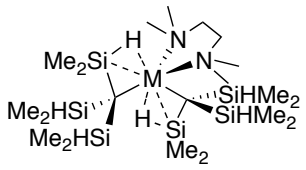

BPh_3, C_6D_6, r.t., 45 min

0.5 $(Me_2Si\text{-}C(SiHMe_2)_2)_2$ + 0.5 $M(HBPh_3)_2TMEDA$ + 0.5 $M(C(SiHMe_2)_3)_2TMEDA$ (3.8)

M = Ca (**3.2-TMEDA**) M = Yb (**3.3-TMEDA**)

M = Ca (**3.8-TMEDA**) M = Yb (**3.9-TMEDA**)

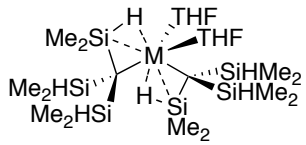

BPh_3, C_6D_6, r.t., 18 h

0.25 $M(C(SiHMe_2)_3)_2THF_2$ + 0.5 $(Me_2Si\text{-}C(SiHMe_2)_2)_2$ + 0.25 $M(HBPh_3)_2THF$ + 0.5 $MC(SiHMe_2)_3(HBPh_3)THF_n$ (3.9)

M = Ca (**3.2-THF$_2$**) M = Yb (**3.3-THF$_2$**)

M = Ca (**3.8-THF**) M = Yb (**3.9-THF**)

M = Ca (**3.10-THF$_n$**) M = Yb (**3.11-THF$_n$**)

The products **3.8-3.9·TMEDA** precipitate or crystallize from the reaction mixtures and are isolated from **3.8-3.9·TMEDA** by filtration. Unfortunately, the compounds **3.8-3.9·TMEDA** are insoluble in pentane, benzene, toluene and THF, precluding characterization in those solvents. In contrast to the IR spectra of the $HB(C_6F_5)_3$ compounds,

the IR spectra of **3.8-3.9·TMEDA** contained four ν_{BH} bands (**3.8·TMEDA**: 2059, 2027, 2008, and 1943 cm^{-1}; **3.9·TMEDA**: 2054, 2024, 2006, and 1940 cm^{-1}). Despite the relatively simple X-ray structure (see below), these signals suggest there are multiple types of M···H···B interactions in these two compounds in the solid state.

X-ray quality crystals of **3.9·TMEDA** are obtained from the reaction mixture, and an X-ray diffraction study confirmed the identity of the product (Figure 3.6).

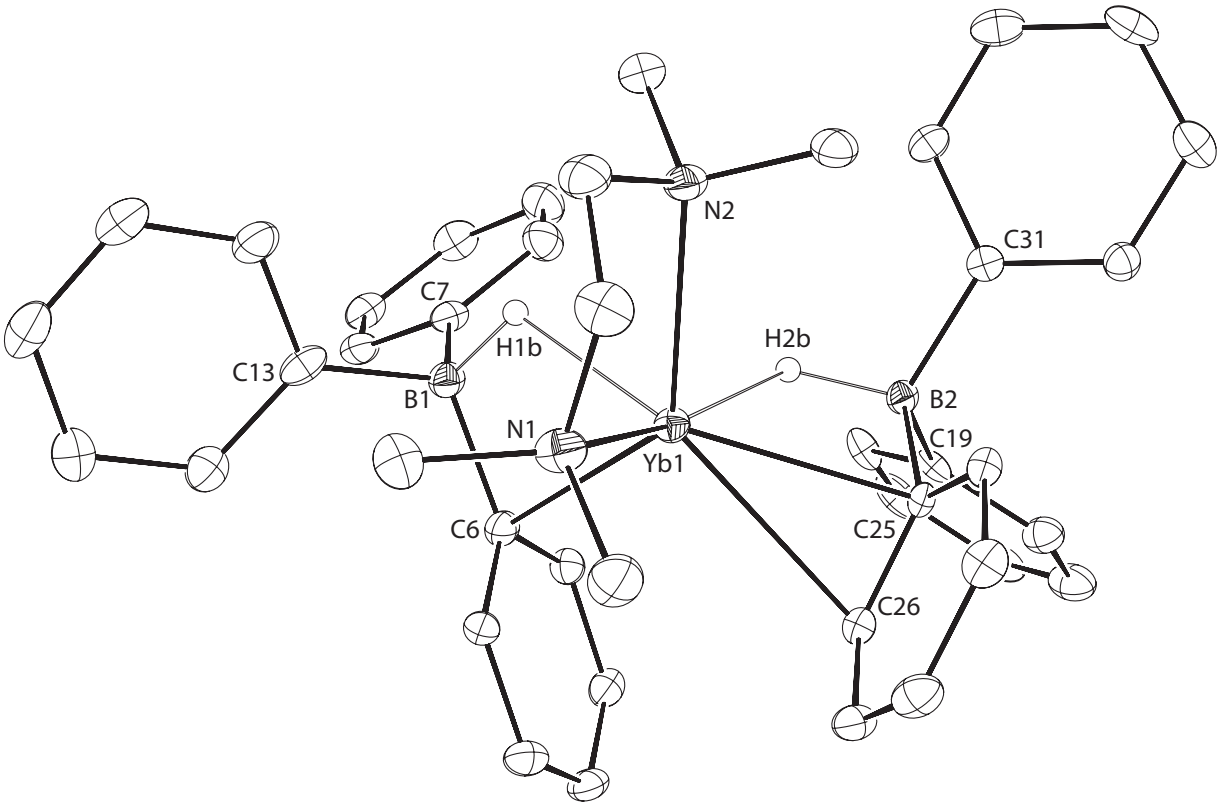

Figure 3.6. ORTEP diagram of $Yb(HBPh_3)_2TMEDA$ (**3.9·TMEDA**). Ellipsoids are plotted at 35% probability, and hydrogen atoms bonded to C_6H_5 and TMEDA groups are not drawn for clarity. Selected interatomic distances (Å): Yb1-H1b, 2.22(5); Yb1-H2b, 2.39(4); Yb1-C6, 2.772(4); Yb1-C25, 2.667(4); Yb1-C26, 2.843(4); B1-H1b, 1.19(5); B2-H2b, 1.22(5);

Yb1-B1, 2.930(5); Yb1-B2, 3.065(4); B1-C6, 1.643(6); B1-C7, 1.621(6); B1-C13, 1.600(6); B2-C19, 1.623(6); B2-C25, 1.648(6); B2-C31, 1.624(6).

The structure of **3.9·TMEDA** contains a bidentate TMEDA ligand and two $HBPh_3$ ligands that have short distances to ytterbium through hydrogen and boron as well as *ipso*- and *ortho*-aryl carbons. Interestingly, the related THF adduct **3.9·THF** contains only one molecule of THF coordinated to ytterbium (Figure 3.7). The $HBPh_3$-ytterbium close interatomic contacts in **3.9·THF** include the H on boron (Yb1-H1b, 2.45(3); Yb1-H2b, 2.22(3) Å), the boron center (Yb1-B1 and Yb1-B2, 2.675(3) Å), and two of the three *ipso*-carbons in each $HBPh_3$ group (Yb1-C6, 2.793(3); Yb1-C18, 2.614(3); Yb1-C24, 2.750(3); Yb1-C36, 2.780(3) Å). Coordination of an anion to BPh_3 tends to lengthen the B-C bonds from 1.58 Å in BPh_3 by 0.05 Å.[40,41,42] This lengthening effect is further enhanced for the phenyl groups of **3.9·TMEDA** and **3.9·THF** in which there is a Yb-C_{ipso} close contact. In **3.9·TMEDA** for example, the pendant phenyl group has a B-C13 distance of 1.600(6) Å, whereas the B-C6 distance for the coordinated phenyl is 1.643(6) Å. Likewise, in **3.9·THF**, coordinated (B2-C36) and non-coordinated (B2-C30) phenyl have distances 1.648(4) and 1.608(4) Å, respectively.

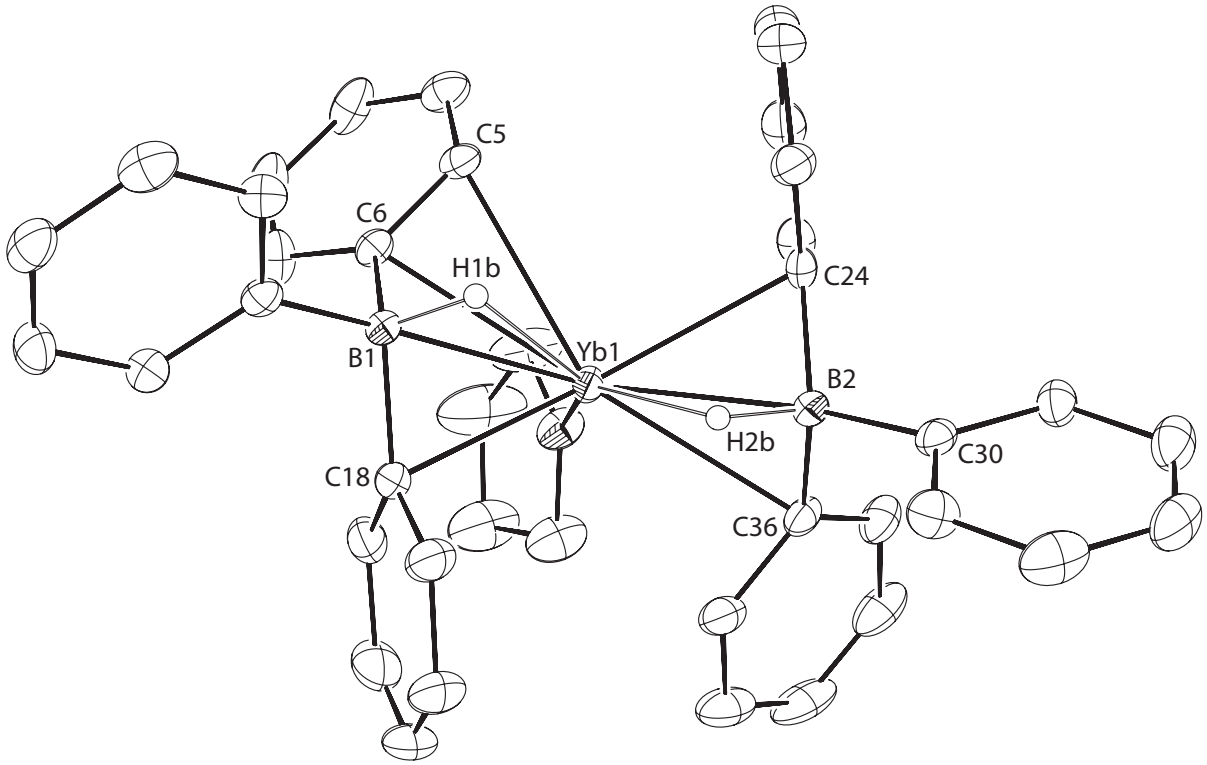

Figure 3.7. ORTEP diagram of $Yb(HBPh_3)_2THF$ (**3.9·THF**). Ellipsoids are plotted at 35% probability, and hydrogen atoms bonded to C_6H_5 and THF groups are not drawn for clarity. Selected interatomic distances (Å): Yb1-H1b, 2.45(3); Yb1-H2b, 2.22(3); Yb1-B1, 2.675(3); Yb1-B2, 2.675(3); Yb1-C5, 2.871(3); Yb1-C6, 2.793(3); Yb1-C18, 2.614(3); Yb1-C24, 2.705(3); Yb1-C36, 2.780(3); B1-C6, 1.642(4).

We know of only two other structurally-characterized compounds that contain the [$HBPh_3$] unit. Reaction of $(C_5H_3t\text{-}Bu_2)_2CeH$ and BPh_3 gives $(C_5H_3t\text{-}Bu_2)_2CeHBPh_3$ which contains a Ce-H-B angle of 139(1)°, a Ce···B distance of 3.423(3) Å, and a B-H distance of 1.26 Å.[42] Additionally, the ruthenium compound $Ru(\eta^6\text{-}C_6H_5)(BHPh_3)(PMe_3)_3$ contains a terminal boron hydrogen; the IR in that case reveals a band at 2270 cm^{-1} assigned to the ν_{BH}.[43]

Additionally, a number of BPh_4^--containing ytterbium(II) and calcium(II) compounds are known,[44] and BPh_4^- is often non-coordinating in these compounds. However, BPh_4^- is known to coordinate to Yb(II) in Yb(η^6-C_6H_5)(η^4-C_6H_5)BPh_2-type structures, where the shortest Yb-C distance is 2.833(3) Å.[45] In Yb{N($SiMe_3$)($SiMe_2CH_2BPh_2$(η^2-C_6H_5)$_2$)}THF_2, short Yb-C_{ipso} distances (2.635(3) and 2.792(3) Å) are similar to the Yb(II)-C distance in **3.9-TMEDA**.[45] Deacon pointed out that these Yb(II)-C_{ipso} distances are in the range observed for bridging Yb-Ph-Yb.[46]

The monoalkyl compounds **3.10-3.11·THF$_n$** are not isolable but are characterized in solution by ^{1}H NMR signals that are distinct from those of the isolable and fully characterized **3.2-3.3·THF$_2$**. In particular, the ^{1}H NMR spectrum of calcium **3.10·THF$_n$** contained resonances at 4.51 ppm ($^1J_{SiH}$ = 152.7 Hz) and 0.41 ppm ($^3J_{HH}$ = 3.5 Hz), assigned to the SiH and $SiMe_2$ groups, respectively.

The species **3.8-3.9·THF** and **3.8-3.9·TMEDA** are independently prepared by the reactions of 2 equiv of BPh_3 and **3.3-3.4·THF$_2$** (eq 3.10). Unlike insoluble **TMEDA** adducts, **3.8-3.9·THF** are soluble in benzene.

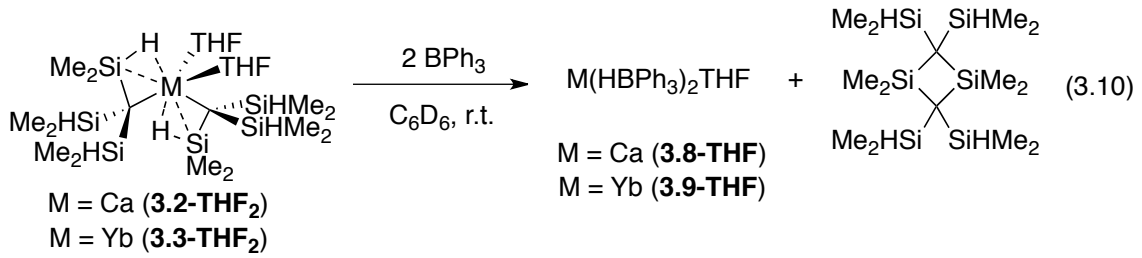

(3.10)

The best procedure to isolate **3.8-3.9·THF** involves evaporation of the reaction mixture followed by pentane washes to remove the 1,3-disilacyclobutane {Me_2Si-C($SiHMe_2$)$_2$}$_2$ by-product. One broad resonance was observed in the ^{11}B NMR spectra of **3.8·THF** (-6.0 ppm), while a broad doublet was detected for **3.9·THF** (-4.0 ppm, $^1J_{BH}$ = 56

Hz). In the $^{1}H\{^{11}B\}$ NMR spectrum, singlet resonances were assigned to the boron hydride (**3.8·THF**: 3.18 ppm; **3.9·THF**: 3.66 ppm), and cross-peaks in ^{1}H-^{11}B HMQC experiments supported these assignments. Two ν_{BH} bands (2021 cm^{-1} and 1936 cm^{-1}) were observed in IR spectrum for **8·THF**, but only one ν_{BH} band (2003 cm^{-1}) was detected for **3.9·THF**.

Reaction of $M\{C(SiHMe_2)_3\}_2L_2$ and Me_3SiI.

As with borane Lewis acids, reactions of **3.2·THF₂** or **3.3·THF₂** and one equiv of Me_3SiI in benzene-d_6 results in β-hydrogen abstraction yielding $HSiMe_3$ and the disilacyclobutane (eq 3.11). The $HSiMe_3$ is characterized by a multiplet at 4.18 ppm and a doublet at 0.01 ppm in ^{1}H NMR spectra of reaction mixtures. Only half of the dialkyl starting material is consumed in the reaction, and a white precipitate is formed that is likely a THF adduct of YbI_2 based on the reaction stoichiometric and the observations for the transformations involving BPh_3.

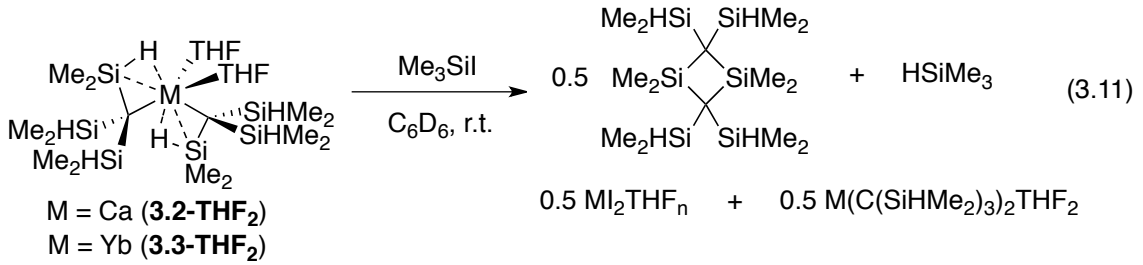

Notably, neither $Me_3Si–C(SiHMe_2)_3$ nor the silylether iodide $Me_3SiO(CH_2)_4I$ product from THF ring opening are formed in these reactions. Alternatively, $Cp^*La\{CH(SiMe_3)_2\}_2THF$ and Me_3SiI were reported to react to give $Me_3SiO(CH_2)_4I$ and $Cp^*La\{CH(SiMe_3)_2\}_2$.[36] The observation of $HSiMe_3$ and disilacyclobutane indicates that

Me_3SiI reacts with the β-H rather than the carbanion $C(SiHMe_3)_3$ through β-H abstraction, similar to reactions with boron-based Lewis acids.

Interestingly, the reaction of Me_3SiI and **3.2-3.3·TMEDA** provides $Me_3Si–C(SiHMe_2)_3$ as the major organic product (eq 3.12). $HSiMe_3$ and the disilacyclobutane $\{Me_2Si\text{-}C(SiHMe_2)_2\}_2$ are formed as minor products (5:2:1), as determined by integration of ^1H NMR spectra of reaction mixtures. Again, an insoluble white precipitate is formed (likely MI_2) and only half of the dialkyl starting material is consumed.

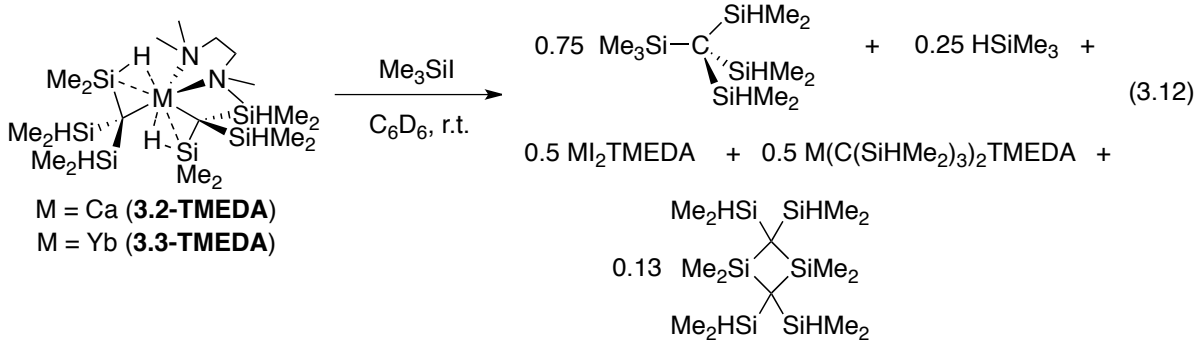

(3.12)

Thus, the central carbon of the $-C(SiHMe_2)_3$ ligands in the TMEDA adducts are accessible for interaction with Me_3SiI. In the ytterbium case, TMEDA adduct contained shorter Yb-Si distances and a longer Yb-C distance than the corresponding THF adducts. Furthermore, the lowest energy ν_{SiH} bands were observed with **3.3·TMEDA** in comparison to **3.2-3.3·THF$_2$**. However, **3.2·TMEDA** also gives Si-C bond formation, even through that compound contains similar distances and spectroscopic features to the THF adducts.

Reaction of $KC(SiHMe_2)_3$ and $B(C_6F_5)_3$.

The bonding interactions between the tris(dimethylsilyl)methyl ligand and calcium(II) or ytterbium(II) have significant polarity. The potassium compound **1** is also highly polar,

and its reactions with $B(C_6F_5)_3$ and Me_3SiI were investigated for comparison with the calcium and ytterbium compounds.

β-Hydrogen abstraction readily occurs in the reaction of $B(C_6F_5)_3$ and $KC(SiHMe_2)_3$ to yield a benzene-insoluble pink solid $KHB(C_6F_5)_3$ (**3.13**) and disilacyclobutane $\{Me_2Si\text{-}C(SiHMe_2)_2\}_2$ (eq 3.13). The product readily dissolves in THF, and **3.13** was characterized in that solvent. Resonances at 3.71 ppm and -27.3 ppm ($^1J_{BH}$ = 93 Hz) in the $^1H\{^{11}B\}$ and ^{11}B NMR spectra were assigned to the hydrogen bonded to boron and the boron center, respectively, and these data are consistent with a hydridoborate moiety. In the IR spectrum, a peak at 2382 cm^{-1} was detected that is similar to the boron-hydrogen stretching frequencies in the calcium and ytterbium hydridoborate compounds described above.

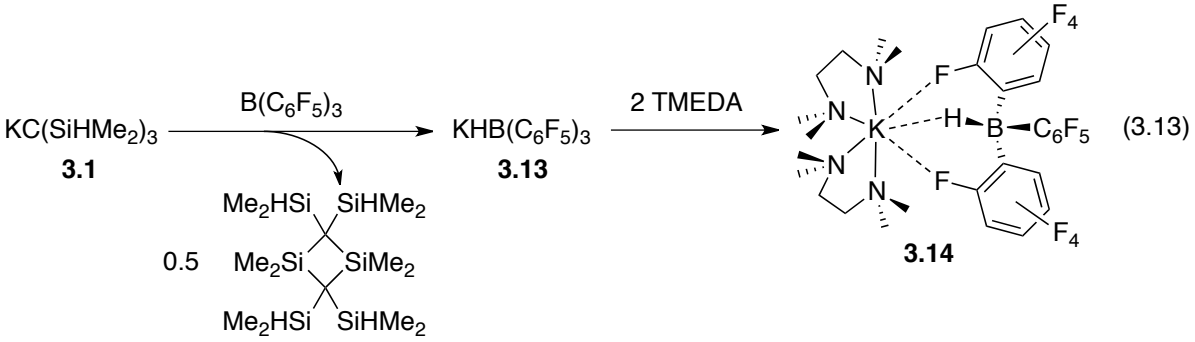

(3.13)

Furthermore, reaction of $KHB(C_6F_5)_3$ and 2 equiv of TMEDA provides the monomeric species $KHB(C_6F_5)_3TMEDA_2$ (**3.13·TMEDA$_2$**). The TMEDA ligand gives solubility to the potassium salt allowing characterization in benzene-d_6. The β-SiH abstraction product is evident as ^{11}B NMR spectrum revealed a doublet resonance at -24.7 ppm ($^1J_{BH}$ = 85 Hz), while the hydrogen bonded to boron was assigned to a resonance at 3.46 ppm in ^1H NMR spectrum. The ν_{BH} band at 2381 cm^{-1} is almost identical to the TMEDA-free

3.13. The monomeric nature of **3.13·TMEDA$_2$** in the solid state is unambiguously demonstrated by an X-ray crystallographic structure determination (Figure 3.8).

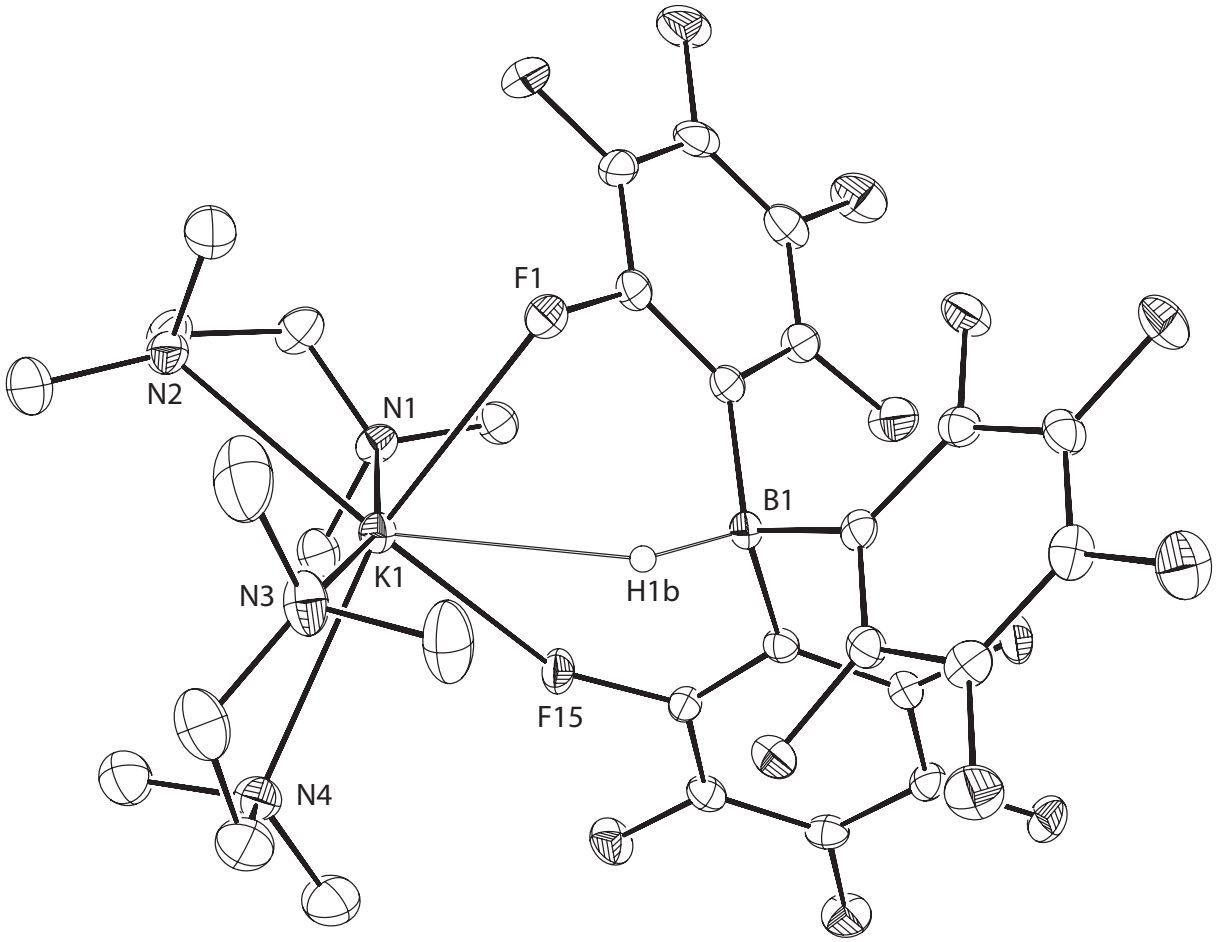

Figure 3.8. ORTEP diagram of K{HB(C_6F_5)$_3$}TMEDA$_2$ (**3.13·TMEDA$_2$**). Ellipsoids are plotted at 35% probability, and hydrogen atoms on the TMEDA ligands are not illustrated for clarity.

The K center is coordinated to two *ortho*-F from the two C_6F_5 rings to form a zwitterionic complex. The structural features of the metal-hydridoperfluorophenylborate interaction to ytterbium, calcium and potassium are similar in dicationic **3.7·TMEDA**, monoalkyl **3.5·THF$_2$**, and **3.13·TMEDA$_2$**. Thus, the reactivity of B(C_6F_5)$_3$ and ionic

tris(dimethylsilyl)methyl metal compounds involves abstraction of β-hydrogen to give the κ^3-$HB(C_6F_5)_3M$ compounds.

Because the ytterbium compound **3.3·TMEDA** and the lithium alkyl $LiC(SiHMe_2)_3$ provide silicon-carbon bond formation upon reaction with Me_3SiCl,[26] and $KC(SiHMe_2)_3$ reacts with MI_2 to give M-C bond formations, the reaction of the potassium alkyl and Me_3SiI was investigated. However, the reaction of $KC(SiHMe_2)_3$ and Me_3SiI gives $HSiMe_3$ and disilacyclobutane as the soluble products; $Me_3Si–C(SiHMe_2)_3$ is not formed.

Conclusion

The β-hydrogen in the tris(dimethylsilyl)methide ligand influences the reaction pathways in reactions of its organometallic compounds with Lewis acids. Two pathways have been observed: β-hydrogen abstraction and ligand group transfer. The favored pathway depends strongly on the identity of the Lewis acid center, but it is also influenced by ancillary ligands and the metal center(s) involved. Thus, reactions of $KC(SiHMe_2)_3$ and MI_2 salts (M = Ca, Yb) result in ligand transfer through salt metathesis. $M\{C(SiHMe_2)_3\}_2TMEDA$ and Me_3SiI give a mixture of alkylation and β-hydrogen abstraction, whereas $M\{C(SiHMe_2)_3\}_2THF_2$ and Me_3SiI react solely through the β-abstraction pathway. Borane electrophiles, such as $B(C_6F_5)_3$ and BPh_3, react with the SiH. The alkylation pathways appear most facile when the partners are sterically less hindered (i.e., MI_2 salts), and β-hydrogen abstraction occurs with bulky Lewis acids (i.e., $B(C_6F_5)_3$). Recently, we have observed a similar effect in the reactions of β-hydrogen containing silazides such as $LiN(SiHMe_2)_2$ and $LiN(SiHMe_2)$*t*-Bu with zirconium halides, where the

sterically most hindered reaction partners give zirconium hydride products rather than silazido zirconium species.[47]

There are similarities between these intermolecular abstraction reactions and intramolecular β-elimination: both form metal-hydrides and both result in the expulsion of an unsaturated organic fragment from the metal alkyl. In the current transformations, a calcium or ytterbium hydridoborate are the products, and dissociation of $B(Aryl)_3$ from the M-H-$B(Aryl)_3$ species would provide a metal hydride, to give final products equivalent with intramolecular β-elimination. Furthermore, it is worth noting that the $B(C_6F_5)_3$ and BPh_3 Lewis acids provide the needed empty orbital that is apparently not present in the calcium or ytterbium alkyl compounds that would allow intramolecular β-elimination or a bimolecular β-abstraction. Considering these points, this abstraction of a β-hydrogen by an external Lewis acid can also be described as a Lewis acid mediated β-hydrogen elimination (Scheme 3.2).

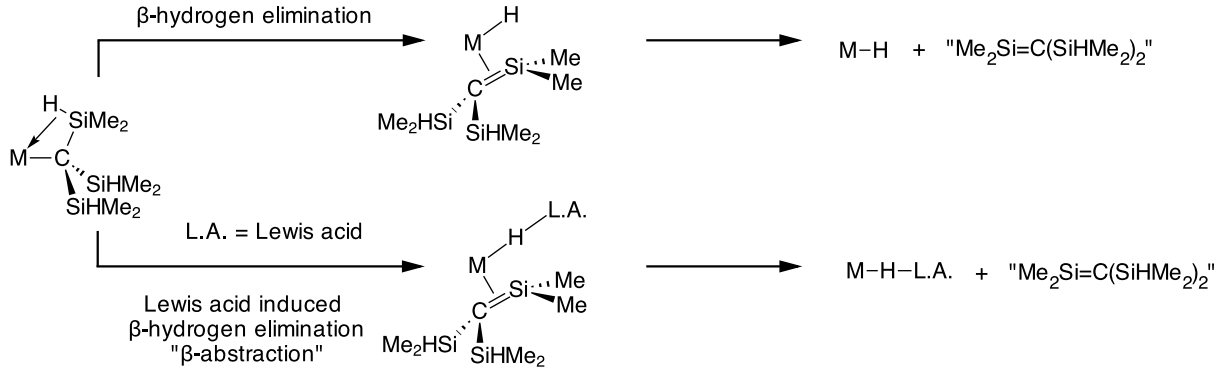

Scheme 3.2. β-hydrogen elimination and intermolecular β-abstraction.

Thus, structural models for intermediates in these β-abstraction reactions are important for understanding the reaction pathway. Intramolecular three-center-two-electron

interactions between β-CH bond and metal centers (i.e., β-agostic interactions) are proposed to provide insight into the pathway for β-elimination and its microscopic reverse, olefin insertion. As noted in the introduction, these abstraction reactions have similar features to intramolecular elimination reactions, as they provide metal hydride and unsaturated organic products. Thus, it is interesting to consider the role of the β-agostic interactions in the potassium, calcium, and ytterbium tris(dimethylsilyl)methyl compounds on the intermolecular β-abstraction reaction. The bridging Si-H groups in the dimeric potassium compound $\{KC(SiHMe_2)_3TMEDA\}_2$, where a third SiH group approaches a potassium center in a side-on β-agostic type interaction, provides a structural model for an arrested intermolecular β-hydrogen abstraction. The "intramolecular" β-agostic interaction in this structure does not interact with the second potassium center, and this may suggest that the reactions of Lewis acids with the ytterbium and calcium alkyl compounds involve abstraction of the terminal SiH groups, rather than the SiH's involved in three-center-two-electron bonding. The presence of the intramolecular silicon-hydrogen-calcium close contacts in this structure, however, may be significant, either for increasing the nucleophilicity of the remaining SiH groups or simply as a spectroscopic and structural marker that shows significant nucleophilic character of all the SiH groups in these hydrosilylalkyl ligands.

Experimental

General Procedures. All reactions were performed under a dry argon atmosphere using standard Schlenk techniques, or under a nitrogen atmosphere in a glovebox unless otherwise indicated. Dry, oxygen-free solvents were used throughout. Benzene, toluene, pentane, and

tetrahydrofuran were degassed by sparging with nitrogen, filtered through activated alumina columns, and stored under N_2. Benzene-d_6, toluene-d_8, THF-d_8 were vacuum transferred from Na/K alloy and stored under N_2 in the glovebox. Anhydrous CaI_2 was purchased from Aldrich and used as received. All organic reagents were purchased from Aldrich. Anhydrous YbI_2,[48] $B(C_6F_5)_3$,[49] and $HC(SiHMe_2)_3$[25a] were prepared as described in literature procedures. We previously reported the following compounds in the supporting information of references 27 in initially communicated work: $KC(SiHMe_2)_3$ (**3.1**), $Ca\{C(SiHMe_2)_3\}_2THF_2$ (**3.2·THF$_2$**), $Yb\{C(SiHMe_2)_3\}_2THF_2$ (**3.3·THF$_2$**), $CaC(SiHMe_2)_3\{HB(C_6F_5)_3\}THF_2$ (**3.4·THF$_2$**), $YbC(SiHMe_2)_3\{HB(C_6F_5)_3\}THF_2$ (**3.5·THF$_2$**), $Ca\{HB(C_6F_5)_3\}_2THF_2$ (**3.6·THF$_2$**), $Yb\{HB(C_6F_5)_3\}_2THF_2$ (**3.7·THF$_2$**), and $Yb(HBPh_3)_2THF$ (**3.9·THF**). 1,1,3,3-tetramethyl-2,2,4,4-tetrakis(dimethylsilyl)-1,3-disilacyclobutane was identified by comparison with literature values[26] and X-ray crystallography (see SI). ^1H, $^{13}C\{^1H\}$, ^{11}B, ^{19}F, and ^{29}SI NMR spectra were collected on Agilent MR-400, Bruker DRX-400, or Bruker AVIII 600, Bruker AVII 700 spectrometers. ^{15}N chemical shifts were determined by ^1H-^{15}N HMBC experiments on a Bruker AVII 600 spectrometer with a Bruker Z-gradient inverse TXI $^1H/^{13}C/^{15}N$ 5mm cryoprobe; ^{15}N chemical shifts were originally referenced to an external liquid NH_3 standard and recalculated to the CH_3NO_2 chemical shift scale by adding -381.9 ppm. $^{29}Si\{^1H\}$ NMR spectra were recorded using DEPT experiments, and assigments were verified by ^1H COESY, ^1H-^{13}C HMQC, ^1H-^{13}C HMBC, and ^1H-^{29}Si HMBC experiments. UV-vis spectral data were measured on a Shimadzu 3101 PC spectrophotometer. Elemental analysis was performed using a Perkin-Elmer 2400 Series II CHN/S by the Iowa State Chemical Instrumentation Facility.

Computational Details. All electronic structure calculations were performed with the NWChem computational chemistry software suite.[50] The 6-311++G** basis set was used for H, C, N, O, and Ca.[51] The small core Stuttgart relativistic effective core potential (RECP) and associated basis set was used for Yb,[52] and the large core Stuttgart RECP and associated basis set was used for Si.[53] Density functional theory with the B3LYP[54] functional was used for both the geometry optimizations and the Hessian (frequency) calculations. The vibrational frequencies were calculated with the harmonic oscillator approximation. C_1 and C_2 symmetries were used in the geometry optimization calculations.

$HC(SiDMe_2)_3$. Lithium aluminum deuteride (1.548 g, 36.88 mmol) was suspended in diethyl ether (50 mL) in a 100 mL Schlenk flask, and the reaction vessel was cooled to 0 °C. A diethyl ether solution (20 mL) of $HC(SiBrMe_2)_3$ (5.249 g, 12.29 mmol) was added slowly. After the addition, the reaction mixture was stirred at room temperature for 12 h and then heated to reflux for 2.5 h. Saturated ammonium chloride solution (15 mL) was added slowly at 0 °C to quench the reaction mixture. The resulting mixture was filtered to remove insoluble salts. The organic phase was separated and washed with water (2 × 10 mL) and brine (1 × 10 mL) and dried with anhydrous sodium sulfate. Evaporation of diethyl ether provided $HC(SiDMe_2)_3$ as a spectroscopically pure colorless oil (2.252 g, 11.6 mmol, 94.7%). ^{2}H NMR ($CDCl_3$, 93.0 MHz, 25 °C): δ 4.15 (br s, SiD).

Tris(dimethylsilyl)methylpotassium-d_3. $KC(SiDMe_2)_3$ (3.1-d_3). The procedure for the synthesis of $KC(SiHMe_2)_3$ was followed:[27] THF (30 mL) was added to a mixture of $HC(SiDMe_2)_3$ (1.841 g, 9.51 mmol) and KCH_2Ph (1.239 g, 9.51 mmol) in a 100 mL Schlenk flask. The dark red mixture was stirred at room temperature for 12 h, and all volatile materials were removed under reduced pressure. The resulting reddish brown gummy solid

was dissolved in minimal amount of toluene and cooled to -30 °C to afford $KC(SiDMe_2)_3$ (1.910 g, 8.25 mmol, 86.7%) as red needles. ^{2}H NMR (benzene-H_6, 93.0 MHz, 25 °C): δ 4.59 (br s, SiD). IR (KBr, cm^{-1}): 1532 (ν_{SiD}), 1417 (ν_{SiD}).

{KC(SiHMe$_2$)$_3$TMEDA}$_2$ {3.1·TMEDA}$_2$. Excess TMEDA (0.35 mL, 2.33 mmol) was added to $KC(SiHMe_2)_3$ (0.175 g, 0.77 mol) dissolved in benzene. The red mixture was stirred for 30 min at room temperature. The volatiles were evaporated under reduced pressure, and the resulting gummy solid was extracted with pentane (10 mL). The pentane extract was concentrated and cooled to -30 °C for recrystallization to obtain yellow needles of $\{KC(SiHMe_2)_3TMEDA\}_2$ {**3.1·TMEDA**}$_2$. (0.093 g, 0.271 mmol, 35.2%). ^{1}H NMR (benzene-d_6, 400 MHz, 25 °C): δ 4.80 (m, 3 H, $^1J_{SiH}$ = 154 Hz, SiH), 1.78 (s, 4 H, NCH_2), 1.74 (s, 12 H, NMe_2), 0.52 (d, 18 H, $^3J_{HH}$ = 3.5 Hz, $SiMe_2$). $^{13}C\{^1H\}$ NMR (benzene-d_6, 100 MHz, 25 °C): δ 57.33 (CH_2), 45.68 (NCH_3), 14.69 (KC), 5.33 ($SiCH_3$). $^{29}Si\{^1H\}$ NMR (benzene-d_6, 79.5 MHz, 25 °C): δ -23.7 (*Si*HMe_2). IR (KBr, cm^{-1}): 2946 s, 2828 m, 2105 m (ν_{SiH}), 2035 m br (ν_{SiH}), 1962 m (ν_{SiH}), 1580 w, 1469 m, 1361 w, 1296 w, 1250 s, 1154 w, 1000 s br, 895 s, 781 s, 699 w, 665 w. Anal. Calcd for $C_{13}H_{37}KSi_3N_2$: C, 45.28; H, 10.82; N, 8.12. Found: C, 44.95; H, 11.32; N, 7.28. Mp 47-53 °C.

{KC(SiDMe$_2$)$_3$TMEDA}$_2$ {3.1-*d*$_3$·TMEDA}$_2$. The procedure for $\{KC(SiHMe_2)_3TMEDA\}_2$ was followed, using $KC(SiDMe_2)_3$ (0.168 g, 0.724 mmol) and TMEDA (0.33 mL, 2.18 mmol) to give $KC(SiDMe_2)_3$(TMEDA) (0.144 g, 0.414 mmol, 57.5%). ^{2}H NMR (benzene-H_6, 93.0 MHz, 25 °C): δ 4.83 (br s, SiD). IR (KBr, cm^{-1}): 1533 (ν_{SiD}), 1462 (ν_{SiD}), 1414 (ν_{SiD}).

Ca{C(SiHMe$_2$)$_3$}$_2$TMEDA (3.2·TMEDA). CaI_2 (0.384 g, 1.31 mmol) and $KC(SiHMe_2)_3$ (0.598 g, 2.62 mmol) were suspended in benzene (10 mL), and TMEDA (0.39 mL, 2.62 mmol) was added. The mixture was allowed to stir at room temperature for 12 h. Evaporation of the benzene, extraction of the residue with pentane (2 × 10 mL), concentration in vacuo, and cooling to -30 °C overnight provided yellow crystals of Ca{C(SiHMe$_2$)$_3$}$_2$TMEDA (**3.2·TMEDA**) (0.166 g, 0.310 mmol, 23.7%). Alternatively, **3.2·TMEDA** can be prepared from CaI_2 (0.165 g, 0.562 mmol) and **3.1·TMEDA** (0.388 g, 1.124 mmol) in benzene (10 mL); stirring for 12 h followed by identical workup gave 51.7% yield (0.156 g, 0.291 mmol). ^{1}H NMR (benzene-d_6, 600 MHz, 25 °C): δ 4.81 (m, 3 H, $^1J_{SiH}$ = 154 Hz, Si*H*Me$_2$), 1.80 (s, 12 H, NCH_3), 1.76 (s, 4 H, NCH_2), 0.53 (d, 18 H, $^3J_{HH}$ = 3.3 Hz, $SiCH_3$). ^{13}C{^{1}H} NMR (benzene-d_6, 150 MHz, 25 °C): δ 57.3 (NCH_2), 45.7 (NCH_3), 5.34 ($^1J_{SiC}$ = 47 Hz, $SiCH_3$), 2.48 (CaC). ^{29}Si{^{1}H} NMR (benzene-d_6, 119.3 MHz, 25 °C): δ -23.6 (SiHMe$_2$). IR (KBr, cm^{-1}): 2949 s br, 2896 s br, 2828 m, 2105 m br (ν_{SiH}), 2038 m br (ν_{SiH}), 1861 m br (ν_{SiH}), 1599 w, 1468 s, 1297 m, 1249 s, 942 s br, 889 s br, 836 s br, 775 s, 670 s. Anal. Calcd for $C_{20}H_{58}Si_6N_2Ca$: C, 44.88; H, 10.92; N, 5.23. Found: C, 44.77; H, 10.83; N, 5.23. Mp 138-140 °C.

Ca{C(SiDMe$_2$)$_3$}$_2$THF$_2$ (3.2-*d*$_6$·THF$_2$). The procedure was similar to the one for the preparation of Ca{C(SiHMe$_2$)$_3$}$_2$THF$_2$,[27b] using CaI_2 (0.157 g, 0.535 mmol) and $KC(SiDMe_2)_3$ (0.248 g, 1.07 mmol) to give Ca{C(SiDMe$_2$)$_3$}$_2$THF$_2$ (0.205 g, 0.360 mmol, 67.4%). ^{2}H NMR (benzene-H$_6$, 93.0 MHz, 25 °C): δ 4.71 (br s, SiD). IR (KBr, cm^{-1}): 1530 (ν_{SiD}), 1493 (ν_{SiD}), 1409 (ν_{SiD}).

Yb{C(SiDMe$_2$)$_3$}$_2$THF$_2$ (3.3-*d*$_6$·THF$_2$). The procedure was similar to the one for Yb{C(SiHMe$_2$)$_3$}$_2$THF$_2$,[27b] using YbI_2 (0.145 g, 0.340 mmol) and $KC(SiDMe_2)_3$ (0.158 g,

0.680 mmol) to give $Yb\{C(SiDMe_2)_3\}_2THF_2$ (0.163 g, 0.234 mmol, 68.9%). ^2H NMR (benzene-H_6, 93.0 MHz, 25 °C): δ 4.77 (br s, SiD). IR (KBr, cm^{-1}): 1506 (ν_{SiD}), 1492 (ν_{SiD}), 1410 (ν_{SiD}).

$Ca\{C(SiDMe_2)_3\}_2$TMEDA (3.2-d_6·TMEDA). The procedure was similar to that for $Ca\{C(SiHMe_2)_3\}_2$TMEDA using CaI_2 (0.143 g, 0.485 mmol), $KC(SiDMe_2)_3$ (0.225 g, 0.970 mmol), and TMEDA (0.15 mL, 0.970 mmol) to give $Ca\{C(SiDMe_2)_3\}_2$TMEDA (0.232 g, 0.434 mmol, 89.4%). ^2H NMR (benzene-H_6, 93.0 MHz, 25 °C): δ 4.71 (br s, SiD). IR (KBr, cm^{-1}): 1510 sh (ν_{SiD}), 1493 (ν_{SiD}), 1411 (ν_{SiD}).

$Yb\{C(SiHMe_2)_3\}_2$TMEDA (3.3·TMEDA). A mixture of $KC(SiHMe_2)_3$ (0.580 g, 2.54 mmol) and YbI_2 (0.542 g, 1.27 mmol) in benzene was allowed to react in the presence of TMEDA (0.38 mL, 2.5 mmol). A similar workup procedure as described above for **3.2·TMEDA** provided a deep red pentane extract; crystallization at -30 °C afforded red crystals of $Yb\{C(SiHMe_2)_3\}_2$TMEDA (**3.3·TMEDA**) (0.253 g, 0.379 mmol, 29.8%). **3.3·TMEDA** can also be prepared from YbI_2 (0.339 g, 0.795 mmol) and **3.1·TMEDA** (0.548 g, 1.590 mmol) in improved yield 70.5% (0.375 g, 0.560 mmol). ^1H NMR (benzene-d_6, 600 MHz, 25 °C): δ 4.76 (m, 3 H, $^1J_{SiH}$ = 148 Hz, Si*H*Me_2), 1.99 (s, 12 H, NMe), 1.72 (s, 4 H, NCH_2), 0.492 (d, 18 H, $^3J_{HH}$ = 2.8 Hz, $SiMe_2$). $^{13}C\{^1H\}$ NMR (benzene-d_6, 150 MHz, 25 °C): δ 57.38 (NCH_2), 47.11 (NMe), 11.94 (YbC), 4.82 ($^1J_{SiC}$ = 50 Hz, $SiMe_2$). $^{29}Si\{^1H\}$ NMR (benzene-d_6, 119.3 MHz, 25 °C): δ -17.9 (*Si*HMe_2, J_{YbSi} = 9.1 Hz). IR (KBr, cm^{-1}): 2949 s br, 2895 s br, 2843 m, 2802 m, 2080 s br (ν_{SiH}), 2038 s br (ν_{SiH}), 1846 s br (ν_{SiH}), 1584 w, 1468 s, 1248 s, 1029 s, 938 s br, 884 s br, 835 s br, 773 s, 670 s. Anal. Calcd for $C_{20}H_{58}Si_6N_2Yb$: C, 35.95; H, 8.75; N, 4.19. Found: C, 35.81; H, 8.74; N, 4.42. Mp 90-95 °C.

Yb{C(SiDMe$_2$)$_3$}$_2$TMEDA (3.3-d_6·TMEDA). The procedure was similar to the one for Yb{C(SiHMe$_2$)$_3$}$_2$TMEDA using YbI_2 (0.143 g, 0.335 mmol), KC(SiDMe$_2$)$_3$ (0.155 g, 0.670 mmol), and TMEDA (0.10 mL, 0.670 mmol) to give Yb{C(SiDMe$_2$)$_3$}$_2$TMEDA (0.164 g, 0.244 mmol, 72.8%). ^{2}H NMR (benzene-H$_6$, 93.0 MHz, 25 °C): δ 4.79 (br s, SiD). IR (KBr, cm^{-1}): 1505 (ν_{SiD}), 1494 (ν_{SiD}), 1380 (ν_{SiD}).

{Yb[C(SiHMe$_2$)$_3$]$_2$THF}$_2$TMEDA ({3.3·THF}$_2$TMEDA). Excess THF (0.45 mL, 5.60 mmol) was added to a benzene solution (5 mL) of **3.3·TMEDA** (0.375 g, 0.560 mol) at room temperature. The red mixture was stirred for 30 min. Evaporation of the volatile materials provided a gummy solid of **({3.3·THF}$_2$TMEDA)** (0.381 g, 0.558 mmol, 99.6%). ^{1}H NMR (benzene-d_6, 600 MHz, 25 °C): δ 4.70 (m, 6 H, $^1J_{SiH}$ = 148 Hz, Si*H*Me$_2$), 3.67 (br s, 4 H, OC*H*$_2$CH$_2$), 1.97 (s, 6 H, NMe), 1.77 (s, 2 H, NCH$_2$), 1.36 (br s, 4 H, OCH$_2$C*H*$_2$), 0.49 (d, 36 H, $^3J_{HH}$ = 2.1 Hz, SiMe$_2$). ^{13}C{^{1}H} NMR (benzene-d_6, 150 MHz, 25 °C): δ 69.46 (OCH$_2$), 57.46 (NCH$_2$), 46.88 (NMe), 25.68 (OCH$_2$*C*H$_2$), 11.81 (YbC), 4.70 ($^1J_{SiC}$ = 50 Hz, SiMe$_2$). ^{29}Si{^{1}H} NMR (benzene-d_6, 119.3 MHz, 25 °C): δ -18.4. IR (KBr, cm^{-1}): 2951 s, 2896 s, 2802 m, 2095 s br (ν_{SiH}), 2039 s br sh (ν_{SiH}), 1850 m br (ν_{SiH}), 1598 w, 1493 m, 1468 w, 1249 s, 1028 s br, 937 s br, 890 s br, 834 s br, 773 s, 670 s. Anal. Calcd for $C_{21}H_{58}Si_6NOYb$: C, 36.97; H, 8.57; N, 2.05. Found: C, 37.04; H, 9.01; N, 1.95.

CaC(SiHMe$_2$)$_3${HB(C$_6$F$_5$)$_3$}TMEDA (3.4·TMEDA). Benzene (5 mL) was added to a mixture of Ca{C(SiHMe$_2$)$_3$}$_2$TMEDA (0.052 g, 0.097 mmol) and B(C$_6$F$_5$)$_3$ (0.050 g, 0.097 mmol). The mixture was stirred for 45 min, and then the volatile components were evaporated under reduced pressure. The yellow solid was washed with pentane (3 × 5 mL) and dried under vacuum to yield CaC(SiHMe$_2$)$_3${HB(C$_6$F$_5$)$_3$}TMEDA as a white solid (0.055

g, 0.064 mmol, 65.7%). ^{1}H NMR (benzene-d_6, 600 MHz, 25 °C): δ 4.44 (m, $^{1}J_{SiH}$ = 144.9 Hz, 3 H, SiH), 3.00-2.27 (br q, 1 H, HB), 1.70 (br s, 12 H, NMe), 1.51 (br s, 4 H, NCH_2), 0.30 (d, $^{3}J_{HH}$ = 3.4 Hz, 18 H, $SiMe_2$). $^{1}H\{^{11}B\}$ NMR (benzene-d_6, 600 MHz, 25 °C): δ 2.64 (br s, HB) (the other signals were unchanged from coupled ^{1}H NMR spectrum). $^{13}C\{^{1}H\}$ NMR (benzene-d_6, 150 MHz, 25 °C): δ 149.78 (br, C_6F_5), 148.30 (br, C_6F_5), 138.83 (br, C_6F_5), 137.12 (br, C_6F_5), 56.72 (NCH_2), 46.37 (br, NMe), 11.69 (CaC), 2.15 ($SiMe_2$). ^{11}B NMR (benzene-d_6, 119.3 MHz, 25 °C): δ -21.8 (d, $^{1}J_{BH}$ = 75.0 Hz). ^{19}F NMR (benzene-d_8, 376 MHz, 25 °C): δ -134.9 (br, 6 F, *ortho*-F), -159.0 (br, 3 F, *para*-F), -163.2 (6 F, *meta*-F). $^{29}Si\{^{1}H\}$ NMR (benzene-d_6, 119.3 MHz, 25 °C): δ -18.9. IR (KBr, cm^{-1}): 2962 m, 2897 m, 2851 m, 2302 m br (ν_{BH}), 2094 m br (ν_{SiH}), 2026 m br (ν_{SiH}), 1918 m br (ν_{SiH}), 1646 m, 1603 w, 1517 s br, 1467 s br, 1373 m, 1283 s, 1253 m, 1124 s, 1078 s, 1024 m, 965 s br, 835 s, 790 s. Anal. Calcd for $BC_{31}F_{15}H_{38}Si_3N_2Ca$: C, 43.36; H, 4.46; N, 3.26. Found: C, 43.15; H, 4.38; N, 3.24. Mp 137-140 °C.

$YbC(SiHMe_2)_3\{HB(C_6F_5)_3\}$TMEDA (3.5·TMEDA). The procedure was similar to that of calcium analog **3.4·TMEDA** above, with $Yb\{C(SiHMe_2)_3\}_2$TMEDA (0.083 g, 0.124 mmol) and $B(C_6F_5)_3$ (0.063 g, 0.124 mmol) affording **3.5·TMEDA** as a yellow solid (0.075 g, 0.076 mmol, 61.2%). ^{1}H NMR (benzene-d_6, 600 MHz, 25 °C): δ 4.51 (m, $^{1}J_{SiH}$ = 147.0 Hz, 3 H, SiH), 3.67-2.82 (br q, 1 H, HB), 1.71 (br s, 12 H, NMe), 1.55 (br s, 4 H, NCH_2), 0.33 (d, $^{3}J_{HH}$ = 2.9 Hz, 18 H, $SiMe_2$). $^{1}H\{^{11}B\}$ NMR (benzene-d_6, 600 MHz, 25 °C): δ 3.22 (br s, HB) (all other resonances were identical to the ^{1}H NMR spectrum). $^{13}C\{^{1}H\}$ NMR (benzene-d_6, 150 MHz, 25 °C): δ 149.88 (br, C_6F_5), 148.34 (br, C_6F_5), 140.84 (br, C_6F_5), 138.93 (br, C_6F_5), 137.17 (br, C_6F_5), 56.65 (NCH_2), 46.18 (br, NMe), 17.41 (YbC), 2.15 ($SiMe_2$). ^{11}B NMR

(benzene-d_6, 119.3 MHz, 25 °C): δ -21.4 (d, $^1J_{BH}$ = 71.6 Hz). ^{19}F NMR (benzene-d_6, 376 MHz, 25 °C): δ -134.7 (br, 6 F, *ortho*-F), -159.3 (br, 3 F, *para*-F), -163.7 (6 F, *meta*-F). ^{29}Si{^{1}H} NMR (benzene-d_6, 119.3 MHz, 25 °C): δ -18.0. IR (KBr, cm^{-1}): 2961 m, 2895 m, 2849 m, 2293 m br (ν_{BH}), 2094 m br (ν_{SiH}), 2027 m br (ν_{SiH}), 1899 m br (ν_{SiH}), 1645 m, 1602 w, 1516 s, 1466 s br, 1373 m, 1326 vw, 1282 m, 1253 m, 1110 s, 1076 s, 1024 m, 965 s br, 894 s br, 837 s, 789 m. Anal. Calcd for $BC_{31}F_{15}H_{38}Si_3N_2Yb$: C, 37.54; H, 3.86; N, 2.82. Found: C, 37.59; H, 3.61; N, 2.75. Mp 120-125 °C.

Ca{HB(C$_6$F$_5$)$_3$}$_2$TMEDA (3.6·TMEDA). Ca{C(SiHMe$_2$)$_3$}$_2$TMEDA (0.095 g, 0.177 mmol) and B(C$_6$F$_5$)$_3$ (0.190 g, 0.371 mmol) were allowed to react in benzene (5 mL). As the mixture was stirred, a light yellow solid precipitated, and the mixture was stirred for an additional 10 mins. The solid was isolated by filtration, washed with benzene (2 × 4 mL) and pentane (1 × 4 mL), and dried under reduced pressure to yield Ca{HB(C$_6$F$_5$)$_3$}$_2$TMEDA as a white solid (0.147 g, 0.124 mmol, 70.3%). ^{1}H NMR (THF-d_8, 600 MHz, 25 °C): δ 4.02-3.33 (br q, 1 H, HB), 2.31 (br s, 4 H, NCH$_2$), 2.15 (br s, 12 H, NMe). ^{1}H{^{11}B} NMR (THF-d_8, 600 MHz, 25 °C): δ 2.64 (br s, HB) (resonances assigned to TMEDA are identical in ^{1}H and ^{1}H{^{11}B} NMR spectra). ^{13}C{^{1}H} NMR (THF-d_8, 150 MHz, 25 °C): δ 150.05 (br, C$_6$F$_5$), 148.47 (br, C$_6$F$_5$), 139.37 (br, C$_6$F$_5$), 138.14 (br, C$_6$F$_5$), 136.14 (br, C$_6$F$_5$), 58.86 (NCH$_2$), 46.23 (br, NMe). ^{11}B NMR (THF-d_8, 119.3 MHz, 25 °C): δ -27.3 (d, $^1J_{BH}$ = 93.2 Hz). ^{19}F NMR (THF-d_8, 376 MHz, 25 °C): δ -136.8 (d, $^3J_{FF}$ = 20.4 Hz, 12 F, *ortho*-F), -169.5 (t, $^3J_{FF}$ = 17.7 Hz, 6 F, *para*-F), -172.1 (t, $^3J_{FF}$ = 22.0 Hz, 12 F, *meta*-F). IR (KBr, cm^{-1}): 2965 m, 2383 m br (ν_{BH}), 1665 m, 1606 m, 1515 s, 1466 s br, 1373 m, 1274 s, 1113 s, 1086 s, 965 s br, 913 m, 828 m,

789 m, 768 m, 685 m, 666 m. Anal. Calcd for $B_2C_{42}F_{30}H_{18}N_2Ca$: C, 42.67; H, 1.53; N, 2.37. Found: C, 43.09; H, 1.79; N, 2.00. Mp 205-211 °C.

Yb{HB(C$_6$F$_5$)$_3$}$_2$TMEDA (3.7·TMEDA). The procedure was similar to the one for **3.7·TMEDA**, using Yb{C(SiHMe$_2$)$_3$}$_2$TMEDA (0.095 g, 0.143 mmol) and B(C$_6$F$_5$)$_3$ (0.153 g, 0.299 mmol) to yield Yb(HB(C$_6$F$_5$)$_3$)$_2$TMEDA as an off-white solid (0.158 g, 0.120 mmol, 84.1%). ^{1}H NMR (THF-d_8, 600 MHz, 25 °C): δ 4.03-3.32 (br q, 1 H, HB), 2.37 (s, 4 H, NCH$_2$), 2.19 (s, 12 H, NMe). ^{1}H{^{11}B} NMR (THF-d_8, 600 MHz, 25 °C): δ 2.64 (br s, HB) (resonances assigned to TMEDA are identical in ^{1}H and ^{1}H{^{11}B} NMR spectra). ^{13}C{^{1}H} NMR (THF-d_8, 150 MHz, 25 °C): δ 150.04 (br, C$_6$F$_5$), 148.51 (br, C$_6$F$_5$), 139.45 (br, C$_6$F$_5$), 138.10 (br, C$_6$F$_5$), 136.52 (br, C$_6$F$_5$), 58.55 (NCH$_2$), 46.05 (br, NMe). ^{11}B NMR (THF-d_8, 119.3 MHz, 25 °C): δ -27.3 (d, $^1J_{BH}$ = 93.3 Hz). ^{19}F NMR (THF-d_8, 376 MHz, 25 °C): δ -136.9 (d, $^3J_{FF}$ = 20.9 Hz, 12 F, *ortho*-F), -169.2 (t, $^3J_{FF}$ = 20.2 Hz, 6 F, *para*-F), -171.9 (t, $^3J_{FF}$ = 19.1 Hz, 12 F, *meta*-F). IR (KBr, cm^{-1}): 3094 w, 2974 w, 2900 w, 2305 m br (ν_{BH}), 1647 m, 1606 m, 1517 s, 1466 s br, 1374 m, 1281 m, 1123 s br, 1083 s, 957 s, 898 m, 789 m, 769 m, 754 m, 685 m, 673 m. Anal. Calcd for $B_2C_{42}F_{30}H_{18}N_2Yb$: C, 38.36; H, 1.38; N, 2.13. Found: C, 38.69; H, 1.24; N, 1.94. Mp 163-170 °C.

Ca(HBPh$_3$)$_2$TMEDA (3.8·TMEDA). Benzene (3 mL) was added to a mixture of Ca{C(SiHMe$_2$)$_3$}$_2$TMEDA (0.077 g, 0.144 mmol) and BPh$_3$ (0.070 g, 0.290 mmol). The colorless solution mixture was thoroughly mixed and allowed to stand at room temperature for 10 h to yield white crystals. The solution was decanted, and the off-white crystals were washed with benzene (3 mL), pentane (2 × 3 mL), and dried under vacuum to give **3.8·TMEDA** as a white, crystalline, benzene-insoluble solid (0.060 g, 0.094 mmol, 65.2%).

IR (KBr, cm^{-1}): 3056 m, 2998 m, 2059 m (ν_{BH}), 2027 m (ν_{BH}), 2008 m (ν_{BH}), 1943 s (ν_{BH}), 1577 m, 1478 m br, 1428 m, 1284 m, 1168 m br, 1066 m, 1027 m, 788 m, 734 s, 707 vs br. Anal. Calcd for $B_2C_{42}H_{48}N_2Ca$: C, 78.51; H, 7.53; N, 4.36. Found: C, 77.97; H, 7.90; N, 3.60. Mp 240-245 °C (dec.).

Yb(HBPh$_3$)$_2$TMEDA (3.9·TMEDA). The procedure followed the one for the calcium analog **3.8·TMEDA**, using Yb{C(SiHMe$_2$)$_3$}$_2$TMEDA (0.087 g, 0.130 mmol) and BPh_3 (0.063 g, 0.261 mmol) to give **3.9·TMEDA** as a red, insoluble, crystalline solid (0.074 g, 0.095 mmol, 73.2%). IR (KBr, cm^{-1}): 3059 s, 3040 s, 2995 s, 2880 m, 2054 s (ν_{BH}), 2024 s (ν_{BH}), 2006 s (ν_{BH}), 1940 s (ν_{BH}), 1582 m, 1464 s, 1428 s, 1284 w, 1158 s br, 1065 m, 943 s, 786 m, 733 s br, 706 s br. Anal. Calcd for $B_2C_{42}H_{48}N_2Yb$: C, 65.05; H, 6.24; N, 3.61. Found: C, 64.84; H, 6.04; N, 3.59. Mp 140-150 °C.

Ca(HBPh$_3$)$_2$THF (3.8·THF). The procedure followed the one for the calcium TMEDA adduct **3.8·TMEDA**, with Ca{C(SiHMe$_2$)$_3$}$_2$THF$_2$ (0.072 g, 0.127 mmol) and BPh_3 (0.062 g, 0.255 mmol) providing **3.8·THF** as a white solid (0.057 g, 0.095 mmol, 74.5%). ^{1}H NMR (benzene-d_6, 600 MHz, 25 °C): δ 7.64 (br, 12 H, *meta*-C_6H_5), 7.24 (br, 12 H, *ortho*-C_6H_5), 7.16 (br, 6 H, *para*-C_6H_5), 3.23 (m, 4 H, CH_2CH_2O), 1.15 (m, br, 4 H, CH_2CH_2O). ^{1}H{^{11}B} NMR (benzene-d_6, 600 MHz, 25 °C): δ 3.18 (br, HB). ^{13}C{^{1}H} NMR (benzene-d_6, 150 MHz, 25 °C): δ 155.2 (*ipso*-CH), 139.3 (*m*-CH), *o*-CH and *p*-CH overlapped with C_6D_6, 69.8 (CH_2CH_2O), 25.4 (CH_2CH_2O). ^{11}B NMR (benzene-d_6, 119.3 MHz, 25 °C): δ -6.0 (br). IR (KBr, cm^{-1}): 3058 m, 2992 m, 2021 m br (ν_{BH}), 1936 m br (ν_{BH}), 1581 m, 1481 m, 1429 m, 1257 w, 1184 m br, 1021 m, 978 m, 880 m br, 737 s, 703 vs. Anal. Calcd for $B_2C_{40}H_{40}OCa$: C, 80.28; H, 6.74. Found: C, 76.09; H, 7.21. Mp 113-116 °C.

$KHB(C_6F_5)_3$ (3.13). Benzene (5 mL) was added to a mixture of $KC(SiHMe_2)_3$ (0.107 g, 0.469 mmol) and $B(C_6F_5)_3$ (0.252 g, 0.492 mmol) and solution was stirred for 10 min. The orange color quickly faded away and a pale pink crystalline solid precipitated. The benzene solution was filtered and the solid was washed with benzene (2 × 5 mL) and pentane (1 × 4 mL). The volatiles were evaporated under reduced pressure to yield a white solid (0.168 g, 0.303 mmol, 64.7%). ^{1}H NMR (THF-d_8, 600 MHz, 25 °C): δ 4.04-3.38 (br q, 1 H, HB). $^{13}C\{^1H\}$ NMR (THF-d_8, 150 MHz, 25 °C): δ 150.1 (br, C_6F_5), 148.5 (br, C_6F_5), 139.5 (br, C_6F_5), 137.9 (br, C_6F_5), 136.5 (br, C_6F_5). ^{11}B NMR (THF-d_8, 119.3 MHz, 25 °C): δ -27.3 (d, $^1J_{BH}$ = 92.5 Hz). ^{19}F NMR (THF-d_8, 376 MHz, 25 °C): δ -136.7 (d, $^3J_{FF}$ = 21.6 Hz, 6 F, *o*-F), -169.8 (t, $^3J_{FF}$ = 20.2 Hz, 3 F, *p*-F), -172.3 (t, $^3J_{FF}$ = 18.9 Hz, 6 F, *m*-F). IR (KBr, cm^{-1}): 3092 w, 3037 w, 2964 w, 2819 w, 2586 vw, 2382 s br (ν_{BH}), 2224 vw, 2178 vw, 2132 vw, 2093 vw, 2027 vw, 1644 vs, 1606 m, 1511 vs, 1450 vs, 1407 m, 1324 vw, 1273 vs, 1114 vs, 1086 vs, 1021 m, 945 vs, 914 vs, 886 s, 843 w, 785 m, 769 s, 752 s, 733 w, 720 vw, 666 s. Anal. Calcd for $BC_{18}F_{15}HK$: C, 39.16; H, 0.18. Found: C, 40.15; H, 0.26. Mp 290-292 °C (dec.).

$KHB(C_6F_5)_3TMEDA_2$ (3.14). $KHB(C_6F_5)_3$ (0.090 g, 0.162 mmol) was suspended in benzene (2 mL) and excess TMEDA (73 ml, 0.486 mmol) was added to yield a clear solution. The mixture was stirred for 10 min and the volatiles were evaporated under reduced pressure to give $KHB(C_6F_5)_3TMEDA_2$ as a white solid (0.125 g, 0.159 mmol, 98.1%). X-ray quality crystals can be grown from a toluene solution of $KHB(C_6F_5)_3(TMEDA)_2$ at -30 C for 3 days. ^{1}H NMR (benzene-d_6, 600 MHz, 25 °C): δ 3.84-3.08 (br q, 1 H, HB), 1.90 (s, 8 H, NCH_2), 1.82 (s, 24 H, NCH_3). $^{13}C\{^1H\}$ NMR (benzene-d_6, 150 MHz, 25 °C): δ 150.0 (br, C_6F_5), 148.5 (br, C_6F_5), 140.1 (br, C_6F_5), 138.5 (br, C_6F_5), 136.9 (br, C_6F_5), 57.5 (NCH_2), 45.4

(NMe). ^{11}B NMR (benzene-d_6, 119.3 MHz, 25 °C): δ -24.7 (d, $^1J_{BH}$ = 83.1 Hz).). ^{19}F NMR (benzene-d_6, 376 MHz, 25 °C): δ -135.9 (d, $^3J_{FF}$ = 21.8 Hz, 6 F, *ortho*-F), -163.2 (t, $^3J_{FF}$ = 20.6 Hz, 3 F, *para*-F), -170.0 (t, $^3J_{FF}$ = 21.8 Hz, 6 F, *meta*-F). IR (KBr, cm^{-1}): 2948 m, 2872 m, 2832 m, 2792 m, 2712 m, 2381 m br (ν_{BH}), 1643 m, 1514 s, 1461 s, 1364 m, 1297 m, 1278 m, 1099 s, 969 s, 907 m, 782 m, 764 m. Calcd for $BC_{30}F_{15}H_{33}K$: C, 45.93; H, 4.24; N, 7.14. Found: C, 46.02; H, 3.84; N, 6.87. Mp 90-92 °C.

Supplementary material

X-ray crystallographic data for $Ca(C(SiHMe_2)_3)_2THF_2$ (**3.2·THF$_2$**).

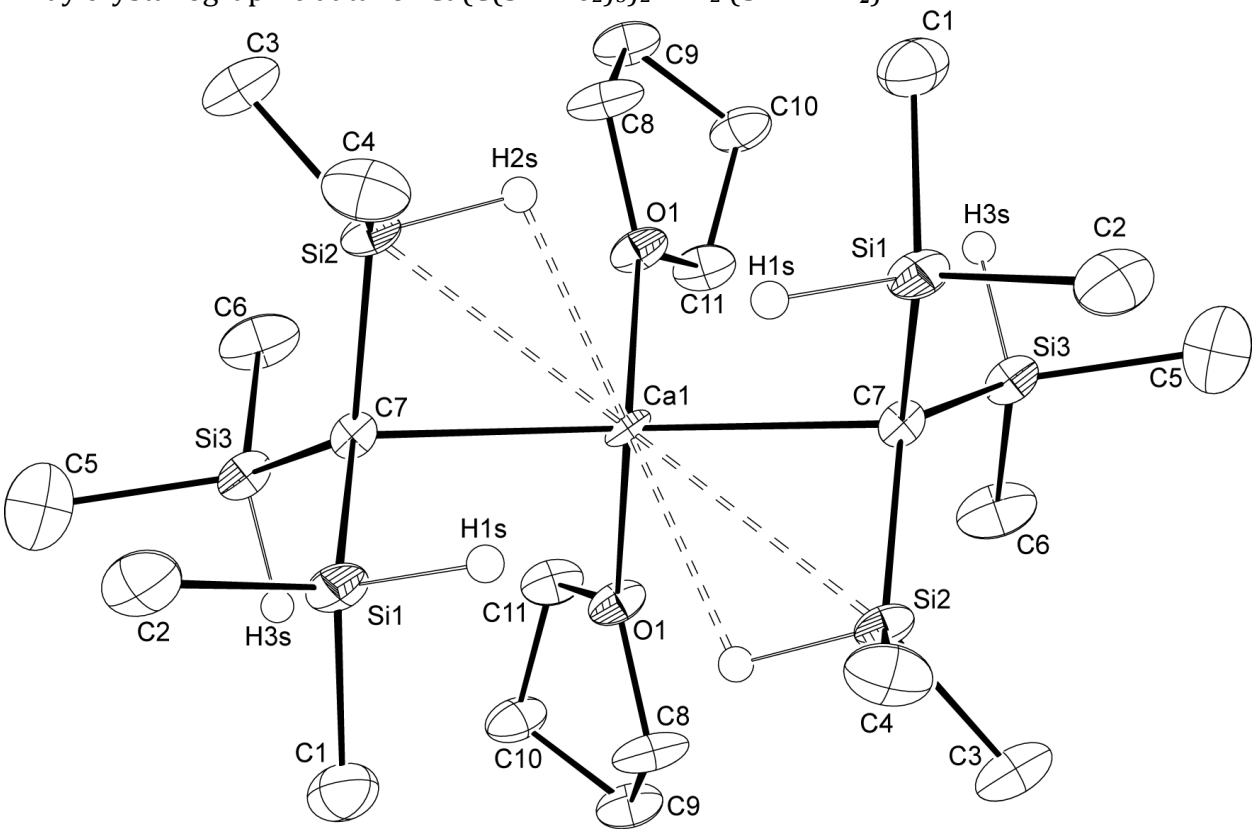

Table 3.S1. Crystal data and structure refinement for $Ca(C(SiHMe_2)_3)_2THF_2$ (**3.2·THF$_2$**).

Empirical formula	$C_{22}H_{58}CaO_2Si_6$
Formula weight	563.30
Temperature	173(2) K

Wavelength	0.71073 Å	
Crystal system	Monoclinic	
Space group	C2/c	
Unit cell dimensions	a = 23.185(7) Å	α= 90°.
	b = 9.352(3) Å	β= 121.49(2)°.
	c = 18.826(6) Å	γ = 90°.

X-ray crystallographic data for $Yb(C(SiHMe_2)_3)_2THF_2$ (**3.3·THF₂**).

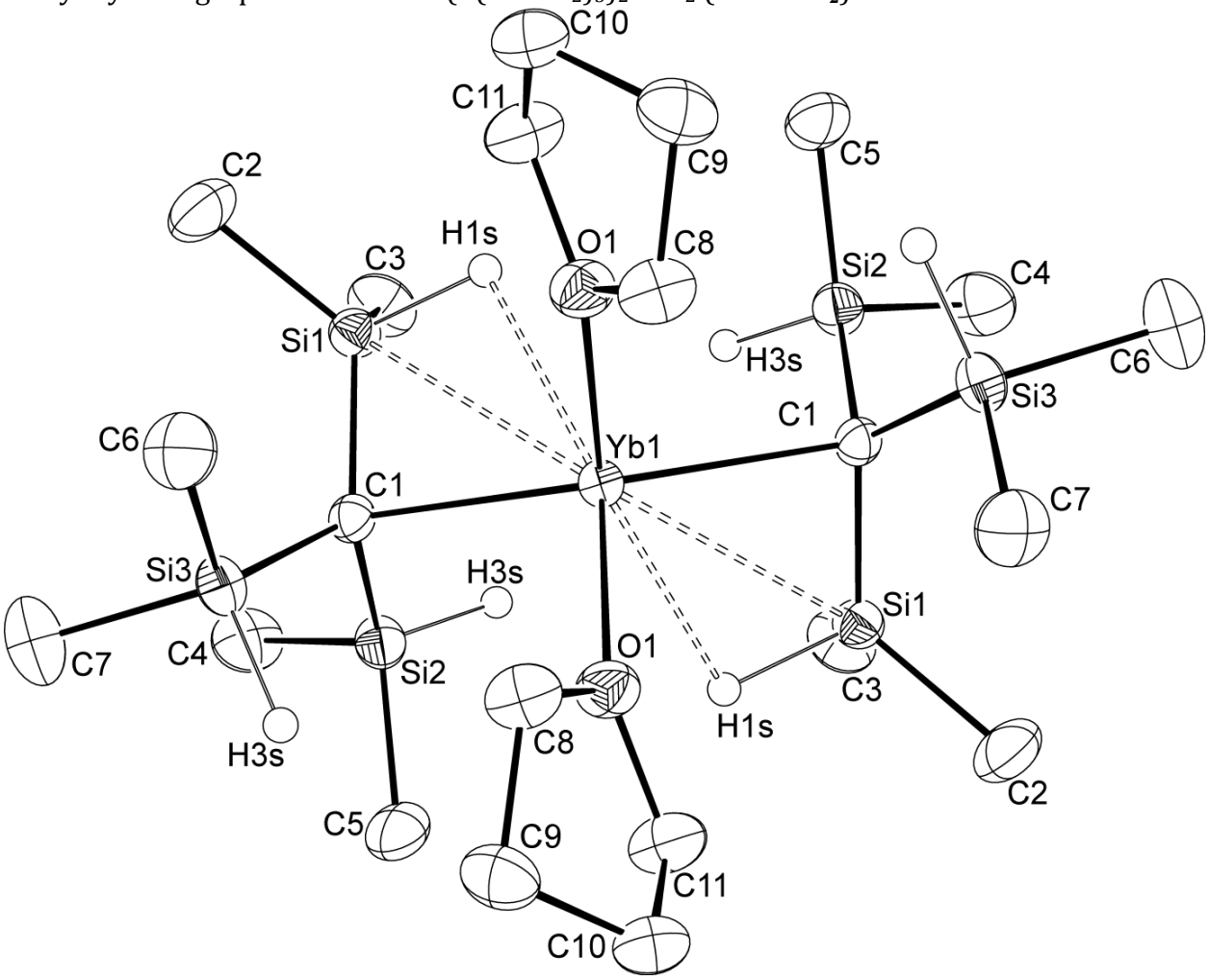

Table 3.S2. Crystal data and structure refinement for $Yb(C(SiHMe_2)_3)_2THF_2$ (**3.3·THF₂**).

Empirical formula	$C_{22}H_{58}O_2Si_6Yb$	
Formula weight	696.26	
Temperature	293(2) K	
Wavelength	0.71073 Å	
Crystal system	Monoclinic	
Space group	C2/c	
Unit cell dimensions	a = 22.792(12) Å	α= 90°.
	b = 9.284(4) Å	β= 121.189(16)°.
	c = 18.655(10) Å	γ = 90°.

X-ray crystallographic data for $YbC(SiHMe_2)_3THF_2[HB(C_6F_5)_3]$ (**3.5·THF₂**).

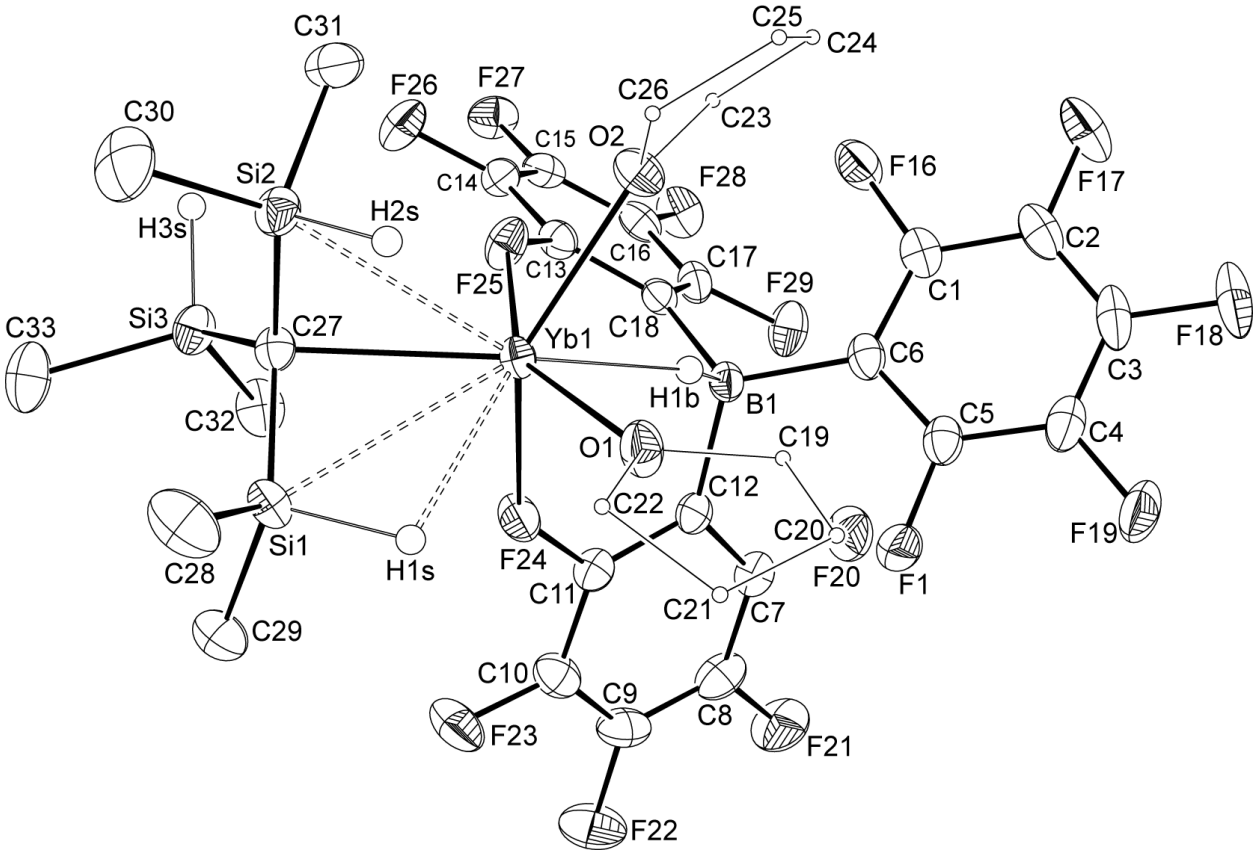

Table 3.S3. Crystal data and structure refinement for $[YbC(SiHMe_2)_3THF_2][HB(C_6F_5)_3]$ (**3.5·THF$_2$**).

Empirical formula	$C_{33}H_{38}BF_{15}O_2Si_3Yb$	
Formula weight	1019.75	
Temperature	123(2) K	
Wavelength	0.71073 Å	
Crystal system	Monoclinic	
Space group	P2(1)/n	
Unit cell dimensions	a = 11.0583(7) Å	α= 90°.
	b = 23.1942(14) Å	β= 97.0320(10)°.
	c = 15.3710(9) Å	γ = 90°.

X-ray crystallographic data for $Ca[HB(C_6F_5)_3]_2THF_2$ (**3.6·THF$_2$**).

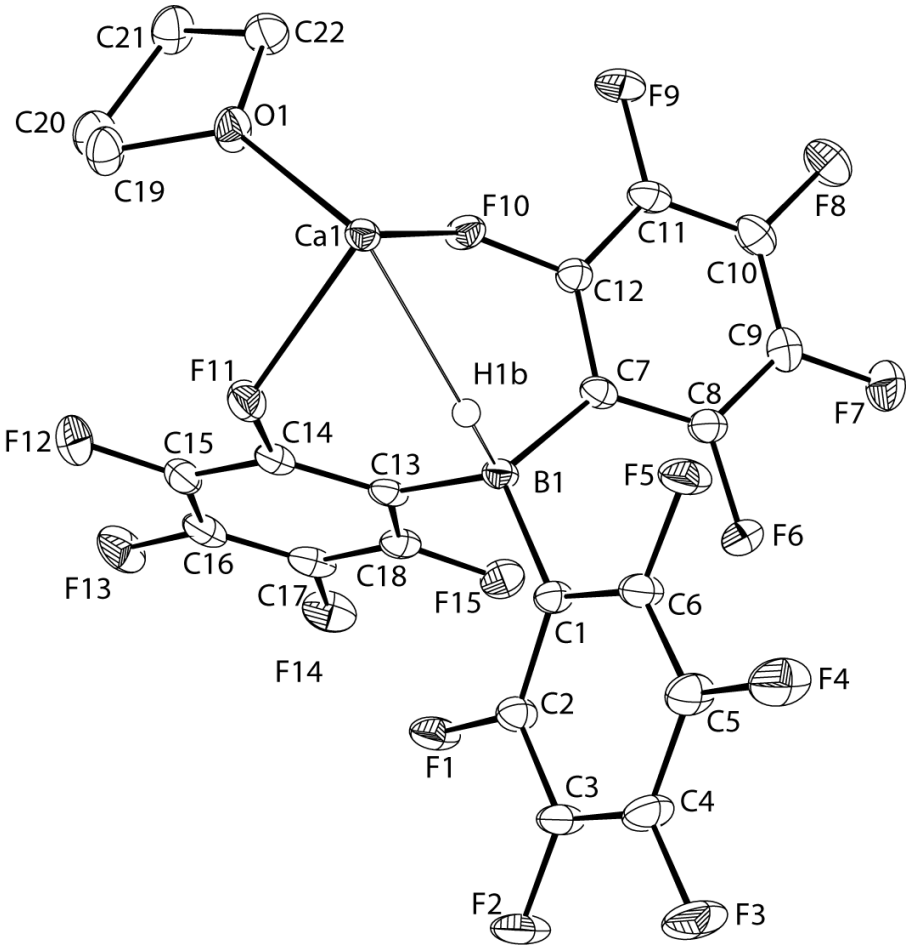

Table 3.S4. Crystal data and structure refinement for $Ca[HB(C_6F_5)_3]_2THF_2$ (**3.6·THF$_2$**).

Empirical formula	$C_{50}H_{24}B_2CaF_{30}O_2$	
Formula weight	1288.39	
Temperature	123(2) K	
Wavelength	0.71073 Å	
Crystal system	monoclinic	
Space group	C 2/c	
Unit cell dimensions	a = 15.9249(9) Å	α= 90°.
	b = 15.7207(9) Å	β= 107.8530(10)°.
	c = 20.7711(12) Å	γ = 90°.

X-ray crystallographic data for $(Me_2SiC(SiHMe_2)_2)_2$.

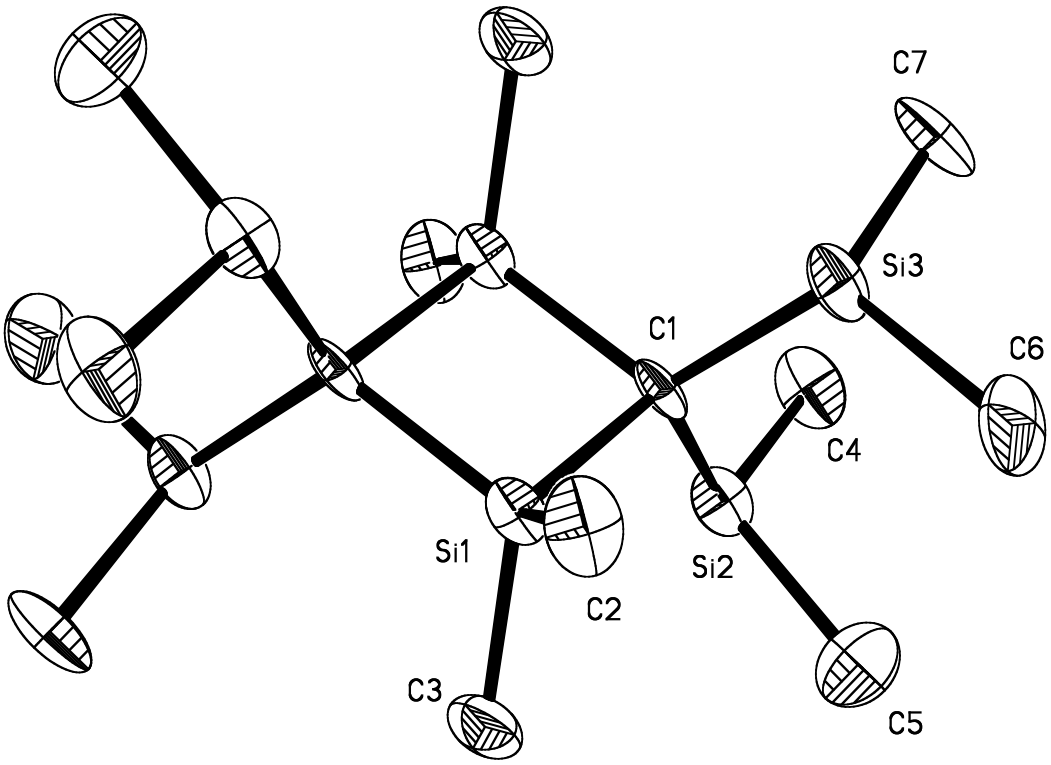

Table 3.S5. Crystal data and structure refinement for $(Me_2SiC(SiHMe_2)_2)_2$.

Empirical formula	$C_{14}H_{40}Si_6$	
Formula weight	377.00	
Temperature	173(2) K	
Wavelength	0.71073 Å	
Crystal system	Triclinic	
Space group	P-1	
Unit cell dimensions	a = 8.512(7) Å	α= 104.555(19)°.
	b = 8.569(7) Å	β= 91.47(2)°.
	c = 9.253(9) Å	γ = 114.49(2)°.

References

1 Collman, J. P.; Hegedus, L. S.; Norton, J. R.; Finke, R. G. *Principles and Applications of Organotransition Metal Chemistry*; University Science Books: Mill Valley, CA, 1987.

2 Chirik, P. J.; Bercaw, J. E. *Organometallics* **2005**, *24*, 5407-5423.

3 a) Finnegan, R. A.; Kutta, H. W. *J. Org. Chem.* **1965**, *30*, 4138-4144. b) Glaze, W. H.; Lin, J.; Felton, E. G. *J. Org. Chem.* **1966**, *31*, 2643-2645. c) Eppley, R. L.; Dixon, J. A. *J. Organomet. Chem.* **1968**, *11*, 174-176.

4 a) Carothers, W. H.; Coffman, D. D. *J. Am. Chem. Soc.* **1929**, *51*, 588-593. b) Morton, A. A.; Newey, H. A. *J. Am. Chem. Soc.* **1942**, *64*, 2247-2250. c) Morton, A. A.; Lanpher, E. J. *J. Org. Chem.* **1955**, *20*, 839-844.

5 a) Fraenkel, G.; Pechhold, E. *Tetrahedron Lett.* **1970**, *11*, 153-156. b) Lochmann, L.; Lím, D. *J. Organomet. Chem.* **1971**, *28*, 153-158.

6 a) Lindsell, W. E. *Magnesium, calcium, strontium, and barium*; 1st ed.; Pergamon Press: Oxford; New York, 1982; Vol. 1. b) Bryce-Smith, D.; Skinner, A. C. *J. Chem. Soc.* **1963**, 577-585.

7 a) Wayda, A. L.; Evans, W. J. *J. Am. Chem. Soc.* **1978**, *100*, 7119-7121. b) Evans, W. J.; Wayda, A. L.; Hunter, W. E.; Atwood, J. L. *J. Chem. Soc., Chem. Commun.* **1981**, 292-293.

8 Evans, W. J.; Meadows, J. H.; Wayda, A. L.; Hunter, W. E.; Atwood, J. L. *J. Am. Chem. Soc.* **1982**, *104*, 2015-2017.

9 a) Hanusa, T. P. *Chem. Rev.* **1993**, *93*, 1023-1036. b) Harder, S. *Chem. Rev.* **2010**, *110*, 3852-3876. c) Zimmermann, M.; Anwander, R. *Chem. Rev.* **2010**, *110*, 6194-6259.

10 a) Feil, F.; Harder, S. *Organometallics* **2000**, *19*, 5010-5015. b) Bambirra, S.; Meetsma, A.; Hessen, B. *Organometallics* **2006**, *25*, 3454-3462. c) Meyer, N.; Roesky, P. W.; Bambirra, S.; Meetsma, A.; Hessen, B.; Saliu, K.; Takats, J. *Organometallics* **2008**, *27*, 1501-1505. d) Torvisco, A.; Ruhlandt-Senge, K. *Inorg. Chem.* **2011**, *50*, 12223-12240.

11 a) Jochmann, P.; Dols, T. S.; Spaniol, T. P.; Perrin, L.; Maron, L.; Okuda, J. *Angew. Chem. Int. Ed.* **2009**, *48*, 5715-5719. b) Chmely, S. C.; Carlson, C. N.; Hanusa, T. P.; Rheingold, A. L. *J. Am. Chem. Soc.* **2009**, *131*, 6344-6345. c) Lichtenberg, C.; Jochmann, P.; Spaniol, T. P.; Okuda, J. *Angew. Chem. Int. Ed.* **2011**, *50*, 5753-5756. d) Jochmann, P.; Spaniol, T. P.; Chmely, S. C.; Hanusa, T. P.; Okuda, J. *Organometallics* **2011**, *30*, 5291-5296.

12 a) Lappert, M. F.; Pearce, R. *J. Chem. Soc., Chem. Commun.* **1973**, 126-126. b) Moorhouse, S.; Wilkinson, G. *J. Organomet. Chem.* **1973**, *52*, C5-C6.

13 a) Atwood, J. L.; Fjeldberg, T.; Lappert, M. F.; Luongthi, N. T.; Shakir, R.; Thorne, A. J. *J. Chem. Soc. Chem. Commun.* **1984**, 1163-1165. b) Avent, A. G.; Caro, C. F.; Hitchcock, P. B.; Lappert, M. F.; Li, Z. N.; Wei, X. H. *J. Chem. Soc., Dalton Trans.* **2004**, 1567-1577.

14 a) Eaborn, C.; Hitchcock, P. B.; Smith, J. D.; Sullivan, A. C. *J. Chem. Soc. Chem. Commun.* **1983**, 827-828. b) Avent, A. G.; Eaborn, C.; Hitchcock, P. B.; Lawless, G. A.; Lickiss, P. D.; Mallien, M.; Smith, J. D.; Webb, A. D.; Wrackmeyer, B. *J. Chem. Soc., Dalton Trans.* **1993**, 3259-3264. c) Eaborn, C.; Hitchcock, P. B.; Izod, K.; Jaggar, A. J.; Smith, J. D. *Organometallics* **1994**, *13*, 753-754. d) Al-Juaid, S. S.; Eaborn, C.; Hitchcock, P. B.; Jaggar, A. J.; Smith, J. D. *J. Organomet. Chem.* **1994**, *469*, 129-133. e) Al-Juaid, S. S.; Eaborn, C.; Hitchcock, P. B.; Kundu, K.; McGeary, C. A.; Smith, J. D. *J. Organomet. Chem.* **1994**, *480*, 199-203. f) Eaborn, C.; Smith, J. D. *J. Chem. Soc., Dalton Trans.* **2001**, 1541-1552.

15 Eaborn, C.; B. Hitchcock, P. *Chem. Commun.* **1997**, 1961-1962.

16 Eaborn, C.; Hitchcock, P. B.; Izod, K.; Smith, J. D. *J. Am. Chem. Soc.* **1994**, *116*, 12071-12072.

17 Cloke, F. G. N.; Hitchcock, P. B.; Lappert, M. F.; Lawless, G. A.; Royo, B. *J. Chem. Soc., Chem. Commun.* **1991**, 724-726.

18 Eaborn, C.; Hitchcock, P. B.; Izod, K.; Lu, Z. R.; Smith, J. D. *Organometallics* **1996**, *15*, 4783-4790.

19 a) Woodward, R. B.; Wendler, N. L.; Brutschy, F. J. *J. Am. Chem. Soc.* **1945**, *67*, 1425-1429. b) Kow, R.; Nygren, R.; Rathke, M. W. *J. Org. Chem.* **1977**, *42*, 826-827. c) Namy, J. L.; Souppe, J.; Collin, J.; Kagan, H. B. *J. Org. Chem.* **1984**, *49*, 2045-2049. d) Campbell, E. J.; Zhou, H.; Nguyen, S. T. *Org. Lett.* **2001**, *3*, 2391-2393.

20 a) Brookhart, M.; Green, M. L. H.; Pardy, R. B. A. *J. Chem. Soc. Chem. Commun.* **1983**, 691-693. b) Schmidt, G. F.; Brookhart, M. *J. Am. Chem. Soc.* **1985**, *107*, 1443-1444. c) Burger, B. J.; Thompson, M. E.; Cotter, W. D.; Bercaw, J. E. *J. Am. Chem. Soc.* **1990**, *112*, 1566-1577.

21 a) Procopio, L. J.; Carroll, P. J.; Berry, D. H. *J. Am. Chem. Soc.* **1991**, *113*, 1870-1872. b) Procopio, L. J.; Carroll, P. J.; Berry, D. H. *J. Am. Chem. Soc.* **1994**, *116*, 177-185.

22 Rees Jr, W. S.; Just, O.; Schumann, H.; Weimann, R. *Angew. Chem., Int. Eng. Ed.* **1996**, *35*, 419-422.

23 a) Herrmann, W. A.; Eppinger, J.; Spiegler, M.; Runte, O.; Anwander, R. *Organometallics* **1997**, *16*, 1813-1815. b) Anwander, R.; Runte, O.; Eppinger, J.; Gerstberger, G.; Herdtweck, E.; Spiegler, M. *J. Chem. Soc. Dalton Trans.* **1998**, 847-858. c) Eppinger, J.; Spiegler, M.; Hieringer, W.; Herrmann, W. A.; Anwander, R. *J. Am. Chem. Soc.* **2000**, *122*, 3080-3096. d) Hieringer, W.; Eppinger, J.; Anwander, R.;

Herrmann, W. A. *J. Am. Chem. Soc.* **2000**, *122*, 11983-11994. e) Klimpel, M. G.; Gorlitzer, H. W.; Tafipolsky, M.; Spiegler, M.; Scherer, W.; Anwander, R. *J. Organomet. Chem.* **2002**, *647*, 236-244.

24 Cundy, C. S.; Lappert, M. F.; Pearce, R. *J. Organomet. Chem.* **1973**, *59*, 161-166.

25 a) Eaborn, C.; Hitchcock, P. B.; Lickiss, P. D. *J. Organomet. Chem.* **1983**, *252*, 281-288. b) Asadi, A.; Avent, A. G.; Coles, M. P.; Eaborn, C.; Hitchcock, P. B.; Smith, J. D. *J. Organomet. Chem.* **2004**, *689*, 1238-1248.

26 Hawrelak, E. J.; Ladipo, F. T.; Sata, D.; Braddock-Wilking, J. *Organometallics* **1999**, *18*, 1804-1807.

27 a) Yan, K.; Pawlikowski, A. V.; Ebert, C.; Sadow, A. D. *Chem. Commun.* **2009**, 656-658. b) Yan, K.; Upton, B. M.; Ellern, A.; Sadow, A. D. *J. Am. Chem. Soc.* **2009**, *131*, 15110-15111.

28 a) Walker, D. A.; Woodman, T. J.; Hughes, D. L.; Bochmann, M. *Organometallics* **2001**, *20*, 3772-3776. b) Milione, S.; Grisi, F.; Centore, R.; Tuzi, A. *Organometallics* **2006**, *25*, 266-274. c) Garner, L. E.; Zhu, H.; Hlavinka, M. L.; Hagadorn, J. R.; Chen, E. Y. X. *J. Am. Chem. Soc.* **2006**, *128*, 14822-14823.

29 Zhu, J.; Mukherjee, D.; Sadow, A. D. *Chem. Commun.* **2012**, *48*, 464-466.

30 Bondi, A. *J. Phys. Chem.* **1964**, *68*, 441-451.

31 a) Olmstead, M. M.; Power, P. P. *J. Am. Chem. Soc.* **1985**, *107*, 2174-2175. b) Harder, S. *Chem. Eur. J.* **2002**, *8*, 3229-3232.

32 Rowland, R. S.; Taylor, R. *J. Phys. Chem.*, **100**, 7384 - 7391, 1996.

33 Brookhart, M.; Green, M. L. H.; Parkin, G. *Proc. Natl. Acad. Sci. U.S.A.* **2007**, *104*, 6908-6914.

34 Corradi, M. M.; Frankland, A. D.; Hitchcock, P.; Lappert, M. F.; Lawless, G. A. *Chem. Commun.* **1996**, 2323-2324.

35 Shannon, R. D. *Acta Cryst. A* **1976**, *32*, 751-767.

36 Van der Heijden, H.; Schaverien, C. J.; Orpen, A. G. *Organometallics* **1989**, *8*, 255-258.

37 Edmiston, C.; Ruedenberg, K. *Rev. Mod. Phys.* **1963**, *35*, 457-465.

38 Evans, W. J.; Forrestal, K. J.; Ansari, M. A.; Ziller, J. W. *J. Am. Chem. Soc.* **1998**, *120*, 2180-2181.

39 Berkefeld, A.; Piers, W. E.; Parvez, M.; Castro, L.; Maron, L.; Eisenstein, O. *J. Am. Chem. Soc.* **2012**, *134*, 10843-10851.

40 Zettler, F.; Hausen, H. D.; Hess, H. *J. Organomet. Chem.* **1974**, *72*, 157-162.

41 Bellamy, D.; G. Connelly, N.; M. Hicks, O.; Guy Orpen, A. *J. Chem. Soc., Dalton Trans.* **1999**, 3185-3190.

42 Werkema, E. L.; Andersen, R. A.; Yahia, A.; Maron, L.; Eisenstein, O. *Organometallics* **2009**, *28*, 3173-3185.

43 Dioumaev, V. K.; Plössl, K.; Carroll, P. J.; Berry, D. H. *Organometallics* **2000**, *19*, 3374-3378.

44 a) Deacon, G. B.; Evans, D. J.; Forsyth, C. M.; Junk, P. C. *Coord. Chem. Rev.* **2007**, *251*, 1699-1706. b) Verma, A.; Guino-o, M.; Gillett-Kunnath, M.; Teng, W.; Ruhlandt-Senge, K. *Z. Anorg. Allg. Chem.* **2009**, *635*, 903-913.

45 Deacon, G. B.; Forsyth, C. M. *Chem. Commun.* **2002**, 2522-2523.

46 M. N. Bochkarev, V. V. Khramenkov, Y. F. RadAkov, L. N. Zhakharov and Y. T. Struchkov, *J. Organomet. Chem.*, 1992, **429**, 27.

47 Yan, K.; Ellern, A.; Sadow, A. D. *J. Am. Chem. Soc.* **2012**, *134*, 9154-9156.

48 Tilley, T. D.; Boncella, J. M.; Berg, D. J.; Burns, C. J.; Andersen, R. A. *Inorg. Syn*. 27, 146

49 Massey, A. G.; Park, A. J., *J. Organomet. Chem.* **1964**, *2*, 245-250.

50 Valiev, M; Bylaska, E.; Govind, N.; Kowalski, K.; Straatsma, T.; Van Dam, H.; Wang, D.; Nieplocha, J.; Apra, E.; Windus, T.; de Jong, W. *Comp. Phys. Comm.* **2010**, *181* 1477.

51 Krishnan, R.; Binkley, J. S.; Seeger, R.; Pople, J. A. *J. Chem. Phys.* **1980**, *72*, 650. Blaudeau, J-P.; McGrath, M. P.; Curtiss, L. A.; Radom, L. *J. Chem. Phys.* **1997**, *107*, 5016.

52 Dolg, M.; Stoll, H.; Preuss, H.; Pitzer, R. M. *J. Phys. Chem.* **1993**, *97*, 5852.

53 Bergner, A.; Dolg, M.; Kuechle, W.; Stoll, H.; Preuss, H. *Mol. Phys.* **1993**, *80*, 1431.

54 Becke, A. D. *J. Chem. Phys.* **2006**, *124*, 16. Lee, C.; Yang, W.; Parr, R. G. *Phys. Rev. B* **1988**, *37*, 785.

Chapter 4: Abstraction reactions of Mixed di(alkyl) magnesium complexes containing Si-H functionality with Lewis acids

Modified from a paper to be submitted to *Organometallics*

KaKing Yan, Brianna M. Upton, Arkady Ellern, Aaron D. Sadow

Department of Chemistry and US Department of Energy Ames Laboratory, Iowa State University, Ames IA, 50011, USA

Abstract. A series of monomeric neutral, zwitterionic and cationic magnesium alkyl compounds containing the tris(dimethylsilyl)methyl -$C(SiHMe_2)_3$, bis(dimethylsilyl)methyl -$CH(SiHMe_2)_2$, and bis(trimethylsilyl)methyl -$CH(SiMe_3)_2$ ligand are described. The magnesium mixed methyl alkyl complexes MeMgR(TMEDA) are synthesized by salt elimination of MeMgBr(TMEDA) with LiR (R = $C(SiHMe_2)_3$, $CH(SiHMe_2)_2$, $CH(SiMe_3)_2$). The synthesis of $MeMgCH(SiHMe_2)_2$(TMEDA) results in contamination of $BrMgCH(SiHMe_2)_2$(TMEDA), which is resulted from possible Schlenk's equilibrium from MeMgBr(TMEDA). The abstraction reactions of MeMgR(TMEDA) (R = $C(SiHMe_2)_3$, $CH(SiMe_3)_2$) with electrophiles, such as $SiMe_3I$, $B(C_6F_5)_3$, $PhB(C_6F_5)_2$ and $[Ph_3C][B(C_6F_5)_4]$ were examined. Mg methyl group abstractions were predominated with all the electrophiles to give the corresponding zwitterionic or cationic Mg species, except in the reaction of $MeMgC(SiHMe_2)_3$(TMEDA) and $B(C_6F_5)_3$, in which a 10:1 ratio of methyl group to β-SiH group abstraction was observed. The spectroscopic data suggests the isolated β-SiH containing zwitterionic or cationic Mg complexes do not process agostic Si—H—Mg interaction.

Introduction

Organomagnesium compounds are important class of reagents in organic and organometallic chemistry. Despite their wide applications in organic synthesis, the understanding of the mechanism involving Grignard reagents is difficult to study, due to their complicated speciation and solution structures. The solution structure of Grignard reagents depends greatly on the nature of groups on Mg, solvent, concentration and temperature. For example, RMgX in Et_2O exist in monomeric form in low concentration but in dimeric or high order in high concentration, despite their monomeric solid-state structure.[1] In addition, the possibility of Schlenk's equilibrium further complicates the actual species in solution. [2] Therefore, the ability to synthesize well-defined monomeric Grignard reagent in solution would greatly provide deep insight on how to control their organic reaction pathways and thus selectivity. Notably, most studies on Grignard are focused on RMgX type where X is halide. Much less attention has been paid to heterolytic Mg compounds RMgX where X is not halide. Other heteroletpic magnesium compounds include Mg alkyl amide, n-BuMg[NDiip($SiMe_3$)]$(THF)_2$, n-BuMgHMDS, and s-BuMgHMDS.[3] These compounds exhibit interesting reactivity, for example, the last two compounds undergo β-H transfer reaction with ketone to give an mixed amide alkoxide ketone-reduced compound [{$(Me_3Si)_2$NMg[μ-OC(H)Ph_2]·(O=CPh_2)}$_2$] and olefins.[4] This interesting result suggested that β-H, not Mg alkyl, on Mg alkyl could be more nuclueophilic in nature.

Recently reported that reaction of MC($SiHMe_2$)$_3$)$_2$THF (M = Ca, Yb) and B(C_6F_5)$_3$ proceed via SiH abstraction rather than abstraction of the entire alkyl group.[5] Furthermore, reactions with two equivalents of Lewis acid gives a 'double' abstraction product, where an H from each of the two -C($SiHMe_2$)$_3$ ligands is abstracted. This selectivity was attributed partly

to steric effects, such that interaction of the electrophile with a sterically hindered carbanion is not possible, whereas the SiH groups are more easily accessed. It is worth considering that no reaction might occur with bulky alkyls and Lewis acids in the absence of SiH groups (e.g. $M(C(SiMe_3)_3)_2$ (rephrase this). Thus, understanding the selectivity for reactions of metal alkyls with Lewis acids where alkyl abstraction is possible to gauge the relative nucleophilicity of β-SiH groups versus unhindered metal alkyls.

Therefore, we are interested in preparing β-H containing organometallic Mg compounds to study their reactivity with Lewis acids in comparison to MgMe group. We have chosen to investigate heteroleptic magnesium dialkyl compounds, since Grignard reagents RMgBr, as their TMEDA adducts, are readily available in monomeric form in solid-state.[6] Although intermetallic anionic ligand exchange is possible for divalent rare earth and alkali earth metal MRR' compounds, we expected those reaction to be less important with the coordinatively saturated tetrahedral TMEDA derivatives. Despite this, few heteroleptic magnesium dialkyl compounds have been reported and/or crystallographically characterized [$PhCH_2MgMe(THF)_2$ is known to form from a reaction of MgMeCl and KBn, but this materal was structurally and analytically characterized.[7] The most prominent complex is CpMgMe, which was formed from disproporation of Cp_2Mg and Me_2Mg, but it is also not structurally characterized.[8] This mixed compound reacted further with aza-crown ether to give cationic species [(AEM)MgMe][Cp].[9] Well-defined cationic magnesium alkyl compounds are rare. Another strategy to synthesize cationic magnesium alkyls is by reaction of cationic ancillary ligand or acid equipped with weakly coordinating anions with MgR_2 to give $[LMg(n\text{-Bu})]^+[BAr_4]^-$[10] and $[(Et_2O)Mg(n\text{-Bu})]^+[B(C_6F_5)_4]^-$.[11] However, direct abstraction of M-R group with Lewis acids was not reported to date for magnesium

chemistry. Here we report the synthesis of rare heteroleptic dialkyl magnesium compounds and our investigations of their reactivity with different borane-based Lewis acids to form cationic Mg alkyl compounds.

Result and discussion.

4.1. Synthesis of $MeMgC(SiHMe_2)_3(TMEDA)$ (4.1).

Salt metathesis reaction of $KC(SiHMe_2)_3$ and MeMgBr(TMEDA) in benzene for 12 h provides $MgC(SiHMe_2)_3Me(TMEDA)$ (**4.1**; eq 4.1) as a light orange crystalline solid.

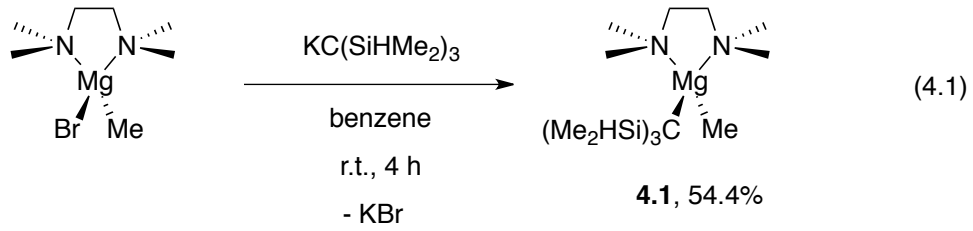

(4.1)

The ^1H NMR spectrum of **4.1** contained resonances at 4.75 ppm ($^1J_{SiH}$ = 169.2 Hz), 0.54 ppm ($^3J_{HH}$ = 3.6 Hz) and 0.91 ppm, assigned to resonances of SiH, $SiMe_2$ and MgMe, respectively. The SiH resonance appears at 4.75 ppm and the $^1J_{SiH}$ is 170 Hz. In comparison, the $^1J_{SiH}$ of $HC(SiHMe_2)_3$ is 184 Hz, and the ^1H NMR chemical shift is 4.33 ppm. Furthermore, the tmeda ligand exhibits diastereotopic resonances for both NMe_2 (2.03 and 1.91 ppm) and NCH_2 (1.65 and 1.59 ppm). This suggests both monodentate[12] and bidentate coordination modes of TMEDA are possible solution structures. Meanwhile, the $^{13}C\{^1H\}$ NMR spectrum contained two signals for the NMe groups at 47.8 and 47.1 ppm and one board signal for the NCH_2 group at 56.8 ppm. The two NMe signals in ^1H NMR spectrum showed cross peaks with the two resonances of NMe groups in ^{13}C spectrum in a ^1H-^{13}C HMBC experiment that unambiguously suggested that both NMe groups are diastereotopic

and both N atoms reside on the Mg center. The ^{29}Si NMR of $MgC(SiHMe_2)_3Me(TMEDA)$ contained one resonance at -20.3 ppm. In comparison, it is relatively closed to that of other TMEDA $-C(SiHMe_2)_3$ anions in $KC(SiHMe_2)_3(TMEDA)$ (-23.7 ppm)[13] and $Ca[C(SiHMe_2)_3]_2(TMEDA)$ (-23.6 ppm) [13]. The IR spectrum showed two absorption bands for the SiH stretching bands at 2076 and 2044 cm^{-1}. The stretching frequency of the SiH bands are lower than that of the free ligand $HC(SiHMe_2)_3$ at 2109 cm^{-1}. Nevertheless, the high $^1J_{SiH}$ coupling constant and high SiH stretching frequency ν_{SiH} imply the Mg---H---Si interaction is not strong, in contrary to the $Y[C(SiHMe_2)_3]_3$[14] and $M[C(SiHMe_2)_3]_2THF_2$ (M = Ca, Yb), which exhibits strong β-SiH agostic interactions.[5]

4.1 can be re-crystallized from a concentrated solution in pentane at -30 °C. Single crystal X-ray diffraction study of $MgMeC(SiHMe_2)_3(TMEDA)$ showed its monomeric nature and the magnesium coordination number to be four and unambiguously showed that both N atoms coordinate to Mg center. **4.1** crystallizes with three crystallographically independent molecules in the unit cell (one is shown in Figure 4.1). The Mg-CH_3 (ave. 2.14) and Mg-C(SiHMe2)3 (ave 2.22) distances are identical within error for the three molecules, as are the C-Mg-C angles (ave. 120°). In the homoleptic $MC(SiHMe_2)_3)_2THF_2$ (M = Ca, Yb) compounds, short M-Si distances and M-C-Si-H torsion angles indicate structures with one β-agostic SiH per alkyl ligand. In contrast, the Mg-Si distances in **4.1** are longer than the sums of ionic or covalent radii for Mg and Si, although shorter than the sum of van der waals radii, which is much smaller than the diviation in the Ca-Si and Yb-Si that occur as a result of one short interaction due to the agostic interaction. Another structural support against β-agostic SiH in the X-ray structure of **1** is the large torsion angles for M-C-Si-H, the smallest of which is 25.79° for Mg3-C29-Si8-HS8.

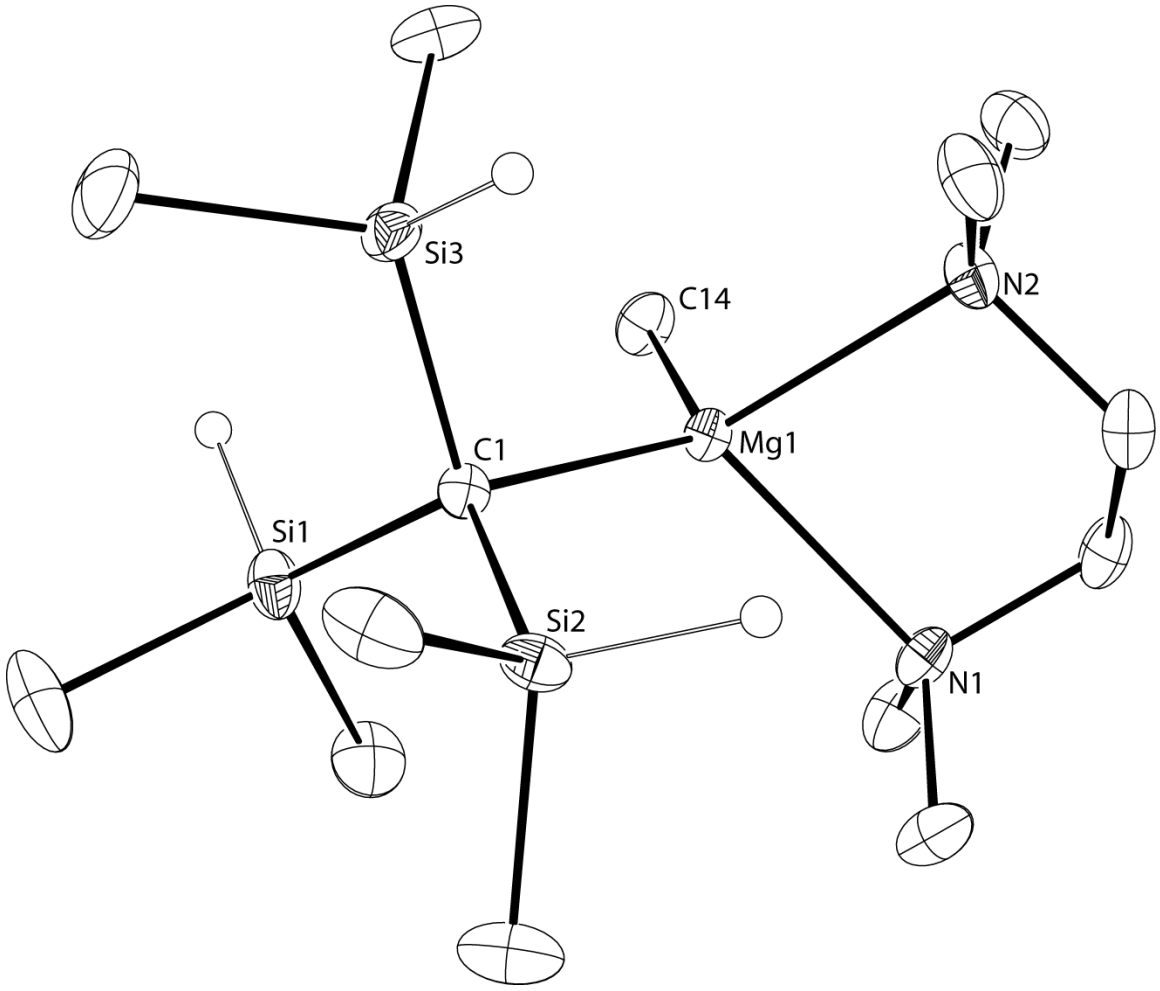

Figure 4.1. ORTEP diagram of one molecule of **4.1**. Ellipsoids are drawn at 35% probability, and the only hydrogen atoms shown are bonded to silicon. The other two, crystallographically independent $MeMgC(SiHMe_2)_3(TMEDA)$ molecules are not shown.

4.2. Synthesis of $MgC(SiHMe_2)_3I(TMEDA)$ (4.2).

Reaction of **4.1** with $SiMe_3I$ in benzene cleanly afforded alkylGrignard $MgIC(SiHMe_2)_3(TMEDA)$ **(4.2)** in good yield (eq 4.2). $SiMe_4$ was observed to evolve in a micromolar scale reaction in benzene-d_6.

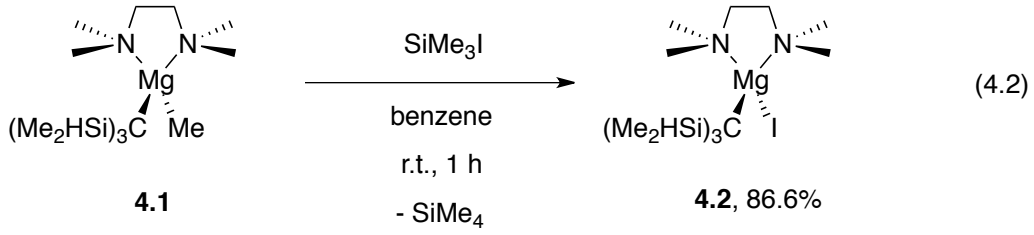

4.1 **4.2**, 86.6% (4.2)

The ^{1}H, ^{13}C and ^{29}Si NMR spectra of **4.2** are very similar to **4.1**, except in the absence of the MgMe resonance. The SiH and SiMe resonances were observed at 4.72 ppm ($^{1}J_{SiH}$ = 169.8 Hz) and 0.57 ppm ($^{3}J_{HH}$ = 3.6 Hz), respectively in ^{1}H NMR spectrum. Similar to **4.1**, TMEDA ligand exhibits diastereotopic resonances for both NMe_2 (2.20 and 1.99 ppm) and NCH_2 (1.79 and 1.49 ppm). Also, the IR spectrum showed two stretching bands for ν_{SiH}, groups at 2078 and 2039 cm^{-1}. Though lower stretching frequency, they are unlikely to contain any secondary interactions.

4.3. Synthesis and characterization of [LiCH(SiHMe$_2$)$_2$](THF) (4.3-Li) and KCH(SiHMe$_2$)$_2$ (4.3-K).

The tris(silyl)anion [$KC(SiHMe_2)_3$] described above is the 'SiH-functionalized' version of the extremely bulky trisyl potassium, we were interested in a less bulky bis(silyl)methyl anion $[CH(SiHMe_2)_2]^-$ as a SiH-containing derivative of bis(trimethylsilyl)methylpotassium. The $CH(SiMe_3)_2$ ligand[15,16] and the N analog of SiH-containing bis(dimethylsilyl)amido ligand $N(SiHMe_2)_2$[17] have been widely used in coordination chemistry in both main group and rare-earth chemistry. The incorporation of two $SiMe_3$ groups for a sterically less hindered environment allow some interesting yet reactive compounds to be insolated. For example, the solvent-free homoleptic trisalkyl lanthanides $Ln[CH(SiMe_3)_2]_3$[16] were synthesized that exclude coordination of solvent

molecules. Moreover, the steric bulk of the ligand also allows isolation of highly reactive moiety, for example, the highly active alkylperoxide group in Al alkylperoxide (Nacnac)AlOO^{t}Bu[CH(SiMe$_3$)$_2$][18] could be stabilized using CH(SiHMe$_2$)$_2$. The ability to engage in M---H---Si interaction allows stabilization of coordinatively unsaturated compounds. [19] In addition, the benefit of having α-H to anchor a β-SiH containing alkyl framework may allow us to study the how the β-SiH affect the acidity of the α-H (α-abstraction reaction).

However, attempts to prepare bis(dimethylsilyl)methyllithium by modification of the route to [LiCH(SiMe$_3$)$_2$] by transmetalation of BrHC(SiHMe$_2$)$_2$ with *n*-BuLi was previously reported to give [(SiHMe$_2$)$_2$CH]SiMe$_2$CH$_2$SiHMe.[20] Instead, we pursued [CH(SiHMe$_2$)$_2$]$^-$ by deprotonation of H$_2$C(SiHMe$_2$)$_2$ based on the effect of β-SiH groups on the acidity of an adjacent CH bond. For example, the acidity of HN(SiHMe$_2$)$_2$ (pKa 22.8) is higher than that of HN(SiMe$_3$)$_2$ (pKa 25.8).[17b] This trend appears to extend to carbon; thus, HC(SiMe$_3$)$_3$ is deprotonated by by MeLi in Et$_2$O/THF mixtures giving 80% yield after 20 h at reflux[21] whereas HC(SiHMe$_2$)$_3$ is deprotonated under less forcing conditions at room temperature after 6 h by lithium diisopropylamide.[22] The analog to the desired bis(dimethylsilyl)methyl anion, bis(trimethylsilyl)methyl anion can be prepared by deprotonation of H$_2$C(SiMe$_3$)$_2$; however, forcing conditions require the use of *t*-BuLi in THF/HMPA mixtures.[23] According to the trend in acidities, we expected that deprotonation of H$_2$C(SiHMe$_2$)$_2$ could be accomplished under milder conditions in the absence of HMPA. In fact, treatment of H$_2$C(SiHMe$_2$)$_2$ with *t*-BuLi in THF at -90 °C affords the desired [LiCH(SiHMe$_2$)$_2$] (eq 9.3). However, this deprotonation reaction is extremely sensitive to the nature of the base and conditions. Initial experiments showed that *n*-BuLi or Schlosser base (MeLi and KO*t*-Bu)[24]

give mixtures of unidentified products. Interestingly, when bis(dimethylsilyl)methane was treated with KCH_2Ph, unexpected silyl group redistribution occurs to yield [$KC(SiHMe_2)_3$] as the major product. Reactions with *t*-BuLi in non-coordinating solvents such as pentane yield only trace amount of the desired lithiated product.

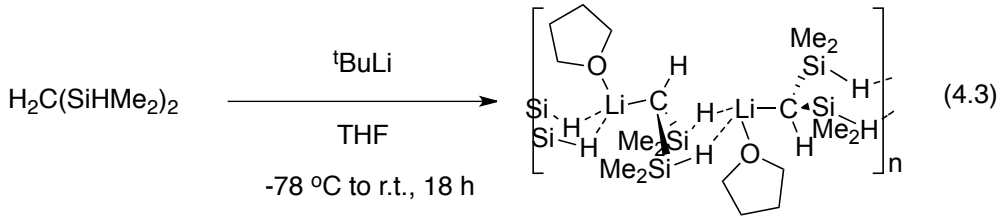

(4.3)

4.3-Li, 36.1%

The formulation of [$LiCH(SiHMe_2)_2(THF)$] is confirmed by NMR and IR spectroscopy as well as X-ray crystallography. The ^1H NMR spectrum contained only one type of SiH group (δ_{SiH} 4.63), but the IR (KBr) spectrum of **4.3-Li** contains two bands assigned to SiH stretching frequencies (ν_{SiH} 2108 and 1986 cm^{-1}). In the solid state of [$LiCH(SiHMe_2)_2THF$], **4.3-Li** forms a linear polymeric structure in the solid state (see Figure 4.1). Such arrangement is rare among lithium alkyl complexes, which typically form small clusters, although both $[NaCH(SiMe_3)_2]_n$ and $[KCH(SiMe_3)_2]_n$ form polymeric chain structure.[25] Unlike solvent -free [$LiCH(SiMe_3)_2$], one molecule of THF is coordinated to lithium in **4.3-Li**. Additionally, short Si—H—Li distances (2.23(4) Å) were observed for both SiH groups to the neighboring lithium center that continues a polymeric structure. Such agostic interaction explains the two ν_{SiH} bands corresponding to the two types of ν_{SiH} in IR.

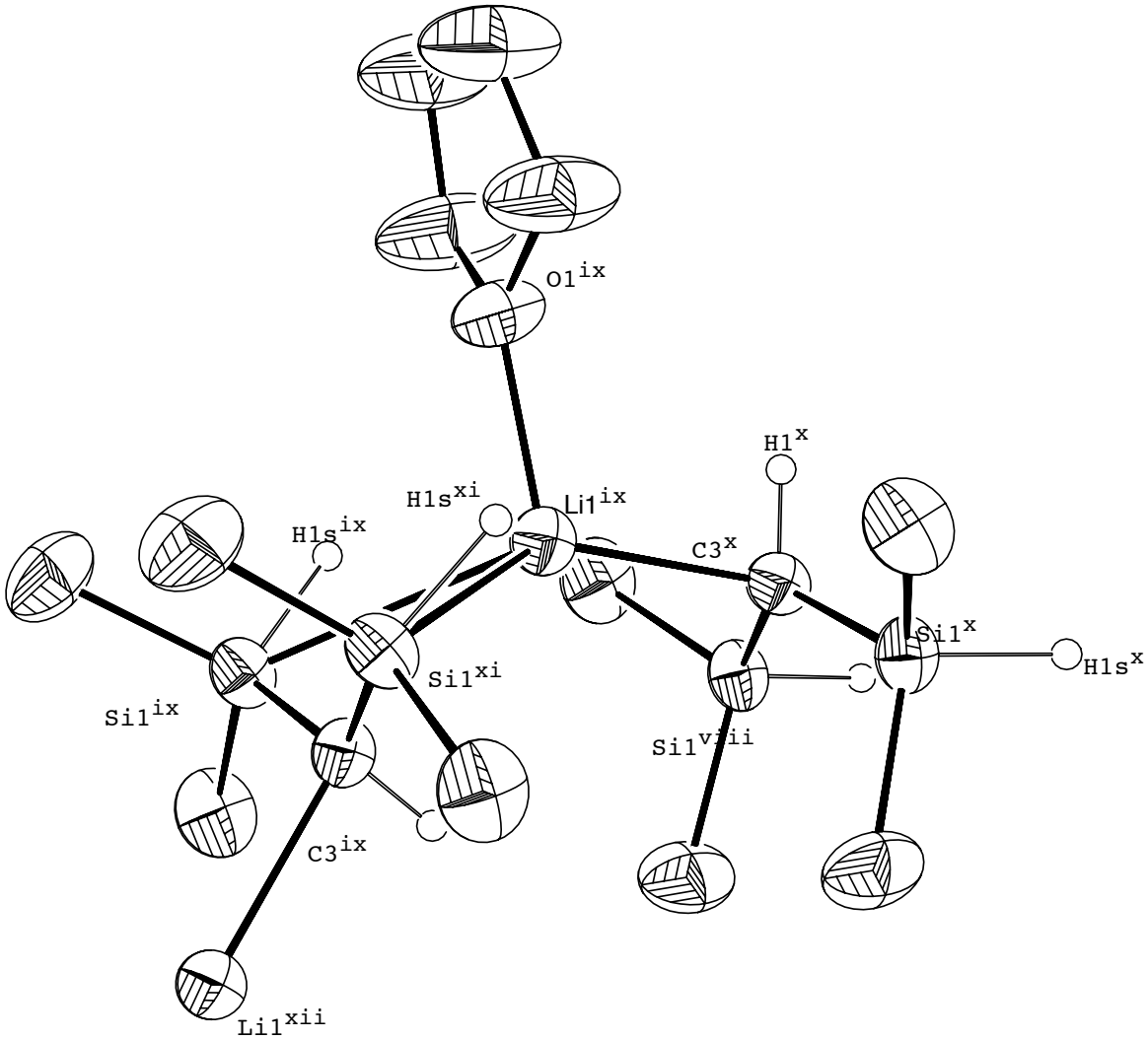

Figure 4.2. ORTEP diagram of one molecule of [LiCH(SiHMe$_2$)$_2$(THF)] (**4.3-Li**). Ellipsoids are drawn at 35% probability, and the only hydrogen atoms shown are bonded to silicon.

Treatment of **4.3-Li** with 1 equiv. of KOtBu in pentane at room temperature affords THF-free [KCH(SiHMe$_2$)$_2$] **(4.3-K)** as a highly moisture and air-sensitive off-white amorphous solid after washing with pentane to remove lithium *t*-butoxide (eq 4.4). NMR

spectra of a freshly prepared sample of **4.3-K** in benzene-d_6 revealed that even at ambient temperature **4.3-K** was slowly decomposed with formation of $H_2C(SiHMe_2)_2$, but it is stable when stored at -30 ^oC in inert atmosphere.

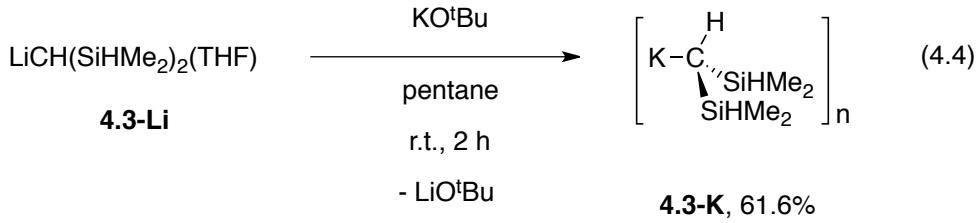

(4.4)

4.3-K is insoluble in aliphatic solvent and is only sparingly soluble in benzene. The ^1H NMR of **4.3-K** in benzene-d_6 contained resonances at 4.73 ($^1J_{SiH}$ = 150.0 Hz), 0.35 and -2.14 ppm that are assigned to SiH, $SiMe_2$ and CH groups, respectively. The chemical shift of the CH group is shifted ca. 0.2 ppm upfield to that of **4.3-Li** and about the same as that of $KCH(SiMe_3)_2(THF)$[25]. In contrast to the SiH resonance in 1H NMR, the IR spectrum of **4.3-K** contained two SiH stretching bands at ν_{SiH} 1854, and 1805 cm^{-1}. The low solubility of **4.3-K** prevents any low-temperature NMR study. Furthermore, the combination of low solubility in aromatic solvent and the absence of THF coordination suggest **4.3-K** in solid state may adopt a polymeric structure analogous to $[KCH(SiMe_3)_2]_n$.

4.4 Synthesis of Mg(CH(SiHMe$_2$)$_2$)Me(TMEDA) (4.4-Me) and Mg(CH(SiHMe$_2$)$_2$)Br(TMEDA) (4.4-Br).

Unfortunately, the analogous salt metathesis reactions between MeMgBr(TMEDA) and $LiCH(SiHMe_2)_2(THF)$ or $KCH(SiHMe_2)_2$ provide a mixture of the desired $MeMgCH(SiHMe_2)_2(TMEDA)$ (**4.4-Me**) and $MgBrCH(SiHMe_2)_2(TMEDA)$ (**4.4-Br**) in a 4.37 : 1 ratio (eq 4.5) based on integration in ^1H NMR spectrum.

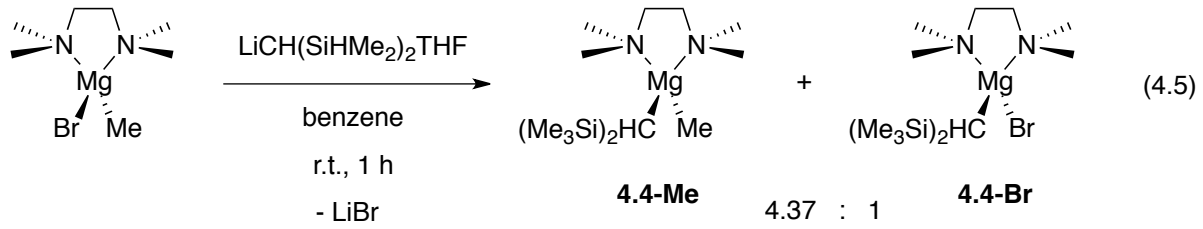

(4.5)

The observed product mixture can be explained by two scenarios: a) **4.4-Me** formed reacts with the by-product LiBr to provide **4.4-Br**; b) MeMgBr(TMEDA) undergoes partial disproportionation reaction to give a mixture of MeMgBr(TMEDA), $MgBr_2$(TMEDA), and $MgMe_2$(TMEDA) prior to the reaction with the Li alkyl. To test the first scenario, the NMR experiment of MeMgBr(TMEDA) and $LiCH(SiHMe_2)_2$(THF) in benzene-d_6 was thermolyzed to 85 ^oC for 4 h after observing the ratio of mixture of **4.4-Me** and **4.4-Br** was developed. However, the product ratio was not affected. To avoid salt contamination, $KCH(SiHMe_2)_2$ was used. KBr is expected to show less solubility than LiBr in benzene, thus less likely to react with **4.4-Me**. The product ratio of **4.4-Me** and **4.4-Br** remains the same. Therefore, the pre-equilibrium of MeMgBr(TMEDA), $MgBr_2$(TMEDA), and $MgMe_2$(TMEDA) may prove problematic in the synthesis of **4.4-Me**, though unexpected, it does not affect the synthesis of **4.1**. Although **4.4-Me** cannot be isolated, its identity can be revealed from the ^1H NMR spectrum, which contained resonances at 0.55 and 0.51 ppm for the diastereotopic $SiMe_2$ groups, 4.77 ppm ($^1J_{SiH}$ = 163.2 Hz) for SiH group and -1.66 ppm for the CH group. The chemical shifts of the $SiHMe_2$ group in **4.4-Me** are not very different than those in **1**. The most interesting feature is the similar $^1J_{SiH}$ between **4.1** and **4.4-Me**. Apparently, although **4.1** processes an extra $SiHMe_2$ group, the electronic natures of in MeMgR(TMEDA) [R = $CH(SiHMe_2)_2$ and $C(SiHMe_2)_3$] are not very different.

A single crystal X-ray diffraction study of **4.4-Me** showed its monomeric nature and the magnesium center unambiguously showed that both N atoms coordinate to Mg center in a tetrahedral fashion. **4.4-Me** crystallizes with two crystallographically independent molecules in the unit cell (one is shown in Figure 4.3). The Mg-C bond distance in MgMe (2.130(2) Å) is a little shorter than the M-C bond in $MgCH(SiHMe_2)_2$ (2.174(2) Å). The Mg-C distance is within error identical to that of **4.1**, but the M-C bond of the silylalkyl ligand in **4.4-Me** is shorter than that of **4.1** by 0.05 Å. The MgMe group is located *trans* to the α-CH group of $–CH(SiHMe_2)_2$, probably as a result from steric pressure imposed by the Me groups on tmeda. Both Hs on the $SiHMe_2$ groups are 3.41(2) and 3.44(2) Å from the Mg center. Though pointing towards Mg, they are unlikely to engage in any secondary Mg—H—Si interactions, similar observation was also observed in $Mg\{N(SiHMe_2)_2\}_2THF_2$.[26] The geometry of the central carbon in $CH(SiHMe_2)_2$ (338.3 °) is distorted from the sp^3 hybridization (328°), resulting from the direct connection to two electropositive Si atoms.

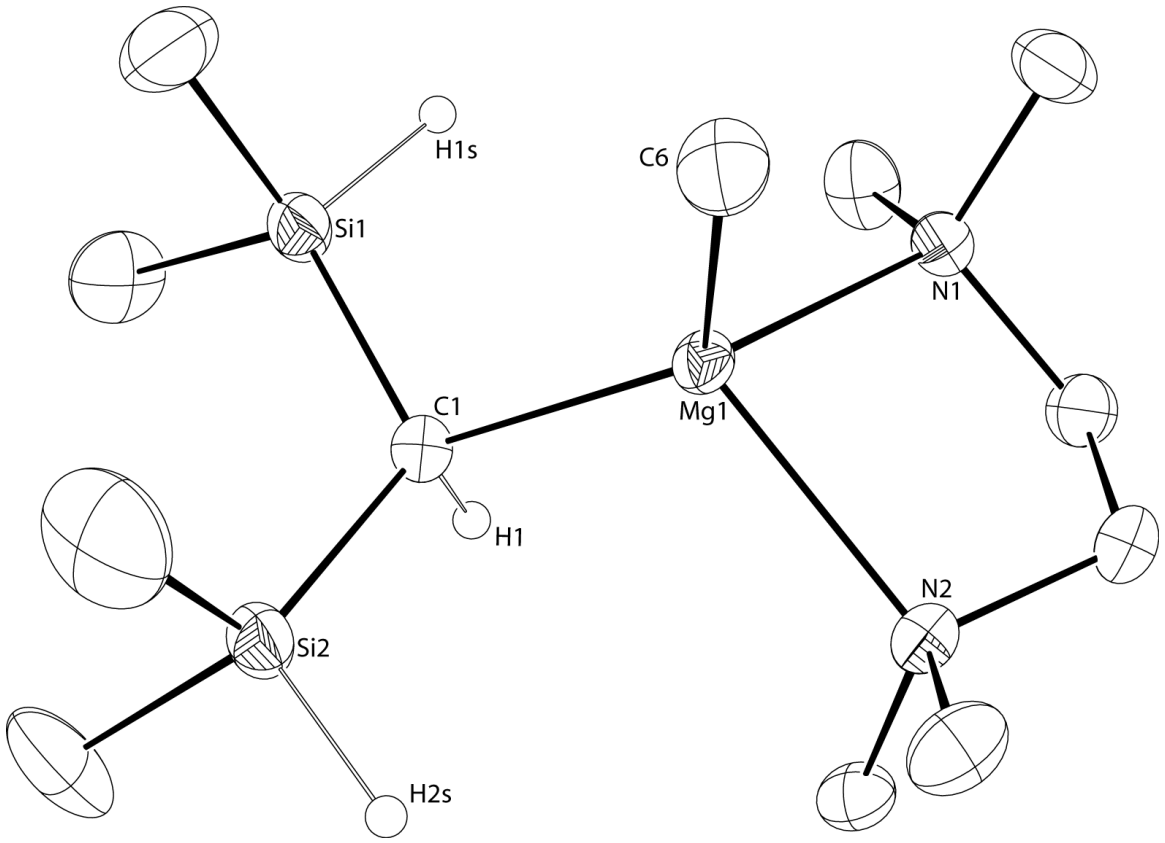

Figure 4.3. ORTEP diagram of $MeMgCH(SiHMe_2)_2(TMEDA)$ (**4.4-Me**). Ellipsoids are drawn at 35% probability. H atoms on TMEDA and on methyl groups are not included for clarity. Selected bond distances (Å): Mg2-Si5, 2.6414(9); Mg2-C32, 2.222(2); Mg-N3, 2.210(2); Mg-N4, 2.213(2). Selected bond angles (°): Si5-Mg2-C32, 120.73(6); N3-Mg2-N4, 82.67(8).

Analytically pure **4.4-Br** can be synthesized by addition of excess amount of $SiMe_3Br$ into a benzene solution of the mixture of **4.4-Me** and **4.4-Br** for 12 h. After removing the by-product $SiMe_4$ and excess $SiMe_3Br$, **4.4-Br** was isolated quantitively as a white crystalline solid (eq 4.6).

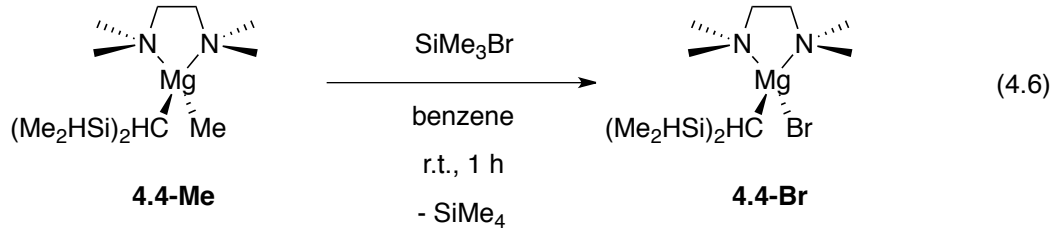

4.4-Me **4.4-Br** (4.6)

The ^{1}H NMR spectrum of **4.4-Br** contained one SiH resonance at 4.73 ppm ($^{1}J_{SiH}$ = 164.9 Hz), two diastereotopic SiMe resonances at 0.60 ppm ($^{3}J_{HH}$ = 3.5 Hz) and 0.50 ppm ($^{3}J_{HH}$ = 3.4 Hz) and one CH resonance at -1.63 ppm. Those chemical shifts are comparable to **4.4-Me**. Furthermore, the ^{29}Si NMR shifts are almost identical (4-Me: 16.7 ppm; 4-Br: 16.9 ppm). The high stretching frequency of SiH group in IR spectroscopy at 2068 cm^{-1} suggests there is no β-SiH agostic interaction with the Mg center either. This suggests that substitution of a methyl to a bromide group does not influence the overall electronic nature of the alkyl framework. Notably, it's worthwhile to consider that the TMEDA ligand in both **4.4-Me** and **4.4-Br** undergoes fast exchange process that results in board TMEDA resonances at room temperature, while this process was not observed in **4.1** that includes a more sterically hindered silylalkyl ligand.

4.5. Synthesis of Mg(CH(SiMe$_3$)$_2$)Me(TMEDA) (4.5).

The analogous Mg mixed alkyls compound without SiH group MeMgCH(SiMe$_3$)$_2$(TMEDA) (**4.5**) was prepared in similar route from MeMgBr(TMEDA) and LiCH(SiMe$_3$)$_2$ in 64.7% yield after recrystallization from pentane (eq 4.7).

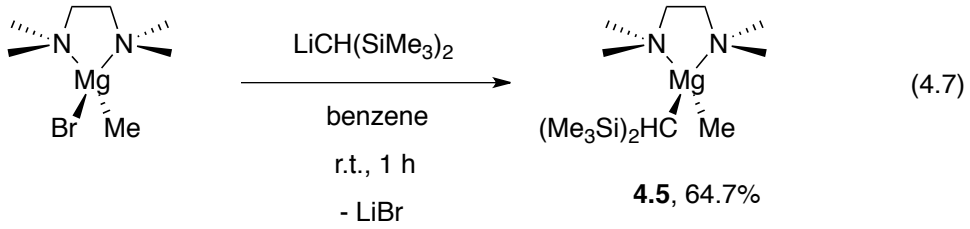

(4.7)

The contamination of Br adduct was not observed in this case. **4.5** was observed as the sole product after re-crystallization. The ^{1}H NMR and ^{13}C NMR spectra were expected for the formulation of **4.5**. One notable feature is that the TMEDA ligand showed as board resonances for NMe_2 and NCH_2 that implied the diamine ligand might undergo fast exchange at room temperature. **4.5** crystallizes with two independent molecules in the unit cell that have the same constitution and connectivity (only 1 is shown in Figure 4.4). There are slight differences in the distances and angles in the compounds that are likely chemically insignificant. For example Mg-CH3 (Mg1-C8, 2.279(2); Mg2-C26, 2.297(2)) and Mg-CH(SiMe3)2 (Mg-C1, 2.186(2); 2.191(3)).

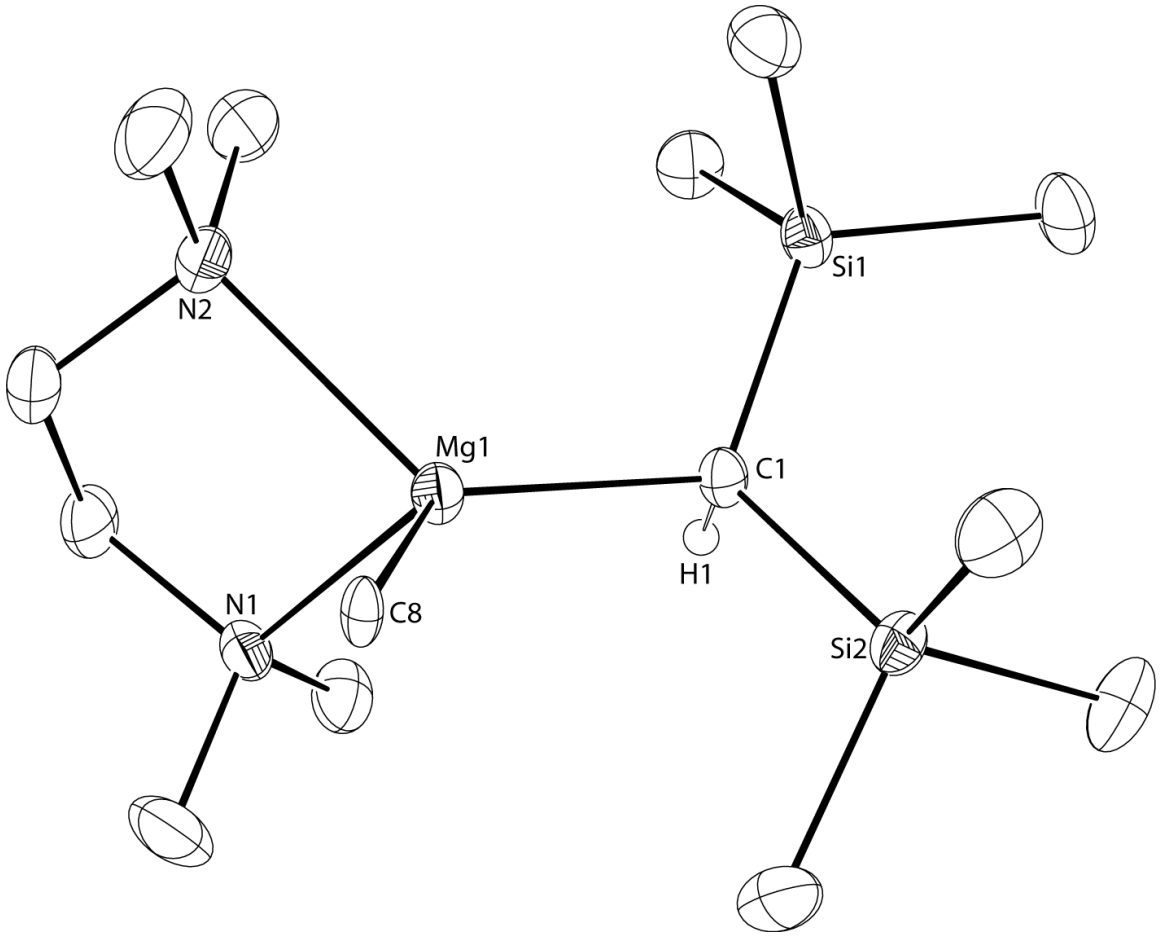

Figure 4.4. ORTEP diagram of $MgMeCH(SiMe_3)_2(TMEDA)$ (**4.5**). Ellipsoids are drawn at 35% probability. H atoms on TMEDA and on methyl groups are not included for clarity. Selected bond distances (Å): Mg2-Si5, 2.6414(9); Mg2-C32, 2.222(2); Mg-N3, 2.210(2); Mg-N4, 2.213(2). Selected bond angles (°): Si5-Mg2-C32, 120.73(6); N3-Mg2-N4, 82.67(8).

4.6. Synthesis of $MgICH(SiMe_3)_2(TMEDA)$ (4.6).

Analoguous to the synthesis of **4.2**, reaction of **4.5** with $SiMe_3I$ in benzene cleanly afforded alkylGrignard $MgICH(SiMe_3)_2(TMEDA)$ (**4.6**; eq 4.8) in good yield. $SiMe_4$ was observed to evolve in a micromolar scale reaction in benzene-d_6.

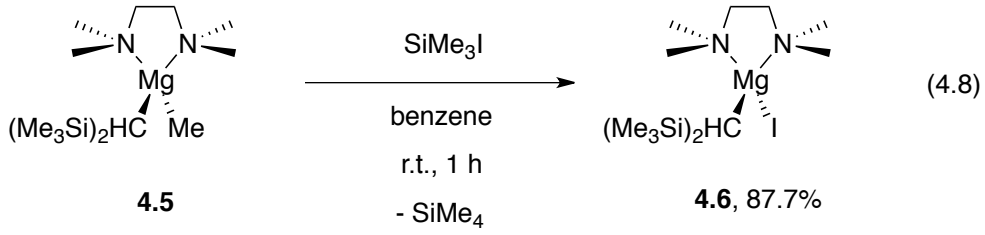

4.5 **4.6**, 87.7% (4.8)

The ^{1}H, ^{13}C and ^{29}Si NMR spectra of **4.6** are very similar to **4.5**, except in the absence of the MgMe resonance. The SiMe and CH resonances were observed at 0.45 and -1.58 ppm respectively in ^{1}H NMR spectrum. It is worthwhile to consider the Mg-C bond distances for the four alkyl ligands Me, $C(SiHMe_2)_3$, $CH(SiHMe_2)_2$, and $CH(SiMe_3)_2$ over the series to evaluate the effect of the different silylmethyl ligands on the Mg-Me distance and the magnesium silylmethyl distance. From Table 4.1, the Mg-Me distances for compounds with dimethylsilylmethyl ligands (either $C(SiHMe_2)_3$ or $CH(SiHMe_2)_2$ are considerable shorter than the Mg-Me distances for the compounds with $CH(SiMe_3)_2$ groups (i.e. lacking β-SiH). This is clearly due to an electronic effect of the β-SiH on the Mg-Me distance, since the steric encumbrance is $C(SiHMe_2)_3$ > $CH(SiMe_3)_2$ > $CH(SiHMe_2)_2$ (based on solid angles, Table 4.2).[27] Alternatively, the Mg-C distance in the silylmethyl ligands correlates with the steric bulk of the ligand *except when CH3 is replaced with I* (Table 4.3).

Table 4.1. Mg-Me and Mg-C bond lengths

Compound	Mg-Me (Å)	M-CSi_n (Å)
$MgMeC(SiHMe_2)_3$(TMEDA) A (**4.1**)	2.147(3)	2.221(3)
$MgMeC(SiHMe_2)_3$(TMEDA) B (**4.1**)	2.142(2)	2.223(3)
$MgMeC(SiHMe_2)_3$(TMEDA) C (**4.1**)	2.140(2)	2.222(3)
$MgMeCH(SiHMe_2)_2$(TMEDA) (**4.4-Me**)	2.126(2)	2.174(2)

$MgMeCH(SiMe_3)_2(TMEDA)$ (**4.5**)	2.296(2)	2.185(2)
$MgIC(SiHMe_2)_3(TMEDA)$ (**4.2**)	n.a.	2.175(5)
$MgIC(SiHMe_2)_3(TMEDA)$ (**4.2**)	n.a.	2.182(5)

Table 4.2. Solid angle for comparing $C(SiHMe_2)_3$, $CH(SiHMe_2)_2$ and $C(SiMe_3)_3$

Compound	Ligand	Solid Angle	alkyl % occupancy
$MeMgC(SiHMe_2)_3TMEDA$ (**4.1**)	C(SiHMe2)3	4.13	32.89
$MeMgCH(SiHMe_2)_2TMEDA$ (**4.4-Me**)	CH(SiHMe2)2	3.15	25.04
$MeMg(CH(SiMe_3)_2)TMEDA$ (**4.5**)	CH(SiMe3)2	3.71	29.56

Table 4.3. Solid angle for Me and TMED for comparing $C(SiHMe_2)_3$, $CH(SiHMe_2)_2$ and $C(SiMe_3)_3$

Compound	Me-Solid Angle	Me % occupancy	TMEDA Solid Angle	TMEDA % occupancy
$MeMgC(SiHMe_2)_3(TMEDA)$ (**4.1**)	1.90	15.14	4.52	35.89
$MeMgCH(SiHMe_2)_2(TMEDA)$ (**4.4-Me**)	1.94	15.42	4.61	36.67
$MeMgCH(SiMe_3)_2(TMEDA)$ (**4.5**)	1.62	12.89	4.53	36.04

4.7. Reaction of $MeMgC(SiHMe_2)_3(TMEDA)$ (4.1) and $MgIC(SiHMe_2)_3(TMEDA)$ (4.2) with Lewis acids.

Alkyl group abstraction by organometallic Lewis acids represents the most general methodology to generate cationic complexes that are important catalysts in polymerization.[28] The commonly used Lewis acid is $B(C_6F_5)_3$ due to its strong electrophilic character and its tendency to form weakly-coordinating anion upon anionic group abstraction. There are few

cationic Mg alkyl compounds reported and the method used to synthesize these elusive compounds was to highly acidic protic reagent with a weakly coordinating anion, such as $[H(OEt_2)][B(C_6F_5)_4]$.[29] Here, we intended to synthesize cationic magnesium alkyl compounds containing β-H containing silylalkyl ligands by anionic group abstraction by Lewis acids. Unfortunately, the reaction between **4.1** and $B(C_6F_5)_3$ in bromobenzene-d_5 gave a mixture of products, including both the desire methide abstracted product, $[MgC(SiHMe_2)_3][MeB(C_6F_5)_3](TMEDA)$ **(4.7)**, and the β-SiH abstracted product, $[MgMe][(\mu\text{-}H)B(C_6F_5)_3](TMEDA)$, in ca. 10:1 ratio, based on the integration of a ^1H NMR spectrum. This is also easily determined by ^{11}B NMR spectroscopy, which exhibits a sharp singlet corresponding to the $MeB(C_6F_5)_3$ anion at -14.4 ppm and a board resonance for the $HB(C_6F_5)_3$ anion at -22.6 ppm. The methyl resonance of $MeB(C_6F_5)_3$ was detected at 0.95 ppm in ^1H NMR spectrum that is more downfield than free $MeB(C_6F_5)_3$ (ca. 0.45 pp,)[30] and **4** could be described better as contacted ion-pair. Another method to identify between zwitterionic species to sovent-separated ion-pair is to measure the $\delta\ para_F - \delta\ meta_F$ in ^{19}F NMR spectrum. The ^{19}F NMR chemical shift difference for *meta* and *para* fluorine resonances in **4.7** is 3.4 ppm. Previously, Horton suggested that a value of $\delta\ para_F - \delta\ meta_F$ less than 3.5 corresponds to a $[X_3Zr][MeB(C_6F_5)_3]$ inner sphere interaction, whereas $\Delta(\delta para_F - \delta meta_F) > 3.5$ indicates that a solvent-separated ion pair is formed.[31] By this measure, **4.7** is best described as $[MgSi(SiMe_3)_3(\mu\text{-}Me)B(C_6F_5)_3](TMEDA)$.

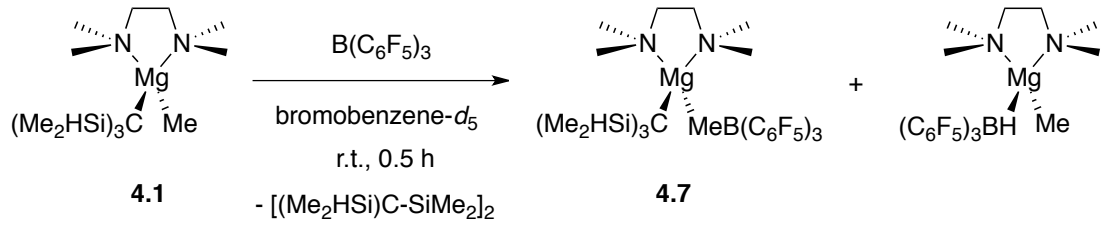

4.1 **4.7** (4.9)

In benzene-d_6, the reaction is less selective. A mixture of [MgC(SiHMe$_2$)$_3$(μ-Me)B(C$_6$F$_5$)$_3$](TMEDA) (**4.7**) and [MeMg(μ-H)B(C$_6$F$_5$)$_3$](TMEDA) was formed in a ~1:1 ratio after 30 min, indicating that MgMe and SiH abstraction occurred. Crosspeaks in ^{1}H-^{11}B HMQC experiments allow the identification of HB(C$_6$F$_5$)$_3$ and MeB(C$_6$F$_5$)$_3$ in the ^{1}H NMR spectrum at xxx and 0.95 ppm, respectively. The ^{1}H NMR spectrum also shows the presence of 1,3-disilacyclobutane that results from head-to-tail dimerization of Me$_2$Si=C(SiHMe$_2$)$_2$.[22] A small amount of HC(SiHMe$_2$)$_3$ is formed, likely due to decomposition of **9.7**. There was no change to the spectra over 16 h in bromobenzene-d_5, and in benzene-d_6, only small increase in disilacyclopbutane was observed. Upon addition of a second equivalent of B(C$_6$F$_5$)$_3$ to the benzene solution, the resonance for C(SiHMe$_2$)$_3$ group was not observed and was completely transformed into disilacylobtane. The other organometallic product [Mg(μ-H)B(C$_6$F$_5$)$_3$(μ-Me)B(C$_6$F$_5$)$_3$](TMEDA) (**4.8**) precipitated out of the solution over a period of 10 min in benzene (eq 4.10).

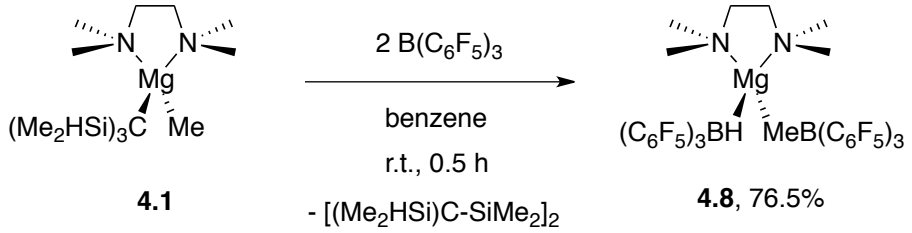

4.1 **4.8**, 76.5% (4.10)

It seems likely that the MgMe is a stronger nucleophile than the SiH groups in MeMgC(SiHMe$_2$)$_3$(TMEDA), however, the SiH group is clearly (and perhaps surprisingly) competitive with the MgMe in the reaction with B(C$_6$F$_5$)$_3$. Therefore, we also looked at the reaction of MgC(SiHMe$_2$)$_3$ group with B(C$_6$F$_5$)$_3$ to examine the reactivity of β-SiH group with a strong Lewis acid. The reaction between MgMe-free **4.2** and B(C$_6$F$_5$)$_3$ in benzene immediately gave 1,3-disilacyclobutane and [MgI(μ-H)B(C$_6$F$_5$)$_3$](TMEDA) (**4.9**; eq 4.11).

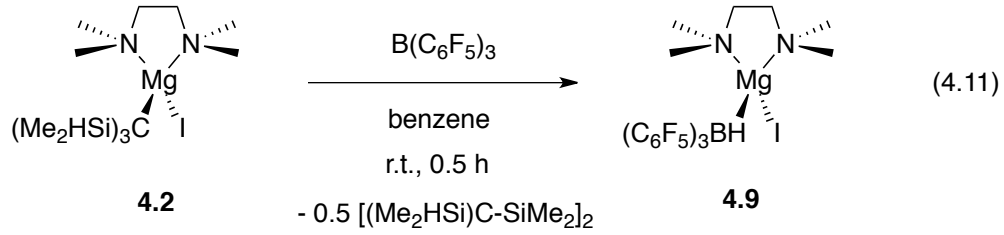

(4.11)

Compound **4.9** appeared to be more soluble in benzene than **4.8**. The hydridoborate moiety was unambiguously assigned by ^{1}H and ^{11}B NMR spectroscopy. The *H*B group was observed as a board quartet at 2.25 ppm in ^{1}H NMR and -20.9 ppm ($^{1}J_{BH}$ = 64.7 Hz) in ^{11}B NMR spectra. The isolation of [MgI(μ-H)B(C_6F_5)$_3$](TMEDA) implied the β-SiH is also susceptible toward β-H abstraction. Thus, other electrophiles including BPh_3 and $PhB(C_6F_5)_2$ were allowed to react with **4.1** for comparison. Because BPh_3 and $PhB(C_6F_5)_2$ are weaker electrophiles than $B(C_6F_5)_3$, its selectivity for the stronger nucleophile is expected to be greater. When BPh3 or $PhB(C_6F_5)_2$ and **4.1** react in benzene-d_6, the methide abstraction product is observed as the sole product, no silene-dimer $[Me_2Si\text{-}C(SiHMe_2)_2]_2$ was detected for possible β-H abstraction by borane. However, the low solubility of resulting adducts resulted in precipitation of **4.10** slowly at room temperature. After further benzene and pentane washes, **4.10** was isolated as a white solid in 62% yield (eq 4.12). The C_6F_5 group enhances the solubility of the adduct, but oily residue of **4.11** slowly formed and precipitated out of the benzene solution overtime (eq 4.12).

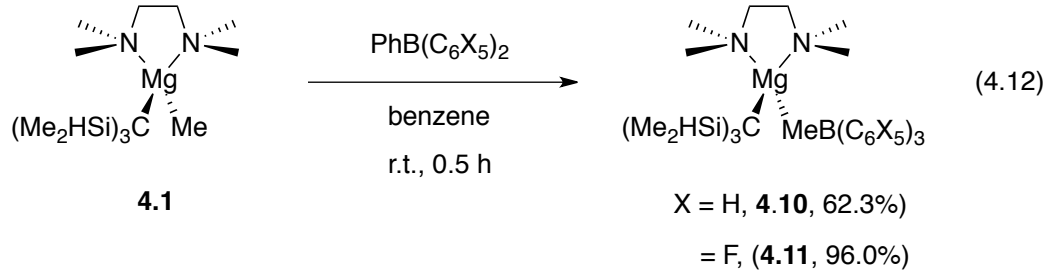

(4.12)

Compound **4.10** is only sparingly soluble in bromobenzene but soluble enough for identification of the product. The ^{1}H NMR of **4.10** in bromobenzene-d_5 consisted of the resonance of methyl borate group at 0.52 ppm. Abstraction reaction from BPh_3 often results in zwitterionic speces formation. For example, contacted ion-pair Yb[(μ-H)BPh_3]$_2$THF was isolated in the reaction of Yb[C(SiHMe_2)$_3$]$_2$THF_2 with BPh_3.[5] The $SiMe_2$ resonance (0.24 ppm, $^{3}J_{HH}$ = 2.4 Hz) also shifted upfield compared to its neutral counterpart. Three IR bands for SiH groups (ν_{SiH}) were detected in IR spectroscopy at 2085, 2067 and 2047 cm^{-1}. Although the SiH groups are not equivalent in solid state, the high $^{1}J_{SiH}$ (171.0 Hz) and high energy for the SiH stretching frequency again suggests **4.10** is absent of β-SiH agostic interaction with Mg center. Also, this has the implications for the preference of methide abstraction over β-H abstraction by BPh_3, as suggested by no further abstraction being observed with more than 1 equiv. of BPh_3 (3 equiv.). The MeB was observed at 0.84 ppm and the SiH resonance is at 4.35 ppm ($^{1}J_{SiH}$ = 166.4 Hz) in benzene-d_6 in ^{1}H NMR, 0.1 ppm downfield to **4.8**. There is only one band in IR spectrum for SiH for **4.9** (ν_{SiH} 2105 cm^{-1}), which is surprisingly high energy compared to **4.1**, **4.5**, **4.7**, and **4.8**, and very close to that of free alkane HC(SiHMe_2)$_3$.

Alternatively, abstraction reactions with [Ph_3C][$B(C_6F_5)_4$] often provide solvent-separated ion pair due to the weakly coordinating $B(C_6F_5)_4$ anion. However, the $B(C_6F_5)_4$ anion is still capable of coordinating to a metal center through fluorine lone pairs, although examples for this coordination mode have only been observed in rare cases and only a very weak interaction is observed. Overall, while both $RBAr_3$ (Ar = Ph or C_6F_5) and $B(C_6F_5)_4$ may be described as "non-coordinating," such description is more appropriate to adducts with $B(C_6F_5)_4$ counterion. Thus, the abstraction reaction of **4.1** and [Ph_3C][$B(C_6F_5)_4$] was also

examined with goal to generate a true cationic Mg alkyl compound. The reaction in benzene-d_6 provided an oil layer; the only observed species was Ph_3CCH_3, indicative of methine abstraction by Ph_3C^+ (eq 4.13). Notably, 1,3-disilacyclobutane was not observed, which suggested β-H of $C(SiHMe_2)_3$ does not compete with MgMe toward Ph_3C^+ abstraction, as observed in the reaction with $B(C_6F_5)_3$. This is interesting since $[Ph_3C][B(C_6F_5)_4]$ is a stronger electrophile than $B(C_6F_5)_3$, one would expect more SiH abstraction be observed if SiH group is nucleophilic enough. Since the abstraction pattern is similar to BPh_3 and the size of both BPh_3 and Ph_3C^+ is also similar, therefore, the competitive abstraction observed using $B(C_6F_5)_3$ may be due to steric of having three C_6F_5 rings that are in close-proximity to the β-SiH when $B(C_6F_5)_3$ approaches to the Mg-Me group.

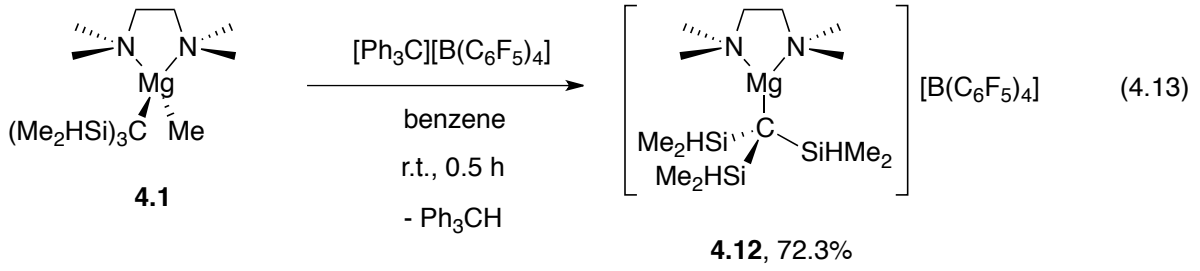

(4.13)

The ^{1}H NMR spectrum in bromobenzene-d_5 contained resonances at 4.23 ($^1J_{SiH}$ = 164.0 Hz), 2.10 and 0.15 ppm for SiH, TMEDA and $SiMe_2$ groups, respectively. Only one SiH band was observed in the IR spectrum at relatively high energy at 2092 cm^{-1}, which is typical for classical 2-center-2-electon Si-H group. The ^{1}H NMR spectrum obtained of $[MgC(SiHMe_2)_3][B(C_6F_5)_4]$(TMEDA) (**4.12**) in bromobenzene-d_5 supports the cationic behavior as the $SiMe_3$ and SiH resonances shifted more upfield (4.23 ($^1J_{SiH}$ = 164.0 Hz) and 0.15 ppm) compared to the neutral compounds $MeMgC(SiHMe_2)_3$(TMEDA). ^{11}B NMR also suggested a single four-coordinated borate product at -16.0 ppm.

Although **4.12** is likely to be a solvent-separated ion pair, surprisingly, the $^{1}J_{SiH}$ and ν_{SiH} in IR does not vary much with the neutral compound **4.1** for zwitterionic compounds **4.7**, **4.10**, and **4.11**. Similar phenomenon was observed for $M[N(SiHMe_2)_2]_2THF_n$ (M = Mg, Ca, Sr, Ba). The $Mg[N(SiHMe_2)_2]_2THF_2$ does not process secondary interaction, highlighted by its high energy IR band for SiH group at 2050 cm^{-1} [Anwander, DT 2012], while the IR of the SiH for heavier congener $Ca[N(SiHMe_2)_2]_2THF_2$ is at 2028, 1959 cm^{-1}, the second low energy band indicates the later compound is stabilized by β-SiH agostic interaction [Carpentier OM 2010]. The lack of b-agostic interaction in the apparent coordinatively unsaturated Mg compounds may be due to its small ionic radii and high electronegativity compared to its heavier Group 2 congeners.

4.8. Reaction of $MeMgC(SiMe_3)_2$(TMEDA) (4.5) with Lewis acids.

In the absence of β-SiH group, the abstraction reactions of **4.5** with either BPh_3 or $B(C_6F_5)_3$ take place specifically on MgMe group to give $[MgC(SiHMe_2)_3(\mu$-Me)$BPh_3]$(TMEDA) **(4.13)** or $[MgC(SiHMe_2)_3(\mu$-Me)$B(C_6F_5)_3]$(TMEDA) **(4.14)** in reasonable yield (eq 4.14).

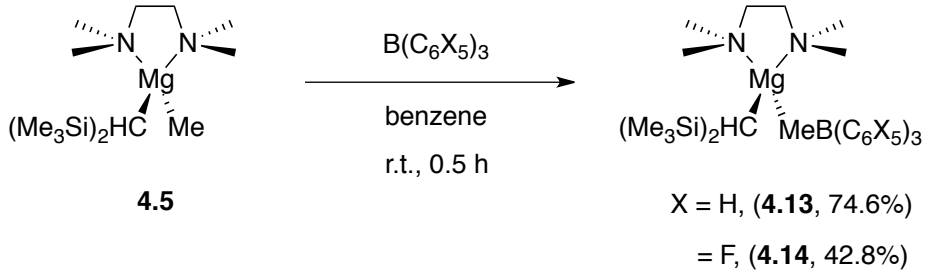

4.5

X = H, (**4.13**, 74.6%)

= F, (**4.14**, 42.8%)

(4.14)

The chemical shift of SiMe group shifted ca. 0.3-0.4 ppm upfield from the neutral analog in ^{1}H NMR spectrum that is typical for cationic compounds. The MgMe resonance

vanished upon abstraction by boranes and a new board resonance (**4.13**, 0.68 ppm; **4.14**, 0.92 ppm) appeared and was assigned to B*Me*. The BMe resonance for **4.13** is more downfield than the free $MeB(C_6F_5)_3^-$ and the ($\Delta\delta m,p$) in ^{19}F NMR spectrum of 3.3 ppm suggested **4.14** is better formulated as zwitterionic [$MgCH(SiMe_3)_2(\mu$-Me)$B(C_6F_5)_3$](TMEDA).

Conclusion.

A series of monomeric neutral, zwitterionic and cationic magnesium alkyl compounds containing the tris(dimethylsilyl)methyl -$C(SiHMe_2)_3$, bis(dimethylsilyl)methyl -$CH(SiHMe_2)_2$, and bis(trimethylsilyl)methyl -$CH(SiMe_3)_2$ ligand are synthesized. Surprisingly, the spectroscopic data (^{1}H NMR chemical shift, $^1J_{SiH}$ coupling constant, and ν_{SiH} IR band) suggests the isolated β-SiH containing zwitterionic or cationic Mg complexes do not process agostic Si—H—Mg interaction. The result is in sharp contrast to the corresponding Ca and Yb complexes with $C(SiHMe_2)_3$ ligand. Also, the preference of Mg methyl group abstraction in opposed to β-SiH abstraction also suggests β-SiH groups in Mg complexes are not "activated" and thus less nucleophilic. Clearly, the coordination to a TMEDA diamine ligand in magnesium generates a less reactive metal center. Meanwhile, although Mg has a small ionic radii (0.57 Å, four-coordinate),[32] the magnesium methyl group is still more accessible than the β-SiH groups, which are well protected by the $SiMe_2$ groups. The argument is supported by reaction of **4.1** with sterically crowded $B(C_6F_5)_3$ group that small amount of β-SiH group abstraction was observed.

Experimental.

General Procedures. All reactions were performed under a dry argon atmosphere using standard Schlenk techniques, or under a nitrogen atmosphere in a glovebox unless otherwise indicated. Dry, oxygen-free solvents were used throughout. Benzene, toluene, pentane, and tetrahydrofuran were degassed by sparging with nitrogen, filtered through activated alumina columns, and stored under N_2. Benzene-d_6 was vacuum transferred from Na/K alloy and stored under N_2 in the glovebox. Bromobenzene-d_5 subjected to three freeze-pumped-thaw cycles and stored over 4 Å molecular sieves. BPh_3 was purchased from Aldrich and was used as received. (TMEDA)MgMeBr,[6] $KC(SiHMe_2)_3$,[14] $LiCH(SiMe_3)_2$,[33] $H_2C(SiHMe_2)_2$,[34] $PhB(C_6F_5)_2$,[35] $B(C_6F_5)_3$,[36] and $[Ph_3C][B(C_6F_5)_4]$[37] were prepared as described in literature procedures. ^1H, $^{13}C\{^1H\}$, $^{29}Si\{^1H\}$ NMR spectra were collected on Bruker DRX-600 MHz or on Varian MR-400 MHz spectrometers. $^{29}Si\{^1H\}$ NMR spectra were recorded using DEPT experiments. Resonance assigments were verified by ^1H COSY, ^1H-^{13}C HMQC, ^1H-^{13}C HMBC, and ^1H-^{29}Si HMBC experiments. Elemental analysis was performed using a Perkin-Elmer 2400 Series II CHN/S by the Iowa State Chemical Instrumentation Facility.

$MeMgC(SiHMe_2)_3(TMEDA)$ (4.1). Benzene (10 ml) was added to a mixture of MgMeBr(TMEDA) (0.269 g, 1.14 mmol) and $KC(SiMe_3)_3$ (0.328 g, 1.14 mmol) at room temperature and stirred for 4 h. The volatiles were evaporated under reduced pressure. The residue was extracted with pentane. The pentane was concentrated and recrystallized at -30 °C to yield $MeMgC(SiHMe_2)_3$(TMEDA) as pale orange block crystals (0.250 g, 0.620 mmol, 54.4 %). ^1H NMR (benzene-d_6, 600 MHz, 25 °C): δ 4.75 (m, 3 H, $^1J_{SiH}$ = 169.2 Hz, SiH), 2.03 (s, 6 H, NMe), 1.91 (s, 6 H, NMe), 1.65 (m, 2 H, NCH_2), 1.59 (m, 2 H, NCH_2), 0.54 (d,

$^{3}J_{HH}$ = 3.6 Hz, 18 H, $SiMe_2$), 0.91 (s, 3 H, MgMe). $^{13}C\{^{1}H\}$ NMR (benzene-d_6, 150 MHz, 25 °C): δ 56.83 (NCH_2), 47.79 (NMe), 47.12 (NMe), 3.72 ($SiMe_2$), -6.90 (MgC), -8.82 (MgMe). $^{29}Si\{^{1}H\}$ NMR (benzene-d_6, 119.3 MHz, 25 °C): δ -20.3. Anal. Calcd for $C_{14}H_{40}Si_3N_2Mg$: C, 48.7; H, 11.7; N, 8.12. Found: C, 46.6; H, 10.6; N, 7.33. IR (KBr, cm^{-1}): 2947 s, 2895 s, 2806 m, 2076 s br (ν_{SiH}), 2044 s br (ν_{SiH}), 1469 s, 1287 m, 1243 s, 1123 m, 1113 m, 1025 s, 1010 m, 891 s br, 794 s, 776 s, 708 m, 677 m.

$MgIC(SiHMe_2)_3(TMEDA)$ (4.2). $SiMe_3I$ (35 μL, 0.248 mmol) was added to a benzene solution (5 ml) of $MeMgC(SiHMe_2)_3(TMEDA)$ (0.078 g, 0.225 mmol) and stirred for 0.5 h. The volatiles were evaporated under reduced pressure. The residue was washed with pentane (1 x 5 ml) and dried under vacuum to yield $MgIC(SiHMe_2)_3(TMEDA)$ as a white crystalline solid (0.089 g, 0.195 mmol, 86.6%). ^{1}H NMR (benzene-d_6, 600 MHz, 25 °C): δ 4.72 (m, 3 H, $^{1}J_{SiH}$ = 169.8 Hz, SiH), 2.20 (s, 6 H, NMe), 1.99 (s, 6 H, NMe), 1.79 (m, 2 H, NCH_2), 1.49 (m, 2 H, NCH_2), 0.57 (d, 18 H, $^{3}J_{HH}$ = 3.6 Hz, $SiMe_2$). $^{13}C\{^{1}H\}$ NMR (benzene-d_6, 150 MHz, 25 °C): δ 56.63 (NCH_2), 50.56 (NMe), 47.03 (NMe), 3.74 ($SiMe_2$), -7.59 (MgC). $^{29}Si\{^{1}H\}$ NMR (benzene-d_6, 119.3 MHz, 25 °C): δ -19.8. Anal. Calcd for $C_{13}H_{37}Si_3N_2IMg$: C, 34.2; H, 8.16; N, 6.13. Found: C, 33.9; H, 7.79; N, 5.78. IR (KBr, cm^{-1}): 2946 s, 2896 s, 2855 s, 2810 m, 2078 s br (ν_{SiH}), 2039 s br (ν_{SiH}), 1468 s, 1284 m, 1248 s, 1121 m, 1061 s, 1042 s, 1020 s, 1006 s, 867 s br, 780 s, 706 s, 680 s.

$Li[CH(SiHMe_2)_2](THF)$ (4.3-Li). Dropwise addition of 1.7 M solution of *t*-BuLi in pentane (12.4 mL, 0.0211 mol) to a THF-solution of $H_2C(SiHMe_2)_2$ (2.786 g, 0.0211 mol) cooled to -78 °C resulted in a visible change in the solution from colorless to yellow. After addition was complete, the reaction mixture was allowed to slowly warm to room temperature and was

stirred for 18 h. Removal of volatile materials under reduced pressure provided a yellow oil. The compound Li[CH(SiHMe$_2$)$_2$](THF) was recrystallized twice from minimum amount of pentane (ca. 3 ml) at -80 °C, to give white crystalline soli (1.604 g, 0.0076 mol, 36.1 %). ^{1}H NMR (benzene-d_6, 600 MHz, 25 °C): δ 4.65 (m, 2 H, $^1J_{SiH}$ = 160.6 Hz, SiH), 3.55 (m, 2 H, OCH$_2$), 1.25 (m, 2 H, OCH$_2$C*H*$_2$), 0.44 (d, $^3J_{HH}$ = 3.4 Hz, 12 H, SiMe$_2$), -1.97 (t, $^3J_{HH}$ = 4.8 Hz, 1 H, LiCH). ^{13}C{^{1}H} NMR (benzene-d_6, 150 MHz, 25 °C): δ 69.17 (OCH), 25.59 (OCH$_2$*C*H$_2$), 3.41 (SiMe$_2$), -4.50 (LiC). ^{29}Si{^{1}H} NMR (benzene-d_6, 119.3 MHz, 25 °C): δ -20.4. IR (KBr, cm^{-1}): 2951 s, 2884 s, 2108 m (ν_{SiH}), 1986 s (ν_{SiH}), 1461 w, 1427 w, 1368 w, 1242 s, 1069 s, 1047 s, 891 s, 828 s, 786 s, 758 s, 681 m.

KCH(SiHMe$_2$)$_2$ (4.3-K). LiCH(SiHMe$_2$)$_2$(THF) (0.560 g, 2.659 mmol) and KO*t*-Bu (0.297 g, 2.649 mmol) were suspended in pentane (10 ml) at room temperature. The mixture was stirred in room temperature for 2 h, and the solution was decanted. The residual white solid was washed with pentane (2 x 10 ml) and dried under reduced pressure to yield KCH(SiHMe$_2$)$_2$ as an off-white solid (0.279 g, 1.637 mmol, 61.6%). ^{1}H NMR (benzene-d_6, 600 MHz, 25 °C): δ 4.73 (m, $^1J_{SiH}$ = 150.0 Hz, 2 H, SiH), 0.35 (s br, 12 H, SiMe$_2$), -2.14 (s br, 1 H, CH). ^{13}C{^{1}H} NMR (benzene-d_6, 150 MHz, 25 °C): δ 4.69 (SiMe$_2$), resonance of CH is not observed due to low solubility of the compound in benzene-d_6. ^{29}Si NMR (benzene-d_6, 119.3 MHz, 25 °C): δ -24.7 (assigned by ^{1}H-^{29}Si HMBC experiment). IR (KBr, cm^{-1}): 2938 s, 2888 s, 1854 s br (ν_{SiH}), 1805 s br (ν_{SiH}), 1430 w, 1249 s, 1090 s, 901 s br, 809 s, 784 m, 728 s, 684 m.

MgCH(SiHMe$_2$)$_2$Me(TMEDA) (4.4-Me). MgMeBr(TMEDA) (0.9062 g, 3.15 mmol) and LiCH(SiHMe$_3$)$_2$THF (0.904 g, 3.15 mmol) were weighed and added to a 100 mL schlenk

flask. Dry benzene was added and the solution mixture was allowed to stir at room temperature for one hour. The benzene solvent was removed under reduced pressure yielding a white crystalline solid (0.928 g) as a mixture of $MeMgCH(SiHMe_2)_2(TMEDA)$ **4.4-Me** and $MgBrCH(SiHMe_2)_2(TMEDA)$ **4.4-Br**. ^1H NMR (benzene-d_6, 600 MHz, 25 °C): δ 4.77 (m, 2 H, $^1J_{SiH}$ = 163.2 Hz, SiH), 1.88 (s br, 12 H, NMe), 1.57 (s br, 4 H, NCH_2), 0.55 (s br, 6 H, $SiMe_2$), 0.51 (s br, 6 H, $SiMe_2$), -1.04 (s, 3 H, MgMe), -1.66 (s br, 1 H, MgCH). $^{13}C\{^1H\}$ NMR (benzene-d_6, 150 MHz, 25 °C): δ 56.34 (NCH_2), 46.73 (br, NMe), 4.25 ($SiMe_2$), 2.01 ($SiMe_2$), -6.99 (MgCH), -13.34 (MgMe). $^{29}Si\{^1H\}$ NMR (benzene-d_6, 119.3 MHz, 25 °C): δ -16.9.

$MgCH(SiHMe_2)_2Br(TMEDA)$ (4.4-Br). The mixture was dissolved in benzene (10 ml) and $SiMe_3Br$ was added. The resulting mixture was stirred at room temperature for 1 h. ^1H NMR (benzene-d_6, 600 MHz, 25 °C): δ 4.73 (m, 2 H, $^1J_{SiH}$ = 164.9 Hz, SiH), 1.94 (s br, 12 H, NMe), 1.57 (s br, 4 H, NCH_2), 0.60 (d, $^3J_{HH}$ = 3.5 Hz, 6 H, $SiMe_2$), 0.50 (d, $^3J_{HH}$ = 3.4 Hz, 6 H, $SiMe_2$), -1.63 (s br, 1 H, MgCH). $^{13}C\{^1H\}$ NMR (benzene-d_6, 150 MHz, 25 °C): δ 56.18 (NCH_2), 46.13 (br, NMe), 3.90 ($SiMe_2$), 1.88 ($SiMe_2$), -7.63 (MgCH). $^{29}Si\{^1H\}$ NMR (benzene-d_6, 119.3 MHz, 25 °C): δ -16.7. Anal. Calcd for $C_{14}H_{40}Si_3N_2Mg$: C, IR (KBr, cm^{-1}): 2952 s, 2896 s, 2068 s br (ν_{SiH}), 1466 s, 1355 w, 1288 m, 1241 s, 1195 w, 1166 w, 1125 m, 1103 w, 1024 s, 894 s br, 838 s, 794 s, 711 m, 679 m.

$MeMgCH(SiMe_3)_2(TMEDA)$ (4.5). Benzene (10 ml) was added to a mixture of MgMeBr(TMEDA) (0.256 g, 1.09 mmol) and $LiCH(SiMe_3)_2$ (0.181 g, 1.09 mmol). The mixture was allowed to stir at room temperature for one hour. The volatiles were removed under reduced pressure. The residue was extracted with pentane (3 x 5ml). The pentane

extract was evaporated in vacuo to give $MeMgCH(SiMe_3)_2(TMEDA)$ as a white crystalline solid (0.275 g, 0.873 mmol, 80.1 %). ^1H NMR (benzene-d_6, 400 MHz, 25 °C): δ 1.84 (s br, 12 H, NMe), 1.75-1.30 (m br, 4 H, CH_2), 0.43 (s, 18 H, $SiMe_3$), -1.04 (MgMe), -1.64 (MgCH). $^{13}C\{^1H\}$ NMR (benzene-d_6, 125 MHz, 25 °C): δ 56.69 (NCH_2), 47.15 (NMe), 6.50 ($SiMe_3$), -1.20 (MgCH), -10.91 (MgMe). $^{29}Si\{^1H\}$ NMR (benzene-d_6, 79.5 MHz, 25 °C): δ -4.3. IR (KBr, cm^{-1}): 2946 m, 2891 m, 2852 m, 1466 s br, 1288 m, 1164 w, 1062 w, 1018 m, 950 w, 850 s br, 793 m, 770 m, 705 m, 677 w.

$MgICH(SiMe_3)_2(TMEDA)$ (4.6). $SiMe_3I$ (45 μL, 0.317 mmol) was added to a benzene (3 ml) solution of **4.5** (0.081 g, 0.256 mmol) and stirred for 0.5 h. The volatiles were removed under reduced pressure to give a sticky white solid. This solid residue was washed with pentane (1 x 5 ml) and dried under vacuum to give $MgICH(SiMe_3)_2(TMEDA)$ as a white solid (0.958 g, 0.224 mmol, 87.7%). ^1H NMR (bromobenzene-d_5, 600 MHz, 25 °C): δ 2.40-1.50 (m br, 16 H, NMe and NCH_2 overlapped), 0.45 (s br, 18 H, $SiMe_3$), -1.58 (s br, 1 H, CH). $^{13}C\{^1H\}$ NMR (benzene-d_6, 125 MHz, 25 °C): δ 56.45 (NCH_2), 48.13 (NMe), 6.58 ($SiMe_3$), -0.51 (MgCH). $^{29}Si\{^1H\}$ NMR (benzene-d_6, 119.3 MHz, 25 °C): δ -3.8 ($SiMe_3$). IR (KBr, cm^{-1}): 3001 m, 2947 m, 2893 m, 1466 m, 1286 w, 1242 m, 1167 w, 1065 w, 1024 m, 948 m, 844 s br, 793 m, 768 m, 723 m, 677 w.

$[Mg(\mu\text{-}H)B(C_6F_5)_3(\mu\text{-}Me)B(C_6F_5)_3](TMEDA)$ (4.8). $B(C_6F_5)_3$ (0.184 g, 0.360 mmol) was added to a benzene solution (5 ml) of $MeMgC(SiHMe_2)_3(TMEDA)$ (0.062 g, 0.180 mmol) and stirred for 0.5 h. White crysyalline solid precipitated and the benzene solution was decanted. The volatiles were evaporated under reduced pressure. The residue was washed with benzene (1 x 3 ml) and pentane (2 x 3 ml) and dried under vacuum to yield [Mg(μ-

H)B(C_6F_5)$_3$(μ-Me)B(C_6F_5)$_3$](TMEDA) as a white solid (0.162 g, 0.138 mmol, 76.5%). IR (KBr, cm^{-1}): 2959 w, 2242 m br (ν_{BH}), 1647 s, 1516 s, 1469 s br, 1375 m, 1284 s br, 1107 s br, 965 s, 942 s, 800 m, 771 m, 756 m, 732 m, 670 m.

[MgI(μ-H)B(C_6F_5)$_3$](TMEDA) (4.9). B(C_6F_5)$_3$ (0.184 g, 0.360 mmol) was added to a benzene solution (5 ml) of MgIC(SiHMe$_2$)$_3$(TMEDA) (0.062 g, 0.180 mmol) and stirred for 0.5 h. White crysyalline solid precipitated and the benzene solution was decanted. The volatiles were evaporated under reduced pressure. The residue was washed with benzene (1 x 3 ml) and pentane (2 x 3 ml) and dried under vacuum to yield [MgI(μ-H)B(C_6F_5)$_3$](TMEDA) as a white solid (0.162 g, 0.138 mmol, 76.5%). ^{1}H NMR (benzene-d_6, 600 MHz, 25 °C): δ 2.51-2.01 (q br, 1 H, BH), 1.77 (s br, 12 H, NMe), 1.47 (s br, 4 H, NCH$_2$). ^{13}C{^{1}H} NMR (benzene-d_6, 150 MHz, 25 °C): δ 149.49 (br, C_6F_5), 147.92 (br, C_6F_5), 141.08 (br, C_6F_5), 139.46 (br, C_6F_5), 138.88 (br, C_6F_5), 137.33 (br, C_6F_5), 55.75 (NCH$_2$), 47.27 (NMe). ^{19}F NMR (benzene-d_6, 564 MHz, 25 °C): δ -135.8 (s br, 6 F, *ortho*-F), -158.3 (s br, 3 F, *para*-F), -163.4 (s br, 6 F, *meta*-F). ^{11}B NMR (benzene-d_6, 119.3 MHz, 25 °C): δ -20.9 (d, $^1J_{BH}$ = 64.7 Hz). IR (KBr, cm^{-1}): 2955 m br, 2361 m br (ν_{BH}), 2280 m br (ν_{BH}), 2125 m br (ν_{BH}), 1647 m, 1517 s, 1466 s br, 1377 m, 1284 s, 1099 s br, 971 s, 907 s, 841 m, 796 m, 763 m, 726 m, 661 m.

[MgC(SiHMe$_2$)$_3$(μ-Me)BPh$_3$](TMEDA) (4.10). BPh$_3$ (0.067 g, 0.278 mmol) was added to a benzene solution (3 ml) of MeMgC(SiHMe$_2$)$_3$(TMEDA) (0.096 g, 0.278 mmol) and stirred for 0.5 h. The volatiles were evaporated under reduced pressure. The residue was washed with benzene (1 x 3 ml) and pentane (2 x 3 ml) and dried under vacuum to yield [MgC(SiHMe$_2$)$_3$(μ-Me)BPh$_3$](TMEDA) as a white solid (0.102 g, 0.173 mmol, 62.3%). ^{1}H

NMR (benzene-d_6, 600 MHz, 25 °C): δ 7.66 (d, $^3J_{HH}$ = 7.2 Hz, 6 H, *ortho*-C_6H_5), 7.24 (t, $^3J_{HH}$ = 7.2 Hz, 6 H, *meta*-C_6H_5), 7.08 (t, $^3J_{HH}$ = 7.1 Hz, 3 H, *para*-C_6H_5), 4.43 (m, $^1J_{SiH}$ = 171.0 Hz, 3 H, SiH), 1.81 (s br, 16 H, NMe and NCH_2 overlapped), 0.52 (s br, 3 H, BMe), 0.24 (d, $^3J_{HH}$ = 2.4 Hz, 18 H, $SiMe_2$). $^{13}C\{^1H\}$ NMR (bromobenzene-d_5, 150 MHz, 25 °C): δ 133.49 (*o*-C_6H_5), 127.22 (*m*-C_6H_5), 121.92 (*p*-C_6H_5), 55.05 (NCH_2), 45.94 (NMe), 11.50 (br, BMe, assigned by ^1H-^{13}C HMQC experiment), 1.92 ($SiMe_2$), -2.61 (MgC). $^{29}Si\{^1H\}$ NMR (bromobenzene-d_5, 119.3 MHz, 25 °C): δ -19.7. ^{11}B NMR (bromobenzene-d_5, 119.3 MHz, 25 °C): δ -9.3. IR (KBr, cm^{-1}): 3056 m, 3038 m, 3002 m, 2950 m, 2899 m, 2806 m, 2085 s br (ν_{SiH}), 2067 s br (ν_{SiH}), 2047 s br (ν_{SiH}), 1878 w, 1816 w, 1471 s, 1427 m, 1283 m, 1249 s, 1152 m, 1117 m, 1018 m, 1001s, 945 s, 894 s br, 795 s, 779 s, 743 s, 706 s.

[MgC(SiHMe$_2$)$_3$(μ-Me)BPh(C$_6$F$_5$)$_2$](TMEDA) (4.11). $PhB(C_6F_5)_2$ (0.114 g, 0.278 mmol) was added to a benzene solution (5 ml) of $MeMgC(SiHMe_2)_3$(TMEDA) (0.093 g, 0.278 mmol) and stirred for 0.5 h. The volatiles were evaporated under reduced pressure. The residue was washed with pentane (2 x 3 ml) and dried under vacuum to yield [$MgC(SiHMe_2)_3$(μ-Me)$BPh(C_6F_5)_2$](TMEDA) as a sticky white solid (0.205 g, 0.267 mmol, 96.0%). ^1H NMR (benzene-d_6, 600 MHz, 25 °C): δ 7.60 (d, $^3J_{HH}$ = 7.3 Hz, 2 H, *ortho*-Ph), 7.34 (t, $^3J_{HH}$ = 7.5 Hz, 1 H, *para*-Ph), 7.20 (t, $^3J_{HH}$ = 7.3 Hz, 2 H, *meta*-Ph), 4.35 (m, 3 H, $^1J_{SiH}$ = 166.4 Hz, SiH), 1.70 (s br, 12 H, NMe), 1.51 (s br, 4 H, NCH_2), 0.84 (s br, 3 H, BMe), 0.21 (d, $^3J_{HH}$ = 2.6 Hz, 18 H, $SiMe_2$). $^{13}C\{^1H\}$ NMR (benzene-d_6, 150 MHz, 25 °C): δ 157.20 (*ipso*-Ph), 150.05 (br, C_6F_5), 148.56 (br, C_6F_5), 139.86 (br, C_6F_5), 138.86 (br, C_6F_5), 137.16 (br, C_6F_5), 133.43 (Ph), 127.58 (Ph), 124.93 (Ph), 56.31 (NCH_2), 46.97 (NMe), 11.0 (br, BMe), 3.20 ($SiMe_2$), -7.58 (MgC). $^{29}Si\{^1H\}$ NMR (benzene-d_6, 119.3 MHz, 25 °C): δ -

19.6. ^{19}F NMR (benzene-d_6, 564 MHz, 25 °C): δ -131.4 (d, $^3J_{FF}$ = 21.2 Hz, 4 F, *ortho*-F), -163.5 (t, $^3J_{FF}$ = 20.4 Hz, 2 F, *para*-F), -166.8 (t, $^3J_{FF}$ = 19.8 Hz, 4 F, *meta*-F). ^{11}B NMR (benzene-d_6, 119.3 MHz, 25 °C): δ -12.2. Anal. Calcd for $C_{13}H_{37}Si_3N_2IMg$: C, 34.2; H, 8.16; N, 6.13. Found: C, 33.9; H, 7.79; N, 5.78. IR (KBr, cm^{-1}): 2956 m, 2903 m, 2105 m br (ν_{SiH}), 1641 m, 1510 s, 1453 s br, 1381 w, 1257 s br, 1081 s br, 968 s, 943 m, 898 s br, 796 s, 739 m, 706 m, 683 m.

[MgC(SiHMe$_2$)$_3$][B(C$_6$F$_5$)$_4$](TMEDA) (4.12). [Ph$_3$C][B(C$_6$F$_5$)$_4$] (0.128 g, 0.139 mmol) was added to a benzene solution (5 ml) of MeMgC(SiHMe$_2$)$_3$(TMEDA) (0.048 g, 0.139 mmol) and stirred for 0.5 h. The solution was separated into two layers. The top layer was decanted and the bottom oily layer was washed with benzene (2 x 3 ml) and pentane (2 x 3ml). The volatiles were evaporated under reduced pressure to yield [MgC(SiHMe$_2$)$_3$][B(C$_6$F$_5$)$_4$](TMEDA) as a white solid (0.101 g, 0.100 mmol, 72.3%). ^{1}H NMR (bromobenzene-d_5, 600 MHz, 25 °C): δ 4.23 (s br, 3 H, $^1J_{SiH}$ = 164.0 Hz, SiH), 2.10 (s br, 16 H, NMe and NCH$_2$ overlapped), 0.15 (s br, 18 H, SiMe$_2$). ^{13}C{^{1}H} NMR (benzene-d_6, 150 MHz, 25 °C): δ 148.22 (br, C$_6$F$_5$), 146.59 (br, C$_6$F$_5$), 138.15 (br, C$_6$F$_5$), 136.29 (br, C$_6$F$_5$), 134.75 (br, C$_6$F$_5$), 54.89 (NCH$_2$), 44.75 (NMe), 1.32 (SiMe$_2$), -5.01 (MgC). ^{29}Si{^{1}H} NMR (benzene-d_6, 119.3 MHz, 25 °C): δ -18.6. ^{19}F NMR (benzene-d_6, 564 MHz, 25 °C): δ -133.0 (s br, 8 F, *ortho*-F), -162.6 (t, $^3J_{FF}$ = 20.4 Hz, 4 F, *para*-F), -166.9 (s br, 8 F, *meta*-F). ^{11}B NMR (benzene-d_6, 119.3 MHz, 25 °C): δ -16.0. Anal. Calcd for $C_{13}H_{37}Si_3N_2IMg$: C, 34.2; H, 8.16; N, 6.13. Found: C, 33.9; H, 7.79; N, 5.78. IR (KBr, cm^{-1}): 2961 m, 2092 s br (ν_{SiH}), 1644 s, 1515 s, 1464 s br, 1374 m, 1276 s br, 1088 s br, 980 m, 943 m, 899 s br, 796 m, 775 m, 756 m, 726 m, 684 m, 662 m.

[MgCH(SiMe$_3$)$_2$(μ-Me)BPh$_3$](TMEDA) (4.13). BPh$_3$ (0.055 g, 0.229 mmol) was added to a benzene solution (3 ml) of MeMgCH(SiMe$_3$)$_3$(TMEDA) (0.072 g, 0.229 mmol) and stirred for 0.5 h. The volatiles were evaporated under reduced pressure. The residue was washed with benzene (1 x 3 ml) and pentane (2 x 3 ml) and dried under vacuum to yield [MgCH(SiMe$_3$)$_2$(μ-Me)BPh$_3$](TMEDA) as a white solid (0.095 g, 0.171 mmol, 74.6%). ^{1}H NMR (benzene-d_6, 600 MHz, 25 °C): δ 7.72 (d, $^3J_{HH}$ = 7.2 Hz, 6 H, *ortho*-C$_6$H$_5$), 7.22 (t, $^3J_{HH}$ = 7.2 Hz, 6 H, *meta*-C$_6$H$_5$), 7.06 (t, $^3J_{HH}$ = 7.2 Hz, 3 H, *para*-C$_6$H$_5$), 1.98 (s, 12 H, NMe), 1.86 (s, 4 H, NCH$_2$), 0.68 (s br, 3 H, BMe), 0.12 (s, 18 H, SiMe$_3$), -1.65 (s, 1 H, CH). ^{13}C{^{1}H} NMR (bromobenzene-d_5, 150 MHz, 25 °C): δ 133.68 (*o*-C$_6$H$_5$), 127.23 (*m*-C$_6$H$_5$), 121.39 (*p*-C$_6$H$_5$), 54.87 (NCH$_2$), 45.61 (NMe), 13.21 (BMe), 4.70 (SiMe$_2$), -2.23 (MgCH). ^{29}Si{^{1}H} NMR (bromobenzene-d_5, 119.3 MHz, 25 °C): δ -3.6. ^{11}B NMR (bromobenzene-d_5, 119.3 MHz, 25 °C): δ -10.6. IR (KBr, cm^{-1}): 3054 w, 3038 w, 3004 m, 2949 m, 2897 m, 1948 w, 1869 w, 1824 w, 1590 m, 1466 s, 1429 m, 1284 m, 1241 s, 1183 w, 1065 w, 1013 s, 944 s, 842 s br, 794 s br, 769 s vbr, 724 s vbr, 663 s vbr.

[MgCH(SiMe$_3$)$_2$(μ-Me)B(C$_6$F$_5$)$_3$](TMEDA) (4.14). B(C$_6$F$_5$)$_3$ (0.105 g, 0.205 mmol) was added to a benzene solution (3 ml) of MgCH(SiMe$_3$)$_2$Me(TMEDA) (0.064 g, 0.203 mmol) and stirred for 0.5 h. The volatiles were evaporated under reduced pressure. The residue was washed with benzene (1 x 3 ml) and pentane (2 x 3 ml) and dried under vacuum to yield [MgCH(SiMe$_3$)$_2$(μ-Me)B(C$_6$F$_5$)$_3$](TMEDA) a sticky white solid (0.072 g, 0.087 mmol, 42.8%). ^{1}H NMR (benzene-d_6, 600 MHz, 25 °C): δ 2.06 (s br, 16 H, NMe and NCH$_2$ overlapped), 0.92 (s br, 3 H, BMe), 0.03 (s br, 18 H, SiMe$_3$), -1.67 (s br, 1 H, CH). ^{13}C{^{1}H} NMR (bromobenzene-d_5, 150 MHz, 25 °C): δ 148.79 (br, C$_6$F$_5$), 146.28 (br, C$_6$F$_5$), 137.89

(br, C_6F_5), 136.92 (br, C_6F_5), 135.50 (br, C_6F_5), 134.41 (br, C_6F_5), 55.02 (NCH_2), 45.34 (NMe), 8.92 (br, BMe), 4.33 ($SiMe_2$), -2.19 (MgC). $^{29}Si\{^1H\}$ NMR (bromobenzene-d_5, 119.3 MHz, 25 °C): δ -3.5. ^{19}F NMR (bromobenzene-d_5, 564 MHz, 25 °C): δ -133.4 (d, $^3J_{FF}$ = 24.7 Hz, 6 F, *ortho*-F), -163.0 (t, $^3J_{FF}$ = 20.5 Hz, 3 F, *para*-F), -166.3 (t, $^3J_{FF}$ = 21.9 Hz, 6 F, *meta*-F). ^{11}B NMR (bromobenzene-d_5, 119.3 MHz, 25 °C): δ -14.5. IR (KBr, cm^{-1}): 2955 m, 1642 m, 1512 s, 1458 s br, 1384 w, 1359 w, 1268 m, 1087 s, 966 m, 951 m, 844 s, 796 m, 735 m, 661 w.

Reference

1 Cannon, K.C.; Krow, G. R. in *Handbook of Grignard Reagents*, eds. Silverman, G. S.; Rakita, P. E. Marcel Dekker, New York, 1996, 271-289.

2 (a) Schlenk, W.; Schlenk, Jr., W. *Chem. Ber.* **1929**, *62*, 920-924. (b) Lindsell, W. E. in *Comprehensive Organometallic Chemistry II*, eds. Wilkinson, G.; Stone, F. G. A.; Abel, E. W. Pregamon Press, Oxford, **1982**, *1*, 155-252. (c) Axten, J.; Troy, J.; Jiang, P.; Trachtman, M.; Bock, C. W. *Struct. Chem.* **1994**, *5*, 99-108. (d) Ehlers, A. W.; van Klink, G. P. M.; van Eis, M. J.; Bickelhaupt, F.; Niederkoorn, P. H. J.; Lammertsma, K. *J. Mol. Model.* **2000**, *6*, 186-194.

3 (a)Forbes, G. C.; Kennedy, A. R.; Mulvey, R. E.; Rodger, P. J. A.; Rowlings, R. B. *J. Chem. Soc., Dalton Trans.* **2001**, 1477-1484. (b) Vargas, W.; Englich, U.; Ruhlandt-Senge, K. *Inorg. Chem.* **2002**, *41*, 5602-5608.

4 Henderson, K. W.; Allan, J. F.; Kennedy, A. R. *Chem. Commun.* **1997**, 1149-1150.

5 Yan, K.; Upton, B. M.; Ellern, A.; Sadow, A. D. *J. Am. Chem. Soc.* **2009**, *131*, 15110-15111.

6 Yousef, R. I.; Walfort, B.; Rüffer, T.; Wagner, C.; Schmidt, H.; Herzog, R.; Steinborn, D. *J. Organomet. Chem.* **2004**, *690*, 1178-1191.

7 Al-Juaid, S. S.; Avent, A. G.; Eaborn, C.; El-Hamruni, S. M.; Hawkes, S. A.; Hill, M. S.; Hopman, M.; Hitchcock, P. B.; Smith, J. D. *J. Organomet. Chem.* **2001**, *631*, 76-86.

8 Jaenschke, A.; Paap, J.; Behrens, U. *Z. Anorg. Allg. Chem.* **2008**, 461-469.

9 Pajerski, A. D.; Squiller, E. P.; Parvez, M.; Whittle, R. R.; Richey, Jr., H. G. *Organometallics* **2005**, *24*, 809-814.

10 Ireland, B. J.; Wheaton, C. A.; Hayes, P. G. *Organometallics* **2010**, *29*, 1079-1084.

11 Sarazin, Y.; Schormann, M.; Bochmann, M. *Organometallics* **2004**, *23*, 3296-3302.

12 a) Jones, C.; Junk, P. C.; Leary, S. G.; Smithies, N. A. *J. Chem. Soc., Dalton Trans.* **2000**, 3186-3190. b) Davies, R. P.; Patel, L.; White, A. J. P. *Inorg. Chem.* **2012**, *51*, 11594-11601.

13 Yan, K.; Schoendorff, G.; Upton, B. M.; Ellern, A.; Windus, T. L.; Sadow, A. D. *Submitted to Organometallics* **2012**.

14 Yan, K.; Pawlikowski, A. V.; Ebert, C.; Sadow, A. D. *Chem. Commun.* **2009**, 656-658.

15 (a) Jeske, G.; Lauke, H.; Mauermann, H.; Swepston, P. N.; Schumann, H.; Marks, T. J. *J. Am. Chem. Soc.* **1985**, *107*, 8091-8103. (b) den Haan, K. H.; de Boer, J. L.; Teuben, J. H.; Spek, A. L.; Kojic-Prodic, B.; Hays, G. R.; Huis, R. *Organometallics* **1986**, *5*, 1726-1733. (c) Schaverien, C. J.; Nesbitt, G. J. *J. Chem. Soc. Dalton Trans.* **1992**, 157-167.

16 Hitchcock, P. B.; Lappert, M. F.; Smith, R. G.; Barlett, R. A.; Power, P. P. *J. Chem. Soc., Chem. Commun.* **1988**, 1007-1009.

17 (a) Herrmann, W. A.; Eppinger, J.; Runte, O.; Spiegler, M.; Anwander, R. *Organometallics* **1997**, *16*, 1813-1815. (b) Eppinger, J.; Spiegler, M.; Hieringer, W.; Herrmann, W. A.; Anwander, R. *J. Am. Chem. Soc.* **2000**, *122*, 3080-3096. (c) Klimpel, M. G.; Gorlitzer, H. W.; Tafipolsky, M.; Spiegler, M.; Scherer, W.; Anwander, R. *J. Organomet. Chem*. **2002**, *647*, 236-244.

18 Uhl, W.; Jana, B. *Chem. Eur. J.* **2008**, *14*, 3067-3071.

19 (a) Anwander, R. *in Lanthanides: Chemistry and Use in Organic Synthesis,* ed. S. Kobayashi, Springer, Berlin, **1999**. (b) Hieringer, W.; Eppinger, J.; Anwander, R.; Hermann, W. A. *J. Am. Chem. Soc.* **2000**, *122*, 11983-11994.

20 Bommers, S., Beruda, H., Paul, M., Schmidbaur, H. *Z. Naturforsch.* **1995**, 50, 821-827.

21 Cook, M. A.; Eaborn, C.; Jukes, A. E.; Walton, D. R. M. *J. Organomet. Chem.* **1970**, *24*, 529-535.

22 Hawrelak, E. J.; Ladipo, F. T.; Sata, D.; Braddock-Wilking, J. *Organometallics* **1999**, *18*, 1804-1807.

23 Groebel, B. T., Seebach, D. *Chem. Ber.* **1977**, 110, 852.

24 Schlosser, M. *Angew. Chem. Int. Ed.* **2005**, *44*, 376-393.

25 (a) Hitchcock, P. B.; Lappert, M. F.; Leung, W.-P.; Diansheng, L.; Shun, T. *J. Chem. Soc., Chem. Commun.* **1993**, 1386-1387. (b) Hitchcock, P. B.; Khvostov, A. V.; Lappert, M. F. *J. Organomet. Chem.* **2002**, *663*, 263-268.

26 Deschner, T.; Klimpel, M.; Tafipolsky, M.; Scherer, W.; Törnroos, K. W.; Anwander, R. *Dalton Trans.* **2012**, *41*, 7319-7326.

27 Guzei, I. A.; Wendt, M. *Dalton Trans.* **2006**, 3991-3999.

28 (a) Walker, D. A.; Woodman, T. J.; Hughes, D. L.; Bochmann, M. *Organometallics* **2001**, *20*, 3772-3776. (b) Milione, S.; Grisi, F.; Centore, R.; Tuzi, A. *Organometallics* **2006**, *25*, 266-274. (c) Garner, L. E.; Zhu, H.; Hlavinka, M. L.; Hagadorn, J. R.; Chen, E. Y. X. *J. Am. Chem. Soc.* **2006**, *128*, 14822-14823.

29 Jutzi, P.; Muller, C.; Stamler, A.; Stammler, H.-G. *Organometallics* **2000**, *19*, 1442-1444.

30 Yang, X.; Stern, C. L.; Marks, T. J. *Angew. Chem. Int. Ed. Engl.* **2003**, *31*, 1375-1377.

31 31(a) Horton, A. D.; de With, J.; van der Linden, A. J.; van de Weg, H. *Organometallics* **1996**, *15*, 2672-2674. (b) Horton, A. D.; de With, J. *Organometallics* **1997**, *16*, 5424-5436.

32 Shannon, R. D. *Acta Cryst. A* **1976**, *32*, 751-767.

33 Davidson, D. J.; Harris, D. H.; Lappert, M. F. *J. Chem. Soc., Dalton Trans.* **1976**, 2268-2274.

34 Bacque, E.; Pillot, J.-P.; Birot, M.; Dunogues, J. *J. Organomet. Chem.* **1988**, *346*, 147-160.

35 Deck, P. A.; Beswick, C. L.; Marks, T. J. *J. Am. Chem. Soc.* **1998**, *120*, 1772-1784.

36 Massey, A. G.; Park, A. J., *J. Organomet. Chem.* **1964**, *2*, 245-250.

37 Scott, V. J.; Celenligil-Cetin, R.; Ozerov, O. V. *J. Am. Chem. Soc.* **2005**, *127*, 2852-2853.

Chapter 5: Zwitterionic and Cationic Magnesium Silyl Compounds from Abstraction reaction of mixed alkyl silyl magnesium complexes with Lewis acids.

A paper to be submitted to *Organometallics*

KaKing Yan, Jing Zhu, Brianna M. Upton, Arkady Ellern, Aaron D. Sadow

Abstract. The reactivity of monomeric magnesium methyl silyl compounds containing the tris(trimethylsilyl)silyl ligand are described and Lewis acids is described. The magnesium mixed methyl silyl $L_2Mg\{Si(SiMe_3)_3\}Me$ (L_2 = tetramethylethylenediamine (**5.2-tmeda**), 1,2-*N*,*N*-dipyrrolidenylethane (**5.2-dpe**)) are synthesized by salt elimination of $L_2MgMeBr$ with $KSi(SiMe_3)_3$. The compounds **5.2** undergo exclusively methyl group abstraction with electrophiles, such as Me_3SiI, $B(C_6F_5)_3$, $[Ph_3C][B(C_6F_5)_4]$, and $HB(C_6F_5)_2$, to provide zwitterionic or cationic Mg silyl complexes, while reaction with MeI or MeOTf gives instead a Si-C bond formation $MeSi(SiMe_3)_3$. Neutral Mg silyl compounds reported here are also relatively stable towards thermal and photolytic conditions, in sharp contrast to Group 4 silyl complexes. The neutral mixed alkyl silyl compound **5.2-tmeda** is also an effective co-transfer agent of silyl and alkyl groups with Cp_2ZrCl_2 to give $Cp_2ZrMe(Si(SiMe_3)_3)$ that initially provide a mixture of $Cp_2ZrSi(SiMe_3)_3Cl$ and $Cp_2ZrMeCl$. The detection of $Cp_2ZrMeCl$ formation in the initial reaction mixture suggests that introduction of diamine ligand enhances the nucleophilicity of Mg methyl group. This observation is in sharp contrast to previously reported system utilizing THF magnesium adducts.

Introduction

The highly polar nature metal-carbon bonds in alkali and alkaline earth metal organometallic compounds are central to their strongly nucleophilic and highly basic character.[1] In comparison to metal alkyl compounds, metal silyl compounds might be expected to have similar nucleophilic and basic character based on their use in salt metathesis chemistry.[2] Some distinctions are evident in d^0 transition metal chemistry, however, as the M-Si bond is expected to be less polar,[3] longer, and weaker[4,5] than corresponding M-C bonds;[5] the latter two points suggest that early metal silyls might be expected to react more rapidly, whereas increased polarity might result in greater reaction rates of related metal alkyls. Direct comparisons are complicated by the difficulty in preparing metal alkyl and metal silyl compounds that are identical with respect to metal center, ancillary ligand, and groups bonded to the carbon or silicon atom.[6] Instead, we decided to initially compare the reactivity of a mixed silyl alkyl magnesium compound with a series of electrophiles.

The compound $(THF)_2MgSi(SiMe_3)_3Me$, prepared by Marschner and co-workers,[7] shows that mixed silyl alkyl magnesium complexes are isolable and might prove suitable for this study. In fact, $(THF)_2MgSi(SiMe_3)_3Me$ provides an initial data point in its salt metathesis reaction with Cp_2ZrCl_2 that forms $Cp_2ZrSi(SiMe_3)_3Cl$ (rather than $Cp_2ZrMeCl$) as an intermediate to the $Cp_2ZrSi(SiMe_3)_3Me$ final product.[8] Thus, the bulkier silyl group transfers faster than the methyl group, although both groups undergo transmetalation. The observation that both Mg-C and Mg-Si bonds react suggests that changes in reaction conditions, ancillary ligands, and identity of the electrophile might change the relative rates of group transfer reaction (and thus the selectivity for C–E versus Si–E (E = electrophile) bond formation.

We have therefore prepared diamine-coordinated derivatives (tmeda)MgSi($SiMe_3$)$_3$Me (tmeda = tetramethylethylenediamine) and (dpe)MgSi($SiMe_3$)$_3$Me (dpe = dipyrrolidine ethane) to stabilize monomeric structures and potentially support lower-coordinate magnesium centers. The interactions of these two monomeric magnesium compounds and the electrophiles have been investigated. Interestingly, reactions of (L_2)MgSi($SiMe_3$)$_3$Me (L_2 = tmeda, dpe) and electrophiles such as B(C_6F_5)$_3$ or [Ph_3C][B(C_6F_5)$_4$] might provide zwitterionic or cationic magnesium silyl or alkyl compounds. Despite the highly electropositive nature of divalent magnesium, few cationic organomagnesium compounds have been described, and we are not aware of cationic compounds containing a Mg-Si bond. These species are interesting because *cationic* alkyl and silyl early transition metal compounds show enhanced reaction rates in comparison to neutral analogs in σ-bond metathesis type reactions involving Si–H and C–H bonds.[9] This trend, however, is less established for neutral versus cationic magnesium alkyls compounds, and in fact relatively few cationic organomagnesium compounds have been reported.[10] Recently, cationic magnesium butyl complexes were shown to be an effective initiator for caprolactone ring-opening polymerization.[10c,d] Here we describe a series of reactions of (L_2)MgSi($SiMe_3$)$_3$Me and electrophiles. Our study demonstrates that the ancillary ligands, the charge, and identity of the electrophile affect the relative reactivity of Mg-C vs. Mg-Si bond. Furthermore, we have found that reactions of (L_2)MgSi($SiMe_3$)$_3$Me with B(C_6F_5)$_3$ and [Ph_3C][B(C_6F_5)$_4$] provide the first examples of cationic compounds that contain a magnesium-silicon bond.

Results and discussion

5.1. Synthesis and characterization of (L)MgSi(SiMe$_3$)$_3$Me.

(tmeda)MgMeBr (**5.1-tmeda**) is a convenient starting material, as it is an isolable, well-defined solid.[11] **5.1-tmeda** and KSi(SiMe$_3$)$_3$ react in benzene to give (tmeda)Mg{Si(SiMe$_3$)$_3$}Me (**2-tmeda**) and KBr (eq 5.1). This route follows a sequence established by Marschner and co-workers for (THF)$_2$Mg{Si(SiMe$_3$)$_3$}Me.[8] We have also prepared (dpe)MgMeBr (dpe = 1,2-*N*,*N*,-dipyrrolidenylethane) (**5.1-dpe**) to provide a magnesium starting material with a bulkier and more electron-donating diamine ligand (see below for a steric comparison) by addition of dpe to a solution of MgMeBr. **5.1-dpe** and KSi(SiMe$_3$)$_3$ react to provide the mixed silyl alkyl compound (dpe)Mg{Si(SiMe$_3$)$_3$}Me (**5.2-dpe)** and KBr (eq 5.1).

The silyl groups of **5.2** have similar ^{1}H, ^{13}C{^{1}H} and ^{29}Si NMR chemical shifts. The magnesium methyls resonanate upfield of tetramethylsilane in both tmeda and dpe compounds (-1.03 and -1.02 ppm, respectively). For comparison, the ^{1}H NMR chemical shift of the magnesium methyl of the previously reported (THF)$_2$Mg{Si(SiMe$_3$)$_3$}Me was detected at -0.8 ppm.[8] The ^{29}Si NMR chemical shifts of the central silicon in *Si*(SiMe$_3$)$_3$ are -175.4 and -177 ppm in the tmeda and dpe magnesium silyl compounds (see Table 5.1), which is expectedly similar to the value reported for (THF)$_2$Mg{Si(SiMe$_3$)$_3$}Me (-174.5 ppm).

Compound	^{29}Si *Si*(SiMe$_3$)$_3$
(tmeda)Mg{Si(SiMe$_3$)$_3$}Me (**5.2-tmeda**)	-175.4
(dpe)Mg{Si(SiMe$_3$)$_3$}Me (**5.2-dpe**)	-177.0
(tmeda)Mg{Si(SiMe$_3$)$_3$}I (**5.3-tmeda**)	-167.9

(dpe)Mg{Si(SiMe$_3$)$_3$}I (**5.3-dpe**)	-168.9
(tmeda)Mg{Si(SiMe$_3$)$_3$}MeB(C$_6$F$_5$)$_3$ (**5.4-tmeda**)	-167.2
(dpe)Mg{Si(SiMe$_3$)$_3$}MeB(C$_6$F$_5$)$_3$ (**5.4-dpe**)	-168.7
[(tmeda)MgSi(SiMe$_3$)$_3$][B(C$_6$F$_5$)$_4$] (**5.6-tmeda**)	-163.4
[(dpe)MgSi(SiMe$_3$)$_3$][B(C$_6$F$_5$)$_4$] (**5.6-dpe**)	-170.8
(tmeda)Mg{Si(SiMe$_3$)$_3$}(μ-H)$_2$B(C$_6$F$_5$)$_2$ (**5.7-tmeda**)	-173.1
(dpe)Mg{Si(SiMe$_3$)$_3$}(μ-H)$_2$B(C$_6$F$_5$)$_2$ (**5.7-dpe**)	-173.1
(tmeda)Mg{Si(SiMe$_3$)$_3$}IB(C$_6$F$_5$)$_3$ (**5.5-tmeda**)	-165.0

Table 5.1. ^{29}Si NMR chemical shifts of magnesium silyl compounds.

A single crystal X-ray diffraction study of **5.2-tmeda** showed its monomeric nature and the magnesium coordination number to be four. The solid-state structure of (THF)$_2$MgSi(SiMe$_3$)$_3$Me was not reported, but those of (tmeda)Mg[Si(SiMe$_3$)$_3$]$_2$, (THF)$_2$MgSi(SiMe$_3$)$_3$Ph and (THF)$_2$ Mg(Si(SiMe$_3$)$_3$)$_2$ were described previously. The chelating tmeda ligand gives N-Mg-N angle of 82.67(8)° for **5.2-tmeda** is similar to (tmeda)Mg[Si(SiMe$_3$)$_3$]$_2$ (81.8(3)°),[8] whereas the unconstrained O-Mg-O angle in (THF)$_2$MgSi(SiMe$_3$)$_3$Ph[8] and (THF)$_2$ Mg(Si(SiMe$_3$)$_3$)$_2$[7] are much wider at 95.41(12)° and 92.0(3)°, respectively. The Si-Mg-C$_{Ph}$ angle in the latter compound of 128.2(1) is greater than the 120.73(6) angle in **5.2-tmeda**. Space-filling models show that there is space between phenyl and tris(trimethyl)silyl groups in (THF)$_2$MgSi(SiMe$_3$)$_3$Ph and between methyl and tris(trimethyl)silyl groups in **5.2-tmeda**. Furthermore, solid angles calculations using the program Solid-G shows tmeda, Me and Si(SiMe$_3$)$_3$ ligands occupy only ca. 80% of the space surrounding the magnesium center in **5.2-tmeda**, and there are no unfavorable inter-ligand interactions.[12] Likewise, only 78% of the space around the magnesium center in

$(THF)_2MgSi(SiMe_3)_3Ph$ is occupied. Thus, intramolecular steric effects are apparently not responsible for the change in Si-Mg-C angles between $(THF)_2MgSi(SiMe_3)_3Ph$ and **5.2-tmeda**.

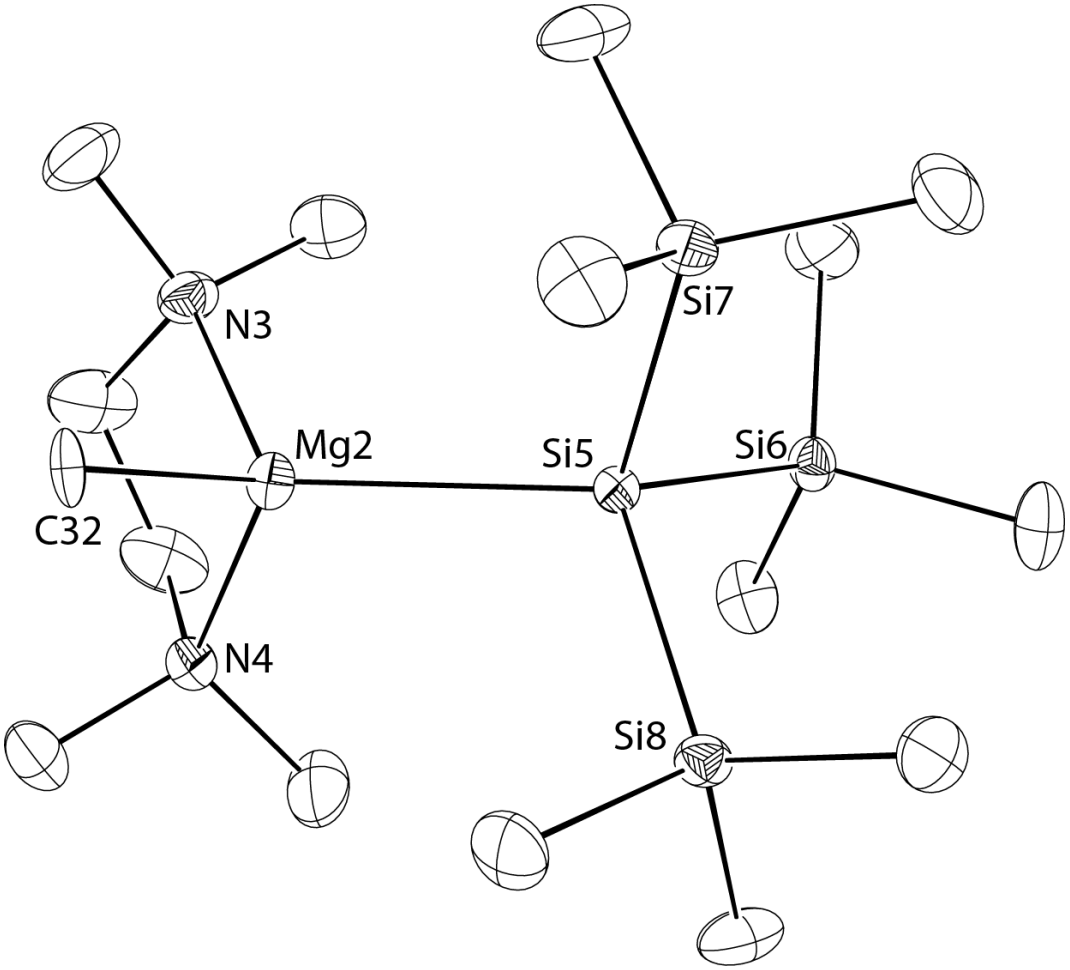

Figure 5.1. ORTEP diagram of **5.2-tmeda**. The unit cell contains two independent molecules, and only one is illustrated. Mg–L distances are identical within error for the two molecules, and the X-Mg-X bond angles are within 1° for the two independent molecules. Hydrogen atoms are not included in the picture. Selected distances (Å): Mg2-Si5, 2.6414(9); Mg2-C32, 2.222(2); Mg-N3, 2.210(2); Mg-N4, 2.213(2). Selected bond angles (°): Si5-Mg2-C32, 120.73(6); N3-Mg2-N4, 82.67(8).

5.2-tmeda is 2.6414(9) Å, and the Mg-Si distances for the crystallographically characterized compounds of this report are listed in Table 5.2. For comparison, the Mg-Si distance in $THF_2MgSi(SiMe_3)_3Ph$ is 2.650(2) Å.[8]

Compound	Mg-Si distance (Å)
(tmeda)Mg{Si(SiMe$_3$)$_3$}Me (**5.2-tmeda**)	2.6414(9)
(dpe)Mg{Si(SiMe$_3$)$_3$}I (**5.3-dpe**)	2.609(2)
(tmeda)Mg{Si(SiMe$_3$)$_3$}MeB(C$_6$F$_5$)$_3$ (**5.4-tmeda**)	2.576(2)
(dpe)Mg{Si(SiMe$_3$)$_3$}MeB(C$_6$F$_5$)$_3$ (**5.4-dpe**)	2.602(2)
(tmeda)Mg{Si(SiMe$_3$)$_3$}(μ-H$_2$)B(C$_6$F$_5$)$_2$ (**5.7-tmeda**)	2.648(1)

Table 5.2. Mg-Si bond distance of magnesium silyl compounds.

5.2. Reactions of $(L_2)MgSi(SiMe_3)_3Me$ and electrophiles.

Reactions of **5.2-tmeda** or **5.2-dpe** and MeOTf afford $(Me_3Si)_3SiMe$ and $(L_2)Mg(OTf)Me$ (L_2 = tmeda or dpe) and (δ 0.20, 0.12 in C_6D_6) within 5 min at room temperature. Addition of excess MeOTf (>2 equiv.) eventually (~30 min) gives ethane (δ 0.8 in C_6D_6) and a white precipitate (presumably $(L_2)Mg(OTf)_2$) in addition to $(Me_3Si)_3SiMe$. Compounds **5.2** and MeI also react at room temperature, but the reactions take longer (18 h at room temperature) to give full conversion to $(Me_3Si)_3SiMe$. The products formed in eq 5.2 follow expectations previously established by the reaction of Cp_2ZrCl_2 and $(THF)_2MgSi(SiMe_3)_3Me$ that initially forms $Cp_2ZrSi(SiMe_3)_3Cl$ rather than $Cp_2ZrMeCl$.[8] That is, salt metathesis with the bulky tris(trimethylsilyl)silyl group is kinetically favored over methyl group transfer.[8] In contrast, reaction of **5.2-tmeda** and Cp_2ZrCl_2 initially affords a mixture of $Cp_2Zr\{Si(SiMe_3)_3\}Cl$, Cp_2ZrMe_2, and $Cp_2Zr\{Si(SiMe_3)_3\}Me$ in a 10:7:1 ratio and a ~1:1 mixture of $(tmeda)Mg\{Si(SiMe_3)_3\}Cl$ and $(tmeda)MgCl_2$. The species

(tmeda)$MgCl_2$ is soluble in the reaction mixture and assigned based on the difference in tmeda resonances in the ^{1}H NMR spectrum from that of a benzene-d_6 solution of tmeda. Interestingly, this mixture is converted to $Cp_2Zr\{Si(SiMe_3)_3\}Me$ as the sole zirconium product after 12 h at room temperature. Meanwhile, the reaction of **5.2-dpe** and Cp_2ZrCl_2 initially gives a mixture of $Cp_2Zr\{Si(SiMe_3)_3\}Cl$, Cp_2ZrMe_2, and $Cp_2Zr\{Si(SiMe_3)_3\}Me$ in a 3.4:5.2:1 ratio. Thus, the ancillary diamine ligand increases the nucleophilicity of the methyl group, especially in the case of dpe ligand, in $(L_2)Mg\{Si(SiMe_3)_3\}Me$ vs. the THF-coordinated compound.[8] These results may be related to the effect of tmeda on the reactivity of organolithium reagents, such that the Li–C bond reacts by insertion of olefins and σ-bond metathesis with H_2.[13]

In contrast, reactions of **5.2-tmeda** or **5.2-dpe** and Me_3SiI afford the sila-Grignard complexes $(L_2)Mg\{Si(SiMe_3)_3\}I$ (L_2 = tmeda (**5.3-tmeda**), dpe (**5.3-dpe**)) and $SiMe_4$ (eq 5.2). The Grignard reagent $(L_2)MgMeI$ and $Si(SiMe_3)_4$ are not detected in the ^{1}H NMR spectrum of the crude reaction mixture. A ^{1}H NMR spectrum of a micromolar scale reaction of 1.1 equiv. of Me_3SiI to **5.2-tmeda** in benzene-d_6, acquired 10 min. after mixing the reagents, revealed rapid and quantitative formation of Me_4Si and new resonances assigned to **5.3-tmeda**.

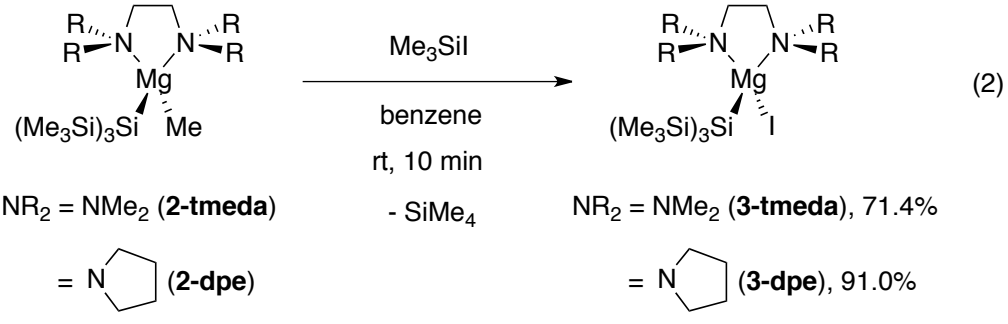

On larger scale, **5.3-tmeda** and **5.3-dpe** are readily isolated by evaporation of the volatile materials and extraction and crystallization from toluene. The X-ray crystal structure of **5.3-dpe** highlights its monomeric nature, as there are no close contacts between (dpe)Mg{Si(SiMe$_3$)$_3$}I molecules. The Mg1-Si1 bond distance of 2.609(2) Å is 0.03 Å shorter than the Mg2-Si5 distance (2.6414(9) Å) in **5.2-tmeda**.

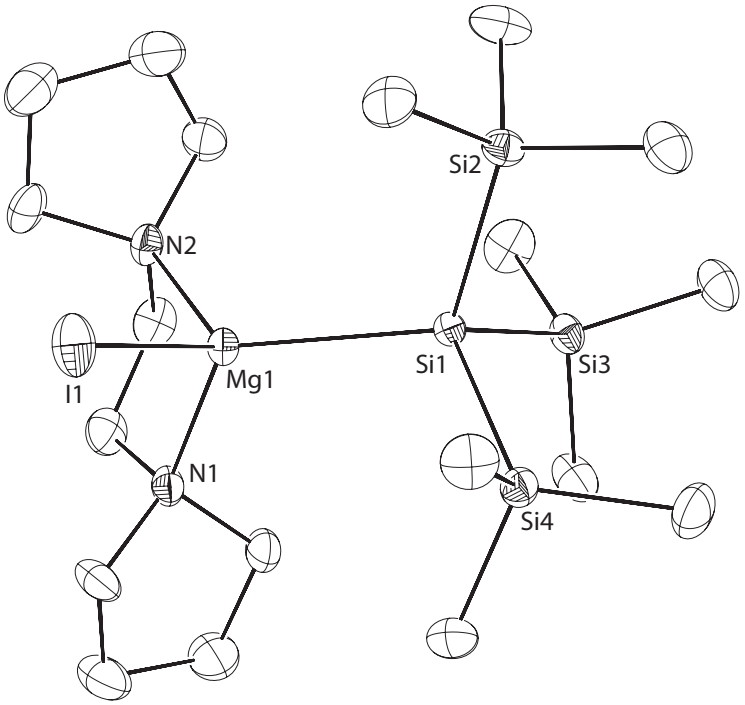

Figure 5.2. ORTEP diagram of **5.3-dpe** at 35% probability. A co-crystallized benzene molecule and hydrogen atoms are not depicted for clarity. Selected interatomic distances (Å): Mg1-Si1, 2.609(2); Mg1-I1, 2.723(2); Mg1-N1, 2.173(4); Mg1-N2, 2.180(4). Selected interatomic angles (°): Si1-Mg1-I1, 114.08(6); N1-Mg1-N2, 83.5(2).

The Mg1-Si1 bond distance of 2.609(2) Å is 0.03 Å shorter than the Mg2-Si5 distance (2.6414(9) Å) in The ^{1}H NMR spectrum of **5.3-tmeda** or **5.3-dpe** dissolved in benzene-d_6 are unchanged after thermolysis at 115 °C for 5 h, and **5.3** is robust in the absence of protic reagents and air, and resistant toward disproportionation to $(L_2)MgI_2$ and

$(L_2)Mg\{Si(SiMe_3)_3\}_2$,[8] as well as dissociation of the diamine ligand. Reactions of 3 equiv of Me_3SiI and **5.2** provide **5.3** as the only observed $(Me_3Si)_3Si$- or L_2Mg-containing compound at room temperature. Upon heating at 83 °C in benzene-d_6, $Si(SiMe_3)_4$ is slowly formed, giving 83% conversion after 28 h. As in the reactions of eq 5.1, $(L_2)MgSi(SiMe_3)_3I$ and MeOTf (2 equiv, r.t., benzene-d_6) react to give $MeSi(SiMe_3)_3$ and $HSi(SiMe_3)_3$ (0.26:1) and a white precipitate (presumable L_2MgX_2). Surprisingly, only starting materials were observed after treatment of either **5.2-tmeda** or **5.2-dpe** with Me_3SiOTf. These interesting results indicate that the magnesium silyl moiety is more reactive to smaller electrophiles (MeOTf) than the methyl group, significantly less reactive toward others (Me_3SiI), and unexpectedly inert toward some electrophiles (Me_3SiOTf). Following this idea, we began to explore reactions with other main group electrophiles to form the zwitterionic or cationic magnesium silyl species.

5.2. Reactions of $L_2MgSi(SiMe_3)_3Me$ and tris(perfluorophenyl)borane.

Reaction of **5.2-tmeda** and $B(C_6F_5)_3$ in benzene provides isolable $(tmeda)Mg\{Si(SiMe_3)_3\}MeB(C_6F_5)_3$ (**5.4-tmeda**) after evaporation of solvent (eq 5.3). The product **5.4-tmeda** is soluble in benzene and toluene. The methyl resonance from $MeB(C_6F_5)_3$ in the ^1H NMR spectrum of **5.4-tmeda** appeared at 1.67 ppm, which was shifted by 2.7 ppm downfield in comparison with the chemical shift of the neutral magnesium methyl (-1.03 ppm). The formation of a B-CH_3 interaction was unambiguously established by a ^1H-^{11}B HMBC experiment that contained a crosspeak between the broad ^1H NMR methyl resonance and the borate resonance at -14.3 ppm in the ^{11}B NMR spectrum. The chemical shifts of the -$Si(SiMe_3)_3$ group in the ^1H and ^{29}Si NMR spectra, however, were similar for **5.2-tmeda**, **5.3-tmeda**, and **5.4-tmeda**. Thus, the data indicates that $B(C_6F_5)_3$ interacts

exclusively with the methyl group. Similarly, reaction of **5.2-dpe** and $B(C_6F_5)_3$ provides (dpe)Mg{Si(SiMe$_3$)$_3$}MeB(C_6F_5)$_3$ (**5.4-dpe**) in 84.6% yield; however, **5.4-dpe** is formed as an insoluble oil that precipitates from benzene.

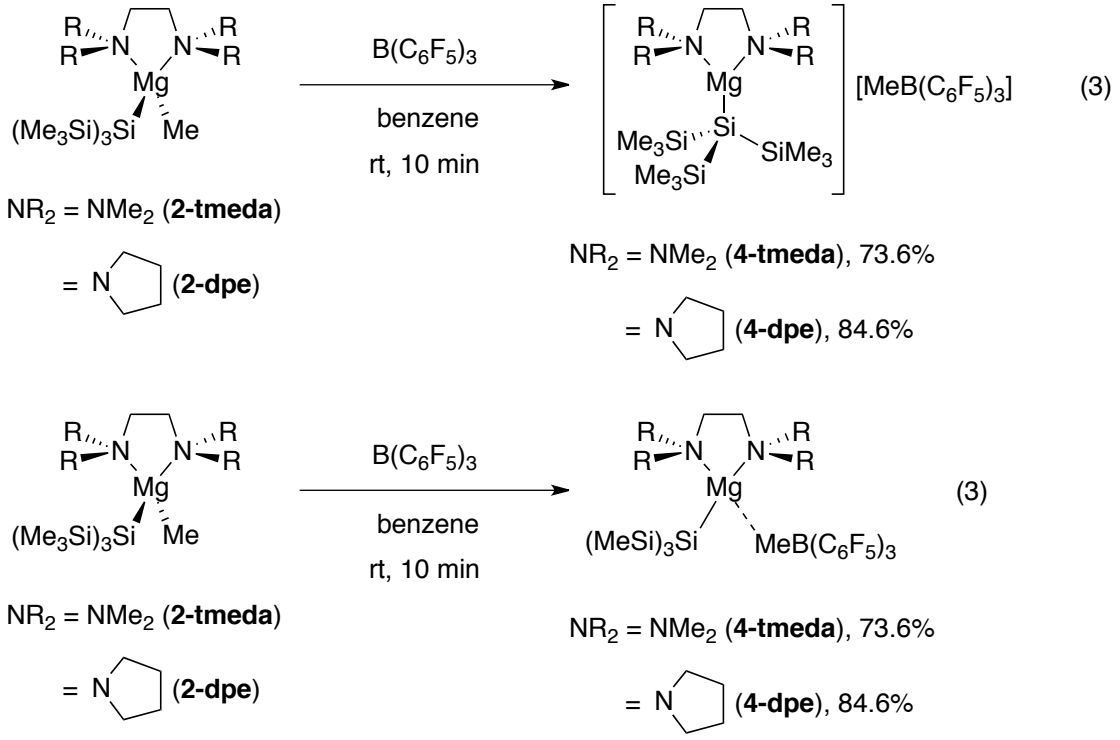

The solution structure of **5.4-tmeda** was probed to identify the magnesium center's coordination environment. The room temperature ^{1}H and ^{13}C NMR spectra of **5.4-tmeda** in benzene-d_6 contains one singlet assigned to four equivalent methyl groups and one singlet assigned to the methylene moiety of the tmeda ligand suggesting effective pseudo-C_{2v} symmetry. In contrast, the NMe_2 groups are inequivalent in four-coordinate compounds **5.2-tmeda** and **5.3-tmeda**. The two ^{1}H NMR resonances for **5.4-tmeda** are broad, but coalesced, at 190 K indicating that tmeda is involved in a rapid, fluxional process even at that temperature. However, this process does not necessarily involve a Mg$\cdots$MeB(C_6F_5) interaction and could instead involve chair-chair interconversions of the five-membered

chelate ring. From 180 K to 295 K, the *Me*B(C_6F_5)$_3$ resonance does not shift and only broadens slightly. Clearly, the solution-phase [Mg]-MeB(C_6F_5)$_3$ interaction in **5.4-tmeda** is, at best, labile. Marks's studies of ($C_5H_3Me_2$)$_2$ZrMe(μ-Me)B(C_6F_5)$_3$ ion pair separation and methide transfer indicate that ion pair separation is 10× faster the borane dissociation in toluene;[14] furthermore, the coalescence of diastereotopic ^{1}H NMR signals in ($C_5H_3Me_2$)$_2$Zr{CH($SiMe_3$)$_2$}[MeB(C_6F_5)$_3$] is also beyond the limits of the low temperature point of toluene-d_6 suggestive of significant ionic character.[14b] .

Still, the ^{19}F NMR chemical shift difference for *meta* and *para* fluorine resonances in **5.4-tmeda** is 3.9 ppm (in bromobenzene-d_5). Previously, Horton suggested that a value of Δ(*para*$_F$–δ*meta*$_F$) greater than 3 corresponds to a X_3Zr(μ-Me)B(C_6F_5)$_3$ inner sphere interaction, whereas Δ(δ*para*$_F$ – δ*meta*$_F$) < 3 indicates that a solvent-separated ion pair is formed.[15] By this measure, **5.4-tmeda** is best described as (tmeda)MgSi($SiMe_3$)$_3$(μ-Me)B(C_6F_5)$_3$, whereas Δ(δ*para*$_F$–δ*meta*$_F$) in **5.4-dpe** is 2.8 ppm (in bromobenzene-d_5) suggesting the structure [(dpe)MgSi($SiMe_3$)$_3$][MeB(C_6F_5)$_3$]. Later, Piers suggested that a correlation between ^{11}B NMR and the separation of the *para*/*meta* ^{19}F NMR resonance is related to the strength of the LB-B(C_6F_5)$_3$ interaction (LB = Lewis base), although this correlation appears to be less meaningful for upfield-shifted ^{11}B NMR signals that would also be associated with the MeB(C_6F_5)$_3$ anion in **5.4**.[16] In this context, it is worth noting the ^{11}B NMR chemical shifts in **5.4-tmeda** (-15.1 ppm, bromobenzene-d_5) and **5.4-dpe** (-14.8 ppm, bromobenzene-d_5), which are not identical but are very similar. Additionally, the diffusion constant values D, measured using PFSG-spin echo experiments in benzene-d_6 at room temperature[17] for [(tmeda)MgSi($SiMe_3$)$_3$] are within error of the values for [MeB(C_6F_5)$_3$] in

5.4-tmeda (the values for [(dpe)MgSi(SiMe$_3$)$_3$] and MeB(C$_6$F$_5$)$_3$ are identical in **5.4-dpe**, but distinct from **5.4-tmeda**). The observation that the cationic and anionic portions of these species diffuse at the same rate suggests that they are associated in solution.

In the solid state, both **5.4-tmeda** and **5.4-dpe** contain zwitterionic, bridging [Mg]-Me-B(C$_6$F$_5$)$_3$ zwitterionic structures (see ORTEP diagrams in Figures 5.3 and 5.4). The Mg-Si bond distance is 0.065 Å shorter in zwitterionic **5.4-tmeda** than neutral **5.2-tmeda** (Table 5.2). The ionic radius of four coordinate magnesium(II) (0.57 Å) is only slightly less than that of hafnium(IV) (0.58 Å) and zirconium(IV) (0.59 Å).[18] In contrast, the Hf-Si distance elongates upon methine abstraction in Cp$_2$Hf(Si^{t}BuPh$_2$)(μ-Me)B(C$_6$F$_5$)$_3$ in 2.851(3) (Cp$_2$Hf(Si^{t}BuPh$_2$)Me: 2.835(2)).[19] The Mg-N bonds are shorter by ca. 0.05 Å in the zwitterionic compounds than the neutral compounds. However, in **5.3-dpe** and **5.4-dpe**, the Mg-Si bond lengths are identical within error. The Mg-N distances are also similar for both dpe and tmeda magnesium compounds. In comparison, the Mg-C distance in **5.4-tmeda** (2.45 Å) elongates by ca. 0.23 Å and the Hf-C bond in Cp$_2$Hf(Si^{t}BuPh$_2$)(μ-Me)B(C$_6$F$_5$)$_3$ is lengthened by 0.19 Å, upon methane abstraction with B(C$_6$F$_5$)$_3$. The objectively located and refined hydrogen atoms on the methyl groups are directed toward the magnesium center in both Mg compounds, **5.4-tmeda** and **5.4-dpe**. The B-C bond distances 1.661(6) and 1.656(1) Å for the two L$_2$MgSi(SiMe$_3$)$_3$(μ-Me)B(C$_6$F$_5$)$_3$ compounds are identical.

Solid state structures of zwitterionic **5.4-tmeda** and **5.4-dpe** clearly are not equivalent to the fluxional solution structures. However, the bridging Mg-Me-B moiety is probably an important component of the solution structures, even if the MeB(C$_6$F$_5$)$_3$ may dissociate from the Mg center to form solvent separate ion-pair. Although the $\Delta(para_F - \delta meta_F)$ of ^{19}F NMR analysis suggested that **5.4-dpe** is solvent-separated ion-pair, this idea was originally applied

to Group 4 $RB(C_6F_5)_3$ (R = Me, CH_2Ph)[15] as solid state structure and solution NMR data indicate **5.4-dpe** as contacted ion-pair. Therefore, we favor both **5.4-tmeda** and **5.4-dpe** as zwitterionic compounds $(L_2)MgSi(SiMe_3)_3(\mu\text{-}Me)B(C_6F_5)_3$.

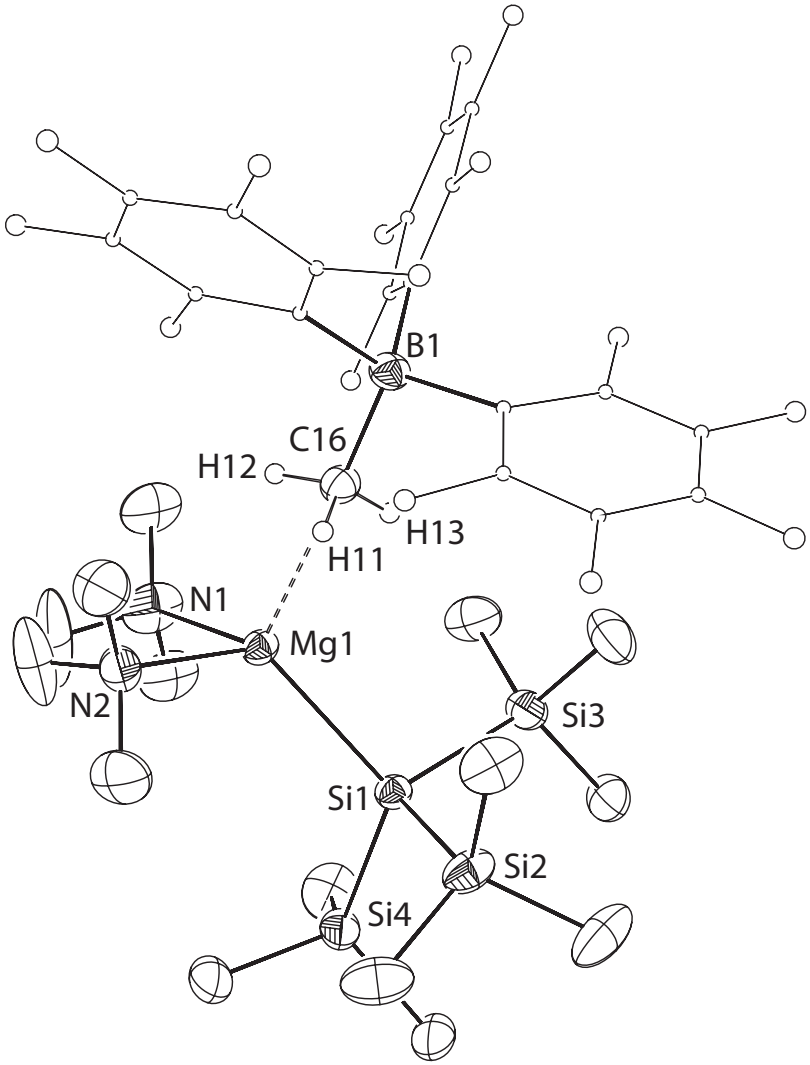

Figure 5.3. ORTEP diagram of **5.4-tmeda** drawn at 35% probability. Hydrogen atoms on the $MeB(C_6F_5)_3$ were found objectively in the electron density map, were refined isotropically, and were included in the plot. All other hydrogen atoms were not included. Fluorine atoms and carbon atoms on $MeB(C_6F_5)_3$ were refined anisotropically and have normal thermal

paramters but are depicted using a ball-and-stick representation for clarity. Selected distances (Å): Mg1-Si1, 2.576(2); Mg1-N1, 2.152(4); Mg1-N2, 2.165(4); Mg1-C16, 2.447; Mg1-H11, 2.30(4); Mg1-H12, 2.25(4); Mg1-H13, 2.40(4); B1-C16, 1.661(6). Selected angles (°): N1-Mg1-N2, 84.7(2); Si1-Mg1-C16, 113.0; Mg1-C16-B1, 175.7.

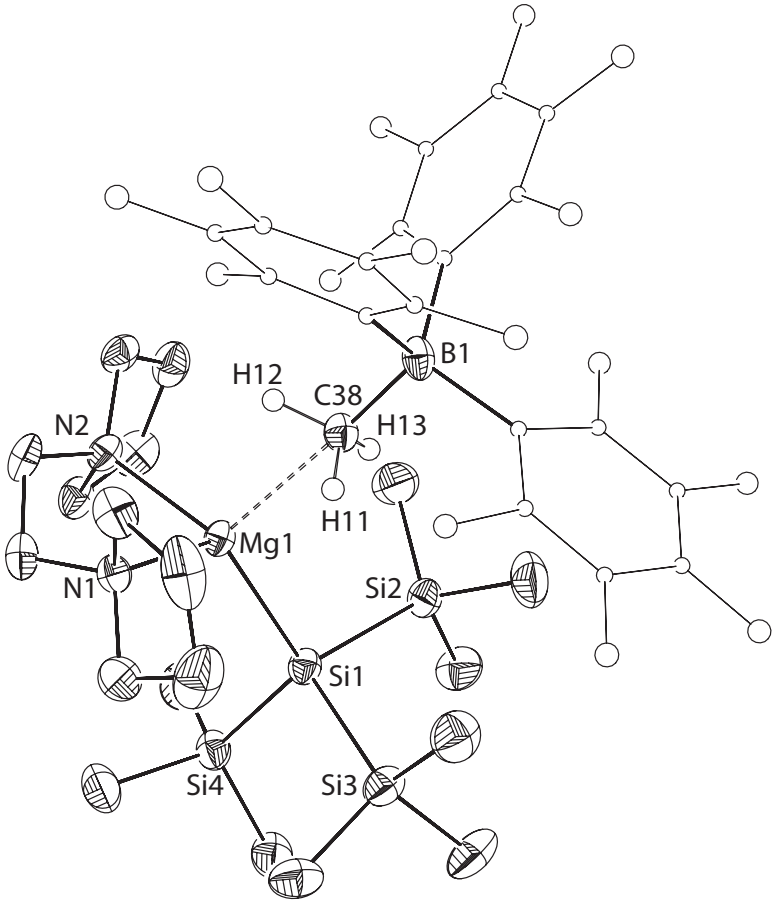

Figure 5.4. ORTEP diagram of **5.4-dpe**. Hydrogen atoms on the $MeB(C_6F_5)_3$ were found objectively in the electron density map, were refined isotropically, and were included in the plot. All other hydrogen atoms were not included. Fluorine atoms and carbon atoms on $MeB(C_6F_5)_3$ were refined anisotropically and have normal thermal paramters but are depicted using a ball-and-stick representation for clarity. Selected distances (Å): Mg1-Si1, 2.602(2); Mg1-N1, 2.191(3); Mg1-N2, 2.177(3); Mg1-C38, 2.459; Mg1-H11, 2.34(3); Mg1-H12,

2.21(3). Selected angles (°): N1-Mg1-N2, 84.5(1); Si1-Mg1-C38, 109.51; Mg1-C38-B1, 174.21.

To further establish the electronic nature of Mg-C bond, reaction of **5.4-tmeda** with electrophile Me_3SiI was also examined. Unexpectedly, the reaction generated $SiMe_4$ and $[(tmeda)MgSi(SiMe_3)_3][IB(C_6F_5)_3]$ (**5.5-tmeda**) after 17 h (eq 5.4).

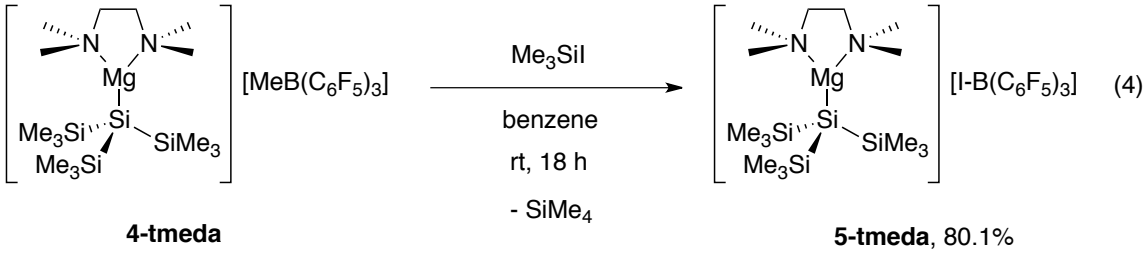

4-tmeda **5-tmeda**, 80.1%

The methyl resonance in $-Si(SiMe_3)_3$ in the ^1H NMR spectrum of **5.5-tmeda** appeared at 0.36 ppm which laid between the neutral Mg iodide and Mg methylborate. Also, the Mg---I---B bridging mode can be confirmed from the inequivalent resonances of the TMEDA ligand in the ^1H NMR spectrum.

Unfortunately, the absence of an X-ray structure fails to confirm the molecular connectivity as multiple recrystallization attempts yielded just oil residues. However, tThe long reaction time (16-18 h vs. 30 min) compared to the reaction of **5.2-tmeda** with Me_3SiI suggests that the methyl group on the neutral complexes **5.2** exhibits stronger nucleophilicity than the methyl group on the methylborate species towards Me_3SiI. This is partly due to a strongly Lewis acidic borane center that quenches out most of the nucleophilicity of the methyl group. In contrast, the reactions with other electrophiles, such as MeI and MeOTf only provide $HSi(SiMe_3)_3$; $MeSi(SiMe_3)_3$ nor ethane were observed in the reactions.

We have also examined the silyl group transfer reactions of **5.4-tmeda** as a convenient route to transition metal silyl. The reactions of 4-tmeda and either Cp_2MCl_2 (M =

Zr, Hf) in bromobenzene-d_5 instantaneously provide $Cp_2M\{Si(SiMe_3)_3\}Cl$ (M = Zr, Hf) and $(tmeda)MgCl\{MeB(C_6F_5)_3\}$. The methyl group or methylborate transfer was not observed. In comparison, the silyl group transfer is faster in **5.4-tmeda** than in **5.2-tmeda**, which indicates the nucleophilicity of the silyl group is enhanced in the cationic species. It has been shown previously cationic hafnium silyl compounds are much more active toward σ-bond metathesis with silanes and arenes than their neutral counterparts.

Reactions 5.3. Reactions of $L_2MgSi(SiMe_3)_3Me$ with trityl tetrakis(perfluorophenyl)borate.

We also examined the reaction of **5.2** with $[Ph_3C][B(C_6F_5)_4]$ in effort to generate cationic Mg silyl complexes with non-coordinating anion. The reactions of **5.2-tmeda** or **5.2-dpe** and $[Ph_3C][B(C_6F_5)_4]$ in benzene give deep brown oily residues that solidify after benzene and pentane washes. The benzene wash revealed the formation of Ph_3CMe, as evidence of methine group abstraction (eq 5.5).

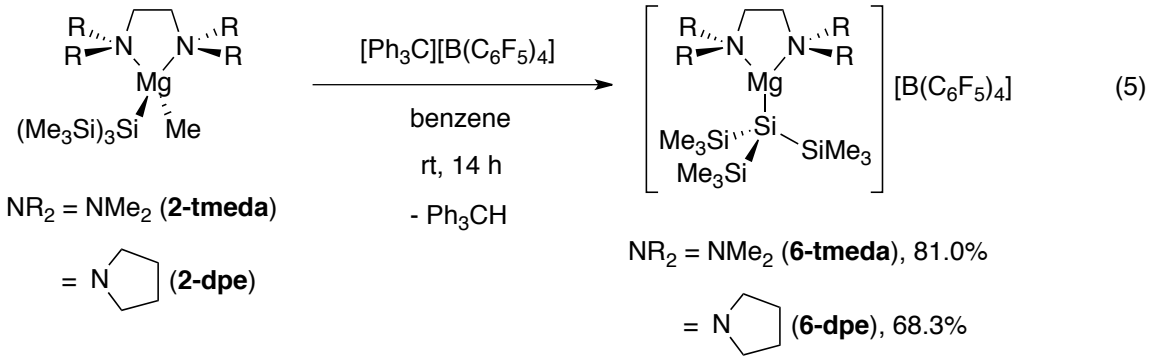

The ^1H NMR spectra of the brown residue in bromobenzene-d_5 supported the cationic character as $SiMe_3$ resonances shifted upfield (0.28 ppm in tmeda adduct and 0.30 ppm in dpe adduct) compared to the neutral compounds **5.2**. ^{11}B NMR data also was also evident of

a single four-coordinated borate product at -15.9 ppm and thus suggested the products as [(tmeda)MgSi(SiMe$_3$)$_3$][B(C$_6$F$_5$)$_4$] (**5.6-tmeda**) and [(dpe)MgSi(SiMe$_3$)$_3$][B(C$_6$F$_5$)$_4$] (**5.6-dpe**). Although X-ray structures of **5.6-tmeda** and **5.6-dpe** are absent, the coordination number on the Mg centers can be established from the splitting pattern of tmeda resonances in ^{1}H NMR spectrum. Similar to **5.4**, the NMe$_2$ and NCH$_2$ resonances displayed as two sets of singlet, suggesting a pseudo-C_{2v} symmetry with the a outer-sphere B(C$_6$F$_5$)$_4^-$ ligand. Besides, the ^{19}F NMR spectrum showed three sets of resonances assigned to *meta*, *para*, and *ortho* fluoride atoms on B(C$_6$F$_5$)$_4$ anion, this can rule out any Mg---F interactions in the solution structure.

5.4. Reactions of L$_2$MgSi(SiMe$_3$)$_3$Me with bis(perfluorophenyl)borane.

We have shown earlier the reactivity and selectivity of **5.2-tmeda** and electrophiles depend on the nature of size (Me vs SiMe$_3$) and leaving groups (I vs OTf). Therefore, we are intrigued with the reaction selectivity with a smaller and weaker Lewis acid in HB(C$_6$F$_5$)$_2$. In the case of Cp$_2$ZrMe(μ-H$_2$)B(C$_6$F$_5$)$_2$, Piers demonstrated HB(C$_6$F$_5$)$_2$ tends to form μ-hydride bridging structure as to stabilize the highly Lewis acidic Zr center without any neutral Lewis base coordination.[iii] When 1 equiv of HB(C$_6$F$_5$)$_2$ was added to **5.2-tmeda** in benzene-d_6, a 1:1 mixture of the comproportionation products (tmeda)MgSi(SiMe$_3$)$_3$(μ-H)$_2$B(C$_6$F$_5$)$_2$ (**5.7-tmeda**) and (tmeda)MgSi(SiMe$_3$)$_3$(μ-Me)$_2$B(C$_6$F$_5$)$_2$ (**5.8-tmeda**) were identified by ^{1}H and ^{11}B NMR spectroscopy (eq 5.6). The expected mixed methylhydridoborate complexes (tmeda)MgSi(SiMe$_3$)$_3${(μ-H)(μ-Me)B(C$_6$F$_5$)$_2$} were not observed.

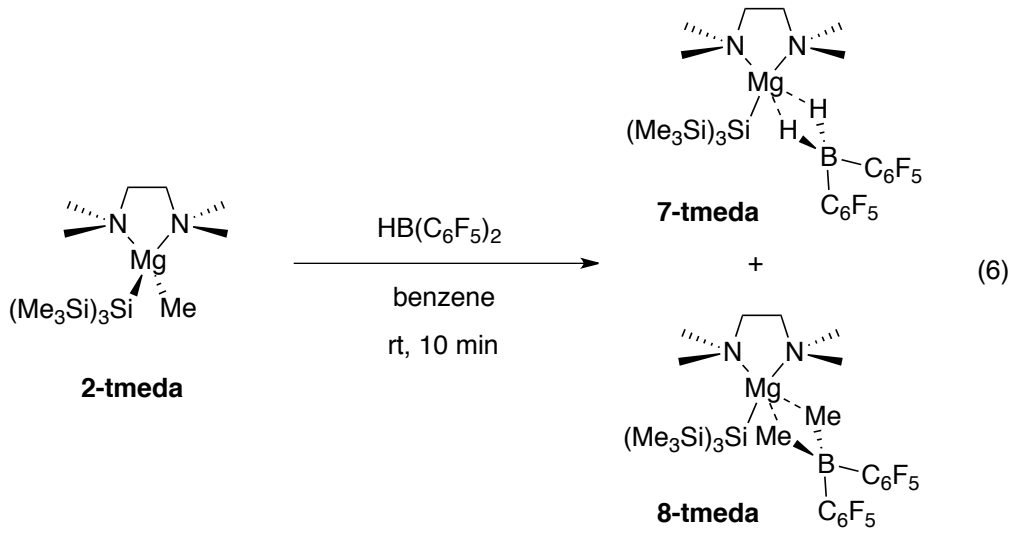

(6)

Two $Si(SiMe_3)_3$ resonances were observed in ^1H NMR spectrum, which suggested two Mg silyl species present in the reaction mixture. A broad quartet at 2.24 ppm and a broad singlet at 0.77 ppm were also observed and were assigned to $H_2B(C_6F_5)_2$ and $Me_2B(C_6F_5)_2$, respectively. Moreover, the ^{11}B NMR spectrum contained a broad singlet (δ -12.9) and a triplet (δ -28.6, $^1J_{BH}$ = 69.6 Hz) that are characteristic of a dimethylborate $Me_2B(C_6F_5)_2$ group and a dihydroborate $H_2B(C_6F_5)_2$ group. The dihydroborate adduct $Cp_2Zr\{(\mu\text{-}H)_2B(C_6F_5)_2\}_2$ is prepared from Cp_2ZrMe_2 and 4 equiv of $HB(C_6F_5)_2$.[19] Interestingly, the ^{11}B NMR shift in **5.7-tmeda** is 15.6 ppm upfield from the signal for $Cp_2Zr\{(\mu\text{-}H)_2B(C_6F_5)_2\}_2$ (-12.9 ppm, $^1J_{BH}$ = 64 Hz).[21] Upon addition of a second equivalent of $HB(C_6F_5)_2$ into a mixture of **5.7-tmeda** and **5.8-tmeda**, the resonances of **5.8-tmeda** in ^1H NMR spectrum are converted quantitatively and rapidly to those of **5.7-tmeda** and $MeB(C_6F_5)_2$ (identified by ^{11}B NMR and ^{19}F NMR to literature). $(L_2)MgSi(SiMe_3)_3(\mu\text{-}H)_2B(C_6F_5)_2$ (L_2 = tmeda (**5.7-tmeda**) or dpe (**5.7-dpe**)) can also be prepared directly from 2 equiv of $HB(C_6F_5)_2$ and **5.2** in good yield (eq 5.7).

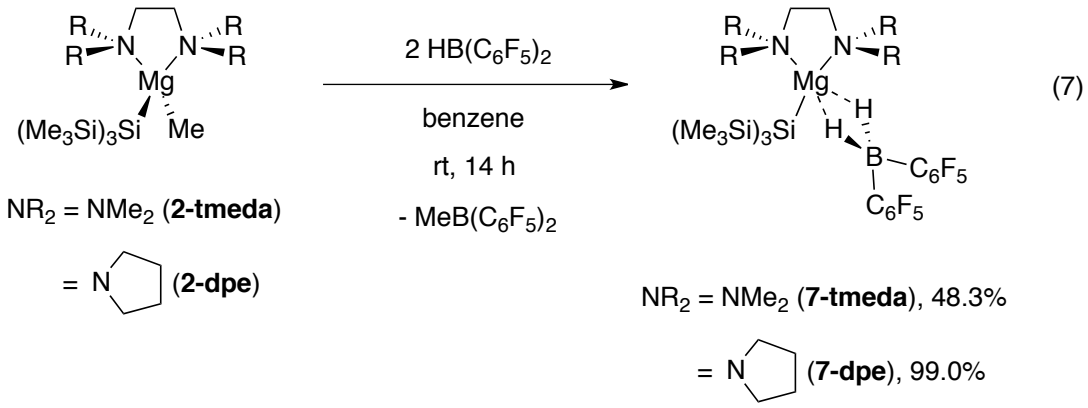

(7)

The ^{1}H NMR spectrum of the isolated dihydridoborate species **5.7-tmeda** contained diastereotopic NMe groups as two sets of singlet at 1.84 and 1.69 ppm and NCH_2 groups as broad resonances at 1.55-1.40 and 1.38-1.25 ppm. The ^{1}H NMR resonance splitting pattern suggests pseudo-tetrahedral geometry on Mg. Furthermore, a board quartet (2.23 ppm, $^1J_{BH}$ = 72.1 Hz) and a sharp singlet (0.28 ppm) were also observed and were assigned to BH and $SiMe_3$ resonances, respectively. The IR spectrum of **5.7-tmeda** (KBr) showed only one band for the ν_{BH} (2268 cm^{-1}), while **5.7-dpe** contained two bands at 2361 and 2333 cm^{-1}. In comparison, $[Li(Et_2O)][B(C_6F_5)_2H_2]$ has two IR bands for BH at 2380 and 2318 cm^{-1},[22] while donor-free Group 4 hydridoborate compounds show lower energy bands, $Cp_2Ti(\mu\text{-}H)_2B(C_6F_5)_2$ (2073, 2008, 1367 cm^{-1})[22] and $Cp_2Zr\{(\mu\text{-}H_2)B(C_6F_5)_2\}_2$ (2184, 2110, 2028 cm^{-1}).[20] Addition of PMe_3 to $Cp_2Ti(\mu\text{-}H)_2B(C_6F_5)_2$ shifts the ν_{BH} to higher energy IR bands in 2361 and 2314 cm^{-1}.[22] Similarly, diamine coordination to Mg contributes to more blue-shifted ν_{BH} IR bands observed in **5.7**.

The solid-state structure suggests **5.7-dpe** as a contact-ion pair that contains a $[Mg](\mu\text{-}H)_2\ B(C_6F_5)_2$ bridging structure (see ORTEP diagram in Figure 5.5). The Mg-Si bond distance is 2.648(1) Å, which is ca. 0.047 Å longer than **5.4-tmeda** but identical to

neutral **5.2-tmeda** (Table 5.2) within 3 e.s.d.'s. The Mg-N bonds are shorter by ca. 0.03 Å in the dihydridoborate compounds than the neutral compounds. The Mg-H distances are 2.09(4) and 2.05(4) Å, well within the sum of Van der Waals radii of Mg and H (Σ_{VDW}(MgH): 2.82 Å) but slightly more than the sum of covalent radii of Mg and H ($\Sigma_{convalent}$(MgH): 1.64 Å).[23] The Mg-B distance of 2.507(4) Å in **5.7-dpe** is on the high end value of that of $Mg(BD_4)_2$ (Mg-B: 2.31(3)-2.53(4)).[24] The B-H bond distances are within error identical to those of $Cp_2Ti(\mu\text{-}H)_2B(C_6F_5)_2$, and the H-B-H angle (109.0(3)°) for **5.7-dpe** falls between $[Li(Et_2O)][B(C_6F_5)_2H_2]$ (111.6(5)°) and $Cp_2Ti(\mu\text{-}H)_2B(C_6F_5)_2$ (100.8(7)°).[22] Meanwhile, the pseudo-five-coordinate Mg center in **5.7-dpe** expected to have a narrower N-Mg-N to accompany the extra coordination of a B-H group. The N-Mg-N angle of **5.7-dpe** (82.9(2)°) is ca. 0.6° and 2° smaller than those of **5.2-tmeda** and **5.4**, respectively.

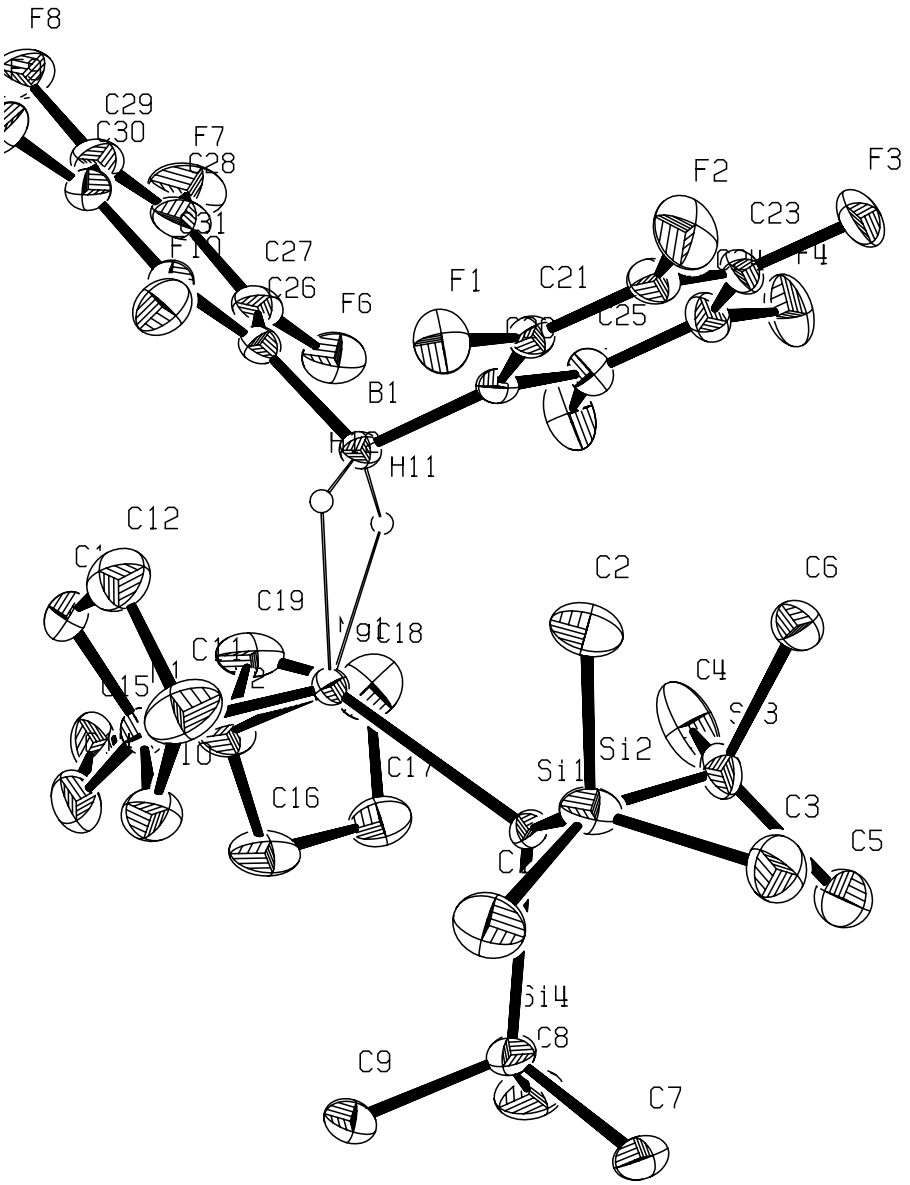

Figure 5.5. ORTEP diagram of **5.7-dpe**. Hydrogen atoms on the H_2 $B(C_6F_5)_2$ were found objectively in the electron density map, were refined isotropically, and were included in the plot. All other hydrogen atoms were not included. Fluorine atoms and carbon atoms on

$H_2B(C_6F_5)_2$ were refined anisotropically and have normal thermal paramters but are depicted using a ball-and-stick representation for clarity. Selected distances (Å): Mg1-Si1, 2.648(1); Mg1-N1, 2.217(4); Mg1-N2, 2.187(4); Mg1-H11, 2.09(4); Mg1-H12, 2.05(4); B1-H11, 1.17(4); B1-H12, 1.12(4). Selected angles (°): N1-Mg1-N2, 82.9(2); Si1-Mg1-B1, 118.1(1).

Tilley reported that M-Si bond of some of the Group 4 silyl complexes are photolytically active. For example, exposure of $CpCp^*Hf[Si(SiMe_3)_3]Cl$ to UV light provides $HSi(SiMe_3)_3$ and $CpCp^*HfCl_2$.[17] In contrast, the syntheses of neutral and cationic magnesium silyl complexes do not require exclusion of light. They can be stored at room light in glovebox for extended period of time without decomposition. Furthermore, neutral magnesium silyl, **5.2-tmeda**, **5.2-dpe**, and **5.3-tmeda** were also exposed to UV light with 450 W medium pressure Hg lamp for 2 h in benzene, and no decomposition was observed.

Conclusion

Relatively few d^0 cationic metal silyl compounds have been prepared for structural, spectroscopic, and reactivity comparisons. The ^{29}Si NMR chemical shifts of $CpCp^*ZrSiH_2PhCl$ and $[Cp_2ZrSiH_2Ph]_2[X]_2$ [X = $B(C_6F_5)_4$; $Bu_nB(C_6F_5)_{4-n}$] were reported to shift downfield for the cationic species (-14.3 vs. 105 ppm),[9a.17] and the cationic species are more active in silane dehydropolymerization than the neutral species. The neutral $Cp_2HfSi^tBuPh_2Me$ vs. $Cp_2HfSi^tBuPh_2(\mu\text{-}Me)B(C_6F_5)_3$ showed only a small downfield ^{29}Si NMR chemical shift for the latter, zwitterionic compound (37.2 vs 39.4 ppm). Significant downfield shifts were reported for zwitterionic $Cp_2HfSi(SiMe_3)_3(\mu\text{-}Me)B(C_6F_5)_3$ (-21.4 ppm) versus neutral $Cp_2HfSi(SiMe_3)_3Me$ (-84.2 ppm).[9e.f] The ^{29}Si NMR chemical shift of the silicon bonded to magnesium is shifted downfield as the ionic character of the other X-type

ligand is increased (Table 1).[7,8] For example, by comparing the ^{29}Si NMR shift of the internal Si, $MgSi(SiMe_3)_3B(C_6F_5)_4$(tmeda) (**5.6-tmeda**) (-163.4 ppm) > $MgSi(SiMe_3)_3MeB(C_6F_5)_3$(tmeda) (**5.4-tmeda**) (-167.2 ppm) > $MgSi(SiMe_3)_3H_2B(C_6F_5)_2$(tmeda) (**5.7-tmeda**) (173.1 ppm) > $MgSi(SiMe_3)_3Me$(tmeda) (**5.2-tmeda**) (-175.4 ppm), the trend nicely follows the expected cationic character of the compound. Furthermore, the chemical shift trend provides a nice parallel to the observed nucleophilicity of Mg silyl in silyl group transfer reaction. For example, zwitterionic Mg silyl (4-tmeda) engages in faster silyl group to Group 4 metal than neutral analogue (2-tmeda). Although utilizing Mg reagents as a silyl group transmetallation agent is reported,[8,25] we have shown here the transfer rate and preference can be enhanced by using cationic Mg silyl reagents and diamine ligands.

Experimental.

General Procedures. All reactions were performed under a dry argon atmosphere using standard Schlenk techniques, or under a nitrogen atmosphere in a glovebox unless otherwise indicated. Dry, oxygen-free solvents were used throughout. Benzene, toluene, pentane, and tetrahydrofuran were degassed by sparging with nitrogen, filtered through activated alumina columns, and stored under N_2. Benzene-d_6, THF-d_8 were vacuum transferred from Na/K alloy and stored under N_2 in the glovebox. (tmeda)Mg(Me)Br,[11] $KSi(SiMe_3)_3$,[2] $B(C_6F_5)_3$,[26] $HB(C_6F_5)_2$,[27] $[Ph_3C][B(C_6F_5)_4]$,[28] and dpe[29] were prepared according to literature procedures. 3.0 M MeMgBr in diethyl ether was purchased from Aldrich and used as received. ^{1}H and $^{13}C\{^1H\}$ NMR spectra were collected on Bruker DRX-400 spectrometer. $^{29}Si\{^1H\}$ NMR spectra were recorded using DEPT experiments, and assigments were verified by ^{1}H

COESY, ^{1}H-^{13}C HMQC, ^{1}H-^{13}C HMBC, and ^{1}H-^{29}Si HMBC experiments. Elemental analysis was performed using a Perkin-Elmer 2400 Series II CHN/S by the Iowa State Chemical Instrumentation Facility.

(tmeda)MgSi(SiMe$_3$)$_3$Me (5.2-tmeda). (tmeda)Mg(Me)Br (0.269 g, 1.14 mmol) and KSi(SiMe$_3$)$_3$ (0.328 g, 1.14 mmol) were dissolved in benzene (10 mL) and the mixture was allowed to stir for 4 h at room temperature. The volatile materials were evaporated under reduced pressure, and the resulting residue was extracted with pentane (3 × 5 mL). The pentane solution was concentrated and cooled to -30 °C to yield **5.2-tmeda** (0.250 g, 0.620 mmol, 54.4%) as a colorless block-like crystal. ^{1}H NMR (benzene-d_6, 600 MHz, 25 °C): δ 1.94 (s, 6 H, NMe), 1.79 (s, 6 H, NMe), 1.56 (s, 4 H, CH$_2$), 0.51 (s, 27 H, SiMe$_3$), -1.03 (s, 3 H, CH$_3$). ^{13}C{^{1}H} NMR (benzene-d$_6$, 150 MHz, 25 °C): δ 56.2 (NCH$_2$), 47.7 (NCH$_3$), 46.6 (NCH$_3$), 6.02 (SiMe$_3$), -11.4 (MgCH$_3$). ^{29}Si{^{1}H} NMR (benzene-d_6, 119.3 MHz, 25 °C): δ -7.1 (SiMe$_3$), -175.4 (*Si*(SiMe$_3$)$_3$). IR (KBr, cm^{-1}): 2994 m, 2944 s, 2887 s, 2852 s, 2806 m, 2778 m, 1465 s, 1288 w, 1236 s, 1027 m, 948 m, 834 s, 677 m. Anal. Calcd for C$_{16}$H$_{46}$Si$_4$N$_2$Mg: C, 47.66; H, 11.50; N, 6.95. Found: C, 47.77; H, 11.51; N, 6.85. mp 179-180 °C.

(dpe)MgMeBr (5.1-dpe). 1,2-*N*,*N*-dipyrrolidenylethane (1.52 g, 9.01 mmol) and 20 mL of diethyl ether were placed in a 100 mL Schlenk flask. In a second Schlenk flask, 3.0 M MgMeBr (2.70 mL, 8.10 mmol) was diluted with 40 mL of diethyl ether. The 1,2-*N*,*N*-dipyrrolidenylethane solution was added dropwise to the MgMeBr solution. Upon addition, a white precipitate formed, and the resulting mixture was allowed to stir for 1 h once the addition was complete. The white solid was isolated by filtration and dried under vacuum to yield **5.1-dpe** (1.94 g, 6.73 mmol, 83.1%) as a white solid. ^{1}H NMR (THF-d_8, 600 MHz, 25

°C): δ 2.71 (s br, 8 H, NCH_2(CH_2)$_2$CH_2), 2.69 (s, 4 H, NCH_2), 1.81 (m, 8 H, NCH_2(CH_2)$_2$$CH_2$), -1.65 (s, 3 H, CH_3). $^{13}C\{^1H\}$ NMR (THF-d_8, 150 MHz, 25 °C): δ 55.7 (N*C*H_2(CH_2)$_2$*C*H_2, NCH_2), 24.0 (NCH_2(*C*H_2)$_2$$CH_2$), -17.3 ($MgCH_3$). IR (KBr, cm^{-1}): 2973 s, 2858 s, 2781 m, 1462 s, 1374 w, 1334 w, 1307 w, 1266 w, 1101 m, 1968 m, 945 m, 863 w. Anal. Calcd for $BrC_{11}H_{23}N_2Mg$: C, 45.95; H, 8.06; N, 9.74. Found: C, 45.00; H, 7.74; N, 9.40. mp 196-197 °C.

(dpe)MgSi(SiMe$_3$)$_3$Me (5.2-dpe). 5.2-dpe was prepared following the procedure for **5.2-tmeda** with **5.1-dpe** (0.906 g, 3.15 mmol) and $KSi(SiMe_3)_3$ (0.904 g, 3.15 mmol) to yield **5.2-dpe** (0.928 g, 2.04 mmol, 64.7%) as a colorless block crystal. ^1H NMR (benzene-d_6, 400 MHz, 25 °C): δ 3.33-3.23 (m, 2 H, NCH_2(CH_2)$_2$CH_2), 3.09-2.99 (m, 2 H, NCH_2(CH_2)$_2$CH_2), 1.93-2.04 (m, 2 H, NCH_2), 1.87-1.71 (m, 2 H, NCH_2 + NCH_2(CH_2)$_2$CH_2), 1.71-1.59 (m, 4 H, NCH_2(CH_2)$_2$$CH_2$), 1.44-1.22 (m, 4 H, NCH_2(CH_2)$_2$$CH_2$), 0.51 (s, 27 H, $SiMe_3$), -1.02 (s, 3 H, MgMe). $^{13}C\{^1H\}$ NMR (benzene-d_6, 125 MHz, 25 °C): δ 57.5 (N*C*H_2(CH_2)$_2$*C*H_2), 55.3 (N*C*H_2(CH_2)$_2$*C*H_2), 55.1 (NCH_2), 23.6 (NCH_2(*C*H_2)$_2$$CH_2$), 23.5 ($NCH_2$(*C*$H_2$)$_2$$CH_2$), 6.2 ($SiMe_3$), -11.9 (MgMe). $^{29}Si\{^1H\}$ NMR (benzene-d_6, 119.3 MHz, 25 °C): δ -7.2 ($SiMe_3$), -177.0 (*Si*($SiMe_3$)$_3$). IR (KBr, cm^{-1}): 2957 s, 2886 m, 2776 m, 2051 w, 1462 w, 1389 w, 1336 w, 1293 w, 1235 m, 1095 w, 1057 w, 950 w, 835 m br, 746 w, 676 m. Calcd for $C_{20}H_{50}Si_4N_2Mg$: C, 52.76; H, 11.07; N, 6.15. Found: C, 52.97; H, 11.31; N, 6.03. mp 226-233 °C.

(tmeda)MgSi(SiMe$_3$)$_3$I (5.3-tmeda). Trimethylsilyl iodide (93.3 μL, 0.658 mmol) was added to a benzene (5 ml) solution of **5.2-tmeda** (0.204 g, 0.506 mmol). The mixture was allowed to stir for 30 min. The volatile materials were evaporated under reduced pressure.

The residue was dissolved in toluene (2 mL) and cooled to -30 °C to give **5.3-tmeda** (0.186 g, 0.362 mmol, 71.4%) as a colorless block crystal. ^{1}H NMR (benzene-d_6, 600 MHz, 25 °C): δ 2.06 (s, 6 H, NMe), 1.88 (s, 6 H, NMe), 1.63-1.67 (m, 2 H, CH_2), 1.43-1.47 (m, 2 H, CH_2), 0.50 (s, 27 H, $SiMe_3$). ^{13}C{^{1}H} NMR (benzene-d_6, 150 MHz, 25 °C): δ 56.0 (NCH_2), 48.9 (NMe_2), 47.2 (NMe_2), 5.84 ($SiMe_3$). ^{29}Si{^{1}H} NMR (benzene-d_6, 119.3 MHz, 25 °C): δ -7.3 ($SiMe_3$), -167.9 ($Si(SiMe_3)_3$). IR (KBr, cm^{-1}): 2994 m, 2956 s, 2891 s, 2810 m, 1465 s, 1287 w, 1260 m, 1238 m, 1023 s br, 948 m, 831 s br, 677 m. Anal. Calcd for $C_{15}H_{43}ISi_4N_2Mg$: C, 34.98; H, 8.41; N, 5.44. Found: C, 34.79; H, 8.50; N, 5.56. mp: 204-205 °C.

(dpe)MgSi(SiMe$_3$)$_3$I (5.3-dpe). 5.3-dpe was prepared following the procedure for **5.3-tmeda** with **5.2-dpe** (0.120 g, 0.263 mmol) and Me_3SiI (39.2 μL, 0.276 mmol) to yield **5.3-dpe** (0.136 g, 0.239 mmol, 91.0%) as a colorless block crystal. ^{1}H NMR (benzene-d_6, 400 MHz, 25 °C): δ 3.54 (m br, 2 H, $NCH_2(CH_2)_2CH_2$), 3.17 (m br, 2 H, $NCH_2(CH_2)_2CH_2$), 1.82 (s, 4 H, NCH_2), 1.78 (m br, 4 H, $NCH_2(CH_2)_2CH_2$; 4 H, $NCH_2(CH_2)_2CH_2$), 1.29 (m br, 4 H, $NCH_2(CH_2)_2CH_2$), 0.51 (s, 27 H, $SiMe_3$). ^{13}C{^{1}H} NMR (benzene-d_6, 125 MHz, 25 °C): δ 57.5 ($NCH_2(CH_2)_2CH_2$), 55.3 ($NCH_2(CH_2)_2CH_2$), 55.1 (NCH_2), 23.4 ($NCH_2(CH_2)_2CH_2$), 23.2 ($NCH_2(CH_2)_2CH_2$), 5.9 ($SiMe_3$). ^{29}Si{^{1}H} NMR (benzene-d_6, 119.3 MHz, 25 °C): δ -7.4 ($SiMe_3$), -168.9 ($Si(SiMe_3)_3$). IR (KBr, cm^{-1}): 2944 m, 2886 m, 1462 m, 1394 w, 1237 s, 1112 w, 1061 w, 945 w, 832 s br, 744 w, 677 m, 622 m. Anal. Calcd for $C_{19}H_{47}ISi_4N_2Mg$: C, 40.24; H, 8.35; N, 4.94. Found: C, 40.14; H, 8.27; N, 5.10. mp 240-243 °C.

[(tmeda)MgSi(SiMe$_3$)$_3$][MeB(C$_6$F$_5$)$_3$] (5.4-tmeda). $B(C_6F_5)_3$ (0.270 g, 0.521 mmol) was added to a benzene solution (5 ml) of **5.2-tmeda** (0.200 g, 0.497 mmol) to give a pale yellow solution. The mixture was stirred for 1.5 h. The volatiles were evaporated under reduced

pressure to give **5.4-tmeda** (0.335 g, 0.366 mmol, 73.6%) as a pale yellow solid. ^{1}H NMR (benzene-d_6, 600 MHz, 25 °C): δ 1.66 (s, 12 H, NMe), 1.44 (m, 4 H, CH_2), 0.94 (s, 3 H, BMe), 0.175 (s, 27 H, $SiMe_3$). $^{13}C\{^{1}H\}$ NMR (benzene-d_6, 150 MHz, 25 °C): δ 56.1 (NCH_2), 46.6 (NMe), 5.1 ($SiMe_3$), BMe resonance was not observed. $^{29}Si\{^{1}H\}$ NMR (benzene-d_6, 119.3 MHz, 25 °C): δ -7.8 ($SiMe_3$), -167.2 ($Si(SiMe_3)_3$). $^{11}B\{^{1}H\}$ NMR (benzene-d_6, 125 MHz, 25 °C): δ -14.3. ^{11}B NMR (bromobenzene-d_5, 79.5 MHz, 25 °C): -15.1. ^{19}F NMR (benzene-d_6, 376 MHz, 25 °C): δ -132.8 (d, $^{3}J_{FF}$ = 22.9 Hz, 6 F, *o*-F), -161.3 (t, $^{3}J_{FF}$ = 21.8 Hz, 3 F, *p*-F), -165.3 (t, $^{3}J_{FF}$ = 18.8 Hz, 6 F, *m*-F). ^{19}F NMR (bromobenzene-d_5, 376 MHz, 25 °C): δ -133.68 (d, $^{3}J_{FF}$ = 23.3 Hz, 6 F, *o*-F), -161.87 (t, $^{3}J_{FF}$ = 20.6 Hz, 3 F, *p*-F), -165.72 (t, $^{3}J_{FF}$ = 20.7 Hz, 6 F, *m*-F). IR (KBr, cm^{-1}): 2954 m, 2896 m, 1644 m, 1513 s, 1459 s br, 1244 m br, 1087 s, 977 s, 836 s br, 757 m. Anal. Calcd for $BC_{34}F_{15}H_{46}Si_4N_2Mg$: C, 44.62; H, 5.07; N, 3.06. Found: C, 44.84; H, 4.90; N, 3.07. mp 130-133 °C

[(dpe)MgSi(SiMe$_3$)$_3$][MeB(C$_6$F$_5$)$_3$] (5.4-dpe). **5.4-dpe** was prepared following the procedure for **5.4-tmeda** using **5.2-dpe** (0.173 g, 2.01 mmol) and $B(C_6F_5)_3$ (0.194 g, 0.379 mmol) to yield **5.4-dpe** (0.311 g, 0.321 mmol, 84.6%) as a pale yellow solid. ^{1}H NMR (bromobenzene-d_5, 400 MHz, 25 °C): δ 3.07 (m br, 4 H, $NCH_2(CH_2)_2CH_2$), 2.35 (s, 4 H, NCH_2), 2.29 (m, 4 H, $NCH_2(CH_2)_2CH_2$), 1.65 (m, 4 H, $NCH_2(CH_2)_2CH_2$), 1.54 (m, 4 H, $NCH_2(CH_2)_2CH_2$), 1.03 (s br, 3 H, $MeB(C_6F_5)_3$), 0.24 (s, 27 H, $SiMe_3$). $^{13}C\{^{1}H\}$ NMR (bromobenzene-d_5, 125 MHz, 25 °C): 148.5 (br, C_6F_5), 146.1 (br, C_6F_5), 138.6 (br, C_6F_5), 137.0 (br, C_6F_5), 136.1 (br, C_6F_5), 134.5 (br, C_6F_5), 54.0 ($NCH_2(CH_2)_2CH_2$), 53.4 (NCH_2), 21.4 ($NCH_2(CH_2)_2CH_2$), 10.8 (br, BMe), 3.5 ($SiMe_3$). ^{11}B NMR (bromobenzene-d_5, 79.5 MHz, 25 °C): -14.8. ^{19}F NMR (bromobenzene-d_5, 376 MHz, 25 °C): δ -132.89 (br), -165.13

(br), -167.92 (br). $^{29}Si\{^{1}H\}$ NMR (bromobenzene-d_5, 119.3 MHz, 25 °C): δ -7.7 ($SiMe_3$), -168.7 ($Si(SiMe_3)_3$). IR (KBr, cm^{-1}): 2960 m, 2890 m, 2811 w, 1642 m, 1514 s, 1460 s, 1379 w, 1261 m, 1244 m, 1087 s, 973 s, 835 s, 803 m, 758 w, 736 w, 648 m. Anal. Calcd for $BC_{38}F_{15}H_{50}Si_4N_2Mg$: C, 47.12; H, 5.21; N, 2.90. Found: C, 47.36; H, 4.71; N, 2.87. mp 71-72 °C.

[(tmeda)MgSi(SiMe$_3$)$_3$IB(C$_6$F$_5$)$_3$] (5.5-tmeda). Me_3SiI (12.5 μl, 0.088 mmol) was added to a benzene (5 ml) solution of **5.4-tmeda** (0.079 g, 0.087 mmol) at room temperature and the mixture was stirred for 17 h. The volatiles of the pale yellow reaction mixture were evaporated under reduced pressure to yield **5.5-tmeda** (0.071 g, 0.069 mmol, 80.1%) as a white solid. ^{1}H NMR (bromobenzene-d_5, 400 MHz, 25 °C): δ 2.32 (s br, 12 H, NMe), 2.23 (s br, 4 H, CH_2), 0.36 (s, 27 H, $SiMe_3$). $^{13}C\{^{1}H\}$ NMR (bromobenzene-d_5, 150 MHz, 25 °C): δ 148.7 (br, C_6F_5), 146.3 (br, C_6F_5), 136.7 (br, C_6F_5), 134.2 (br, C_6F_5), 54.7 (NCH_2), 46.1 (NCH_3), 4.0 ($SiMe_3$). $^{29}Si\{^{1}H\}$ NMR (bromobenzene-d_5, 119.3 MHz, 25 °C): δ -7.6 ($SiMe_3$), -165.0 ($Si(SiMe_3)_3$). $^{11}B\{^{1}H\}$ NMR (bromobenzene-d_5, 125 MHz, 25 °C): δ -14.3. ^{19}F NMR (bromobenzene-d_5, 376 MHz, 25 °C): δ -131.5 (d, t, $^{3}J_{FF}$ = 20.3 Hz, 6 F, *o*-F), -163.3 (t, $^{3}J_{FF}$ = 21.1 Hz, 3 F, *p*-F), -166.0 (t, $^{3}J_{FF}$ = 19.6 Hz, 6 F, *m*-F). Calcd for $BC_{33}F_{15}H_{43}ISi_4N_2Mg$: C, 38.59; H, 4.22; N, 2.73. Found: C, 38.52; H, 3.97; N, 2.83.

[(tmeda)MgSi(SiMe$_3$)$_3$][B(C$_6$F$_5$)$_4$] (5.6-tmeda). $[Ph_3C][B(C_6F_5)_4]$ (0.250 g, 0.271 mmol) was added to a benzene solution of **5.2-tmeda** (0.104 g, 0.258 mmol). The reaction mixture was stirred overnight to give an oily residue. The benzene solvent (top layer) was decanted from the precipitate. The oily residue was washed with benzene (3 × 5 ml) and pentane (3 × 5 ml) to remove Ph_3CMe. The remaining material was dried under reduced pressure to give

5.6-tmeda (0.223 g, 0.209 mmol, 81.0 %) as light brown solid. ^{1}H NMR (bromobenzene-d_5, 400 MHz, 25 °C): δ 2.20 (s br, 4 H, CH_2), 2.12 (s br, 12 H, NMe), 0.28 (s, 27 H, $SiMe_3$). $^{13}C\{^{1}H\}$ NMR (bromobenzene-d_5, 150 MHz, 25 °C): δ 148.6 (br, C_6F_5), 146.2 (br, C_6F_5), 138.5 (br, C_6F_5), 136.7 (br, C_6F_5), 136.0 (br, C_6F_5), 134.3 (br, C_6F_5), 54.5 (NCH_2), 44.4 (NCH_3), 3.6 ($SiMe_3$). $^{29}Si\{^{1}H\}$ NMR (bromobenzene-d_5, 119.3 MHz, 25 °C): δ -7.9 ($SiMe_3$), -163.4 ($Si(SiMe_3)_3$). $^{11}B\{^{1}H\}$ NMR (bromobenzene-d_5, 125 MHz, 25 °C): δ -15.9. ^{19}F NMR (bromobenzene-d_5, 376 MHz, 25 °C): δ -131.5 (s br, 6 F, *o*-F), -160.9 (t, $^{3}J_{FF}$ = 20.7 Hz, 3 F, *p*-F), -165.5 (s br, 6 F, *m*-F). IR (KBr, cm^{-1}): 2951 m, 2895 w, 2181 w, 1644 s, 1515 s, 1464 s br, 1374 m, 1278 s, 1244 m, 1091 s br, 980 s br, 834 s br, 769 m, 756 m, 684 s. Calcd for $BC_{39}F_{20}H_{43}Si_4N_2Mg$: C, 43.89; H, 4.06; N, 2.62. Found: C, 43.93; H, 3.84; N, 2.62. mp 103-105°C.

[(dpe)MgSi(SiMe$_3$)$_3$][B(C$_6$F$_5$)$_4$] (5.6-dpe). A modified procedure for **5.6-tmeda** was followed, using **5.2-dpe** (0.101 g, 0.223 mmol) and $[Ph_3C][B(C_6F_5)_4]$ (0.216 g, 0.234 mmol) to yield **5.6-dpe** (0.170 g, 0.152 mmol, 68.3%) as a light brown solid. ^{1}H NMR (bromobenzene-d_5, 400 MHz, 25 °C): δ 3.09-2.85 (m br, 4 H, $NCH_2(CH_2)_2CH_2$), 2.60-2.20 (m br, 4 H, NCH_2; 4 H, $NCH_2(CH_2)_2CH_2$), 1.69 (s br, 8 H, $NCH_2(CH_2)_2CH_2$), 0.30 (s, 27 H, $SiMe_3$). $^{13}C\{^{1}H\}$ NMR (bromobenzene-d_5, 150 MHz, 25 °C): δ 144.6 (br, C_6F_5), 142.2 (br, C_6F_5), 134.4 (br, C_6F_5), 132.7 (br, C_6F_5), 132.0 (br, C_6F_5), 130.2 (br, C_6F_5), 49.8 ($NCH_2(CH_2)_2CH_2$), 49.4 ($NCH_2(CH_2)_2CH_2$), 49.2 (NCH_2), 49.1 (NCH_2), 17.5 ($NCH_2(CH_2)_2CH_2$), 17.4 ($NCH_2(CH_2)_2CH_2$), -0.3 ($SiMe_3$). $^{29}Si\{^{1}H\}$ NMR (bromobenzene-d_5, 119.3 MHz, 25 °C): δ -7.9 ($SiMe_3$), -170.8 ($Si(SiMe_3)_3$).$^{11}B\{^{1}H\}$ NMR (bromobenzene-d_5, 125 MHz, 25 °C): δ -15.9. ^{19}F NMR bromobenzene-d_5, 376 MHz, 25 °C): δ -131.7 (d,

$^{3}J_{FF}$ = 9.4 Hz, 8 F, *o*-F), -161.3 (t, $^{3}J_{FF}$ = 20.7 Hz, 4 F, *p*-F), -165.6 (t, $^{3}J_{FF}$ = 19.2 Hz, 4 F, *m*-F). IR (KBr, cm^{-1}): 3092 w, 3072 w, 3037 w, 2952 s, 2891 s, 2622 vw, 2596 vw, 2551 vw, 2331 vw, 2177 w, 2088 vw, 2046 vw, 1966 vw, 1825 vw, 1643 s, 1515 s, 1464 s, 1277 s, 1243 s, 1091 s, 1037 s, 980 s, 940 s, 904 s, 834 s, 684 s, 661 s. Calcd for $BC_{43}F_{20}H_{47}Si_4N_2Mg$: C, 46.14; H, 4.23; N, 2.50. Found: C, 46.29; H, 4.01; N, 2.38. mp 70-73 °C.

(tmeda)MgSi(SiMe$_3$)$_3$(μ-H)$_2$B(C$_6$F$_5$)$_2$ (5.7-tmeda). $HB(C_6F_5)_2$ (0.293 g, 0.271 mmol) was added to a benzene solution of **5.2-tmeda** (0.123 g, 0.258 mmol) at room temperature. After stirring for 0.5 h, volatile of the clear reaction mixture was evaporated under reduced pressure, followed by pentane wash (2 x 5 ml) and evaporated under vacuum to yield **5.7-tmeda** (0.137g, 0.186 mmol, 52.5 %) as a pale white solid. ^{1}H NMR (benzene-d_6, 400 MHz, 25 °C): δ 2.23 (q, $^{1}J_{BH}$ = 72.1 Hz, 2 H, BH_2), 1.84 (s, 6 H, NMe), 1.69 (s, 6 H, NMe), 1.55-1.40 (m br, 2 H, NCH_2) , 1.38-1.25 (m br, 2 H, NCH_2), 0.28 (s, 27 H, $SiMe_3$). $^{13}C\{^{1}H\}$ NMR (benzene-d_6, 150 MHz, 25 °C): δ 149.8 (br, C_6F_5),147.4 (br, C_6F_5), 141.7 (br, C_6F_5), 139.2 (br, C_6F_5), 136.8 (br, C_6F_5), 56.4 (NCH_2), 47.9 (NCH_3), 46.5 (NCH_3), 5.4 ($SiMe_3$).). $^{29}Si\{^{1}H\}$ NMR (benzene-d_6, 119.3 MHz, 25 °C): δ -7.7 ($SiMe_3$), -173.1 ($Si(SiMe_3)_3$).$^{11}B\{^{1}H\}$ NMR (benzene-d_6, 125 MHz, 25 °C): δ -28.5 (t, $^{1}J_{BH}$ = 72.1 Hz).). ^{19}F NMR (benzene-d_6, 376 MHz, 25 °C): δ -132.7 (d, $^{3}J_{FF}$ = 21.8 Hz, 6 F, *o*-F), -161.6 (s br, 3 F, *p*-F), -165.4 (s br, 6 F, *m*-F). IR (KBr, cm^{-1}): 2959 m, 2894 w, 2855 w, 2268 w br (ν_{BH}), 1645 m, 1512 s, 1469 s br, 1286 w, 1262 w, 1293 w, 1109 m, 1089 m, 1023 m, 972 m, 832 m, 796 m, 682 w. Calcd for $BC_{25}F_{10}H_{39}Si_4N_2Mg$: C, 44.12; H, 6.17; N, 3.81. Found: C, 43.53; H, 6.61; N, 3.66. mp 195-196 °C.

(dpe)MgSi(SiMe$_3$)$_3$(μ-H)$_2$B(C$_6$F$_5$)$_2$ (5.7-dpe). **5.7-dpe** was prepared following the procedure for **5.7-tmeda** with **5.2-dpe** (0.057 g, 0.125 mmol) and HB(C$_6$F$_5$)$_2$ (0.089 g, 0.257 mmol to give **5.7-dpe** as a pale white solid. (0.098g, 0.124 mmol, 99.0%) ^{1}H NMR (benzene-d_6, 400 MHz, 25 °C): 3.10 (m, 2 H, NC*H*$_2$(CH$_2$)$_2$C*H*$_2$), 2.93 (m, 2 H, NC*H*$_2$(CH$_2$)$_2$C*H*$_2$), 2.31 (q, $^1J_{BH}$ = 72.4 Hz, 2 H, BH$_2$), 1.82 (m, 2 H, NC*H*$_2$(CH$_2$)$_2$C*H*$_2$), 1.73 (m, 4 H, NCH$_2$), 1.59 (m br, 4 H, NCH$_2$(C*H*$_2$)$_2$*C*H$_2$), 1.48 (m, 2 H, NC*H*$_2$(CH$_2$)$_2$C*H*$_2$), 1.21 (m br, 4 H, NCH$_2$(C*H*$_2$)$_2$CH$_2$), 0.30 (s, 27 H, SiMe$_3$). ^{13}C NMR (benzene-d_6, 125 MHz, 25 °C): 149.8 (br, C$_6$F$_5$), 147.4 (br, C$_6$F$_5$), 139.2 (br, C$_6$F$_5$), 136.8 (br, C$_6$F$_5$), 56.1 (N*C*H$_2$(CH$_2$)$_2$*C*H$_2$), 55.9 (N*C*H$_2$(CH$_2$)$_2$*C*H$_2$), 54.9 (NCH$_2$), 23.2 (NCH$_2$(*C*H$_2$)$_2$CH$_2$), 22.9 (NCH$_2$(*C*H$_2$)$_2$CH$_2$), 5.5 (SiMe$_3$). ^{29}Si{^{1}H} NMR (benzene-d_6, 119.3 MHz, 25 °C): δ -7.6 (SiMe$_3$), -173.1 (*Si*(SiMe$_3$)$_3$).^{11}B{^{1}H} NMR (benzene-d_6, 125 MHz, 25 °C): δ -29.5 (t, $^1J_{BH}$ = 72.5 Hz). ^{19}F NMR (benzene-d_6, 376 MHz, 25 °C): δ -130.0 (s br, 4 F, *o*-F), -159.0 (t, $^3J_{FF}$ = 19.9 Hz, 2 F, *p*-F), -163.7 (t, $^3J_{FF}$ = 17.7 Hz, 4 F, *m*-F). IR (KBr, cm^{-1}): 2956 m, 2919 m, 2851 m, 2361 vw (ν_{BH}), 2333 vw br (ν_{BH}), 1642 s, 1514 s, 1460 s, 1379 w, 1261 m, 1244 m, 1087 s, 973 s, 835 s, 803 m, 736 w, 684 w, 647 w. Calcd for BC$_{31}$F$_{10}$H$_{49}$Si$_4$N$_2$Mg: C, 47.30; H, 6.27; N, 3.56. Found: C, 46.80; H, 5.96; N, 3.46. mp 193-196 °C.

Reference

1 Tilley, T. D. in *The Silicon–Heteroatom Bond*, eds. Patai, S.; Rappoport, Z. Wiley, Chichester, 1991.

2 Marschner, C. *Eur. J. Inorg. Chem.* **1998**, 221-226.

3 Roddick, D. M.; Heyn, R. H.; Tilley, T. D. *Organometallics* **1989**, *8*, 324-330.

4 (a) Jiang, Q.; Pestana, D. C.; Carroll, P. J.; Berry, D. H. *Organometallics* **1994**, *13*, 3679-3691. (b) Koga, N.; Morokuma, K. *J. Am. Chem. Soc.* **1993**, *115*, 6883-6892. (c) Yu, X.; Morton, L. A.; Xue, Z.-L. *Organometallics* **2004**, *23*, 2210-2224.

5 (a) King, W. A.; Marks, T. J. *Inorg. Chim. Acta.* **1995**, *229*, 343-354. (b)

6 Corey, J. Y. *Chem. Rev.* **2011**, *111*, 863-1071.

7 Farwell, J. D.; Lappert, M. F.; Marschner, C.; Strissel, C.; Tilley, T. D. *J. Organomet. Chem.* **2000**, *603*, 185-188.

8 Gaderbauer, W.; Zirngast, M.; Baumgartner, J.; Marschner, C.; Tilley, T. D. *Organometallics* **2006**, *25*, 2599-2606.

9 (a) Dioumaev, V. K.; Harrod, J. F. *Organometallics* **1994**, *13*, 1548-1550. (b) Jordan, R. F.; Taylor, D. F.; Baenziger, N. C. *Organometallics* **1990**, *9*, 1546-1557. (c) Wu, F.; Jordan, R. F. *Organometallics* **2005**, *24*, 2688-2697. (d) Sadow, A. D.; Tilley, T. D. *J. Am. Chem. Soc.* **2002**, *124*, 6814-6815. (f) Sadow, A. D.; Tilley, T. D. *J. Am. Chem. Soc.* **2003**, *125*, 9462-9475.

10 (a) Fabicon, R. M.; Pajerski, A. D.; Richey, Jr., H. G. *J. Am. Chem. Soc.* **1993**, *115*, 9333-9334. (b) Pajerski, A. D.; Squiller, E. P.; Parvez, M.; Whittle, R. R.; Richey, Jr., H. G. *Organometallics* **2005**, *24*, 809-814. (c) Ireland, B. J.; Wheaton, C. A.; Hayes, P. G. *Organometallics* **2010**, *29*, 1079-1084. (d) Sarazin, Y.; Schormann, M.; Bochmann, M. *Organometallics* **2004**, *23*, 329603302. (e) Layfield, R. A.; Bullock, T. H.; García, F.; Humphrey, S. M.; Schüler, P. *Chem. Commun.* **2006**, 2039-2041. f) Sarazin, Y.; Poirier, V.; Roisnel, T.; Carpentier, J.-F. *Eur. J. Inorg. Chem.* **2010**, 3423-3428. g) Brignou, P.; Guillaume, S. M.; Roisnel, T.; Bourissou, D.; Carpentier, J.-F. *Chem. Eur. J.* **2012**, *18*,

9360-9370. h) Sarazin, Y.; Liu, B.; Roisnel, T.; Maron, L.; Carpentier, J.-F. *J. Am. Chem. Soc.* **2011**, *133*, 9069-9087.

11 Yousef, R. I.; Walfort, B.; Rüffer, T.; Wagner, C.; Schmidt, H.; Herzog, R.; Steinborn, D. *J. Organomet. Chem.* **2004**, *690*, 1178-1191.

12 Guzei, I. A.; Wendt, M. *Dalton Trans.* **2006**, 3991-3999.

13 Vitale, A. A.; San Filippo, Jr., J. *J. Am. Chem. Soc.* **1982**, *104*, 7341-7343.

14 a) Deck, P. A.; Beswick, C. L.; Marks, T. J. *J. Am. Chem. Soc.* **1998**, *120*, 1772-1784. b) Beswick, C. L.; Marks, T. J. *J. Am. Chem. Soc.* **2000**, *122*, 10358-10370.

15 (a) Horton, A. D.; de With, J.; van der Linden, A. J.; van de Weg, H. *Organometallics* **1996**, *15*, 2672-2674. (b) Horton, A. D.; de With, J. *Organometallics* **1997**, *16*, 5424-5436.

16 Piers, W. E. *Adv. Organomet. Chem.* **2005**, *52*, 1-76.

17 Pregosin, P. S.; Martínez-Viviente, E.; Kumar, P. G. H. *Dalton Trans.* **2003**, 4007-4014; (b) Valentini, M.; Pregosin, P. S.; Ruegger, H. *Organometallics* **2000**, *19*, 2551-2555.

18 Shannon, R. D. *Acta Cryst* **1976**, *A32*, 751-767.

19 Sadow, A. D.; Tilley, T. D. *J. Am. Chem. Soc.* **2003**, *125*, 9462-9475.

20 von H. Spence, R. E.; Piers, W. E.; Sun, Y.; Parvez, M.; MacGillivray, L. R.; Zaworotko, M. J. *Organometallics* **1998**, *17*, 2459-2469.

21 von H. Spence, R. E.; Parks, D. J.; Piers, W. E.; MacDonald, M.-A.; Zaworotko, M. J.; Rettig, S. J. *Angew. Chem. Int. Ed. Engl.* **1995**, *34*, 1230-1233.

22 Douthwaite, R. E. *Polyhedron* **2000**, *19*, 1579-1583.

23 Cordero, B.; Gómez, V.; Platero-Prats, A. E.; Revés, M.; Echeverría, J.; Cremades, E.; Barragán, F.; Alvarez, S. *Dalton Trans.* **2008**, 2832-2838.

24 Černý, R.; Filinchuk, Y.; Hagemann, H.; Yvon, K. *Angew. Chem. Int. Ed.* **2007**, *46*, 5765-5767.

25 a) Fischer, R.; Zirngast, M.; Flock, M.; Baumgartner, J.; Marschner, C. *J. Am. Chem. Soc.* **2005**, *127*, 70-71. b) Zirngast, M.; Flock, M.; Baumgartner, J.; Marschner, C. *J. Am. Chem. Soc.* **2009**, *131*, 15952-15962. c) Arp, H.; Baumgartner, J.; Marschner, C.; Zark, P.; Müller, T. *J. Am. Chem. Soc.* **2012**, *134*, 10864-10875.

26 Massey, A. G.; Park, A. J., *J. Organomet. Chem.* **1964**, *2*, 245-250.

27 Park, D. J.; Piers, W. E.; Yap, G. P. A. *Organometallics* **1998**, *17*, 5492-5503.

28 Scott, V. J.; Celenligil-Cetin, R.; Ozerov, O. V. *J. Am. Chem. Soc.* **2005**, *127*, 2852-2853.

29 Remenar, J. F.; Lucht, B. L.; Collum, D. B. *J. Am. Chem. Soc.* **1997**, *119*, 5567-5572.

Chapter 6: Non-classical β-Hydrogen Elimination of Agostic Hydrosilazido Zirconium Compounds

Modified from a paper published in *J. Am. Chem. Soc.*[4]

KaKing Yan, Arkady Ellern, and Aaron D. Sadow

Department of Chemistry and US Department of Energy Ames Laboratory, Iowa State University, Ames IA, 50011, USA

Abstract. Salt metathesis reactions of $Cp_2(NR_2)ZrX$ (X = Cl, I, OTf) and lithium hydrosilazide ultimately afford hydride products $Cp_2(NR_2)ZrH$ that suggest unusual β-hydrogen elimination processes. A likely intermediate in one of these reactions, $Cp_2Zr[N(SiHMe_2)t\text{-}Bu][N(SiHMe_2)_2]$, is isolated under controlled synthetic conditions. Addition of alkali metal salts to this zirconium hydrosilazide compound produces the corresponding zirconium hydride. However as conditions are varied, a number of other pathways are also accessible, including C-H/Si-H dehydrocoupling, γ-abstraction of a CH, and β-abstraction of a SiH. Our observations suggest that the conversion of (hydrosilazido)zirconocene to zirconium hydride does not follow the classical four-center β-elimination mechanism.

Introduction

β-elimination reactions are central to the stoichiometric and catalytic chemistry of organometallic compounds. However, the corresponding elimination of a metal amide

[4] *J. Am. Chem. Soc.* **2012**, *134*, 9154-9156.

(MNR_2) to form a metal hydride (M-H) and an imine is considerably less facile and less common.[1] For example, a few highly reactive three-coordinate tris(anilido) d^2 group 5 and d^3 group 6 complexes are masked as metallaziridine hydride compounds by a rare, reversible β-elimination[2] while β-eliminations of d^0 metal amides are virtually unknown. Instead, d^0 metal amide compounds undergo α-, β-, and γ-abstraction processes to give metal imido,[3,4] azometallocyclopropane (η^2-imine),[5] and azametallocyclobutane products.[6] The distinct reactivity of alkyl and amide ligands was recently suggested to be related to their dissimilar β-agostic structures.[7] In short, β-agostic amides generally contain long N-C bonds, large (ca. ~120 °) ∠M-N-C angles, and short β-C-H distances,[7] whereas β-agostic alkyls contain short C-C bonds, acute ∠M-C-C angles, and long β-CH bonds.[8] In the analysis of alkyl and amide reactivity, the relationship between β-agostic structures and β-elimination is tied to the idea that agostic alkyls represent arrested intermediates on the reaction coordinate for elimination. Because β-agostic amides do not give those features, β-elimination is not the favored pathway.

Interestingly, hydrosilazide ligands [$N(SiHR_2)R$] have the typical reactivity associated with early-metal amides, undergoing α-abstraction,[9] β-abstraction,[10] and γ-abstraction, even though the structural features of β-agostic hydrosilazides (small ∠M-N-Si angles, short N-Si distances) are closer to those of alkyl ligands rather than aliphatic amides.[11] Thus, 'β-hydridic' silazides might be more reactive toward β-elimination. In fact, examples from the main group, where β-eliminations are typically uncommon (even of alkyls), hint at this reactivity. Reaction of a diketimimate zinc chloride and $LiNR_2BH_3$ gives a zinc hydride,[12] and a four-coordinate zinc tetramethyldisilazide is converted to a the zinc

hydride in the presence of LiCl.[13] Furthermore, dehydrogenation of hydrosilazanes occurs upon addition of *n*-butyllithium followed by chlorosilanes.[14]

Result and discussion

Thus, we were intrigued by the reaction of $LiN(SiHMe_2)t$-Bu and $Cp_2Zr[N(SiHMe_2)t$-Bu]X [X = I (**6.1**), OTf (**6.2**)] that provides $Cp_2Zr[N(SiHMe_2)t$-Bu]H (**3**), LiX, and [*t*-BuN-$SiMe_2]_2$ (eq 6.1). The products suggest a sequence involving salt metathesis followed by β-hydrogen elimination, where [*t*-BuN-$SiMe_2]_2$ likely forms via head-to-tail dimerization of the silanimine *t*-BuN=$SiMe_2$.

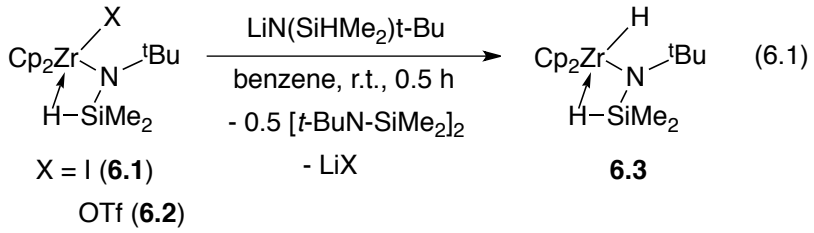

(6.1)

The product is identical to authentic samples of **6.3** prepared by treatment of $[Cp_2ZrHCl]_n$ with $LiN(SiHMe_2)t$-Bu.[10,11a] Its ^1H NMR spectrum contained a ZrH (δ 5.53) and upfield SiH (δ 1.21, $^1J_{SiH}$ = 113 Hz) that is consistent with a β-agostic structure, as previously described by Berry and co-workers. The starting materials, $Cp_2Zr[N(SiHMe_2)t$-Bu]X (X = I,[11a] OTf) also contain β-agostic hydrosilazides (δ_{SiH}: (**6.1**) 1.71 and (**6.2**) 1.29). Thus, both the starting and product zirconium hydrosilazido compounds contain β-agostic SiH structures.

Compound **6.3** is also conveniently obtained by treatment of Cp_2ZrCl_2 with 2 equiv. of $LiN(SiHMe_2)t$-Bu (eq 6.2). Additionally, Cp_2HfCl_2 and 2 equiv. of $LiN(SiHMe_2)t$-Bu provides the congener $Cp_2Hf[N(SiHMe_2)t$-Bu]H (**6.4**) and [*t*-BuN-$SiMe_2]_2$, while Cp_2TiCl_2

and 2 equiv. of LiN(SiHMe$_2$)*t*-Bu gives paramagnetic titanium species as well as the elimination by-product [*t*-BuN-SiMe$_2$]$_2$.

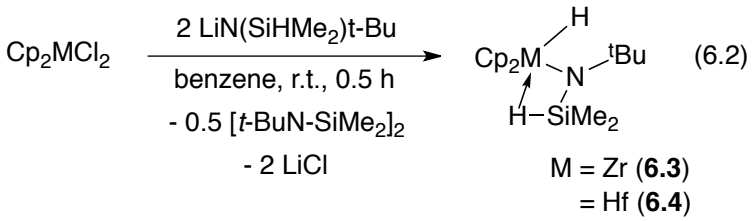

(6.2)

The SiH and HfH resonances in the ^{1}H NMR spectrum of **6.4** (δ_{SiH} 1.35, $^1J_{SiH}$ = 118 Hz; δ_{HfH} 10.12) are downfield compared to the zirconium analog. In the IR spectrum (KBr), the ν_{SiH} (1907 cm^{-1}) and ν_{HfH} (1640 cm^{-1}) were observed.

A possible pathway for formation of **6.3** and **6.4** that avoids β-elimination might involve β- or γ-abstraction followed by hydrogenolysis by adventitious H_2. For example, [Cp$_2$ZrClH]$_n$ and LiN(SiMe$_3$)$_2$ react at room temperature to give the azasilazirconacyclobutane Cp$_2$Zr[κ^2-*N*,*C*-N(SiMe$_3$)SiMe$_2$CH$_2$].[6b] In fact, thermolysis of **6.3** at 140 °C in a sealed flask forms H_2 and Cp$_2$Zr[κ^2-*N*,*C*-N(*t*-Bu)SiHMeCH$_2$] (**6.5a**) showing that mechanism is viable. However, isobutylene and species assigned as imido [Cp$_2$Zr(μ-NSiHMe$_2$)]$_n$ (**6.5b**) are also formed (eq 6.3). The irreversible formation of [Cp$_2$Zr(μ-NSiHMe$_2$)]$_n$ rules out the γ-abstraction pathway as a route to **6.3**, which also does not account for [*t*-BuN-SiMe$_2$]$_2$ produced in the apparent β-elimination.

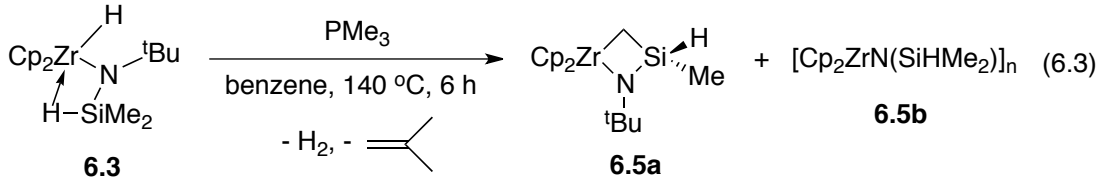

(6.3)

Thus, β-abstraction products are not observed from hydride **6.3**, which contrasts the mild conditions needed for β-abstraction from $Cp_2Zr[N(SiHMe_2)t\text{-}Bu](CH_2SiMe_3)$ (in the presence of PMe_3) to give $Cp_2Zr[\eta^2\text{-}N(t\text{-}Bu)SiMe_2](PMe_3)$ (**6.6**). Interestingly, β-hydrogen abstraction occurs upon reaction of $Cp_2Zr[N(SiHMe_2)t\text{-}Bu]OTf$ and $LiN(SiMe_3)_2$ or $LiN(SiMe_3)CH_2Ph$ to give **6.6** and $HN(SiMe_3)_2$ or $HN(SiMe_3)CH_2Ph$ (eq 6.4). This transformation is also not involved in the formation of **6.3**, because **6.6** and $HN(SiHMe_2)t\text{-}Bu$ do not provide **6.3** and $[t\text{-}BuN\text{-}SiMe_2]_2$ as would be expected if β-abstraction is the initial step on a pathway to form the zirconium hydride.

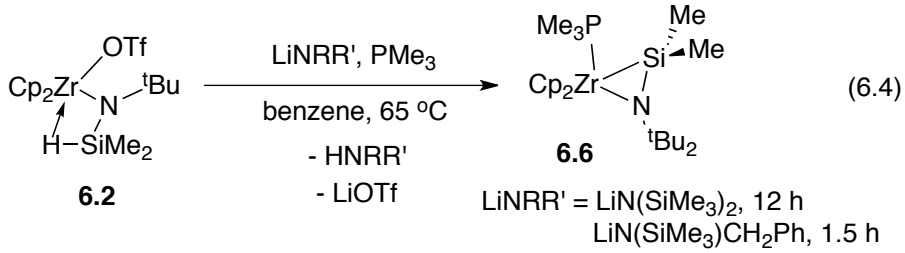

(6.4)

These experiments suggest that the SiH group in $LiN(SiHMe_2)t\text{-}Bu$ diverts the reaction from abstraction to elimination. The effect of the SiH in the lithium hydrosilazide was further tested by the reaction of **6.2** and $LiN(SiHMe_2)_2$. That reaction gives a mixture of **6.3** from elimination and the mixed diamide $Cp_2Zr[N(SiHMe_2)t\text{-}Bu][N(SiHMe_2)_2]$ (**6.7**; eq 6.5) from salt metathesis in a 1:1.4 ratio.

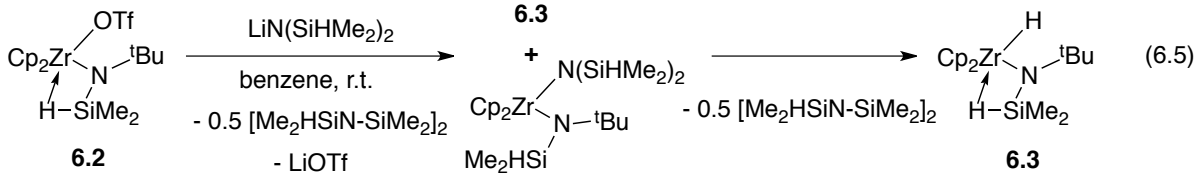

(6.5)

The formation of compound **6.7** was later verified by its independent preparation and characterization (see below). Micromolar scale reactions of **6.2** and $LiN(SiHMe_2)_2$ in

toluene-d_8, monitored by ^{1}H NMR spectroscopy from 216 to 363 K, showed signals consistent with **6.7** at 233 K. Upon warming to 283 K, this species rapidly but *only partially* converts to **6.3**.

Similarly, $Cp_2Zr[N(SiHMe_2)_2]OTf$ (**6.8**) and $LiN(SiHMe_2)$*t*-Bu react in benzene to give a mixture of **6.3**: **6.7**:$Cp_2Zr[N(SiHMe_2)_2]H$ (**6.9**, eq 6.6) in a 1.0:10.4:0.7 ratio. Interestingly, thermolysis of this mixture at 50 °C gives a mixture of **6.3**: **6.9** in a ratio (11.4:0.7) derived from the intermediate mixture (**6.7**+**6.3**): **6.9**. Thus, **6.7** is a intermediate that affords zirconium hydride **6.3** but not hydride **6.9**.

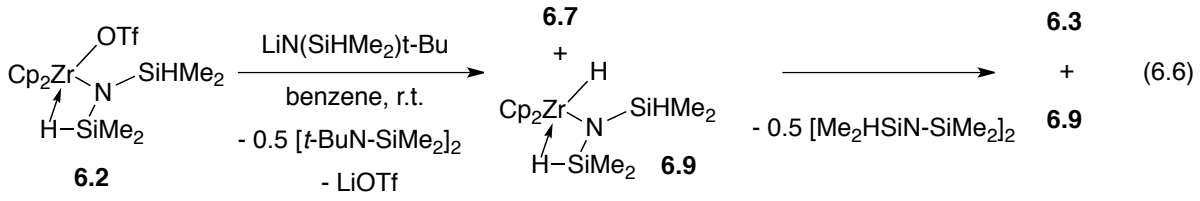

(6.6)

These experiments suggest that two pathways provide zirconium hydride products. The first pathway involves the direct interaction of the metal triflate and lithium hydrosilazide (the first step of eq 6.5 and 6.6 that provides **6.3** and **6.9**, respectively). In the second pathway, compound **6.7** appears to be a precursor to compound **6.3**. Thus, isolated zirconium bis(disilazide) was required to better study the conversion of **6.7** to **6.3**.

After a number of experiments, we found that compound **6.2** and the potassium disilazide $KN(SiHMe_2)_2$ react in benzene to form **6.7** (eq 6.7). The ^{1}H NMR spectrum of **6.7** contained two resonances assigned to SiH groups (δ 4.98, $^1J_{SiH}$ = 173 Hz; δ 4.90, $^1J_{SiH}$ = 185 Hz) in a 1:2 integrated ratio.

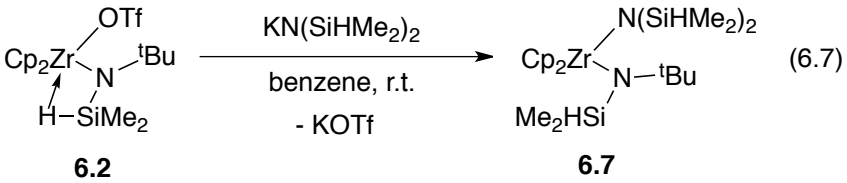

6.2 **6.7**

In a surprising contrast to the conversion of **6.7** to **6.3** in eq 6.5, thermolysis of isolated **6.7** in benzene results in H_2 elimination and inter-ligand coupling between a Si-H bond of the $N(SiHMe_2)_2$ and the C-H bond of a C_5H_5 to form constrained-geometry-like $\{Me_2Si(C_5H_4)N(SiHMe_2)\}CpZrN(SiHMe_2)$*t*-Bu (**6.10**, eq 6.8).

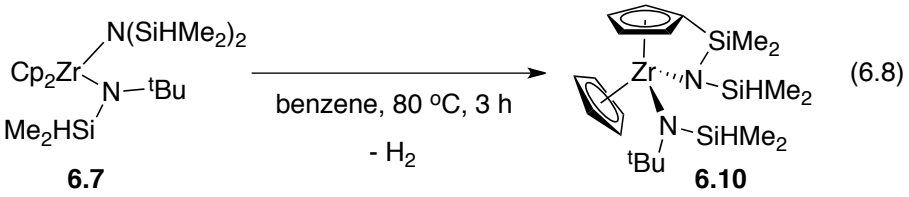

6.7 **6.10**

The ^1H NMR spectrum of **6.10** showed the C_5H_4 group as four multiplets. Two SiH signals (δ 5.16, $^1J_{SiH}$ = 196 Hz; δ 4.07, $^1J_{SiH}$ = 167 Hz) were observed in a 1:1 ratio. The monomeric structure of **6.10** was confirmed by X-ray crystallography (see Supporting Information). We considered a possible mechanism for formation of **6.10** based on the thermolysis of $[Cp_2ZrHCl]_n$ that involves intermolecular activation of a C_5H_5 ligand to give $[Cp(Cl)Zr(\mu\text{-}\eta^1\text{:}\eta^5\text{-}C_5H_4)]_2$ and H_2.[15] However, this mechanism is ruled out by a plot of [**6.7**] vs. time that follows an exponential decay for 3 half-lives (see SI), which is inconsistent with a dimeric intermediate. The same conversion of **6.7** into **6.9** occurs at room temperature in benzene (0.5 h; 52.5% based on a cyclooctane internal standard) in the presence of $Li[B(C_6F_5)_4](OEt_2)_{2.5}$ (1 or 0.5 equiv.) suggesting that the transformation involves a Lewis acid activation.

However, LiCl or KOTf in a THF/benzene solvent mixture diverts the conversion of **6.7** from the C-H bond activation pathway, instead forming the β-hydrogen elimination products **6.3** and $(Me_2Si\text{-}NSiHMe_2)_2$ quantitatively. Thus, a sufficiently soluble salt containing both a cation (Li^+ or K^+) and a coordinating counteranion Cl^-, I^-, or OTf^- is required for hydrogen transfer to zirconium. Likely, the intermediate salt adduct that precedes the hydride transfer is also accessed upon treatment of [Zr]X with $LiN(SiHMe_2)_2$.

Interestingly, both the starting materials and products $Cp_2Zr[N(SiHMe_2)R]X$ (X = H, Cl, I, OTf; R = *t*-Bu, $SiHMe_2$) contain β-agostic SiH groups, yet the β-agostic silazide ligands in **6.1**, **6.2**, and **6.8** do not undergo elimination. Instead, the incoming lithium silazide transfers a SiH to zirconium and eliminates LiX and silanimine. This transfer appears to occur through a pathway that is sensitive to the nature of the incoming group and ancillary ligands. Thus, the most hindered of interactions, $LiN(SiHMe_2)$*t*-Bu with **6.1** or **6.2**, forms only hydride **6.3**, whereas the reaction of less hindered $LiN(SiHMe_2)_2$ and **6.1** or **6.2** gives a mixture of **6.3** and diamide **6.7**. The initial hydride to amide ratio is produced under kinetic control that reflects the relative (and sterically-influenced) nucleophilicity of the nitrogen versus the β-H in a lithium hydrosilazide. Additionally, hydride transfer reactions are clearly facilitated under conditions where salt metathesis is reversible (i.e., the salt byproduct is soluble).

Conclusion

Direct hydride transfer, as an alternative to the classic β-elimination, was suggested for the reaction of Cp^*TaMe_3Cl and lithium amides.[2] Additionally, side reduction products in late-metal-catalyzed Buchwald-Hartwig C-N cross-couplings, are often attributed to β-

elimination from a metal-amide intermediate.[1,16] In those systems, the choice of base and solvent (i.e., the solubility of the salt) significantly influences the ratio of C-N to C-H bond formation, suggesting that a related direct hydride attack may be important.[1b] The features of the reactions reported here, including the effect of a soluble salt on the favored pathway (among many transformations) and the observation that the β-elimination event does not involve the β-agostic SiH, provide strong evidence for direct attack of the β-hydrogen of an amide on a metal center. Furthermore, the reactions described here provide an alternative strategy for the synthesis of catalytically important d^0 metal hydride compounds.

Experimental.

General. All manipulations were performed under a dry argon atmosphere using standard Schlenk techniques or under a nitrogen atmosphere in a glovebox unless otherwise indicated. Water and oxygen were removed from benzene, toluene, pentane, diethyl ether, and tetrahydrofuran solvents using an IT PureSolv system. Benzene-d_6 and tetrahydrofuran-d_8 were heated to reflux over Na/K alloy and vacuum-transferred. The compounds Cp_2ZrHCl,[18] [*t*-BuN-$SiMe_2$]$_2$,[19] LiN($SiHMe_2$)*t*-Bu,[20] Cp_2Zr[N($SiHMe_2$)*t*-Bu]I (**6.1**),[21] LiN($SiMe_3$)CH_2Ph,[21] LiN($SiMe_3$)$_2$,[21] LiN($SiHMe_2$)$_2$,[22] KN($SiHMe_2$)$_2$,[23] LiB(C_6F_5)$_4$(Et_2O)$_{2.5}$,[24] and Cp_2HfCl_2[25] were prepared following literature procedures. Cp_2ZrCl_2 was purchased from Strem and used as received. PMe_3 and MeOTf were purchased from Aldrich and used as received. LiCl and KOTf were heated under vacuum overnight at 120 °C before use.

^1H, $^{13}C\{^1H\}$, ^{11}B and $^{29}Si\{^1H\}$ NMR spectra were collected on an Agilent MR400 spectrometer. ^{11}B NMR spectra were referenced to an external sample of $BF_3{\cdot}Et_2O$. ^{15}N chemical shifts were determined either by ^1H-^{15}N HMBC experiments on a Bruker Avance II

700 spectrometer with a Bruker Z-gradient inverse TXI $^{1}H/^{13}C/^{15}N$ 5mm cryoprobe or by ^{1}H-^{15}N CIGARAD experiments on an Agilent MR400 spectrometer; ^{15}N chemical shifts were originally referenced to liquid NH_3 and recalculated to the CH_3NO_2 chemical shift scale by adding -381.9 ppm. Assignments of resonances are supported by ^{1}H-^{1}H and heteronuclear correlation NMR experiments. Infrared spectra were measured on a Bruker IFS66v FTIR. Elemental analyses were performed using a Perkin-Elmer 2400 Series II CHN/S. X-ray diffraction data was collected on a Bruker APEX II diffractometer.

$Cp_2Zr[N(SiHMe_2)t\text{-}Bu]OTf$ (6.2). $Cp_2Zr[N(SiHMe_2)t\text{-}Bu]H$ (0.111 g, 0.315 mmol) and MeOTf (38.0 μL, 0.346 mmol) were allowed to react in benzene for 10 min. The volatile materials were evaporated from the resulting yellow solution under vacuum to give $Cp_2Zr[N(SiHMe_2)t\text{-}Bu]OTf$ as a yellow solid in excellent yield (0.142 g, 0.284 mmol, 90.1%). Recrystallization from toluene at -30 °C provided X-ray quality crystals of $Cp_2Zr[N(SiHMe_2)t\text{-}Bu]OTf$. ^{1}H NMR (benzene-d_6, 400 MHz, 25 °C): δ 5.97 (s, 10 H, C_5H_5), 1.29 (m, 1 H, SiH), 1.16 (s, 9 H, *t*-Bu), -0.016 (d, $^{3}J_{SiH}$ = 2.4 Hz, 6 H, SiHMe_2). $^{13}C\{^{1}H\}$ NMR (benzene-d_6, 125 MHz): δ 120.5 (q, $^{1}J_{FC}$ = 317.7 Hz, OSO_2CF_3), 113.7 (C_5H_5), 57.7 (CMe_3), 34.6 (CMe_3), 1.4 ($SiHMe_2$). $^{15}N\{^{1}H\}$ NMR (benzene-d_6, 61 MHz, 25 °C): δ -242.9. ^{19}F NMR (benzene-d_6, 376 MHz, 25 °C): δ -77.1. $^{29}Si\{^{1}H\}$ NMR (benzene-d_6, 119.3 MHz, 25 °C): δ -47.1. IR (KBr, cm^{-1}): 3115 br m, 2962 m, 2089 w, 1917 s br, 1756 m, 1453 m, 1328 s, 1235 br vs, 1053 s, 1016 vs, 823 s, 803 s, 633 s. Anal. Calcd for $C_{17}F_3H_{26}SiNO_3SZr$: C, 40.77; H, 5.23; N, 2.80. Found: C, 41.15; H, 5.08; N, 2.80. Mp 115-119 °C (dec.).

$Cp_2Zr[N(SiHMe_2)t\text{-}Bu]H$ (6.3). Compound **6.3** was originally prepared by Procopio and Berry from $(Cp_2ZrHCl)_n$ and $LiN(SiHMe_2)t\text{-}Bu$ according to reference 21. Here we describe

several synthetic procedures (where the identity of the zirconium starting material is varied) that afford $Cp_2Zr[N(SiHMe_2)t\text{-}Bu]H$. The materials obtained by these procedures have identical spectroscopic features to $Cp_2Zr[N(SiHMe_2)t\text{-}Bu]H$ obtained with the literature procedure.

Method A: A mixture of $Cp_2Zr[N(SiHMe_2)t\text{-}Bu]OTf$ (0.116 g, 0.232 mmol) and $LiN(SiHMe_2)t\text{-}Bu$ (0.032 g, 0.233 mmol) was stirred in benzene (6 mL) at room temperature for 30 min. The volatile materials were removed under reduced pressure to leave an orange solid residue, which was extracted with 10 mL of pentane. The pentane extract was concentrated and cooled to -30 °C to yield $Cp_2Zr[N(SiHMe_2)t\text{-}Bu]H$ (0.060 g, 0.170 mmol, 73.3%).

Method B: A mixture of $Cp_2Zr[N(SiHMe_2)t\text{-}Bu]I$ (0.102 g, 0.213 mmol) and $LiN(SiHMe_2)t\text{-}Bu$ (0.029 g, 0.211 mmol) in benzene (6 ml) was stirred at room temperature for 30 min. The reaction mixture was worked-up following the procedure of Method A to yield $Cp_2Zr[N(SiHMe_2)t\text{-}Bu]H$ (0.048 g, 0.136 mmol, 63.8%).

Method C: A mixture of Cp_2ZrCl_2 (0.302 g, 1.03 mmol) and $LiN(SiHMe_2)t\text{-}Bu$ (0.284 g, 2.07 mmol) in benzene (6 ml) was stirred at room temperature for 30 min. The reaction mixture was worked-up following the procedure of Method A to yield $Cp_2Zr[N(SiHMe_2)t\text{-}Bu]H$ (0.235 g, 0.666 mmol, 64.7%). ^1H NMR (benzene-d_6, 400 MHz, 25 °C): δ 5.71 (s, 10 H, C_5H_5), 5.54 (s, 1 H, ZrH), 1.24 (s, 9 H, CMe_3), 1.20 (m, 1 H, SiH, overlapped with *t*-Bu), 0.05 (d, $^3J_{CH}$ = 2.8 Hz, 6 H, SiHMe_2). $^{13}C\{^1H\}$ NMR (benzene-d_6, 125 MHz): δ 105.9 (C_5H_5), 55.5 (CMe_3), 35.1 (CMe_3), 0.87 ($SiHMe_2$). $^{15}N\{^1H\}$ NMR (benzene-d_6, 61 MHz): δ -259.7. $^{29}Si\{^1H\}$ NMR (benzene-d_6, 119.3 MHz, 25 °C): δ -73.9. IR (KBr, cm^{-1}): 3079 m br,

2950 s, 1888 s (ν_{SiH}), 1598 s br (ZrH), 1437 s, 1349 s, 1244 s, 1204 s br, 1061 s, 1015 s, 793 s br.

$Cp_2Hf[N(SiHMe_2)t\text{-}Bu]H$. (**6.4**) A suspension of Cp_2HfCl_2 (0.219 g, 0.58 mmol) and $LiN(SiHMe_2)t$-Bu (0.158 g, 1.16 mmol) in benzene (5 mL) was stirred under nitrogen at room temperature for 1.5 h. The volatile materials were evaporated, giving an off-white solid residue that was extracted with pentane (10 mL). The pentane extract was concentrated and cooled to -30 °C to yield $Cp_2Hf[N(SiHMe_2)t$-Bu]H (0.152 g, 0.35 mmol, 59.4%). ^{1}H NMR (benzene-d_6, 400 MHz, 25 °C): δ 10.12 (s, 1 H, HfH), 5.69 (s, 10 H, C_5H_5), 1.35 (m, 1 H, $^1J_{SiH}$ = 118 Hz, SiH), 1.24 (s, 9 H, CMe_3) 0.09 (d, 6 H, $^3J_{HH}$ = 3.2 Hz, $SiHMe_2$). $^{13}C\{^1H\}$ NMR (benzene-d_6, 125 MHz): δ 105.6 (C_5H_5), 55.9 (CMe_3), 35.5 (CMe_3), 0.23 ($SiHMe_2$). $^{15}N\{^1H\}$ NMR (benzene-d_6, 61 MHz, 25 °C): δ -269.6. $^{29}Si\{^1H\}$ NMR (benzene-d_6, 119.3 MHz, 25 °C): δ -74.3. IR (KBr, cm^{-1}): 3082 m br, 2951 s, 1907 s (ν_{SiH}), 1640 s br (ν_{HfH}), 1438 s, 1377 s, 1245 s, 1206 s, 1044 s, 1016 s, 795 s br. Anal. Calcd for $C_{16}HfH_{27}SiN$: C, 43.68; H, 6.19; N, 3.18. Found: C, 43.25; H, 6.14; N, 3.15. Mp 130-134 °C.

$Cp_2Zr[\kappa^2\text{-}N,C\text{-}N(t\text{-}Bu)SiHMeCH_2]$ (6.5a) and $[Cp_2ZrNSiHMe_2]_n$ (6.5b). A sealable flask with a Teflon valved was charged with $Cp_2Zr[N(SiHMe_2)t$-Bu]H (0.062 g, 0.175 mmol), PMe_3 (1.1 equiv.; 20 ml, 0.193 mmol) and benzene (1 mL). The tube was sealed and heated to 150 °C for 12 h. The reaction was cooled and then degassed by freeze-pump-thaw cycles (3×). The reaction mixture was then heated at 150 °C for another 12 h. The reaction was allowed to cool, and then the volatile materials were evaporated to yield a brownish-purple solid. Spectroscopic analysis revealed this solid to be a mixture of compounds **6.5a** and **6.5b** in a 1:1.4 ratio. Attempts to separate these two compounds by crystallization were not

successful. Parallel micromolar scale reactions in toluene-d_8 contained isobutylene, unbound PMe_3, and compounds **6.5a** and **6.5b**. The identities of **6.5a** and **6.5b** are assigned by 1D and 2D multinuclear NMR spectroscopy, symmetry, reaction stoichiometry (isobutylene: **6.5b** = 1:1), and the similarity of the formation pathway and spectroscopy of **6.5a** with the compound $Cp_2Zr[k^2$-*N*,*C*-$N(SiHMe_2)SiHMeCH_2]$. IR (KBr, cm^{-1}): 2959 m br, 2053 m br (ν_{SiH}), 1440 w, 1355 m, 1246 m, 1199 m, 1015 s, 879 s br, 794 s br. **6.5a**: ^{1}H NMR (benzene-d_6, 400 MHz, 25 °C): δ 5.85 (s, 5 H, C_5H_5), 5.85 (s, 5 H, C_5H_5), 4.33 (m, $^1J_{SiH}$ = 198 Hz, 1 H, SiH), 2.29 (dd, $^2J_{HH}$ = 4.4 Hz, $^3J_{SiH}$ = 12.0 Hz, 1 H, CH_2), 1.83 (dd, $^2J_{HH}$ = 2.0 Hz, $^3J_{SiH}$ = 12.0 Hz, 1 H, CH_2), 1.10 (s, CMe_3), 0.28 (d, $^3J_{HH}$ = 2.4 Hz, 3 H, SiH*Me*$_2$). $^{13}C\{^1H\}$ NMR (benzene-d_6, 125 MHz, 25 °C): δ 111.7 (C_5H_5), 111.7 (C_5H_5), 56.8 (*C*Me_3), 41.2 (CH_2), 35.0 (C*Me*$_3$), 3.0 ($SiHMe_2$). $^{29}Si\{^1H\}$ NMR (benzene-d_6, 119.3 MHz, 25 °C): δ -75.8. **6.5b**: ^{1}H NMR (benzene-d_6, 400 MHz, 25 °C): δ 6.18 (s, 10 H, C_5H_5), 4.81 (m, $^1J_{SiH}$ = 189 Hz, 1 H, SiH), 0.13 (d, $^3J_{HH}$ = 3.6 Hz, 6 H, SiH*Me*$_2$). $^{13}C\{^1H\}$ NMR (benzene-d_6, 125 MHz, 25 °C): d 112.9 (C_5H_5), 4.7 (SiH*Me*$_2$). $^{29}Si\{^1H\}$ NMR (benzene-d_6, 119.3 MHz, 25 °C): δ -36.7.

$Cp_2Zr[\eta^2$-$NSiMe_2$(*t*-Bu)]PMe_3 (6.6). Compound **6.6** was originally prepared from $Cp_2Zr[N(SiHMe_2)$*t*-Bu]I, $LiCH_2SiMe_3$, and PMe_3 according to reference 21. Here we describe two syntheses from lithium silazides (rather than alkyllithiums) that afford spectroscopically authentic **6.6**.

Method A: PMe_3 (54 mL, 0.52 mmol) was dissolved in benzene (15 mL). This solution was added to a solid mixture of $Cp_2Zr[N(SiHMe_2)$*t*-Bu]OTf (0.235 g, 0.47 mmol) and $LiN(SiMe_3)_2$ (0.079 g, 0.047 mmol) in a re-sealable storage tube equipped with a Teflon valve. The yellow mixture was stirred at 65 °C for 12 h. The volatiles were removed under

reduced pressure, and the sticky solid was extracted with pentane (2 × 10 mL). The pentane extract was concentrated and cooled to -30 °C to yield $Cp_2Zr[\eta^2\text{-}NSiMe_2(t\text{-}Bu)]PMe_3$ (0.113 g, 0.27 mmol, 56.3%) as a light orange crystalline material.

Method B: A solution of PMe_3 (31 mL, 0.30 mmol) in benzene (10 mL) was added to a solid mixture of $Cp_2Zr[N(SiHMe_2)t\text{-}Bu]OTf$ (0.135 g, 0.27 mmol) and $LiN(SiMe_3)CH_2Ph$ (0.050 g, 0.27 mmol) in a storage tube equipped with a Teflon valve. The yellow mixture was stirred at 65 °C for 1.5 h. Workup as described in Method A affords $Cp_2Zr[\eta^2\text{-}NSiMe_2(t\text{-}Bu)]PMe_3$ in similar yield (0.066 g, 0.15 mmol, 57.7%).

$Cp_2Zr[N(SiHMe_2)t\text{-}Bu][N(SiHMe_2)_2]$ (6.7). A mixture of $Cp_2Zr[N(SiHMe_2)t\text{-}Bu]OTf$ (0.120 g, 0.24 mmol) and $KN(SiHMe_2)_2$ (0.041 g, 0.24 mmol) was stirred in benzene (6 mL) at room temperature for 30 min. Evaporation of the solvent left an orange solid residue, which was then extracted with 10 mL of pentane. The pentane was evaporated yielding $Cp_2Zr[N(SiHMe_2)t\text{-}Bu][N(SiHMe_2)_2]$ (0.072 g, 0.13 mmol, 52.6%) as an analytically pure yellow solid. ^{1}H NMR (benzene-d_6, 400 MHz, 25 °C): δ 6.13 (s, 10 H, C_5H_5), 4.98 (m, $^1J_{SiH}$ = 172.5 Hz, 1 H, SiH), 4.90 (m, $^1J_{SiH}$ = 184.8 Hz, 2 H, Si*H*), 1.29 (s, 9 H, CMe_3), 0.38 (d, $^3J_{HH}$ = 3.2 Hz, 6 H, N(SiH*Me*$_2$)*t*-Bu), 0.34 (d, $^3J_{HH}$ = 3.2 Hz, 12 H, Si(H*Me*$_2$)$_2$). ^{13}C{^{1}H} NMR (benzene-d_6, 125 MHz): δ 113.1 (C_5H_5), 60.0 (*C*Me$_3$), 36.0 (C*Me*$_3$), 3.8 (N(SiH*Me*$_2$)*t*-Bu), 2.8 ($N(SiHMe_2)_2$). ^{15}N{^{1}H} NMR (benzene-d_6, 61 MHz, 25 °C): δ -230.7 ($N(SiHMe_2)t$-Bu), -287.3 ($N(SiHMe_2)_2$). ^{29}Si{^{1}H} NMR (benzene-d_6, 119.3 MHz, 25 °C): δ -19.4 (N(SiHMe)*t*-Bu), -33.4 ($N(SiHMe)_2$). IR (KBr, cm^{-1}): 2951 m br, 2130 s (ν_{SiH}), 2072 s (ν_{SiH}), 1450 m, 1358 m, 1247 s, 1180 s, 1028 s, 923 s br, 802 s br, 756 s. Anal. Calcd for

$C_{20}H_{40}Si_3N_2Zr$: C, 49.63; H, 8.33; N, 5.79. Found: C, 49.47; H, 8.48; N, 5.84. Mp 108-110 °C.

$Cp_2Zr[N(SiHMe_2)_2]OTf$ (6.8). $Cp_2Zr[N(SiHMe_2)_2]H$ (0.106 g, 0.301 mmol) was dissolved in benzene (10 mL). MeOTf (35.4 μL, 0.313 mmol) was added to give a yellow solution, which was stirred for 10 min. The volatile materials were removed under reduced pressure, and the isolated yellow solid was analytically pure $Cp_2Zr[N(SiHMe_2)_2]OTf$ (0.144 g, 0.286 mmol, 95.3%). ^{1}H NMR (benzene-d_6, 400 MHz, 25 °C): δ 6.02 (s, 10 H, C_5H_5), 3.80 (m, $^1J_{SiH}$ = 170.0 Hz, 2 H, SiH), 0.16 (d, $^3J_{HH}$ = 3.2 Hz, 12 H, SiH*Me*$_2$). ^{1}H NMR (toluene-d_8, 600 MHz, -88 °C): δ 5.84 (s, 10 H, C_5H_5), 4.96 (s br, $^1J_{SiH}$ = 194.6 Hz, 1 H, non-agostic $SiHMe_2$), 1.12 (br s, $^1J_{SiH}$ = 115.1 Hz, 1 H, agostic SiH), 0.36 (s br, 6 H, agostic $SiHMe_2$), -0.13 (s br, 6 H, nonagostic SiH*Me*$_2$). $^{13}C\{^1H\}$ NMR (benzene-d_6, 125 MHz): δ 115.4 (C_5H_5), 1.1 ($SiHMe_2$). $^{13}C\{^1H\}$ NMR (toluene-d_8, 125 MHz, -88 °C): δ 113.5 (C_5H_5), 1.6 (nonagostic $SiHMe_2$), -0.97 (agostic $SiHMe_2$). $^{15}N\{^1H\}$ NMR (benzene-d_6, 61 MHz, 25 °C): δ -266.5. ^{19}F NMR (benzene-d_8, 376 MHz, 25 °C): δ -77.2. ^{19}F NMR (toluene-d_8, 376 MHz, -88 °C): δ -78.2. $^{29}Si\{^1H\}$ NMR (benzene-d_6, 119.3 MHz, 25 °C): δ -24.1. $^{29}Si\{^1H\}$ NMR (toluene-d_8, 119.3 MHz, -88 °C): δ -14.1 (agostic $SiHMe_2$), -35.8 (nonagostic $SiHMe_2$). IR (KBr, cm^{-1}): 3115 m br, 2955 m, 2901 w, 2119 m (ν_{SiH}), 2054 m (ν_{SiH}), 1884 m br (ν_{SiH}), 1771 w (ν_{SiH}), 1428 m, 1327 vs, 1235 vs, 1207 s br, 1187 vs, 1014 s br, 891 vs, 807 vs br, 633 vs. br. Anal. Calcd for $C_{15}H_{24}F_3NO_3SSi_2Zr$: C, 35.83; H, 4.81; N, 2.79; Found: 35.41; H, 4.68; N, 2.81. Mp 70-72 °C.

$Cp_2Zr[N(SiHMe_2)_2]H$ (6.9). A suspension of $[Cp_2ZrHCl]_n$ (0.909 g, 3.53 mmol) and $LiN(SiHMe_2)_2$ (0.491 g, 3.53 mmol) was stirred for 30 min in benzene (15 mL) at room

temperature. The volatile materials were removed under reduced pressure to leave an off-white solid residue, which was extracted with pentane (15 mL). The pentane extract was concentrated and cooled to -30 °C to yield $Cp_2ZrH(N(SiHMe_2)_2$ (0.931 g, 2.62 mmol, 74.4%). ^{1}H NMR (benzene-d_6, 400 MHz, 25 °C): δ 5.78 (s, 10 H, C_5H_5), 5.60 (s, 1 H, ZrH), 3.78 (m, $^1J_{SiH}$ = 161.0 Hz, 2 H, SiH), 0.18 (d, $^3J_{HH}$ = 3.2 Hz, SiMe). ^{13}C{^{1}H} NMR (benzene-d_6, 125 MHz): δ 107.6 (C_5H_5), 1.8 (SiMe). ^{15}N{^{1}H} NMR (benzene-d_6, 61 MHz, 25 °C): δ -292.4. ^{29}Si{^{1}H} NMR (benzene-d_6, 119.3 MHz, 25 °C): δ -40.7. IR (KBr, cm^{-1}): 3099 w br, 2955 m, 2895 w, 2047 s br (ν_{SiH}), 1907 m br (ν_{SiH}), 1559 m br (ν_{ZrH}), 1441 w, 1246 s, 1014 s, 890 s, 798 s br, 765 s br, 650 s br. Anal. Calcd for $C_{14}H_{25}NSi_2Zr$: C, 47.40; H, 7.10; N, 3.95. Found: C, 47.02; H, 6.96; N, 3.92. Mp 104-106 °C.

{η^5:η^1-Me$_2$Si(C$_5$H$_4$)N(SiHMe$_2$)}CpZrN(SiHMe$_2$)*t*-Bu (6.10). A benzene solution (5 mL) of $Cp_2Zr[N(SiHMe_2)t\text{-Bu}][N(SiHMe_2)_2]$ (0.062 g, 0.128 mmol) was heated in a sealed flask at 90 °C for 4 h. The volatiles were evaporated to yield a yellow, analytically pure solid of {η^5:η^1-$Me_2Si(C_5H_4)N(SiHMe_2)$}$CpZrN(SiHMe_2)t$-Bu (**6.10**) (0.059 g, 0.122 mmol, 95.5%). X-ray quality crystals were grown in a concentrated pentane solution at -30 °C overnight. ^{1}H NMR (benzene-d_6, 400 MHz, 25 °C): δ 6.39 (m, 1 H, C_5H_4), 6.33 (m, 1 H, C_5H_4), 6.20 (m, 1 H, C_5H_4), 6.12 (s, 5 H, C_5H_5), 5.50 (m, 1 H, C_5H_4), 5.16 (m, $^1J_{SiH}$ = 196 Hz, 1 H, SiH), 4.07 (m, $^1J_{SiH}$ = 166.7 Hz, 1 H, SiH), 1.28 (s, 9 H, CMe_3), 0.53 (s, 3 H, $C_5H_4SiMe_2SiHMe_2$), 0.37 (s, 3 H, $C_5H_4SiMe_2SiHMe_2$), 0.35 (d, $^3J_{HH}$ = 3.2 Hz, 3 H, $C_5H_4SiMe_2NSiHMe_2$), 0.31 (d, $^3J_{HH}$ = 3.2 Hz, 3 H, $N(SiHMe_2)t$-Bu), 0.28 (d, $^3J_{HH}$ = 3.2 Hz, 3 H, $N(SiHMe_2)t$-Bu), 0.26 (d, $^3J_{HH}$ = 3.2 Hz, 3 H, $C_5H_4SiMe_2SiHMe_2$). ^{13}C{^{1}H} NMR (benzene-d_6, 125 MHz): δ 123.2 (C_5H_4), 119.1 (C_5H_4), 115.33 (C_5H_4), 113.1 (*ipso*-$C_5H_4SiMe_2$), 112.8 (C_5H_5), 112.2 (C_5H_4), 56.5

(*C*Me$_3$), 36.2 (C*Me*$_3$), 4.3 (SiMe$_2$NSiH*Me*$_2$), 3.9 (N(SiH*Me*$_2$)*t*-Bu), 3.5 (Si*Me*$_2$NSiHMe$_2$), 2.7 (SiMe$_2$NSiH*Me*$_2$), 2.6 (N(SiH*Me*$_2$)*t*-Bu), 2.3 (Si*Me*$_2$NSiHMe$_2$). ^{15}N{^{1}H} NMR (benzene-d_6, 61 MHz, 25 °C): δ -226.6 (ZrNSiMe$_2$C$_5$H$_4$), -266.6 (ZrN(SiHMe$_2$)*t*-Bu). ^{29}Si{^{1}H} NMR (benzene-d_6, 119.3 MHz, 25 °C): δ -10.2 (SiMe$_2$N*Si*HMe$_2$), -16.9 (*Si*Me$_2$NSiHMe$_2$), -36.7 (N(SiHMe$_2$)*t*-Bu). IR (KBr, cm^{-1}): 2952 m br, 2900 m, 2139 s (ν_{SiH}), 2106 s (ν_{SiH}), 1357 m, 1251 s, 1181 s, 915 s br, 799 s br. Anal. Calcd for $C_{20}H_{38}N_2Si_3Zr$: C, 49.84; H, 7.95; N, 5.81. Found: C, 49.13; H, 8.14; N, 5.78. Mp 103-107 °C.

Kinetics measurements were conducted by monitoring concentrations of reactants and products with ^{1}H NMR spectroscopy using a Bruker DRX400 NMR spectrometer. Cp$_2$Zr[N(SiHMe$_2$)*t*-Bu][N(SiHMe$_2$)$_2$] (**6.7**) (0.0125 g, 0.026 mmol, 0.048 M) and cyclooctane (0.027 g, 0.242 mmol, 0.451 M) was weighed out in a glass vial. Toluene-d_8 (0.505 mL, weighed out on balance) was added by a 1 mL syringe to the mixture (0.005 g, 0.010 mmol). The resulting solution was quickly transferred to a NMR tube. The NMR tube was immediately placed in the NMR probe, which was preset at 353 K. Single scan spectra were acquired automatically at preset time intervals. The concentration of **6.7** and product **6.10** at any given time were determined by integration of substrate and product resonances relative to the integration of the internal standard. These values of substrate concentrations (M) at different times (s) were plotted for the determination of the order of the substrate.

Figure 6.S1. Plot of the concentration of $Cp_2Zr[N(SiHMe_2)t\text{-}Bu][N(SiHMe_2)_2]$ (**6.7**) while heating at 80 °C in benzene-d_6 to give $\{\eta^5{:}\eta^1\text{-}Me_2Si(C_5H_4)N(SiHMe_2)\}CpZrN(SiHMe_2)t\text{-}Bu$ (**10**).

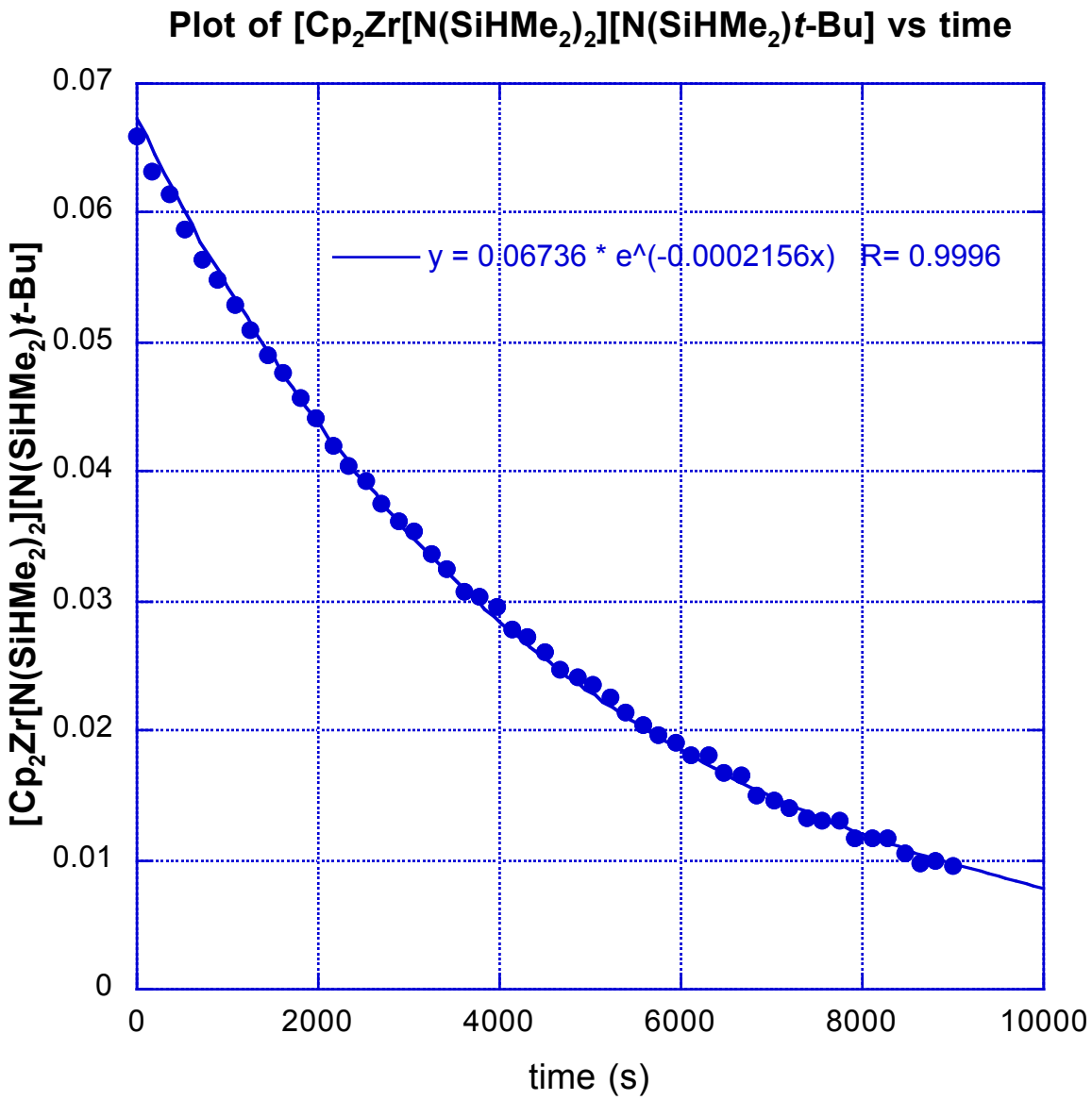

Reference

1 (a) Hartwig, J. F. *J. Am. Chem. Soc.* **1996**, *118*, 7010-7011. (b) Hartwig, J. F.; Richards, S.; Barañano, D.; Paul, F. *J. Am. Chem. Soc.* **1996**, *118*, 3626-3633. (c) Ishiyama, T.; Hartwig, J. *J. Am. Chem. Soc.* **2000**, *122*, 12043-12044. (d) Matas, I.; Cámpora, J.; Palma, P.; Álvarez, E. *Organometallics* **2009**, *28*, 6515-6523.

2 (a) Mayer, J. M.; Curtis, C. J.; Bercaw, J. E. *J. Am. Chem. Soc.* **1983**, *105*, 2651-2660. (b) Tsai, Y.-C.; Johnson, M. J. A.; Mindiola, D. J.; Cummins, C. C.; Klooster, W. T.; Koetzle, T. F. *J. Am. Chem. Soc.* **1999**, *121*, 10426-10427. (c) Figueroa, J. S.; Cummins, C. C. *J. Am. Chem. Soc.* **2003**, *125*, 4020-4021.

3 Walsh, P. J.; Hollander, F. J.; Bergman, R. G. *J. Am. Chem. Soc.* **1988**, *110*, 8729-8731.

4 (a) Nugent, W. A.; Mayer, J. M. Metal-ligand multiple bonds; Wiley: New York, **1988**, 52-61. (b) Zarubin, D. N.; Ustynyuk, N. A. *Russ. Chem. Rev.* **2006**, *75*, 671.

5 Buchwald, S. L.; Watson, B. T.; Wannamaker, M. W.; Dewan, J. C. *J. Am. Chem. Soc.* **1989**, *111*, 4486-4494.

6 (a) Bennett, C. R.; Bradley, D. C. *J. Chem. Soc., Chem. Commun.* **1974**, 29-30. (b) Simpson, S. J.; Andersen, R. A. *Inorg. Chem.* **1981**, *20*, 3627-3629. (c) Simpson, S. J.; Turner, H. W.; Andersen, R. A. *Inorg. Chem.* **1981**, *20*, 2991-2995. (d) Berno, P.; Gambarotta, S. *Organometallics* **1994**, *13*, 2569-2571. (e) Horton, A. D.; de With, J. *Chem. Commun.* **1996**, 1375-1376. (f) Bott, S. G.; Hoffman, D. M.; Rangarajan, P. *J. Chem. Soc., Dalton Trans.* **1996**, 1979-1982. (g) Gerlach, C. P.; Arnold, J. *Organometallics* **1997**, *16*, 5148-5157. (h) Dehnicke, K.; Greiner, A. *Angew. Chem. Int. Ed.* **2003**, *42*, 1340-1354. (i) Cai, H.; Yu, X.; Chen, T.; Chen, X.-T.; You, X.-Z.; Xue, Z.

Can. J. Chem. **2003**, *81*, 1398-1405. (j) Niemeyer, M. *Inorg. Chem.* **2006**, *45*, 9085-9095.

7 Scherer, W.; Wolstenholme, D. J.; Herz, V.; Eickerling, G.; Brück, A.; Benndorf, P.; Roesky, P. W. *Angew. Chem. Int. Ed.* **2010**, *49*, 2242-2246.

8 Brookhart, M.; Green, M. L. H.; Parkin, G. *Proc. Natl. Acad. Sci.* **2007**, *104*, 6908-6914.

9 Cummins, C. C.; Baxter, S. M.; Wolczanski, P. T. *J. Am. Chem. Soc.* **1988**, *110*, 8731-8733.

10 Procopio, L. J.; Carroll, P. J.; Berry, D. H. *J. Am. Chem. Soc.* **1991**, *113*, 1870-1872.

11 (a) Procopio, L. J.; Carroll, P. J.; Berry, D. H. *J. Am. Chem. Soc.* **1994**, *116*, 177-185. (b) Herrmann, W. A.; Eppinger, J.; Spiegler, M.; Runte, O.; Anwander, R. *Organometallics* **1997**, *16*, 1813-1815. (c) Eppinger, J.; Spiegler, M.; Hieringer, W.; Herrmann, W. A.; Anwan-der, R. *J. Am. Chem. Soc.* **2000**, *122*, 3080-3096.

12 Spielmann, J.; Piesik, D.; Wittkamp, B.; Jansen, G.; Harder, S. *Chem. Commun.* **2009**, 3455-3456.

13 Mukherjee, D.; Ellern, A.; Sadow, A. D. *J. Am. Chem. Soc.* **2010**, *132*, 7582-7583.

14 Wiseman, G. H.; Wheeler, D. R.; Seyferth, D. *Organometallics* **1986**, *5*, 146-152. (b) Kosse, P.; Popowski, E. *Z. Anorg. Allg. Chem.* **1992**, *613*, 137-148.

15 Choukroun, R.; Raoult, Y.; Gervais, D. *J. Organomet. Chem.* **1990**, *391*, 189-194.

16 (a) Wolfe, J. P.; Wagaw, S.; Buchwald, S. L. *J. Am. Chem. Soc.* **1996**, *118*, 7215-7216. (b) Driver, M. S.; Hartwig, J. F. *J. Am. Chem. Soc.* **1996**, *118*, 7217-7218. (c)

17 Wolfe, J. P.; Wagaw, S.; Marcoux, J.-F.; Buchwald, S. L. *Acc. Chem. Res.* **1998**, *31*, 805-818.

18 Buchwald, S. L., LaMaire, S. J., Nielsen, R. B., Watson, B. T., King, S. M. *Org. Synth., Coll. Vol. 7*, **1998**, *9*, 162-165.

19 Wiseman, G. H., Wheeler, D. R., Seyferth, D. *Organometallics* **1986**, *5*, 146-152.

20 Kim, J., Bott, S. G., Hoffman, D. M. *Inorg. Chem.* **1998**, *37*, 3835-3841.

21 (a) Procopio, L. J., Carroll, P. J., Berry, D. H. *J. Am. Chem. Soc.* **1991**, *113*, 1870-1872. (b) Procopio, L. J., Carroll, P. J., Berry, D. H. *J. Am. Chem. Soc.* **1994**, *116*, 177-185.

22 G. R. Willey, T. J. Woodman and M. G. B. Drew, *Polyhedron* **1997**, *16*, 3385-3393.

23 Eppinger, J., Herdtweck, E., Anwander, R. *Polyhedron* **1998**, *17*, 1195 – 1201.

24 Kuprat, M., Lehmann, M., Axel Schulz, A., Villinger, A. *Organometallics* **2010**, *29*, 1421–1427.

25 Druce, P. M., Kingston, B. M., Lappert, M. F., Spalding, Srivastava, R. C. *J. Chem. Soc. A.* **1969**, 2106-1220.

Supplementary information.

Ortep figure for **6.2**.

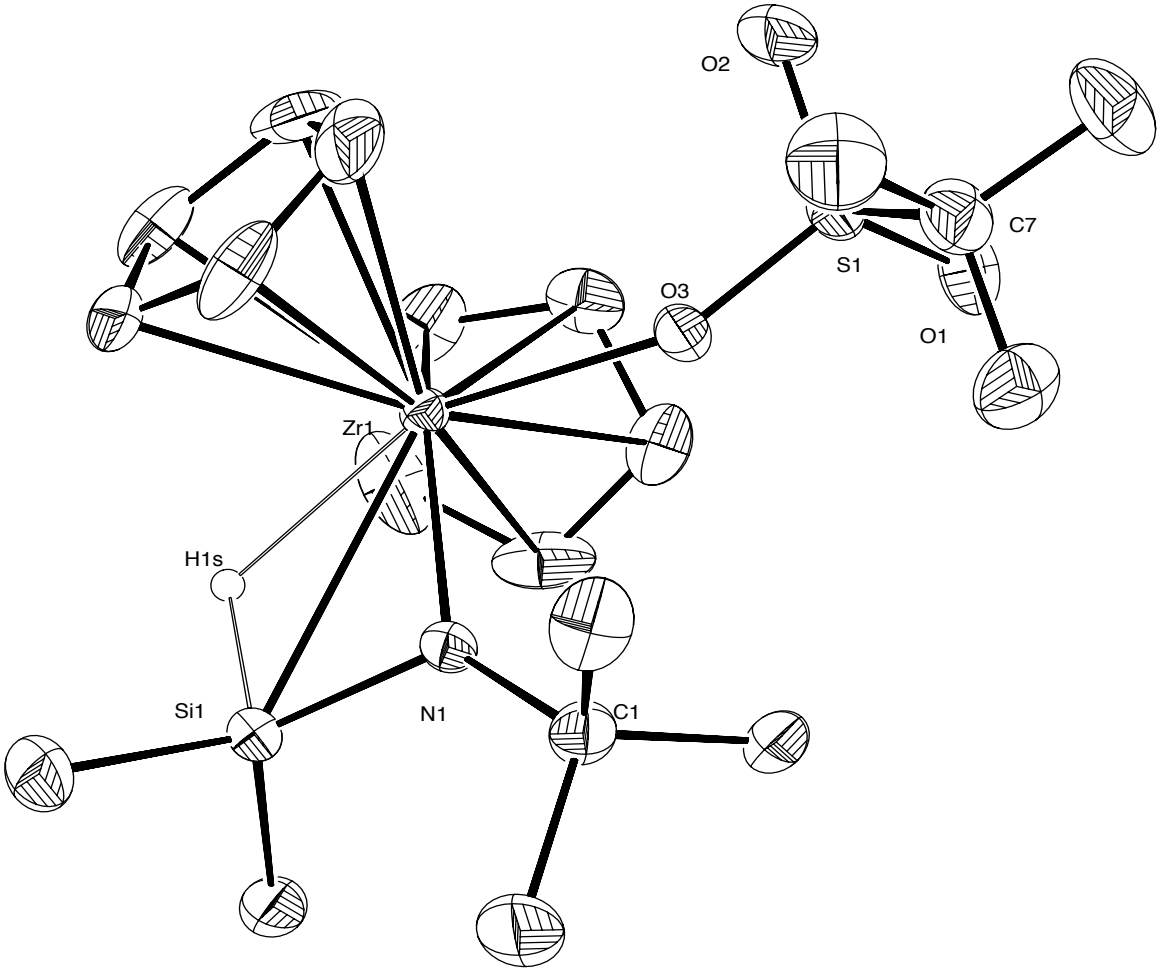

Ortep figure for **6.10**.

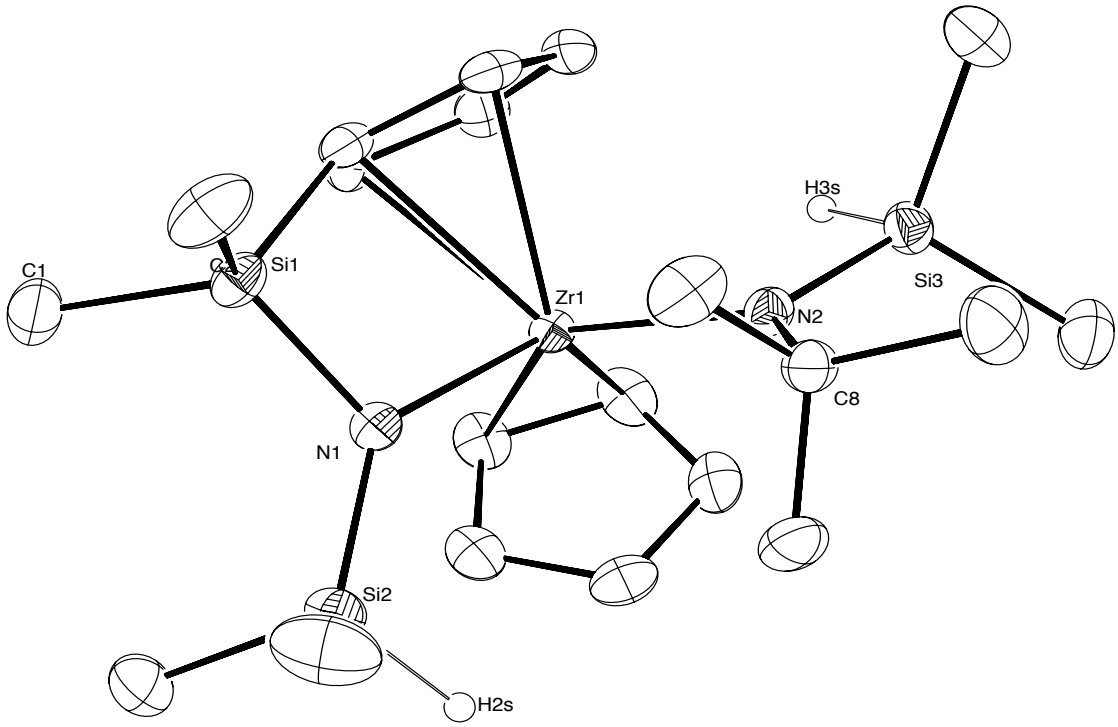

Chapter 7: C-H Bond activation of ethylene by a zirconacycle

Modified from a paper published in *Chem. Commun.*[5]

KaKing Yan, and Aaron D. Sadow

Department of Chemistry and US Department of Energy Ames Laboratory, Iowa State University, Ames IA, 50011, USA

Abstract. The reaction of C_2H_4 and β-SiH containing azasilazirconacycle $Cp_2Zr\{\kappa^2\text{-}N(SiHMe_2)SiHMeCH_2\}$ (7.3), formed via a γ-abstraction reaction of $Cp_2Zr\{N(SiHMe_2)_2\}H$ (7.1), follows an unusual pathway in which a rare σ-bond metathesis reaction of ethylene generates a vinyl intermediate. That species undergoes a β-hydrogen abstraction under the reaction conditions to form a zirconium silanimine ethylene adduct en route to the metallacyclopentane product.

Introduction

β-Hydrogen elimination and abstraction reactions are central to synthetic organometallic chemistry and catalysis, although these processes are often associated with unwanted side reactions including alkyl group decompositions, chain transfer in polymerizations, and reduction rather than bond formation in cross couplings. Inhibition of these unwanted side reactions will allow access to productive elementary steps, such as σ-bond metathesis and insertion, that can be used to develop new transformations. In one approach, ligand design strategies and catalytic reaction partners have simply avoided β-

[5] *Chem. Commun.* **2013***, 49*, 3212-3214.

hydrogen. However, the β-hydrogen-rich tetramethyldisilazide ligand $N(SiHMe_2)_2$[1] has found recent application in groups 2 and 3 and f element chemistry,[2] possibly because β-elimination is slow in those systems.[3] Despite the rich rare earth chemistry, the reactivity of tetramethyldisilazido zirconium compounds is essentially unexplored.[4] Early metal and rare earth β-SiH containing silazides often form agostic-type structures,[2,5,6] while $Cp_2Zr\{N(SiHMe_2)t\text{-}Bu\}CH_2SiMe_3$ reacts by H-abstraction to give a zirconium-stabilized silanimine (Scheme 7.1).[7] *N*-Alkyl amido zirconocenes also react via β-hydrogen abstraction, even in the presence of γ-hydrogen.[8] In contrast, a key reaction of β-hydrogen-free d^0 and f^nd^0 $[M]N(SiMe_3)_2$ compounds is γ-H abstraction to form azametallasilacyclobutanes.[9]

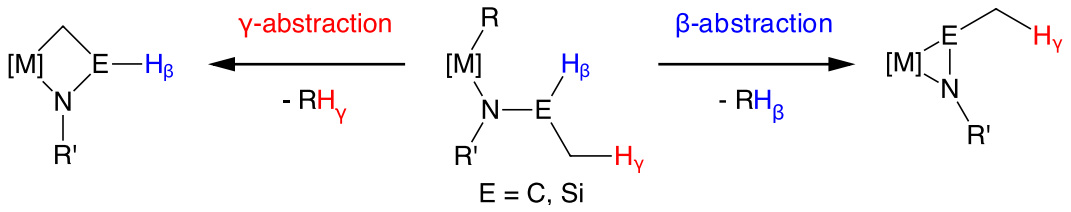

Scheme 7.1. Hydrogen abstraction processes. Amido ligands with both β- and γ-hydrogen typically react by β-hydrogen abstraction.

Here, we describe β- and γ-hydrogen abstraction reactions of $Cp_2Zr\{N(SiHMe_2)_2\}R$ that provide β-SiH containing zirconasilanimines and azasilazirconacyclobutanes. γ-Abstraction is favored for R = H and Me, while β-abstraction is observed when R = Et and $CH{=}CH_2$. Furthermore, the Zr-C bond in the metallocyclobutane mediates a rare and reversible C-H bond activation of ethylene through σ-bond metathesis.

Result and discussion

Disilazido zirconium hydride and methyl compounds $Cp_2Zr\{N(SiHMe_2)_2\}R$ (R = H; Me) have dissimilar ground state structures. $Cp_2Zr\{N(SiHMe_2)_2\}H$ (**7.1**) contains one side-on coordinated SiH and one terminal SiH that exchange at room temperature, while the spectroscopy of $Cp_2Zr\{N(SiHMe_2)_2\}Me$ (**7.2**) is consistent with two classical SiHs. Still, thermolysis of **7.1** or **7.2** in a sealed tube affords the azasilazirconacycle $Cp_2Zr\{\kappa^2\text{-}N(SiHMe_2)SiHMeCH_2\}$ (**7.3**) with H_2 or CH_4 elimination through γ-abstraction (eq 7.1).

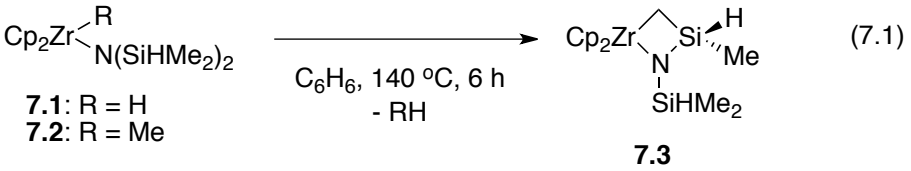

(7.1)

The ^1H NMR spectrum of **7.3** contained resonances at 4.84 ppm ($^1J_{SiH}$ = 193.4 Hz) and 4.37 ppm ($^1J_{SiH}$ = 204.0 Hz) assigned to inequivalent SiH moieties. Doublet of doublet resonances at 1.97 and 1.61 ppm (1 H each) were assigned to the diastereotopic CH_2. In the IR spectrum, a single ν_{SiH} band at 2074 cm^{-1} was observed.

This γ-H abstraction occurs in the presence of β-hydrogen, and the observed selectivity is unusual for amides. In fact, labeling studies of alkylamides suggest that kinetics and thermodynamics both favor β-abstraction over γ-abstraction, based on the incorporation of deuterium in only the β-position in a reversible system.[10] In an interesting contrast, H/D exchange studies indicate that early transition metal alkoxides react via (reversible) γ-abstraction.[10a]

Ethylene is a small, non-polar, unsaturated substrate that could undergo Zr-C bond insertion. Instead, compound **7.3** and C_2H_4 (1 atm) react at 150 °C over 1 week to give

$Cp_2Zr\{\kappa^2\text{-}N(SiHMe_2)SiMe_2CH_2CH_2\}$ (**7.4**; eq 7.2).

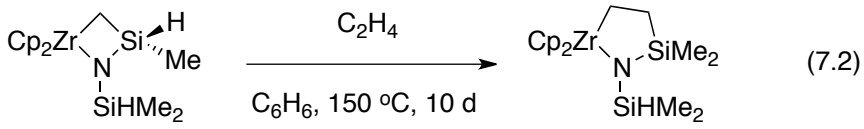

7.3 **7.4** (7.2)

Compound **7.4** is prepared by the reaction of **7.1** and ethylene (1 atm) at 150 °C for 1 d. *In situ* NMR experiments on micromolar-scale reactions of **7.1** and C_2H_4 in benzene-d_6 revealed a mixture of **7.3**, **7.4**, H_2 and ethane. The ratio of **7.3** to **7.4** was 1.4:1 after 45 min., and 0.13:1 after 190 min, and quantitative for **7.4** after 1 d. The conversion of **7.3** to **7.4** is greatly facilitated by H_2, but there is no clear route to give H_2 as an intermediate in the interaction of **7.3** and C_2H_4. Substoichiometric quantities of H_2 do not catalyze the transformation. In contrast, only starting materials are observed after heating $Cp_2Zr\{\kappa^2\text{-}N(SiMe_3)SiMe_2CH_2\}$ and ethylene at 150 °C for several days. Apparently, the SiH groups are critical to the reaction of equation 7.2.

We considered two possible mechanisms for the H_2-free transformation (Scheme 7.1). In Pathway **A**, Lewis acid-mediated hydrosilylation of ethylene generates a SiEt moiety. Subsequent δ-abstraction would provide the ring expansion product. In fact, olefin hydrosilylation catalyzed by $B(C_6F_5)_3$ is proposed to involve SiH abstraction.[11] Alternatively, Pathway **B** is based on the known reaction of silanimine $Cp_2Zr\{\eta^2\text{-}N(t\text{-}Bu)SiMe_2\}$ and ethylene that forms $Cp_2Zr\{N(t\text{-}Bu)SiMe_2CH_2CH_2\}$.[7] C-H Bond activation of ethylene by a ring-opening reaction of **7.3** would provide the vinyl intermediate $Cp_2Zr\{N(SiHMe_2)_2\}CH{=}CH_2$. β-H abstraction then generates a silanimine intermediate. However C-H bond activation of ethylene is uncommon,[12] particularly for organometallic

systems known for olefin insertion. For example, the compound $Cp^*_2Th(\kappa^2\text{-}CH_2CMe_2CH_2)$ reacts with CH_4 by C-H bond activation but C_2H_4 inserts into a Th-C bond.[12g]

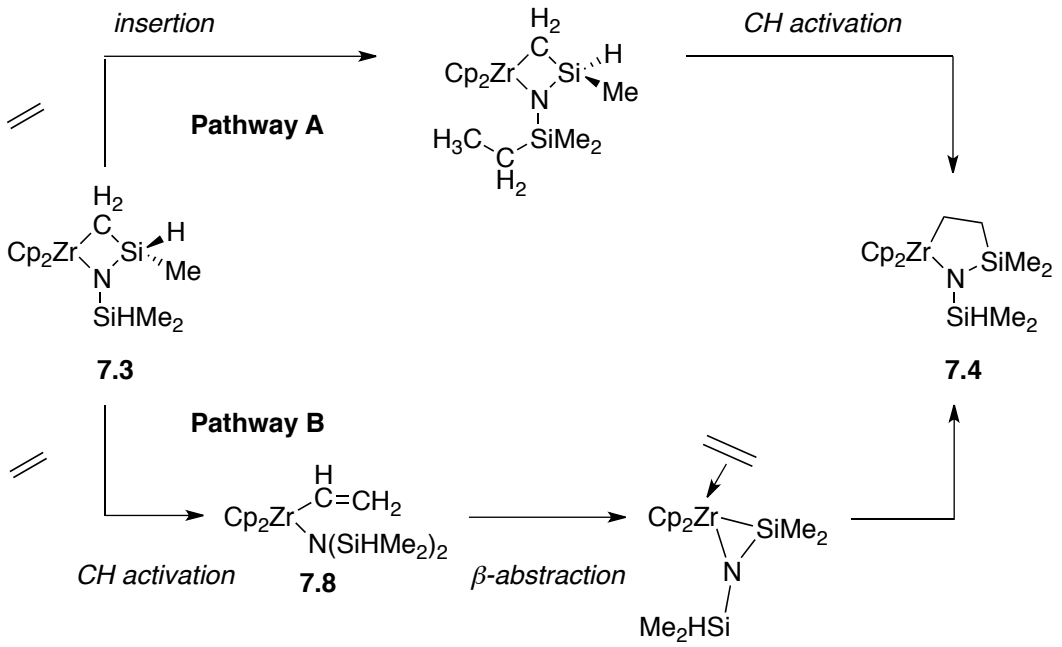

Scheme 7.2. Possible H_2-free pathways for conversion of **7.3** to **7.4**.

Additionally, vinylic organometallic compounds are often inert relative to alkyls, and a β-abstraction reaction of $Cp_2Zr\{N(SiHMe_2)_2\}CH{=}CH_2$ requires experimental justification. In support of pathway B, β-abstraction by a zirconium acetylide was proposed in the rearrangement of an alkyl acetylide to a zirconacyclopentene.[13]

Only starting materials and products were detected in the conversion of **7.3** to **7.4**, therefore, model compounds and plausible intermediates were studied. To investigate Pathway **A**, we prepared $Cp_2Zr\{N(SiEtMe_2)_2\}H$ (**7.5**) by reaction of Cp_2ZrHCl and $LiN(SiEtMe_2)_2$ in benzene. Thermolysis of **7.5** for 1 h at 110 °C, or standing at room temperature for 9 h,[9c] gives full conversion to the γ-abstraction product $Cp_2Zr\{N(SiEtMe_2)SiMeEtCH_2\}$ (**7.6**, eq 7.3).

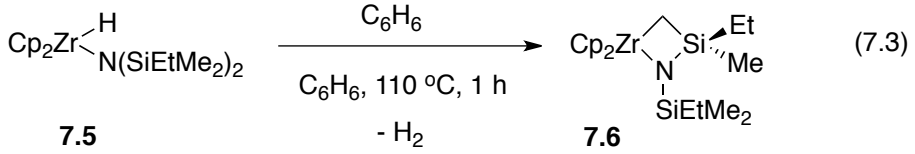

7.5 **7.6** (7.3)

Treatment of **7.6** at 180 °C for 5 days in a sealed tube (1 atm N_2 or 1 atm C_2H_4) returns metallacycle **7.6** in quantitative NMR yield. Thus, Pathway **A** appears unlikely. Instead, a labeling experiment supports Pathway **B**. Reaction of C_2D_4 and **7.1** provides **7.4**-d_n, with partial deuteration of SiMe and the [Zr]CD_2CD_2Si moieties.

Reaction of **7.3** and the terminal alkyne HC≡$CSiMe_3$ at 150 °C over 1 day forms $Cp_2Zr\{N(SiHMe_2)_2\}C{\equiv}CSiMe_3$ (**7.7**) as a model for the C-H bond activation of ethylene proposed in Pathway **B**. This type of σ-bond metathesis reaction is unusual for zirconium. While rare earth alkyls and terminal acetylene readily react,[14] few σ-bond metathesis reactions of 16-electron zirconium alkyl compounds and alkynes have been described. For example, CpCp*Zr{$Si(SiMe_3)_3$}Me is inert to acetylene at room temperature for one day, even though the Zr-Si bond readily reacts with organosilanes via σ-bond metathesis under those conditions.[15] Most alkynylzirconium species are formed by salt metathesis involving alkali metal acetylides[16] or from reactions of terminal acetylenes with zirconium-heteroatom bonds.[17,18,19] Low electron count metal alkyl compounds, however, react directly with acetylenes.[20] Zr-C bonds in strained 3-membered zirconacycles also form [Zr]CCR through C-H bond addition to zirconium(II) species.[13,21] While $Cp^*_2Zr(CH{=}CHMe)_2$ reacts with acetylenes to give zirconium alkynyl compounds, labelling studies implicate a $Cp^*_2Zr(\eta^2$-HCCMe) intermediate rather than a σ-bond metathesis reaction.[22]

Acetylide **7.7** is inert under the conditions that give **7.4** (i.e., 1 atm. C_2H_4, 150 °C).

Therefore, $Cp_2Zr\{N(SiHMe_2)_2\}CH=CH_2$ (**7.8**) was sought as an intermediate. Reaction of $Cp_2Zr(CH=CH_2)Cl$ and $LiN(SiHMe_2)_2$ affords **7.8** as a red-brown gummy solid. The ^1H NMR spectrum of the solid contained the characteristic ABX pattern for the zirconium vinyl group ($^3J_{HH}$ = 19.2 Hz, $^3J_{HH}$ = 14.4 Hz, $^2J_{HH}$ = 3.6 Hz). The downfield chemical shift and large $^1J_{SiH}$ coupling constant (4.48 ppm, $^1J_{SiH}$ = 186.5 Hz) suggest classical-bonded SiH groups. We examined the thermal reactivity of **7.8** as the proposed intermediate in the reaction of **7.3** and ethylene. Thermolysis of **7.8** in benzene-d_6 at 90 °C for 4 h provides **7.3** and **7.4** in 1:5 ratio (eq 7.4).

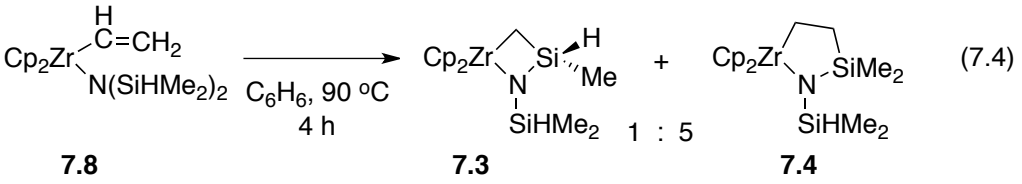

(7.4)

σ-Bond metathesis of ethylene is the microscopic reverse of γ-abstraction by **7.8**, and formation of **7.3** implies that the C-H bond activation of C_2H_4 is reversible. Interestingly, only **7.4** is observed upon thermolysis of **7.8** in the presence of ethylene. However, in the presence of excess C_2D_4 (ca. 3 atm), a mixture of **7.4** and **7.4**-d_4 are formed in a 3.4:1 ratio; that ratio is unchanged after 24 h at 120 °C. Additionally, the conversion of **7.8** to **7.3** and **7.4** is much faster than the reaction of **7.3** and excess ethylene, which suggests the product distribution in equation 7.4 may describe a kinetic competition between β- and γ-abstraction processes. Thus, while γ-abstraction is favoured with H_2 and CH_4 as departing groups, β-abstraction from $[Zr]C_2H_3$ gives $Cp_2Zr(\eta^2\text{-}C_2H_4)\{\eta^2\text{-}NSiMe_2(SiHMe_2)\}$ as an apparent intermediate (Scheme 7.2).

To check if $[Zr](\eta^2\text{-}C_2H_4)$ formation influences the relative rate of β- vs. γ-

abstraction, $Cp_2Zr\{N(SiHMe_2)_2\}Et$ (**7.9**) was thermalized at 60 °C to afford ethane and $Cp_2Zr\{k^2\text{-}NSiMe_2(SiHMe_2)\}$ (**7.10**, eq 7.5).

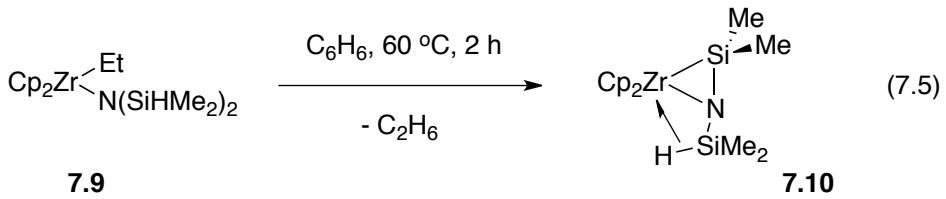

7.9 **7.10** (7.5)

The ^{1}H NMR spectrum of **7.10** contained a singlet (0.55 ppm) and a doublet (-0.04 ppm, $^3J_{HH}$ = 1.5 Hz) for the $SiMe_2$ and $SiH\mathit{Me}_2$, respectively. The unusually upfield SiH multiplet at -2.23 ppm ($^1J_{SiH}$ = 89 Hz) is consistent with a β-agostic structure. Upon addition of PMe_3, the SiH resonance in **7.10** shifts dramatically downfield to 5.19 ppm, which suggests PMe_3 disrupts the β-agostic structure. Neither **7.10** nor **7.10**·PMe_3 could be isolated free of impurities, but both compounds react with C_2H_4 to afford **7.4**, providing further support for the Pathway **B**.

Conclusion

Several points are worth noting. First, the β-SiH moieties provide a pathway for the chemistry described here, which is distinct from that of $N(SiMe_3)_2$ analogues. Second, the relative reactivity toward β-abstraction decreases following the series alkyl (ethyl) > vinyl (ethenyl) >> alkynyl, and we are currently testing the generality of this trend. Third, the metalation of ethylene is generally challenging because compounds that are capable of C-H bond activation by σ-bond metathesis are also often highly reactive toward ethylene insertion and polymerization. The chemistry with ethylene of **7.3** extends intermolecular σ-bond metathesis reactions involving C-H bonds for the first time to neutral 16-electron zirconocene

compounds.

The C-H bond activation chemistry of ethylene by **7.3** may depend on a combination of factors including the electronic and steric limitations of a sixteen-electron complex, the strain associated with the four-membered metallacycle, the presence of a β-Si-H to trap the vinyl product, and thermal stability of compound **7.3**. Nevertheless, this work shows that introduction of β-SiH groups in a metallocyclobutane significantly alters the outcome of small molecule chemistry. These results may lead to new catalytic hydrosilylation mechanism and provide new ways for C-H bond functionalization of challenging substrates.

Experimental

General. All manipulations were performed under a dry argon atmosphere using standard Schlenk techniques or under a nitrogen atmosphere in a glovebox unless otherwise indicated. Water and oxygen were removed from benzene, toluene, pentane, diethyl ether, and tetrahydrofuran solvents using an IT PureSolv system. Benzene-d_6 and tetrahydrofuran-d_8 were heated to reflux over Na/K alloy and vacuum-transferred. The compounds $Cp_2ZrMeCl$,[23] Cp_2ZrHCl,[24] (*E*)-$Cp_2Zr(CH{=}CH_2SiMe_3)Cl$,[25] $LiN(SiMe_3)_2$,[26] $LiN(SiHMe_2)_2$,[27] $LiN(SiEtMe_2)_2$,[28] $B(C_6F_5)_3$,[29] $Cp_2Zr[N(SiHMe_2)_2]H$,[5] $Cp_2Zr(CH{=}CH_2)Cl$,[30] and $Cp_2ZrEtCl$[31] were prepared following literature procedures.

^1H, $^{13}C\{^1H\}$, ^{11}B and $^{29}Si\{^1H\}$ NMR spectra were collected on an Agilent MR400 spectrometer. ^{11}B NMR spectra were referenced to an external sample of $BF_3{\cdot}Et_2O$. ^{15}N chemical shifts were determined either by ^1H-^{15}N HMBC experiments on a Bruker Avance II 700 spectrometer with a Bruker Z-gradient inverse TXI $^1H/^{13}C/^{15}N$ 5mm cryoprobe or by ^1H-^{15}N CIGARAD experiments on an Agilent MR400 spectrometer; ^{15}N chemical shifts were

originally referenced to liquid NH_3 and recalculated to the CH_3NO_2 chemical shift scale by adding -381.9 ppm. Assignments of resonances are supported by ^1H-^1H and heteronuclear correlation NMR experiments. Infrared spectra were measured on a Bruker IFS66v FTIR. Elemental analyses were performed using a Perkin-Elmer 2400 Series II CHN/S. X-ray diffraction data was collected on a Bruker APEX II diffractometer.

$Cp_2Zr[N(SiHMe_2)_2]H$ (7.1). The synthesis of $Cp_2Zr[N(SiHMe_2)_2]H$ was previously reported in reference 8; here we give the low temperature ^1H, ^{13}C and ^{29}Si NMR spectra that provide support for a β-agostic interaction. The synthetic procedure and room temperature spectroscopic data is repeated here for the reader's convenience. A suspension of $[Cp_2ZrHCl]_n$ (0.909 g, 3.53 mmol) and $LiN(SiHMe_2)_2$ (0.491 g, 3.53 mmol) was stirred for 30 min in benzene (15 mL) at room temperature. The volatile materials were removed under reduced pressure to leave an off-white solid residue, which was extracted with pentane (15 mL). The pentane extract was concentrated and cooled to -30 °C, yielding $Cp_2Zr[N(SiHMe_2)_2]H$ (0.931 g, 2.62 mmol, 74.4%). ^1H NMR (benzene-d_6, 400 MHz, 25 °C): δ 5.78 (s, 10 H, C_5H_5), 5.60 (s, 1 H, ZrH), 3.78 (m, $^1J_{SiH}$ = 161.0 Hz, 2 H, SiH), 0.18 (d, $^3J_{HH}$ = 3.2 Hz, 12 H, SiH*Me*$_2$). $^{13}C\{^1H\}$ NMR (benzene-d_6, 125 MHz, 25 °C): δ 107.58 (C_5H_5), 1.76 (SiMe). $^{15}N\{^1H\}$ NMR (benzene-d_6, 61 MHz, 25 °C): δ -292.4. $^{29}Si\{^1H\}$ NMR (benzene-d_6, 119.3 MHz, 25 °C): δ -40.7. ^1H NMR (toluene-d_8, 600 MHz, -82 °C): δ 5.67 (s, 10 H, C_5H_5), 5.48 (s, 1 H, ZrH), 4.99 (s br, $^1J_{SiH}$ = 179.6 Hz, 1 H, $SiH^{anagostic}$), 2.13 (s br, $^1J_{SiH}$ = 129.7 Hz, 1 H, $SiH^{agostic}$), 0.49 (s br, 6 H, SiMe), 0.06 (s br, 6 H, SiMe). $^{13}C\{^1H\}$ NMR (toluene-d_8, 125 MHz, -82 °C): δ 106.58 (C_5H_5), 2.96 ($SiH^{anagostic}Me_2$), -1.13 ($SiH^{agostic}Me_2$). $^{29}Si\{^1H\}$ NMR (toluene-d_8, 119.3 MHz, -82 °C): δ -23.1 ($SiH^{anagostic}Me_2$), -62.9

($SiH^{agostic}Me_2$). IR (KBr, cm^{-1}): 3099 w br, 2955 m, 2895 w, 2047 s br ($\nu_{SiH\text{-}anagostic}$), 1907 m br ($\nu_{SiH\text{-}agostic}$), 1559 m br ($\nu_{ZrH}$), 1441 w, 1246 s, 1014 s, 890 s, 798 s br, 765 s br, 650 s br. Anal. Calcd for $C_{14}H_{25}NSi_2Zr$: C, 47.40; H, 7.10; N, 3.95. Found: C, 47.02; H, 6.96; N, 3.92. mp 104-106 °C.

$Cp_2Zr[N(SiHMe_2)_2]Me$ (7.2). $Cp_2ZrMeCl$ (0.716 g, 2.63 mmol) and $LiN(SiHMe_2)_2$ (0.367 g, 0.264 mmol) were suspended in benzene (15 mL). This mixture was stirred at room temperature for 13 h. Evaporation of the volatile materials provided an off-white solid. Extraction with pentane (15 mL), concentration, and cooling of the saturated solution to -30 °C yielded crystals of $Cp_2Zr[N(SiHMe_2)_2]Me$. The mother liquor was further concentrated and cooled to provide a second crop of crystals in good overall yield (0.823 g, 2.23 mmol, 84.8%). ^{1}H NMR (benzene-d_6, 400 MHz, 25 °C): δ 5.82 (s, 10 H, C_5H_5), 4.44 (m, $^1J_{SiH}$ = 180.8 Hz, 2 H, SiH), 0.47 (s, 3 H, ZrMe), 0.22 (d, $^3J_{HH}$ = 3.2 Hz, 12 H, SiMe). $^{13}C\{^1H\}$ NMR (benzene-d_6, 125 MHz, 25 °C): δ 112.41 (C_5H_5), 34.46 (ZrMe), 1.96 (SiMe). $^{15}N\{^1H\}$ NMR (benzene-d_6, 61 MHz, 25 °C): δ -277.4. $^{29}Si\{^1H\}$ NMR (benzene-d_6, 119.3 MHz, 25 °C): δ -27.6 (SiMe). IR (KBr, cm^{-1}): 3104 m br, 2954 s br, 2074 s br (SiH), 1815 w br, 1718 w br, 1616 w br, 1247 s, 1015 s, 901 s br, 800 s br, 763 s br. Anal. Calcd for $C_{15}H_{27}Si_2NZr$: C, 48.85; H, 7.38; N, 3.80. Found: C, 49.15; H, 7.20; N, 3.79. mp 185-191 °C.

$Cp_2Zr[\kappa^2\text{-}N(SiHMe_2)SiHMeCH_2]$ (7.3). A benzene solution of **5.2** (0.332 g, 0.90 mmol) was heated at 135 °C for 3 h in a sealed reaction vessel. The color quickly turned from pale yellow to green. After 6 h, the reaction mixture was evaporated to provide **5.3** as an analytically-pure, yellow-green oil in excellent yield (0.310 g, 0.879 mmol, 97.6%). ^{1}H NMR (benzene-d_6, 400 MHz, 25 °C): δ 5.84 (s, 5 H, C_5H_5), 5.81 (s, 5 H, C_5H_5), 4.84 (m, $^1J_{SiH}$ =

193.4 Hz, 1 H, NSi*H*Me$_2$), 4.37 (m, $^1J_{SiH}$ = 204.0 Hz, 1 H, ZrCH$_2$Si*H*Me), 1.97 (dd, $^2J_{HH}$ = 12.4 Hz, $^3J_{HH}$ = 4.4 Hz, 1 H, CH$_2$), 1.61 (dd, $^2J_{HH}$ = 12.4 Hz, $^3J_{HH}$ = 2.4 Hz, 1 H, CH$_2$), 0.28 (d, $^3J_{HH}$ = 2.4 Hz, 3 H, SiMe), 0.22 (d, $^3J_{HH}$ = 3.2 Hz, 3 H, SiMe$_2$), 0.20 (d, $^3J_{HH}$ = 3.2 Hz, 3 H, SiMe$_2$). ^{13}C{^{1}H} NMR (benzene-d_6, 125 MHz, 25 °C): δ 112.24 (C$_5$H$_5$), 112.20 (C$_5$H$_5$), 36.44 (ZrCH$_2$), 2.54 (SiMe$_2$), 2.09 (SiMe$_2$), 1.58 (CH$_2$SiH*Me*). ^{15}N{^{1}H} NMR (benzene-d_6, 61 MHz, 25 °C): δ -250.8. ^{29}Si{^{1}H} NMR (benzene-d_6, 119.3 MHz, 25 °C): δ -19.9 (NSiHMe$_2$), -68.3 (CH$_2$SiHMe). IR (KBr, cm^{-1}): 3097 w br, 2950 m br, 2895 m, 2074 s br (SiH), 1598 w br, 1441 m, 1247 s, 1168 w, 1015 s, 910 s br, 795 s br, 715 m, 678 m. Anal. Calcd for C$_{14}$H$_{23}$Si$_2$NZr: C, 47.67; H, 6.57; N, 3.97. Found: C, 47.31; H, 6.80; N, 4.00.

Cp$_2$Zr[κ^2-N(SiHMe$_2$)SiMe$_2$CH$_2$CH$_2$] (7.4). Compound **7.1** (0.129 g, 0.364 mmol) was dissolved in benzene (10 mL) in a 100 mL reaction flask equipped with a Teflon valve. The solution was degassed with three freeze-pump-thaw cycles. The flask was then charged with ethylene (1 atm), sealed, and heated to 150 °C overnight. The volatiles were removed under reduced pressure to provide analytically pure **7.4** as light brown oily residue (0.127 g, 0.335 mmol, 92.0%). ^{1}H NMR (benzene-d_6, 400 MHz, 25 °C): δ 5.85 (s, 10 H, C$_5$H$_5$), 3.94 (m, $^1J_{SiH}$ = 174.8 Hz, 1 H, NSi*H*Me$_2$), 1.50 (m, 2 H, CH$_2$), 1.34 (m, 2 H, CH$_2$), 0.13 (overlapping s and d, 12 H, SiMe$_2$ and SiH*Me*$_2$). ^{13}C{^{1}H} NMR (benzene-d_6, 125 MHz, 25 °C): δ 112.12 (C$_5$H$_5$), 37.86 (ZrCH$_2$), 18.70 (*C*H$_2$SiMe$_2$), 3.55 (SiMe$_2$), 1.87 (CH$_2$Si*Me*$_2$). ^{15}N{^{1}H} NMR (benzene-d_6, 61 MHz, 25 °C): δ -255.9. ^{29}Si{^{1}H} NMR (benzene-d_6, 119.3 MHz, 25 °C): δ -33.3 (*Si*Me). IR (KBr, cm^{-1}): 2951 s, 2900 s br, 2062 s br (SiH), 1800 w, 1704 w, 1602 w, 1441 s, 1406 s, 1366 m, 1247 s, 1166 s, 1015 s, 917 s br, 795 s br. Anal. Calcd for C$_{16}$H$_{27}$Si$_2$NZr: C, 50.47; H, 7.15; N, 3.68. Found: C, 50.79; H, 6.89; N, 3.63.

$Cp_2Zr[N(SiEtMe_2)_2]H$ (7.5). This compound was prepared and characterized in situ; all attempts to isolate **7.5** afforded mixtures of **7.5** and the cyclometallated $Cp_2Zr[\kappa^2$-$N(SiEtMe_2)SiMeEtCH_2]$ (**7.6**). A solution of $LiN(SiEtMe_2)_2$ (0.028 g, 0.102 mmol) in benzene-d_6 (0.5 mL) was added to Cp_2ZrHCl (0.020 g, 0.102 mmol) in an NMR tube. Cyclooctane (10 μL) was added to the NMR tube as an internal standard, and the reaction mixture was agitated on a vortex stirrer. After 75 min., $Cp_2Zr[N(SiEtMe_2)_2]H$ was detected. The yield was estimated by ^{1}H NMR spectroscopy as 52.3% based on integration relative to the internal standard. At room temperature, hindered rotation renders the $SiMe_2Et$ groups inequivalent. ^{1}H NMR (benzene-d_6, 400 MHz, 25 °C): δ 5.88 (s, 10 H, C_5H_5), 5.64 (s, 1 H, Zr*H*), 1.04 (t, $^3J_{HH}$ = 7.8 Hz, 3 H, $SiCH_2CH_3$), 0.98 (t, $^3J_{HH}$ = 5.2 Hz, 3 H, $SiCH_2CH_3$), 0.77 (q, $^3J_{HH}$ = 7.8 Hz, 2 H, $SiCH_2CH_3$), 0.56 (q, $^3J_{HH}$ = 5.2 Hz, 2 H, $SiCH_2CH_3$), 0.24 (s, 6 H, $SiEtMe_2$), 0.06 (s, 6 H, $SiEtMe_2$). $^{13}C\{^1H\}$ NMR (benzene-d_6, 150 MHz, 25 °C): δ 109.54 (C_5H_5), 15.25 ($SiCH_2CH_3$), 13.94 ($SiCH_2CH_3$), 9.07 ($SiCH_2CH_3$), 8.66 ($SiCH_2CH_3$), 4.58 (SiMe), 4.00 (SiMe). $^{15}N\{^1H\}$ NMR (benzene-d_6, 61 MHz, 25 °C): δ -256.7. $^{29}Si\{^1H\}$ NMR (benzene-d_6, 119.3 MHz, 25 °C): δ -6.8, -13.3.

$Cp_2Zr[\kappa^2$-$N(SiEtMe_2)SiMeEtCH_2]$ (7.6). A suspension of $[Cp_2ZrHCl]_n$ (0.087 g, 0.338 mmol) and $LiN(SiEtMe_2)_2$ (0.066 g, 0.338 mmol) was stirred for 24 h in benzene (2 mL) at room temperature. The volatile materials were removed under reduced pressure leaving an off-white solid residue, which was extracted with pentane (2 × 2 mL). The pentane extract was evaporated to dryness to yield **7.6** as a yellow oil (0.081 g, 0.199 mmol, 58.8%). ^{1}H NMR (benzene-d_6, 600 MHz, 25 °C): δ 5.84 (s, 5 H, C_5H_5), 5.83 (s, 5 H, C_5H_5), 1.86 (d, $^2J_{HH}$ = 12.1, 1 H, CH_2), 1.72 (d, $^2J_{HH}$ = 12.1 Hz, 1 H, CH_2), 1.13 (t, $^3J_{HH}$ = 7.9 Hz, 3 H,

$CH_2SiMeCH_2CH_3$), 1.02 (t, $^3J_{HH}$ = 7.9 Hz, 3 H, $SiMe_2CH_2CH_3$), 0.73 (m, 1 H, $CH_2SiMeCH_2CH_3$), 0.51 (q, $^3J_{HH}$ = 8.4 Hz, 2 H, $SiMe_2CH_2CH_3$), 0.42 (m, 1 H, $CH_2SiMeCH_2CH_3$), 0.18 (s, 3 H, SiMe), 0.06 (s, 3 H, $SiMe_2$), 0.06 (s, 3 H, $SiMe_2$). $^{13}C\{^1H\}$ NMR (benzene-d_6, 150 MHz): δ 112.04 (C_5H_5), 111.97 (C_5H_5), 40.29 ($ZrCH_2$), 13.11 ($SiMe_2CH_2CH_3$), 12.07 ($CH_2SiMeCH_2CH_3$), 9.23 ($CH_2SiMeCH_2CH_3$), 8.76 ($SiMe_2CH_2CH_3$), 2.34 ($SiMe_2$), 2.33 ($SiMe_2$), 1.58 (CH_2SiMe). $^{15}N\{^1H\}$ NMR (benzene-d_6, 61 MHz, 25 °C): δ -239.1. $^{29}Si\{^1H\}$ NMR (benzene-d_6, 119.3 MHz, 25 °C): δ -4.2 ($SiMe_2Et$), -52.5 ($CH_2SiMeEt$). IR (KBr, cm^{-1}): 2951 s, 2872 s, 1459 m, 1249 s, 1180 w, 1014 s, 985 s, 794 s br. Anal. Calcd for $C_{18}H_{31}Si_2NZr$: C, 52.88; H, 7.64; N, 3.43. Found: C, 52.20; H, 7.02; N, 3.80.

$Cp_2Zr[N(SiHMe_2)_2]C{\equiv}CSiMe_3$ (7.7). $Cp_2Zr[\kappa^2\text{-}N(SiHMe_2)SiHMeCH_2]$ (0.082 g, 0.231 mmol) was dissolved in benzene (5 mL), and $SiMe_3C{\equiv}CH$ (0.33 ml, 2.34 mmol) was added by syringe. The reaction mixture was heated at 150 °C for 17 h. The volatiles were evaporated under reduced pressure to provide analytically pure **7.7** as a light brown microcrystalline solid (0.104 g, 0.231 mmol, 99.8%). ^1H NMR (benzene-d_6, 600 MHz, 25 °C): δ 6.01 (s, 10 H, C_5H_5), 4.47 (m, $^1J_{SiH}$ = 172.2 Hz, 2 H, $SiHMe_2$), 0.38 (d, $^3J_{HH}$ = 3.2 Hz, 12 H, $SiHMe_2$), 0.31 (s, 9 H, $SiMe_3$). $^{13}C\{^1H\}$ NMR (benzene-d_6, 150 MHz, 25 °C): δ 161.48 ($ZrC{\equiv}CSiMe_3$), 131.39 ($ZrC{\equiv}CSiMe_3$), 113.03 (C_5H_5), 1.71 ($SiHMe_2$), 0.94 ($SiMe_3$). $^{15}N\{^1H\}$ NMR (benzene-d_6, 61 MHz, 25 °C): δ -267.3. $^{29}Si\{^1H\}$ NMR (benzene-d_6, 119.3 MHz, 25 °C): δ -24.3 ($SiMe_3$), -28.3 ($SiHMe_2$). IR (KBr, cm^{-1}): 2956 m, 2897 w, 2076 m br (SiH), 2031 w (C≡C), 1442 w, 1245 s, 1018 s, 905 s br, 842 s br, 798 s br, 744 s br, 681 s br.

Anal. Calcd for $C_{19}H_{33}Si_3NZr$: C, 50.61; H, 7.38; N, 3.11. Found: C, 50.24; H, 7.01; N, 2.74. mp 87-93 °C.

$Cp_2Zr[N(SiHMe_2)_2](CH=CH_2)$ (7.8). The procedure described above for **7.2** was used, starting from $Cp_2Zr(CH=CH_2)Cl$ (0.037g, 0.130 mmol) and $LiN(SiHMe_2)_2$ (0.018 g, 0.130 mmol) to afford **7.8** (0.044 g, 0.114 mmol, 87.9%) as light brown gummy solid. ^{1}H NMR (benzene-d_6, 600 MHz, 25 °C): δ 7.68 (dd, $^3J_{HH}$ = 19.2 Hz, $^3J_{HH}$ = 14.4 Hz, 1 H, ZrCH), 6.39 (dd, $^3J_{HH}$ = 14.4 Hz, $^2J_{HH}$ = 3.6 Hz, 1 H, *cis*-ZrCH=CH), 5.89 (s, 10 H, C_5H_5), 5.63 ($^3J_{HH}$ = 19.2 Hz, $^2J_{HH}$ = 3.6 Hz, 1 H, *trans*-ZrCH=CH), 4.48 (m, $^1J_{SiH}$ = 186.5 Hz, 2 H, SiH), 0.24 (d, $^3J_{HH}$ = 3.0 Hz, 12 H, SiMe). $^{13}C\{^1H\}$ NMR (benzene-d_6, 150 MHz, 25 °C): δ 187.22 (ZrCH), 128.82 (ZrCH=*C*H_2), 112.78 (C_5H_5), 1.93 (SiMe). $^{15}N\{^1H\}$ NMR (benzene-d_6, 61 MHz, 25 °C): δ -274.5. $^{29}Si\{^1H\}$ NMR (benzene-d_6, 119.3 MHz, 25 °C): δ -27.3. IR (KBr, cm^{-1}): 3100 w, 2951 m, 2897 m, 2071 m br (ν_{SiH}), 1600 w, 1441 m ($\nu_{C=C}$), 1408 w, 1367 w, 1246 s, 1166 w, 1015 s, 989 s, 915 s, 842 s, 795 s, 703 m, 674 m, 603 m. Anal. Calcd for $C_{19}H_{35}Si_3NZr$: C, 50.47; H, 7.15; N, 3.68. Found: C, 50.83; H, 7.64; N, 3.71.

$Cp_2Zr[N(SiHMe_2)_2]Et$ (7.9). The procedure described above for **7.2** was used, starting from $Cp_2ZrEtCl$ (0.426 g, 1.490 mmol) and $LiN(SiHMe_2)_2$ (0.208 g, 1.490 mmol) to afford **7.9** (0.478 g, 1.248 mmol, 83.7%) as light brown solid. ^{1}H NMR (benzene-d_6, 600 MHz, 25 °C): δ 5.84 (s, 10 H, C_5H_5), 4.46 (m, $^1J_{SiH}$ = 183.2 Hz, 2 H, SiH), 1.41 (t, $^3J_{HH}$ = 7.4 Hz, 3 H, $ZrCH_2C\mathit{H}_3$), 1.10 (q, $^3J_{HH}$ = 7.4 Hz, 2 H, $ZrC\mathit{H}_2CH_3$), 0.22 (d, $^3J_{HH}$ = 3.1 Hz, 12 H, SiMe). $^{13}C\{^1H\}$ NMR (benzene-d_6, 150 MHz, 25 °C): δ 112.38 (C_5H_5), 47.66 ($ZrCH_2$), 18.44 (CH_3), 2.28 (SiMe). $^{15}N\{^1H\}$ NMR (benzene-d_6, 61 MHz, 25 °C): δ -277.4. $^{29}Si\{^1H\}$ NMR (benzene-d_6, 119.3 MHz, 25 °C): δ -25.8. IR (KBr, cm^{-1}): 3092 w, 2951 m, 2896 m, 2854 m,

2090 m (ν_{SiH}), 2055 m (ν_{SiH}), 1443 w, 1370 w, 1246 s, 1172 w, 1139 w, 1016 s, 901 s, 844 m, 800 s, 762 s, 699 s, 679 s, 633 m, 598 m. mp 79-83 °C.

$Cp_2Zr[\eta^2$-N(SiHMe$_2$)SiMe$_2$] (7.10). Compound 7.9 (0.034 g, 0.088 mmol) was dissolved in benzene-d_6 (0.6 ml) and added to a NMR tube equipped with a J-Young valve. Cyclooctane as an internal standard (0.5 ml) was also added to the mixture. The reaction mixture was heated to 65 °C for 2 h to give a brown color solution and the NMR yield was calculated in comparison to the integration of the internal standard (37.2%). ^{1}H NMR (benzene-d_6, 600 MHz, 25 °C): δ 5.31 (s, 10 H, C_5H_5), 0.55 (s, 6 H, $SiMe_2$), -0.04 (d, $^3J_{HH}$ = 5.5 Hz, 6 H, SiH*Me*), -2.23 (m, $^1J_{SiH}$ = 89.1 Hz, 1 H, SiH). ^{13}C{^{1}H} NMR (benzene-d_6, 150 MHz, 25 °C): δ 101.14 (C_5H_5), 3.71 ($SiMe_2$), -0.16 (SiHMe). ^{15}N{^{1}H} NMR (benzene-d_6, 61 MHz, 25 °C): δ -355.6. ^{29}Si{^{1}H} NMR (benzene-d_6, 119.3 MHz, 25 °C): δ -8.7 ($SiMe_2$), -61.5 ($SiHMe_2$).

$Cp_2Zr[\eta^2$-N(SiHMe$_2$)SiMe$_2$](PMe$_3$) (7.10·PMe$_3$). Compound 7.9 (0.022 g, 0.057 mmol) and PMe_3 (6.4 μl, 0.063 mmol) were dissolved in benzene-d_6 (0.6 ml) and added to a NMR tube equipped with a J-Young valve. Cyclooctane as an internal standard (0.5 ml) was also added to the mixture. The reaction mixture was heated to 65 °C for 2.5 h to give a deep red solution and the NMR yield was calculated in comparison to the integration of the internal standard (74.3%). ^{1}H NMR (benzene-d_6, 600 MHz, 25 °C): δ 5.40 (s, 10 H, C_5H_5), 5.18 (br, 1 H, SiH), 0.93 (d, $^2J_{PH}$ = 9 Hz, 9 H, PMe), 0.42 (d, $^3J_{HH}$ = 4.8 Hz, 6 H, SiH*Me*), 0.40 (s, 6 H, $SiMe_2$). ^{13}C{^{1}H} NMR (benzene-d_6, 150 MHz, 25 °C): δ 104.72 (C_5H_5), 20.98 (d, $^1J_{PC}$ = 21.8 Hz, PMe), 3.62 ($SiMe_2$ and SiHMe overlapped). ^{15}N{^{1}H} NMR (benzene-d_6, 61 MHz, 25 °C): δ -331.1. ^{31}P NMR (benzene-d_6, 243 MHz, 25 °C): δ 18.67. ^{29}Si{^{1}H} NMR (benzene-d_6, 119.3 MHz, 25 °C): δ -12.9 ($^1J_{SiH}$ = 177.0 Hz, $SiHMe_2$), -26.9 ($^2J_{PSi}$ = 74.0 Hz, $SiMe_2$).

Reference

1 Mainz, V. V.; Andersen, R. A. *Inorg. Chem.* **1980**, *19*, 2165-2169.

2 (a) Herrmann, W. A.; Eppinger, J.; Spiegler, M.; Runte, O.; Anwander, R. *Organometallics* **1997**, *16*, 1813-1815. (b) Anwander, R.; Runte, O.; Eppinger, J.; Gerstberger, G.; Herdtweck, E.; Spiegler, M. *J. Chem. Soc. Dalton Trans.* **1998**, 847-858. (c) Eppinger, J.; Spiegler, M.; Hieringer, W.; Herrmann, W. A.; Anwander, R. *J. Am. Chem. Soc.* **2000**, *122*, 3080-3096. (d) Klimpel, M. G.; Görlitzer, H. W.; Tafipolsky, M.; Spiegler, M.; Scherer, W.; Anwander, R. *J. Organomet. Chem.* **2002**, *647*, 236-244. (e) Liu, B.; Roisnel, T.; Guégan, J.-P.; Carpentier, J.-F.; Sarazin, Y. *Chem. Eur. J.* **2012**, *18*, 6289-6301.

3 (a) Hartwig, J. F. *J. Am. Chem. Soc.* **1996**, *118*, 7010-7011. (b) Scherer, W.; Wolstenholme, D. J.; Herz, V.; Eickerling, G.; Brück, A.; Benndorf, P.; Roesky, P. W. *Angew. Chem., Int. Ed.* **2010**, *49*, 2242-2246.

4 (a) Herrmann, W. A.; Huber, N. W.; Behn, J. *Chem. Ber.* **1992**, *125*, 1405-1407. (b) Hasan, P.; Potts, S. E.; Carmalt, C. J.; Palgrave, R. G.; Davies, H. O. *Polyhedron* **2008**, *27*, 1041-1046. (c) Yan, K.; Ellern, A.; Sadow, A. D. *J. Am. Chem. Soc.* **2012**, *134*, 9154-9156.

5 Procopio, L. J.; Carroll, P. J.; Berry, D. H. *J. Am. Chem. Soc.* **1994**, *116*, 177-185.

6 Rees Jr., W. S.; Just, O.; Schumann, H.; Weimann, R. *Angew. Chem., Int. Ed.* **1996**, *35*, 419-422.

7 (a) Procopio, L. J.; Carroll, P. J.; Berry, D. H. *J. Am. Chem. Soc.* **1991**, *113*, 1870-1872. (b) Procopio, L. J.; Carroll, P. J.; Berry, D. H. *Polyhedron* **1995**, *14*, 45-55.

8 Buchwald, S. L.; Watson, B. T.; Wannamaker, M. W.; Dewan, J. C. *J. Am. Chem. Soc.* **1989**, *111*, 4486-4494.

9 (a) Bennett, C. R.; Bradley, D. C. *J. Chem. Soc., Chem. Commun.* **1974**, 29-30. (b) Simpson, S. J.; Turner, H. W.; Andersen, R. A. *J. Am. Chem. Soc.* **1979**, *101*, 7728-7729. (c) Simpson, S. J.; Andersen, R. A. *Inorg. Chem.* **1981**, *20*, 3627-3629. (d) Bradley, D. C.; Chudzynska, H.; Backer-Dirks, J. D. J.; Hursthouse, M. B.; Ibrahim, A. A.; Motevalli, M.; Sullivan, A. C. *Polyhedron* **1990**, *9*, 1423-1427. (e) Berno, P.; Minhas, R.; Hao, S.; Gambarotta, S. *Organometallics* **1994**, *13*, 1052-1054. (f) Gerlach, C. P.; Arnold, J. *Organometallics* **1996**, *15*, 5260-5262. (g) Cai, H.; Yu, X.; Chen, T.; Chen, X.-T.; You, X.-Z.; Xue, Z. *Can. J. Chem.* **2003**, *81*, 1398-1405. (h) Niemeyer, M. *Inorg. Chem.* **2006**, *45*, 9085-9095. (i) Bénaud, O.; Berthet, J.-C.; Thuéry, P.; Ephritikhine, M. *Inorg. Chem.* **2010**, *49*, 8117-8130.

10 (a) Nugent, W. A.; Ovenall, D. W.; Holmes, S. J. *Organometallics* **1983**, *2*, 161-162. (b) Herzon, S. B.; Hartwig, J. F. *J. Am. Chem. Soc.* **2007**, *129*, 6690-6691. (c) Herzon S. B.; Hartwig, J. F. *J. Am. Chem. Soc.* **2008**, *130*, 14940-14941.

11 Rubin, M.; Schwier, T.; Gevorgyan, V. *J. Org. Chem.* **2002**, *67*, 1936-1940.

12 (a) Stoutland, P. O.; Bergman, R. G. *J. Am. Chem. Soc.* **1985**, *107*, 4581-4582. (b) Bergman, R. G.; Seidler, P. F.; Wenzel, T. T. *J. Am. Chem. Soc.* **1985**, *107*, 4358-4359. (c) Baker, M. V.; Field, L. D. *J. Am. Chem. Soc.* **1986**, *108*, 7436-7438. (d) Stoutland, P. O.; Bergman, R. G. *J. Am. Chem. Soc.* **1988**, *110*, 5732-5744. (e) Schaller, C. P.; Cummins, C. C.; Wolczanski, P. T. *J. Am. Chem. Soc.* **1996**, *118*, 591-611. (f) Kennedy, A. R.; Klett, J.; Mulvey, R. E.; Wright, D. S. *Science* **2009**, *326*, 706-708. (g) Fendrick, C. M.; Marks, T. J. *J. Am. Chem. Soc.* **1986**, *108*, 425-437.

13 Kissounko, D.; Epshteyn, A.; Fettinger, J. C.; Sita, L. R. *Organometallics* **2005**, *25*, 531-535.

14 (a) Thompson, M. E.; Baxter, S. M.; Bulls, A. R.; Burger, B. J.; Nolan, M. C.; Santarsiero, B. D.; Schaefer, W. P.; Bercaw, J. E. *J. Am. Chem. Soc.* **1987**, *109*, 203-219. (b) Nolan, S. P.; Stern, D.; Marks, T. J. *J. Am. Chem. Soc.* **1989**, *111*, 7844-7853.

15 (a) Woo, H.-G.; Don Tilley, T. *J. Organomet. Chem.* **1990**, *393*, C6-C9. (b) Woo, H.-G.; Heyn, R. H.; Tilley, T. D. *J. Am. Chem. Soc.* **1992**, *114*, 5698-5707.

16 (a) Jimenez, R.; Barral, M. C.; Moreno, V.; Santos, A. *J. Organomet. Chem.* **1979**, *182*, 353-359. (b) Reger, D. L.; Tarquini, M. E.; Lebioda, L. *Organometallics* **1983**, *2*, 1763-1769. (c) Erker, G.; Froemberg, W.; Benn, R.; Mynott, R.; Angermund, K.; Krueger, C. *Organometallics* **1989**, *8*, 911-920. (d) Ferreira, H.; Dias, A. R.; Duarte, M. T.; Ascenso, J. R.; Martins, A. M. *Inorg. Chem.* **2007**, *46*, 750-755.

17 (a) Jenkins, A. D.; Lappert, M. F.; Srivastava, R. C. *J. Organomet. Chem.* **1970**, *23*, 165-172. (b) Black, D. G.; Swenson, D. C.; Jordan, R. F.; Rogers, R. D. *Organometallics* **1995**, *14*, 3539-3550.

18 (a) Hou, Z.; Breen, T. L.; Stephan, D. W. *Organometallics* **1993**, *12*, 3158-3167. (b) Bernskoetter, W. H.; Pool, J. A.; Lobkovsky, E.; Chirik, P. J. *J. Am. Chem. Soc.* **2005**, *127*, 7901-7911. (c) Munhá, R. F.; Veiros, L. F.; Duarte, M. T.; Fryzuk, M. D.; Martins, A. M. *Dalton Trans.* **2009**, 7494-7508.

19 Hoyt, H. M.; Bergman, R. G. *Angew. Chem., Int. Ed.* **2007**, *46*, 5580-5582.

20 (a) Roering, A. J.; Maddox, A. F.; Elrod, L. T.; Chan, S. M.; Ghebreab, M. B.; Donovan, K. L.; Davidson, J. J.; Hughes, R. P.; Shalumova, T.; MacMillan, S. N.; Tanski, J. M.; Waterman, R. *Organometallics* **2009**, *28*, 573-581. (b) Munhá, R. F.; Antunes, M. A.;

Alves, L. G.; Veiros, L. F.; Fryzuk, M. D.; Martins, A. M. *Organometallics* **2010**, *29*, 3753-3764. (c) Roering, A. J.; Leshinski, S. E.; Chan, S. M.; Shalumova, T.; MacMillan, S. N.; Tanski, J. M.; Waterman, R. *Organometallics* **2010**, *29*, 2557-2565.

21 Horácek, M.; Stepnicka, P.; Kubista, J.; Gyepes, R.; Mach, K. *Organometallics* **2004**, 23, 3388-3397.

22 McDade, C.; Bercaw, J. E. *J. Organomet. Chem.* **1985**, *279*, 281-315.

23 Walsh, P. J.; Hollander, F. J.; Bergman, R. G. *J. Am. Chem. Soc.* **1988**, *110*, 8729-8731.

24 Buchwald, S. L.; LaMaire, S. J.; Nielsen, R. B.; Watson, B. T.; King, S. M. *Org. Synth. Coll. Vol. 7*, **1998**, *9*, 162-165.

25 Hyla-Kryspin, I.; Gleiter, R.; Kruger, C.; Zwettler, C. R.; Erker, G. *Organometallics* **1990**, *9*, 517-523.

26 Li, B.-L.; Engenito, Jr., J. S.; Neilson, R. H.; Wisian-Neilson, P. *Inorg. Chem.* **1983**, *22*, 575-579.

27 Willey, G. R.; Woodman, T. J.; Drew, M. G. B. *Polyhedron* **1997**, *16*, 3385-3393.

28 Broomhall-Dillard, R. N. R.; Gordon, R. G.; Wagner, V. A. *Mater. Res. Soc. Symp. Proc.* **2000**, *606*, 139-145.

29 (a) Massey, A. G.; Park, A. J. *J. Organomet. Chem.* **1964**, *2*, 245. (b) Chien, J. C. W.; Tsai, W.-M.; Rausch, M. D. *J. Am. Chem. Soc.* **1991**, *113*, 8570.

30 Erker, G.; Kropp, K.; Atwood, J. L.; Hunter, W. E. *Organometallic* **1983**, *2*, 1555-1561.

31 Chirik, P. J.; Day, M. W.; Labinger, J. A.; Bercaw, J. E. *J. Am. Chem. Soc.* **1999**, *121*, 10308-10317.

Chapter 8: Nucleophilicity of β-SiH containing zirconacycle

KaKing Yan, Arkady Ellern, Aaron D. Sadow

Department of Chemistry and US Department of Energy Ames Laboratory, Iowa State University, Ames IA, 50011, USA

Abstract. The β-SiH groups in azasilazirconacycle $Cp_2Zr[\kappa^2\text{-}N(SiHMe_2)SiHMeCH_2]$ **8.1** provide access to new pathways for sixteen-electron zirconium alkyl compounds. First, the pendent β-SiH in **8.1** reacts with paraformaldehyde through an uncatalyzed hydrosilylation to form an exocyclic methoxysilyl moiety, while the zirconium-carbon bond in **8.1** is surprisingly inert toward formaldehyde. Still, the Zr-C moiety in **8.1** is available for chemistry, and it interacts with the carbon monoxide and strong electrophile $B(C_6F_5)_3$ to provide 1,1-CO insertion product $Cp_2Zr[\kappa^2\text{-}OC(=CH_2)SiMeHN(SiHMe_2)]$ **8.3** and zwitterionic nonclassical $Cp_2Zr[N(SiHMe_2)SiHMeCH_2B(C_6F_5)_3]$ **8.4**. Addition of DMAP to **8.4** results in coordination to a Si center and hydrogen migration to zirconium to give a mixture of the zwitterionic isomers $Cp_2ZrH[N\{SiHMeCH_2B(C_6F_5)_3\}(SiMe_2DMAP)]$ **8.7a** and $Cp_2ZrH[N\{SiMe(DMAP)CH_2B(C_6F_5)_3\}(SiHMe2)]$ **8.7b** in a 1.65:1 ratio. However, addition of $OPEt_3$ results in $OPEt_3$ coordination to give a classical zwitterionic Zr product $Cp_2Zr(OPEt_3)$ $[N(SiHMe_2)SiHMeCH_2B(C_6F_5)_3]$ **8.8**.

Introduction

β-Hydrogen elimination in metal alkyl systems often results in catalyst decomposition in catalytic transformations. As a rule of thumb, catalyst designs often avoid incoporation of β-hydrogen containing ligands. However, important aspects of transition metal-ligand

bonding and reactivity may be overlooked in the absence of studies of β-hydrogen-containing complexes. In sharp contrary to early transition metal alkyl chemistry, β-H elimination in metal amide sysyems are rare. Instead, β-hydrogen-free early transition metal and f-element [M]-N($SiMe_3$)$_2$ compounds often undergo γ-H abstraction that form azametallasilacyclobutanes.[1] These metallacycles are highly active in reactions at with unsaturated organic small molecules (e.g., nitriles, isonitriles, and CO) with the M-C moiety.[1e,2] A related zirconacyclobutane $Cp_2Zr[CH_2SiMe_2CH_2]$ and formaldehyde react to give a monoinsertion product.[3] Enhanced reactivity in some cases may be ascribed to strained four-membered rings or carbene character associated with retrocycloadditions. Recently, we have reported that the selectivity between alkyl group and β-H abstraction in a zirconocene alkyl silazide compound is highly dependent to the steric hindrance of the Zr alkyl. Meanwhile, azazirconacycle $Cp_2Zr[\kappa^2$-$N(SiHMe_2)SiHMeCH_2]$ (**8.1**) contains β-SiH group and a strained cyclometallated alkyl group reminiscent of the structral motif in $Cp_2ZrN(SiHMe_2)_2(R)$; however, spectroscopic data suggests that both β-SiH groups are best described as classical Si-H (two-center-two-electron bond). Interestingly, **8.1** promotes unusual C-H bond activation of ethylene instead of undergoing insertion.

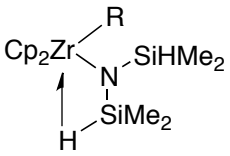

Zr silazide with unstrained alkyl group

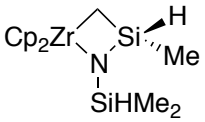

8.1

Zr silazide with strained cyclometallated alkyl group

In light of this reseult, we herein describe the inherent dissimilar spectroscopic property in **8.1** promotes vastly different reactivity to small molecules in comparison to

$Cp_2ZrN(SiHMe_2)_2(R)$. For example, the Zr-C bond of **8.1** engages reactions with CO and $B(C_6F_6)_3$, while the pendent, anagostic β-SiH of the exocyclic $SiHMe_2$ group reacts by an unusual addition reaction of formaldehyde. Such diverse reactivity in **8.1** highlights the rich chemistry in small molecule activation by zirconacycle **8.1** that contains β-hydrogen moiety.

Results and Discussion

Metallocyle $Cp_2Zr[\kappa^2\text{-}N(SiHMe_2)SiHMeCH_2]$ (**8.1**) and paraformaldehyde $(H_2CO)_n$ react in benzene at 80 °C over 9 h to give $Cp_2Zr[\kappa^2\text{-}N(SiMe_2OMe)SiHMeCH_2]$ (**8.2**) in 95% yield (eq 8.1). In this transformation, the methoxy group is formed by a hydrosilylation of formaldehyde.

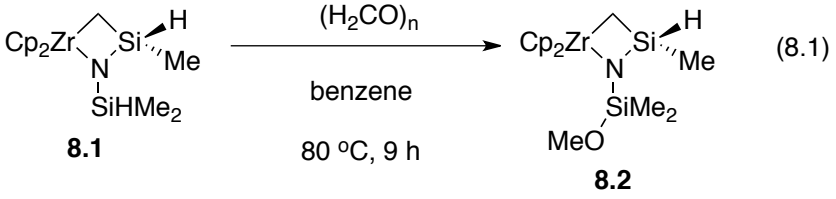

(8.1)

A new singlet resonance at 3.29 ppm in the ^1H NMR spectrum of **8.2** was assigned to the methoxy group, and only one SiH signal was detected at 4.50 ppm. That signal was assigned by ^1H-^{29}Si HMQC and COSY experiments; the latter showed scalar coupling to the $ZrCH_2$. As in **8.1**, the $(C_5H_5)_2Zr$, CH_2, and $SiMe_2$ groups are diastereotopic. Two SiMe resonances (3 H each) assigned to the Si*Me*$_2$OMe group appeared as singlets rather than the doublets observed for **8.1**. The reaction product and approximate rate of conversion are not affected when the reaction is performed in acetonitrile or in the presence of donor ligands such as PMe_3, $OPEt_3$ or *para*-dimethylaminopyridine (DMAP). Meanwhile, only starting materials are observed upon treatment of **8.1** with benzophenone, acetophenone, or

cyclohexanecarbaldehyde. Reaction with acetone provides multiple unidentified products. Benzaldehyde gives a mixture of at least three products, one of which is tentatively assigned as the Zr-C insertion product. Upon thermolysis of **8.1** with excess benzaldehyde at 60 °C, a small amount of toluene is generated (2.2%) among unidentified zirconium-containing products. Compound **8.2** is inert toward further formaldehyde insertions under the conditions of eq 8.1. For comparison, reaction of the $Cp_2ZrN(SiHMe_2)_2(Me)$ and formaldehyde provides unreacted $Cp_2ZrN(SiHMe_2)_2(Me)$ as the major product and a complex mixture of products after 9 h at 85 °C in benzene-d_6, while $Cp_2ZrN(SiHMe_2)_2(H)$ affords the zirconium methoxide $Cp_2Zr[N(SiHMe_2)_2]OMe$ in which the SiH moieties are unreacted. Notably, reaction of $Cp_2ZrN(SiHMe_2)_2(H)$ and excess OCH_2 under this condition does not provide further conversion of the $N(SiHMe_2)_2$ group. Similarly, zirconium hydride silazide containing one β-SiH group $Cp_2Zr(N(SiHMe_2)$*t*-Bu)H also undergoes insertion with paraformaldehyde exlcusively into Zr-H bond to give $Cp_2Zr(N(SiHMe_2)$*t*-Bu)OMe. Interestingly, reaction of azazirconacyclobutane containing one inner-ring SiH $Cp_2Zr[k^2$-*N*,*C*-N(*t*-Bu)$SiHMeCH_2]$ with paraformaldehyde in benzene-d_6 at 120 °C for 12 h only provides unreacted $Cp_2Zr[k^2$-*N*,*C*-N(*t*-Bu)$SiHMeCH_2]$. However, β-SiH containing azazironacyclopentane $Cp_2Zr[\kappa^2$-$N(SiHMe_2)SiMe_2CH_2CH_2]$ undergoes slow insertion with paraformaldehyde to give $Cp_2Zr[\kappa^2$-$N(SiOMeMe_2)SiMe_2CH_2CH_2]$ (**8.2**; eq 8.2) under harsh condition (120 °C, 6 h), which suggests that pendent SiH group is essential for formaldehyde insertion.

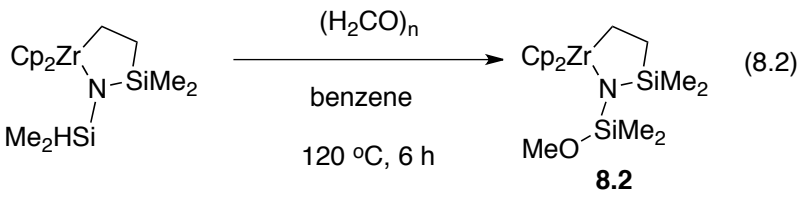

(8.2)

8.2

The interaction of formaldehyde and the exocyclic SiH, rather than the Zr-C bond, was unexpected because (a) the reactive site in polar organometallic compounds is typically the M-C bond, (b) zirconium is particularly oxophilic and electronically unsaturated, and (c) a related silazirconacyclobutane reacts via insertion.[3] While hydrosilylation mechanisms involving metal-centered oxidation can be ruled out, zirconocene-type olefin hydrosilylations involve reduced metal centers.[4] Likewise, Ti-catalyzed carbonyl hydrosilylation involves low-valent titanium, and these mechanisms are unlikely in the current system. Carbonyl hydrosilylation catalyzed by the strong Lewis acid, $B(C_6F_5)_3$, is proposed to involve SiH-abstraction by $B(C_6F_5)_3$ to give a silyl cation that interacts with the carbonyl oxygen.[5] The $B(C_6F_5)_3$-carbonyl interaction is observed but it is not implicated in those Si-O bond formations. In compound **8.1**, the anagostic SiH structures are reinforced by the rigid four-membered ring, and unimolecular hydrogen transfer from silicon to zirconium (based on the $B(C_6F_5)_3$ mechanism) appears unlikely.

We therefore explored other possible mechanisms for the observed hydrosilylation. First, coordination of a Lewis base to a silicon center can enhance hydridic character of the SiH, and this has been used in carbonyl hydrosilylation.[6] Additionally, we have recently suggested that β-hydrogen transfer from a five-coordinate silicon center to a magnesium center is involved in a catalytic Si-N bond formation.[7] Alternatively, a molybdenum compound has been proposed to activate carbonyl substrates toward intermolecular hydrosilylation based partly on BF_3-catalyzed hydrosilylations.[8,9] Meerwein-Pondorff-Verley

(MPV) carbonyl reduction involves b-hydrogen abstraction from metal alkoxides, and recently a Mo catalyst for hydrosilylation has been implicated in MPV type β-hydrogen abstraction.[10] Based on these suggestions and our observations that rule out typical zirconium-catalyzed hydrosilylations, we considered three pathways (Scheme 8.1).

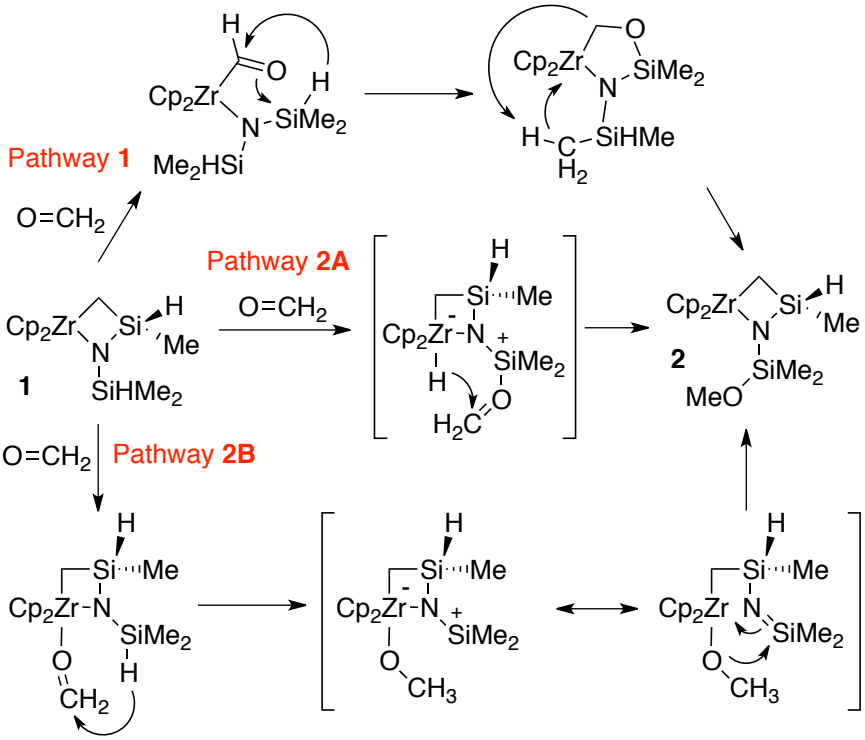

Scheme 8.1. Possible pathways for conversion of **8.1** to **8.2**.

Pathway **8.1** consists of C-H bond activation of formaldehyde to form a formyl species, and hydrosilylation of formayl carbonyl, followed by γ-abstraction. Pathway **2A** involves SiH transfer to Zr upon interaction of the carbonyl and the silicon center (e.g., a Lewis-based induced β-elimination). Alternatively, a MPV-type hydrogen transfer to a Zr-coordinated carbonyl is suggested in Pathway **2B**. Thus, the reactivity of **8.1** was further explored to test for chemistry involving the zirconacycle versus the exocyclic $SiHMe_2$ moiety.

The reaction of $Cp_2ZrN(SiHMe_2)_2(H)$ with 1 atm of CO rapidly turns bright yellow in benzene-d_6. The ^1H NMR spectrum of this solution contained a singlet at 4.6 ppm that is consistent to a formyl CH resonance.[11] In the ^1H-^{13}C HMQC experiments, the 4.6 ppm 1H resonance was correlated with a ^{13}C NMR signal at 103.3 ppm assigned to formyl *C*=O. However, the formyl compound is not stable upon exposure to excess CO. Thermolysis of the resulting formyl compound $Cp_2ZrN(SiHMe_2)_2(CHO)$ (**8.3**) at 88 °C led to formation of $Cp_2ZrN(SiHMe_2)_2(OMe)$ in 46.1% based on **8.3**, and **8.2** was not observed as one of the product. Besides, deuterium labeling experiments using paraformaldehyde-d_3 resulted in deuterium incorporation solely into the methoxy group. Thus, Pathway **1A** can be ruled out.

Next, the accessibility of the zirconium center toward ligands was probed. Reaction of **8.1** and CO at 85 °C for 3 h gives an insertion product containing a five-membered ring, a Zr-O bond, and an exocyclic methylene group (**8.4**; eq 8.3). Related reactions of CO and azametallasilacyclobutanes (for group 4, Th and U centers)[12] were previously suggested to involve 1,1-insertion of CO to give an acyl that rearranges to the product through 1,2-silyl migration of an oxycarbene intermediate.[1e,i,2]

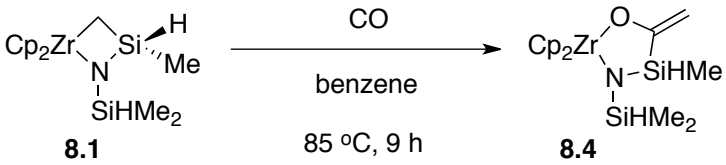

8.1 **8.4** (8.3)

^1H NMR resonances at 4.91 and 4.48 ppm were assigned to the exocyclic methylene, and these gave crosspeaks in one-bond and multiple-bond ^1H-^{13}C heteronuclear correlation spectra to signals at 173.4 and 98.4 assigned to terminal and disubstituted vinylic carbon centers. This transformation shows that small molecules can access the zirconium center in **8.1**.

Because the (presumably nucleophilic) zirconium alkyl group in **8.1** does not give a detectable interaction with H_2CO, while CO insertion takes place into Z-C bond, the nucleophilicity of **8.1** was investigated. The strong Lewis acid tris(perfluorophenyl)borane is known to interact with organosilanes to give $[R_3Si\text{-}H\text{-}B(C_6F_5)_3]$-type species, while organometallic alkyl and hydride compounds L_nMR react to form $[L_nM\text{-}R\text{-}B(C_6F_5)_3]$. Furthermore, β-SiH-containing organometallic compounds such as $M[C(SiHMe_2)_3]_2(THF)_2$ (M = Ca, Yb) react with $B(C_6F_5)_3$ by hydrogen abstraction.[13] Although there are multiple sites in **8.1** that could react with $B(C_6F_5)_3$, selective alkyl abstraction is observed (which contrasts the reaction with formaldehyde). Thus, **8.1** and $B(C_6F_5)_3$ react to give the zwitterionic $Cp_2Zr[N(SiHMe_2)SiHMeCH_2B(C_6F_5)_3]$ (**8.5**; eq 8.4).

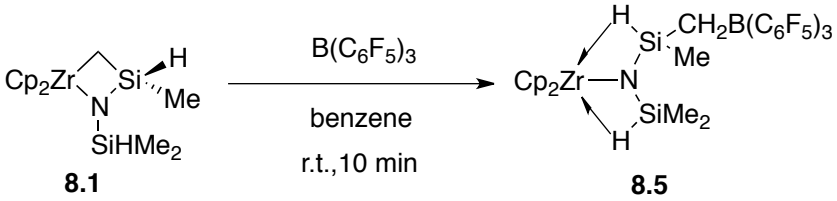

8.1 **8.5** (8.4)

The ^{11}B NMR spectrum contained a singlet at -14.4 ppm rather than a doublet associated with a hydridoborate. In the ^1H NMR spectrum, two SiH resonances were detected far upfield at 0.02 ($^1J_{SiH}$ = 81 Hz) and -0.54 ppm ($^1J_{SiH}$ = 83 Hz) consistent with a rare diagostic-type structure. Such agostic interaction was also compromised by a low energy SiH band ν_{SiH} at 1737 cm^{-1} in IR spectrum.[14] Diagostic d^0 amido compounds were previously reported in their neutral form.[15] **8.5** represents a rare zwitterionic diagostic complex reported. Unfortunately, multiple attempts to obtain X-ray quality crystals gave oily material. However, **8.5** reacts with two equiv. of acetone in methylene chloride to give Si-H insertion product $Cp_2Zr[N(SiO^iPrMe_2)SiO^iPrMeCH_2B(C_6F_5)_3]$ (**8.6**; eq 8.5) in quantitative yield.

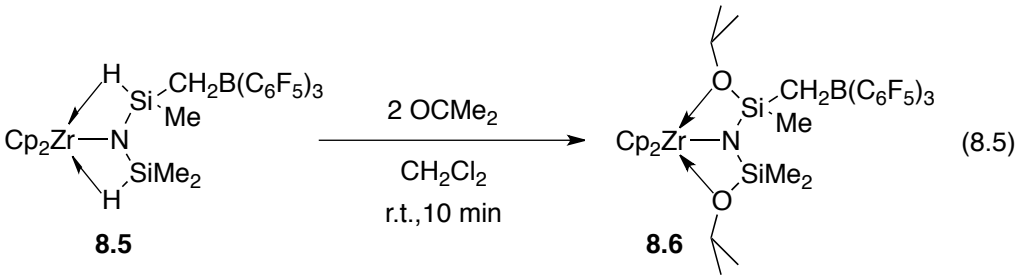

(8.5)

The ^{1}H NMR spectrum consisted of four sets of doublets at 1.53, 1.52, 1.49, and 1.29 ppm for the diastereotopic methyl resonances for two isopropyl groups. Besides, three sets of singlet (0.31, 0.13, -0.21 ppm) were also observed for the SiMe groups. ^{1}H-^{1}H COSY and ^{29}Si INEPT experiments supported the insertion of carbonyl into both β-agostic SiHs to give two SiOiPr groups. X-ray quality crystals of **8.6** were grown from methylene chloride solution at room temperature that unambiguously shows the methyleneborate moiety (see supplementary information).

Unlike **8.1**, addition of DMAP to **8.5** results in DMAP-initiated β-SiH group migration from β-Si to Zr to give a mixture of isomers and $Cp_2ZrN\{SiHMeCH_2B(C_6F_5)_3\}(SiMe_2DMAP)(H)$ (**8.7a**, 62.3%) and $Cp_2ZrN\{SiMe(DMAP)CH_2B(C_6F_5)_3\}(SiHMe2)(H)$ (**8.7b**, 37.7%; Scheme 8.2). A ^{1}H NMR spectrum acquired at room temperature in methylene chloride-d_2 was slightly broad, but the complete disappearance of **8.5** and the formation of two new species can be identified.

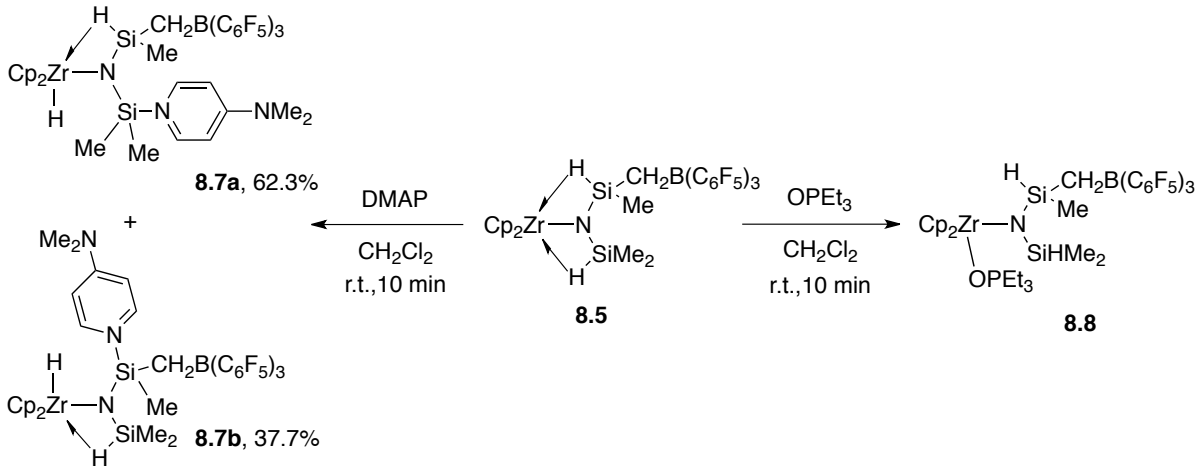

Scheme 8.2. Divergent reactivity of **8.5** with DMAP and $OPEt_3$.

The low temperature NMR spectra of **8.7** were sharper and better resolved. At 220 K, four ^{29}Si resonances were observed at 11.4, -4.6, -61.1 and -63.9 ppm. Only the signals at -61.1 ppm ($^{1}J_{SiH}$ = 115 Hz) and -63.9 ppm ($^{1}J_{SiH}$ = 112 Hz) was observed in a ^{29}Si INEPT experiment optimized for J_{SiH} = 120 Hz, and the signals at 11.4 ppm and -4.6 ppm were only detected in a ^{29}Si INEPT experiment optimized for long range proton coupling (J_{SiH} = 7 Hz). In a ^{1}H-^{29}Si HMBC experiment optimized for long range ^{1}H-^{29}Si coupling (J_{SiH} = 7 Hz), the -63.9 ppm ^{29}Si resonance was correlated with a ^{1}H NMR signal at -0.25 ppm assigned to a SiH*Me* and the -61.1 ppm ^{29}Si resonance was correlated with a ^{1}H NMR signal at 0.39 ppm and 0.27 ppm, which are assigned to a SiH*Me*$_2$. In that experiment, crosspeaks from the ^{29}Si signal of the major product at -4.6 ppm were correlated to $SiMe_2$ resonances (0.53 ppm and 0.48 ppm), the signal at 3.93 ppm (1 H) assigned to the ZrH, and the aromatic resonances assigned to DMAP (7.87 ppm) in the ^{1}H NMR spectrum. Similarly, crosspeaks from the ^{29}Si signal of the minor product at 11.4 ppm were correlated to a second SiMe resonance (0.39 ppm), the signal at 3.99 ppm (1 H) assigned to the ZrH, and the aromatic resonances assigned to DMAP (7.48 ppm). The correlations between the silicon atom and the aromatic signals

provide convincing evidence that DMAP is coordinated to silicon rather than zirconium. We assign the ^{1}H NMR signal at 3.93 ppm and 3.99 ppm to zirconium hydride groups based on a correlation in a COSY experiment between that signal and the resonance at 0.95 ppm assigned to a β-Si-H→Zr. A board band at 1845 cm^{-1} was observed in the crude mixture of **8.7a** and **8.7b** that suggests the nonclassical nature of β-SiH groups in **8.7**. The formation of two isomers is due to the addition of DMAP to two different β-Si groups ($SiHMe_2$ vs SiHMe) and the DMAP coordination to the sterically less hindered Si position is favored (**8.7a**, 62%).

In contrast, reaction of **8.5** with $OPEt_3$ affords $Cp_2Zr(OPEt_3)[N(SiHMe_2)SiHMeCH_2B(C_6F_5)_3]$ (**8.8**, Scheme 8.2). The structure of **8.8** is readily distinguished from the DMAP adduct **8.7** by NMR and IR spectroscopy. In the ^{1}H NMR spectrum of **8.8**, two doublet resonances assigned to $SiHMe_2$ and SiHM groups were observed at 0.27 ppm ($^{3}J_{HH}$ = 3.0 Hz) and -0.45 ppm ($^{3}J_{HH}$ = 2.3 Hz). Furthermore, two signals at 4.09 ppm ($^{1}J_{SiH}$ 169 Hz; 1 H) and 3.82 ppm (1JSiH 177 Hz) were assigned as a Si*H*Me_2 and Si*H*Me groups, respectively, based on their correlation to the $SiMe_2$ and SiMe signals in a COSY experiment. The $^{1}J_{SiH}$ value suggests that **8.8** contains terminal silicon hydride groups. The observation of NMR signals assigned to $SiHMe_2$ and SiHMe groups provide evidence that $OPEt_3$ is coordinated to Zr center instead of either β-Si positions. Similar reactivity was previously observed in the reactions of cationic zirconium β-SiH containing silazide $[Cp_2ZrN(SiHMe_2)_2]^{+}$ with DMAP and $OPEt_3$.

Conclusion

The small molecule activation by zirconacycle **8.1** takes place in both Zr-C and β-SiH groups. The reaction of formaldehyde exclusively involves the exocyclic $SiHMe_2$ group. Because the zirconium center in **8.1** is accessible to CO, we favor a mechanism for formaldehyde hydrosilylation that involves a [Zr]-O=CH_2 interaction followed by a β-SiH abstraction (Pathway **2B** in Scheme 1). Still, we are not able to rule out nucleophilic attack at the β-$SiHMe_2$ group (Pathway **2A** in Scheme 1), and we are currently investigating related systems to trap the kinetic products of nucleophiles and β-hydrogen-containing organometallics. Nevertheless, this work shows that introduction of β-SiH groups in a metallocyclobutane significantly alters the outcome of small molecule chemistry.

Experimental.

General. All manipulations were performed under a dry argon atmosphere using standard Schlenk techniques or under a nitrogen atmosphere in a glovebox unless otherwise indicated. Water and oxygen were removed from benzene, toluene, pentane, diethyl ether, and tetrahydrofuran solvents using an IT PureSolv system. Benzene-d_6 and tetrahydrofuran-d_8 were heated to reflux over Na/K alloy and vacuum-transferred. PMe_3, triethylphosphine oxide, DMAP, benzophenone, paraformaldehyde and paraformaldehyde-d_3 were purchased from Aldrich and were used as received. Acetone, acetophenone, and cyclohexanecarbaldehyde were degassed and stored over 4 Å molecular sieves before use. The compounds $Cp_2ZrN(SiHMe_2)_2(H)$,[19] $Cp_2ZrN(SiHMe_2)_2(Me)$,[20] $B(C_6F_5)_3$,[7] $Cp_2Zr[\kappa^2$-$N(SiHMe_2)SiHMeCH_2]$ (**8.1**)[20] were prepared following literature procedures.

^{1}H, $^{13}C\{^{1}H\}$, ^{11}B and $^{29}Si\{^{1}H\}$ NMR spectra were collected on an Agilent MR400 spectrometer. ^{11}B NMR spectra were referenced to an external sample of $BF_3{\cdot}Et_2O$. ^{15}N chemical shifts were determined either by ^{1}H-^{15}N HMBC experiments on a Bruker Avance II 700 spectrometer with a Bruker Z-gradient inverse TXI $^{1}H/^{13}C/^{15}N$ 5mm cryoprobe or by ^{1}H-^{15}N CIGARAD experiments on an Agilent MR400 spectrometer; ^{15}N chemical shifts were originally referenced to liquid NH_3 and recalculated to the CH_3NO_2 chemical shift scale by adding -381.9 ppm. Assignments of resonances are supported by ^{1}H-^{1}H and heteronuclear correlation NMR experiments. Infrared spectra were measured on a Bruker IFS66v FTIR. Elemental analyses were performed using a Perkin-Elmer 2400 Series II CHN/S. X-ray diffraction data was collected on a Bruker APEX II diffractometer.

$Cp_2Zr[\kappa^2$-N(SiMe$_2$OMe)SiHMeCH$_2$] (8.1). $Cp_2Zr[\kappa^2$-N(SiHMe$_2$)SiHMeCH$_2$] (0.115 g, 0.326 mmol) and formaldehyde (0.010 g, 0.33 mmol) were suspended in benzene and heated to 80 °C for 5.5 h. The reaction mixture was filtered, and the volatile components of the soluble portion were evaporated under reduced pressure to give a yellow oil. Extraction with pentane and evaporation of the pentane provided **8.1** as viscous yellow oil (0.119 g, 0.31 mmol, 95.4%). ^{1}H NMR (benzene-d_6, 600 MHz, 25 °C): δ 5.91 (s, 5 H, C_5H_5), 5.87 (s, 5 H, C_5H_5), 4.50 (m, $^{1}J_{SiH}$ = 202 Hz, 1 H, NSi*H*Me), 3.29 (s, 3 H, SiMe$_2$O*Me*), 1.90 (dd, $^{2}J_{HH}$ = 12.4 Hz, $^{3}J_{HH}$ = 4.0 Hz, 1 H, CH_2), 1.55 (dd, $^{2}J_{HH}$ = 12.4 Hz, $^{3}J_{HH}$ = 2.2 Hz, 1 H, CH_2), 0.32 (d, $^{3}J_{HH}$ = 2.4 Hz, 3 H, CH$_2$SiH*Me*), 0.12 (s, 3 H, Si*Me*$_2$OMe), 0.10 (s, 3 H, Si*Me*$_2$OMe). $^{13}C\{^{1}H\}$ NMR (benzene-d_6, 150 MHz, 25 °C): δ 112.32 (C_5H_5), 112.29 (C_5H_5), 50.02 (SiMe$_2$O*Me*), 35.56 (ZrCH$_2$), 2.14 (CH$_2$SiH*Me*), 1.26 (Si*Me*$_2$OMe), 0.80 (Si*Me*$_2$OMe). $^{15}N\{^{1}H\}$ NMR (benzene-d_6, 61 MHz, 25 °C): δ -246.8. $^{29}Si\{^{1}H\}$ NMR (benzene-d_6, 119.3

MHz, 25 °C): δ -6.4 ($SiMe_2OMe$), -65.9 (SiHMe). IR (KBr, cm^{-1}): 2952 m, 2827 w, 2072 m br (SiH), 1597 w, 1443 w, 1249 s, 1087 s, 1016 s, 900 s, 796 s br, 720 s. Anal. Calcd for $C_{15}H_{25}Si_2NOZr$: C, 47.07; H, 6.58; N, 3.66. Found: C, 47.37; H, 6.59; N, 3.44.

$Cp_2ZrN(SiHMe_2)_2(CHO)$ (8.3). Excess Carbon monoxide (3 atm) was charged into a NMR tube with a J-Young valve containing $Cp_2ZrN(SiHMe_2)_2(H)$ (0.0XX, mmol) in benzene-d_6 (0.6 ml) at 77 K. The solution was slowly thawed and stayed at room temperature for 5 min. The excess CO was purged away with argon. The bright yellow solution was transferred to a vial and all the volatiles were evaporated under reduced pressure to give **8.3** as a yellow gummy solid.

^{1}H NMR (benzene-d_6, 600 MHz, 25 °C): δ 6.10 (s, 10 H, C_5H_5), 4.55 (br, 3 H, SiH and CHO overlapped, assigned by 1H-13C HMQC experiment), 0.32 (br, 6 H, $SiMe_2$). $^{13}C\{^1H\}$ NMR (benzene-d_6, 150 MHz, 25 °C): δ 112.66 (C_5H_5), 103.27 (OCH), 2.79 ($SiMe_2$). $^{29}Si\{^1H\}$ NMR (benzene-d_6, 119.3 MHz, 25 °C): δ -23.6 ($^1J_{SiH}$ = 201.1 Hz).

$Cp_2Zr[\kappa^2$-$OC(=CH_2)SiMeHN(SiHMe_2)]$ (8.4). $Cp_2Zr[\kappa^2$-$N(SiHMe_2)SiHMeCH_2]$ (0.116 g, 0.329 mmol) was dissolved in benzene (15 mL), and the solution was degassed with freeze-pump-thaw cycles (3×). The vessel was charged with CO (1 atm), and the reaction mixture was heated to 85 °C for 9 h. Evaporation of the volatile components, extraction of the resulting yellow residue with pentane, and evaporation of the pentane provided **4** as yellow microcrystalline solid (0.045 g, 0.12 mmol, 36%). ^{1}H NMR (benzene-d_6, 400 MHz, 25 °C): δ 6.09 (s, 5 H, C_5H_5), 6.06 (s, 5 H, C_5H_5), 5.43 (m, $^1J_{SiH}$ = 207 Hz, 1 H, NSi*H*Me), 4.91 (s br, 1 H, CH_2), 4.48 (s br, 1 H, CH_2), 4.27 (m, $^1J_{SiH}$ = 190 Hz, 1 H, NSi*H*Me_2), 0.41 (d, $^3J_{HH}$ = 3.2 Hz, 3 H, OCNSiH*Me*) 0.24 (d, $^3J_{HH}$ = 3.1 Hz, 3 H, ZrNSiH*Me*$_2$), 0.18 (d, $^3J_{HH}$ = 3.2 Hz, 3 H,

ZrNSiH*Me*$_2$). ^{13}C{^{1}H} NMR (benzene-d_6, 125 MHz, 25 °C): δ 173.42 (O*C*CH$_2$), 115.31 (C_5H_5), 115.27 (C_5H_5), 98.41 (OC*C*H$_2$), 3.35 (OCSiH*Me*), 2.27 (SiMe$_2$), 0.73 (SiMe$_2$). ^{29}Si{^{1}H} NMR (benzene-d_6, 119.3 MHz, 25 °C): δ -10.5 (SiHMe), -24.6 (SiHMe$_2$). IR (KBr, cm^{-1}): 3083 w, 2953 s, 2075 s br (SiH), 1609 m, 1576 s (C=C), 1442 s, 1361 m, 1249 s, 1176 s, 1015 s, 916 s br, 796 s br. Anal. Calcd for $C_{15}H_{23}Si_2NOZr$: C, 47.32; H, 6.09; N, 3.68. Found: C, 47.73; H, 5.85; N, 3.28. mp 120 °C (decomp).

Cp$_2$Zr[N(SiHMe$_2$)SiHMeCH$_2$B(C$_6$F$_5$)$_3$] (8.5). Cp$_2$Zr[κ^2-N(SiHMe$_2$)SiHMeCH$_2$] (0.082 g, 0.232 mmol) and B(C_6F_5)$_3$ (0.125 g, 0.244 mmol) were allowed to react in benzene (5 mL) in a vial. A light yellow oily layer precipitated from the benzene solution. The top benzene layer was removed with a pipet. The remaining oil was washed with benzene (2 × 5 mL) and pentane (2 × 5 mL). The resulting material was then dried under vacuum to give **8.5** as a pale green solid (0.159 g, 0.184 mmol, 79.2%). ^{1}H NMR (bromobenzene-d_5, 600 MHz, 25 °C): δ 5.54 (s, 5 H, C_5H_5), 5.46 (s, 5 H, C_5H_5), 1.64 (br d, $^2J_{HH}$ = 15 Hz, 1 H, CH$_2$), 0.61 (br d, $^2J_{HH}$ = 13.0 Hz, 1 H, CH$_2$), 0.02 (br overlapping signal, $^1J_{SiH}$ = 81 Hz, 4 H, ZrNSiH*Me*$_2$ and Si*H*MeCH$_2$B(C_6F_5)$_3$), -0.04 (br s, 3 H, ZrNSiH*Me*$_2$), -0.07 (br s, 3 H, SiH*Me*CH$_2$B(C_6F_5)$_3$), -0.54 (br s, $^1J_{SiH}$ = 83 Hz, 1 H, Si*H*Me$_2$). ^{13}C{^{1}H} NMR (bromobenzene-d_5, 150 MHz, 25 °C): δ 148.23 (C_6F_5), 146.65 (C_6F_5), 138.08 (C_6F_5), 136.49 (C_6F_5), 134.90 (C_6F_5), 108.17 (C_5H_5), 107.74 (C_5H_5), 8.87 (ZrCH$_2$), -2.05 (SiMe$_2$), -2.80 (CH$_2$Si*Me*$_2$), -2.88 (SiMe$_2$). ^{11}B NMR (bromobenzene-d_5, 119.3 MHz, 25 °C): -14.4. ^{19}F NMR (bromobenzene-d_5, 564 MHz, 25 °C): δ -131.9 (d, $^3J_{FF}$ = 21.3 Hz, 6 F, *o*-F), -162.2 (t, $^3J_{FF}$ = 21.5 Hz, 3 F, *p*-F), -165.7 (t, $^3J_{FF}$ = 19.9 Hz, 6 F, *m*-F). ^{29}Si{^{1}H} NMR (bromobenzene-d_5, 119.3 MHz, 25 °C): δ -36.2 (SiMe), -47.3 (SiMe$_2$). IR (KBr, cm^{-1}): 3125 w, 2963 w, 2905 w, 1737 m (SiH), 1641 s, 1579 m br,

1512 s, 1456 vs br, 1257 s, 1169 s, 1101 s, 1081 s, 1017 s, 972 s, 925 s, 860 s, 811 s, 778 s, 750 m. Anal. Calcd for $BC_{32}F_{15}H_{23}Si_2NZr$: C, 44.45; H, 2.68; N, 1.62. Found: C, 44.01; H, 2.51; N, 1.51. mp 113-120 °C.

$Cp_2Zr[N(SiMe_2O^iPr)(SiMeO^iPrCH_2B(C_6F_5)$ (8.6). Acetone (32.5 μl, 0.444 mmol) was added to a methylene chloride (10 ml) solution of **8.5** (0.128 g, 0.148 mmol) and the mixture was stirred for 20 min. Volatiles were removed under reduced pressure. The residue was washed with pentane (2 x 2 ml). The volatiles were evaporated under reduced pressure to give **8.6** as a yellow solid. (0.141 g, 0.144 mmol, 97.4%) ^{1}H NMR (methylene chloride-d_2, 600 MHz, 25 °C): δ 6.47 (s, 5 H, C_5H_5), 6.32 (s, 5 H, C_5H_5), 4.13 (m, 1 H, Me_2SiOCH), 3.95 (m, 1 H, BCH_2SiOCH), 1.53 (d, $^3J_{HH}$ = 6.3 Hz, 3 H, $BCH_2SiOCH(CH_3)_2$), 1.52 (d, $^3J_{HH}$ = 6.2 Hz, 3 H, $Me_2SiOCH(CH_3)_2$), 1.49 (d, $^3J_{HH}$ = 6.5 Hz, 3 H, $Me_2SiOCH(CH_3)_2$), 1.29 (d, $^3J_{HH}$ = 6.5 Hz, 3 H, $BCH_2SiOCH(CH_3)_2$), 0.31 (s br, 3 H, $SiMe_2$), 0.13 (s br, 3 H, $SiMe_2$), -0.21 (s br, 3 H, SiMe). $^{13}C\{^1H\}$ NMR (methylene chloride-d_2, 150 MHz): δ 149.54 (br, C_6F_5), 147.95 (br, C_6F_5), 139.36 (br, C_6F_5), 137.90 (br, C_6F_5), 136.39 (br, C_6F_5), 116.26 (C_5H_5), 115.29 (C_5H_5), 75.07 (Me_2SiOCH), 74.91 (BCH_2SiOCH), 25.44 ($Me_2SiOCH(CH_3)_2$), 25.15 ($BCH_2SiOCH(CH_3)_2$), 24.77 ($Me_2SiOCH(CH_3)_2$), 24.29 ($BCH_2SiOCH(CH_3)_2$), 4.29 ($SiMe_2$), 4.20 ($SiMeCH$), 4.15 ($SiMe_2$). $^{29}Si\{^1H\}$ NMR (methylene chloride-d_2, 119.3 MHz, 25 °C): δ 13.8 ($SiMe_2$), 5.7 ($SiMeCH_2$). ^{19}F NMR (methylene chloride-d_2, 376 MHz, 25 °C): δ -133.1 (d, $^3J_{FF}$ = 22.1 Hz, 6 F, *o*-F), -165.2 (t, $^3J_{FF}$ = 20.4 Hz, 3 F, *p*-F), -168.3 (t, $^3J_{FF}$ = 20.5 Hz, 6 F, *m*-F). ^{11}B NMR (methylene chloride-d_2, 79.5 MHz, 25 ºC): δ -15.1. Calcd for $BC_{38}F_{15}H_{35}Si_2NO_2Zr$: C, 46.53; H, 3.60; N, 1.43. Found: C, 46.34; H, 4.00; N, 1.14. mp 77-85 °C.

$Cp_2Zr(H)N\{SiHMeCH_2B(C_6F_5)_3\}(SiMe_2DMAP)$ (8.7a) and $Cp_2Zr(H)N(SiHMe_2)\{SiMeCH_2B(C_6F_5)_3(DMAP)\}$ (8.7b). 8.5 and DMAP were allowed to react in methylene chloride (2 mL) in a vial to form a yellow solution and the solution was stirred for 5 min. The resulting material was then dried under vacuum and washed with pentane (2 × 5 mL). The volatiles were removed under reduced pressure to give $Cp_2Zr(H)N(SiHMe_2)\{SiMeCH_2B(C_6F_5)_3(DMAP)\}$ and $Cp_2Zr(H)N\{SiHMeCH_2B(C_6F_5)_3\}(SiMe_2DMAP)$ as a yellow crystalline solid in a 1.65:1 ratio as determined by integration of the 1H NMR spectrum. **8.7a**: ^{1}H NMR (methylene chloride-d_2, 600 MHz, 25 °C): δ 7.87 (d, $^3J_{HH}$ = 7.3 Hz, 2 H, α-$NC_5H_4NMe_2$), 6.72 (d, $^3J_{HH}$ = 7.2 Hz, 2 H, β-$NC_5H_4NMe_2$), 5.61 (s, 5 H, C_5H_5), 5.60 (s, 5 H, C_5H_5), 3.93 (br s, 1 H, ZrH), 3.17 (s, 6 H, NMe_2), 1.17 (br d, $^2J_{HH}$ = 8.2 Hz, 2 H, BCH_2), 0.53 (s, 3 H, $SiMe_2$), 0.48 (s, 3 H, $SiMe_2$) 0.28 (overlapped with $SiHMe_2$ resonance, assigned by ^{1}H-^{1}H COSY experiment, SiH), 0.25 (br s, 6 H, $SiHMe_2$). $^{13}C\{^1H\}$ NMR (methylene chloride-d_2, 125 MHz, 25 °C): δ 155.28 (*ipso*-$NC_5H_4NMe_2$), 142.31 (α-$NC_5H_4NMe_2$), 105.39 (C_5H_5), 105.01 (C_5H_5), 40.13 ($NC_5H_4NMe_2$), 8.3 (br, BCH_2), 1.05 ($SiMe_2$), 1.03 ($SiMe_2$), -1.96 ($SiHMe_2$). ^{11}B NMR (methylene chloride-d_2, 119.3 MHz, 25 °C): δ -14.7. $^{15}N\{^1H\}$ NMR (methylene chloride-d_2, 61 MHz, 25 °C): δ -193.8 ($NC_5H_4NMe_2$), -295.8 ($NC_5H_4NMe_2$), -317.7 (ZrN). ^{19}F NMR (methylene chloride-d_2, 564 MHz, 25 °C): δ -133.3 (br, 6 F, *ortho*-F), -164.4 (t, $^3J_{FF}$ = 20.2 Hz, 3 F, *para*-F), -167.7 (d, $^3J_{FF}$ = 21.1 Hz, 6 F, *meta*-F). $^{29}Si\{^1H\}$ NMR (methylene chloride-d_2, 119.3 MHz, 25 °C): δ -4.6 ($SiMe_2DMAP$), -63.9 (d, $^1J_{SiH}$ = 112.3 Hz, $SiHMe_2$). **8.7b**: ^{1}H NMR (methylene chloride-d_2, 600 MHz, 25 °C): δ 7.48 (d, $^3J_{HH}$ = 6.8 Hz, 2 H, α-$NC_5H_4NMe_2$), 6.53 (d, $^3J_{HH}$ = 6.5 Hz, 2 H, β-$NC_5H_4NMe_2$), 5.86 (s, 5 H, C_5H_5), 5.47 (s, 5 H,

C_5H_5), 3.99 (br s, 1 H, ZrH), 3.17 (s, 6 H, NMe_2), 1.33 (br d, $^2J_{HH}$ = 14.1 Hz, 2 H, BCH_2), 1.29 (br, 1 H, SiH), 0.39 (br s, 6 H, SiMe and SiHMe_2), 0.27 (br s, 3 H, SiHMe_2). $^{13}C\{^1H\}$ NMR (methylene chloride-d_2, 125 MHz, 25 °C): δ 156.08 (*ipso*-N$C_5H_4NMe_2$), 142.47 (α-N$C_5H_4NMe_2$), 105.81 (C_5H_5), 105.21 (C_5H_5), 40.20 ($NC_5H_4NMe_2$), 10.5 (br, BCH_2), -0.47 ($SiMe_2$), -1.20 ($SiMe_2$), -1.96 ($SiHMe_2$). ^{11}B NMR (methylene chloride-d_2, 119.3 MHz, 25 °C): δ -14.7. $^{15}N\{^1H\}$ NMR (methylene chloride-d_2, 61 MHz, 25 °C): δ -192.3 ($NC_5H_4NMe_2$), -295.8 ($NC_5H_4NMe_2$), -311.8 (ZrN). ^{19}F NMR (methylene chloride-d_2, 564 MHz, 25 °C): δ -135.3 (d, $^3J_{FF}$ = 22.3 Hz, 6 F, *ortho*-F), -164.7 (t, $^3J_{FF}$ = 20.2 Hz, 3 F, *para*-F), -167.5 (br, 6 F, *meta*-F). $^{29}Si\{^1H\}$ NMR (methylene chloride-d_2, 119.3 MHz, 25 °C): δ 11.4 ($SiMe_2$DMAP), -61.1 (d, $^1J_{SiH}$ = 115.0 Hz, $SiHMe_2$). IR (KBr, cm^{-1}): 2959 m br, 1845 m vbr (ν_{SiH}), 1641 m (ν_{C6F5}), 1601 m, 1565 s, 1511 s (ν_{C6F5}), 1458 s br (ν_{C6F5}), 1403 m, 1309 m, 1255 m, 1233 m, 1102 s br, 1069 s br, 1030 m, 972 s, 846 m, 804 s br, 681 m.

$Cp_2Zr[N(SiHMe_2)SiHMeCH_2B(C_6F_5)_3](OPEt_3)$ (8.8). 8.5 and OPEt were allowed to react in methylene chloride (2 mL) in a vial to form a yellow solution and the solution was stirred for 5 min. The resulting material was then dried under vacuum and washed with pentane (2 × 5 mL). The volatiles were removed under reduced pressure to give **8.8** as a yellow crystalline solid. ^1H NMR (methylene chloride-d_2, 600 MHz, 25 °C): δ 6.37 (s, 5 H, C_5H_5), 6.24 (s, 5 H, C_5H_5), 4.09 (m, $^1J_{SiH}$ = 169.4 Hz, 1 H, SiHMe$_2$), 3.82 (m, $^1J_{SiH}$ = 177 Hz, 1 H, SiHMe), 1.98 (m, 6 H, PCH_2), 1.19 (m, 9 H, PCH_2CH_3), 0.47 (d, $^3J_{HH}$ = 2.8 Hz, 3 H, SiHMe_2), 0.37 (br, 2 H, CH_2), 0.27 (d, $^3J_{HH}$ = 3.0 Hz, 3 H, SiHMe_2), -0.45 (d, $^3J_{HH}$ = 2.3 Hz, 3 H, SiHMe). $^{13}C\{^1H\}$ NMR (methylene chloride-d_2, 150 MHz, 25 °C): δ 149.65 (C_6F_5), 148.05 (C_6F_5), 139.17 (C_6F_5), 137.82 (C_6F_5), 137.48 (C_6F_5), 136.26 (C_6F_5), 115.13 (C_5H_5), 114.96 (C_5H_5),

18.79 (d, $^{1}J_{PC}$ = 65.5 Hz, P*C*H$_2$CH$_3$), 11.57 (br, BCH$_2$), 5.94 (d, $^{2}J_{PC}$ = 4.7 Hz, PCH$_2$*C*H$_3$), 2.79 (SiHMe), 2.06 (SiHMe$_2$), 1.34 (SiHMe$_2$). ^{11}B NMR (methylene chloride-d_2, 119.3 MHz, 25 °C): -14.7. ^{19}F NMR (methylene chloride-d_2, 564 MHz, 25 °C): δ -133.5 (br, 6 F, *o*-F), -165.9 (t, $^{3}J_{FF}$ = 19.9 Hz, 3 F, *p*-F), -168.8 (br, 6 F, *m*-F). ^{31}P NMR (methylene chloride-d_2, 243 MHz, 25 °C): 101.9. ^{29}Si{^{1}H} NMR (methylene chloride-d_2, 119.3 MHz, 25 °C): δ -7.7 (SiHMe), -26.3 (SiHMe$_2$). IR (KBr, cm^{-1}): 2956 m, 2914 w, 2890 w, 2135 m br (ν_{SiH}), 2099 m br (ν_{SiH}), 1641 m (ν_{C6F5}), 1511 s (ν_{C6F5}), 1457 s br (ν_{C6F5}), 1271 m, 1250 m, 1166 m, 1082 s br, 1016 m, 973 s, 930 s, 861 s, 804 s, 681 m.

Reference

1 (a) Bennett, C. R.; Bradley, D. C. *J. Chem. Soc., Chem. Commun.* **1974**, 29-30. (b) Simpson, S. J.; Turner, H. W.; Andersen, R. A. *J. Am. Chem. Soc.* **1979**, *101*, 7728-7729. (c) Simpson, S. J.; Andersen, R. A. *Inorg. Chem.* **1981**, *20*, 3627-3629. (d) Bradley, D. C.; Chudzynska, H.; Backer-Dirks, J. D. J.; Hursthouse, M. B.; Ibrahim, A. A.; Motevalli, M.; Sullivan, A. C. *Polyhedron* **1990**, *9*, 1423-1427. (e) Berno, P.; Minhas, R.; Hao, S.; Gambarotta, S. *Organometallics* **1994**, *13*, 1052-1054. (f) Gerlach, C. P.; Arnold, J. *Organometallics* **1996**, *15*, 5260-5262. (g) Cai, H.; Yu, X.; Chen, T.; Chen, X.-T.; You, X.-Z.; Xue, Z. *Can. J. Chem.* **2003**, *81*, 1398-1405. (h) Niemeyer, M. *Inorg. Chem.*, **2006**, *45*, 9085-9095. (i) Bénaud, O.; Berthet, J.-C.; Thuéry, P.; Ephritikhine, M. *Inorg. Chem.* **2010**, *49*, 8117-8130.

2 (a) Simpson, S. J.; Andersen, R. A. *J. Am. Chem. Soc*. **1981**, *103*, 4063-4066. (b) Planalp, R. P.; Andersen, R. A. *Organometallics* **1983**, *2*, 1675-1680. (c)

Sonnenberger, D. C.; Mintz, E. A.; Marks, T. J.*J. Am. Chem. Soc.* **1984**, *106*, 3484-3491.

3 Tikkanen, W. R.; Petersen, J. L.*Organometallics* **1984**, *3*, 1651-1655.

4 (a) Harrod, J. F.; Yun, S. S. *Organometallics*, **1987**, *6*, 1381-1387. (b) Kesti, M. R.; Abdulrahman, M.; Waymouth, R. M. *J. Organomet. Chem.* **1991**, *417*, C12-C15. (c) Kesti, M. R.; Waymouth, R. M. *Organometallics* **1992**, *11*, 1095-1103.

5 (a) Parks, D. J.; Piers, W. E. *J. Am. Chem. Soc.* **1996**, *118*, 9440-9441. (b) Parks, D. J.; Blackwell, J. M.; Piers, W. E. *J. Org. Chem.* **2000**, *65*, 3090-3098. (c) Piers, W. E.; Marwitz, A. J. V.; Mercier, L. G. *Inorg. Chem.* **2011**, *50*, 12252-12262.

6 (a) Arya, P.; Boyer, J.; Corriu, R. J. P.; Lanneau, G. F.; Perrot, M. *J. Organomet. Chem.* **1988**, *346*, C11-C14.

7 Dunne, J. F.; Neal, S. R.; Engelkemier, J.; Ellern, A.; Sadow, A. D. *J. Am. Chem. Soc.* **2011**, *133*, 16782-16785.

8 Shirobokov, O. G.; Kuzmina, L. G.; Nikonov, G. I. *J. Am. Chem. Soc.* **2011**, *133*, 6487-6489.

9 (a) Doyle, M. P.; West, C. T.; Donnelly, S. J. McOsker, C. C. *J. Organomet. Chem.*, **1976**, *117*, 129-140. (b) Fry, J. L.; Orfanopoulos, M.; Adlington, M. G.; Dittman Jr., W. P. Silverman, S. B. *J. Org. Chem.* **1978**, *43*, 374-375.

10 Khalimon, A. Y.; Ignatov, S. K.; Simionescu, R.; Kuzmina, L. G.; Howard, J. A. K.;. Nikonov, G. I. *Inorg. Chem.* **2011**, *51*, 754-756.

11 Fryzuk, M. D.; Mylvaganam, M.; Zaworotko, M. J.; MacGillivray, L. R. *Organometallics* **1996**, *15*, 1134-1138.

12 Yang, X.; Stern, C. L.; Marks, T. J. *J. Am. Chem. Soc.* **1994**, *116*, 10015-10031.

13 Yan, K.; Upton, B. M.; Ellern, A.; Sadow, A. D. *J. Am. Chem. Soc.* **2009**, *131*, 15110-15111.

14 (a) Ohff, A.; Kosse, P.; Baumann, W.; Tillack, A.; Kempe, R.; Gorls, H.; Burlakov, V. V.; Rosenthal, U. *J. Am. Chem. Soc.* **1995**, *117*, 10399-10400. (b) Lamač, M.; Spannenberg, A.; Baumann, W.; Jiao, H.; Fischer, C.; Hansen, S.; Arndt, P.; Rosenthal, U. *J. Am. Chem. Soc.* **2010** *132*, 4369-4380.

15 (a) Herrmann, W. A.; Eppinger, J.; Runte, O.; Spiegler, M.; Anwander, R. *Organometallics* **1997**, *16*, 1813-1815. (b) Eppinger, J.; Spiegler, M.; Hieringer, W.; Herrmann, W. A.; Anwander, R. *J. Am. Chem. Soc.* **2000**, *122*, 3080-3096. (c) Klimpel, M. G.; Gorlitzer, H. W.; Tafipolsky, M.; Spiegler, M.; Scherer, W.; Anwander, R. *J. Organomet. Chem*. **2002**, *647*, 236-244.

16 Stephan, D. W.; Erker, G. *Angew. Chem. Int. Ed.* **2010,** *49*, 46-76.

17 Geier, S. J.; Gille, A. L.; Gilbert, T. M.; Stephan, D. W. *Inorg. Chem.* **2009**, *48*, 10466-10474.

18 Chapter 9 in this thesis and Yan, K.; Ellern, A.; Sadow, A. D. *Manuscript in preparation.*

19 Yan, K.; Ellern, A.; Sadow, A. D. *J. Am. Chem. Soc.* **2012**, *134*, 9154-9156.

20 Chapter 7 in this thesis and Yan, K.; Sadow, A. D. *Manuscript in preparation.*

21 Massey, A. G.; Park, A. J., *J. Organomet. Chem.* **1964**, *2*, 245-250.

Supplementary information

Ortep figure for $Cp_2Zr[N(SiMe_2O^iPr)(SiMeO^iPrCH_2B(C_6F_5)$ **(8.6)**.

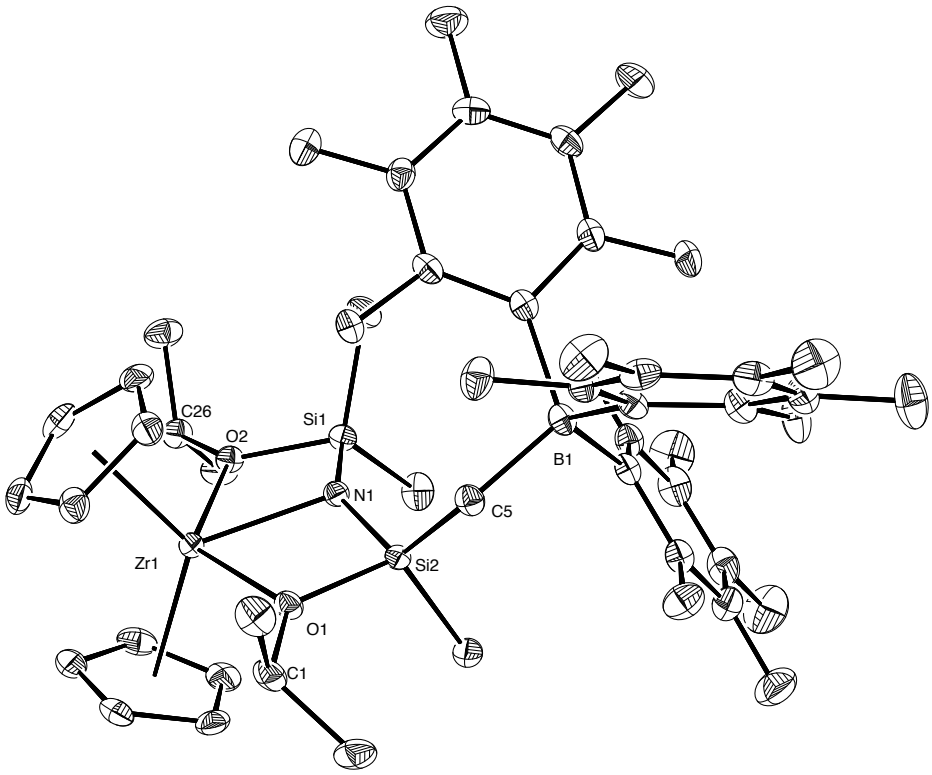

Chapter 9: Lewis base mediated β-hydrogen elimination and Lewis acid mediated insertion reactions of disilazido zirconium compounds

Modified from a paper to be submitted to J. Am. Chem. Soc.

*KaKing Yan, Juan Duchimaza, Arkady Ellern, Mark S. Gordon and Aaron D. Sadow**

Department of Chemistry and US Department of Energy Ames Laboratory, Iowa State University, Ames IA, 50011, USA

ABSTRACT. The reactivity of a series of cationic disilazido zirconocene complexes is dominated by the migration of anionic groups (hydrogen, alkyl, halide, OTf) between the zirconium and silicon centers. These migrations are controlled by addition of two-electron donors (Lewis bases) and two-electron acceptors (Lewis acids). The cationic non-classical $[Cp_2Zr\{N(SiHMe_2)_2\}]^+$ $[\mathbf{9.2}]^+$ is prepared from $Cp_2Zr\{N(SiHMe_2)_2\}H$ (**9.1**) and $B(C_6F_5)_3$, while reactions of $B(C_6F_5)_3$ and zirconium alkyl tetramethyldisilazide $Cp_2Zr\{N(SiHMe_2)_2\}R$ (R = Me (**9.6**), Et (**9.8**), *n*-C_3H_7 (**9.10**), CH=CHSiMe$_3$ (**9.12**)) provide a mixture of $[\mathbf{9.2}]^+$ and $[Cp_2Zr\{N(SiHMe_2)(SiRMe_2)\}]^+$. The latter product is formed through $B(C_6F_5)_3$ abstraction of a β-SiH and R group migration from Zr to the b-Si group. The selectivity for the alkyl group migration pathway to $[Cp_2Zr\{N(SiHMe_2)(SiRMe_2)\}]^+$ increases following the trend Me < Et < *n*-C_3H_7 < CH=CHSiMe$_3$. Related β-SiH group abstraction and X group migration reactions are observed for $Cp_2Zr\{N(SiHMe_2)_2\}X$ (X = Cl (**9.19**), OTf (**9.14**), OMe (**9.25**), O*i*-C_3H_7 (**9.26**)). Resonance structures for the proposed intermediates include a transient silylium moiety and a cationic alkylzirconocene coordinated by a silanimine, and the latter resonance structure suggests parallels to classical migratory insertion reactions. In contrast, addition of DMAP to $[\mathbf{9.2}]^+$ results in coordination to a Si center and hydrogen migration to zirconium to

give the cationic complex $[Cp_2ZrH\{N(SiHMe_2)(SiMe_2DMAP)\}]^+$. Related hydrogen migration occurs from $[Cp_2Zr\{N(SiHMe_2)(SiMe_2OCHMe_2)\}]^+$ to give $[Cp_2ZrH\{N(SiMe_2DMAP)(SiMe_2OCHMe_2)\}]^+$, whereas X-group migration is observed upon addition of DMAP to $[Cp_2Zr\{N(SiHMe_2)(SiMe_2X)\}]^+$ (X = Cl, OTf). Addition of $B(C_6F_5)_3$ to these cationic [Zr]-X species provides the [Zr]-$N(SiHMe_2)(SiXMe_2)$ starting material, indicating the Lewis base induced X-group and H migrations are reversible upon loss of DMAP. The species involved in these transformations are described by resonance structures that, by analogy to corresponding hydrocarbyl chemistry, are suggestive of β-hydrogen elimination. Notably, such pathways are previously unknown in early-metal amide chemistry, which is dominated by formally reductive β-hydrogen abstraction and γ-hydrogen abstractions. Finally, these reversible migrations facilitate SiH addition to carbonyls (hydrosilylation) through a proposed pathway that previously had been reserved for later transition metal compounds.

Introduction

β-Elimination and its microscopic reverse, 1,2-migratory insertion of an unsaturated moiety into a M-R bond (R = H, alkyl), are central to bond forming and breaking processes. These reactions are well studied for many metal-ligand pairs; however, the formation of new C-E bonds through insertion reactions into M-E bonds (E = halide, OR, NR_2) remains a major challenge in chemistry. New elementary steps could provide enabling strategies, including catalytic methods, for the synthesis of functionalized organic compounds (e.g., enantioselective hydration, halogenation) or the selective defunctionalization of organic compounds (e.g. for the conversion of biorenewables).

When the migrating ligand is hydrogen, β-agostic species are the proposed intermediates on this pathway.[1] Detailed structural and spectroscopic studies of these compounds are suggested to provide a description of the species on the reaction coordinate between the alkyl to the olefin. The bonding nature of agostic interactions, the chemical interpretations offered to describe the interactions, and the anticipated reactions associated with the structures, however, vary with the relative position of a C-H with respect to the metal (α, β, etc.), the metal center and its valence, and the other elements present in the agostic ligand.[2] On one end of the continuum, such 3-center-2-electron (3c-2e) interactions of aromatic C-H bonds and electron rich metal centers may be viewed as an arrested C-H bond oxidative addition.[3] Similarly, β-agostic organometallics containing a low valent metal center may be viewed as an intermediate between the metal alkyl and the 2-electron-oxidized metallacyclopropane hydride, or the olefin-hydride resonance form, where olefin coordination involves 2-electron π-back donation.[4] On the other hand, high valent metals containing β-agostic C-H bonds are characterized as arrested intermediates on the path to an isovalent metal hydride and olefin.[4a,5] β-agostic main group alkyls, are at the other end of the continuum, and electron-density analysis suggests the metal-CH interaction is mainly electrostatic;[4a] β-hydrogen elimination is least facile in the main group systems. These electrostatic agostic structures are not established as intermediates on pathways for insertion or elimination.

Thus, among agostic structures, β-agostic species have a special relationship with the pathways involving insertion of unsaturated organics into M-H bonds and β-hydrogen elimination. However, strong Lewis acidic metal centers and polarizable E-E' bonds (e.g., E-

E' = Si-H, Si-C, B-H) are well-known to form side-on interactions.[2,6,7,8] For example, the rare earth disilazides such as $Cp^*_2LaN(SiHMe_2)_2$ contain a unusual structure characterized by obtuse Si-N-Si angle, upfield SiH resonances and low $^1J_{SiH}$ (ca 120 Hz), and low energy ν_{SiH} bands in the IR spectra (1900 cm-1).[9] Bonding may be silimilar in a related bis(catacolborane) compound $Cp_2Ti(\eta^2\text{-HBcat})_2$ that contains two side-on HBcat ligands.[10]

A key question associated with these bridging structures involves their relationship to the insertion-elimination reactivity. It has been suggested that rarity of β-eliminations for transition-metal amido compounds[11] is related to the nature of agostic β-CH structures of amide ligands that is distinct in geometry and spectroscopy from the agostic alkyls.[12] For example, β-agostic amides generally feature long N-C bonds, large (ca. ~120 °) ∠M-N-C angles, and short β-C-H distances,[11] whereas β-agostic alkyls contain short C-C bonds, acute ∠M-C-C angles, and elongated β-CH bonds.[4b] As the microscopic reverse of β-elimination, the insertion of olefins into more polar M-X bonds (e.g., M-F, M-Cl, M-OR, $M\text{-}NR_2$) are vary from unknown to rare.[13] Interestingly, a Si-N bond forming reaction was recently described in the reaction of $[Sc]\{N(SiHMe_2)_2\}_2$ and Ph_3C^+ that gives $[Sc]N(SiHMe_2)SiMe_2N(SiHMe_2)_2$.[14]

Here, we present a study of a cationic disilazidozirconium compound $[Cp_2Zr\{N(SiHMe_2)_2\}]^+$ $[\mathbf{9.2}]^+$ that possesses extreme spectroscopic and structural features attributed to the side-on interaction of two SiH groups with a zirconium center. The analogy of the side-on β-Si-H→Zr interaction with agostic β-CH organometallic compounds is supported by pathways to form $[\mathbf{9.2}]^+$ and its reactivity. This cationic disilazidozirconium reacts with DMAP to give a zirconium hydride through an apparent β-hydrogen elimination

process. Addition of the Lewis acid $B(C_6F_5)_3$ to $Cp_2Zr\{N(SiHMe_2)_2\}R$ results in Si-C bond formation through an apparent migratory insertion reaction. Furthermore, $[Cp_2ZrN(SiHMe_2)_2]^+$ reacts with carbonyls to give the hydrosilylation products; the pathway for this reaction is explored through the study of migration chemistry of β-OR, β-OTf, and β-Cl migration between zirconium and silicon centers (Scheme 9.1).

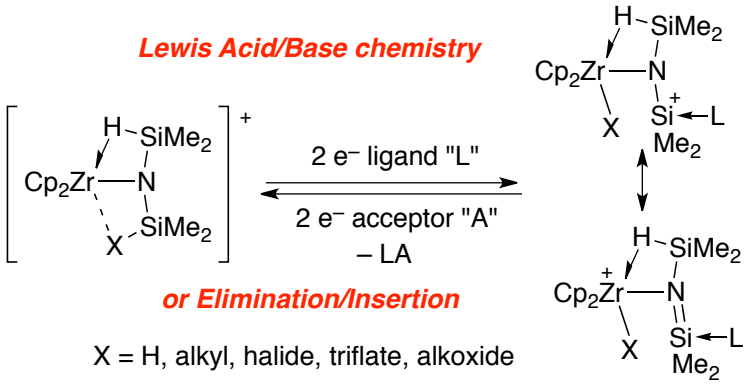

Scheme 9.1. General scheme illustrating 2-electron donor/acceptor mediated anionic group transfer based on resonance structures that depend on the relative charges on zirconium and silicon.

In fact, the reactivity of the β-groups on the disilazido ligand, in response to 2-electron donors and 2-electron acceptors, provides connections to β-elimination and insertion chemistry reminiscent of late transition-metal β-agostic alkyl systems. In addition, these compounds react with carbonyls, resulting in hydrosilylation. The mechanism of this hydrosilylation is shown to be related to the hydrogen shuttling between Zr and Si centers.

Results

Synthesis of the neutral precursor of $Cp_2Zr\{N(SiHMe_2)_2\}H$.

We recently reported the formation of $Cp_2Zr\{N(SiHMe_2)_2\}H$ (**9.1**) as a side product in the reaction of $Cp_2Zr\{N(SiHMe_2)_2\}OTf$ and $LiN(SiHMe_2)t$-Bu. Identification of **9.1** in that reaction required its independent synthesis,[15] which was achieved by reaction of Cp_2ZrHCl and $LiN(SiHMe_2)_2$. We have also briefly communicated its solution-phase structure in the context of an unusual γ-abstraction reaction.[16] Surprisingly, $[ZrCl\{N(SiHMe_2)_2\}_2(\mu\text{-}Cl)]_2$ is the only other reported zirconium complex containing the $N(SiHMe_2)_2$ moiety,[17] even though this hydrosilazide ligand is widely used in Group 3 and lanthanide chemistry,[18] and the related hexamethyldisilazide ligand ($N(SiMe_3)_2$) is important in transition-metal, lanthanide, and main group chemistry.[19] We describe this compound here because the spectroscopy associated with the non-classical SiH zirconium interaction represents a starting point for comparison to the unique compounds described here.

The ^{1}H NMR spectrum of **9.1** contained the expected resonances including the ZrH (5.60 ppm) and SiH (3.78 ppm, $^1J_{SiH}$ = 161.0 Hz). The slightly upfield silicon hydride resonance and moderately low $^1J_{SiH}$ (cf. $HN(SiHMe_2)_2$, $^1J_{SiH}$ = 170 Hz) suggest a possible side-on Si-H interaction with Zr,[20] however, the $SiMe_2$ groups are equivalent in the ^{1}H, $^{13}C\{^1H\}$, and ^{29}Si NMR spectra acquired at room temperature.

Therefore, ^{1}H NMR spectra of **9.1** in toluene-d_8 were recorded from 298 to 191 K. The SiH and SiMe resonances broaden to the coalescence point at 210 K. At 191 K, the ^{1}H NMR spectrum contains two SiH resonances and two $SiMe_2$ signals. The two SiH resonances were assigned as non-classical SiH (2.13 ppm, $^1J_{SiH}$ = 129.7 Hz) and terminal SiH (4.99 ppm, $^1J_{SiH}$ = 179.6 Hz) based on the $^1J_{SiH}$ coupling constants. At 191 K, the ^{29}Si NMR spectrum was resolved to show resonances at -23.1 and -62.9 ppm, which were assigned to silicon atoms with terminal and bridging hydrogen, respectively, by a ^{1}H-^{29}Si HMBC

experiment. A similar upfield ^{29}Si NMR resonance was reported for the non-classical $Cp_2Zr\{N(SiHMe_2)t\text{-}Bu\}H$ (-73.4 ppm),[21] while the downfield signal is comparable to ^{29}Si NMR resonance of the SiH in $Y\{N(SiHMe_2)_2\}_3(NHC)_2$ (δ -22.5, $^1J_{SiH}$ = 172 Hz, NHC = 1,3-dimethylimidazolin-2-ylidene) which contains short Y-Si distances (Y-Si ~ 3.13 Å; Y-N-Si = 105.1(3)°) and a low energy ν_{SiH} (2041 cm^{-1}).[22] Bands at 2047 and 1907 cm^{-1} in the infrared spectrum of **9.1** further indicate a non-classical interaction, and IR also provides support for the ZrH (1559 cm^{-1}).

Interestingly, the reaction of deuterium-labeled Cp_2ZrDCl and $LiN(SiHMe_2)_2$ provides an isotopically-scrambled mixture of $Cp_2Zr\{N(SiDMe_2)(SiHMe_2)\}H$ and $Cp_2Zr\{N(SiHMe_2)_2\}D$ (eq 9.1).

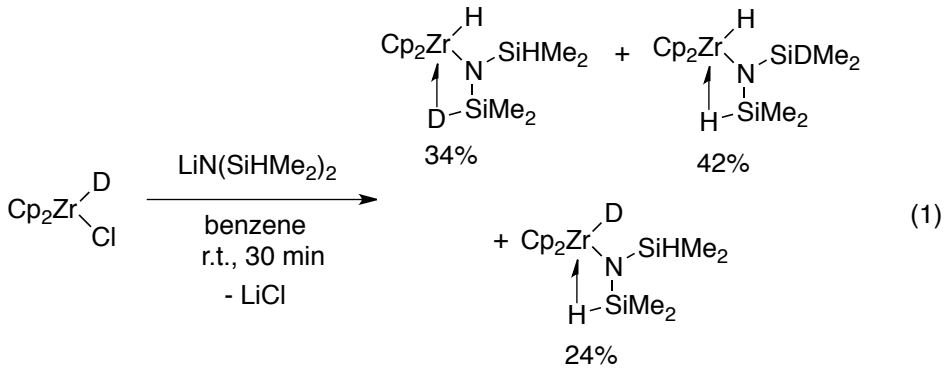

As expected, the deuterium distribution favors its localization in the most tightly bonded position based on IR analysis.[23]

Synthesis of the cationic $[Cp_2ZrN(SiHMe_2)_2]^+$.

Cationic $[Cp_2ZrN(SiHMe_2)_2]^+$ (**[9.2]$^+$**) is synthesized from reactions of **9.1** and $B(C_6F_5)_3$ or $[Ph_3C][B(C_6F_5)_4]$ as $[HB(C_6F_5)_3]^-$ or $[B(C_6F_5)_4]^-$ salts (eq 9.2). The reactions are quantitative in bromobenzene-d_5 on micromolar scale, but benzene is preferable as solvent in preparatory scale reactions for easy separation of [**9.2**]$^+$ as an insoluble oil.

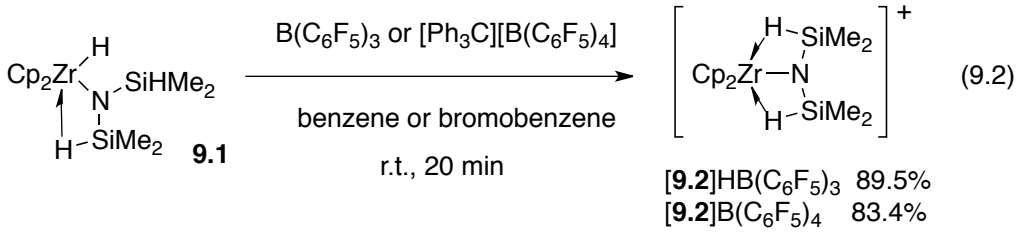

(9.2)

The unusual NMR spectroscopic features of the $N(SiHMe_2)_2$ ligand in $[\mathbf{9.2}]^+$ are similar in both the $[HB(C_6F_5)_3]^-$ and $[B(C_6F_5)_4]^-$ compounds, and the spectroscopic data here is given for the $[B(C_6F_5)_4]^-$ salt.[24] The SiH in $[\mathbf{9.2}]^+$ was characterized by a far upfield ^1H NMR signal at -0.48 ppm and an unusually low $^1J_{SiH}$ (89.3 Hz). For comparison, the ^1H NMR spectrum of the isoelectronic *rac*-Me_2Si(2-Me-Benz-Ind)$_2$]$YN(SiHMe_2)_2$ contained upfield SiH (2.65 ppm) and low $^1J_{SiH}$ (133 Hz).[9] The spectroscopy of $[\mathbf{9.2}]^+$ is consistent with a C_{2v} symmetric compound. One ^{29}Si NMR signal was observed at -43 ppm; the ^{29}Si NMR resonance of $[\mathbf{9.2}]^+$ is upfield of terminal SiH groups in **9.1**, but downfield of the nonclassical SiH in **9.1**. In the IR spectrum of $[\mathbf{9.2}][B(C_6F_5)_4]$, two bands are observed at 1738 and 1659 cm^{-1} may be assigned to ν_{SiH}. These energies are significantly lower than 2c-2e SiH's in the classical $[Cp_2Zr\{N(SiHMe_2)_2\}OPEt_3]^+$ (2122 cm^{-1}, see below) or the neutral mixed classical/non-classical **9.1** (2047 and 1907 cm^{-1}).

X-ray quality crystals of $[\mathbf{9.2}][HB(C_6F_5)_3]$ are obtained by slow diffusion of pentane into a concentrated bromobenzene solution at -30 °C. In the solid state structure, the cationic portion $[Cp_2Zr(N(SiHMe_2)_2]^+$ is separated from the $[HB(C_6F_5)_3]^-$ anion, and the shortest distance in the ion pair is 3.27 Å between an aryl fluoride and one of the silicon centers (Σ_{SiF}^{VDW} = 3.57 Å). The solid state structure contains a significant, almost perfectly symmetrical distortion of the $N(SiHMe_2)_2$ ligand. The short Zr-Si distances (Zr1-Si1: 2.8740(8) and Zr1-Si2: 2.8706(7) Å) and the N-Si distances are equivalent within error

(1.661(2) and 1.662(2) Å). For comparison, the Zr-Si distance in an authentic zirconium silyl $Cp_2ZrSiMe_3(S_2CNEt_2)$ is 2.815(1) Å,[25] while the Zr-Si distance in $Cp_2Zr\{\eta^2$-N(*t*-Bu)$SiMe_2\}PMe_3$ is 2.654(1) Å.[26] The latter distances are ca. 0.05 Å shorter than the Si-N distance associated with the terminal $SiHMe_2$ in **9.1** (1.710(2) Å), and ca. 0.02 Å shorter than the Si-N distance of 1.863(2) associated with the non-classical β-$SiHMe_2$ group. The ∠Zr-N-Si angles are small (95.4(1) and 95.3(1)°), and the ∠Si-N-Si angle approaches linearity at 168.9(2)°.

Interestingly, the Zr-N distance of 2.193(2) Å is 0.05 Å longer than that in $Cp_2ZrHN(SiHMe_2)_2$. The hydrogen atoms on the $SiHMe_2$ (as well as the $HB(C_6F_5)_3$ group) were located in the Fourier difference map and refined; the Zr-N bond and the two Si-H bonds are essentially coplanar, as indicated by the torsion angles Zr1-N1-Si1-H1s (0(1)°), the Zr1-N1-Si2-H2s (-3(1)°), and H1s-Si1-Si2-H2s (3(2)°).

The Zr-H (2.06(3) Å) distances in $[\mathbf{9.2}]^+$ are long in comparison to the Zr-H distance for the zirconium hydride in **9.1** (1.90(3) Å). Although it is significantly shorter than the Zr-H(Si) distance of the non-classical SiH in that compound (2.469 Å), while the terminal Si-H distance and the non-classical Si-H distance in **9.1** are 1.53(4) and 1.47(4) Å, respectively. The observed spectroscopic and structural features provide support for significant non-classical Zr-$N(SiHMe_2)_2$ interactions in the electron-poor metal complex.[9,17]

Furthermore, the $HB(C_6F_5)_3$ counterion has minimal, but tantalizing, impact on the distances and angles of the $N(SiHMe_2)_2$ ligand. The Zr-H (2.06(3) Å) and Si-H (1.54(4) Å) distances of the $SiHMe_2$ with the fluorine-silicon close contact are within 3 e.s.d.s of the distances in the other $SiHMe_2$ (2.09(3) and 1.69(3) Å, respectively).

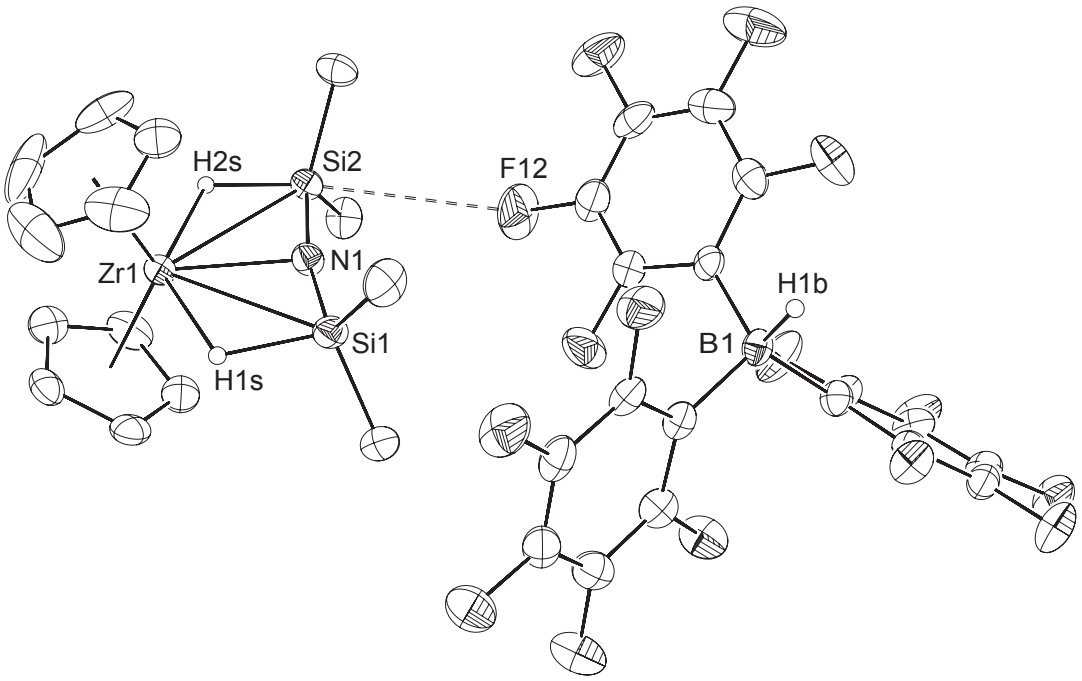

Figure 9.1. ORTEP diagram of $[Cp_2ZrN(SiHMe_2)_2][HBC_6F_5)_3]$ [**9.2**][$HB(C_6F_5)_3$]. Ellipsoids are drawn at 35% probability. The dashed line between Si2 and F12 indicates the shortest contact between the cation and anion. Significant interatomic distances (Å): Zr1-N1, 2.193(2); Zr1-Si1, 2.8740(8); Zr1-H1s, 2.09(3); Si1-H1s, 1.69(3); Zr1-Si2, 2.8706(7); Zr1-H2s, 2.06(3); Si2-H2s, 1.54(4); N1-Si1, 1.662(2); N1-Si2, 1.661(2). Selected interatomic angles (°): Zr1-N1-Si1, 95.4(1); Zr1-N1-Si2, 95.3(1); Si1-N1-Si2, 168.9(1); H1s-Zr1-H2s, 137(x); Zr1-N1-Si1-H1s, 0(1); Zr1-N1-Si2-H2s, -3(1), H1s-Si1-Si2-H2s. 3(2).

Computational model of $[Cp_2Zr\{N(SiHMe_2)_2]^+$

More insight into the relationship between the structural features of $[Cp_2Zr\{N(SiHMe_2)_2]^+$ and its spectroscopic properties is provided by a computational study. The optimized geometry of the cationic portion of $[Cp_2ZrN(SiHMe_2)_2]^+$ shown in Figure 9.2 is in good agreement with the coordinates obtained from X-ray crystallographic structure determination.

For example, the Zr-Si distances, calculated to be 2.861 Å, match the experimental Zr-Si distances. The calculated Zr-N distance of 2.22 Å is slightly longer than the experimental value. The bridging hydrogen atoms are of particular interest, and the calculated Zr-H and Si-H distances are 2.06 and 1.57 Å, respectively.

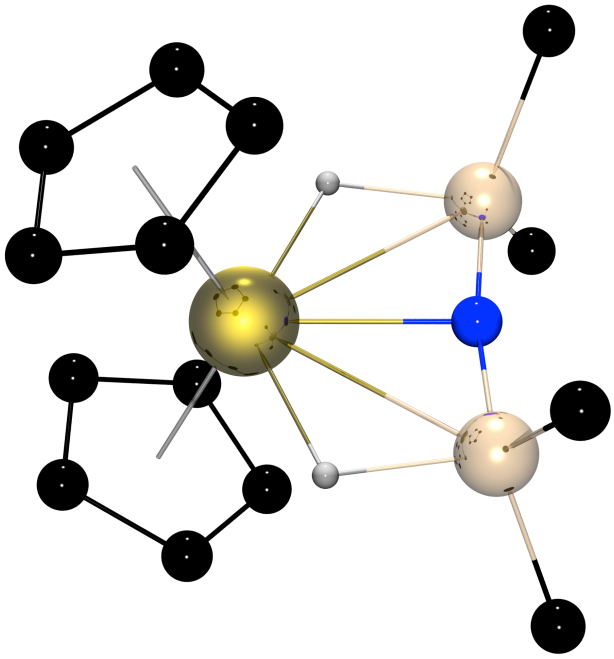

Figure 9.2. Rendered illustration of MP2-optimized coordinates of $[Cp_2ZrN(SiHMe_2)_2]^+$. Hydrogen atoms on methyl and cyclopentadienyl groups are not included in the image.

The vibrational calculation verified that this structure is a ground state on the potential energy surface. Two normal modes are associated with the bridging Zr–H-Si structure; these are symmetric and asymmetric SiH stretching motion at 1800 and 1743 cm^{-1}. These energies compare well to the bands in IR spectrum of $[\mathbf{9.2}]^+$; furthermore, the motion is parallel to the Si-H bond vector rather than along the Zr-H vector.

Reactions $Cp_2Zr\{N(SiHMe_2)_2\}R$ with $B(C_6F_5)_3$.

Two pathways could provide [**9.2**]$^+$ from **9.1** and $B(C_6F_5)_3$: (**A**) abstraction of the ZrH and (**B**) β-hydrogen abstraction to give a silylium intermediate followed by ZrH migration. Although labeled $Cp_2Zr\{N(SiHMe_2)_2\}D$ could resolve this issue, attempted synthesis **9.1**-d_1 from Cp_2ZrDCl and $LiN(SiHMe_2)_2$ provides a mixture with $Cp_2Zr\{N(SiHMe_2)_2$-$d_1\}H$. Thus, SiH/ZrH exchange occurs and labeling cannot distinguish the two pathways. Alkyl disilazido zirconium compounds could provide a means for distinguishing the abstraction pathways; furthermore, variation of the alkyl group is a means to control the nucleophilic site in the zirconium compound as probed by reactions with $B(C_6F_5)_3$.

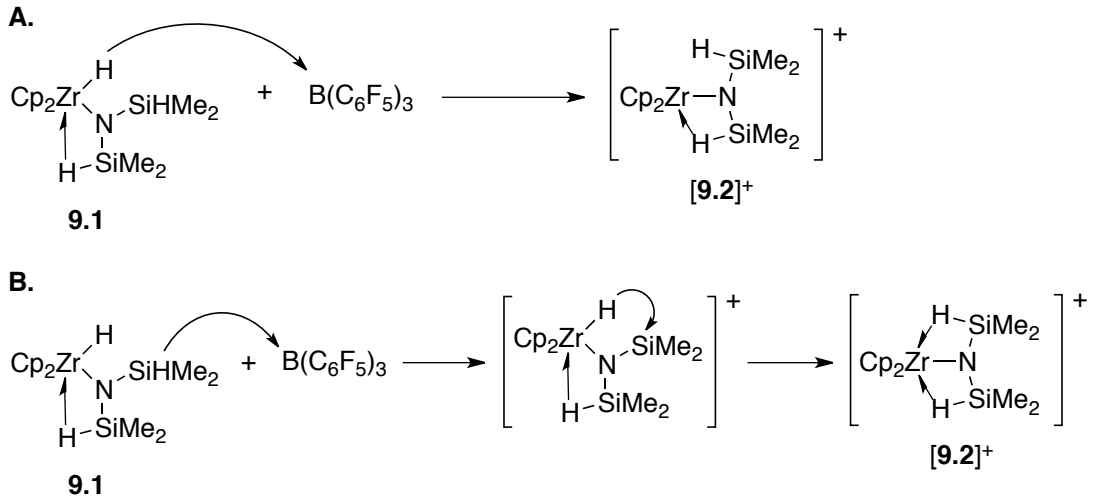

Scheme 9.2. Possible pathways for formation of [**9.2**]$^+$. (A) ZrH abstraction or (B) SiH abstraction followed by intramolecular ZrH abstraction.

Treatment of zirconium methyl $Cp_2Zr\{N(SiHMe_2)_2\}Me$ (**9.3**) with $B(C_6F_5)_3$ gives [**9.2**][$MeB(C_6F_5)_3$] as the major product (70%) and [$Cp_2Zr\{N(SiHMe_2)(SiMe_3)\}$][$HB(C_6F_5)_3$] ([**9.4**][$HB(C_6F_5)_3$]) is also formed in 30% yield (eq 9.3).

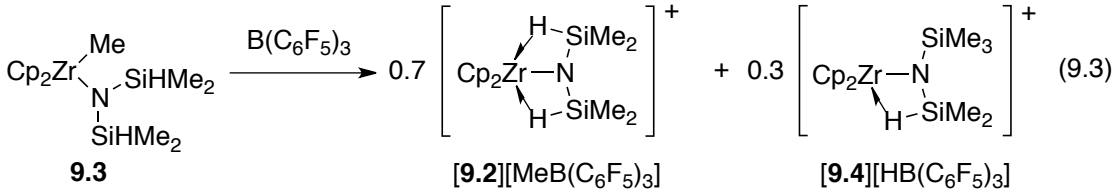

9.3 [**9.2**][MeB(C$_6$F$_5$)$_3$] [**9.4**][HB(C$_6$F$_5$)$_3$] (9.3)

In the reaction mixture, two ^{11}B NMR resonances were observed at -14.2 ppm (singlet; major) and -24.8 ppm ($^1J_{BH}$ = 81.5 Hz; minor). A ^{1}H-^{11}B HMQC experiment contained a crosspeak between the resonance at -14.2 ppm and a broad ^{1}H NMR resonance at 1.11 ppm (3 H) assigned to a [MeB(C$_6$F$_5$)$_3$] group. Integration of the resonances for [**9.2**]$^+$ and [MeB(C$_6$F$_5$)$_3$] is the basis for assignment of the major product as [**9.2**][MeB(C$_6$F$_5$)$_3$]. The minor product [**9.7**][HB(C$_6$F$_5$)$_3$], meanwhile, contained a doublet (0.31 ppm, $^3J_{HH}$ = 2.4 Hz, 6 H) and a singlet 0.27 ppm (9 H) assigned to SiMe$_2$ and SiMe$_3$ groups and a multiplet at 0.64 ppm ($^1J_{SiH}$ = 94.4 Hz) assigned to a non-classical β-Si-H→Zr.

The proposed pathway to the minor product [**9.7**]$^+$ involves b-hydrogen abstraction from the disilazido ligand to give a silylium center followed by ZrMe migration. Based on this idea, the reaction of B(C$_6$F$_5$)$_3$ and sterically hindered alkyl groups should be disfavored with respect to β-hydrogen abstraction. The compounds Cp$_2$Zr{N(SiHMe$_2$)$_2$}R (R = Et (**9.5**), *n*-C$_3$H$_7$ (**9.7**), CH=CHSiMe$_3$ (**9.9**)) were allowed to react with B(C$_6$F$_5$)$_3$ to give mixtures of [Cp$_2$Zr{N(SiHMe$_2$)(SiRMe$_2$)}]$^+$ (R = Et (**9.6**), *n*-C$_3$H$_7$ (**9.8**), CH=CHSiMe$_3$ (**9.10**)) and [**9.2**]$^+$ (Scheme 9.3). Importantly, the ratio of [Cp$_2$Zr{N(SiHMe$_2$)(SiRMe$_2$)}]$^+$ to [**9.2**]$^+$ increases following the trend Me < Et < *n*-C$_3$H$_7$ < CH=CHSiMe$_3$.

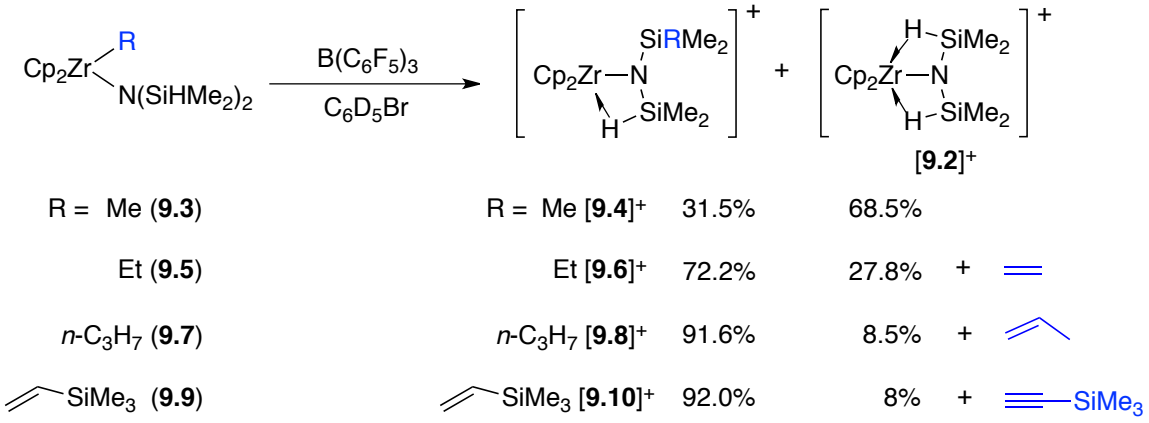

Scheme 9.3. Competition between [Zr]R abstraction and β-hydrogen abstraction in reactions of mixed alkyl disilazido zirconium compounds and $B(C_6F_5)_3$.

Although [**9.4**]$^+$, [**9.6**]$^+$, [**9.8**]$^+$, and [**9.10**]$^+$ could not be separated from the side product [**9.2**]$^+$, the assignments of Si-C bond formation are unambiguously supported by ^{1}H-^{29}Si HMBC and COSY experiments. For example in compound [**9.10**]$^+$, a crosspeak is detected between the ^{29}Si NMR signal at -12.9 ppm and the ^{1}H NMR vinylic signals at 6.43 and 6.75 ppm.

Interestingly, $B(C_6F_5)_3$ reacts with the ethyl, *n*-propyl, and trimethylsilylvinyl zirconium compounds to give $[HB(C_6F_5)_3]^-$ as the only counterion in the reaction mixture. Meanwhile, the corresponding byproducts ethylene, propylene, and trimethylacetylene are formed. Thus, β-hydrogen abstraction (as part of either SiH or CH groups) is favored with respect to alkyl group abstraction.[27] Previously, we observed a concentration dependence on β-hydrogen abstraction vs alkyl group abstraction in reactions of ZnR_2 and bis(4,4-dimethyl-2-oxazolinyl)phenyl borane.[28] However, in the current system carbon-boron bond formation was below ^{1}H and ^{11}B NMR detection limits, and the product ratios were similar in reaction performed at concentrations from 2.4 mM to 9.6 mM.

Reactions $Cp_2Zr\{N(SiHMe_2)_2\}X$ with $B(C_6F_5)_3$.

Zirconium alkyls, and likely a zirconium hydride, migrate to the β-silicon center. Therefore, we were interested to study the migration of other anionic groups, such as OR, Cl and OTf.

The compounds $Cp_2Zr\{N(SiHMe_2)_2\}X$ (X = OTf (**9.11**), Cl (**9.13**), OMe (**9.15**), $OCHMe_2$ (**9.16**)) react with $B(C_6F_5)_3$ or $[Ph_3C][B(C_6F_5)_4]$ in benzene to give $[Cp_2ZrN(SiHMe_2)(SiMe_2\text{-}\mu\text{-}X)]^+$ (X = OTf $[\mathbf{9.12}]^+$, Cl $[\mathbf{9.14}]^+$, OMe $[\mathbf{9.17}]^+$, $OCHMe_2$ $[\mathbf{9.18}]^+$) (Scheme 9.4).

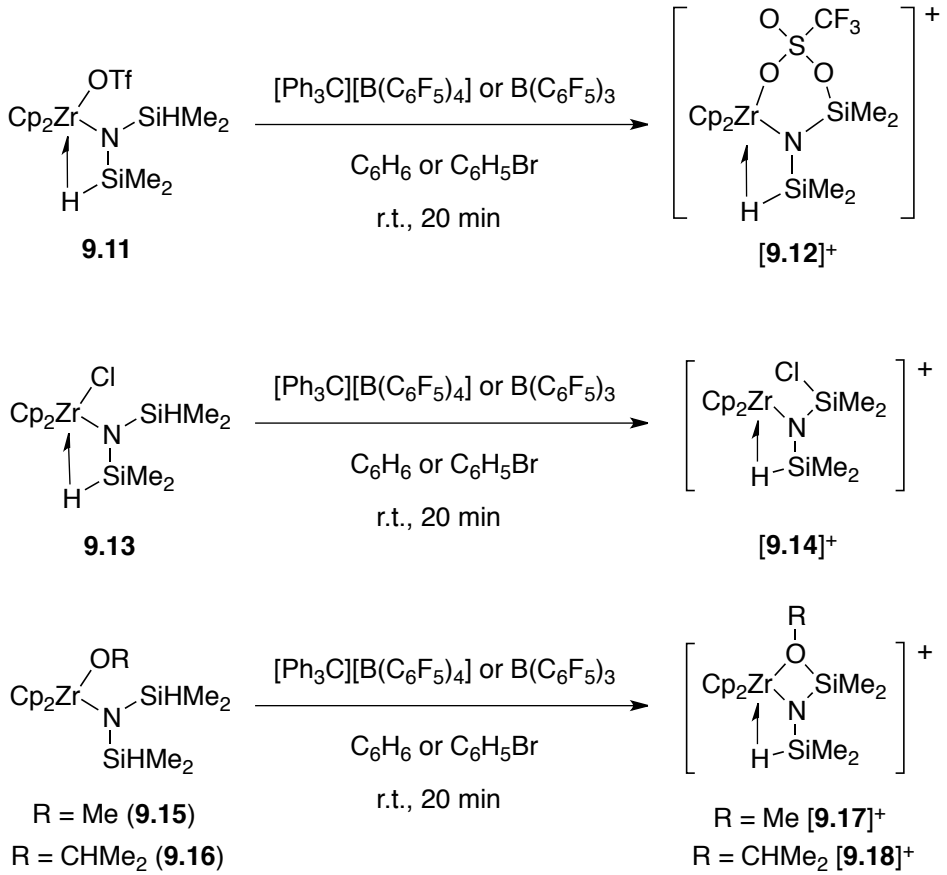

Scheme 9.4. β-Hydrogen abstraction reactions of zirconium disilazido triflate, chloride, and alkoxide compounds.

In all cases, hydrogen abstraction is supported by formation of $[HB(C_6F_5)_3]^-$ (^{11}B NMR: -24.8, $^1J_{BH}$ = 87.1 Hz) or Ph_3CH. The series of products [**9.12**]$^+$, [**9.14**]$^+$, [**9.17**]$^+$ and [**9.18**]$^+$ contain similar spectroscopic features for the $N(SiHMe_2)(SiXMe_2)$ ligand. The cationic $[Cp_2ZrN(SiHMe2)(SiMe_2X)]^+$ is C_s symmetric, as two $SiMe_2$ and one C_5H_5 resonance were observed in the ^1H NMR spectrum. All the compounds feature upfield-shifted ^1H NMR resonances for the β-SiH, extremely low $^1J_{SiH}$ values, and ^{29}Si NMR resonances for the β-SiH ranging from -26 to -32 ppm (Table 9.1). These assignments are supported by ^1H-^{29}Si HMBC experiments.

Table 9.1. ^1H and ^{29}Si NMR data of cationic β-SiH containing zirconium silazide.

Compound[a]	δ Si*H*	$^1J_{SiH}$ (Hz)	δ *Si*HMe_2	δ *Si*Me_2X
$[Cp_2ZrN(SiHMe_2)_2][HB(C_6F_5)_3]$ [**9.2**][$HB(CF_5)_3$]	-0.44	107	-42.7	n.a.
$[Cp_2ZrN(SiHMe_2)_2][B(C_6F_5)_4]$ [**9.2**][$B(C_6F_5)_4$]	-0.48	89	-43.7	n.a.
$[Cp_2ZrN(SiHMe_2)(SiMe_3)]^+$ [**9.4**]$^+$	0.64	94	8.2	-0.2
$[Cp_2ZrN(SiHMe_2)(SiMe_2Et)]^+$ [**9.6**]$^+$	0.5	94	7.4	5.6
$[Cp_2ZrN(SiHMe_2)(SiMe_2\text{-}C_3H_7)]^+$ [**9.8**]$^+$	0.46	87	5.2	6.0
$[Cp_2ZrN(SiHMe_2)(SiMe_2\text{-}CHCHSiMe_3)]^+$ [**9.10**]$^+$	0.56	89	-11.5	-5.2
$[Cp_2ZrN(SiHMe_2)(SiMe_2\text{-}\mu\text{-}\kappa^2\text{-}OTf)][HB(C_6F_5)_3]$ [**9.12**][$HB(C_6F_5)_3$]	0.22	107	-25.9	21.4
[**9.12**][$B(C_6F_5)_4$]	0.18	99	-25.2	21.4

$[Cp_2ZrN(SiHMe_2)(SiMe_2\text{-}\mu\text{-}Cl)]^+$ [**9.14**]$^+$	0.65	89	-32.5	29.6
$Cp_2ZrN(SiHMe_2)(SiMe_2\text{-}\mu\text{-}OMe)]^+$ [**9.17**]$^+$	0.34	96	-29.7	20.4
$Cp_2ZrN(SiHMe_2)(SiMe_2\text{-}\mu\text{-}OCHMe_2)]^+$ [**9.18**]$^+$	0.41	94	-33.0	13.2
$[Cp_2Zr\{N(SiHMe_2)(SiMe_2\text{-DMAP})\}H]^+$ [**9.19**]$^+$	0.95	118[b]	-63.6	-0.6
$[Cp_2Zr\{N(SiHMe_2)(SiMe_2\text{-DMAP})\}Cl]^+$ [**9.20**]$^+$	3.04	155	-34.2	5.7
$[Cp_2Zr\{N(SiHMe_2)(SiMe_2py)\}OTf]^+$ [**9.25**]$^+$	1.27	115	-24.0	14.4
$[Cp_2Zr\{N(SiHMe_2)(SiMe_2\text{-DMAP})\}OTf]^+$ [**9.26**]$^+$	1.37	115	-26.6	7.7
$[Cp_2Zr\{N(SiHMe_2)(SiMe_2\text{-}OPEt_3)\}OTf]^+$ [**9.27**]$^+$	1.35	115	-29.1	2.4

[a]All compounds are $[HB(C_6F_5)_3]$ salts unless otherwise noted. [b]Acquired at -88 °C.

The upfield SiH chemical shifts and $^1J_{SiH}$ values for both salts of [**9.12**]$^+$ provide support for the non-classical structure. The ^{29}Si NMR resonances at 21.4 ppm ($SiMe_2OTf$) and -25.9 ppm ($SiHMe_2$) were assigned by ^{1}H-^{29}Si HMBC experiments. For comparison, the Me_3SiOTf ^{29}Si NMR chemical shift is +43.5 ppm and the $Me_2(Et_2N)_2SiOTf$ ^{29}Si NMR chemical shift is -19.[29]

X-ray quality crystals of [**9.12**][$HB(C_6F_5)_3$] were obtained from a concentrated bromobenzene solution layered with pentane cooled to -30 °C. A single crystal X-ray diffraction study shows the OTf^- is bridging between Zr and a β-Si center (Figure 9.3). In addition, there is a short Zr1-Si2 distance of 2.89 Å, respectively. The Zr1-H1g distance (of the nonclassical SiH) of 2.20(3) Å is in between the related distances in neutral **9.1** and cationic **9.2**. However, [**9.12**]$^+$ does not display the other unusual structural features of [**9.2**]$^+$, namely the Si1-N1-Si2 angle is normal (127.7(2)°) and the Zr1-Si1 distance is long (3.59 Å). Thus, the features of the Zr←H-Si structure are in between those of neutral **9.1** and [**9.2**]$^+$.

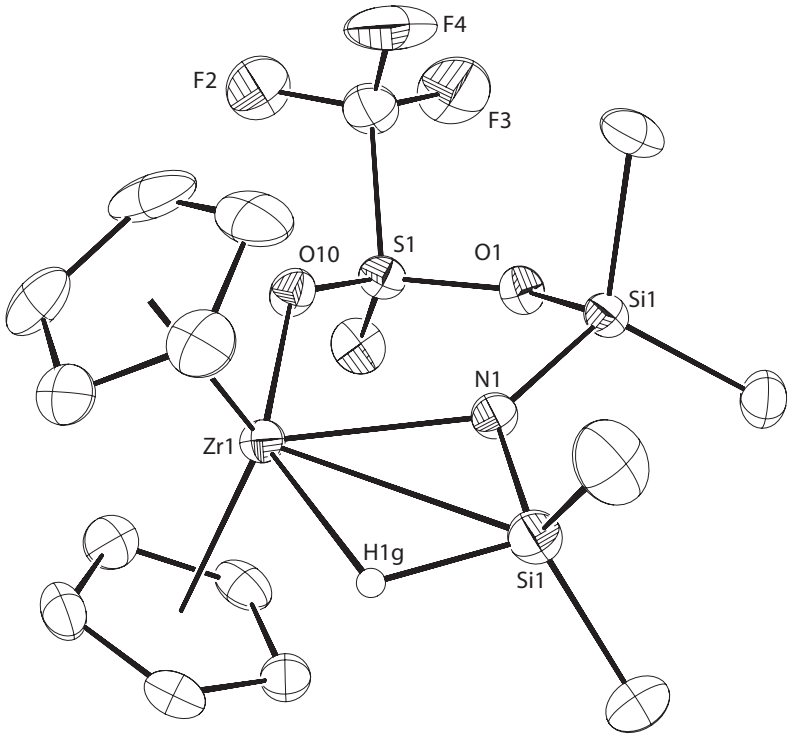

Figure 9.3. ORTEP diagram of [$Cp_2ZrN(SiHMe_2)(SiMe_2$-μ-κ^2-OTf)][$HB(C_6F_5)_3$] ([**9.12**][$HB(C_6F_5)_3$]). The cationic portion of the structure is illustrated, and only the bridging hydrogen atom is plotted. All other hydrogen atoms, the $HB(C_6F_5)_3$ counterion, and a disordered C_6H_5Br molecule are not included for clarity.

In addition, the Zr1-O10 distance of 2.313(2) Å is slightly longer than the Zr-OTf distance in $[Cp_2Zr(\kappa^1\text{-OTf})(\mu\text{-H})]_2$ (2.205(2) Å).[30] The Si1-O1 distance of 1.788(2) Å is within the sum of covalent radii.[31] These distances, the ^{29}Si NMR chemical shift of the SiOTf center, and the short Zr-H and Zr-Si distances argue for greater positive charge localization on Zr rather than on the Si center.

Similarly, reaction of $Cp_2Zr\{N(SiHMe_2)_2\}Cl$ and $B(C_6F_5)_3$ gives $[Cp_2ZrN(SiHMe_2)(SiMe_2\text{-}\mu\text{-Cl})]^+$ ([**9.14**][$HB(C_6F_5)_3$]) via β-hydrogen abstraction. The ^{29}Si NMR chemical shift for the $SiMe_2Cl$ moiety is 29.6 ppm; for comparison the value for Me_3SiCl is 30.2 ppm,[32] and the value for Me_2NSiMe_2Cl is 13.9 ppm.[33]

Finally, reactions of **9.1** and paraformaldehyde or acetone provide the alkoxide (disilazido)zirconium compounds $Cp_2Zr\{N(SiHMe_2)_2\}OR$ (R = Me (**9.15**); $CHMe_2$ (**9.16**)). Notably, reactions of **9.1** and excess ketone or aldehyde do not involve insertion into Si-H bonds in the $N(SiHMe_2)_2$ group under these conditions. The bonding of the $N(SiHMe_2)_2$ group in neutral $Cp_2Zr\{N(SiHMe_2)_2\}OR$ is classical, as evidenced by downfield SiH chemical shifts (δ 4.71 and 4.77), high SiH coupling constants ($^1J_{SiH}$ = 180 and 182 Hz), and high energy ν_{SiH} bands (**9.15**: 2078 cm^{-1}; **9.16**: 2113 and 2051 cm^{-1}). The structure is further supported by a single crystal X-ray diffraction study of **9.16**.[34] The ∠Zr1-N1-Si1 and ∠Zr1-N1-Si2 angles are 121.4(1) and 122.2(1)° , respectively; the Zr1-Si1 and Zr1-Si2 distances are 3.37 Å and 3.38 Å. In addition, the Zr1-O1 distance is 1.937(2) Å while the O1-Si1 distance is 3.35 Å.

The reactions of methoxyzirconium **9.15** and $B(C_6F_5)_3$ or $[Ph_3C][B(C_6F_5)_4]$ provide $[Cp_2ZrN(SiHMe_2)(SiMe_2\text{-}\mu\text{-OMe})]^+$ [**9.17**]$^+$. Likewise, the reactions of isopropoxyzirconium

9.16 and $B(C_6F_5)_3$ or $[Ph_3C][B(C_6F_5)_4]$ yield $[\mathbf{9.18}]^+$ (Scheme 9.4). Compounds $[\mathbf{9.17}]^+$ and $[\mathbf{9.18}]^+$, remarkably, also feature spectroscopic features associated with nonclassical Zr-H-Si structures. This, perhaps, is most notable because the neutral precursors **9.15** and **9.16** contain only 2c-2e SiH moieties. Abstraction of a β-hydrogen and formation of a Zr-O-Si bridging interaction might be expected to geometrically limit possible Zr-H-Si interactions. Instead, the structure of $[Cp_2ZrN(SiMe_2OCHMe_2)_2]^+$ suggests that the $N(SiMe_2OCHMe_2)$ moiety is best described as a β-silylether, and this permits a long Zr-O distance (see below). Overall, the addition of Lewis acids to $Cp_2Zr\{N(SiHMe_2)_2\}X$-type compounds results in β-hydrogen abstraction and Si-X bond formation, accompanied by the formation of nonclassical Zr←H-Si structures.

Reactions with Lewis bases. Hydride migration.

Interestingly, the cationic disilazide compounds $[\mathbf{9.2}]^+$ reacts with 4-dimethylaminopyridine (DMAP) to give $[Cp_2ZrH\{N(SiHMe_2)(SiMe_2DMAP)\}]^+$ ($[\mathbf{9.19}]^+$; X = $HB(C_6F_5)_3$, $B(C_6F_5)_4$) (eq 9.4); the product contains only one β-Si-H→Zr and a new zirconium hydride.

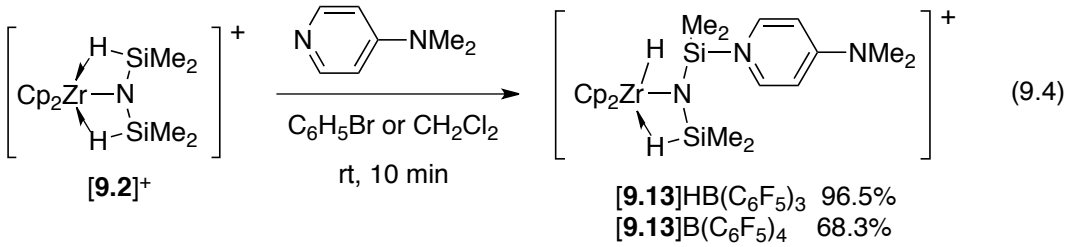

$[\mathbf{9.2}]^+$

$[\mathbf{9.13}]HB(C_6F_5)_3$ 96.5%
$[\mathbf{9.13}]B(C_6F_5)_4$ 68.3%

(9.4)

A ^1H NMR spectrum acquired at room temperature in methylene chloride-d_2 was slightly broad but the $SiMe_2$ groups (0.51 and 0.21 ppm), ZrH (4.43 ppm), SiH (1.27 ppm), and aromatic (pyridine) CH resonances (7.93 and 6.78 ppm) were readily assigned. The

resonances assigned to the C_5H_5 (5.81 ppm) and NMe_2 (3.21 ppm) were sharp (all assignments are supported by COSY experiments, chemical shift, and integration). However, we were unable to detect ^{29}Si NMR resonances at room temperature using ^{29}Si INEPT experiments.

The low temperature NMR spectra of [**9.19**]$^+$ were sharper and better resolved. At 185 K, two ^{29}Si resonances were observed at -0.5 and -63.6 ppm. Only the signal at -63.6 ppm ($^1J_{SiH}$ = 118 Hz) was observed in a ^{29}Si INEPT experiment optimized for J_{SiH} = 120 Hz, and the signal at -0.5 ppm was only detected in a ^{29}Si INEPT experiment optimized for long range proton coupling (J_{SiH} = 7 Hz). In a ^{1}H-^{29}Si HMBC experiment optimized for long range ^{1}H-^{29}Si coupling (J_{SiH} = 7 Hz) shown in Figure 9.2, the -63.6 ppm ^{29}Si resonance was correlated with a ^{1}H NMR signal at 0.21 ppm assigned to a $SiMe_2$. In that experiment, crosspeaks from the ^{29}Si signal at -0.5 were correlated to a second $SiMe_2$ (0.51 ppm), the signal at 3.95 ppm (1 H) assigned to the ZrH, and the aromatic resonances assigned to DMAP (7.93 ppm). The correlations between the silicon atom and the aromatic signals provide convincing evidence that DMAP is coordinated to silicon rather than zirconium. Further evidence for Si-N bond formation is the ^{1}H-^{15}N HMBC experiments that showed a correlation between the pyridine nitrogen and the $SiMe_2$ at 0.51 ppm. We assign the ^{1}H NMR signal at 3.95 to a zirconium hydride based on a correlation in a COSY experiment between that signal and the resonance at 0.95 ppm assigned to a β-Si-H→Zr. The extent of interaction between the ZrH and the silicon center in the $SiMe_2$DMAP group is considerably less than in [**9.2**]$^+$ ($^1J_{SiH}$ = 89 Hz). The chemical shift of 3.95 ppm is upfield relative to the signal for the zirconium hydride in **9.1** (5.60 ppm). However, zirconium hydrides have been assigned to signals at 3.12-3.61 ppm in $Cp_2Zr(H)NH_2BH_3$.[35] Although spectra were obtained for [**9.19**]$^+$

in methylene chloride-d_2, after solutions are heated to 120 °C for 45 min in that solvent, a reaction occurs to provide $[Cp_2Zr\{N(SiMe_2DMAP)(SiHMe_2)\}Cl]^+$ ([**9.20**]$^+$). The identity of [**9.20**]$^+$ is supported by its independent synthesis (see below).

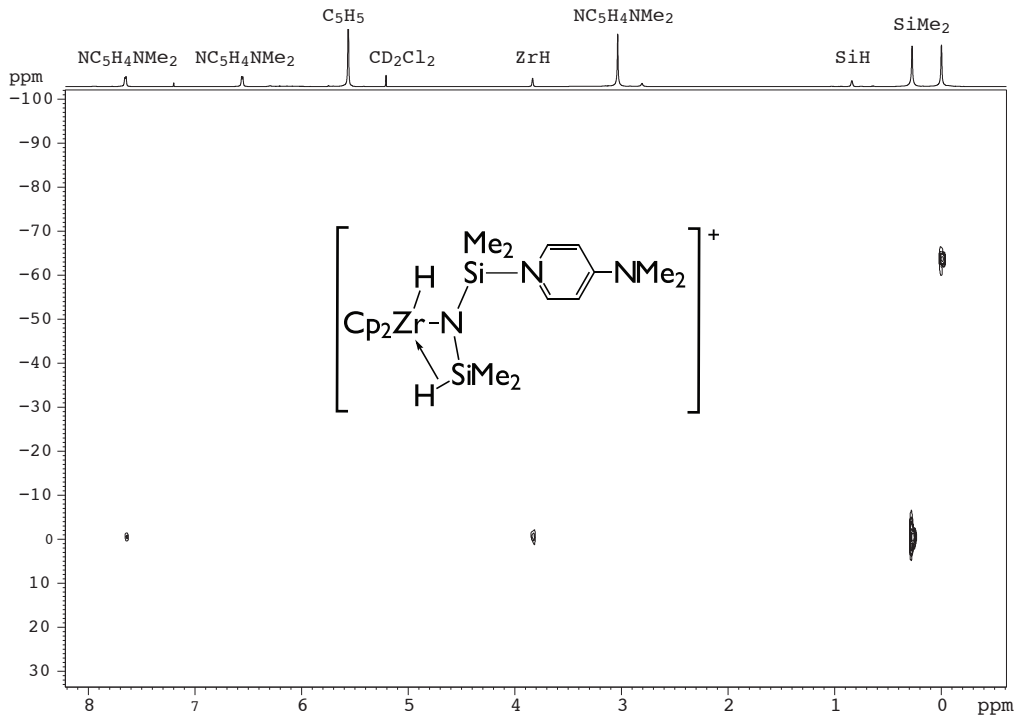

Figure 9.2. ^{1}H-^{29}Si HMBC experiment on $Cp_2Zr\{N(SiHMe_2)(SiMe_2DMAP)\}[HB(C_6F_5)_3]$ [**9.19**][$HB(C_6F_5)_3$] in methylene chloride-d_2 optimized for J_{SiH} = 7 Hz and acquired at 185 K. The experiment is optimized for long-range bonding, so there is no crosspeak for the SiH; the crosspeak between ZrH and SiMe$_2$DMAP shows small scalar coupling.

The broad, room temperature ^{1}H NMR spectrum for compound [**9.3**]$^+$ suggests a fast exchange process involving the silyl groups, the zirconium hydride and DMAP. In an EXSY experiment performed at room temperature, a crosspeak between the $SiMe_2$ and $SiHMe_2$ groups and a crosspeak between ZrH and SiH showed exchange involving hydrogen transfer

between Zr and both silicon centers. However, this fast exchange process significantly slows down at low temperature.

In contrast, reactions of [**9.2**]$^+$ and triethylphosphine oxide afford [$Cp_2Zr\{N(SiHMe_2)_2\}OPEt_3$]$^+$ ([**9.21**]$^+$, eq 9.5).

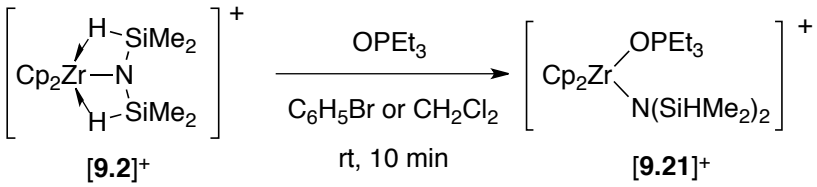

[**9.2**]$^+$ [**9.21**]$^+$ (9.5)

The structure of [**9.21**]$^+$ is readily distinguished from the DMAP adduct [**9.19**]$^+$ by NMR spectroscopy. In the ^{1}H NMR spectrum of [**9.21**]$^+$, a single resonance assigned to equivalent SiMe groups was observed at 0.11 ppm ($^3J_{HH}$ = 4.2 Hz; 12 H), and a signal at 4.09 ppm ($^1J_{SiH}$ 181.8 Hz; 2 H) was assigned as a SiH based on its correlation to the $SiMe_2$ signal in a COSY experiment. The typical chemical shift and $^1J_{SiH}$ value suggests that [**9.21**]$^+$ contains terminal silicon hydride groups. A single ^{29}Si NMR signal was detected at -19.2 ppm. In addition, compound [**9.19**]$^+$ and $OPEt_3$ react to give [**9.21**]$^+$ and free DMAP, while starting materials are observed in the reaction of [**9.21**]$^+$ and DMAP.

Based on the interesting results in reactions of [**9.2**]$^+$ with two electron donors, we also examined reactions of [**9.18**]$^+$ with coordinating ligands. The reaction of [**9.18**]$^+$ with DMAP in CH_2Cl_2 forms [$Cp_2ZrH\{N(SiMe_2OCHMe_2)(SiMe_2DMAP)\}$]$^+$ (**9.22**; Scheme 9.5).

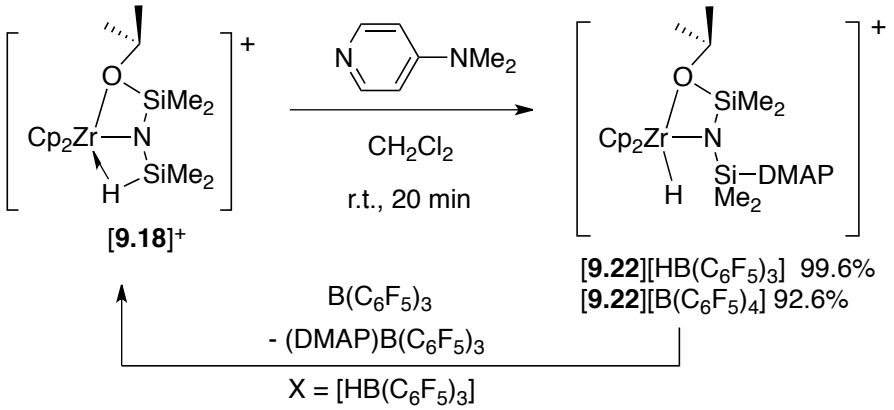

Scheme 9.5. Reversible hydrogen migration between Zr and Si is controlled by the addition or removal of a two-electron donor.

In contrast to the NMR spectroscopy of [**9.3**]$^+$, the ^{1}H, ^{13}C and ^{29}Si NMR spectra of [**9.22**]$^+$ were sharp at room temperature. The ^{1}H NMR resonances of the ZrH, $SiMe_2$DMAP and $SiMe_2OCHMe_2$ of [**9.27**][$HB(C_6F_5)_3$] were observed at 4.44 (1 H), 0.39 (6 H) and -0.06 ppm (6 H), respectively. Coordination of DMAP to the silicon center was supported by crosspeaks between the ^{1}H NMR signals of DMAP and a $SiMe_2$ group in a COSY experiment. In contrast, the ZrH signal at 4.44 ppm did not show any correlation to either $SiMe_2$ signal in COSY experiments. Two ^{29}Si NMR resonances were detected at 16.6 and -11.0 ppm with INEPT experiments. ^{1}H-^{29}Si HMBC experiments (optimized for J_{SiH} = 7 Hz) contained crosspeaks between the ^{29}Si signal at 16.6 ppm and the resonances assigned to one $SiMe_2$, the OC*H*Me_2 and the ZrH; the upfield ^{29}Si resonance (-11.0 ppm) was correlated to the other Si*Me*$_2$, the ZrH and the α-CH protons of the DMAP. The latter crosspeak supports the structural assignment involving a DMAP-silicon interaction. Moreover, the long-range correlations between the Zr-H proton and *both* Si atoms ($SiMe_2$DMAP and $SiMe_2OCHMe_2$) in the ^{1}H-^{29}Si HMBC experiment provides support for a Zr-H that is formed via DMAP-induced hydrogen elimination.

Interestingly, this migration is reversible. Addition of $B(C_6F_5)_3$ to a methylene chloride solution of [**9.22**][$HB(C_6F_5)_3$] provides [**9.18**][$HB(C_6F_5)_3$] and (DMAP)$B(C_6F_5)_3$.

Furthermore, compound [**9.22**]$^+$ reacts similarly to related zirconium hydride **9.1**, as well as $Cp_2Zr\{N(SiMe_3)_2\}H$, by undergoing γ-hydrogen abstraction.[15,36] Thus, thermolysis of [**9.22**]$^+$ in a sealed glass tube at 140 °C for 4 h affords H_2 and [$Cp_2ZrN(SiMe_2OCHMe_2)SiMe(DMAP)CH_2$]$^+$ ([**9.23**]$^+$; eq 9.6).

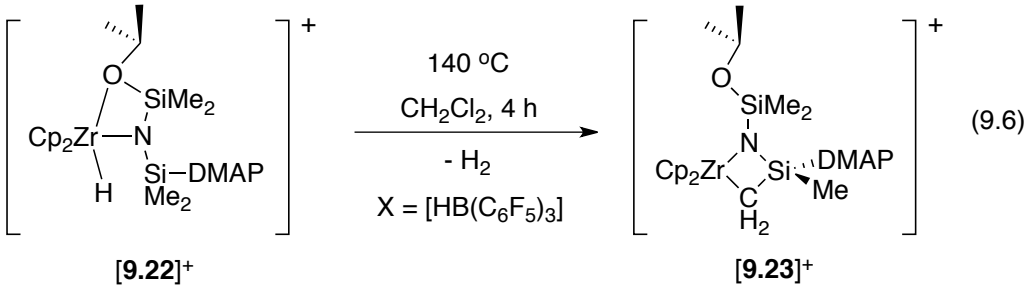

[**9.22**]$^+$ [**9.23**]$^+$ (9.6)

The ^{1}H NMR spectrum of [**9.23**]$^+$ contained signals assigned to a diastereotopic isopropyl group (1.32 ppm, $^3J_{HH}$ = 6.1 Hz; 1.29 ppm, $^3J_{HH}$ = 6.1 Hz) and a diastereotopic $ZrCH_2$ (1.14 ppm, $^2J_{HH}$ = 13.4 Hz; 0.95 ppm, $^2J_{HH}$ = 13.3 Hz), as well as three SiMe signals (0.44, 0.17, and 0.14 ppm). ^{1}H-^{29}Si HMBC experiment revealed correlations from the chiral Si center to the aromatic α-CH proton of DMAP and the diastereotopic CH_2, which unambiguously confirms the connectivity between $ZrCH_2$*Si* and DMAP.

As in the reaction of [**9.2**]$^+$ and $OPEt_3$, phosphine oxide coordinates to the zirconium center in [**9.18**]$^+$ to give [$Cp_2Zr\{N(SiHMe_2)(SiMe_2OCHMe_2)\}OPEt_3$]$^+$ ([**9.24**]$^+$; eq 9.7). The NMR spectroscopy of [**9.24**]$^+$, particularly the SiH (d 4.04, $^1J_{SiH}$ = 187 Hz) distinguishes its connectivity from the silicon-coordinated DMAP [**9.22**]$^+$.

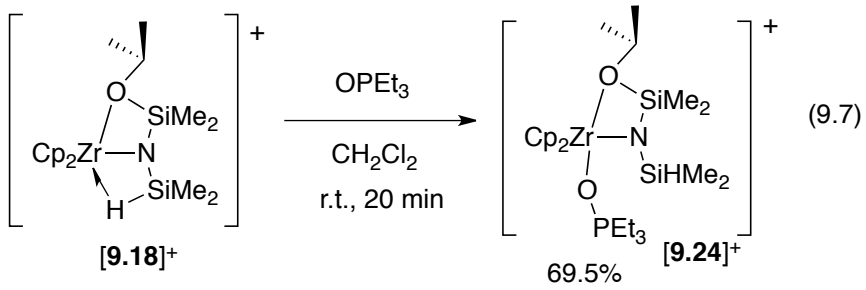

In a COSY experiment, the ^{1}H NMR resonance at 0.12 ppm (6 H) assigned to the $SiMe_2$ correlated with the SiH resonance at 4.04 ppm. Two ^{29}Si resonances were detected in ^{29}Si INEPT and ^{1}H-^{29}Si HMBC experiments at -5.1 and -21.9 ppm. In the latter experiments, crosspeaks between the ^{29}Si resonance at -5.1 ppm and the methine proton (3.74 ppm) of the $OCHMe_2$ group and $OSiMe_2$ protons (0.06 ppm, 6 H) provided evidence for Si-O-C linkage in the $SiOCHMe_2$ moiety.

Halide and pseudo halide migration

Reactions of [**9.12**]$^{+}$ with DMAP, pyridine or $OPEt_3$ result migration of OTf^{-} to zirconium to provide the series of compounds $[Cp_2Zr\{N(SiHMe_2)(SiMe_2L\}OTf]^{+}$ (L = py ([**9.25**]$^{+}$), DMAP ([**9.26**]$^{+}$); $OPEt_3$ ([**9.27**]$^{+}$), eq 9.8).

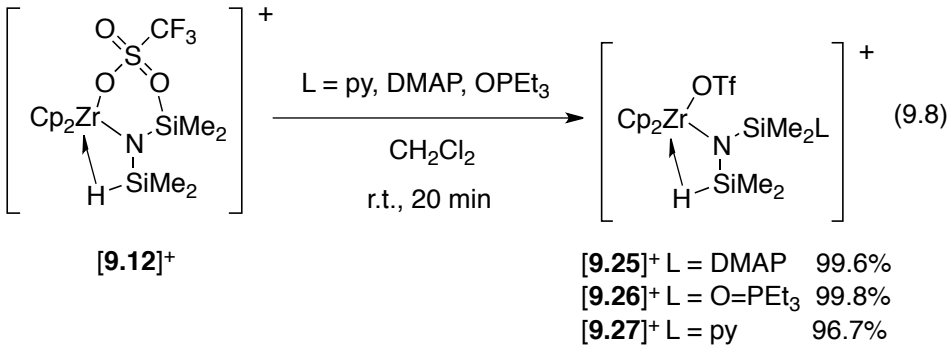

The ^{1}H NMR spectra of [**9.25**]$^{+}$, [**9.26**]$^{+}$, and [**9.27**]$^{+}$ contain resonances in the region 1.27-1.37 ppm assigned to SiH groups; the upfield chemical shift and the $^{1}J_{SiH}$ values of 115

Hz establish the nonclassical Zr-H-Si structures. ^{1}H-^{29}Si HMBC experiments revealed two silicon signals for [**9.16**]$^{+}$-[**9.18**]$^{+}$; correlations between the further downfield signals and aromatic resonances of pyridine and DMAP established Si-L bond formation. These correlations are not available for $OPEt_3$, and in that case we relied on the similarity in other spectral features of [**9.27**]$^{+}$ with [**9.25**]$^{+}$ and [**9.26**]$^{+}$. The upfield ^{29}Si NMR resonances correlated in ^{1}H-^{29}Si HMBC experiments to the upfield ^{1}H NMR peaks assigned to the SiH in [**9.16**]$^{+}$-[**9.18**]$^{+}$. The ^{19}F NMR chemical shifts of the signals assigned to OTf^{-} for compounds [**9.25**]$^{+}$-[**9.27**] varied only 0.3 ppm from -78.5 to -78.8 ppm, whereas the signal for bridging OTf^{-} in [**9.12**]$^{+}$ appears at -75.0 ppm. The monodentate OTf^{-} in **9.11** is -78.2 ppm. Thus, of three possible outcomes that include coordination to zirconium, coordination to silicon with hydrogen migration, and coordination to silicon with OTf^{-} migration, the observed products are consistent with the last pathway.

Likewise, reaction of [**9.14**]$^{+}$ and DMAP gives $Cp_2Zr\{N(SiHMe_2)(SiMe_2DMAP)\}Cl]^{+}$ ([**9.20**]$^{+}$). Interestingly, [**9.20**]$^{+}$ is also prepared quantitatively through the thermolysis of [**9.19**]$^{+}$ in methylene chloride. Similarly, reaction of [**9.19**]$^{+}$ and MeOTf gives [**9.26**]$^{+}$ and methane.

Synthesis of cationic $[Cp_2ZrN(SiMe_2OR)_2]^{+}$.

The implications of the nonclassical structure of [**9.2**]$^{+}$ on reactivity was further explored with carbonyl reagents. Compound [**9.2**]$^{+}$ and 2 equiv of paraformaldehyde react at 80 °C in bromobenzene to yield $[Cp_2ZrN(SiMe_2OMe)_2]^{+}$ ([**9.28**]$^{+}$) (eq 9.9).

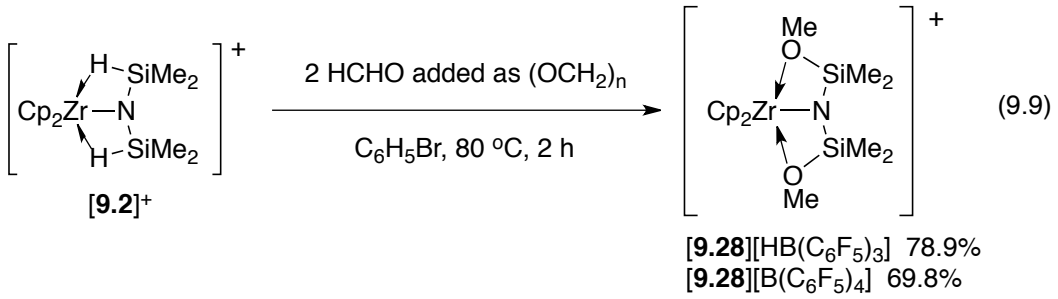

[**9.2**]$^+$

[**9.28**][$HB(C_6F_5)_3$] 78.9%
[**9.28**][$B(C_6F_5)_4$] 69.8%

In the ^{1}H NMR spectrum of [**9.28**]$^+$, a resonance at 2.99 ppm (3 H) in the ^{1}H NMR spectrum is characteristic of a methoxy group. A single ^{29}Si NMR signal at 9.6 ppm was observed that is >50 ppm further downfield than the corresponding resonance at -43 ppm in the starting material [**9.2**]$^+$. The formation of a SiOMe group was unambiguously supported by a ^{1}H-^{29}Si HMBC experiment that contained a crosspeak between the methoxy group and the silicon center. The methoxy group, however, is likely bridging silicon and zirconium, as shown below in the structure of $[Cp_2ZrN(SiMe_2OCHMe_2)_2]^+$.

The preparation of [**9.28**]$^+$ requires elevated temperature to dissolve and depolymerize paraformaldehyde. In contrast, the reaction of [**9.2**]$^+$ and 2 equiv of acetone occurs within 10 min at room temperature in bromobenzene or methylene chloride to give $[Cp_2ZrN(SiMe_2OCHMe_2)_2]^+$ ([**9.29**]$^+$) (Scheme 9.6).

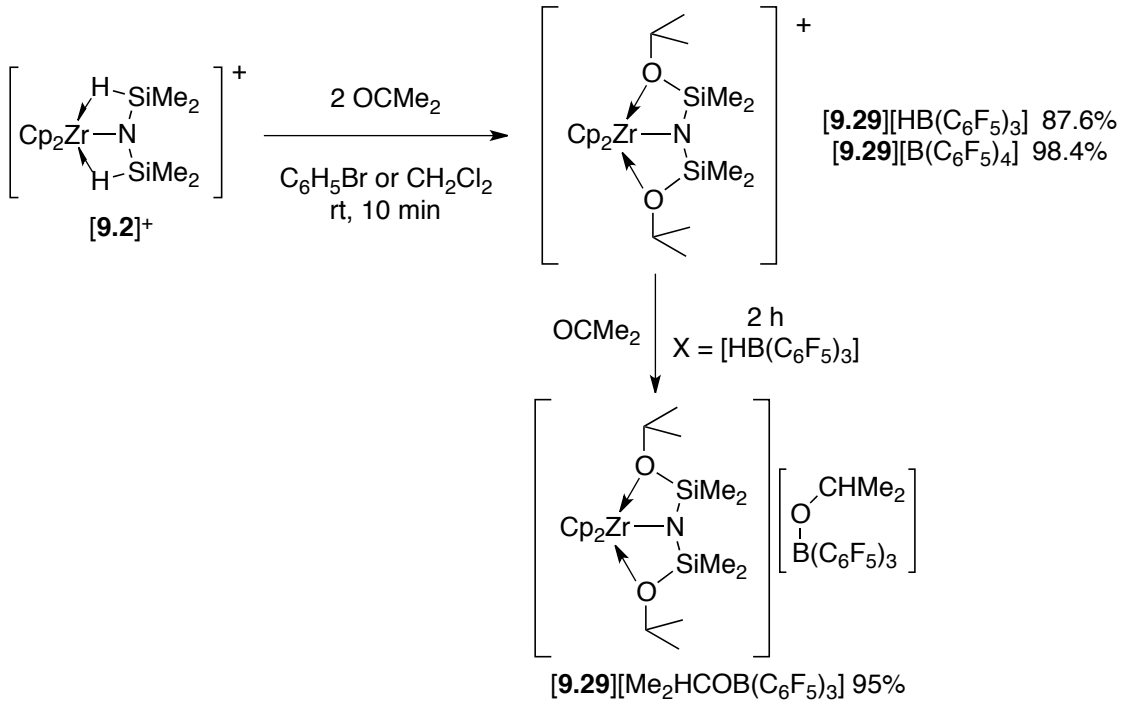

Scheme 9.6. Hydrosilylation of [**9.2**]$^+$ with acetone, followed by slower hydroboration of acetone with $HB(C_6F_5)_3^-$.

The ^{1}H NMR spectrum of [**9.29**]$^+$ contained a multiplet at 4.14 ppm (2 H) and a doublet at 1.51 ppm ($^3J_{HH}$ = 6.5 Hz, 12 H) that are characteristic of the isopropoxy group. One ^{29}Si resonance was detected by ^{29}Si INEPT experiments at 5.2 ppm, and this signal correlated to ^{1}H NMR signals of the $SiMe_2$ (12 H) and the OC*H*Me_2 in ^{1}H-^{29}Si HMBC experiments. Thus, the spectroscopy unambiguously identified the $SiOCHMe_2$ moiety.

X-ray quality crystals of [**9.29**][$HB(C_6F_5)_3$] are obtained from a concentrated methylene chloride solution cooled to -30 °C. Hydrosilylation of the acetone is confirmed, and the resulting isopropoxy groups bridge between the silicon and zirconium centers. The Zr1-O1 and Zr1-O2 distances of 2.385(4) and 2.333(3) Å are similar to other distances in three-coordinated oxygen centers bonded to silicon and zirconium where the O center is unambiguously described as an L-type ligand,[37] such as $\{(C_6H_{11}NSiMe_2)_2O\}Zr(CH_2Ph)_2$

which feature a Zr-O distance of 2.381(2) Å.[38] The Si1-O1 and Si2-O2 distances of 1.711(4) and 1.699(4) are slightly longer than the distances in that compound. For comparison, the Zr-O distance in neutral $Cp_2Zr\{N(SiHMe_2)_2\}OCHMe_2$ (**9.16**) is 1.937(2) Å,[32] while the Zr-O and Si-O distances in $Cp_2Zr(OSiMe_2CH_2Cl)Cl$ are and 1.943(3) and 1.609(3) Å, respectively.[39] Based on these structural comparisons, [**9.22**]$^+$ is probably best described as a $N(SiMe_2OCHMe_2)_2$ tridentate L_2X-type ligand coordinated to the Zr center through an amide and two silyl ether groups.

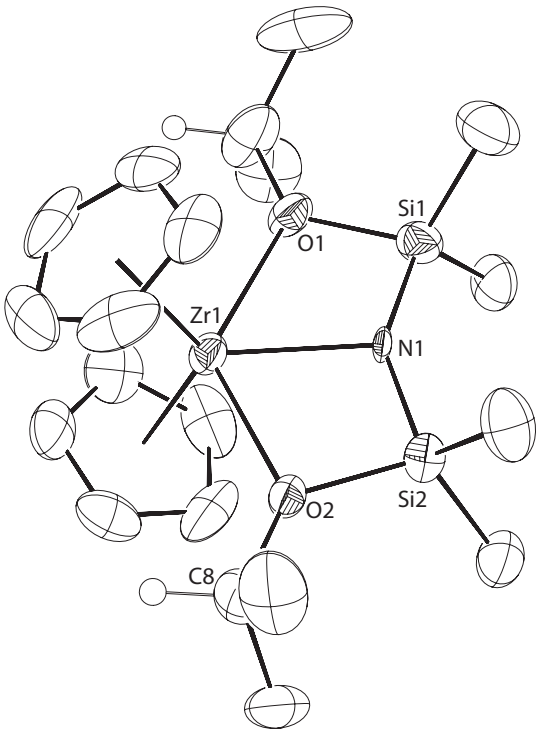

Figure 9.3. ORTEP diagram of the cationic portion of [**9.22**]$^+$ with ellipsoids plotted at 50% probability. The $HB(C_6F_5)_3$ and a CH_2Cl_2 solvent molecule are not illustrated. The hydrogen on the C_5H_5 and methyl groups are not shown for clarity. Significant interatomic distances (Å): Zr1-N1, 2.121(4); Zr1-O1, 2.385(4); Zr1-O2, 2.333(3); N1-Si1, 1.642(4); N1-Si2, 1.712(4); Si1-O1, 1.711(4); Si2-O2, 1.699(4). Selected interatomic angles (°): Zr1-N1-Si1,

108.5(2); Zr1-N1-Si2, 104.88(19); Si1-N1-Si2, 146.6(2); O1-Zr1-O2, 130.65(12); Zr1-N1-Si1-O1, -1.4(2); Zr1-N1-Si2-O2, -2.3(2), O1-Si1-Si2-O2. -4.0(2).

Addition of excess acetone (> 3 equiv) to [**9.2**][$HB(C_6F_5)_3$] yields [$Cp_2ZrN(SiMe_2OCHMe_2)_2$][($Me_2HCOB(C_6F_5)_3$] ([**9.29**][$Me_2HCOB(C_6F_5)_3$]) over 2 h (Scheme 9.6). The formation of [**9.22**][$HB(C_6F_5)_3$] as an intermediate occurs within 5 min, followed by slow conversion of [$HB(C_6F_5)_3$] into [$Me_2HCOB(C_6F_5)_3]^-$. The ^{1}H NMR spectrum of [**9.29**][$Me_2HCOB(C_6F_5)_3$] contained two sets of isopropoxy resonances in a 2:1 ratio assigned to the Me_2HCOSi (1.51 ppm, $^3J_{HH}$ = 6.5 Hz; 4.14 ppm) and the Me_2HCOB (0.88 ppm, $^3J_{HH}$ = 5.9 Hz; 3.60 ppm). Furthermore, the resonance in the ^{11}B NMR spectrum at -3.4 is characteristic of formation of an alkoxyborate moiety.[40] Interestingly, the rate of insertion to non-classical SiH group (10 min) is much faster than B-H bond (2 h). Furthermore, conversion of [$HB(C_6F_5)_3$] in [**9.29**]$^+$ into the [$Me_2HCOB(C_6F_5)_3$] anion is not detected in the absence of excess acetone.

Discussion

9.1. Migrations from Zr to Si

The migration of an anionic group (H, alkyl, halide, triflate, alkoxide) from zirconium to a β-silicon center can be described as an X-group abstraction by a transient cationic β-silylium electrophile generated by hydrogen abstraction of a β-hydrogen by a Lewis acid. This description is based on a resonance structure of the transient where charge is localized on silicon center (Scheme 9.7, structure I.A.). Additionally, silylium cations are known as strong Lewis acids in hydride and halide abstractions.[41]

An alternative resonance structure of the cationic transient shows localization of charge on the electropositive Zr center, in which case the intermediate is described as a cationic zirconium-coordinated silanimine complex (Scheme 9.7, I.B.). Notably, reactions of β-SiH containing alkyl moieties $MC(SiHMe_2)_3$ and $B(C_6F_5)_3$ produce $M\text{-}H\text{-}B(C_6F_5)_3$ and disilacyclobutane (Scheme 9.7, II.).[42] The latter species is postulated to form via 2π+2π cyclodimerization of the silene intermediate that forms upon β-hydrogen abstraction. Likewise, reactions of $M\text{-}N(SiHMe_2)_2$ and $B(C_6F_5)_3$ afford $M\text{-}H\text{-}B(C_6F_5)_3$ and diazadisilacyclobutane, where the reactive silanimine undergoes 2π+2π cyclodimerization.[43] Furthermore, abstraction of a β-hydrogen from an alkyl ligand in $Cp_2Zr\{N(SiHMe_2)_2\}R$ provides the olefin, as noted above. The intermediacy of a coordinated $Me_2Si{=}NSiHMe_2$ in the present system is thus supported by the selective dimerization observed in the absence of a reactive M-X group.

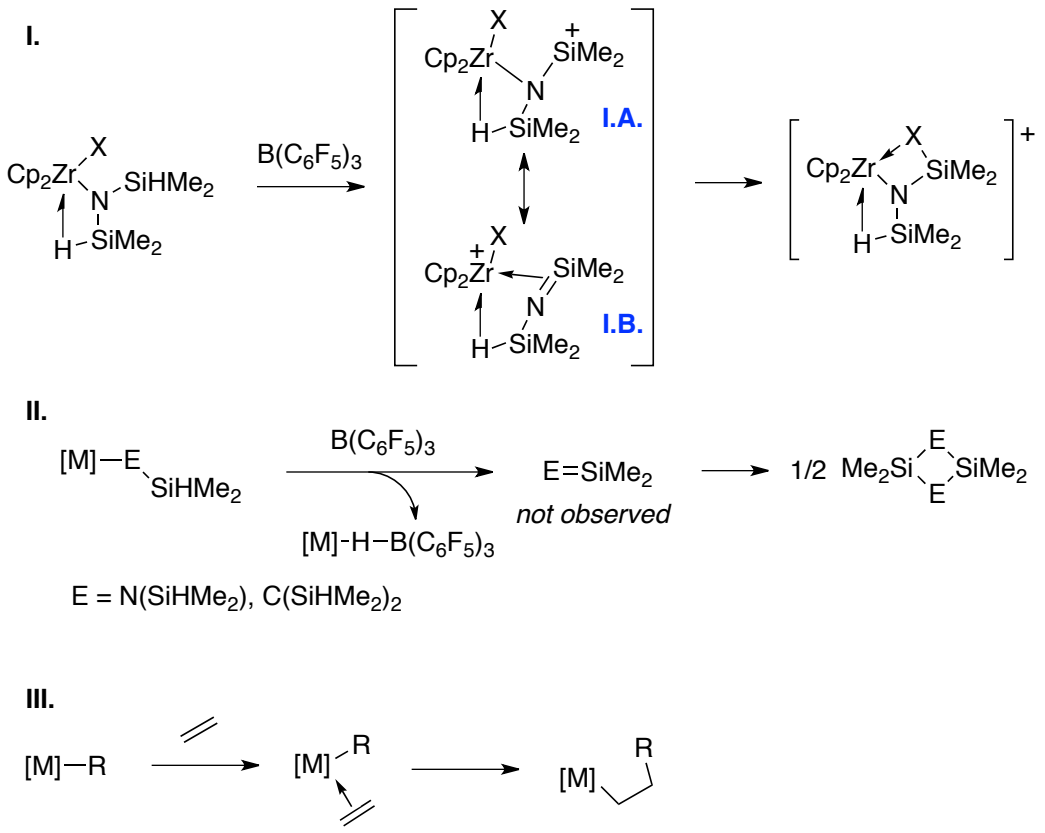

Scheme 9.7. Comparisons between (I) borane-induced X-group migration through a silanimine, (II) β-hydrogen abstraction to generate transient R'N=SiR_2 or $Me_2Si=C(SiHMe_2)_2$, and (III) insertion of an olefin into a M-C bond.

In addition, both 1,1-insertions and 1,2-insertions are better described as migrations of a X-type ligand to an electrophilic, metal-coordinated carbon center (Scheme 9.7, III.), as evidenced by stereochemical studies of insertion reactions.[44,45] Thus, formation of Si-X bonds from the polarized silanimine/silylium in $[Cp_2Zr\{N(SiMe_2)(SiHMe_2)\}]^+$ is best understood with both resonance structures that highlight polarization of unsaturated moieties as an important component of insertion reactions.

The influence of the alkyl group R on reactions of $Cp_2Zr\{N(SiHMe_2)_2\}R$ and Lewis acids provides data to compare the interpretation of abstraction. In these reactions, four

pathways may be postulated based on structures of the products: a) alkyl group abstraction by the Lewis acid; b) β-hydrogen abstraction from the alkyl group; c) β-hydrogen abstraction from the disilazido group followed by β-hydrogen abstraction by the transient silylium electrophile; and d) β-hydrogen abstraction from the disilazido group followed by alkyl group migration (Scheme 9.8).

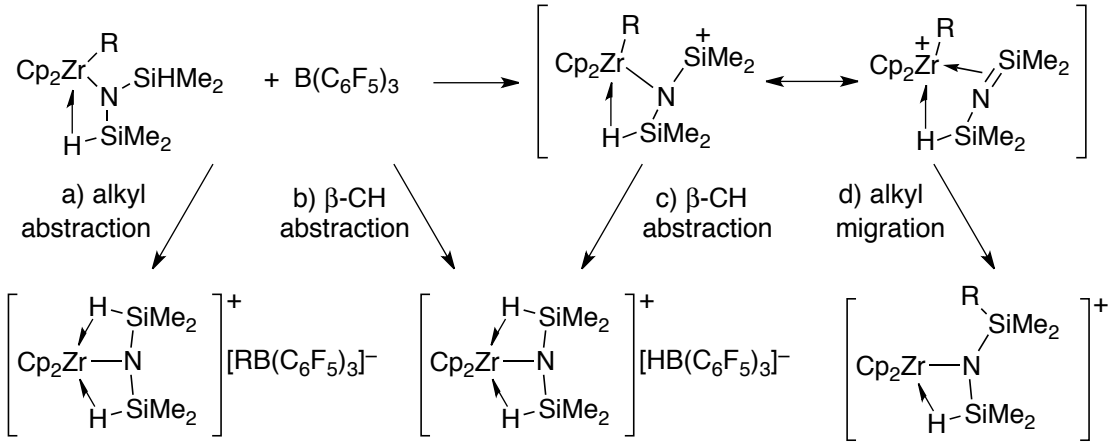

Scheme 9.8. Possible reaction pathways in the reactions of $Cp_2Zr\{N(SiHMe_2)_2\}R$ and $B(C_6F_5)_3$.

With larger R groups (e.g., *n*-C_3H_7) the pathway that provides Si-C bond formation (alkyl migration) is the most favored, and alkyl group abstraction products (pathway a) are not detected. β-CH abstraction (pathways b and c) as a minor pathway is evident by the formation of [**9.2**]$^+$ and the corresponding olefin. It is important that alkyl group migration is favored over β-CH abstraction. The dominance of alkyl migration suggests that the silanimine resonance structure is a more important contributor than the silylium structure in Scheme 9.8; the latter would be expected to react by β-hydrogen abstraction because the well-defined Lewis acid $B(C_6F_5)_3$ reacts by β-hydrogen abstraction in this system.[26]

Related X-group migration was also observed for chloride, triflate, methoxide, and isopropoxide. In the final products, bridging Zr-X-Si structures are obtained. In these bridging compounds, the X group on X-$SiMe_2$ behaves as a L-type, two-electron donor to the electron-deficient Zr center. This assignment is supported by ^{29}Si NMR spectroscopy and X-ray diffraction studies of [**9.22**]$^+$.

In addition, a recent report documents a related $N(SiHMe_2)_2$ migration from a scandium center to a β-Si upon addition of a Lewis acid, and a similar sequential hydrogen abstraction/silazide migration sequence was proposed.[8] These similarities indicate that the reactivity pattern described in the current contribution is not simply limited to the Cp_2Zr-system.

9.2. Migrations from Si to Zr

The entry-points to the Si-to-Zr migration chemistry in all cases are bridging Si-X-Zr structures. DMAP induces migration of a monovalent group from silicon to the zirconium center. The migrating group may be hydrogen, alkoxide, chloride, or triflate. In the systems where both β-H and β-X (X = Cl, OTf) are present, migration of X rather than H is observed, whereas competition between β-H and β-OR results in hydrogen migration. Other nucleophilic ligands coordinate, such as $OPEt_3$ and pyridine, and the binding site varies between Si and Zr depending on the identity of the migrating X group. There are similarities in these donor-assisted migrations to β-elimination as well as to Lewis base-induced cleavage reactions. The comparison between β-elimination versus Lewis acid/base chemistry is evaluated through analogies to main group and transition-metal chemistry and through analysis of the microscopic reverse reaction.

A related Lewis-base induced hydride transfer is reported for the reaction of symmetrical hydrogen-bridged, cationic disilyl $[(\mu\text{-H})(Me_2Si(CH_2)_3SiMe_2]^+$ and acetonitrile that gives $[(Me_2HSi(CH_2)_3SiMe_2(NCMe)]^+$.[46]

In contrast to the $[Si\text{-}H\text{-}Si]^+$ system, the atoms in the bridging Zr←H-Si moieties are inequivalent. In these structures, a coordinating ligand may interact with the zirconium center or the silicon center and disrupt the M-H-Si interaction. These bridging structures, and their interactions with ligands, may be compared to bona fide M-H-LA adducts (LA = Lewis acid). In that case as a typical example, THF or pyridine binds to metal center rather than the LA center.[47]

It should also be noted that the nucleophilicity of a hydrosilane is proposed to be enhanced by coordination of a Lewis base such as F^-, for example, to facilitate the hydrosilylation of a carbonyl compound.[48]

Alternatively, rare earth metal tetraalkylaluminate adducts react with pyridine to form metal alkyls.[49,50] Although aluminum-pyridine adducts are formed in these reactions, both a [M]-Me bond and an [Al]-Me bond are broken during the transformation; in addition, both bridging methyl groups are engaged in electron-deficient bonding, and therefore elimination gives saturated products (as opposed to unsaturated products). While $[Cp_2ZrMe_2AlMe_2]^+$ are proposed to dissociate $AlMe_3$ to generate active $[Cp_2ZrMe]^+$ catalytic species, the only donors present in such polymerizations are olefins.[51] Additionally, a yttrium hydridoaluminate is converted to a $[Y(\mu\text{-H})]_2$ species in the presence of excess DIBAH.[52] That conversion occurs without an additional two-electron donor.

Thus, the present example of DMAP coordination to the β-silicon of the disilazido ligand is distinguished from typical Lewis base chemistry of bridging aluminates or borates.

Here, it should be noted that β-hydrogen elimination in transition-metal amido compounds is rare,[10] and β-eliminations of amides from d^0 transition-metal and rare earth centers are unknown. Still, there are also similarities in the present system to the β-elimination chemistry of transition-metal alkyls.[4a,11]

The unsaturated β-elimination products from reactions of low valent transition-metal alkyls are stabilized by two-electron π back-donation to give metallacyclopropyl resonance structures. In the cationic zirconium disilazido compounds, two electrons from DMAP serve as a surrogate for metal-based π back-donation to stabilize the silanimine (Scheme 9.9).

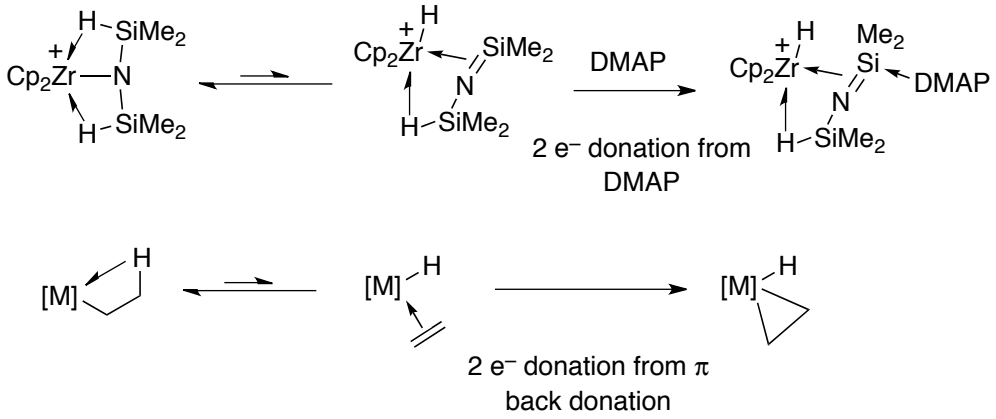

Scheme 9.9. Comparison of resonance structures for H migration products in (A) DMAP induced reactions and (B) low valent β-eliminations.

β-Hydrogen elimination and insertion into a M-H bond are related by the principle of microscopic reversibility. Likewise, this Si-to-Zr migration and its microscopic reverse of Zr-to-Si migrations are controlled by the addition of Lewis acids or Lewis bases. Thus, the zirconium hydride DMAP adduct [**9.22**]$^+$ and $B(C_6F_5)_3$ react to reform β-SiH-containing [**9.18**]$^+$ and (DMAP)$B(C_6F_5)_3$.

The migration of halide, alkoxide, and triflate from Si to Zr of Scheme 9.4 should also be considered in the context of abstraction vs. elimination. While the lone pair electrons on X argue for the Lewis acid model, several other comparisons are worth noting. First, β-Cl eliminations from metal chloroalkyls limit vinyl chloride polymerizations (indeed this reaction limits many transition-metal vinyl chloride eliminations).[53] Moreover, similar β-X elimination reactions were observed from $Cp^*_2ScCH_2CH_2X$ (X = PPh_2, OEt, F).[54] In these systems, as well as in the current cationic zirconium compounds, β-X elimination products are formed instead of β-H (at least as the isolated products).

Finally, it is remarkable that the non-classical Zr←H-Si interactions in [**9.2**]$^+$ reacts as if it is an intermediate on the reaction coordinate for β-hydrogen elimination. This comparison further reinforces the description of the reaction as a Lewis base mediated β-hydrogen elimination and highlights the similarities between these bridging SiH groups and β-agostic alkyls.

9.3. Carbonyl hydrosilylation.

Given the observations of hydrogen migration between silicon and zirconium centers, several pathways for the formation of silyl ethers from the carbonyl compounds may be considered. First, (Pathway A) a carbonyl oxygen may coordinate to the zirconium center, disrupting the nonclassical Zr←H-Si structure, as was observed in the interaction of [**9.2**]$^+$ and $OPEt_3$. Transfer of hydrogen to the carbonyl carbon, followed by alkoxide migration to silicon would then provide the hydrosilylated product. Alternatively, (Pathway B) the carbonyl may coordinate to the silicon center to induce migration of hydrogen from silicon to

form a ZrH, which subsequently is transferred to the carbon of the coordinated carbonyl. A third possible mechanism (Pathway C) again invokes the carbonyl-assisted ZrH formation, which is then followed by insertion of a second carbonyl into the ZrH bond to give a zirconium alkoxide. Dissociation of the coordinated carbonyl from the silicon center, followed by migration of the alkoxide to silicon, would then provide the product. In general, Lewis acid assisted hydrosilylation reactions involve hydrogen abstraction from silane, coordination of the carbonyl oxygen to a silylium center, and transfer of hydride from silicon to the resulting carbocation.[55] Note that the cationic components of complexes containing $[HB(C_6F_5)_3]^-$ or $[B(C_6F_5)_4]^-$ react similarly, and the hydroboration of the carbonyls by $[HB(C_6F_5)_3]$ is slow relative to the hydrosilylation. These observations rule out a $B(C_6F_5)_3$-catalyzed process and hydride transfer from $[HB(C_6F_5)_3]^-$, as proposed by Piers (not shown in Scheme 9.10).[56]

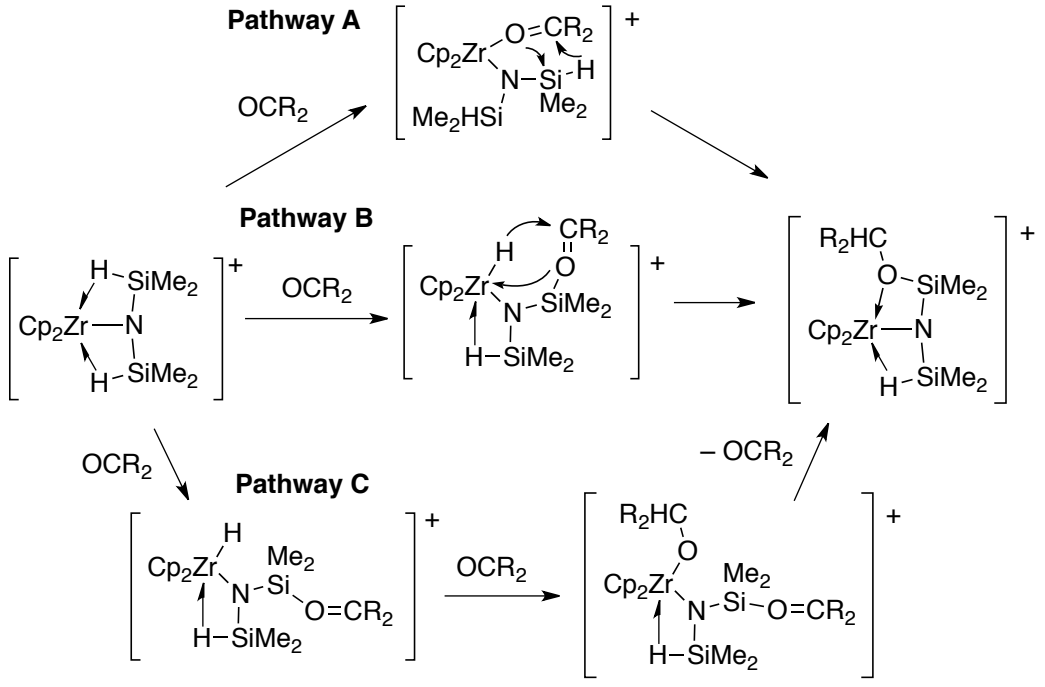

Scheme 9.10. Possible pathways for the hydrosilylation of carbonyl compounds by [**9.2**]$^+$.

Attempts to distinguish these pathways through kinetic studies were not successful, because the reaction of [**9.2**]$^+$ and acetone is finished before it can be measured even at 200 K. Furthermore, kinetic studies were limited by the heterogeneous nature of the reaction between [**9.2**]$^+$ and paraformaldehyde. Other carbonyl compounds, including bulky aldehydes and ketones, also were not useful for kinetic studies.

Thus, alternative tests are needed probe the pathway(s) by which hydrosilylation occurs. While the Zr-H in **9.1** reacts with acetone and paraformaldehyde to form **9.15** and **9.16**, the β-SiH groups in these molecules do not react with either substrate (at least under the conditions tested). We then attempted to block the zirconium center by $OPEt_3$ coordination. In fact, reactions of the $OPEt_3$ adduct $[Cp_2Zr\{N(SiHMe_2)_2\}OPEt_3]^+$ [**9.21**]$^+$ with paraformaldehyde or acetone provided the hydrosilylation products, albeit qualitatively slower than in the absence of $OPEt_3$. Still, $OPEt_3$ is displaced from zirconium in the final product.

Similarly, reactions of DMAP adduct [**9.19**]$^+$ and paraformaldehyde provide [**9.28**]$^+$. Again, these reactions are slower than the corresponding reaction of [**9.2**]$^+$ and the carbonyls, suggesting that the silicon site is involved in the hydrosilylation pathway. Interestingly, an additional product $[Cp_2ZrN(SiMe_2OCMeCH_2)_2]^+$ and H_2 are obtained (from reactions of DMAP adduct [**9.19**]$^+$ and acetone; these products correspond to deprotonation of acetone and formation of an enolate (the ratio of enolate:insertion = 1.8:1). Enolate formation is not observed in reactions of [**9.2**]$^+$ and acetone, nor in reactions of $OPEt_3$ adduct $[Cp_2Zr\{N(SiHMe_2)_2\}OPEt_3]^+$ and acetone. This observation suggests that the ZrH can react with acetone through two routes, insertion or deprotonation/enolate formation. Because

enolate formation is not observed in reactions of [**9.2**]$^+$, it seem unlikely that Pathway C is dominant.

These experiments suggest that both sites are necessary for the hydrosilylation. In accordance with this idea, compounds [**9.25**]$^+$, [**9.26**]$^+$ and [**9.27**]$^+$, which contain OTf bonded to the zirconium center, a Lewis base coordinated to a silicon center, and a non-classical β-SiH are unchanged in the presence of acetone, even at elevated temperature (85 °C). In those compounds, excess DMAP does not induce migration of hydrogen to zirconium.

We rule out Pathway 1 because it should be available for compounds such as [**9.25**]$^+$ that feature a non-classical Zr–H-Si structure that could be disrupted by carbonyl coordination to zirconium. Yet, no hydrosilylation is observed with [**9.25**]$^+$. Furthermore, the $OPEt_3$ adduct [**9.21**]$^+$, as a model for the intermediate on Pathway A, features classical 2c-2e SiH moieties that should not be reactive in hydrosilylation.[54] Although coordination of a carbonyl to a Lewis acid Mo center was recently proposed as a pathway for hydrosilylation based on an isotopic labeling experiment,[57] this mechanism seems unlikely in the current case.

Instead, a pathway in which hydride migrates to zirconium is favored, as suggested by Pathways B and C. The formation of enolates from the cationic ZrH DMAP-adduct [**9.19**]$^+$ suggests that Pathway C should also feature enolate formation in general. Because [**9.2**]$^+$ and acetone react to give enolate-free products, we rule out Pathway C for the hydrosilylation of carbonyls by [**9.2**]$^+$.

The remaining mechanism, Pathway B, features formation of a Si-O bond and Zr-H bond, followed by hydrogen transfer to the electrophilic carbonyl site. The proposed pathway

is similar to the one proposed by Abu-Omar and co-workers for the Re(V)-catalyzed hydrosilylation of carbonyls, based on elimination of a mechanism involving carbonyl insertion into a Re^{V}-H.[58] A related proposed mechanism is described by Brookhart that features an Ir^{III}-(η^1-H-SiR_3) that transfers R_3Si^+ to the carbonyl oxygen.[59] Notably, the zirconium center in [**9.2**]$^+$ is d^0 and thus p back-donation is not available to stabilize the M-(η^2-$HSiR_3$) interaction or to populate the σ*-orbital to assist in the Si-H bond cleavage.

Conclusion

The non-classical Zr⬸H-Si in compounds [**9.2**]$^+$ and its derivatives provide a connection between the insertion/β-agostic CH/elimination organometallic reaction pathways and inorganic Lewis acid/Lewis base chemistry of silylium, boranes and trialkylaluminum/tetraalkylaluminate adducts. This comparison is important, particularly with respect to the transfer of anionic hydride and alkyl ligands between Lewis acidic centers. Furthermore, the addition of a two-electron donor to facilitate hydrogen migration shows the connection between the two seemingly unrelated organometallic systems in terms of reactivity. The transformation from non-classical Zr⬸H-Si to a trapped β-eliminated product is noteworthy.

In addition, the non-classical structures in [**9.2**]$^+$ are central to the observed carbonyl hydrosilylation reaction. Here, it is seen that the non-classical structure facilitates the overall addition reaction without generating an enolate side product, as is observed with the cationic ZrH [**9.19**]$^+$. The similarities between the chemistry of [**9.2**]$^+$ and the proposed catalytic mechanisms based on Re^{V} and Ir^{III} catalysts further support the generality of the pathway across the transition metal series.

Experimental

General Procedures. All reactions were performed under a dry argon atmosphere using standard Schlenk techniques, or under a nitrogen atmosphere in a glovebox unless otherwise indicated. Dry, oxygen-free solvents were used throughout. Benzene, toluene, pentane, and methylene chloride solvents were degassed by sparging with nitrogen, filtered through activated alumina columns, and stored under N_2. Benzene-d_6 and toluene-d_8 were vacuum transferred from Na/K alloy and stored under N_2 in the glovebox. Methylene chloride-d_2 was dried over CaH_2 and filtered and stored over 4 Å molecular sieve under N_2 in the glovebox. Bromobenzene-d_5, pyridine, acetone were degassed in three freeze-pump-thaw cycles and stored over 4 Å molecular sieve under N_2 in the glovebox. All organic reagents were purchased from Aldrich and used as received. $Cp_2ZrMeCl$,[60] $Cp_2ZrEtCl$,[61] $Cp_2Zr(n\text{-}C_3H_7)Cl$,[59] $Cp_2Zr\{(E)\text{-}CH{=}CHSiMe_3\}Cl$,[62] $Cp_2Zr\{N(SiHMe_2)_2\}H$ (**9.1**),[63] $Cp_2Zr\{N(SiHMe_2)_2\}Me$ (**9.3**),[64] $Cp_2Zr\{N(SiHMe_2)_2\}OTf$,[61] $B(C_6F_5)_3$,[65] and $[Ph_3C][B(C_6F_5)_4]$[66] were prepared as described in literature procedures. ^1H, $^{13}C\{^1H\}$, ^{11}B, ^{19}F, and ^{29}Si NMR spectra were collected on Agilent MR-400, Bruker DRX-400, or Bruker AVIII 600 NMR spectrometers. ^{15}N chemical shifts were determined by ^1H-^{15}N HMBC experiments on a Bruker AVII 600 spectrometer with a Bruker Z-gradient inverse TXI $^1H/^{13}C/^{15}N$ 5mm cryoprobe; ^{15}N chemical shifts were originally referenced to an external liquid NH_3 standard and recalculated to the CH_3NO_2 chemical shift scale by adding -381.9 ppm. $^{29}Si\{^1H\}$ NMR spectra were recorded using DEPT experiments, and assignments were verified by ^1H COESY, ^1H-^{13}C HMQC, ^1H-^{13}C HMBC, and ^1H-^{29}Si HMBC experiments. Elemental analysis was performed using a Perkin-Elmer 2400 Series II CHN/S by the Iowa

State Chemical Instrumentation Facility. X-ray diffraction data was collected on a Bruker APEX II diffractometer.

$Cp_2Zr[N(SiHMe_2)_2]H$ (9.1). The synthesis and characterization data of **9.1** was previously reported in reference 61; the low temperature ^1H, ^{13}C and ^{29}Si NMR spectra that provide support for a β-agostic interaction were recently reported in reference **Error! Bookmark not defined.**. The synthetic procedure and spectroscopic data is repeated here for the reader's convenience in comparison with the cationic compounds. A suspension of $[Cp_2ZrHCl]_n$ (0.909 g, 3.53 mmol) and $LiN(SiHMe_2)_2$ (0.491 g, 3.53 mmol) was stirred for 30 min in benzene (15 mL) at room temperature. The volatile materials were removed under reduced pressure to leave an off-white solid residue, which was extracted with pentane (15 mL). The pentane extract was concentrated and cooled to -30 °C, yielding **9.1** (0.931 g, 2.62 mmol, 74.4%). ^1H NMR (benzene-d_6, 400 MHz, 25 °C): δ 5.78 (s, 10 H, C_5H_5), 5.60 (s, 1 H, ZrH), 3.78 (m, $^1J_{SiH}$ = 161.0 Hz, 2 H, SiH), 0.18 (d, $^3J_{HH}$ = 3.2 Hz, 12 H, SiH*Me*$_2$). $^{13}C\{^1H\}$ NMR (benzene-d_6, 125 MHz, 25 °C): δ 107.58 (C_5H_5), 1.76 (SiMe). $^{15}N\{^1H\}$ NMR (benzene-d_6, 61 MHz, 25 °C): δ -292.4. $^{29}Si\{^1H\}$ NMR (benzene-d_6, 119.3 MHz, 25 °C): δ -40.7. ^1H NMR (toluene-d_8, 600 MHz, -82 °C): δ 5.67 (s, 10 H, C_5H_5), 5.48 (s, 1 H, ZrH), 4.99 (s br, $^1J_{SiH}$ = 179.6 Hz, 1 H, $SiH^{terminal}$), 2.13 (s br, $^1J_{SiH}$ = 129.7 Hz, 1 H, $SiH^{agostic}$), 0.49 (s br, 6 H, SiMe), 0.06 (s br, 6 H, SiMe). $^{13}C\{^1H\}$ NMR (toluene-d_8, 125 MHz, -82 °C): δ 106.58 (C_5H_5), 2.96 ($SiH^{terminal}Me_2$), -1.13 ($SiH^{agostic}Me_2$). $^{29}Si\{^1H\}$ NMR (toluene-d_8, 119.3 MHz, -82 °C): δ -23.1 ($SiH^{terminal}Me_2$), -62.9 ($SiH^{agostic}Me_2$). IR (KBr, cm^{-1}): 3099 w br, 2955 m, 2895 w, 2047 s br ($\nu_{SiH\text{-}terminal}$), 1907 m br ($\nu_{SiH\text{-}agostic}$), 1559 m br ($\nu_{ZrH}$), 1441 w, 1246 s,

1014 s, 890 s, 798 s br, 765 s br, 650 s br. Anal. Calcd for $C_{14}H_{25}NSi_2Zr$: C, 47.40; H, 7.10; N, 3.95. Found: C, 47.02; H, 6.96; N, 3.92. mp 104-106 °C.

[$Cp_2ZrN(SiHMe_2)_2$][$HB(C_6F_5)_3$] ([9.2][$HB(C_6F_5)_3$]). Compound **9.1** (0.098 g, 0.277 mmol) and $B(C_6F_5)_3$ (0.142 g, 0.278 mmol) were dissolved in benzene (10 mL). The reaction mixture was stirred at room temperature for 20 min, and a light yellow oil layer precipitated from the solvent. The top layer was decanted, and the oil layer was washed with benzene (4 × 5 mL) and pentane (2 × 5 mL). All the volatile materials were removed under reduced pressure to yield [**9.3**][$HB(C_6F_5)_3$] (0.215 g, 0.248 mmol, 89.5%) as a light yellow solid. X-ray quality crystals were grown from a concentrated bromobenzene solution at -30 °C. ^{1}H NMR (bromobenzene-d_5, 600 MHz, 25 °C): δ 5.64 (s, 10 H, C_5H_5), 4.25 (q br, 1 H, HB), 0.11 (s br, 12 H, SiMe), -0.44 (m, $^1J_{SiH}$ = 106.8 Hz, 2 H, SiH). ^{13}C{^{1}H} NMR (bromobenzene-d_5, 150 MHz, 25 °C): δ 148.68 (br, C_6F_5), 146.28 (br, C_6F_5), 137.96 (br, C_6F_5), 136.86 (br, C_6F_5), 135.52 (br, C_6F_5), 134.50 (br, C_6F_5), 108.65 (C_5H_5), -2.55 (SiMe). ^{11}B NMR (bromobenzene-d_5, 119.3 MHz, 25 °C): δ -24.8 (d, $^1J_{BH}$ = 91.2 Hz). ^{15}N{^{1}H} NMR methylene chloride-d_2, 61 MHz, 25 °C): δ -314.9. ^{19}F NMR (bromobenzene-d_5, 376 MHz, 25 °C): δ -131.9 (d, $^3J_{FF}$ = 22.2 Hz 6 F, *ortho*-F), -162.5 (t, $^3J_{FF}$ = 20.7 Hz, 3 F, *para*-F), -165.5 (t, $^3J_{FF}$ = 19.6 Hz, 6 F, *meta*-F). ^{29}Si{^{1}H} NMR (bromobenzene-d_5, 119.3 MHz, 25 °C): δ -42.7. IR (KBr, cm^{-1}): 3120 w, 2962 w, 2368 br m (ν_{BH}), 1742 m, 1665 br s (ν_{SiH}), 1642 s (ν_{C6F5}), 1605 m, 1510 s, 1463 s br (ν_{C6F5}), 1377 m, 1275 s, 1259 s, 1184 s, 1103 s, 1067 s, 1021 m, 969 s br, 905 m, 865 m, 827 s, 803 s, 781 s, 763 m. Anal. Calcd for $BC_{32}F_{15}H_{25}Si_2NZr$: C, 44.34; H, 2.91; N, 1.62. Found: C, 44.51; H, 3.51; N, 1.53. mp 159-160 °C.

[$Cp_2ZrN(SiHMe_2)_2$][$B(C_6F_5)_4$] ([9.2][$B(C_6F_5)_4$]). The procedure described above for [**9.3**][$HB(C_6F_5)_3$] was used, starting from **9.1** (0.149 g, 0.420 mmol) and [Ph_3C][$B(C_6F_5)_4$] (0.387 g, 0.420 mmol) to afford [**9.3**][$B(C_6F_5)_4$] (0.361 g, 0.350 mmol, 83.4%) as a light yellow solid. ^{1}H NMR (bromobenzene-d_5, 400 MHz, 25 °C): δ 5.60 (s, 10 H, C_5H_5), 0.10 (br s, 12 H, SiMe,), -0.48 (br m, $^1J_{SiH}$ = 89.3 Hz, 2 H, SiH). ^{13}C{^{1}H} NMR (bromobenzene-d_5, 125 MHz, 25 °C): δ 148.68 (br, C_6F_5), 146.26 (br, C_6F_5), 138.47 (br, C_6F_5), 136.59 (br, C_6F_5), 134.26 (br, C_6F_5), 108.56 (C_5H_5), -2.57 (SiMe). ^{11}B NMR (bromobenzene-d_5, 119.3 MHz, 25 °C): δ -15.9. ^{15}N{^{1}H} NMR (methylene chloride-d_2, 61 MHz, 25 °C): δ -314.5. ^{19}F NMR (bromobenzene-d_5, 376 MHz, 25 °C): δ -131.4 (s br, 8 F, *ortho*-F), -161.6 (t, $^3J_{FF}$ = 21.1 Hz, 4 F, *para*-F), -165.4 (t, $^3J_{FF}$ = 17.7 Hz, 8 F, *meta*-F). ^{29}Si{^{1}H} NMR (bromobenzene-d_5, 119.3 MHz, 25 °C): δ -43.1. IR (KBr, cm^{-1}): 3134 w, 2963 w, 1738 m, 1659 s sh (ν_{SiH}), 1644 s (ν_{C6F5}), 1609 m, 1515 s (ν_{C6F5}), 1463 br s (ν_{C6F5}), 1382 m, 1264 s br, 1180 s, 1087 s br, 1021 s, 979 s br, 863 s, 816 s br, 775 s, 756 s, 726 s. Anal. Calcd for $BC_{38}F_{20}H_{24}Si_2NZr$: C, 44.19; H, 2.34; N, 1.36. Found: C, 43.86; H, 2.27; N, 1.30. mp 85-88 °C.

$Cp_2Zr\{N(SiHMe_2)_2\}Me$ (9.3). The orginal synthesis was given in reference 62; the procedure is repeated here because this preparation is the model for the series of $Cp_2Zr\{N(SiHMe_2)_2\}R$ compounds. $Cp_2ZrMeCl$ (0.716 g, 2.63 mmol) and $LiN(SiHMe_2)_2$ (0.367 g, 0.264 mmol) were suspended in benzene (15 mL). This mixture was stirred at room temperature for 13 h. Evaporation of the volatile materials provided an off-white solid. Extraction with pentane (15 mL), concentration of the solution in vacuo, and cooling of the saturated solution to -30 °C yielded crystals of $Cp_2Zr\{N(SiHMe_2)_2\}Me$. The mother liquor

was further concentrated and cooled to provide a second crop of crystals in good overall yield (0.823 g, 2.23 mmol, 84.8%). ^{1}H NMR (benzene-d_6, 400 MHz, 25 °C): δ 5.82 (s, 10 H, C_5H_5), 4.44 (m, $^{1}J_{SiH}$ = 180.8 Hz, 2 H, SiH), 0.47 (s, 3 H, ZrMe), 0.22 (d, $^{3}J_{HH}$ = 3.2 Hz, 12 H, SiMe). ^{13}C{^{1}H} NMR (benzene-d_6, 125 MHz, 25 °C): δ 112.41 (C_5H_5), 34.46 (ZrMe), 1.96 (SiMe). ^{15}N{^{1}H} NMR (benzene-d_6, 61 MHz, 25 °C): δ -278.2. ^{29}Si{^{1}H} NMR (benzene-d_6, 119.3 MHz, 25 °C): δ -27.6. IR (KBr, cm^{-1}): 3104 br m, 2954 s br, 2074 br s (ν_{SiH}), 1815 w br, 1718 br w, 1616 br w, 1247 s, 1015 s, 901 br s, 800 br s, 763 br s. Anal. Calcd for $C_{15}H_{27}Si_2NZr$: C, 48.85; H, 7.38; N, 3.80. Found: C, 49.15; H, 7.20; N, 3.79. mp 185-191 °C.

[$Cp_2ZrN(SiMe_3)(SiHMe_2)$][$HB(C_6F_5)_3$] ([9.4]$^+$). Compound **9.3** (0.011 g, 0.029 mmol) and $B(C_6F_5)_3$ (0.015 g, 0.029 mmol) were dissolved in bromobenzene-d_5 (0.6 mL). The mixture was subjected to multinuclear NMR analysis, which revealed a mixture of two Cp_2Zr-containing species and two $RB(C_6F_5)_3$ anions. Compound [**9.4**]$^+$ and $[HB(C_6F_5)_3]^-$ were formed in equal amounts; [**9.2**]$^+$ and $[MeB(C_5F_5)_3]^-$ were formed in equal amounts. The spectral data here describes [**9.4**]$^+$. Attempts to separate [**9.2**]$^+$ and [**9.4**]$^+$ by crystallization were not successful. ^{1}H NMR (bromobenzene-d_5, 600 MHz, 25 °C): δ 6.13 (s, 10 H, C_5H_5), 0.64 (m, $^{1}J_{SiH}$ = 94.4 Hz, 1 H, SiH), 0.31 (s br, 6 H, SiH*Me*$_2$), 0.27 (s, 9 H, $SiMe_3$). ^{13}C{^{1}H} NMR (bromobenzene-d_5, 150 MHz, 25 °C): δ 116.29 (C_5H_5), 1.50 ($SiMe_3$), 0.31 ($SiHMe_2$). ^{15}N{^{1}H} NMR (bromobenzene-d_5, 61 MHz, 25 °C): δ -209.8. ^{29}Si{^{1}H} NMR (bromobenzene-d_5, 119.3 MHz, 25 °C): δ 8.21 (SiH), -0.17 ($SiMe_3$).

$Cp_2Zr\{N(SiHMe_2)_2\}Et$ (9.5). The procedure described above for **9.3** was used, starting from $Cp_2ZrEtCl$ (0.074 g, 0.259 mmol) and $LiN(SiHMe_2)_2$ (0.036 g, 0.258 mmol) to afford **5**

(0.081 g, 0.211 mmol, 81.8%) as light brown solid. ^{1}H NMR (benzene-d_6, 400 MHz, 25 °C): δ 5.84 (s, 10 H, C_5H_5), 4.46 (m, $^{1}J_{SiH}$ = 183.2 Hz, 2 H, SiH), 1.41 (t, $^{3}J_{HH}$ = 7.4 Hz, 3 H, $ZrCH_2C\mathit{H}_3$), 1.10 (q, $^{3}J_{HH}$ = 7.4 Hz, 2 H, $ZrC\mathit{H}_2CH_3$), 0.22 (d, $^{3}J_{HH}$ = 3.1 Hz, 12 H, SiMe). $^{13}C\{^{1}H\}$ NMR (benzene-d_6, 125 MHz, 25 °C): δ 112.38 (C_5H_5), 47.66 ($ZrCH_2$), 18.44 (CH_3), 2.28 (SiMe). $^{15}N\{^{1}H\}$ NMR (benzene-d_6, 61 MHz, 25 °C): δ -277.4. $^{29}Si\{^{1}H\}$ NMR (benzene-d_6, 119.3 MHz, 25 °C): δ -25.8. IR (KBr, cm^{-1}): 3104 m br, 2954 s br, 2074 s br (ν_{SiH}), 1815 w br, 1718 w br, 1616 w br, 1247 s, 1015 s, 901 s br, 800 s br, 763 s br. Anal. Calcd for $C_{16}H_{29}Si_2NZr$: C, 50.20; H, 7.64; N, 3.66. Found: C, 50.46; H, 7.42; N, 3.56. mp 79-83 °C.

[$Cp_2ZrN(SiMe_2Et)(SiHMe_2)$][$HB(C_6F_5)_3$] ([9.6]$^+$). Compound **9.5** (0.011 g, 0.029 mmol) and $B(C_6F_5)_3$ (0.015 g, 0.029 mmol) were dissolved in bromobenzene-d_5. The mixture was transferred to a NMR tube for analysis, which showed a mixture of two Cp_2Zr-containing species and $HB(C_6F_5)_3$, as well as C_2H_4. Compounds [**9.6**]$^+$ and [**9.2**]$^+$ were observed in a 2.6:1 ratio. The spectral data here describes [**9.6**]$^+$. Attempts to separate [**9.6**]$^+$ and [**9.2**]$^+$ by crystallization were not successful. ^{1}H NMR (bromobenzene-d_5, 600 MHz, 25 °C): δ 6.14 (s, 10 H, C_5H_5), 0.55 (t, $^{3}J_{HH}$ = 7.8, 4 H, $SiCH_2C\mathit{H}_3$ and SiH resonances were overlapped), 0.32 (d, $^{3}J_{HH}$ = 2.1 Hz, 6 H, $SiH\mathit{Me}_2$), 0.09 (q, $^{3}J_{HH}$ = 7.7 Hz, 2 H, $SiC\mathit{H}_2CH_3$), -0.28 (s, 6 H, $Si\mathit{Me}_2Et$). $^{13}C\{^{1}H\}$ NMR (bromobenzene-d_5, 150 MHz, 25 °C): δ 115.88 (C_5H_5), 9.89 ($SiCH_2$), 7.34 ($SiCH_2\mathit{C}H_3$), 0.33 ($Si\mathit{Me}_2Et$), -1.00 ($SiHMe_2$). $^{15}N\{^{1}H\}$ NMR (bromobenzene-d_5, 61 MHz, 25 °C): δ -215.3. ^{29}Si NMR (bromobenzene-d_5, 119.3 MHz, 25 °C): δ 5.64 (SiEt), 7.35 ($^{1}J_{SiH}$ = 94.4 Hz, SiH).

$Cp_2Zr\{N(SiHMe_2)_2\}(n\text{-}C_3H_7)$ (9.7). The procedure described above for **9.3** was used, starting from $Cp_2Zr(n\text{-}C_3H_7)Cl$ (0.172 g, 0.573 mmol) and $LiN(SiHMe_2)_2$ (0.080 g, 0.574 mmol) to afford **9.7** (0.195 g, 0.491 mmol, 85.9%) as light brown solid. ^{1}H NMR (benzene-d_6, 400 MHz, 25 °C): δ 5.84 (s, 10 H, C_5H_5), 4.47 (m, $^1J_{SiH}$ = 183.3 Hz, 2 H, SiH), 1.51 (m, 2 H, $ZrCH_2CH_2CH_3$), 1.10 (m, 5 H, $ZrCH_2CH_2CH_3$), 0.23 (d, $^3J_{HH}$ = 3.2 Hz, 12 H, $SiHMe_2$). $^{13}C\{^1H\}$ NMR (benzene-d_6, 125 MHz, 25 °C): δ 112.28 (C_5H_5), 59.67 ($ZrCH_2$), 27.77 ($CH_2CH_2CH_3$), 22.23 ($CH_2CH_2CH_3$), 2.34 ($SiHMe_2$). $^{15}N\{^1H\}$ NMR (benzene-d_6, 61 MHz, 25 °C): δ -277.0. $^{29}Si\{^1H\}$ NMR (benzene-d_6, 119.3 MHz, 25 °C): δ -25.6. IR (KBr, cm^{-1}): 3361 w, 3090 w, 2952 s, 2896 m, 2084 s br (ν_{SiH}), 1892 w, 1586 m, 1440 m, 1366 m, 1247 s, 1173 m, 1015 s, 908 s, 797 s, 595 m. Anal. Calcd for $C_{17}H_{31}Si_2NZr$: C, 51.45; H, 7.87; N, 3.53. Found: C, 51.72; H, 7.47; N, 3.51. mp 64-67 °C.

$[Cp_2ZrN\{SiMe_2(n\text{-}C_3H_7)\}(SiHMe_2)][HB(C_6F_5)_3]$ ($[\mathbf{9.8}]^+$). Compound **9.7** (0.012 g, 0.029 mmol) and $B(C_6F_5)_3$ (0.015 g, 0.029 mmol) were dissolved in bromobenzene-d_5, and the product mixture was analyzed by NMR spectroscopy. Compound $[\mathbf{9.8}]^+$ was formed as a mixture with $[\mathbf{9.2}]^+$ in a 10.7:1 ratio, along with the counterion $[HB(C_6F_5)_3]^-$ and propylene. The spectral data here describes $[\mathbf{9.8}]^+$. Attempts to separate $[\mathbf{9.8}]^+$ and $[\mathbf{9.2}]^+$ by crystallization were not successful. ^{1}H NMR (bromobenzene-d_5, 600 MHz, 25 °C): δ 6.11 (s, 10 H, C_5H_5), 0.91 (t, $^3J_{HH}$ = 7.1, 3 H, $SiCH_2CH_2CH_3$), 0.46 (m, 3 H, $SiCH_2CH_2CH_3$ and SiH resonances were overlapped, as determined by ^{1}H-^{29}Si HMQC and COSY experiments), 0.31 (d, $^3J_{HH}$ = 2.2 Hz, 6 H, $SiHMe_2$), 0.13 (m, 2 H, $SiCH_2CH_2CH_3$), -0.24 (s, 6 H, $SiHMe_2$). $^{13}C\{^1H\}$ NMR (bromobenzene-d_5, 150 MHz, 25 °C): δ 115.41 (C_5H_5), 20.30 ($SiCH_2CH_2CH_3$), 19.92 ($SiCH_2CH_2CH_3$), 16.99 ($SiCH_2CH_2CH_3$), 0.26 (SiMe), -0.24

($SiHMe_2$). $^{15}N\{^1H\}$ NMR (bromobenzene-d_5, 61 MHz, 25 °C): δ -218.8. ^{29}Si NMR (bromobenzene-d_5, 119.3 MHz, 25 °C): δ 6.0 (Si(*n*-C_3H_7)Me_2), 5.2 ($^1J_{SiH}$ = 87.1 Hz, $SiHMe_2$).

$Cp_2Zr\{N(SiHMe_2)_2\}\{(E)$-CH=CHSiMe$_3\}$ (9.9). The procedure described above for **9.3** was used, starting from $Cp_2Zr\{(E)$-CH=$CH_2SiMe_3\}Cl$ (0.13 g, 0.364 mmol) and $LiN(SiHMe_2)_2$ (0.050 g, 0.359 mmol) to afford **9.9** (0.154 g, 0.339 mmol, 95.3%) as a green solid. ^1H NMR (benzene-d_6, 600 MHz, 25 °C): δ 8.26 (d, $^3J_{HH}$ = 20.8 Hz, 1 H, ZrC*H*=CHSiMe$_3$), 6.63 (d, $^3J_{HH}$ = 20.8 Hz, 1 H, ZrCH=C*H*SiMe$_3$), 5.89 (s, 10 H, C_5H_5), 4.46 (m, $^1J_{SiH}$ = 179 Hz, 2 H, SiH), 0.26 (s, 9 H, $SiMe_3$), 0.24 (d, $^3J_{HH}$ = 3.2 Hz, 12 H, SiH*Me*$_2$). $^{13}C\{^1H\}$ NMR (benzene-d_6, 150 MHz, 25 °C): δ 201.94 (Zr*C*H=CHSiMe$_3$), 147.30 (ZrCH=*C*HSiMe$_3$), 112.95 (C_5H_5), 1.94 ($SiHMe_2$), -0.55 ($SiMe_3$). $^{15}N\{^1H\}$ NMR (benzene-d_6, 61 MHz, 25 °C): δ -276.6. $^{29}Si\{^1H\}$ NMR (benzene-d_6, 119.3 MHz, 25 °C): δ -11.2 ($SiMe_3$), -27.2 ($SiHMe_2$). IR (KBr, cm^{-1}): 2952 s, 2895 s, 2084 s br (ν_{SiH}), 1706 w, 1605 w, 1508 w ($\nu_{C=C}$), 1441 m, 1244 s, 1014 s, 903 s br, 795 s br, 735 s br, 686 s br. Anal. Calcd for $C_{19}H_{36}Si_3NZr$: C, 50.27; H, 7.99; N, 3.09. Found: C, 50.49; H, 7.89; N, 3.17. mp 45-50 °C.

$[Cp_2ZrN\{Si((E)$-CH=CHSiMe$_3)Me_2\}(SiHMe_2)][HB(C_6F_5)_3]$ ($[\mathbf{9.10}]^+$). Compound **9.9** (0.013 g, 0.029 mmol) and $B(C_6F_5)_3$ (0.015 g, 0.029 mmol) were dissolved in bromobenzene-d_5, and the product mixture was analyzed by NMR spectroscopy. The resulting mixture contained compounds [**9.10**]$^+$ and [**9.3**]$^+$ in a 11.5:1 ratio, the counterion $[HB(C_6F_5)_3]^-$, and trimethylsilylacetylene. The spectral data given here describes [**9.10**]$^+$. Attempts to separate [**9.10**]$^+$ and [**9.2**]$^+$ by crystallization were not successful. ^1H NMR (bromobenzene-d_5, 600 MHz, 25 °C): δ 6.75 (d, $^3J_{HH}$ = 22.7 Hz, 1 H, CH=C*H*SiMe$_3$), 6.43 (d, $^3J_{HH}$ = 22.7 Hz, 1 H,

C*H*=CHSiMe$_3$), 6.08 (s, 10 H, C_5H_5), 0.56 (m, $^1J_{SiH}$ = 89.2 Hz, 1 H, SiH), 0.26 (d, $^3J_{HH}$ = 2.2 Hz, 6 H, SiH*Me*$_2$), 0.10 (s, 9 H, SiMe$_3$), -0.05 (s, 6 H, SiMe$_2$). $^{13}C\{^1H\}$ NMR (bromobenzene-d_5, 150 MHz, 25 °C): δ 160.02 (*C*H=CHSiMe$_3$), 142.99 (CH=*C*HSiMe$_3$), 114.27 (C_5H_5), -0.29 (SiHMe$_2$), -0.50 (SiMe$_2$), -2.91 (SiMe$_3$). $^{15}N\{^1H\}$ NMR (bromobenzene-d_5, 61 MHz, 25 °C): δ -236.4. $^{29}Si\{^1H\}$ NMR (bromobenzene-d_5, 119.3 MHz, 25 °C): δ -5.2 (SiMe$_3$), -11.5 (SiH), -12.9 (SiMe$_2$).

[Cp$_2$ZrN(SiHMe$_2$)SiMe$_2$-μ-κ^2-OTf][HB(C$_6$F$_5$)$_3$] ([9.12][HB(C$_6$F$_5$)$_3$]). Cp$_2$Zr{N(SiHMe$_2$)$_2$}OTf (0.091 g, 0.181 mmol) and B(C_6F_5)$_3$ (0.097 g, 0.190 mmol) were dissolved in benzene (5 mL). The mixture was stirred for 20 min to give a biphasic solution. The top clear layer was decanted and the bottom yellow oil layer was washed with benzene (3 × 3 mL) and pentane (2 × 3 mL). All the volatiles were evaporated to dryness under reduced pressure to give [**9.12**][HB(C_6F_5)$_3$] (0.065 g, 0.0641 mmol, 35.4%) as a yellow solid. ^1H NMR (bromobenzene-d_5, 600 MHz, 25 °C): δ 5.91 (s, 10 H, C_5H_5), 4.22 (s br, 1 H, HB), 0.22 (s br, 7 H, Si*HMe*$_2$), 0.13 (s br, 6 H, SiMe). $^{13}C\{^1H\}$ NMR (bromobenzene-d_5, 150 MHz, 25 °C): δ 148.64 (br, C_6F_5), 146.30 (br, C_6F_5), 136.82 (br, C_6F_5), 134.23 (br, C_6F_5), 113.04 (C_5H_5), 0.96 (br, SiMe$_2$OTf), -1.60 (br, SiHMe$_2$). ^{11}B NMR (bromobenzene-d_5, 119.3 MHz, 25 °C): δ -24.8 (d, $^1J_{BH}$ = 87.1 Hz). $^{15}N\{^1H\}$ NMR (bromobenzene-d_5, 61 MHz, 25 °C): δ -294.6. ^{19}F NMR (bromobenzene-d_5, 564 MHz, 25 °C): δ -75.0 (s, OTf), -132.1 (br s, 6 F, *ortho*-F), -162.7 (br s, 3 F, *para*-F), -165.7 (br s, 6 F, *meta*-F). $^{29}Si\{^1H\}$ NMR (bromobenzene-d_5, 119.3 MHz, 25 °C): δ 21.4 (SiMe$_2$OTf), -25.9 ($^1J_{SiH}$ = 106.7 Hz, SiHMe$_2$). IR (KBr, cm^{-1}): 3117 m br, 2964 w, 2915 w, 2383 s br (ν_{BH}), 1817 m br, 1737 s, 1640 s (ν_{C6F5}), 1603 s, 1550 s, 1511 s (ν_{C6F5}), 1462 s br (ν_{C6F5}), 1371 s br, 1268 s, 1240 s,

1125 s, 969 s, 817 s br, 632 s. Anal. Calcd for $BC_{33}F_{18}H_{24}Si_2NO_3SZr$: C, 39.06; H, 2.38; N, 1.38; Found: 39.01; H, 2.43; N, 1.40. mp 94-98 °C.

[$Cp_2ZrN(SiHMe_2)(SiMe_2$-μ-κ^2-OTf)][$B(C_6F_5)_4$] ([9.12][$B(C_6F_5)_4$]). A similar procedure was used to the one described for [**9.12**][$HB(C_6F_5)_3$], starting from $Cp_2Zr\{N(SiHMe_2)_2\}OTf$ (0.081 g, 0.160 mmol) and [Ph_3C][$B(C_6F_5)_4$] (0.155 g, 0.168 mmol) to afford [**9.12**][$B(C_6F_5)_4$] (0.145 g, 0.122 mmol, 76.5 %) as a yellow solid. ^{1}H NMR (bromobenzene-d_5, 600 MHz, 25 °C): δ 5.85 (s br, C_5H_5, 10 H), 0.18 (br s, 7 H, Si*HMe*$_2$), 0.10 (br s, Si*Me*$_2$OTf, 6 H). $^{13}C\{^1H\}$ NMR (bromobenzene-d_5, 150 MHz, 25 °C): δ 148.30 (br, C_6F_5), 146.70 (br, C_6F_5), 138.24 (br, C_6F_5), 136.55 (br, C_6F_5), 134.61 (br, C_6F_5), 112.96 (C_5H_5), 0.57 (br, $SiMe_2$), -1.73 (br, $SiHMe_2$). ^{11}B NMR (bromobenzene-d_5, 119.3 MHz, 25 °C): δ -15.9. $^{15}N\{^1H\}$ NMR (bromobenzene-d_5, 61 MHz, 25 °C): δ -293.4. ^{19}F NMR (bromobenzene-d_5, 564 MHz, 25 °C): δ -76.3 (s, OTf), -132.9 (s br, 8 F, *ortho*-F), -163.1 (t, $^3J_{FF}$ = 20.8 Hz, 4 F, *para*-F), -167.0 (s br, 8 F, *meta*-F). ^{29}Si NMR (bromobenzene-d_5, 119.3 MHz, 25 °C): δ 21.4 ($SiMe_2OTf$), -25.2 ($^1J_{SiH}$ = 99.2 Hz, $SiHMe_2$). IR (KBr, cm^{-1}): 3126 w br, 2965 w, 1826 m br, 1741 m, 1644 s (ν_{C6F5}), 1599 m, 1515 s (ν_{C6F5}), 1464 s br (ν_{C6F5}), 1374 s, 1270 s, 1239 s, 1126 s 1090 s, 980 s, 819 s br. Anal. Calcd for $BC_{39}F_{23}H_{23}Si_2NO_3SZr$: C, 39.67; H, 1.96; N, 1.19; Found: 39.95; H, 1.91; N, 1.19. mp 77-80 °C.

$Cp_2Zr\{N(SiHMe_2)_2\}Cl$ (9.13). Compound **9.1** (0.228 g, 0.642 mmol) was stirred in methylene chloride (3 mL) for 4 h. The volatiles were evaporated under reduced pressure. The yellow solid was extracted with benzene (3 mL); evaporation of the solid provided $Cp_2Zr\{N(SiHMe_2)_2\}Cl$ as an analytically and spectroscopically pure pale yellow solid (0.243

g, 0.624 mmol, 97.2%). ^{1}H NMR (benzene-d_6, 600 MHz, 25 °C): δ 5.99 (s, 10 H, C_5H_5), 4.52 (m, $^{1}J_{SiH}$ = 178.5 Hz, 2 H, SiH), 0.36 (d, $^{3}J_{HH}$ = 3.1 Hz, 12 H, SiH*Me*$_2$). ^{13}C{^{1}H} NMR (benzene-d_6, 150 MHz, 25 °C): δ 115.35 (C_5H_5), 1.39 (SiMe). ^{15}N{^{1}H} NMR (benzene-d_6, 61 MHz, 25 °C): δ -270.4. ^{29}Si{^{1}H} NMR (benzene-d_6, 119.3 MHz, 25 °C): δ -22.8. IR (KBr, cm^{-1}): 3107 m, 2954 m, 2896 m, 2107 s (ν_{SiH}), 2071 s (ν_{SiH}), 1736 w, 1628 w, 1439 m, 1247 s, 1013 s, 943 s, 895 s, 854 s, 807 s, 797 s, 702 s, 638 s. Anal. Calcd for $C_{14}H_{24}Si_2NClZr$: C, 43.21; H, 6.22; N, 3.60. Found: C, 43.32; H, 5.81; N, 3.53. mp 140-143 °C.

[Cp$_2$Zr{N(SiHMe$_2$)(SiMe$_2$-μ-Cl)][HB(C$_6$F$_5$)$_3$] ([9.14][HB(C$_6$F$_5$)$_3$]). The procedure described above for [**9.12**][HB(C_6F_5)$_3$] was used, starting from $Cp_2Zr\{N(SiHMe_2)_2\}Cl$ (0.205 g, 0.526 mmol) and B(C_6F_5)$_3$ (0.269 g, 0.526 mmol) to afford [**9.12**][HB(C_6F_5)$_3$] (0.396 g, 0.440 mmol, 83.6%) as a yellow solid. ^{1}H NMR (methylene chloride-d_2, 600 MHz, 25 °C): δ 6.38 (s, 10 H, C_5H_5), 3.60 (br, 1 H, HB), 0.65 (br, 7 H, Si*H*Me$_2$ and Si*Me*$_2$Cl), 0.59 (br, 6 H, SiH*Me*$_2$). ^{13}C{^{1}H} NMR (bromobenzene-d_5, 150 MHz, 25 °C): δ 149.59 (br, C_6F_5), 148.00 (br, C_6F_5), 137.86 (br, C_6F_5), 136.29 (br, C_6F_5), 114.91 (C_5H_5), 6.34 ($SiMe_2Cl$), 0.18 ($SiHMe_2$). ^{11}B NMR (bromobenzene-d_5, 119.3 MHz, 25 °C): δ -25.3 (d, $^{1}J_{BH}$ = 87.4 Hz). ^{15}N{^{1}H} NMR (methylene chloride-d_2, 61 MHz, 25 °C): δ -295.2. ^{19}F NMR (bromobenzene-d_5, 564 MHz, 25 °C): δ -135.4 (6 F, *ortho*-F), -165.8 (3 F, *para*-F), -168.7 (6 F, *meta*-F). ^{29}Si NMR (bromobenzene-d_5, 119.3 MHz, 25 °C): δ 29.6 ($SiMe_2Cl$), -32.5 ($^{1}J_{SiH}$ = 89.0 Hz, $SiHMe_2$). IR (KBr, cm^{-1}): 3120 m, 2975 w, 2911 w, 2377 s (ν_{BH}), 1765 m (ν_{SiH}), 1673 s, 1642 s (ν_{C6F5}), 1605 s, 1511 s (ν_{C6F5}), 1464 s (ν_{C6F5}), 1375 m, 1262 s, 1184 s, 1089 s, 1024

m, 968 s, 915 m, 867 m, 805 s, 722 m, 660 m, 602 w. Anal. Calcd for $C_{32}H_{24}BNF_{15}Si_2ClZr$: C, 42.65; H, 2.68; N, 1.55. Found: C, 43.00; H, 2.43; N, 1.50. mp 121-123 °C.

$Cp_2Zr\{N(SiHMe_2)_2\}OMe$ (9.15). Paraformaldehyde (0.010 g, 0.327 mmol) and $Cp_2Zr\{N(SiHMe_2)_2\}H$ (0.105 g, 0.296 mmol) were suspended in benzene (1 mL) at room temperature. The mixture was heated at 85 °C for 6 h. The resulting yellow solution was filtered, and the benzene supernatant was evaporated to dryness under reduced pressure to afford **9.22** as an analytically and spectroscopically pure yellow oil (0.110 g, 0.286 mmol, 96.7%). ^{1}H NMR (benzene-d_6, 600 MHz, 25 °C): δ 5.96 (s, 10 H, C_5H_5), 4.71 (br m, $^1J_{SiH}$ = 179.6 Hz, 2 H, Si*H*Me$_2$), 3.62 (s, 3 H, O*Me*), 0.31 (d, $^3J_{HH}$ = 3.6 Hz, 12 H, SiH*Me*$_2$). ^{13}C{^{1}H} NMR (benzene-d_6, 150 MHz, 25 °C): δ 112.95 (C_5H_5), 62.22 (OMe), 1.91 (SiHMe$_2$). ^{15}N{^{1}H} NMR (benzene-d_6, 61 MHz, 25 °C): δ -296.2. ^{29}Si{^{1}H} NMR (benzene-d_6, 119.3 MHz, 25 °C): δ -20.1. IR (KBr, cm^{-1}): 3100 w, 2952 s, 2913 s, 2807 s, 2078 s (ν_{SiH}), 1800 w, 1694 w, 1596 w, 1444 m, 1244 s, 1139 s br, 912 s br, 795 s br, 701 s. Anal. Calcd for $C_{15}H_{27}Si_2NOZr$: C, 46.82; H, 7.07; N, 3.64. Found: C, 46.70; H, 7.42; N, 3.46.

$Cp_2Zr\{N(SiHMe_2)_2\}OCHMe_2$ (9.16). Acetone (0.049 mL, 0.663 mmol) was added to a benzene (5 mL) solution of **9.1** (0.214 g, 0.603 mmol). The very pale yellow solution was stirred for another 30 min. The volatiles were evaporated under reduced pressure to give **9.14** as an analytical and spectroscopically pure pale yellow solid (0.242 g, 0.586 mmol, 97.3%). X-ray quality crystal was grown from concentrated pentane solution at -30 °C. ^{1}H NMR (benzene-d_6, 600 MHz, 25 °C): δ 6.01 (s, 10 H, C_5H_5), 4.77 (m, $^1J_{SiH}$ = 182.4 Hz, 2 H, SiH), 4.10 (m, 1 H, OC*H*Me$_2$), 1.02 (d, $^3J_{HH}$ = 6.1 Hz, 6 H, OC*H*Me$_2$), 0.35 (d, $^3J_{HH}$ = 2.9 Hz, 12 H, SiH*Me*$_2$). ^{13}C{^{1}H} NMR (benzene-d_6, 150 MHz, 25 °C): δ 112.84 (C_5H_5), 75.94 (O*C*HMe$_2$), 26.74 (OCH*Me*$_2$), 2.32 (SiHMe$_2$). ^{15}N{^{1}H} NMR (benzene-d_6, 61 MHz, 25 °C):

δ -297.7. ^{29}Si{^{1}H} NMR (benzene-d_6, 119.3 MHz, 25 °C): δ -19.5. IR (KBr, cm^{-1}): 3107 w, 2964 s, 2899 m, 2861 m, 2113 s (ν_{SiH}), 2051 s (ν_{SiH}), 1808 w, 1701 w, 1597 w, 1445 m, 1374 m, 1362 m, 1335 m, 1242 s, 1138 s, 1003 s, 956 s, 900 s br, 845 s, 797 s, 763 s, 700 s. Anal. Calcd for $C_{17}H_{31}Si_2NOZr$: C, 49.46; H, 7.57; N, 3.39. Found: C, 49.96; H, 7.43; N, 3.37. mp 57-59 °C.

[Cp$_2$ZrN(SiHMe$_2$)(SiMe$_2$-μ-OMe)][HB(C$_6$F$_5$)$_3$] ([9.17][HB(C$_6$F$_5$)$_3$]). $Cp_2Zr\{N(SiHMe_2)_2\}OMe$ (0.059 g, 0.154 mmol) and $B(C_6F_5)_3$ (0.079 g, 0.154 mmol) were dissolved in benzene (3 mL). The mixture was stirred for 20 min to give a biphasic solution. The top clear layer was decanted, and the bottom yellow oil layer was washed with benzene (3 × 2 mL) and pentane (2 × 2 mL). All the volatiles were evaporated from the oil to dryness under reduced pressure to give [**9.13**][$HB(C_6F_5)_3$] (0.101 g, 0.113 mmol, 73.2%) as a light yellow solid. ^{1}H NMR (bromobenzene-d_5, 600 MHz, 25 °C): δ 5.83 (s, 10 H, C_5H_5), 4.31 (br, 1 H, HB), 3.07 (s, 3 H, OMe), 0.34 (br m, $^{1}J_{SiH}$ = 95.5 Hz, 1 H, SiH), 0.18 (d, $^{3}J_{HH}$ = 1.9 Hz, 6 H, SiH*Me*$_2$), -0.03 (s, 6 H, $SiMe_2$). ^{13}C{^{1}H} NMR (bromobenzene-d_5, 150 MHz, 25 °C): δ 148.27 (br, C_6F_5), 146.67 (br, C_6F_5), 136.55 (br, C_6F_5), 134.81 (br, C_6F_5), 111.90 (C_5H_5), 53.32 (OMe), -1.26 (Si*Me*$_2$OMe), -1.56 (SiH*Me*$_2$). ^{11}B NMR (bromobenzene-d_5, 119.3 MHz, 25 °C): δ -24.4 (br). ^{15}N{^{1}H} NMR (benzene-d_6, 61 MHz, 25 °C): δ -294.2. ^{19}F NMR (bromobenzene-d_5, 564 MHz, 25 °C): δ -132.8 (s br, 8 F, *ortho*-F), -163.0 (t, $^{3}J_{FF}$ = 20.9 Hz, 4 F, *para*-F), -166.9 (s br, 8 F, *meta*-F). ^{29}Si{^{1}H} NMR (bromobenzene-d_5, 119.3 MHz, 25 °C): δ 20.4 ($SiMe_2OMe$), -29.7 ($SiHMe_2$). IR (KBr, cm^{-1}): 2961 m, 2363 m br (ν_{BH}), 1642 s (ν_{C6F5}), 1605 m, 1511 s (ν_{C6F5}), 1459 s (ν_{C6F5}), 1375 s, 1263 s, 1188 s, 1103 s br, 1047 s br,

970 s br, 869 s, 814 s br, 734 s br, 661 m. Anal. Calcd for $C_{33}H_{27}BNO_2F_{15}Si_2Zr$: C, 44.20; H, 3.03; N, 1.56. Found: C, 43.69; H, 2.86; N, 1.47. mp 129-132 °C.

[$Cp_2ZrN(SiHMe_2)(SiMe_2$-μ-$OMe)][B(C_6F_5)_4]$ ([9.17][$B(C_6F_5)_4$]). The procedure described above for [**9.13**][$HB(C_6F_5)_3$] was used, starting from $Cp_2Zr\{N(SiHMe_2)_2\}OMe$ (0.054 g, 0.141 mmol) and [Ph_3C][$B(C_6F_5)_4$] (0.130 g, 0.141 mmol) to afford [**9.13**][$B(C_6F_5)_4$] (0.130 g, 0.122 mmol, 86.9%) as a light yellow solid. ^{1}H NMR (bromobenzene-d_5, 600 MHz, 25 °C): δ 5.79 (s, 10 H, C_5H_5), 3.01 (s, 3 H, OMe), 0.30 (br m, $^1J_{SiH}$ = 87.1 Hz, 1 H, SiH), 0.17 (s, 6 H, Si*Me*$_2$OMe), -0.03 (s br, 6 H, $SiHMe_2$). $^{13}C\{^1H\}$ NMR (bromobenzene-d_5, 150 MHz, 25 °C): δ 148.28 (br, C_6F_5), 146.69 (br, C_6F_5), 138.14 (br, C_6F_5), 136.29 (br, C_6F_5), 134.65 (br, C_6F_5), 111.80 (C_5H_5), 53.18 (OMe), -1.30 (Si*Me*$_2$OMe), -1.58 (SiH*Me*$_2$). ^{11}B NMR (bromobenzene-d_5, 119.3 MHz, 25 °C): δ -15.9. $^{15}N\{^1H\}$ NMR (bromobenzene-d_5, 61 MHz, 25 °C): δ -294.2. ^{19}F NMR (bromobenzene-d_5, 564 MHz, 25 °C): δ -132.8 (br s, 6 F, *ortho*-F), -163.9 (br s, 3 F, *para*-F), -166.6 (br s, 6 F, *meta*-F). $^{29}Si\{^1H\}$ NMR (bromobenzene-d_5, 119.3 MHz, 25 °C): δ 20.1 ($MeOSiMe_2$), -29.8 ($SiHMe_2$). IR (KBr, cm^{-1}): 3367 w, 3093 w, 3037 w, 2960 m, 2852 w, 2360 w, 1762 m (ν_{SiH}), 1644 s (ν_{C6F5}), 1514 s (ν_{C6F5}), 1464 s (ν_{C6F5}), 1374 m, 1264 s, 1186 s, 1088 s, 1047 s, 980 s, 907 m, 869 m, 815 s, 794 s, 775 s, 756 s, 727 m, 683 s, 661 s, 610 w. Anal. Calcd for $C_{39}H_{26}BNOF_{20}Si_2Zr$: C, 44.07; H, 2.47; N, 1.32. Found: C, 44.34; H, 2.19; N, 1.16. mp 90-92 °C.

[$Cp_2ZrN(SiHMe_2)(SiMe_2$-μ-$OCHMe_2)][HB(C_6F_5)_3]$ ([9.18][$HB(C_6F_5)_3$]). The compound $Cp_2Zr\{N(SiHMe_2)_2\}OCHMe_2$ (0.136 g, 0.330 mmol) and $B(C_6F_5)_3$ (0.178 g, 0.347 mmol) were dissolved in benzene (5 mL). The mixture was stirred for 20 min to give a biphasic solution. The top clear layer was decanted and the bottom yellow oil layer was washed with

benzene (3 × 3 mL) and pentane (2 × 3 mL). All the volatiles were evaporated to dryness under reduced pressure to give [**9.14**][$HB(C_6F_5)_3$] (0.257 g, 0.278 mmol, 84.2%) as a light yellow solid. X-ray quality crystal was grown from concentrated methylene chloride solution at -30 °C. ^{1}H NMR (bromobenzene-d_5, 600 MHz, 25 °C): δ 5.87 (s, C_5H_5, 10 H), 4.34 (br, HB, 1 H), 3.66 (m, 1 H, OC*H*Me_2), 0.99 (d, $^3J_{HH}$ = 6.4 Hz, 6 H, OCH*Me*$_2$), 0.41 (br m, $^1J_{SiH}$ = 93.6 Hz, 1 H, SiH), 0.16 (d, $^3J_{HH}$ = 1.9 Hz, 6 H, SiH*Me*$_2$), 0.02 (s, 6 H, Si*Me*$_2$OCHMe_2). ^{13}C{^{1}H} NMR (bromobenzene-d_5, 150 MHz, 25 °C): δ 148.33 (br, C_6F_5), 146.76 (br, C_6F_5), 136.65 (br, C_6F_5), 136.38 (br, C_6F_5), 136.03 (br, C_6F_5), 134.76 (br, C_6F_5), 112.09 (C_5H_5), 74.14 (O*C*HMe_2), 22.90 (OCH*Me*$_2$), 2.55 (SiMe_2OCHMe_2), -1.66 (SiHMe_2). ^{11}B NMR (bromobenzene-d_5, 119.3 MHz, 25 °C): δ -24.8 (d, $^1J_{BH}$ = 89.0 Hz). ^{15}N{^{1}H} NMR (methylene chloride-d_2, 61 MHz, 25 °C): δ -286.8. ^{19}F NMR (bromobenzene-d_5, 564 MHz, 25 °C): δ -133.6 (d, $^3J_{FF}$ = 21.6 Hz, 6 H, *ortho*-F), -164.5 (t, $^3J_{FF}$ = 21.0 Hz, 3 F, *para*-F), -167.4 (t, $^3J_{FF}$ = 19.8 Hz, 6 F, *meta*-F). ^{29}Si{^{1}H} NMR (bromobenzene-d_5, 119.3 MHz, 25 °C): δ 13.2 (SiMe_2OCHMe_2), -33.0 (SiHMe_2). IR (KBr, cm^{-1}): 3123 m, 2994 s, 2381 s br (ν_{BH}), 1767 s, 1689 s br, 1641 s (ν_{C6F5}), 1603 s, 1510 s (ν_{C6F5}), 1463 s br (ν_{C6F5}), 1376 s, 1263 s br, 1180 s, 1109 s br, 1068 s, 1013 s, 970 s br, 813 s br, 713 s. Anal. Calcd for $BC_{35}F_{15}H_{31}Si_2NOZr$: C, 45.46; H, 3.38; N, 1.51. Found: C, 45.97; H, 3.47; N, 1.48. mp 105-110 °C.

[$Cp_2ZrN(SiHMe_2)(SiMe_2$-μ-$OCHMe_2)$][$B(C_6F_5)_4$] ([9.18][$B(C_6F_5)_4$]). The procedure described above for [**9.14**][$HB(C_6F_5)_3$] was used, starting from $Cp_2Zr\{N(SiHMe_2)_2\}OMe$ (0.011 g, 0.266 mmol) and [Ph_3C][$B(C_6F_5)_4$] (0.238 g, 0.258 mmol) to afford [**9.14**][$B(C_6F_5)_4$] (0.091 g, 0.084 mmol, 78.5%) as a light yellow solid. ^{1}H NMR

(bromobenzene-d_5, 600 MHz, 25 °C): δ 5.83 (s, 10 H, C_5H_5), 3.61 (m, 1 H, OC*H*Me_2), 0.99 (d, $^3J_{HH}$ = 6.2 Hz, 6 H, OCH*Me*$_2$), 0.37 (m br, $^1J_{SiH}$ = 92.7 Hz, 1 H, SiH), 0.16 (br, 6 H, SiH*Me*$_2$), 0.03 (s, 6 H, $SiMe_2$). $^{13}C\{^1H\}$ NMR (bromobenzene-d_5, 150 MHz, 25 °C): δ 148.26 (br, C_6F_5), 146.63 (br, C_6F_5), 136.26 (br, C_6F_5), 135.45 (br, C_6F_5), 134.65 (br, C_6F_5), 111.98 (C_5H_5), 74.08 (O*C*HMe_2), 22.88 (OCH*Me*$_2$), 2.47 (Si*Me*$_2$OCHMe_2), -1.70 ($SiHMe_2$). ^{11}B NMR (bromobenzene-d_5, 119.3 MHz, 25 °C): δ -15.9. $^{15}N\{^1H\}$ NMR (methylene chloride-d_2, 61 MHz, 25 °C): δ -289.1. ^{19}F NMR (bromobenzene-d_5, 564 MHz, 25 °C): δ -132.9 (s br, 8 H, *ortho*-F), -162.9 (t, $^3J_{FF}$ = 20.9 Hz, 4 F, *para*-F), -166.9 (s br, 8 F, *meta*-F). $^{29}Si\{^1H\}$ NMR (bromobenzene-d_5, 119.3 MHz, 25 °C): δ 13.9 ($SiMe_2OCMe_2$), -32.6 ($SiHMe_2$). IR (KBr, cm^{-1}): 3125 w, 2977 m, 2381 s, 1764 m, 1690 m, 1644 s (ν_{C6F5}), 1603 m, 1514 s (ν_{C6F5}), 1464 s br (ν_{C6F5}), 1376 s, 1265 s br, 1177 s, 1091 s br, 980 s br, 814 s br, 792 s. Anal. Calcd for $BC_{41}F_{20}H_{30}Si_2NOZr$: C, 45.14; H, 2.77; N, 1.28. Found: C, 45.28; H, 2.38; N, 1.12. mp 115-120 °C.

[$Cp_2Zr\{N(SiHMe_2)(SiMe_2DMAP)\}H$][$HB(C_6F_5)_3$] ([9.19][$HB(C_6F_5)_3$]). The cationic compound [**9.2**][$HB(C_6F_5)_3$] (0.113 g, 0.130 mmol) and 4-dimethylaminopyridine (0.016 g, 0.130 mmol) were dissolved in methylene chloride (5 mL) at room temperature. The mixture was stirred for 20 min. The solvent was removed under reduced pressure and the residue was washed with pentane (2 × 2 mL). All the volatile materials were evaporated to dryness under reduced pressure to give [**9.19**][$HB(C_6F_5)_3$] as a light yellow sticky solid. (0.126 g, 0.126 mmol, 96.5%) ^1H NMR (methylene chloride-d_2, 600 MHz, 25 °C): d 7.93 (d, $^3J_{HH}$ = 6.0 Hz, 2 H, α-$NC_5H_4NMe_2$), 6.78 (d, $^3J_{HH}$ = 6.2 Hz, 2 H, β-$NC_5H_4NMe_2$), 5.81 (s, 10 H, C_5H_5), 4.43 (br s, 1 H, ZrH), 3.21 (s, 6 H, NMe_2), 1.27 (br, 1 H, SiH), 0.51 (s, 6 H, $SiMe_2$), 0.21 (s br, 6

H, SiH*Me*$_2$). ^{1}H NMR (methylene chloride-d_2, 600 MHz, -88 °C): d 7.76 (d, $^3J_{HH}$ = 6.6 Hz, 2 H, α-NC$_5$*H*$_4$NMe$_2$), 6.67 (d, $^3J_{HH}$ = 7.2 Hz, 2 H, β-NC$_5$*H*$_4$NMe$_2$), 5.67 (s, 10 H, C$_5$H$_5$), 3.95 (br s, 1 H, ZrH), 3.15 (s, 6 H, NMe$_2$), 0.95 (br, $^1J_{SiH}$ = 118.1 Hz, 1 H, SiH), 0.39 (s, 6 H, SiMe$_2$), 0.11 (d, $^3J_{HH}$ = 2.4 Hz, 6 H, SiH*Me*$_2$). ^{13}C{^{1}H} NMR (methylene chloride-d_2, 125 MHz, 25 °C): d 157.15 (*ipso*-N*C*$_5$H$_4$NMe$_2$), 149.55 (br, C$_6$F$_5$), 147.98 (br, C$_6$F$_5$), 143.42 (α-N*C*$_5$H$_4$NMe$_2$), 139.16 (br, C$_6$F$_5$), 137.77 (br, C$_6$F$_5$), 136.21 (br, C$_6$F$_5$), 106.56 (β-N*C*$_5$H$_4$NMe$_2$), 106.56 (C$_5$H$_5$), 40.37 (NC$_5$H$_4$N*Me*$_2$), 1.82 (SiMe$_2$), -0.54 (SiHMe$_2$). ^{11}B NMR (methylene chloride-d_2, 119.3 MHz, 25 °C): δ -25.4 (d, $^1J_{BH}$ = 91.7 Hz). ^{15}N{^{1}H} NMR (methylene chloride-d_2, 61 MHz, -88°C): δ -197.3 (*N*C$_5$H$_4$NMe$_2$), -292.5 (NC$_5$H$_4$*N*Me$_2$), -327.8 (ZrN). ^{19}F NMR (methylene chloride-d_2, 564 MHz, 25 °C): δ -135.2 (d, $^3J_{FF}$ = 21.7 Hz, 6 F, *ortho*-F), -165.9 (t, $^3J_{FF}$ = 20.0 Hz, 3 F, *para*-F), -168.8 (t, $^3J_{FF}$ = 19.0 Hz, 6 F, *meta*-F). ^{29}Si{^{1}H} NMR (methylene chloride-d_2, 119.3 MHz, -88 °C): δ -0.6 (SiMe$_2$DMAP), -63.6 (SiHMe$_2$). IR (KBr, cm^{-1}): 3116 w, 2958 m, 2376 m br (ν_{BH}), 1889 m br (ν_{SiH}), 1640 s (ν_{C6F5}), 1568 s (ν_{DMAP}), 1509 s (ν_{C6F5}), 1464 s (ν_{C6F5}), 1404 m, 1373 m, 1348 w, 1310 s, 1272 s, 1104 s, 1072 s, 1030 s, 968 s, 907 m, 857 m, 800 s, 725 s, 659 m. Anal. Calcd for BC$_{39}$F$_{15}$H$_{35}$Si$_2$N$_3$Zr: C, 47.37; H, 3.57; N, 4.25. Found: C, 46.85; H, 3.96; N, 4.29. mp 80-86 °C.

[Cp$_2$Zr{N(SiHMe$_2$)(SiMe$_2$DMAP)}H][B(C$_6$F$_5$)$_4$] ([9.19][B(C$_6$F$_5$)$_4$]). A similar procedure as described for the preparation of [**9.19**][HB(C$_6$F$_5$)$_3$] was used, starting from [**9.2**][B(C$_6$F$_5$)$_4$] (0.071 g, 0.069 mmol) and DMAP (0.008 g, 0.069 mmol) to afford [**9.5**][B(C$_6$F$_5$)$_4$] (0.055 g, 0.047 mmol, 68.3%) as a light yellow sticky solid. ^{1}H NMR (bromobenzene-d_5, 600 MHz, 25 °C): δ 7.65 (br, 2 H, α-NC$_5$*H*$_4$NMe$_2$), 6.17 (br, 2 H, β-NC$_5$*H*$_4$NMe$_2$), 5.61 (s, 10 H, C$_5$H$_5$),

4.40 (br s, 1 H, ZrH), 2.54 (s, 6 H, $NC_5H_4NMe_2$), 0.89 (br, $^1J_{SiH}$ = 120.7 Hz, 1 H, SiH), 0.32 (s, 6 H, SiMe_2DMAP), -0.03 (br, 6 H, SiHMe_2). $^{13}C\{^1H\}$ NMR (bromobenzene-d_5, 150 MHz, 25 °C): δ 154.80 (*ipso*-$NC_5H_4NMe_2$), 148.25 (br, C_6F_5), 146.65 (br, C_6F_5), 141.19 (α-$NC_5H_4NMe_2$), 138.13 (br, C_6F_5), 136.22 (br, C_6F_5), 134.60 (br, C_6F_5), 105.35 (β-$NC_5H_4NMe_2$), 104.72 (C_5H_5), 37.84 ($NC_5H_4NMe_2$), 0.12 (SiMe_2DMAP), -2.22 ($SiHMe_2$). ^{11}B NMR (bromobenzene-d_5, 119.3 MHz, 25 °C): δ -16.2. $^{15}N\{^1H\}$ NMR (methylene chloride-d_2, 61 MHz, -73 °C): δ -195.5 ($NC_5H_4NMe_2$), -292.9 ($NC_5H_4NMe_2$), -323.1 (ZrN). ^{19}F NMR (bromobenzene-d_5, 564 MHz, 25 °C): δ -133.1 (d, $^3J_{FF}$ = 17.5 Hz, 8 F, *ortho*-F), -163.3 (t, $^3J_{FF}$ = 20.9 Hz, 4 F, *para*-F), -167.2 (t, $^3J_{FF}$ = 19.7 Hz, 8 F, *meta*-F). $^{29}Si\{^1H\}$ NMR (methylene chloride-d_2, 119.3 MHz, -73 °C): δ -0.4 ($SiMe_2$), -63.5 ($SiHMe_2$). IR (KBr, cm^{-1}): 3074 w, 2960 m, 2619 w, 1889 m (ν_{SiH}), 1643 s (ν_{C6F5}), 1568 s (ν_{DMAP}), 1514 s (ν_{C6F5}), 1464 s (ν_{C6F5}), 1405 m, 1374 m, 1349 w, 1310 s, 1274 s, 1234 s, 1087 s, 1031 s, 979 s, 906 m, 858 m, 814 s, 774 s, 756 s, 726 s, 683 s, 661 s, 601 w, 573 m. Anal. Calcd for $BC_{45}F_{20}H_{34}Si_2N_3Zr$: C, 46.80; H, 2.97; N, 3.64. Found: C, 46.35; H, 3.08; N, 3.64. mp 68-73 °C.

$[Cp_2Zr\{N(SiMe_2DMAP)(SiHMe_2)\}Cl][HB(C_6F_5)_3]$ ([9.20][$HB(C_6F_5)_3$]). The procedure described above for the synthesis of [**9.19**][$HB(C_6F_5)_3$] was used, with [$Cp_2ZrN(SiHMe_2)(SiMe_2$-μ-Cl)][$HB(C_6F_5)_3$] ([**9.14**][$HB(C_6F_5)_3$]; 0.170 g, 0.188 mmol) and 4-dimethylaminopyridine (0.023 g, 0.188 mmol) to afford [**9.20**][$HB(C_6F_5)_3$] (0.191 g, 0.187 mmol, 99.4%) as a yellow gummy solid. ^1H NMR (methylene chloride-d_2, 600 MHz, 25 °C): δ 7.87 (d, $^3J_{HH}$ = 7.8 Hz, 2 H, α-$NC_5H_4NMe_2$), 6.77 (d, $^3J_{HH}$ = 7.8 Hz, 2 H, β-$NC_5H_4NMe_2$), 6.23 (s, C_5H_5, 10 H), 3.21 (br q, 1 H, BH), 3.21 (s, 6 H, NMe_2), 3.04 (m, $^1J_{SiH}$ = 154.7 Hz, 1

H, SiH), 0.60 (s, 6 H, Si*Me*$_2$DMAP), 0.48 (d, $^3J_{HH}$ = 2.9 Hz, 6 H, SiH*Me*$_2$). ^{13}C{^{1}H} NMR (methylene chloride-d_2, 150 MHz, 25 °C): δ 157.34 (*ipso*-*C*NMe$_2$), 149.54 (br, C_6F_5), 147.98 (br, C_6F_5), 143.32 (α-N*C*$_5$H$_4$NMe$_2$), 139.16 (br, C_6F_5), 137.66 (br, C_6F_5), 136.27 (br, C_6F_5), 116.68 (C_5H_5), 107.59 (β-N*C*$_5$H$_4$NMe$_2$), 40.43 (NC$_5$H$_4$N*Me*$_2$), 3.22 (Si*Me*$_2$DMAP), 1.00 (SiHMe$_2$). ^{11}B NMR (methylene chloride-d_2, 119.3 MHz, 25 °C): δ -25.4 (d, $^1J_{BH}$ = 88.3 Hz). ^{15}N{^{1}H} NMR (methylene chloride-d_2, 61 MHz, 25 °C): δ -197.7 (*N*C$_5$H$_4$NMe$_2$), -294.2 (NC$_5$H$_4$*N*Me$_2$), -301.8 (ZrN). ^{19}F NMR (methylene chloride-d_2, 564 MHz, 25 °C): δ -135.2 (d, $^3J_{FF}$ = 21.3 Hz, 6 F, *ortho*-F), -165.9 (t, $^3J_{FF}$ = 20.0 Hz, 3 F, *para*-F), -168.8 (t, $^3J_{FF}$ = 18.9 Hz, 6 F, *meta*-F). ^{29}Si{^{1}H} NMR (methylene chloride-d_2, 119.3 MHz, 25 °C): δ 5.7 (SiMe$_2$DMAP), -34.2 (SiHMe$_2$). IR (KBr, cm^{-1}): 3117 m, 2960 s, 2375 m br (ν_{BH}), 1930 m br (ν_{SiH}), 1639 s (ν_{C6F5}), 1569 s (ν_{DMAP}), 1509 s (ν_{C6F5}), 1467 s (ν_{C6F5}), 1405 s, 1374 s, 1272 s, 1232 s, 1077 s br, 970 s br, 908 s br, 811 s br. Anal. Calcd for $C_{39}H_{34}BN_3F_{15}Si_2ClZr$: C, 45.77; H, 3.35; N, 4.11. Found: C, 46.02; H, 3.46; N, 3.98. mp 127-139 °C.

[Cp$_2$Zr{N(SiHMe$_2$)$_2$}OPEt$_3$][B(C$_6$F$_5$)$_4$] ([9.21][B(C$_6$F$_5$)$_4$]). The procedure described above for [**9.19**][HB(C$_6$F$_5$)$_3$] was used, starting from [**9.2**][B(C$_6$F$_5$)$_4$] (0.103 g, 0.100 mmol) and triethylphosphine oxide (0.013 g, 0.100 mmol) to afford [**9.21**][B(C$_6$F$_5$)$_4$] (0.091 g, 0.078 mmol, 78.3%) as a light yellow oil. ^{1}H NMR (bromobenzene-d_5, 600 MHz, 25 °C): δ 5.98 (br s, 10 H, C_5H_5), 4.09 (br s, $^1J_{SiH}$ = 181.8 Hz, 2 H, SiH), 1.52 (m, 6 H, PC*H*$_2$CH$_3$), 0.82 (m, 9 H, PCH$_2$C*H*$_3$), 0.11 (d, $^3J_{HH}$ = 4.2 Hz, 12 H, SiMe$_2$). ^{13}C{^{1}H} NMR (bromobenzene-d_5, 125 MHz, 25 °C): δ 148.29 (br, C_6F_5), 146.64 (br, C_6F_5), 138.04 (br, C_6F_5), 136.34 (br, C_6F_5), 134.67 (br, C_6F_5), 113.56 (C_5H_5), 16.53 (d, $^1J_{PC}$ = 64.8 Hz, P*C*H$_2$CH$_3$), 3.93 (d, $^2J_{PC}$ = 4.8 Hz, PCH$_2$*C*H$_3$), 0.81 (SiHMe$_2$). ^{11}B NMR (bromobenzene-d_5, 119.3 MHz, 25 °C): δ -15.9.

$^{15}N\{^{1}H\}$ NMR (methylene chloride-d_2, 61 MHz, 25 °C): δ -256.3. ^{19}F NMR (bromobenzene-d_5, 564 MHz, 25 °C): δ -132.8 (d, $^{3}J_{FF}$ = 17.5 Hz, 8 F, *ortho*-F), -163.0 (t, $^{3}J_{FF}$ = 20.9 Hz, 4 F, *para*-F), -166.9 (t, $^{3}J_{FF}$ = 20.3 Hz, 8 F, *meta*-F). $^{29}Si\{^{1}H\}$ NMR (bromobenzene-d_5, 119.3 MHz, 25 °C): δ -19.2. ^{31}P NMR (bromobenzene-d_5, 243 MHz, 25 °C): δ 103.1. IR (KBr, cm^{-1}): 3129 w, 2956 m, 2361 w, 2122 m br (ν_{SiH}), 1644 m (ν_{C6F5}), 1515 s (ν_{C6F5}), 1464 s (ν_{C6F5}), 1411 m, 1374 m, 1276 s, 1092 s, 1016 m, 980 s, 937 s, 880 s, 809 s, 773 s, 756 m, 726 m, 683 s, 661 s, 603 w. Anal. Calcd for $BC_{44}F_{20}H_{39}Si_2NOPZr$: C, 45.29; H, 3.37; N, 1.20. Found: C, 45.13; H, 3.40; N, 1.16. mp 65-69 °C.

$[Cp_2Zr\{N(SiMe_2OCHMe_2)(SiMe_2DMAP)\}H][HB(C_6F_5)_3]$ ([9.22][$HB(C_6F_5)_3$]). Compound [**9.18**][$HB(C_6F_5)_3$] (0.076 g, 0.082 mmol) and 4-dimethylaminopyridine (0.010 g, 0.082 mmol) were dissolved in methylene chloride (5 mL). The mixture was stirred for 20 min. The solvent was removed under reduced pressure, and the residue was washed with pentane (2 mL × 2). All the volatile materials were evaporated to dryness under reduced pressure to give [**9.22**][$HB(C_6F_5)_3$] as a crystalline white solid (0.085 g, 0.081 mmol, 99%). ^{1}H NMR (bromobenzene-d_5, 600 MHz, 25 °C): δ 7.66 (d, $^{3}J_{HH}$ = 6.8 Hz, 2 H, α-$NC_5H_4NMe_2$), 6.25 (d, $^{3}J_{HH}$ = 6.8 Hz, 2 H, β-$NC_5H_4NMe_2$), 5.61 (s, 10 H, C_5H_5), 4.44 (s, 1 H, ZrH), 4.29 (q br, 1 H, BH), 3.77 (m, 1 H, OC*H*Me_2), 2.56 (s, 6 H, NMe_2), 1.05 (d, $^{3}J_{HH}$ = 9.6 Hz, 6 H, OCH*Me*$_2$), 0.39 (s, 6 H, $SiMe_2$DMAP), -0.06 (s, 6 H, Si*Me*$_2$$OCHMe_2$). $^{13}C\{^{1}H\}$ NMR (bromobenzene-d_5, 150 MHz, 25 °C): δ 154.53 (*ipso*-N*C*$_5H_4Me_2$), 148.65 (br, C_6F_5), 146.36 (br, C_6F_5), 141.62 (α-N*C*$_5H_4NMe_2$), 137.96 (br, C_6F_5), 136.81 (br, C_6F_5), 134.25 (br, C_6F_5), 105.77 (C_5H_5), 105.39 (β-N*C*$_5H_4NMe_2$), 69.88 (O*C*HMe_2), 37.83 (NMe_2), 23.38 (OCH*Me*$_2$), 3.47 (Si*Me*$_2$$OCHMe_2$), 1.38 (Si*Me*$_2$DMAP). ^{11}B NMR (bromobenzene-d_5, 119.3

MHz, 25 °C): δ -24.9 (d, $^{1}J_{BH}$ = 88.2 Hz, BH). $^{15}N\{^{1}H\}$ NMR (methylene chloride-d_2, 61 MHz, 25 °C): δ -195.4 (NC$_5$H$_4$NMe$_2$), -295.4 (NMe$_2$), -310.2 (ZrN). ^{19}F NMR (bromobenzene-d_5, 564 MHz, 25 °C): δ -136.6 (d, $^{3}J_{FF}$ = 21.2 Hz, 6 H, *ortho*-F), -164.7 (t, $^{3}J_{FF}$ = 21.1 Hz, 3 F, *para*-F), -167.5 (t, $^{3}J_{FF}$ = 19.0 Hz, 6 F, *meta*-F). $^{29}Si\{^{1}H\}$ NMR (bromobenzene-d_5, 119.3 MHz, 25 °C): δ 16.6 (SiMe$_2$OCHMe$_2$), -11.0 (SiMe$_2$DMAP). IR (KBr, cm^{-1}): 3099 m, 2962 s, 2376 m br (ν_{BH}), 1709 m sh, 1640 s (ν_{C6F5}), 1566 s (ν_{DMAP}), 1509 s (ν_{C6F5}), 1464 s br (ν_{C6F5}), 1374 m, 1258 s, 1100 s, 1071 s, 967 s br, 862 s, 794 s br. Anal. Calcd for BC$_{42}$F$_{15}$H$_{41}$Si$_2$N$_3$OZr: C, 48.18; H, 3.95; N, 4.01. Found: C, 48.51; H, 3.46; N, 3.64. mp 55-58 °C.

[Cp$_2$Zr{N(SiMe$_2$OCHMe$_2$)(SiMe$_2$DMAP)}H][B(C$_6$F$_5$)$_4$] ([9.22][B(C$_6$F$_5$)$_4$]). The procedure described above for [**9.22**][HB(C$_6$F$_5$)$_3$] was used, starting from [**9.18**][B(C$_6$F$_5$)$_4$] (0.091 g, 0.084 mmol) and 4-dimethylaminopyridine (0.010 g, 0.084 mmol) to afford [**9.22**][B(C$_6$F$_5$)$_4$] (0.094 g, 0.095 mmol, 92.6%) as a crystalline white solid. ^{1}H NMR (bromobenzene-d_5, 600 MHz, 25 °C): δ 7.65 (br, 2 H, α-NC$_5$$H_4NMe_2$), 6.17 (br, 2 H, β-NC$_5$$H_4NMe_2$), 5.61 (s, 10 H, C$_5H_5$), 4.40 (s, 1 H, ZrH), 3.78 (m, 1 H, OCHMe$_2$), 2.52 (s, 6 H, NMe$_2$), 1.06 (d, $^{3}J_{HH}$ = 6.3 Hz, 6 H, OCHMe_2), 0.38 (s, 6 H, SiMe_2DMAP), -0.05 (s, 6 H, SiMe_2OCHMe$_2$). $^{13}C\{^{1}H\}$ NMR (methylene chloride-d_2, 150 MHz, 25 °C): δ 158.20 (*ipso*-NC$_5$H$_4$NMe$_2$), 149.51 (br, C$_6$F$_5$), 147.90 (br, C$_6$F$_5$), 144.20 (α-NC$_5$H$_4$NMe$_2$), 137.67 (br, C$_6$F$_5$), 136.05 (br, C$_6$F$_5$), 119.96 (β-NC$_5$H$_4$NMe$_2$), 107.51 (C$_5$H$_5$), 71.96 (OCHMe$_2$), 40.22 (NMe$_2$), 25.31 (OCHMe_2), 5.23 (SiMe_2OCHMe$_2$), 3.00 (SiMe_2DMAP). ^{11}B NMR (bromobenzene-d_5, 119.3 MHz, 25 °C): δ -15.9. $^{15}N\{^{1}H\}$ NMR (methylene chloride-d_2, 61 MHz, 25 °C): δ -192.6 (NC$_5$H$_4$NMe$_2$), -295.4 (NMe$_2$), -311.8 (ZrN). ^{19}F NMR (bromobenzene-d_5, 564 MHz, 25 °C):

δ -132.8 (br, 8 H, *ortho*-F), -163.1 (t, $^{3}J_{FF}$ = 20.3 Hz, 4 F, *para*-F), -167.0 (s br, 8 F, *meta*-F). $^{29}Si\{^{1}H\}$ NMR (bromobenzene-d_5, 119.3 MHz, 25 °C): δ 16.8 ($SiMe_2OCHMe_2$), -10.8 ($SiMe_2$DMAP). IR (KBr, cm^{-1}): 3093 w, 2968 s, 2619 w, 1643 s (ν_{C6F5}), 1566 m (ν_{DMAP}), 1514 s (ν_{C6F5}), 1464 s (ν_{C6F5}), 1403 m, 1374 m, 1274 s, 1233 s, 1088 s, 1016 m, 980 s, 861 m, 812 s, 775 s, 756 s, 727 m, 683 s, 661 s, 610 w, 573 w. Anal. Calcd for $BC_{48}F_{20}H_{40}Si_2N_3OZr$: C, 47.53; H, 3.32; N, 3.46. Found: C, 47.81; H, 3.10; N, 3.36. mp 56-60 °C.

$Cp_2ZrN(SiMe_2OCHMe_2)SiMe(DMAP)CH_2][HB(C_6F_5)_3]$ ([9.23][$HB(C_6F_5)_3$]). **[9.22][$HB(C_6F_5)_3$]** (0.088 g, 0.084 mmol) was dissolved in methylene chloride (2 ml) and transfer to a storage tube with a Teflon valve. The mixture was heated to 140 °C for 4 h. The volatiles were removed under reduced pressure to give [**9.23**][$HB(C_6F_5)_3$] (0.080 g, 0.077 mmol, 90.7%) as a yellow solid. ^{1}H NMR (methylene chloride-d_2, 600 MHz, 25 °C): δ 8.09 (d, $^{3}J_{HH}$ = 7.8 Hz, 2 H, α-$NC_5H_4NMe_2$), 6.76 (d, $^{3}J_{HH}$ = 7.0 Hz, 2 H, β-$NC_5H_4NMe_2$), 6.28 (s, 5 H, C_5H_5), 6.13 (s, 5 H, C_5H_5), 4.07 (m, 1 H, OC*H*Me_2), 3.60 (q br, 1 H, BH), 3.20 (s, 6 H, NMe_2), 1.32 (d, $^{3}J_{HH}$ = 6.1 Hz, 3 H, OCH*Me*$_2$), 1.29 (d, $^{3}J_{HH}$ = 6.1 Hz, 3 H, OCH*Me*$_2$), 1.14 (d br, $^{2}J_{HH}$ = 13.4 Hz, 1 H, $ZrCH_2$), 0.95 (d br, $^{2}J_{HH}$ = 13.3 Hz, 1 H, $ZrCH_2$), 0.44 (s, 3 H, Si*Me*DMAP), 0.17 (s, 3 H, Si*Me*$_2$$OCHMe_2$), 0.14 (s, 3 H, Si*Me*$_2$$OCHMe_2$). $^{13}C\{^{1}H\}$ NMR (methylene chloride-d_2, 150 MHz, 25 °C): δ 157.29 (*ipso*-$CNMe_2$), 149.90 (br, C_6F_5), 147.52 (br, C_6F_5), 143.07 (α-$NC_5H_4NMe_2$), 139.48 (br, C_6F_5), 138.03 (br, C_6F_5), 137.09 (br, C_6F_5), 107.95 (β-$NC_5H_4NMe_2$), 113.48 (C_5H_5), 113.39 (C_5H_5), 67.14 (Me_2SiOCH), 40.41 (NMe_2), 25.91 ($Me_2SiOCH(CH_3)_2$), 25.77 ($Me_2SiOCH(CH_3)_2$), 23.69 ($ZrCH_2$), 3.18 (Si*Me*$_2$$OCHMe_2$), 2.95 (Si*Me*DMAP), 2.03 (Si*Me*$_2$$OCHMe_2$). $^{29}Si\{^{1}H\}$ NMR (methylene chloride-d_2, 119.3

MHz, 25 °C): δ -1.8 ($SiMe_2OCHMe_2$), -22.7 (SiMeDMAP). ^{19}F NMR (methylene chloride-d_2, 376 MHz, 25 °C): δ -135.3 (d, $^3J_{FF}$ = 22.5 Hz, 6 F, *ortho*-F), -166.1 (t, $^3J_{FF}$ = 20.4 Hz, 3 F, *para*-F), -168.9 (t, $^3J_{FF}$ = 19.2 Hz, 6 F, *meta*-F). ^{11}B NMR (methylene chloride-d_2, 79.5 MHz, 25 °C): δ -25.4 (d, $^1J_{BH}$ = 88.0 Hz). $^{15}N\{^1H\}$ NMR (methylene chloride-d_2, 61 MHz, 25 °C): δ -194.6 ($NC_5H_4NMe_2$), -266.7 (ZrN), -295.7 (NMe_2). IR (KBr, cm^{-1}): 2970 m, 2376 m (ν_{BH}), 1640 s (ν_{C6F5}), 1567 m (ν_{DMAP}), 1509 s (ν_{C6F5}), 1464 s (ν_{C6F5}), 1402 w, 1373 w, 1260 m, 1233 m, 1172 w, 1103 m, 1072 m, 1015 m, 968 s, 803 s, 726 m, 659 m. Anal. Calcd for $C_{42}H_{39}BN_3OF_{15}Si_2Zr$: C, 48.28; H, 3.76; N, 4.02. Found: C, 48.14; H, 3.59; N, 3.88. mp 65-67 °C.

$[Cp_2Zr\{N(SiHMe_2)(SiMe_2OCHMe_2)\}OPEt_3][HB(C_6F_5)_3]$ ([9.24][$HB(C_6F_5)_3$]). The procedure described above for [**9.22**][$HB(C_6F_5)_3$] was used, starting from [**9.18**][$HB(C_6F_5)_3$] (0.103 g, 0.111 mmol) and triethylphosphine oxide (0.015 g, 0.111 mmol) to afford [**9.24**][$HB(C_6F_5)_3$] (0.082 g, 0.077 mmol, 69.5%) as a light yellow oil. ^1H NMR (bromobenzene-d_5, 600 MHz, 25 °C): δ 6.04 (s, C_5H_5, 10 H), 4.27 (q br, 1 H, BH), 4.04 (br s, $^1J_{SiH}$ = 186.9 Hz, 1 H, SiH), 3.74 (br s, 1 H, OC*H*Me_2), 1.59 (m, 6 H, PCH_2CH_3), 1.07 (d, $^3J_{HH}$ = 6.1 Hz, 6 H, OCHMe_2), 0.87 (m, 9 H, PCH_2CH_3), 0.12 (s br, 6 H, SiHMe_2), 0.06 (s, 6 H, SiMe_2OCHMe_2). $^{13}C\{^1H\}$ NMR (bromobenzene-d_5, 150 MHz, 25 °C): δ 148.31 (br, C_6F_5), 146.74 (br, C_6F_5), 137.68 (br, C_6F_5), 136.34 (br, C_6F_5), 136.04 (br, C_6F_5), 134.73 (br, C_6F_5), 113.88 (C_5H_5), 63.90 (O*C*HMe_2), 24.12 (OCHMe_2), 16.70 (d, $^1J_{PC}$ = 64.7 Hz, P*C*H_2CH_3), 4.07 (d, $^2J_{PC}$ = 4.6 Hz, PCH_2CH_3), 2.11 (SiMe_2OCHMe_2), 1.18 ($SiHMe_2$). ^{11}B NMR (bromobenzene-d_5, 119.3 MHz, 25 °C): δ -24.9 (br). $^{15}N\{^1H\}$ NMR (methylene chloride-d_2, 61 MHz, 25 °C): δ -291.5. ^{19}F NMR (bromobenzene-d_5, 564 MHz, 25 °C): δ -

132.4 (d, $^{3}J_{FF}$ = 21.8 Hz, 6 F, *ortho*-F), -163.2 (t, $^{3}J_{FF}$ = 20.7 Hz, 3 F, *para*-F), -166.1 (t, $^{3}J_{FF}$ = 19.9 Hz, 6 F, *meta*-F). ^{29}Si{^{1}H} NMR (bromobenzene-d_5, 119.3 MHz, 25 °C): δ -5.1 ($SiMe_2OCHMe_2$), -21.9 ($SiHMe_2$). ^{31}P NMR (bromobenzene-d_5, 243 MHz, 25 °C): δ 102.5. IR (KBr, cm^{-1}): 2975 m, 2375 m (ν_{BH}), 2146 s (ν_{SiH}), 1641 m (ν_{C6F5}), 1509 s (ν_{C6F5}), 1464 s (ν_{C6F5}), 1371 m, 1273 s, 1095 s, 1015 m, 968 s, 893 m, 808 s, 729 m, 648 w, 603 w. Anal. Calcd for $BC_{41}F_{15}H_{46}Si_2NO_2PZr$: C, 46.50; H, 4.38; N, 1.32. Found: C, 46.49; H, 4.77; N, 1.33.

[Cp_2Zr{$N(SiHMe_2)(SiMe_2py)$}OTf][$HB(C_6F_5)_3$] ([9.25][$HB(C_6F_5)_3$]). The procedure described above for [**9.22**][$HB(C_6F_5)_3$]) was used, starting from [$Cp_2ZrN(SiHMe_2)(SiMe_2$-μ-κ^2-OTf)][$HB(C_6F_5)_3$] ([**9.12**][$HB(C_6F_5)_3$]) (0.091 g, 0.090 mmol) and pyridine (7.5 mL, 0.090 mmol) to afford [**9.25**][$HB(C_6F_5)_3$] (0.095 g, 0.087 mmol, 96.7%) as a gummy yellow solid. ^{1}H NMR (methylene chloride-d_2, 600 MHz, 25 °C): δ 8.61 (br, 2 H, *ortho*-NC_5H_5), 8.48 (br, 1 H, *para*-NC_5H_5), 8.04 (br, 2 H, *meta*-NC_5H_5), 6.39 (s, 10 H, C_5H_5), 3.61 (br q, 1 H, BH), 1.27 (br s, $^{1}J_{SiH}$ = 115.3 Hz, 1 H, SiH), 0.69 (s, 6 H, Si*Me*$_2NC_5H_5$), 0.67 (br s, 6 H, SiH*Me*$_2$). ^{13}C{^{1}H} NMR (methylene chloride-d_2, 150 MHz, 25 °C): δ 149.78 (br, C_6F_5), 147.47 (br, C_6F_5), 144.97 (*ortho*-NC_5H_5), 139.53 (br, C_6F_5), 138.35 (br, C_6F_5), 137.09 (br, C_6F_5), 135.91 (br, C_6F_5), 128.50 (*para*-NC_5H_5), 114.47 (C_5H_5), 117.52 (*meta*-NC_5H_5), 2.78 (Si*Me*$_2$py), 1.01 ($SiHMe_2$). ^{11}B NMR (methylene chloride-d_2, 119.3 MHz, 25 °C): δ -25.4 (d, $^{1}J_{BH}$ = 90.0 Hz). ^{15}N{^{1}H} NMR (methylene chloride-d_2, 61 MHz, 25 °C): δ -154.0 (NC_5H_5), -309.5 (ZrN). ^{19}F NMR (methylene chloride-d_2, 564 MHz, 25 °C): δ -78.8 (s, OTf), -135.2 (d, $^{3}J_{FF}$ = 21.5 Hz, 6 F, *ortho*-F), -165.8 (t, $^{3}J_{FF}$ = 20.5 Hz, 3 F, *para*-F), -168.7 (t, $^{3}J_{FF}$ = 17.5 Hz, 6 F, *meta*-F). ^{29}Si NMR (methylene chloride-d_2, 119.3 MHz, 25 °C): δ 14.4 (SiMe), -24.0

(SiHMe). IR (KBr, cm^{-1}): 3121 m, 2962 m, 2920 w, 2373 m (ν_{BH}), 2131 w, 1880 m, 1767 m, 1642 w (ν_{C6F5}), 1624, 1511 s (ν_{C6F5}), 1465 s (ν_{C6F5}), 1373 m, 1339 s, 1270 s, 1237 s, 1206 s, 1102 s, 1018 s, 968 s, 910 m, 861 s, 818 s, 766 m. Anal. Calcd for $BC_{40}F_{18}H_{34}Si_2N_3O_3SZr$: C, 41.72; H, 2.67; N, 2.56. Found: C, 42.27; H, 2.22; N, 2.34. mp 77-86 °C.

[$Cp_2Zr\{N(SiHMe_2)(SiMe_2DMAP)\}OTf$][$HB(C_6F_5)_3$] ([9.26][$HB(C_6F_5)_3$]). The procedure described above for ([**9.22**][$HB(C_6F_5)_3$]) was used, starting from [$Cp_2ZrN(SiHMe_2)(SiMe_2$-μ-κ^2-OTf)][$HB(C_6F_5)_3$] ([**9.12**][$HB(C_6F_5)_3$]) (0.118 g, 0.116 mmol) and 4-dimethylaminopyridine (0.014 g, 0.116 mmol) to afford [**9.30**][$HB(C_6F_5)_3$] (0.131 g, 0.116 mmol, 99.6%) as a gummy yellow solid. ^{1}H NMR (methylene chloride-d_2, 600 MHz, 25 °C): δ 7.89 (d, $^3J_{HH}$ = 7.6 Hz, 2 H, a-$NC_5H_4NMe_2$), 6.80 (d, $^3J_{HH}$ = 7.2 Hz, 2 H, b-$NC_5H_4NMe_2$), 6.37 (s, 10 H, C_5H_5), 3.61 (br q, 1 H, BH), 3.21 (s, 6 H, NMe_2), 1.37 (s br, $^1J_{SiH}$ = 115.3 Hz, 1 H, SiH), 0.58 (d, $^3J_{HH}$ = 2.4 Hz, 6 H, SiH*Me*$_2$), 0.54 (s br, 6 H, Si*Me*$_2$DMAP). ^{13}C{^{1}H} NMR (methylene chloride-d_2, 150 MHz, 25 °C): δ 157.47 (*ipso*-N*C*$_5$H$_4$NMe$_2$), 149.86 (br, C_6F_5), 147.50 (br, C_6F_5), 142.47 (α-N*C*$_5$H$_4$NMe$_2$), 139.46 (br, C_6F_5), 138.18 (br, C_6F_5), 137.07 (br, C_6F_5), 135.70 (br, C_6F_5), 114.36 (C_5H_5), 108.22 (β-N*C*$_5$H$_4$NMe$_2$), 40.48 (NMe_2), 2.32 ($SiMe_2$DMAP), 0.89 ($SiHMe_2$). ^{11}B NMR (methylene chloride-d_2, 119.3 MHz, 25 °C): δ -25.4 (d, $^1J_{BH}$ = 91.1 Hz). ^{15}N{^{1}H} NMR (methylene chloride-d_2, 61 MHz, 25 °C): δ -201.8 (*N*$C_5H_4NMe_2$), -292.3 (NMe_2), -302.8 (ZrN). ^{19}F NMR (methylene chloride-d_2, 564 MHz, 25 °C): δ -78.7 (s, OTf), -135.2 (d, $^3J_{FF}$ = 20.9 Hz, 6 F, *ortho*-F), -165.8 (t, $^3J_{FF}$ = 20.7 Hz, 3 F, *para*-F), -168.8 (t, $^3J_{FF}$ = 18.3 Hz, 6 F, *meta*-F). ^{29}Si{^{1}H} NMR (methylene chloride-d_2, 119.3 MHz, 25 °C): δ 7.7 ($SiMe_2$DMAP), -26.6 ($SiHMe_2$). IR (KBr, cm^{-1}): 3119 m br, 2961 m br, 2375 m br (ν_{BH}), 1881 m br, 1770 w, 1639 s (ν_{C6F5}), 1570 s (ν_{DMAP}), 1509 s (ν_{C6F5}),

1464 s (ν_{C6F5}), 1405 m, 1373 m, 1337 m, 1312 s, 1271 s, 1235 s, 1203 s, 1102 s, 1078 s, 1031 s, 1001 s, 819 s. Anal. Calcd for $BC_{40}F_{18}H_{34}Si_2N_3O_3SZr$: C, 42.26; H, 3.01; N, 3.70. Found: C, 42.06; H, 2.85; N, 3.43. mp 60-65 °C.

[$Cp_2Zr\{N(SiHMe_2)(SiMe_2OPEt_3)\}OTf][HB(C_6F_5)_3]$ ([9.27][$HB(C_6F_5)_3$]). The procedure described above for [**9.22**][$HB(C_6F_5)_3$] was used, starting from [**9.12**][$HB(C_6F_5)_3$] (0.101 g, 0.099 mmol) and triethylphosphine oxide (0.0133 g, 0.099 mmol) to afford ([**9.27**][$HB(C_6F_5)_3$] (0.114 g, 0.099 mmol, 99.8%) as a yellow gummy solid. Unlike the pyridine and DMAP compounds [**9.25**]$^+$ and [**9.26**]$^+$, 1D and 2D NMR spectroscopy does not distinguish [Si]-$OPEt_3$ coordination from [Zr]-$OPEt_3$. However in [**9.25**]$^+$ and [**9.26**]$^+$, the [Si]-L adduct is well-supported by COSY experiments; in these compounds an non-classical SiH is observed. An agostic SiH is observed here in [**9.31**]$^+$, and by analogy we assign this compound as a [Si]-$OPEt_3$ adduct. In contrast, when $OPEt_3$ coordinates to zirconium in $[Cp_2Zr\{N(SiHMe_2)_2\}OPEt_3]^+$ ([**9.21**]$^+$) and $[Cp_2Zr\{N(SiHMe_2)(SiMe_2OCHMe_2)\}OPEt_3]^+$ [**9.24**]$^+$, the resulting adduct contains only classical SiH moieties. ^{1}H NMR (methylene chloride-d_2, 600 MHz, 25 °C): δ 6.34 (s, C_5H_5, 10 H), 3.62 (br q, 1 H, BH), 2.23 (m, 6 H, PCH_2CH$_3$), 1.35 (s br, $^1J_{SiH}$ = 114.5 Hz, 1 H, SiH), 1.26 (m, 9 H, PCH_2CH_3), 0.52 (s br, 6 H, SiHMe_2), 0.37 (s, 6 H, SiMe_2OPEt$_3$). $^{13}C\{^1H\}$ NMR (methylene chloride-d_2, 150 MHz, 25 °C): δ 149.92 (br, C_6F_5), 147.59 (br, C_6F_5), 139.41 (br, C_6F_5), 138.16 (br, C_6F_5), 137.15 (br, C_6F_5), 135.74 (br, C_6F_5), 114.28 (C_5H_5), 17.75 (d, $^1J_{PC}$ = 62.5 Hz, PCH_2CH_3), 5.50 (d, $^2J_{PC}$ = 4.6 Hz, PCH_2CH_3), 3.99 ($SiMe_2$), 0.88 ($SiHMe_2$). ^{11}B NMR (methylene chloride-d_2, 119.3 MHz, 25 °C): δ -25.3 (d, $^1J_{BH}$ = 93.1 Hz). $^{15}N\{^1H\}$ NMR (methylene chloride-d_2, 61 MHz, 25 °C): δ -291.5. ^{19}F NMR (methylene chloride-d_2, 564 MHz, 25 °C): δ -78.5 (s, OTf), -135.2 (d, $^3J_{FF}$ = 21.2 Hz, 6 F, *ortho*-F), -165.8 (t, $^3J_{FF}$ = 20.9 Hz, 3 F, *para*-F), -168.8 (t, $^3J_{FF}$

= 19.3 Hz, 6 F, *meta*-F). $^{29}Si\{^{1}H\}$ NMR (methylene chloride-d_2, 119.3 MHz, 25 °C): δ 2.4 ($SiMe_2OPEt_3$), -29.1 ($SiHMe_2$). ^{31}P NMR (methylene chloride-d_2, 243 MHz, 25 °C): δ 105.1. IR (KBr, cm^{-1}): 3126 m, 2985 m, 2959 m, 2920 m, 2362 m (ν_{BH}), 1880 s, 1766 m, 1642 s (ν_{C6F5}), 1603 w, 1511 s (ν_{C6F5}), 1463 s (ν_{C6F5}), 1411 m, 1374 m, 1329 s, 1262 s, 1236 s, 1205 s, 1079 s, 1037 s, 969 s, 906 m, 861 s, 818 s. Anal. Calcd for $BC_{39}F_{18}H_{39}Si_2NO_4PSZr$: C, 40.77; H, 3.42; N, 1.22. Found: C, 40.85; H, 3.50; N, 1.20.

Reference

1 a) Schmidt, G. F.; Brookhart, M. *J. Am. Chem. Soc.* **1985**, *107*, 1443-1444. b) Doherty, N. M.; Bercaw, J. E. *J. Am. Chem. Soc.* **1985**, *107*, 2670-2682. c) Burger, B. J.; Thompson, M. E.; Cotter, W. D.; Bercaw, J. E. *J. Am. Chem. Soc.* **1990**, *112*, 1566-1577.

2 Clot, E.; Eisenstein, O. In *Principles and Applications of Density Functional Theory in Inorganic Chemistry II*; Kaltsoyannis, N., McGrady, J. E., Eds.; Springer, Berlin: 2004; 113, p. 1-36.

3 a) Green, M. L. H.; Ohare, D. *Pure Appl. Chem.* **1985**, *57*, 1897-1910. b) Ryabov, A. D. *Chem. Rev.* **1990**, *90*, 403-424. b) Shilov, A. E.; Shul'pin, G. B. *Chem. Rev.* **1997**, *97*, 2879-2932.

4 a) Scherer, W.; Herz, V.; Brück, A.; Hauf, C.; Reiner, F.; Altmannshofer, S.; Leusser, D.; Stalke, D. *Angew. Chem. Int. Ed.* **2011**, *50*, 2845-2849. b) Brookhart, M.; Green, M. L. H.; Parkin, G. *Proc. Natl. Acad. Sci.* **2007**, *104*, 6908-6914. c) Crabtree, R. H. in *The Organometallic Chemistry of the Transition Metals*, 2nd ed.; Wiley: New York, **1994**, 53-54 and 188-190.

5 a) Burger, B. J.; Thompson, M. E.; Cotter, W. D.; Bercaw, J. E. *J. Am. Chem. Soc.* **1990**, *112*, 1566-1577. b) Dawoodi, Z.; Green, M. L. H.; Mtetwa, V. S. B.; Prout, K. *J. Chem.* Soc., *Chem. Commun.***1982**, 802-803.

6 a) Nikonov, G. I. In *Adv. Organomet. Chem.*; Robert West, A. F. H., Stone, F. G. A., Eds.; Academic Press: 2005; Vol. Volume 53, p 217-309. b) Corey, J. Y. *Chem. Rev.* **2011**, *111*, 863-1071.

7 Tilley, T. D.; Andersen, R. A.; Zalkin, A. *Inorg. Chem.* **1984**, *23*, 2271-2276.

8 a) Lin, Z. In *Contemporary metal boron chemistry. I, Borylenes, boryls, borane σ-complexes, and borohydrides*; Marder, T. B., Lin, Z., Eds.; Springer,: Berlin, 2008, p. 151-202. b) Besora, M.; Lledós, A. In *Contemporary metal boron chemistry. I, Borylenes, boryls, borane σ-complexes, and borohydrides*; Marder, T. B., Lin, Z., Eds.; Springer,: Berlin, 2008; Vol. 130, p 203-214.

9 Eppinger, J.; Spiegler, M.; Hieringer, W.; Herrmann, W. A.; Anwander, R. *J. Am. Chem. Soc.* **2000**, *122*, 3080-3096.

10 a) Hartwig, J. F.; Muhoro, C. N.; He, Xiaoming. *J. Am. Chem. Soc.* **1996**, *118*, 10936-10937. b) Lam, W.-H.; Lin, Z. *Organometallics* **2000**, *19,* 2625-2628.

11 Hartwig, J. F. *J. Am. Chem. Soc.* **1996**, *118*, 7010-7011.

12 Scherer, W.; Wolstenholme, D. J.; Herz, V.; Eickerling, G.; Brück, A.; Benndorf, P.; Roesky, P. W. *Angew. Chem. Int. Ed.* **2010**, *49*, 2242-2246.

13 Hanley, P.S.; Hartwig, J.F. *J. Am. Chem. Soc.* **2011**, *133*, 15661-15673. b) Neukom, J. D.; Perch, N. S.; Wolfe, J. P. *Organometallics* **2011**, *30*, 1269-1277. c) Hanley, P.S.; Markovic, D.; Hartwig, J.F. *J. Am. Chem. Soc.* **2010**, *132*, 6302–6303. d) Neukom, J. D.; Perch, N. S.; Wolfe, J. P. *J. Am. Chem. Soc.* **2010**, *132*, 6276-6277.

14 Chen, F.; Fan, S.; Wang, Y.; Chen, J.; Luo, Y. *Organometallics* **2012**, *31*, 3730-3735.

15 Yan, K.; Ellern, A.; Sadow, A. D. *J. Am. Chem. Soc.* **2012**, *134*, 9154-9156.

16 Yan, K.; Sadow, A. D. *Chem. Commun.* **2013**, *49*, 3212-3214.

17 Herrmann, W. A.; Huber, N. W.; Behm, J. *Chem. Ber.* **1992**, 1405-1407.

18 (a) Herrmann, W. A.; Eppinger, J.; Runte, O.; Spiegler, M.; Anwander, R. *Organometallics* **1997**, *16*, 1813-1815. (b) Klimpel, M. G.; Gorlitzer, H. W.; Tafipolsky, M.; Spiegler, M.; Scherer, W.; Anwander, R. *J. Organomet. Chem*. **2002**, *647*, 236-244.

19 a) Harris, D. H.; Lappert, M. F. in *Organometallic Chemistry Reviews: Organosilicon Reviews: Organosilicon Reviews*, Elsevier Scientific Publishing Company, Amsterdam, **1976**, p. 13. b) Bradley, D. C.; Chisholm, M. H. *Acc. Chem. Res.* **1976**, *9*, 273-280. c) Ghotra, J. S.; Hursthouse, M. B.; Welch, A. J. *J. Chem. Soc., Chem. Commun.* **1973**, 669-700. d) Andersen, R. A.; Templeton, D. H.; Zalkin, A. *Inorg. Chem.* **1978**, *17*, 2317-2319. e) Bradley, D. C.; Ghotra, J. S.; Hart, F. A.; Hursthouse, M. B.; Raithby, P. R. *J. Chem. Soc., Chem. Commun.* **1972**, 1225-1226.

20 Anwander, R.; Runte, O.; Eppinger, J.; Gerstberger, G.; Herdtweck, E.; Spiegler, M. *J. Chem. Soc. Dalton Trans.* **1998**, 847-858.

21 Procopio, L. J.; Carroll, P. J.; Berry, D. H. *J. Am. Chem. Soc.* **1994**, *116*, 177-185.

22 Herrmann, W. A.; Munck, F. C.; Artus, G. R. J.; Runte, O.; Anwander, R. *Organometallics* **1997**, *16*, 682-688.

23 Wolfsberg, M. *Acc. Chem. Res.* **1972**, *5*, 225-233.

24 See SI for full characterization of [HB(C6F5)3]- and [B(C6F5)4]- salts.

25 Tilley, T. D. *Organometallics* **1985**, *4*, 1452-1457.

26 Procopio, L. J.; Carroll, P. J.; Berry, D. H. *J. Am. Chem. Soc.* **1991**, *113*, 1870-1872.

27 Walker, D. A.; Woodman, T. J.; Hughes, D. L.; Bochmann, M. *Organometallics* **2001**, *20*, 3772–3776. (b) Milione, S.; Grisi, F.; Centore, R.; Tuzi, A. *Organometallics* **2006**, *25*, 266–274. (c) Yan, K.; Upton, B. M.; Ellern, A.; Sadow, A. D. *J. Am. Chem. Soc.* **2009**, *131*, 15110–15111. (d) Garner, L. E.; Zhu, H.; Hlavinka, M. L.; Hagadorn, J. R.; Chen, E. Y. X. *J. Am. Chem. Soc.* **2006**, *128*, 14822–14823.

28 Zhu, J.; Mukherjee, D.; Sadow, A. D. *Chem. Commun.* **2012**, *48*, 464-466.

29 Uhlig, W.; Tretner, C. *J. Organomet. Chem.* **1994**, *467*, 31-35.

30 Luinstra, G. A.; Rief, U.; Prosenc, M. H. *Organometallics* **1995**, *14*, 1551-1552.

31 Cordero, B.; Gómez, V.; Platero-Prats, A. E.; Revés, M.; Echeverría, J.; Cremades, E.; Barragán, F.; Alvarez, S. *Dalton Trans.* **2008**, 2832-2838.

32 Chaudhry, S. C.; Kummer, D. *J. Organomet. Chem.* **1988**, *339*, 241-251.

33 Passarelli, V.; Zanella, P. *Eur. J. Inorg. Chem.* **2004**, *2004*, 4439-4446.

34 See Supporting Information.

35 Forster, T. D.; Tuononen, H. M.; Parvez, M.; Roesler, R. *J. Am. Chem. Soc.* **2009**, *131*, 6689-6691.

36 Simpson, S. J.; Andersen, R. A. *Inorg. Chem.* **1981**, *20*, 3627-3629.

37 Green, M. L. H. *J. Organomet. Chem.* **1995**, *500*, 127-148.

38 Male, N. A. H.; Thornton-Pett, M.; Bochmann, M. *J. Chem. Soc., Dalton Trans.* **1997**, 2487-2494.

39 Enders, M.; Fink, J.; Maillant, V.; Pritzkow, H. *Z. Anorg. Allg. Chem.* **2001**, *627*, 2281-2288.

40 Kidd, R. G. *Boron-11 in NMR of Newly Accessible Nuclei*, Vol. 2, Laszlo, P., eds, Academic Press, NY, **1983**, Ch. 3.

41 Lambert, J. B.; Zhang, S.; Stern, C. L.; Huffman, J. C. *Science* **1993**, *260*, 1917-1918. b) Reed, C. A.; Kim, K.-C.; Bolskar, R. D.; Mueller, L. J. *Science* 2000, *289*, 101–104. c) Reed, C. A. *Acc. Chem. Res.* 1998, *31*, 325–332. d) Douvris, C.; Ozerov, O. V. *Science* 2008, *321*, 1188–1190. e) Parks, D. J.; Blackwell, J. M.; Piers, W. E. *J. Org. Chem.* **2000**, *65,* 3090-3098. f) Panisch, R.; Bolte, M.; Müller, T. *J. Am. Chem. Soc.* **2006**, *128*, 9676-9682. g) Klare, H. F. T.; Bergander, K.; Oestreich, M. *Angew. Chem. Int. Ed.* **2009**, *48*, 9077-9079.

42 Yan, K.; Upton, B. M.; Ellern, A.; Sadow, A. D. *J. Am. Chem. Soc.* **2009**, *131*, 15110-15111.

43 ToMZnN(SiHMe2)2 and B(C6F5)3 provide ToMZnHB(C6F5)3 and [Me2Si-N(SiHMe2)]2, Mukherjee, D.; Lampland, N. L.; Sadow, A. D. unpublished results.

44 a) Collman, J. P.; Hegedus, L. S. *Principles and Applications of Organotransition Metal Chemistry*, Kelly, A., eds, University Science Books, CA, **1980**, Ch. 5.1. b) Calderazzo, F. Angew. Chem. Int. Ed. Engl. **1977**, *16*, 299-311. c) Berke, H.; Hoffman, R. *J. Am. Chem. Soc.* **1978**, *100*, 7224-7236.

45 Brintzinger, H. H.; Fischer, D.; Mülhaupt, R.; Rieger, B.; Waymouth, R. M. *Angew. Chem. Int. Ed. Eng.* **1995**, *34*, 1143-1170.

46 Müller, T. *Angew. Chem. Int. Ed.* **2002**, *40*, 3033-3036.

47 Yan, K.; Schoendorff, G.; Ellern, A.; Upton, B. M.; Windus, T.; Sadow, A. D. *Organometallics* **2013**, *32*, 1300-1316.

48 Corriu, R. J. P.; Perz, R.; Réye, C. *Tetrahedron*, **1983**, *39*, 999-1009.

49 Holton, J.; Lappert, M. F.; Ballard, D. G. H.; Pearce, R.; Atwood, J. L.; Hunter, W. E. *J. Chem. Soc. Dalton Trans.* **1979**, 54-61.

50 a) Watson P, L.; Herskovitz, T. In *Initiation of Polymerization*; ACS: 1983; Vol. 212, p 459-479. b) Watson, P. L.; Parshall, G. W. *Acc. Chem. Res.* **1985**, *18*, 51-56.

51 Bochmann, M.; Lancaster, S. J. *Angew. Chem. Int. Ed.* **1994**, *33*, 1634-1637.

52 Klimpel, M. G.; Sirsch, P.; Scherer, W.; Anwander, R. *Angew. Chem. Int. Ed.* **2003**, *42*, 574-577.

53 Stockland, Jr., R. A.; Jordan, R. F. *J. Am. Chem. Soc.* **2000**, *122*, 6315-6316.

54 Burger, B. J. Thesis, California Institute of Technology 1987.

55 Parks, D. J.; Piers, W. E. *J. Am. Chem. Soc.* **1996**, *118,* 9440-9441.

56 Parks, D. J.; Blackwell, J. M.; Piers, W. E. *J. Org. Chem.* **2000**, *65,* 3090-3098.

57 Shirobokov, O. G.; Kuzmina, L. G.; Nikonov, G. I. *J. Am. Chem. Soc.* **2011**, *133*, 6487-6489.

58 a) Du, G.; Abu-Omar, M. M. *Organometallics* **2006**, *25*, 4920-4923. b) Du, G.; Fanwick, P. E.; Abu-Omar, M. M. *J. Am. Chem. Soc.* **2007**, *129*, 5180-5187.

59 a) Yang, J.; White, P. S.; Schauer, C. K.; Brookhart, M. *Angew. Chem. Int. Ed.* **2008**, *47*, 4141-4143. b) Park, S.; Brookhart, M. *Organometallics* **2010**, *29*, 6057-6064.

60 Walsh, P. J.; Hollander, F. J.; Bergman, R. G. *J. Am. Chem. Soc.* **1988**, *110*, 8729-8731.

61 Chirik, P. J.; Day, M. W.; Labinger, J. A.; Bercaw, J. E. *J. Am. Chem. Soc.* **1999**, *121*, 10308-10317.

62 Hyla-Kryspin, I.; Gleiter, R.; Krueger, C.; Zwettler, R.; Erker, G. *Organometallics* **1990**, *9*, 517-523.

63 Yan, K.; Ellern, A.; Sadow, A. D. *J. Am. Chem. Soc.* **2012**, *134*, 9154-9156.

64 Yan, K.; Sadow, A. D. *Chem. Commun.* **2013**, *49*, 3212-3214.

65 Massey, A. G.; Park, A. J., *J. Organomet. Chem.* **1964**, *2*, 245-250.

66 Scott, V. J.; Celenligil-Cetin, R.; Ozerov, O. V. *J. Am. Chem. Soc.* **2005**, *127*, 2852-2853.

Chapter 10: A facile synthesis to constrained-geometry complexes facilitated by $B(C_6F_5)_3$.

Modified from a paper to be submitted to *Organometallics*

KaKing Yan, Arkady Ellern, Aaron D. Sadow

Abstract. Cationic zirconocene amido compounds containing the dimethylsilyl(t-butyl)amido ligand $[Cp_2ZrN(SiHMe_2)t\text{-}Bu]^+$ $[\mathbf{10.2}]^+$ are prepared by Zr-H abstraction from $Cp_2Zr\{N(SiHMe_2)(t\text{-}Bu\}H$ (**10.1**) with Lewis acids. The β-SiH agostic structure in $[\mathbf{10.2}]^+$ is characterized by NMR and IR spectroscopy and X-ray diffraction study. Low $^1J_{SiH}$ coupling constants in the NMR spectra, and low-energy ν_{SiH} band in the IR spectra, and short M-Si distances and acute M-N-Si angles in the X-ray structure suggest non-classical three-center-two-electron bonding mode on $N(SiHMe_2)(t\text{-}Bu)$ ligand in $[\mathbf{10.2}]^+$. Addition of DMAP to $[\mathbf{10.2}]^+$ provides a mixture of products that includes a azaziconasilacyclobutane product $[Cp_2Zr\{CH_2SiMe(DMAP)Nt\text{-}Bu\}][HB(C_6F_5)_3]$ ($[\mathbf{3}][HB(C_6F_5)_3]$) and H_2 from a sequence of b-SiH migration to Zr, and g-H abstraction. The reactions of $Cp_2Zr\{N(SiHMe_2)(t\text{-}Bu\}X$ (X = Cl (**10.4**), I (**10.5**), OTf (**10.6**)) and $B(C_6F_5)_3$ give C-H/Si-H dehydrocoupling constrained-geometry complex (cgc) $\{Me_2Si(C_5H_4)N(t\text{-}Bu)\}Zr(C_5H_5)X$ (X = Cl (**10.7**), I (**10.8**), OTf (**10.9**)) and hydrogen from a silicon cation-induced electrophilic aromatic substitution.

Introduction

Silicon element multiple-bonded species ($R_2E{=}SiR'_2$) (E = C, Si, N) have been intensively studied for their remarkably reactive nature, in comparison with the relatively inert carbon analogues, and their possible roles in bond-formation reactions with organosilanes. An organometallic approach to stabilize these reactive fragments is by coordination to transition metal centers to generate π-type complexes.[1] In particular, silanimine adduct is postulated as a key intermediate in hydrosilylation of ketone by Group 6 imido catalysts. Addition of silane to molybdenum imido complex provides silanimine adduct.[2] Berry et. al demonstrated in his seminal work that unsaturated molecules, such as CO, CO_2 and formaldehyde, insert into Zr-Si bond in zirconium η^2-silanimine.[2f,3] Although such silanimine adduct can be drawn in resonance forms between two extreme scenarios: Zr(IV) metallocycle with sp^3-hybridized Si and Zr(II) η^2-silanimine with sp^2-hybridized Si center (Scheme 10.1).[2f] Spectroscopic and DFT calculation[4] data suggested that it's best to describe Berry's silanimine as Zr(IV) metallocycle.

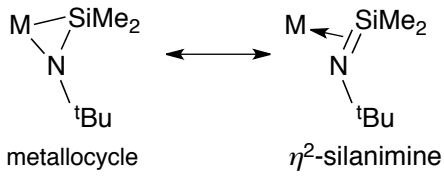

Scheme 10.1. General scheme for the resonance structures of η^2-silanimine organometallic complexes.

Meanwhile, it's well documented that SiH group in organosilanes can be abstracted by strong Lewis acids. Hydrosilylation of carbonyl catalyzed by $B(C_6F_5)_3$ represents a prime example of this strategy in catalysis.[5] Recently, we reported the preparation of silene head to

tail dimer $[(Me_2HSi)_2C{=}SiMe_2]_2$ facilitated by β-SiH abstraction with Lewis acid.[6] Therefore, inspired by Berry's effort, we proposed to prepare a Zr(IV) η^2-silanimine by β SiH group abstraction by Lewis acid with $Cp_2Zr\{N(SiHMe_2)t\text{-}Bu\}X$ (X = H, halides) (Scheme 10.2).

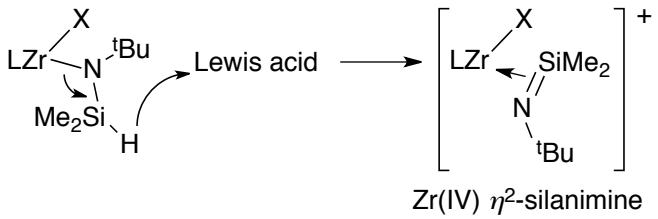

Scheme 10.2. General scheme for our approach to general cationic η^2-silanimine zirconium complexes.

Herein we report our attempt to prepare Zr(IV) η^2-silanimine from the reaction of $Cp_2Zr\{N(SiHMe_2)t\text{-}Bu\}X$ (X = H, halides) and Lewis acids. Instead of β-SiH abstraction in $Cp_2Zr\{N(SiHMe_2)t\text{-}Bu\}(H)$ (**10.1**), hydride abstraction was observed to give cationic silazidozirconium compound that features unusual spectroscopic and structural motif with a side-on interaction of a SiH group with a zirconium center in an agostic type structure. Furthermore, when X is a halide group, a constrained-geometry complex (cgc) and hydrogen were observed. β-SiH abstraction was proposed to give a transient silicon cation that activates a cyclopentadienyl ring and undergoes a C-H/Si-H dehydrocoupling reaction for C-Si bond formation.

Result and Discussion

Reactions of $Cp_2Zr[N(SiHMe_2)t\text{-}Bu](H)$ with $B(C_6F_5)_3$ and $[Ph_3C][B(C_6F_5)_4]$.

The reactions of **10.1** and $B(C_6F_5)_3$ or $[Ph_3C][B(C_6F_5)_4]$ give $[Cp_2ZrN(SiHMe_2)t\text{-}Bu]^+$ ($[\mathbf{10.2}][HB(C_6F_5)_3]$ or $[\mathbf{10.2}][B(C_6F_5)_4]$) respectively (eq 10.1). These cationic tert-butylsilazidozirconocene compounds readily form purple crystals upon slow diffusion of pentane into bromobenzene solution or the oil that precipitates from the reaction in benzene.

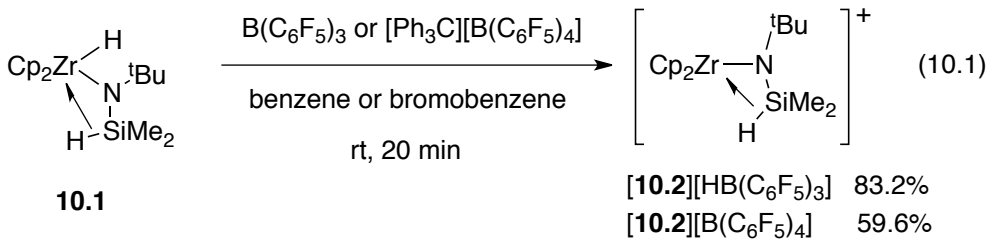

10.1

(10.1)

$[\mathbf{10.2}][HB(C_6F_5)_3]$ 83.2%
$[\mathbf{10.2}][B(C_6F_5)_4]$ 59.6%

The upfield ^1H NMR chemical shifts at 0.46 and 0.35 ppm in $[\mathbf{10.2}][HB(C_6F_5)_3]$ and $[\mathbf{10.2}][B(C_6F_5)_4]$ were assigned to the SiH moiety based on crosspeaks to $SiMe_2$ resonances in COSY experiments. These upfield signals are characterized by very low one-bond silicon-hydrogen coupling constants ($^1J_{SiH}$ = 90.7 and 90.4 Hz). The SiH resonances of $[\mathbf{10.2}]^+$ are shifted upfield by 0.8 ppm in comparison to neutral **1**, which is also assigned a b-agostic ground state structure.[2f] Meanwhile, ^1H NMR spectra of $Cp_2Z(N(SiHMe_2)t\text{-}Bu)X$ (X = F, Cl, Br, I, OTf) contain SiH resonances from 1.3-2.8 ppm and $^1J_{SiH}$ from 119-135 Hz.[2f] In fact, the low $^1J_{SiH}$ value for $[\mathbf{10.2}]^+$ is similar to that in $Cp_2Ti(Me_2HSiCCt\text{-}Bu)$ (δ_{SiH} -7.32 ppm, $^1J_{SiH}$ = 93 Hz at 193 K), although the δ_{SiH} in $[\mathbf{10.2}]^+$ is further downfield.[7] In addition, ^{29}Si NMR signals were detected at -7.5 and -7.6 ppm for $[\mathbf{10.2}][HB(C_6F_5)_3]$ and $[\mathbf{10.2}][B(C_6F_5)_4]$, respectively. These signals are dramatically downfield of the chemical shift of the agostic precursor **10.1** (-73.9 ppm). In the ^{11}B NMR spectrum, $HB(C_6F_5)_3$ was identified (-23.6 ppm, $^1J_{BH}$ = 91.2 Hz) in $[\mathbf{10.2}][HB(C_6F_5)_3]$. Ph_3CH was detected in reactions that give $[\mathbf{10.2}][B(C_6F_5)_4]$. Further evidence of a $Zr(\eta^2\text{-}HSi)$ interaction in $[\mathbf{10.2}]^+$ comes from the observation of exceedingly low energy IR bands assigned to the ν_{SiH} at 1709 and 1703 cm^{-1},

respectively. For comparison, $Cp_2Zr\{N(SiHMe_2)t\text{-}Bu\}X$ (X = H, F, Cl, Br, I) contain ν_{SiH} bands from 1912-1998 cm^{-1},[8] while the ν_{SiH} in $Er[N(SiHMe_2)t\text{-}Bu]_3$ appeared at 1858 cm^{-1}.[9]

X-ray quality crystals of [**10.2**][$B(C_6F_5)_4$] were obtained from a concentrated bromobenzene solution cooled to 0 °C. The solid-state structure confirmed the separation of [**10.2**]$^+$ and $B(C_6F_5)_4$. The closest F-Si distance is 4.580(4) that suggests the anion is well-separated from the cation. Both the Zr1-N1 distance (2.056(2) Å) and N-Si distance (1.617(2) Å) are shorter than those in **10.2** (Zr-N1: 2.143(2) and N1-Si1: 1.709(6) A) in **10.2**. The N-Si distance is also shorter than that in the silanimine compound $Cp_2Zr\{\eta^2\text{-}N(t\text{-}Bu)SiMe_2\}PMe_3$ by ~0.04 Å.[2f] The β-silicon center and the three substituents are approaching planarity in [**10.2**]$^+$. The sums of the C-Si-C angle and N-Si-C angels are 349.9°. [**10.2**]$^+$ salts are robust in solid state and solution. The intensity of resonances corresponding to [**10.2**][$HB(C_6F_5)_3$] in ^{1}H NMR spectrum decreases upon heating at 85 °C for 36 h, however, the resonances of silaimine product corresponding to β-hydrogen elimination are not observed.

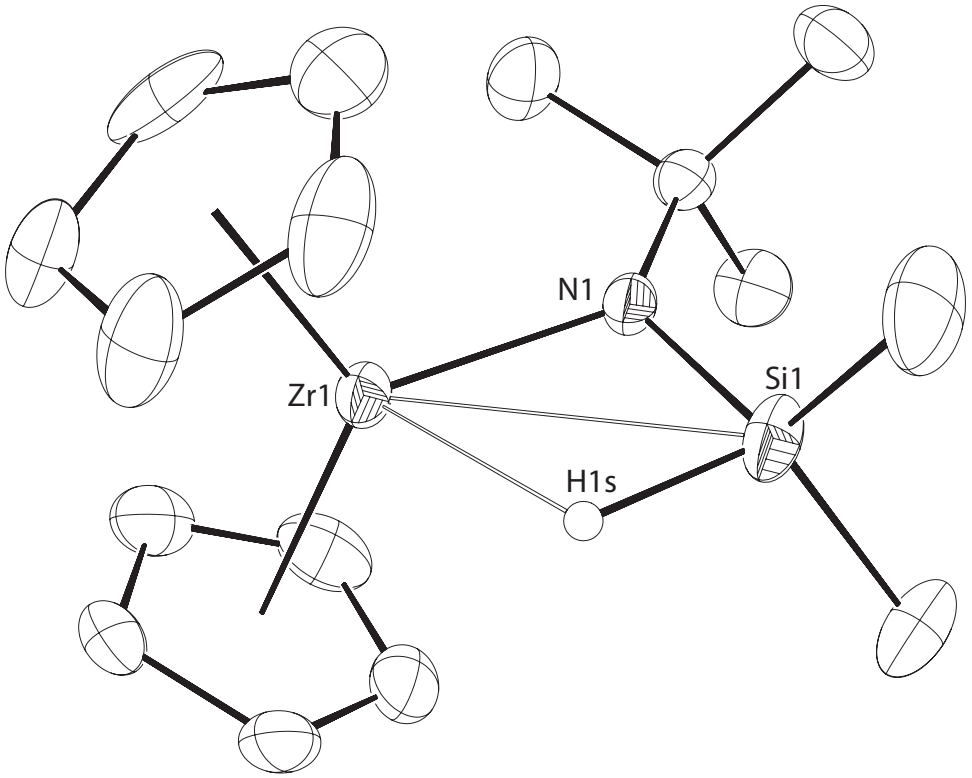

Figure 10.1. ORTEP diagram illustrating the cationic portion of $[Cp_2ZrN(SiHMe_2)t\text{-}Bu][B(C_6F_5)_4]$ ([**10.2**][$B(C_6F_5)_4$]). Only hydrogen bonded to silicon are illustrated. Selected interatomic distances (Å): Zr1-H1s, 2.03(4); Zr1-N1, 2.058(3); Zr-Si1, 2.836(1); Si1-H1s, 1.53(5); N1-Si1, 1.697(3); N1-C3, 1.476(6). Selected interatomic angles (°): Zr1-Si1-N1, 46.0(1); Si1-Zr1-N1, 36.41(8); Zr1-N1-Si1, 97.6(1); Si1-N1-C3, 129.4(3).

Reaction of *tert*-butylsilazide [**10.2**][$HB(C_6F_5)_3$] and DMAP in methylene chloride at room temperature gives an inseparable mixture of products over one day. A combination of 1D and 2D multinuclear NMR experiments allowed the assignment of the major product as $[Cp_2Zr\{CH_2SiMe(DMAP)Nt\text{-}Bu\}][HB(C_6F_5)_3]$ ([**10.3**][$HB(C_6F_5)_3$]; Scheme 10.3).

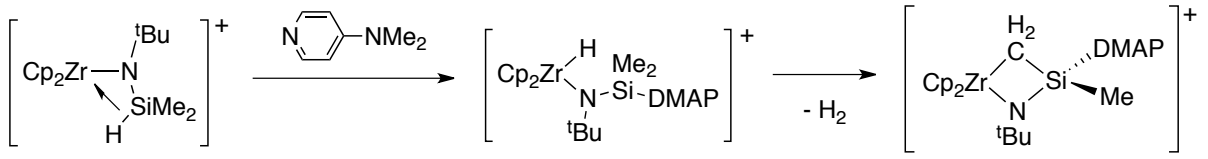

[**10.2**][$HB(C_6F_5)_3$] [**10.3**][$HB(C_6F_5)_3$] 49%

Scheme 10.3. The proposed pathway for formation of [**10.3**][$HB(C_6F_5)_3$] from [**10.2**][$HB(C_6F_5)_3$].

In the ^{1}H NMR spectrum of the reaction mixture, H_2 (4.46 ppm) was detected; however, a silicon hydride was not observed. Characteristic ^{1}H NMR doublet resonances at 1.70 and 1.62 ppm ($^2J_{HH}$ = 13.2 Hz, 1 H each) were correlated in a COSY experiment and assigned as diastereotopic hydrogens in a methylene unit adjacent to a chiral center. A ^{1}H-^{29}Si HMBC experiment (optimized for J_{SiH} = 7 Hz) showed correlations between the Si center and the CH_2, Me, and α-aromatic CH protons of the DMAP group, and confirmed the connectivity of the assigned structure. A plausible pathway for the formation of [**10.3**]$^+$ involves coordination of DMAP to the silicon center and a 1,3-hydride shift to form $[Cp_2Zr\{N(Si(DMAP)Me_2)t\text{-}Bu\}H]^+$, followed by β-hydrogen abstraction.

Reactions of $Cp_2Zr[N(SiHMe_2)t\text{-}Bu](OTf)$ with $B(C_6F_5)_3$.

Zirconium hydride abstraction has been shown to be a predominant pathway with $B(C_6F_5)_3$ in the presence of β-SiH moiety. In order to favor β-SiH abstraction, the reactivity with borane were examined with mixed halide amide compounds $Cp_2ZrN(SiHMe_2)t$-Bu(X) (X = Cl (**10.4**), I (**10.5**), OTf (**10.6**)). The syntheses of **10.4** and **10.5** were previously reported.[9] The desired mixed triflate amide adduct $Cp_2ZrN(SiHMe_2)t$-Bu(OTf) (**10.4**) was prepared from **10.1** and MeOTf in benzene (eq 10.2). Instantaneous formation of methane was observed in ^{1}H NMR spectra upon monitoring micromolar scale reactions in benzene-d_6.

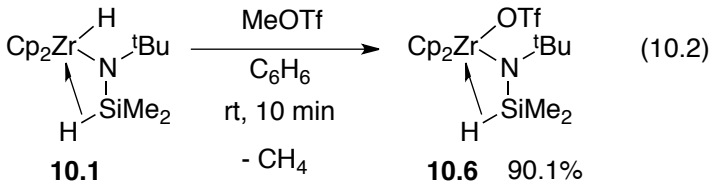

10.1 **10.6** 90.1% (10.2)

The ^{1}H NMR spectrum of **10.6** contained equivalent C_5H_5 (5.97 ppm), SiH (1.29 ppm, $^1J_{SiH}$ = 112.2 Hz), *t*-Bu (1.16 ppm) and $SiMe_2$ (-0.02 ppm, $^3J_{HH}$ = 2.4 Hz) moieties. The low $^1J_{SiH}$ of **10.6** is in good agreement with other halide analogues (119-135 Hz). Besides, one ν_{SiH} band was observed for **10.6** at 1917 cm^{-1}. Both $^1J_{SiH}$ and ν_{SiH} are lower than other halide adducts by at least 6.5 Hz and 33 cm^{-1}, respectively. This suggests the electon-withdrawing triflate group affects the electronic property of SiH group.

In contrast to the chemistry of tetramethyldisilazido zirconocene, the tert-butyl monosilazide compound **10.6** and $B(C_6F_5)_3$ react to give H_2 and a C_5H_5-activated product $\{Me_2Si(C_5H_4)N(t\text{-}Bu)\}Zr(C_5H_5)OTf$ (**10.7**; eq 10.3).

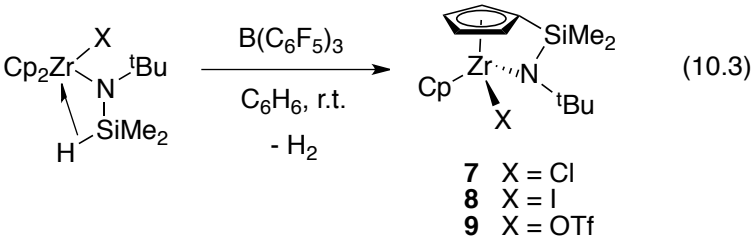

7 X = Cl
8 X = I
9 X = OTf (10.3)

The product **10.9** is soluble in benzene, and only a small amount of oily precipitate was formed. In contrast, all of the cationic disilazido compounds are insoluble in benzene and precipitate from reaction mixtures as oils. In micromolar scale reactions in benzene-d_6 that give **10.9**, a broad ^{11}B NMR resonance at 55 ppm was assigned to $B(C_6F_5)_3$, and a downfield resonance normally assigned to $[HB(C_6F_5)_3]^-$ was absent. Still, one equivalent of $B(C_6F_5)_3$ is required for conversion of $Cp_2Zr\{N(SiHMe_2)t\text{-}Bu\}X$ (X = I, OTf) to **10.8** or **10.9** and H_2. Unfortunately, the product is contaminated with $B(C_6F_5)_3$, and this route does not

provide analytically pure **10.8** and **10.9**. The reaction of **10.6** and $B(C_6F_5)_3$ is much slower than the reaction with **10.5**. The conversion from **10.6** to **10.9** takes one day at room temperature for complete conversion, while the reaction with **10.5** is complete within 5 min. One possibility for slow reactivity may result from possible coordination of $B(C_6F_5)_3$ to one of the S-O group in triflate group. Similar borane-sulfonate interaction was previous observed in a palladium complex equipped with a sulfonate-functionalized NHC ligand.[10]

In the ^{1}H NMR spectrum of **10.9**, a singlet (5.93 ppm, 5 H) and four multiplets (4 H total) in the cyclopentadienyl region suggested that one of C-H bond on a Cp ring is activated. A tert-butyl singlet (1.13 ppm) and two singlets at 0.49 and 0.19 (3 H each) for the diastereotopic $SiMe_2$ were also observed; the ^{1}H resonances of the SiMe groups showed correlation with the *ipso*-C_5H_4 signal in a ^{1}H-^{13}C HMBC experiment that is indicative of a Si-C bond formation. The spectroscopy data of **10.9** is very similar to the previously reported $\{Me_2Si(C_5H_5)N(t\text{-Bu})\}Zr(C_5H_5)Cl$ (**10.7**).[11] **10.7** can also be synthesized through the $B(C_6F_5)_3$-mediated reaction of $Cp_2Zr\{N(SiHMe_2)t\text{-Bu}\}Cl$, however micromolar reaction in benzene-d_6 as the major component in a mixture of products, further confirming the identity of **10.9**.

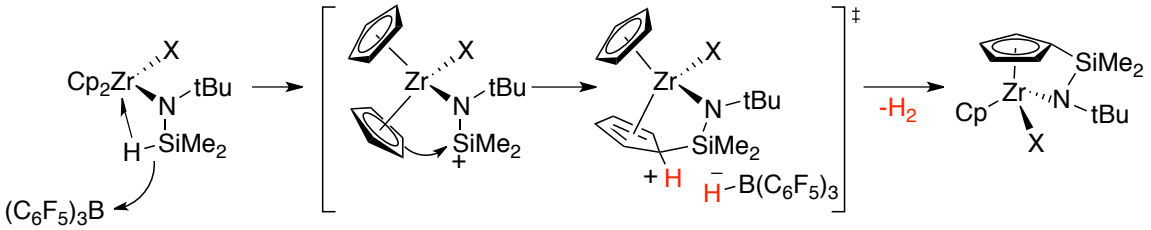

Scheme 10.4. Proposed pathway for Lewis acid-mediated constrained geometry complex formation.

Related $B(C_6F_5)_3$-mediated electrophilic substitution reactions of a cyclopentadienyl group were previously observed in a chromocene and a zirconocene-diene system facilitated by $CpB(C_6F_5)_3$ formation.[12] Previously, we have shown that H_2 elimination and interligand coupling between a Si−H bond of a silazide and the C−H bond of Cp is facilitated by Lewis acid.[13] The formation of constrained geometry framework is proposed to involve a C-H/Si-H dehydrogenative coupling reaction catalyzed by $B(C_6F_5)_3$ takes place (Scheme 10.4). β-SiH abstraction generates silicon cation similar to first step in Scheme 10.3, which is in close proximity to the Cp ring than the triflate group, or else the major product could be the formation of triflate migration product $[Cp_2Zr(OTfSiMe_2)N\textit{t}\text{-Bu}]^+$. Instead, the key step here is the Cp ring attack to the silicon cation following an electrophilic aromatic substitution type mechanism. This follows a deprotonation by borohydride to give constrained geometry production and extrudes H_2. The β-SiH group directed C-Si bond formation catalyzed by $B(C_6F_5)_3$ might provide new synthetic route to arylsilane.

Conclusion

The Zr-H-Si interaction in [**10.2**]$^+$ represents a ground state agostic structure model on the coordinate to β-H elimination. While this β-elimination reaction is not initiated by thermolysis, addition of a two-electron donor promotes this reaction to take place. Although the β-H elimination product is not observed by NMR spectroscopy, its subsequent intramolecular g-abstraction reaction product is identified. Using the four-center transition state pioneered by Bercaw in the description for β-H elimination, positive charge builds up on the β-Si position. Unlike its carbon congener, silicon cation species are highly reactive

and its generation during a reaction is thermodynamically unfavorable. Thus, it may explain why β-H elimination is not an observable pathway in the thermolysis of [**10.2**]$^+$. However, the introduction of DMAP stabilizes transient silicon cation by inductive effect and resonance (Scheme 10.5).

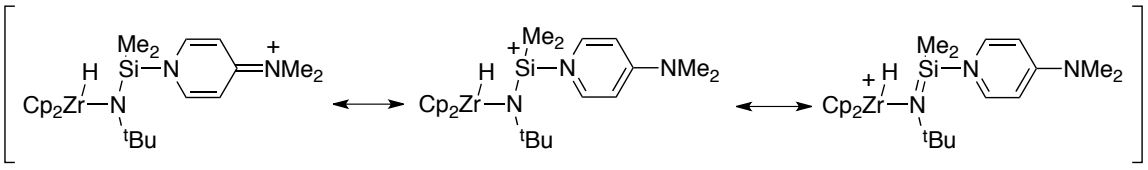

Scheme 10.5. Resonance structure in the reaction of [**10.2**]$^+$ and DMAP.

Meanwhile, the reaction of $B(C_6F_5)_3$ with zirconium amido halide **10.4**-**10.6** gave constrained geometry complexes **10.7**-**10.9**, through a transient silicon cation intermediate. The inhibition of intramolecular abstraction of a Zr halide by silicon cation is probably due to the formation of a highly electron-deficient fourteen-electron complex. Thus, Cp ring activation is observed instead. Constrained-geometry complexes play an important role in industrial α-olefin polymerization process. Our work here represents a facile approach to generate cgc ligand motif facilitated by $B(C_6F_5)_3$. The β-SiH group directed C-Si bond formation catalyzed by $B(C_6F_5)_3$ might provide new synthetic route to arylsilane.

Experimental

General Procedures. All reactions were performed under a dry argon atmosphere using standard Schlenk techniques, or under a nitrogen atmosphere in a glovebox unless otherwise indicated. Dry, oxygen-free solvents were used throughout. Benzene and pentane solvents were degassed by sparging with nitrogen, filtered through activated alumina columns, and stored under N_2. Benzene-d_6 and toluene-d_8 were vacuum transferred from Na/K alloy and

stored under N_2 in the glovebox. Bromobenzene-d_5, was degassed in three freeze-pump-thaw cycles and stored over 4 Å molecular sieve under N_2 in the glovebox. All organic reagents were purchased from Aldrich and used as received. $Cp_2Zr\{N(SiHMe_2)t\text{-}Bu\}H$ (**10.2**),[2f,9] $Cp_2Zr\{N(SiHMe_2)t\text{-}Bu\}OTf$,[14] $B(C_6F_5)_3$,[14] and $[Ph_3C][B(C_6F_5)_4]$[15] were prepared as described in literature procedures. ^1H, $^{13}C\{^1H\}$, ^{11}B, ^{19}F, and ^{29}SI NMR spectra were collected on Agilent MR-400, Bruker DRX-400, or Bruker AVIII 600 NMR spectrometers. ^{15}N chemical shifts were determined by ^1H-^{15}N HMBC experiments on a Bruker AVII 600 spectrometer with a Bruker Z-gradient inverse TXI $^1H/^{13}C/^{15}N$ 5mm cryoprobe; ^{15}N chemical shifts were originally referenced to an external liquid NH_3 standard and recalculated to the CH_3NO_2 chemical shift scale by adding -381.9 ppm. $^{29}Si\{^1H\}$ NMR spectra were recorded using DEPT experiments, and assignments were verified by ^1H COESY, ^1H-^{13}C HMQC, ^1H-^{13}C HMBC, and ^1H-^{29}Si HMBC experiments. Elemental analysis was performed using a Perkin-Elmer 2400 Series II CHN/S by the Iowa State Chemical Instrumentation Facility. X-ray diffraction data was collected on a Bruker APEX II diffractometer.

$[Cp_2ZrN(SiHMe_2)t\text{-}Bu][HB(C_6F_5)_3]$ ([10.2][$HB(C_6F_5)_3$]). Compound **10.1** (0.066 g, 0.188 mmol) and $B(C_6F_5)_3$ (0.096 g, 0.188 mmol) were dissolved in benzene (10 mL). The reaction mixture was stirred at room temperature for 20 min, and a light yellow oil layer precipitated from the solvent. The top layer was decanted, and the oil layer was washed with benzene (4 × 5 mL) and pentane (2 × 5 mL). All the volatile materials were removed under reduced pressure to yield [**10.2**][$HB(C_6F_5)_3$] (0.135 g, 0.157 mmol, 83.2%) as a light purple solid. ^1H NMR (bromobenzene-d_5, 400 MHz, 25 °C): δ 6.17 (s, 10 H, C_5H_5), 4.24 (br q, 1 H, HB), 0.72 (s, 9 H, C_4H_9), 0.46 (m, $^1J_{SiH}$ = 90.7 Hz, 1 H, SiH), 0.29 (d, $^3J_{HH}$ = 3.2 Hz, 6 H, SiMe). $^{13}C\{^1H\}$ NMR (bromobenzene-d_5, 125 MHz, 25 °C): δ 148.68 (br, C_6F_5), 146.34 (br, C_6F_5),

138.07 (br, C_6F_5), 136.82 (br, C_6F_5), 135.65 (br, C_6F_5), 134.42 (br, C_6F_5), 116.28 (C_5H_5), 61.26 (CMe_3), 31.85 (CMe_3), 0.26 (SiMe). ^{11}B NMR (bromobenzene-d_5, 119.3 MHz, 25 °C): δ - 24.4 (br). ^{15}N{^{1}H} NMR (methylene chloride-d_2, 61 MHz, 25 °C): δ -199.3. ^{19}F NMR (bromobenzene-d_5, 376 MHz, 25 °C): δ -131.8 (d, $^3J_{FF}$ = 24.4 Hz, 6 F, *ortho*-F), -162.5 (t, $^3J_{FF}$ = 20.7 Hz, 3 F, *para*-F), -165.4 (t, $^3J_{FF}$ = 17.7 Hz, 6 F, *meta*-F). ^{29}Si{^{1}H} NMR (bromobenzene-d_5, 119.3 MHz, 25 °C): δ -7.5. IR (KBr, cm^{-1}): 3135 m, 3105 m, 2963 m, 2367 m br (ν_{BH}), 1709 m (ν_{SiH}), 1644 s (ν_{C6F5}), 1602 m, 1513 s (ν_{C6F5}), 1457 br s (ν_{C6F5}), 1377 m, 1365 m, 1276 s, 1253 s, 1237 s, 1219 s, 1113 s, 1070 s, 1023 s, 1014 s, 970 s br, 906 s, 858 s, 818 s, 762 s, 720 m. Anal. Calcd for $BC_{34}F_{15}H_{27}SiNZr$: C, 47.23; H, 3.15; N, 1.62. Found: C, 47.29; H, 3.60; N, 1.52. mp 132-135 °C.

[$Cp_2ZrN(SiHMe_2)$*t*-Bu][$B(C_6F_5)_4$] ([10.2][$B(C_6F_5)_4$]). Compound **10.1** (0.084 g, 0.239 mmol) and [Ph_3C][$B(C_6F_5)_4$] (0.221 g, 0.239 mmol) were dissolved in benzene (10 mL). The reaction mixture was stirred at room temperature for 20 min, and a purple layer precipitated from the solvent. The top layer was decanted, and the oil layer was washed with benzene (4 × 5 mL) and pentane (2 × 5 mL). All the volatile materials were removed under reduced pressure to yield [**10.2**][$B(C_6F_5)_4$] (0.147 g, 0.142 mmol, 59.6%) as a light purple solid. Purple X-ray quality crystals were grown from concentrated bromobenzene at -30 °C. ^{1}H NMR (bromobenzene-d_5, 400 MHz, 25 °C): δ 6.11 (s, 10 H, C_5H_5), 0.72 (s, 9 H, C_4H_9), 0.35 (m, $^1J_{SiH}$ = 90.4 Hz, 1 H, SiH), 0.28 (s, 6 H, SiMe). ^{13}C{^{1}H} NMR (bromobenzene-d_5, 125 MHz, 25 °C): δ 148.70 (C_6F_5), 146.32 (C_6F_5), 138.56 (C_6F_5), 136.69 (C_6F_5), 136.11 (C_6F_5), 134.24 (C_6F_5), 116.14 (C_5H_5), 61.37 (CMe), 31.78 (CMe), 0.21 (SiMe). ^{11}B NMR (bromobenzene-d_5, 119.3 MHz, 25 °C): δ -16.0. ^{15}N{^{1}H} NMR (methylene chloride-d_2, 61

MHz, 25 °C): δ -198.5. ^{19}F NMR (bromobenzene-d_5, 376 MHz, 25 °C): δ -131.6 (br, 8 F, *ortho*-F), -161.6 (t, $^{3}J_{FF}$ = 22.0 Hz, 4 F, *para*-F), -165.5 (t, $^{3}J_{FF}$ = 19.2 Hz, 8 F, *meta*-F). ^{29}Si{^{1}H} NMR (bromobenzene-d_5, 119.3 MHz, 25 °C): δ -7.6. IR (KBr, cm^{-1}): 3123 w, 2968 m, 1763 w, 1703 w (ν_{SiH}), 1644 s (ν_{C6F5}), 1600 m, 1515 s (ν_{C6F5}), 1463 s br (ν_{C6F5}), 1375 m, 1365 m, 1275 s br, 1219 m, 1189 m, 1086 s br, 1019 m, 980 s br, 906 m, 857 m, 810 s br, 775 s, 756 s, 725 m. Calcd for $BC_{40}F_{20}H_{26}SiNZr$: C, 46.61; H, 2.54; N, 1.36. Found: C, 46.83; H, 2.50; N, 1.27. mp 145-148 °C.

Cp(CpSiMe$_2$N*t*-Bu)ZrOTf (9.30). A benzene (10ml) solution of $Cp_2ZrOTfN$*t*-$BuSiHMe_2$ (0.102 g, 0.204 mmol) and $B(C_6F_5)_3$ (0.105 g, 0.204 mmol) was stirred at room temperature for 24 h. The volatiles were evaporated under reduced pressure to yield a yellow solid. The yellow solid was extracted with pentane (2 x 5 ml). The pentane extract was concentrated and cooled to -30 ºC to give **9.30** as a white solid (0.097 g, 0.194 mmol) ^{1}H NMR (benzene-d_6, 400 MHz, 25 °C): δ 6.84 (m br, C_5H_5, 1 H), 6.41 (m br, C_5H_5, 1 H), 6.06 (m br, C_5H_5, 1 H), 5.93 (s, C_5H_5, 5 H), 5.21 (m br, C_5H_5, 1 H), 1.13 (s, C_4H_9, 9 H), 0.49 (s, Si*Me*, 3 H), 0.19 (s, Si*Me*, 3 H). ^{13}C{^{1}H} NMR (benzene-d_6, 125 MHz, 25 °C): δ 125.09 (C_5H_4), 120.80 (C_5H_4), 118.35 (C_5H_4), 115.26 (C_5H_5), 113.16 ($SiMe_2C_5H_4$), 112.21 (C_5H_4), 59.96 (*C*CH3), 35.20 (C*C*H$_3$), 4.68 (Si*Me*), 1.59 (Si*Me*).^{19}F NMR (benzene-d_6, 376 MHz, 25 °C): δ -77.4. ^{29}Si{^{1}H} NMR (benzene-d_6, 119.3 MHz, 25 °C): d -23.3 (*Si*Me). ^{15}N{^{1}H} NMR (benzene-d_6, 61 MHz, 25 °C): δ -266.5.

Cp(CpSiMe$_2$N*t*-Bu)ZrI (8-I). A benzene (10 ml) solution of Cp_2ZrIN*t*-$BuSiHMe_2$ (0.096 g, 0.201 mmol) and $B(C_6F_5)_3$ (0.103 g, 0.201 mmol) was stirred at room temperature for 1 h. The volatiles were evaporated under reduced pressure to yield a yellow solid. The yellow

solid was extracted with pentane (2 x 5 ml). The pentane extract was concentrated and cooled to -30 ºC to give Cp(CpSiMe$_2$N*t*-Bu)ZrI as a bright yellow solid (0.091 g, 0.191 mmol, 95.0 %). ^{1}H NMR (benzene-d_6, 400 MHz, 25 °C): δ 7.07 (m br, C_5H_5, 1 H), 6.32 (m br, C_5H_5, 1 H), 5.97 (s, C_5H_5, 5 H), 5.72 (m br, C_5H_5, 1 H), 5.47 (m br, C_5H_5, 1 H), 1.21 (s, C_4H_9, 9 H), 0.51 (s, Si*Me*, 3 H), 0.27 (s, Si*Me*, 3 H). ^{13}C{^{1}H} NMR (benzene-d_6, 125 MHz, 25 °C): δ 125.09 (C_5H_4), 118.65 (C_5H_4), 118.24 (C_5H_4), 115.09 (C_5H_5), 112.66 (SiMe$_2C_5H_4$), 112.11 (C_5H_4), 59.82 (*C*CH3), 35.10 (C*C*H$_3$), 4.62 (Si*Me*), 2.09 (Si*Me*). ^{29}Si{^{1}H} NMR (benzene-d_6, 119.3 MHz, 25 °C): δ -23.9 (*Si*Me). ^{15}N{^{1}H} NMR (benzene-d_6, 61 MHz, 25 °C): δ -141.9.

Reference

1 For transition metal silene: a) Campion, B. K.; Heyn, R. H.; Tilley, T. D. *J. Am. Chem. Soc.* **1988**, *110*, 7558-7560. b) Campion, B. K.; Heyn, R.; Tilley, T. D. *J. Am. Chem. Soc.* **1990**, *112*, 4079. c) Pannell, K. H. *J. Organomet. Chem.* **1970**, *21*, P17. d) Koloski, T. S.; Carroll, P. J.; Berry, D. H. *J. Am. Chem. Soc.* **1990**, *112*, 6405-6406. For transition metal disilene: d) Pham, E. K.; West, R. *J. Am. Chem. Soc.* **1989**, *111*,7667-7668. e) Berry, D. H.; Chey, J. H.; Zipin. H. S.; Carroll, P. J. *J. Am. Chem. Soc.* **1990**, *112*, 452. For transition metal and f-element silanimine: f) Procopio, L. J.; Carroll, P. J.; Berry, D. H. *J. Am. Chem. Soc.* **1991**, *113*, 1870-1872. g) Chen, Y.; Song, H.; Cui, C. *Angew. Chem. Int. Ed.* **2010**, *49*, 8958-8961.

2 Khalimon, A. Y.; Simionescu, R.; Kuzmina, L. G.; Howard, J. A. K.; Nikonov G. I. *Angew. Chem. Int. Ed.* **2008**, *47*, 7701-7704. Khalimon, A. Y.; Simionescu, R.; Nikonov, G. I. *J. Am. Chem. Soc.* 2011, *133*, 7033-7053.

3 Procopio, L. J.; Carroll, P. J.; Berry, D. H. *Organometallics* **1993**, *12*, 3087-3093.

4 Bi, S.; Zhu, S.; Zhang, Z. *Eur. J. Inorg. Chem.* ***2007***, 2046–2054.

5 a) Parks, D. J.; Piers, W. E. *J. Am. Chem. Soc.* **1996**, *118,* 9440-9441. b) Parks, D. J.; Blackwell, J. M.; Piers, W. E. *J. Org. Chem.* **2000**, *65,* 3090-3098.

6 a) Yan, K.; Upton, B. M.; Ellern, A.; Sadow, A. D. *J. Am. Chem. Soc.* **2009**, *131*, 15110–15111. b) Yan, K.; Schoendorff, G.; Upton, B. M.; Ellern, A.; Windus, T. L.; Sadow, A. D. *Organometallics* **2013**, *32*, 1300-1316.

7 Ohff, A.; Kosse, P.; Baumann, W.; Tillack, A.; Kempe, R.; Goerls, H.; Burlakov, V. V.; Rosenthal, U. *J. Am. Chem. Soc.* **1995**, *117*, 10399-10400.

8 Procopio, L. J.; Carroll, P. J.; Berry, D. H. *J. Am. Chem. Soc.* **1994**, *116*, 177-185.

9 Rees Jr., W. S.; Just, O.; Schumann, H.; Weimann, R. *Angew. Chem. Int. Ed.* **1996**, *35*, 419-422.

10 Zhou, Z.; Jordan, R. F. *Organometallics* **2011**, *30*, 4632-4642.

11 a) Carpenetti, D. W.; Kloppenburg, L.; Kupec, J. T.; Petersen, J. L. *Organometallics* **1996**, *15*, 1572-1581. b) Braun, L. F.; Dreier, T.; Christy, M.; Petersen, J. L. *Inorg. Chem.* **2004**, *43*, 3976-3987. c) Petrisor, C. E.; Frutos, L. M.; Castaño, O.; Mosquera, M. E. G.; Royo, E.; Cuenca, T. *Dalton Trans.* **2008**, 2670-2673.

12 a) Shapiro, P. J.; Sinnema, P.-J.; Perrotin, P.; Budzelaar, P. H. M.; Weihe, H.; Twamley, B.; Zehnder, R. A.; Nairn, J. J. *Chem. Eur. J.* **2007**, *13*, 6212-6222. b) Ruwwe, J.; Erker, G.; Fröhlich, R. *Angew. Chem. Int. Ed. Engl.* **1996**, *35*, 80-82.

13 Yan, K.; Ellern, A.; Sadow, A. D. *J. Am. Chem. Soc.* **2012**, *134*, 9154-9156.

14 Massey, A. G.; Park, A. J. *J. Organomet. Chem.* **1964**, *2*, 245-250.

15 Scott, V. J.; Celenligil-Cetin, R.; Ozerov, O. V. *J. Am. Chem. Soc.* **2005**, *127*, 2852-2853.

Chapter 11: General conclusion

Development and understanding of fundamental reaction pathwayas remains an important aspect of organometallic chemistry and experimental organometallic chemistry is still full of surprises. Understanding the role of β-H containing ligand in stoichiometric and catalytic reactions provides valuable insight into how these metal complexes behave intramolecularly and intermolecularly with substrates or co-catalysts, and their decomposition pathway. The major challenge in olefin polymerization is to control the rate between olefin insertion and β-H elimination. Both processes originate from organometallic species that contain β-hydrogen and vacant *cis* coordination site.

From my work, we have introduced a new multiple β-hydrogens containing alkyl ligand $C(SiHMe_2)_3$ for coordination chemistry in main group, early transition metal and rare earth metals. The three SiH groups also provide excellent spectroscopic probe. One compound that I synthesized was $Y[C(SiHMe_2)_3]_3$ that all nine SiHs are equivalent at 298K. However, an unprecedented six β-agostic SiHs (2 agostic Si-H for each $C(SiHMe_2)_3$) was observed by NMR spectroscopy at 190K. This compound shows no sign of β-H elimination even at elevated temperature that was often considered as the catalyst degradation pathway in other early metal alkyl complexes bearing β-H. To investigate if the lack of open site for β-H elimination to proceed in the Y case, we prepared the less sterically crowded $M[C(SiHMe_2)_3]_2THF_2$ M=Ca, Yb. The IR and NMR spectroscopy show that the compounds do bear weaker agostic SiH interaction than the Y analog, so we expect β-elimination to be more facile. However, thermolysis study revealed no sign of β-H elimination either. As a result, we

reacted $M[C(SiHMe_2)_3]_2THF_2$ M = Ca, Yb with Lewis acids (LA = BPh_3, $B(C_6F_5)_3$, $[Ph_3C][B(C_6F_5)_4]$) to attempt to open up a vacant site to facilitate such elimination. Unexpectedly, the most nucleophilic site in the complexes is not the carbanic carbon, but the Si-H bond to form the H-abstracted byproduct silene dimer $[Me_2SiC(SiHMe_2)_2]_2$ and zwitterionic species $[MC(SiHMe_3)_3THF_2][H\text{-}LA]$. $[MC(SiHMe_3)_3THF_2][HB(C_6F_5)_3]$ does eliminate silene at 100 ^oC, but the actual mechanism is still under investigation. We favored the transition state of being the silene-bound hydrido species illustrated below.

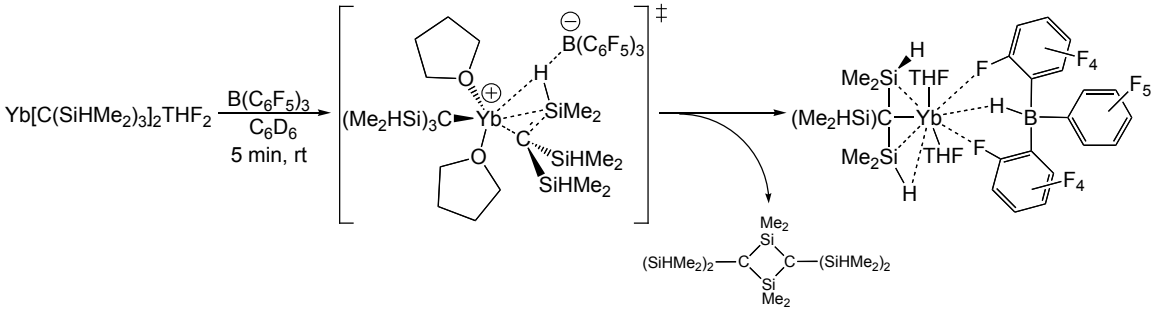

The questions remain to be answered in this project is: Can we trap the intermediate? Which Si-H is responsible for the abstraction, agostic Si-H or nonagostic Si-H? These fundamental questions have not been addressed in literature and could be important in aspects such as catalyst-activation and chain-walking on olefin polymerization.

Although my work is more related to stoichiometric reactivity, the research plan is to understand what is going on in stoichiometric reaction, the structure of the intermediates, and then apply the complexes to homogeneous catalysis. However, heterogeneous catalysis is the ultimate goal to utilize the silica surface (act as an immobilized ancillary ligand) to isolate reactive species, such as $(SiO)_{3-n}Ln\text{-}(H)_n$. Related species (ex. $(Cp'YH_2)_4$ cluster) have displayed amazing reactivity as homogeneous polymerization catalysts. Also, the redox ability in Yb or other related Ln(II) metals can also be tuned to study the reactivity of these β-SiH containing complexes upon oxidation. In that regard, we have attempted the oxidation

of Yb bis(alkyl) with $[Cp_2Fe][BPh_4]$, but only oxidation of alkyl group was observed. Therefore, an oxidant with the right redox potential is crucial for the development of this end of this chemistry. On the other hand, we have also synthesized another β-SiH containing alkyl ligand $CH(SiHMe_2)_2$, a β-H containing analog of a widely used $CH(SiMe_3)_2$ ligand. Preliminary works show that we can synthesize new rare-earth alkyl with this ligand and their reactivity with Lewis acids would be investigated in the near future.

Another part of my thesis is to investigate the reactivity of β-H containing zirconium amido complexes. Prior to my work, surprisingly, there was only one example of Group 4 complex that contains $N(SiHMe_2)_2$ ligand. Coordination chemistry with $N(SiHMe_2)_2$ has been widely studied for Group 3 and rare-earth and more recently main group and late metal systems. By using this ligand, we have successfully introduced a couple first examples of β-H elimination reaction for d^0 amido systems promoted by 1) alkali-metal salt, and 2) 2-electron donor. More importantly in the second example, d^0 amide complexes are suggested to be resistant to β-H elimination and further, Bercaw demonstrated that complexes with β-agostic interactions are even less prone to b-H elimination due to a stabilization effect in their ground state structures. We showed that highly bis(agostic) Zr(IV) amide cationic complexes undergo a formally β-H elimination at room temperature promoted by Lewis base. These findings provide unqiue examples for the exception of the general belief. This is why chemistry in general and organometallic chemistry in particular in this case are endlessly interesting because conventional wisdom is always being challenged and questioned even in well-studied systems. Every new example is unique and best of all, surprises lurk around

almost every corner. As Nobel Laureate Arthur Kornberg once said, "I never met a dull enzyme".